Development of α-Helix-like α/β/γ Foldamers

By

Younghee Shin

A dissertation submitted in partial fulfillment of

the requirements for the degree of

Doctor of Philosophy

(Chemistry)

at the

UNIVERSITY OF WISCONSIN-MADISON

2015

Date of final oral examination: 01/16/2015

The dissertation is approved by the following members of the Final Oral Committee:

Samuel H. Gellman, Professor, Chemistry
Judith N. Burstyn, Professor, Chemistry
Tehshik P. Yoon, Professor, Chemistry
Eric R. Strieter, Assistant Professor, Chemistry
Sandro Mecozzi, Associate Professor, Pharmaceutical Sciences

Acknowledgements:

First and foremost, I would like to thank my advisor, Prof. Sam Gellman. I was very lucky to learn from him, who is an excellent scientist and mentor. He helped me to think by myself about scientific topics and projects. Sometimes with a challenge but always with patience, he guided me to grow up as a scientist. I would like to thank all the Gellman group members who are enthusiastic about research and science. It will be an unforgettable experience for me to work and study with such an intelligent and energetic people. I also would like to thank my classmates. We supported each other with warm hearts and cookies, went to gym together, and were happy for growing up together. I am grateful to my parents and family, who are always in my side with positive mind and love, and have helped me to get through my life in abroad. I would like to thank my husband Naechul, who always encouraged me with love. Lastly, I thank God for leading my life.

Editorial Assistance
Professor Sam Gellman
Marlies Hager
Brian Fisher
Ross Cheloha
James Checco
Leslie Rank
Melissa MacDonald

Dissertation Committee
Professor Sam Gellman
Professor Judith Burstyn
Professor Eric Strieter
Professor Tehshik Yoon
Professor Sandro Mecozzi

Facilities
Dr. Charlie Fry – Chemistry NMR
Dr. Martha Vestling – Chemistry Mass Spectrometry
Dr. Darrell McCaslin – Biophysics Instrumentation Facility

Crystallography
Dr. Katrina Forest & Dr. Kenneth Satyshur
David Mortenson

Table of Contents

Chapter 1. Introduction: α-Helical Peptidomimetics and γ-Amino Acids as New Building Blocks

1.1 α-Helix-mimicry

Protein-protein interactions (PPIs) that regulate a variety of cellular processes are mediated by helical interfaces.[1-4] Several examples of clinically interesting helix-mediated interactions are shown in Figure 1.1. In each case, disruption of the interaction could be therapeutically beneficial.

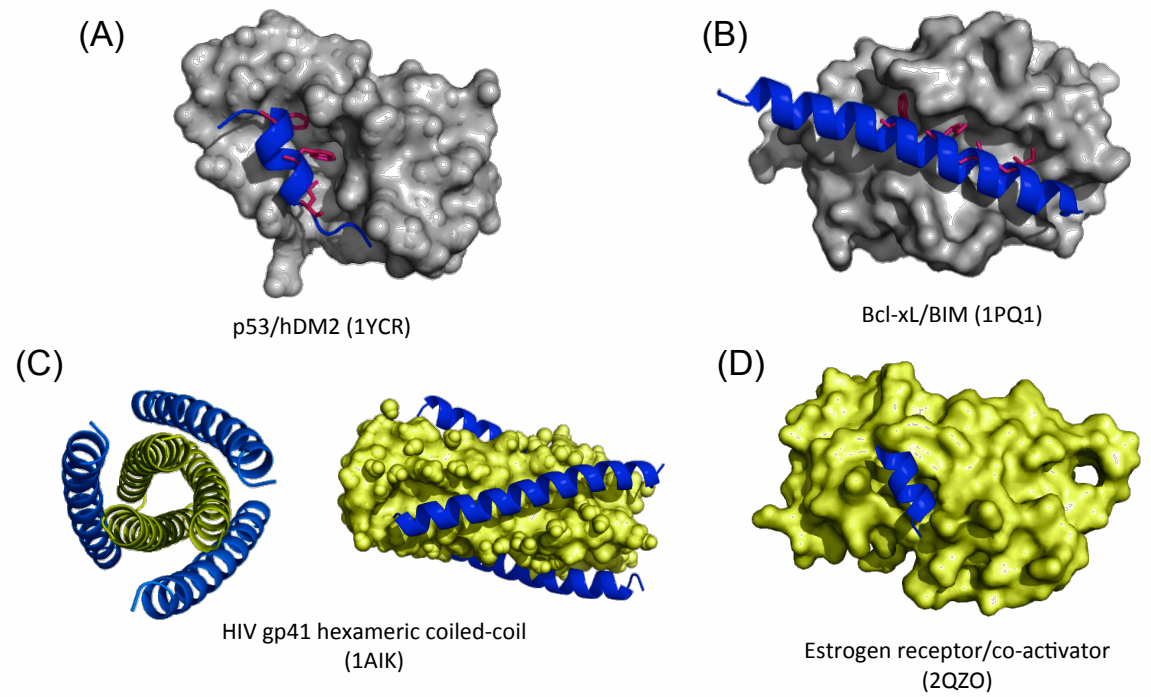

Figure 1.1 α-Helix-mediated protein-protein interactions (A) p53/hDM2 (tumour protein 53–human double minute 2) interaction (PDB ID: 1YCR), key residues of p53 segment involved in binding shown in pink. (B) Bcl-xL/BIM (B-cell lymphoma 2) interaction (PDB ID: 1PQ1), key residues involved in binding shown in pink. (C) Top and side view of HIV gp41 hexameric coiled-coil fusion complex (PDB ID: 1AIK). (D) Estrogen receptor/co-activator interaction (PDB ID: 2QZO).

To serve as therapeutically useful helical peptidomimetics, synthetic oligomers must mimic the spatial arrangement of functional groups in the original α-helix to retain target affinity, and should be stable in physiological environments to be able to reach

their targets. Important physical parameters include solubility, resistance to proteolytic degradation, and membrane permeability for intracellular targets. Employing small molecules (molecular weight < 500) to modulate helix-mediated interactions is very challenging, due to the large contact area involved at helical interfaces. Non-small molecule strategies for designing helical peptidomimetics have been extensively explored.[2,4] Systems examined include terphenyls, peptoids, miniproteins, β-peptides, α/β-peptides, and α-helices stabilized by cross-linked side-chains or backbone (hydrogen bond surrogate, HBS) (Figure 1.2).[1,3,4]

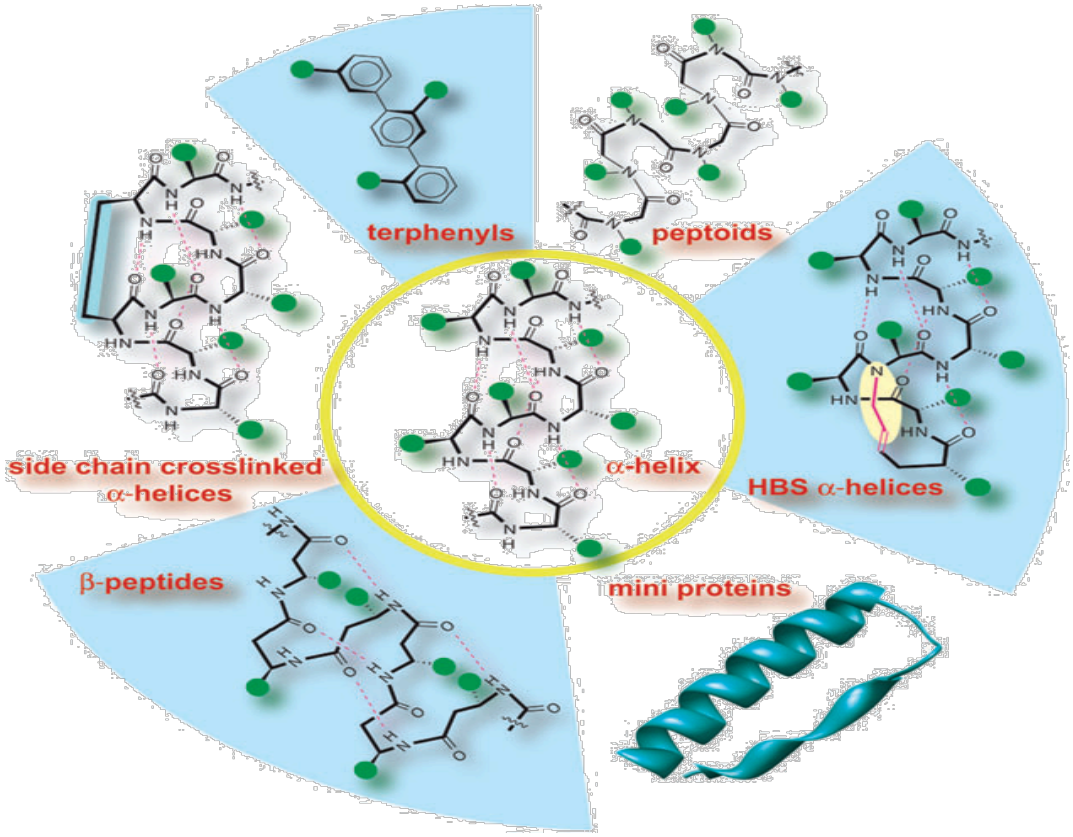

Figure 1.2 Strategies for non-natural helix mimetic design and α-helix stabilization. Green circles indicate functional groups. The image was reproduced with permission from reference 3 [*Molecular Biosystems* **2009**, *5*, 924-926.] Copyright [2009] Royal Society of Chemistry.

1.2 α/β Foldamers to mimic α-helices

A critical limitation of canonical α-peptides for biomedical applications is their rapid proteolytic degradation under physiological conditions. The Gellman group has developed foldamers, unnatural oligomers with well-defined folding behavior, containing non-natural backbone subunits such as β-amino acids (Figure 1.3).[5-7] Foldamers containing β-amino acids have been shown to adopt helical conformations with significantly increased resistance to proteolysis relative to analogous .[5-11] Thorough structural analyses of β-peptides (containing exclusively β-residues) and α/β-peptides (heterogeneous backbone with α- and β-residues) have led to the successful design of α/β-peptide foldamers to manipulate PPIs involving helical interfaces (Figure 1.3).[12-18] Selective incorporation of five-membered ring-constrained β-amino acids into helical α/β-peptides has been shown to enhance affinity for the target proteins, presumably due to the pre-organization of the helical backbone caused by ring-constraints on the β-amino acid residues (Figure 1.3).[11,15-19] One example of α/β-peptide foldamers mimicking α-helical peptide function is shown in Figure 1.3.[9] The α/β-peptide **1.1** was derived from the CHR domain of HIV protein gp41 and is an effective inhibitor of HIV infection in a cell-based assay. This activity presumably results from effective biomimicry of the long α-helix formed by the gp41 CHR domain. α/β **1.1** presented an improved stability to proteolytic degradation compared to the corresponding α-peptide T-2635, and exhibited a reasonable affinity for gp41-5, an engineered five-helix bundle protein that contains three NHR segments and two CHR segments (Figure 1.3).

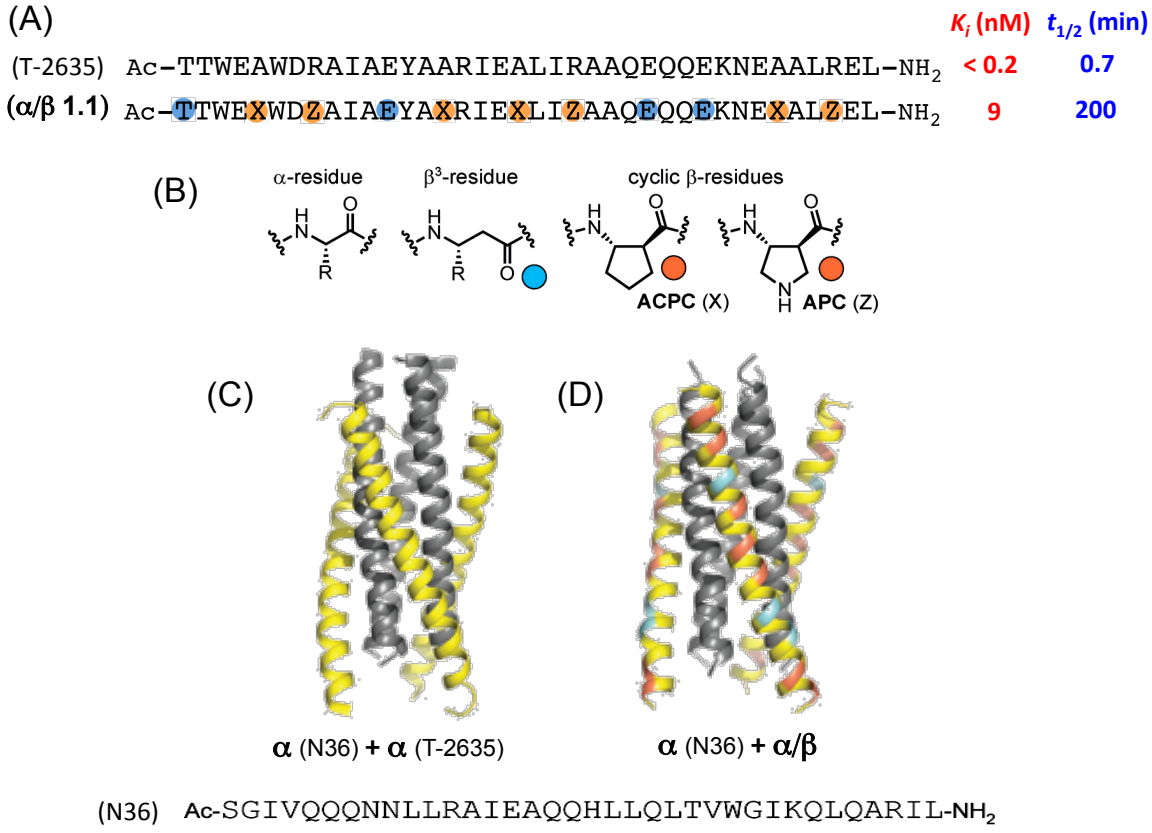

Figure 1.3 α-Helix mimicry using an α/β-peptide. (A) Sequences of α-peptide T-2635 and α/β-peptide **1.1**, dissociation constants (K_i) for binding to the protein gp41–5 as determined by competition FP experiments, and half-life ($t_{1/2}$) of a 20 μM solution of peptide in TBS in the presence of 10 μg/mL proteinase K. (B) Structures of an α-amino acid residue, the corresponding β^3 residue analogue, and cyclic β residues ACPC and APC. (C and D) Crystal structure of the six-helix bundles formed by NHR α-peptide N36 in complex with α-peptide T-2635, PDB 3F4Y, and N36 with the α/β-peptide **1.1**, PDB 3O43. Blue for β^3, peach for cyclic β residues. [9]

1.3 γ-Amino acids as new building blocks for helical foldamers

Other building blocks besides β-amino acids for a non-natural peptide might also display discrete conformational properties, which may result in useful function. γ-Amino acids are appealing extension beyond β-amino acid building blocks.[20-30] The study of γ-residue-containing foldamers lags behind the study of β-residue-containing foldamers, perhaps due to the challenges of synthesizing enantiopure γ-amino acids.

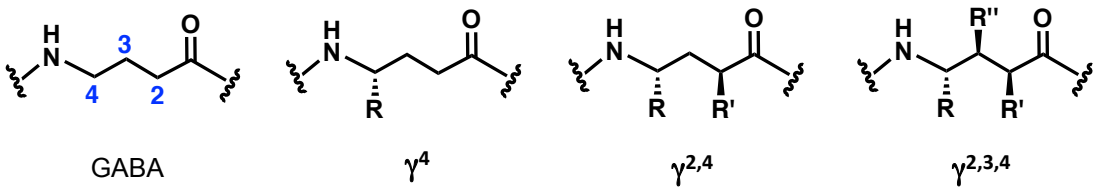

Figure 1.4 Structures of acyclic γ-amino acids.

Several research groups have examined helical foldamers containing acyclic γ-amino acids in organic solvents (Figure 1.4). In the 1990's Hanessian *et al.* and Seebach *et al.* reported in separate studies that γ-peptides containing γ^4-, $\gamma^{2,4}$-, or $\gamma^{2,3,4}$-amino acid residues adopt helical conformations in organic solvents. These helices contain 14-membered C=O(i)--H-N(i+3) hydrogen bonds, and are therefore referred to as 14-helices based on H-bond ring size (Figure 1.4).[21-23] γ^4-Amino acids, such as γ^4-hAla, γ^4-hLeu, and γ^4-hPhe, contain side chains at the γ-position, and can be viewed as analogous to L-α-amino acids in canonical peptides. This type of γ residues have been incorporated into α/γ-peptides by Balaram *et al.* and Gopi *et al.*. These α/γ-peptides adopt helical conformation in organic solvents.[24-28] However, analogous structural

evaluations have not been yet performed in water. Studies in water require substantial conformational stability and are important for biological applications of foldamers.

The Gellman group has developed ring-constrained γ-amino acids (Figure 1.5).[20-30] One central hypothesis is that in the absence of ring-constraints on γ-residues, peptides containing acyclic γ-residues may be too flexible to adopt a helical conformation in water.[31-36] The Gellman group has developed five- and six-membered ring-constrained β-amino acids, and the residues exhibited excellent ability to promote helical folding of α/β-peptides.[6,9,37] Using ring-constrained β-amino acids as inspiration, we are interested in γ-amino acids containing a five- or six-membered-ring on the Cβ-Cγ bond or the Cα-Cβ bond, with either *cis*- or *trans*-ring configuration (Figure 1.5A).

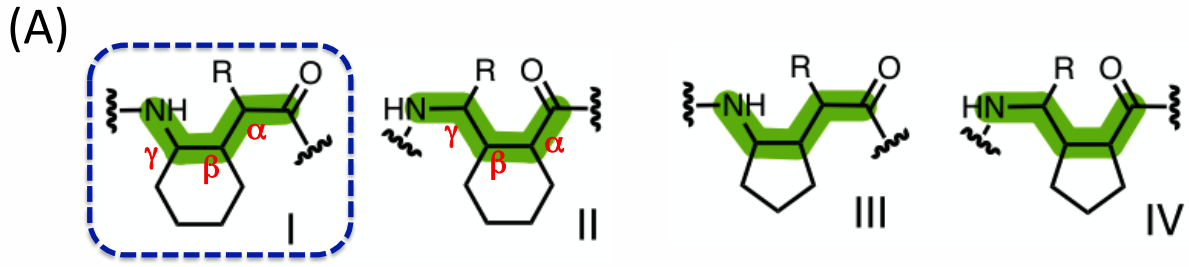

Figure 1.5 (A) Structures of constrained γ-residues of interest. Configurations are not shown since all the possible configurations are worthy of evaluation for their folding propensities. (B) Structure of EtACHA.[35,36]

Among the various γ-amino acids shown in Figure 1.5A, several constrained γ-amino acids have been successfully synthesized in enantiopure form by Guo and by Giuliano (Figure 1.5B). [31-36,38] Giuliano *et al.* prepared γ-amino acids containing *trans*-cyclopentyl or *trans*-cyclohexyl ring-constraints across the Cα-Cβ bond (Figure 1.5A, **II** and **IV**) by organo-catalyzed Michael addition of nitroalkanes to α/β-unsaturated aldehydes (Figure 1.6B). These γ-residues, containing *trans* rings on the Cα-Cβ bonds, have been incorporated into peptide with a 1:1 α:γ alteration. The resulting α/γ peptides display distinct helical folding with *alternating* H-bond directionalities. In contrast, H-bonded helices in α-peptides feature a *uniform* H-bonding directionality, N-terminal side C═O to C-terminal side NH.[31,39]

Guo *et al.* synthesized constrained γ-amino acids with *cis* or *trans* cyclohexyl rings on the Cβ-Cγ bond and R groups on the Cα position (Figure 1.5A, **I**) by organo-catalyzed Michael addition of aldehydes to nitroalkenes (Figure 1.6A). The *cis* ring-constrained γ-amino acids consistently support helical structures in a pure γ-amino acid backbone[34] and for 1:1 α/γ- and 1:1 β/γ-backbones.[35,36] X-ray crystallographic results revealed that γ-, α/γ-, and β/γ-peptides containing EtACHA (Figure 1.7) resembled an α-peptide 3_{10} helix in terms of hydrogen bonding pattern, with 14-atom, 12-atom, and 13-atom-ring C=O(i)/H-N(i+3) hydrogen bonds, respectively (Figure 1.7).[34-36]

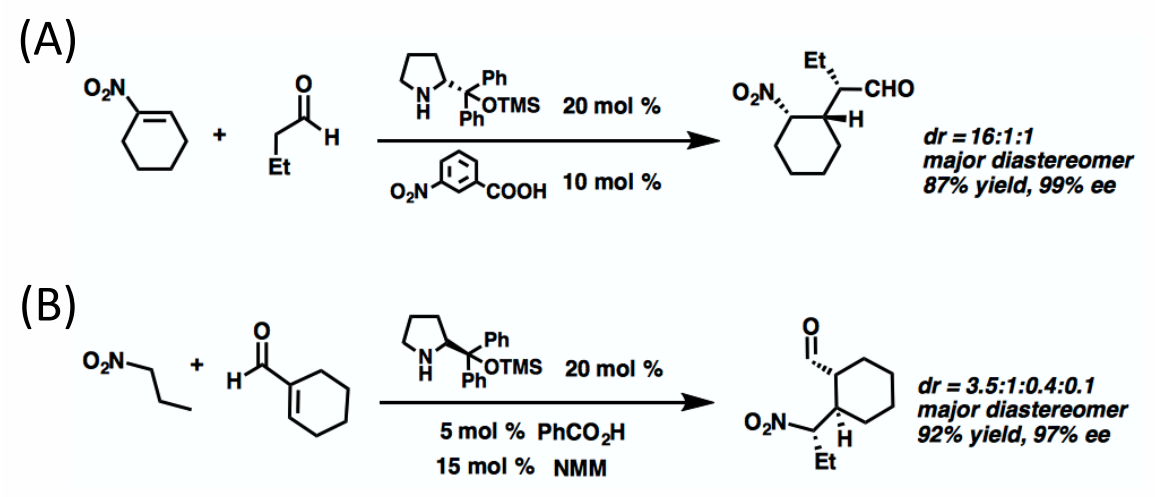

Figure 1.6 Key steps for the syntheses of ring constrained γ amino acids (types **I** and **II** shown in Figure 1.5). (A) Catalytic Michael addition of butanal to 1-nitrocyclohexene to yield a γ-nitro aldehyde to lead to *cis* type **I** residue, with R = ethyl (EtACHA).[36] (B) Catalytic Michael addition of 1-nitropropane to the enal yields a γ-nitro aldehyde to lead to *trans* type **II** residue, with R = ethyl.[39] (NMM: *N*-methylmorpholine)

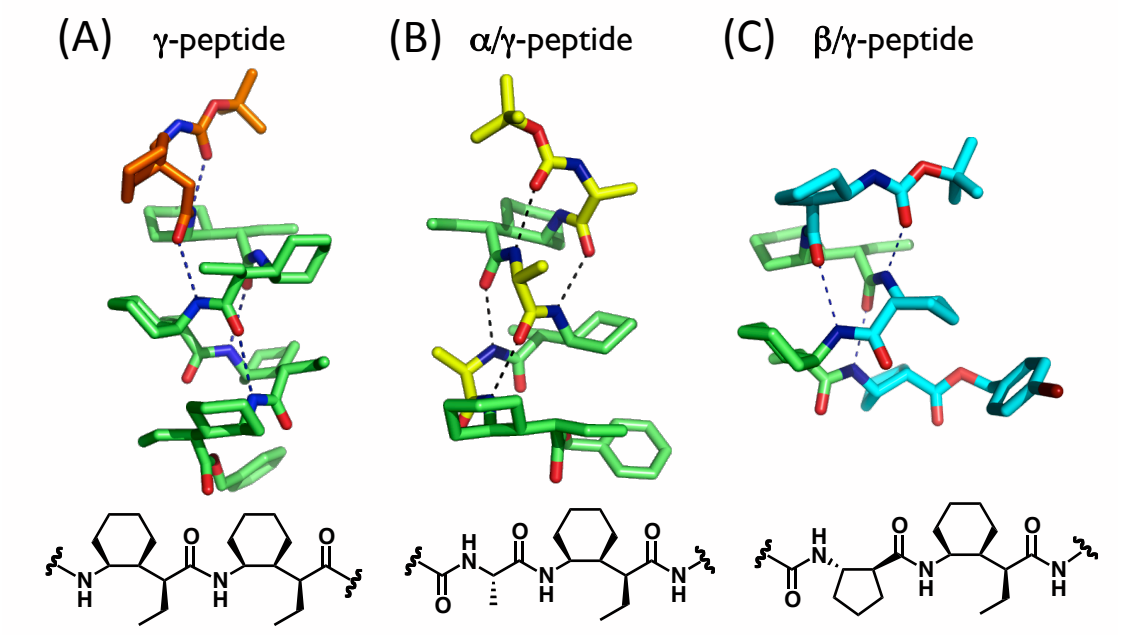

Figure 1.7 Crystal structures of (A) a γ-peptide, (B) a α/γ-peptide, and (C) a β/γ-peptide containing EtACHA (cyclic γ). Green is γ, yellow is α, cyan is β residue.[35,36]

1.4 Helical α/β/γ-peptide

Sawada and Gellman found that an α/β/γ-peptide containing ring-constrained β- and γ-residues in an αγααβα hexad pattern yielded a stable α-helix-like conformation.[20,40] The αγααβα hexad design is based on the idea that the number of backbone atoms from three α-amino acid residues corresponds to the number found in one β- and one γ-amino acid residue collectively (9 atoms = α + α + α = β + γ). This relationship replaces seven α-residues in the α-peptide heptad repeat with one β-, one γ-, and four α-residues in the α/β/γ-peptide hexad repeat (Figure 1.8A). The αγααβα pattern is intended to align β- and γ-residues along one side of the helix, allowing the α-residues (*a, d, e* and *g* positions on the helical wheel) to define the other face of the helix. Thus, the αγααβα pattern is proposed to allow mimicry of the recognition surface of a natural α-helix (Figure 1.8).

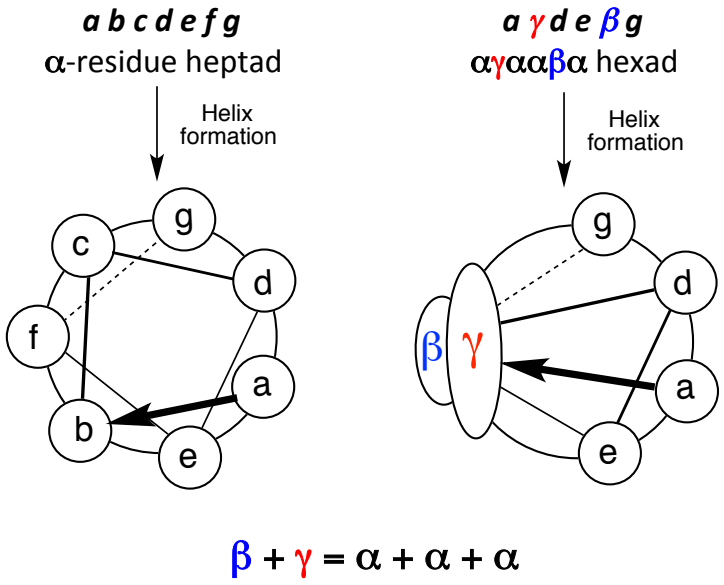

Figure 1.8 (A) Helical wheel diagrams of an αααααααα heptad (α-helix) and an αγααβα hexad (α/β/γ-helix).[40]

To test the hexad concept, Sawada and Gellman designed α/β/γ-peptide **1.2**, which incorporates ring-constrained β- and γ-residues in an αγααβα pattern. The analogous α-peptide **1.3** was not helical in aqueous solution. For the α/β/γ-peptide **1.2**, however, numerous medium-range NOEs (Nuclear Overhauser Effect) from non-adjacent residues were detected in water (acetate buffer), and the NMR structure based on the NOE-restraints showed an α-helix-like conformation (Figure 1.9B and C).[20,40]

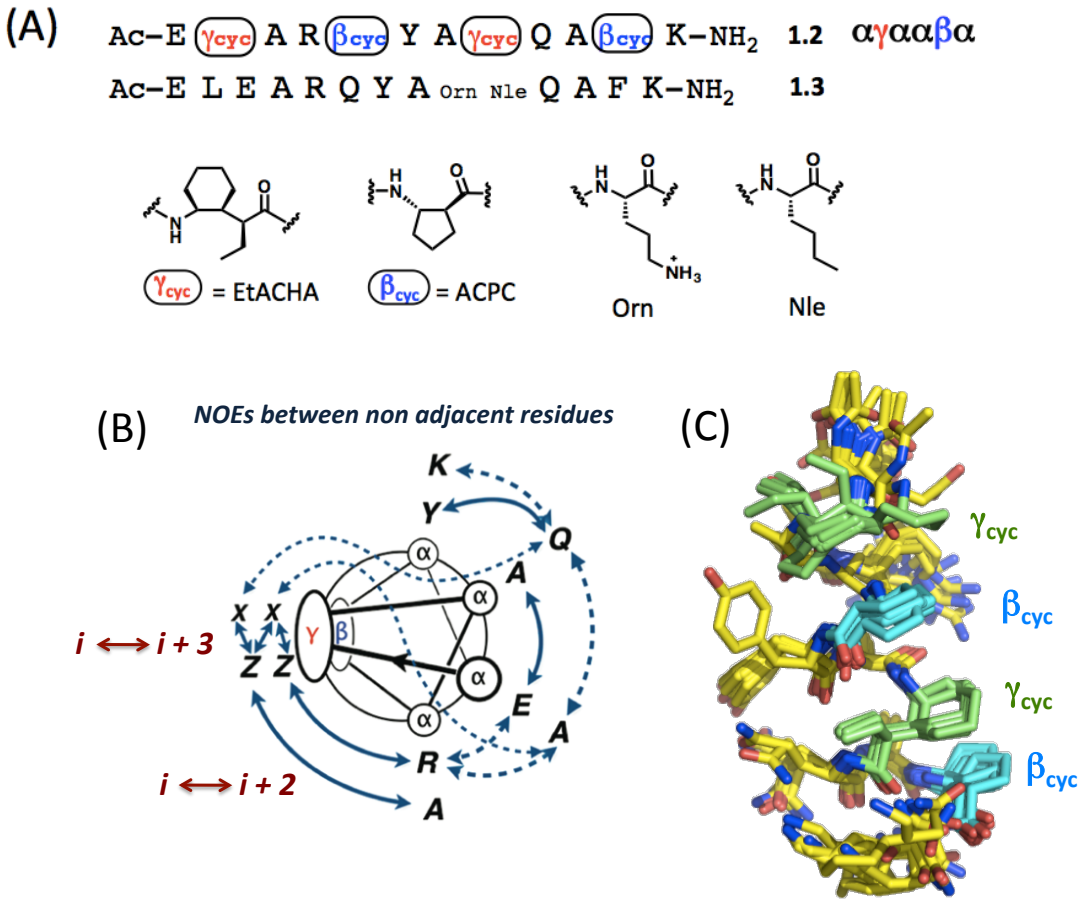

Figure 1.9 (A) Sequence of α/β/γ-peptide **1.2**, and structures of cyclic γ- and cyclic β-amino acids. (B) Helical wheel diagram of **1.2** with non-adjacent NOEs shown as curved arrows; plain curve-strong NOEs, dashed curve-medium NOEs (8 mM peptide in 9:1 H_2O/D_2O, 100 mM acetate buffer, pH 3.8). (C) NMR structures calculated based on the NOE-restraints. [40]

1.5 Foreword to Thesis Work

Further characterization of α-helix-mimicking α/β/γ-peptides is necessary to pursue biomedical applications of these potential peptidomimetics. This thesis details development of α-helix-like α/β/γ foldamers. Chapters 2 and 3 discuss biophysical investigations of helical α/β/γ-peptides. Chapter 4 discusses efforts to establish an α + α/β/γ coiled-coil system for use in thermodynamic analysis of α + α/β/γ coiled-coil folding propensities, and Chapter 5 discusses efforts toward developing functional α/β/γ-peptides to modulate apoptosis-regulating protein-protein interactions.

1.6 References

(1) Bullock, B. N.; Jochim, A. L.; Arora, P. S. Assessing Helical Protein Interfaces for Inhibitor Design. *Journal of the American Chemical Society* **2011**, *133*, 14220-14223.

(2) Jochim, A. L.; Arora, P. S. Systematic Analysis of Helical Protein Interfaces Reveals Targets for Synthetic Inhibitors. *Acs Chemical Biology* **2010**, *5*, 919-923.

(3) Jochim, A. L.; Arora, P. S. Assessment of helical interfaces in protein-protein interactions. *Molecular Biosystems* **2009**, *5*, 924-926.

(4) Azzarito, V.; Long, K.; Murphy, N. S.; Wilson, A. J. Inhibition of alpha-helix-mediated protein-protein interactions using designed molecules. *Nature Chemistry* **2013**, *5*, 161-173.

(5) Gellman, S. H. Foldamers: A manifesto. *Accounts of Chemical Research* **1998**, *31*, 173-180.

(6) Horne, W. S.; Gellman, S. H. Foldamers with Heterogeneous Backbones. *Accounts of Chemical Research* **2008**, *41*, 1399-1408.

(7) Johnson, L. M.; Mortenson, D. E.; Yun, H. G.; Horne, W. S.; Ketas, T. J.; Lu, M.; Moore, J. P.; Gellman, S. H. Enhancement of alpha-Helix Mimicry by an alpha/beta-Peptide Foldamer via Incorporation of a Dense Ionic Side-Chain Array. *Journal of the American Chemical Society* **2012**, *134*, 7317-7320.

(8) Johnson, L. M.; Gellman, S. H.: alpha-Helix Mimicry with alpha/beta-Peptides. In *Methods in Protein Design*; Keating, A. E., Ed.; Methods in Enzymology, 2013; Vol. 523; pp 407-429.

(9) Horne, W. S.; Johnson, L. M.; Ketas, T. J.; Klasse, P. J.; Lu, M.; Moore, J. P.; Gellman, S. H. Structural and biological mimicry of protein surface recognition by alpha/beta-peptide foldamers. *Proceedings of the National Academy of Sciences of the United States of America* **2009**, *106*, 14751-14756.

(10) Horne, W. S.; Boersma, M. D.; Windsor, M. A.; Gellman, S. H. Sequence-based design of alpha/beta-peptide foldamers that mimic BH3 domains. *Angewandte Chemie-International Edition* **2008**, *47*, 2853-2856.

(11) Horne, W. S.; Price, J. L.; Keck, J. L.; Gellman, S. H. Helix bundle quaternary structure from alpha/beta-peptide foldamers. *Journal of the American Chemical Society* **2007**, *129*, 4178.

(12) Cheloha, R. W.; Maeda, A.; Dean, T.; Gardella, T. J.; Gellman, S. H. Backbone modification of a polypeptide drug alters duration of action in vivo. *Nature Biotechnology* **2014**, *32*, 653.

(13) Boersma, M. D.; Haase, H. S.; Peterson-Kaufman, K. J.; Lee, E. F.; Clarke, O. B.; Colman, P. M.; Smith, B. J.; Horne, W. S.; Fairlie, W. D.; Gellman, S. H. Evaluation of Diverse alpha/beta-Backbone Patterns for Functional alpha-Helix Mimicry: Analogues of the Bim BH3 Domain. *Journal of the American Chemical Society* **2012**, *134*, 315-323.

(14) Choi, S. H.; Guzei, I. A.; Spencer, L. C.; Gellman, S. H. Crystallographic Characterization of 12-Helical Secondary Structure in beta-Peptides Containing Side Chain Groups. *Journal of the American Chemical Society* **2010**, *132*, 13879-13885.

(15) Choi, S. H.; Guzei, I. A.; Spencer, L. C.; Gellman, S. H. Crystallographic Characterization of Helical Secondary Structures in 2:1 and 1:2 alpha/beta-Peptides. *Journal of the American Chemical Society* **2009**, *131*, 2917-2924.

(16) Giuliano, M. W.; Horne, W. S.; Gellman, S. H. An alpha/beta-Peptide Helix Bundle with a Pure beta(3)-Amino Acid Core and a Distinctive Quaternary Structure. *Journal of the American Chemical Society* **2009**, *131*, 9860.

(17) Choi, S. H.; Guzei, I. A.; Spencer, L. C.; Gellman, S. H. Crystallographic characterization of helical secondary structures in alpha/beta-peptides with 1 : 1 residue alternation. *Journal of the American Chemical Society* **2008**, *130*, 6544-6550.

(18) Choi, S. H.; Guzei, I. A.; Gellman, S. H. Crystallographic Characterization of the alpha/beta-Peptide 14/15-Helix. *Journal of the American Chemical Society* **2007**, *129*, 13780.

(19) Price, J. L.; Home, W. S.; Gellman, S. H. Heterogeneous helix-bundle quaternary structure formed by alpha/beta-peptide foldamers and alpha-peptides. *Biopolymers* **2007**, *88*, 568-568.

(20) Shin, Y.-H.; Mortenson, D. E.; Satyshur, K. A.; Forest, K. T.; Gellman, S. H. Differential Impact of beta and gamma Residue Preorganization on alpha/beta/gamma-Peptide Helix Stability in Water. *Journal of the American Chemical Society* **2013**, *135*, 8149-8152.

(21) Hanessian, S.; Luo, X. H.; Schaum, R.; Michnick, S. Design of secondary structures in unnatural peptides: Stable helical gamma-tetra-, hexa-, and octapeptides and consequences of alpha-substitution. *Journal of the American Chemical Society* **1998**, *120*, 8569-8570.

(22) Seebach, D.; Brenner, M.; Rueping, M.; Schweizer, B.; Jaun, B. Preparation and determination of X-ray-crystal and NMR-solution structures of gamma(2,3,4)-peptides. *Chemical Communications* **2001**, 207-208.

(23) Hintermann, T.; Gademann, K.; Jaun, B.; Seebach, D. gamma-peptides forming more stable secondary structures than alpha-peptides: Synthesis and helical NMR-solution structure of the gamma-hexapeptide analog of H-(Val-Ala-Leu)(2)-OH. *Helvetica Chimica Acta* **1998**, *81*, 983-1002.

(24) Sonti, R.; Dinesh, B.; Basuroy, K.; Raghothama, S.; Shamala, N.; Balaram, P. C-12 Helices in Long Hybrid (alpha gamma)(n) Peptides Composed Entirely of Unconstrained Residues with Proteinogenic Side Chains. *Organic Letters* **2014**, *16*, 1656-1659.

(25) Basuroy, K.; Dinesh, B.; Shamala, N.; Balaram, P. Promotion of Folding in Hybrid Peptides through Unconstrained gamma Residues: Structural Characterization of

Helices in (alpha gamma gamma)(n) and (alpha gamma alpha)(n) Sequences. *Angewandte Chemie-International Edition* **2013**, *52*, 3136-3139.

(26) Basuroy, K.; Dinesh, B.; Shamala, N.; Balaram, P. Structural Characterization of Backbone-Expanded Helices in Hybrid Peptides: (alpha gamma)(n) and (alpha beta)(n) Sequences with Unconstrained beta and gamma Homologues of L-Val. *Angewandte Chemie-International Edition* **2012**, *51*, 8736-8739.

(27) Bandyopadhyay, A.; Jadhav, S. V.; Gopi, H. N. alpha/gamma(4)-Hybrid peptide helices: synthesis, crystal conformations and analogy with the alpha-helix. *Chemical Communications* **2012**, *48*, 7170-7172.

(28) Bandyopadhyay, A.; Gopi, H. N. Hybrid Peptides: Direct Transformation of alpha/alpha, beta-Unsaturated gamma-Hybrid Peptides to alpha/gamma-Hybrid Peptide 12-Helices. *Organic Letters* **2012**, *14*, 2770-2773.

(29) Sharma, G. V. M.; Chandramouli, N.; Choudhary, M.; Nagendar, P.; Ramakrishna, K. V. S.; Kunwar, A. C.; Schramm, P.; Hofmann, H.-J. Hybrid Helices: Motifs for Secondary Structure Scaffolds in Foldamers. *Journal of the American Chemical Society* **2009**, *131*, 17335-17344.

(30) Baldauf, C.; Gunther, R.; Hofmann, H. J. Helix formation in alpha,gamma- and beta,gamma-hybrid peptides: Theoretical insights into mimicry of alpha- and beta-Peptides. *Journal of Organic Chemistry* **2006**, *71*, 1200-1208.

(31) Giuliano, M. W.; Maynard, S. J.; Almeida, A. M.; Reidenbach, A. G.; Guo, L.; Ulrich, E. C.; Guzei, I. A.; Gellman, S. H. Evaluation of a Cyclopentane-Based gamma-Amino Acid for the Ability to Promote alpha/gamma-Peptide Secondary Structure. *Journal of Organic Chemistry* **2013**, *78*, 12351-12361.

(32) Guo, L.; Zhang, W.; Guzei, I. A.; Spencer, L. C.; Gellman, S. H. Helical secondary structures in 2:1 and 1:2 alpha/gamma-peptide foldamers. *Tetrahedron* **2012**, *68*, 4413-4417.

(33) Guo, L.; Zhang, W.; Guzei, I. A.; Spencer, L. C.; Gellman, S. H. New Preorganized gamma-Amino Acids as Foldamer Building Blocks. *Organic Letters* **2012**, *14*, 2582-2585.

(34) Guo, L.; Zhang, W.; Reidenbach, A. G.; Giuliano, M. W.; Guzei, I. A.; Spencer, L. C.; Gellman, S. H. Characteristic Structural Parameters for the gamma-Peptide 14-Helix: Importance of Subunit Preorganization. *Angewandte Chemie-International Edition* **2011**, *50*, 5843-5846.

(35) Guo, L.; Almeida, A. M.; Zhang, W.; Reidenbach, A. G.; Choi, S. H.; Guzei, I. A.; Gellman, S. H. Helix Formation in Preorganized beta/gamma-Peptide Foldamers: Hydrogen-Bond Analogy to the alpha-Helix without alpha-Amino Acid Residues. *Journal of the American Chemical Society* **2010**, *132*, 7868.

(36) Guo, L.; Chi, Y.; Almeida, A. M.; Guzei, I. A.; Parker, B. K.; Gellman, S. H. Stereospecific Synthesis of Conformationally Constrained gamma-Amino Acids: New Foldamer Building Blocks That Support Helical Secondary Structure. *Journal of the American Chemical Society* **2009**, *131*, 16018.

(37) Horne, W. S.; Price, J. L.; Gellman, S. H. Interplay among side chain sequence, backbone composition, and residue rigidification in polypeptide folding and assembly. *Proceedings of the National Academy of Sciences of the United States of America* **2008**, *105*, 9151-9156.

(38) Li, G.; Weicheng, Z.; Reidenbach, A. G.; Giuliano, M. W.; Guzei, I. A.; Spencer, L. C.; Gellman, S. H. Characteristic structural parameters for the gamma-peptide 14-helix: Importance of subunit preorganization. *Angewandte Chemie International Edition* **2011**, *50*, 5843-5846.

(39) Giuliano, M. W.; Maynard, S. J.; Almeida, A. M.; Guo, L.; Guzei, I. A.; Spencer, L. C.; Gellman, S. H. A gamma-Amino Acid That Favors 12/10-Helical Secondary Structure in alpha/gamma-Peptides. *Journal of the American Chemical Society* **2014**, *136*, 15046-15053.

(40) Sawada, T.; Gellman, S. H. Structural Mimicry of the alpha-Helix in Aqueous Solution with an Isoatomic alpha/beta/gamma-Peptide Backbone. *Journal of the American Chemical Society* **2011**, *133*, 7336-7339.

Chapter 2: Effects of Ring Constrained γ- and β-residues on Helical α/β/γ-Peptides

Portions of this chapter were published as:

Shin, Y.-H.; Mortenson, D. E.; Satyshur, K. A.; Forest, K. T.; Gellman, S. H., "Differential Impact of β and γ Residue Preorganization on α/β/γ-Peptide Helix Stability in Water", *Journal of the American Chemical Society,* **2013**, *135*, 8149.

2.1 Introduction

2.1.1 Helical peptidomimetics

The surfaces of folded proteins often bear identifying information that is encoded in specific side chain arrangements and recognized by other proteins.[1-3] Oligomers that can mimic these molecular messages while displaying superiority to conventional peptides in other aspects (e.g., diminished susceptibility to enzymatic degradation, enhanced conformational stability) can be useful as antagonists of specific protein-protein associations or agonists of polypeptide-activated receptors.[4-9] Gellman *et al.* have previously shown that α/β-peptides generated from a prototype sequence by replacing 25-33% of the original α-amino acid residues with β-amino acid residues, at sites that are dispersed along the backbone, can adopt a conformation very similar to the α-helix and bind tightly to recognition surfaces that evolved to bind natural α-helices.[10-15] In some cases, affinity can be enhanced by use of cyclic β residues, presumably because the extra backbone bond introduced with each α→β replacement raises the entropic cost of folding unless that bond is appropriately constrained.[10-16] The effective α-helix mimicry manifested by these α/β-peptides is somewhat surprising because they contain at least one additional backbone atom per helical turn relative to a true α-helix.

2.1.2 Helical α/β/γ-peptide

Sawada and Gellman proposed that the recognition surface of a natural α-helix could be mimicked by replacement of α heptads, which form two full helical turns, with αγααβα hexads (Figure 2.1A).[17] The β- and γ- residues, collectively, contain the same

number of backbone atoms as the three α-residues they replace. This design strategy built upon pioneering studies of the folding of γ-residue-containing oligomers by other groups.[18-31] The αγααβα arrangement allows the α-residues to define one face of the helix. 2D NMR data showed that α/β/γ-peptide 12-mer **2.1** in aqueous solution adopts a conformation resembling an α-helix, and that this conformation is considerably more stable than the true α-helix formed by analogous α-peptide 14-mer **2.2**.[17] Sawada and Gellman originally postulated that this high conformational stability in water arises from the backbone preorganization of both the β- and γ- residues provided by the five- and six-membered rings, respectively. Here we test this hypothesis and show it to be only partially correct.

2.2 Peptide design for this study

To evaluate the contribution of the β-residue and γ-residue preorganization independently, we prepared three α/β/γ-peptide analogues of **2.1** (Figure 2.1B and C). In **2.3**, the γ-residue constraints have been relaxed, because γ^4-hAla occurs in place of the two cyclohexane-based residues of **2.1**. In **2.4**, the β-residue constraints have been relaxed, because β^3-hGln and β^3-hPhe replace the trans-2-aminocyclopentanecarboxylic acid (ACPC) residues. In **2.5**, the β- and γ-residues constraints are relaxed simultaneously (Figure 2.1).

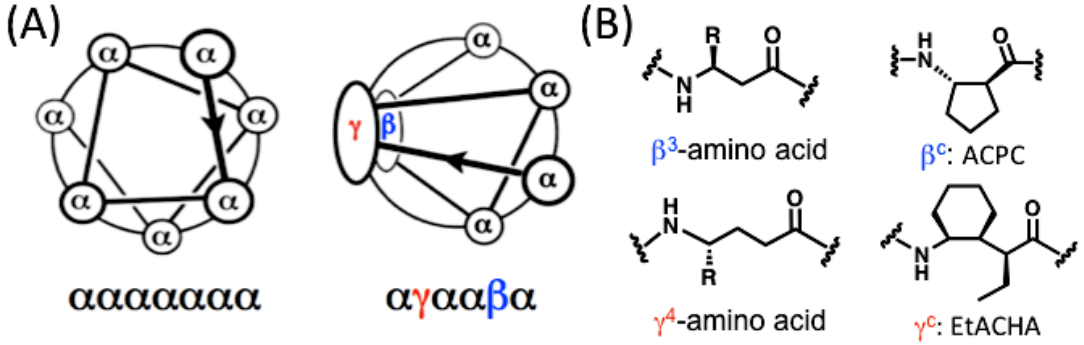

(C)

Ac-Glu γ^c Ala Arg β^c Tyr Ala γ^c Gln Ala β^c Lys-NH_2	2.1
Ac-Glu Leu Glu Ala Arg Gln Tyr Ala Orn Nle Gln Ala Phe Lys-NH_2	2.2
Ac-Glu γ^4Ala Ala Arg β^c Tyr Ala γ^4Ala Gln Ala β^c Lys-NH_2	2.3
Ac-Glu γ^c Ala Arg β^3Gln Tyr Ala γ^c Gln Ala β^3Phe Lys-NH_2	2.4
Ac-Glu γ^4Ala Ala Arg β^3Gln Tyr Ala γ^4Ala Gln Ala β^3Phe Lys-NH_2	2.5

(D)

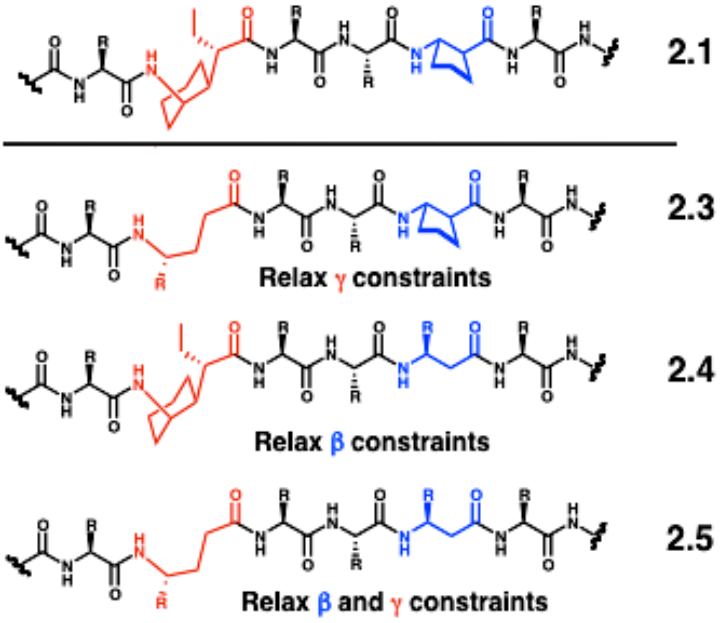

Figure 2.1 (A) Helical wheel diagrams for the αααααααα heptad and the αγααβα hexad. (B) Structures of β-and γ-amino acids. (C) Sequences of α/β/γ-peptides and α-peptide **2.2**. Superscript 'c' indicates a ring-constrained residue. (D) Backbones of αγααβα hexads from α/β/γ–peptides; β- and γ- residues are shown in blue and red, respectively.

2.3 Experimental Analysis

2.3.1 Circular Dichroism

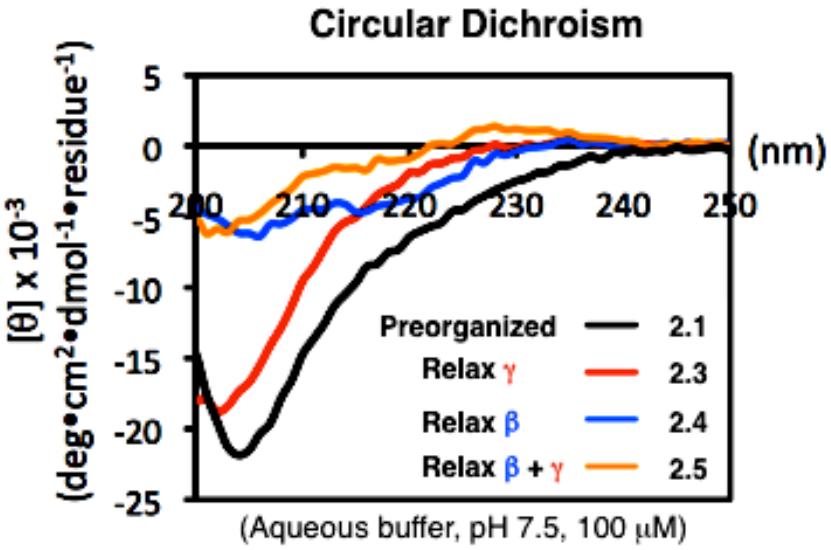

Figure 2.2 Circular dichroism data for α/β/γ-peptides **2.1** and **2.3**-**2.5** measured in PBS buffer, pH 7.5 at 20 °C. Peptide concentration is 0.1 mM for all spectra.

Circular dichroism was used for an initial comparison of new α/β/γ-peptides **2.3**-**2.5** with **2.1** in aqueous buffer (Figure 2.2). The strong minimum at 204 nm seen for **2.1** was previously assigned to the α-helix-like conformation because 2D NMR data reveal a network of medium-range NOEs consistent with this conformation under the same conditions.[17] For α/β/γ-peptide **2.5**, the very limited CD intensity suggests little or no helix formation, as we expected for a backbone lacking β- or γ- residue constraints. Similar behavior is observed for **2.4**, which indicates that the β -residue constraint provided by the ring in ACPC is important for helical folding; this observation is consistent with previous demonstrations that incorporation of ACPC or similar cyclic β-residues is crucial for helical folding of α/β-peptides in aqueous media.[10,13,16,32,33] The

CD data for **2.3**, however, were surprising: the strong minimum near 202 nm implies a significant population of peptide in a helical conformation, despite the absence of γ-residue constraints.

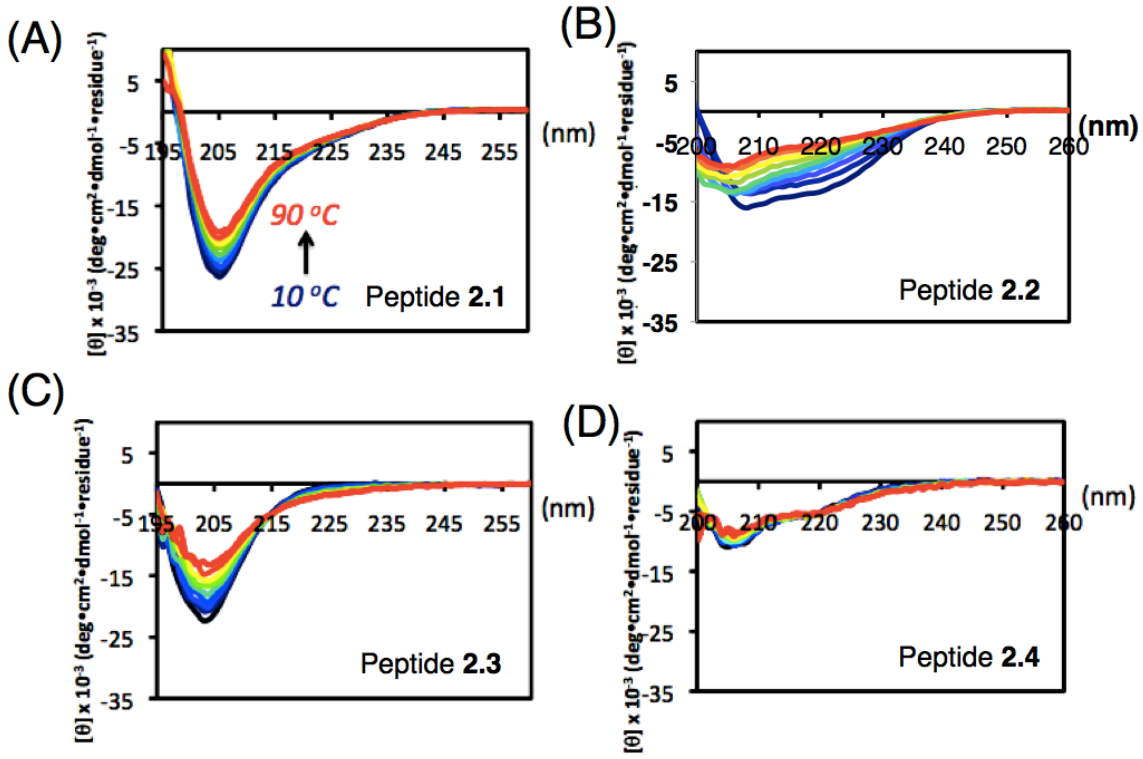

Figure 2.3 Circular dichroism data for (A) α/β/γ-peptide **2.1**, (B) α-peptide **2.2** (C) α/β/γ-peptide **2.3**, and (D) α/β/γ-peptide **2.4** measured in 50% MeOH/ 50% H_2O at varied temperatures from 10 °C to 90 °C. Peptides concentration is 0.1 mM for all spectra.

Previous thermal denaturation study of α/β/γ-peptide **2.1** showed that 6-membered-ring constrained γ-amino acids and 5-memebred-ring β-amino acids together yielded a very stable helical conformation (Figure 2.3A).[17] To compare the conformational stability of ring-relaxed α/β/γ-peptides to ring-constrained α/β/γ-peptide **2.1**, the helicities of **2.1**, **2.2**, **2.3** and **2.4** were monitored by CD upon varying the temperature from 10 °C to 90 °C in 50% methanol/water solution (Figure 2.3). Because

α-peptide **2.2** did not show helical folding in water based on CD, 50% methanol/water solution was used, in order to induce and thermally denature a helical conformation of α-peptide **2.2**. As expected, thermal denaturation behavior was shown by peptides **2.1** - **2.4**: helical folding at low temperature, with decreased helicity as temperature increases. Peptide **2.3** containing ring-relaxed γ-residues presented considerably reduced CD minima intensities at higher temperature, implying that the helical conformation of **2.3** is not as rigid as that of **2.1** (Figure 2.3A and C). Peptide **2.4**, containing cyclic γ-residues but without ring-constraints on β-residues, did not fold into a helical structure even in 50 % methanol solution at low temperature, and no change was observed in CD spectra while increasing temperature (Figure 2.3D).

To encourage increased helicity in α/β/γ-peptides **2.3**-**2.5**, trifluoroethanol (TFE), which promotes secondary structures of peptides with debatable mechanisms, was added to peptide solutions[34], and changes were monitored by CD (Figure 2.4). Interestingly, we could not observe significant changes in CD intensity for α/β/γ-peptide **2.1**, whereas improved helicity was observed for **2.3**, **2.4** and **2.5**. These data suggest that α/β/γ-peptide **2.1**, which has ring-constraints on both β- and γ-residues, is almost fully folded into a helical structure in water. The rigid folding deduced for **2.1** could be desirable for helical peptidomimetics; however, **2.3**, which manifests significant helicity in water despite the lack of constrained γ residues, might be also promising for future design of α/β/γ peptidomimetics.

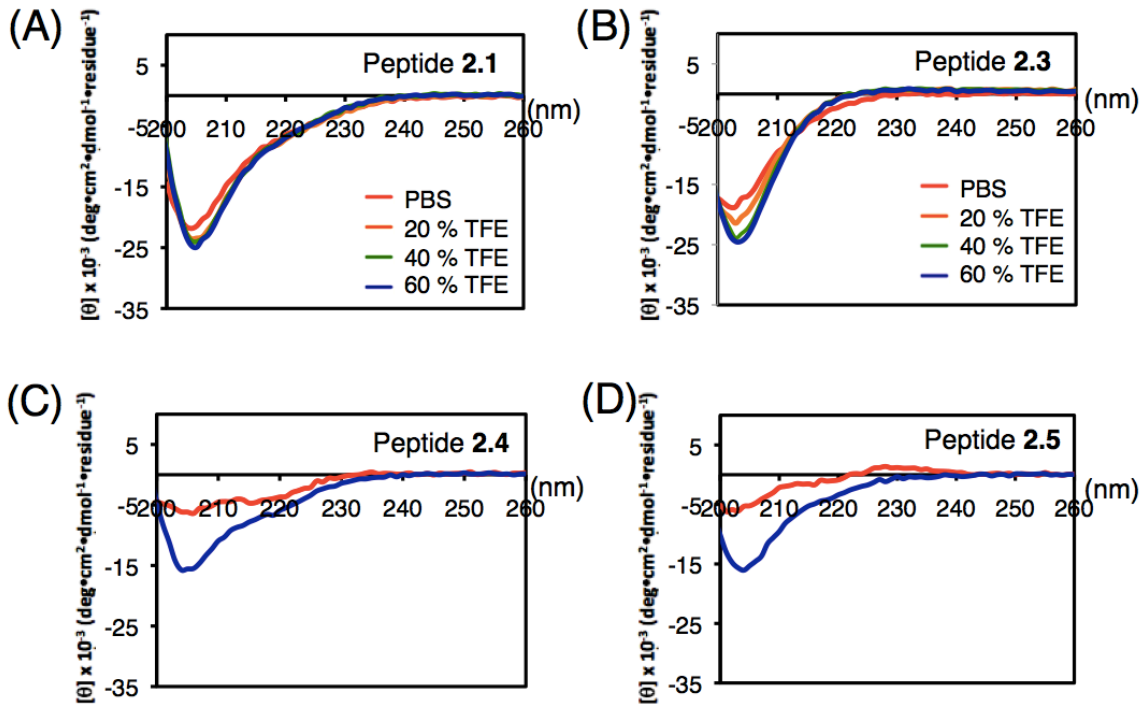

Figure 2.4 Circular dichroism data for α/β/γ-peptides **2.1** and **2.3**-**2.5** measured in 0 % to 60 % of TFE in PBS buffer (pH 7.5) at 20 °C. Peptide concentration is 0.1 mM for all spectra.

2.3.2 2D-NMR studies of 2.3

NMR analysis was undertaken to probe the behavior of α/β/γ-peptide **2.3** in more detail (Figure 2.5), because CD can provide only low-resolution insight on molecular structure. Previously, the fully preorganized α/β/γ-peptide **2.1** was found to display numerous NOEs between protons from residues with i, i+2 and i, i+3 sequence relationships in both aqueous buffer and methanol; these medium-range NOEs were all consistent with an α-helix-like conformation.[17] For **2.3**, in which the cyclic γ-residues have been replaced by unconstrained γ^4-hAla residues, a smaller set of i, i+2 and i, i+3 NOEs was observed in methanol relative to **2.1** in methanol, and an even smaller set of medium-range NOEs was detected for **2.3** in aqueous solution (Figure 2.5). However, the NOEs observed for **2.3** in water included both of the possible γ-residue CγH(*i*) – β-residue NH(*i+3*) NOEs and both γ-residue CγH(*i*) – α-residue NH(*i+2*) NOEs, which provides strong evidence for a significant population of the helical state. Thus, the 2D NMR data indicate that removing the γ-residue constraints, to generate **2.3**, causes some diminution in helix population relative to fully preorganized **2.1**, but that the unconstrained γ^4-hAla residues nevertheless manifest a significant helical propensity, more so than unconstrained β^3-residues.

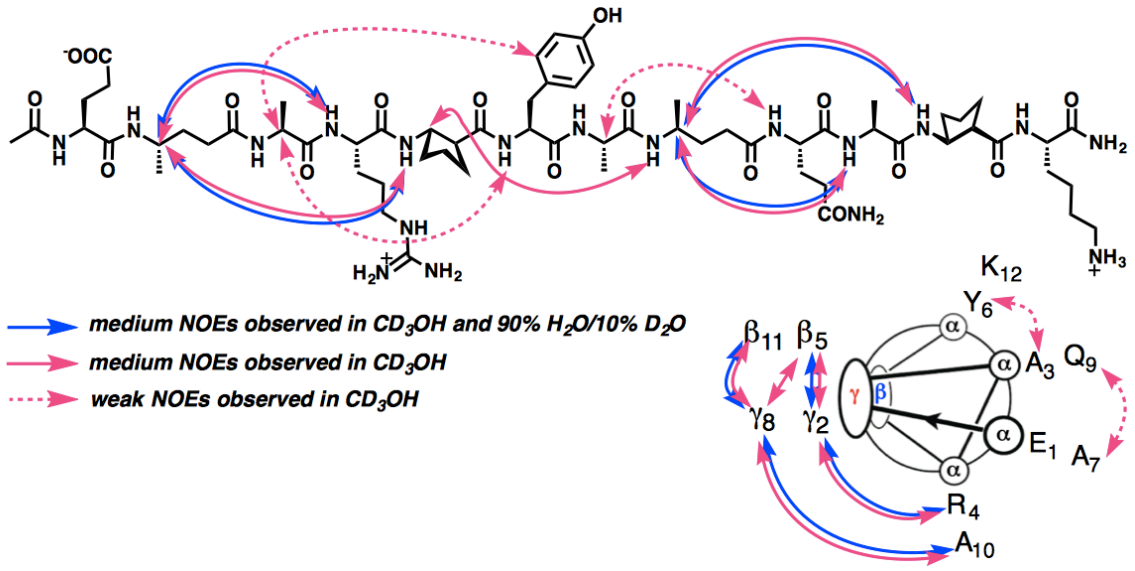

Figure 2.5 NOEs observed between nonadjacent residues for α/β/γ-peptide **2.3** in CD_3OH (blue and pink, peptide concentration 6 mM), or in water (blue, peptide concentration 2 mM) at 10 °C. Medium (2.6~3.5 Å) and weak (3.6~5.5 Å) NOEs are shown as curved arrows on the peptide structure and on the helical wheel diagram.

2.4 Crystallography

2.4.1 Peptide design based on GCN4-pLI model

In order to gain higher-resolution insight regarding accommodation of the αγααβα motif in an α-helix-like conformation, we designed oligomers intended to provide crystallographic data. The 12-mer α/β/γ-peptides **2.1** and **2.3** did not provide high quality crystals for X-ray crystallography (Figure 2.6). GCN4-pLI is a 33-residue α-peptide derived from the dimerization domain of the yeast transcriptional regulator GCN4.[35] The pLI version forms a very stable tetrameric α-helix bundle, while the native sequence prefers lower oligomerization states.[36,37] Many α/β-peptides derived from GCN4-pLI have been crystallized in four-helix bundle assemblies that are remarkably similar to the quaternary structure of GCN4-pLI itself.[18,38,39] We therefore prepared a series of α/β/γ-peptides based on this sequence, which contain varying numbers of αγααβα hexads in different locations (Figure 2.7).

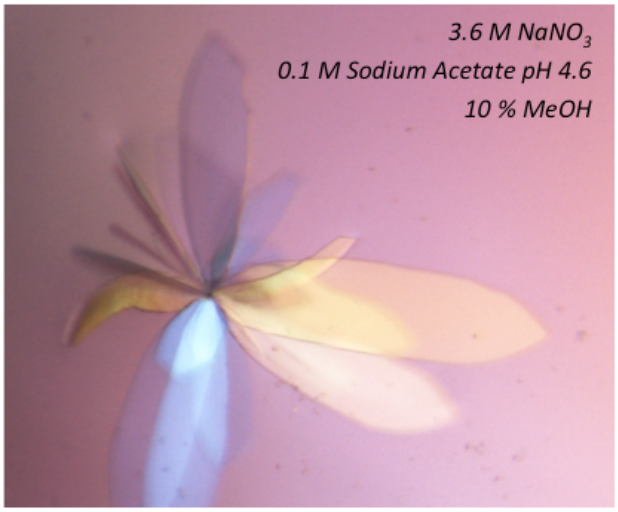

Figure 2.6 Peptide **2.1** was observed to crystallize with a thin, plate-like morphology. Even after extensive optimization attempts, these crystals were found to be unsuitable for collection of useful X-ray diffraction data.

(A)

	Ac–RMKQIEDKLEEILSKLYHIENELARIKKLLGER–OH	GCN4-pLI
	Ac–RM(γcyc)IEZKL(γcyc)IIZKL(γcyc)IEZEL(γcyc)IKZLL(γcyc)R–OH	2.8
★	Ac–RMKQIEDKLEEILSKLYHIEZEL(γcyc)IKZLLGER–OH	2.6
	Ac–RMKQIEDKLEEIIZKL(γcyc)IEZELARIKKLLYER–OH	2.9
	Ac–RMKQIEDKLEEIIZKL(γcyc)IEZEL(γcyc)IKZLLYER–OH	2.10
	Ac–RMKQIEDKLEEILYKL(γcyc)IEZEL(γcyc)IKZLL(γcyc)R–OH	2.11
★	Ac–RMKQIEDKLEEIIXKLγ⁴hAIEXELARIKKLLYER–OH	2.7
	Ac–RMKQIEDKLEEIIZKLγ⁴hAIEZELγ⁴hAIKZLLYER–OH	2.12
	Ac–RMKQIEDKLEEILYKLγ⁴hAIEXELγ⁴hAIKXLLγ⁴hAR–OH	2.13

(B)

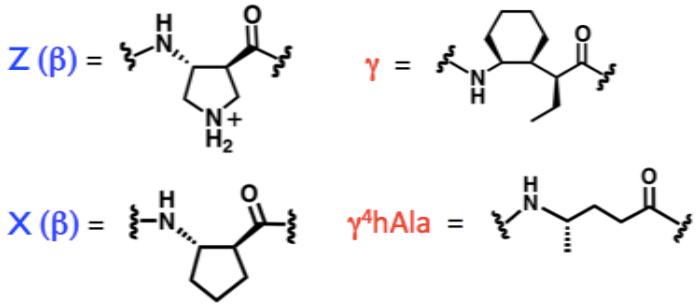

(C)

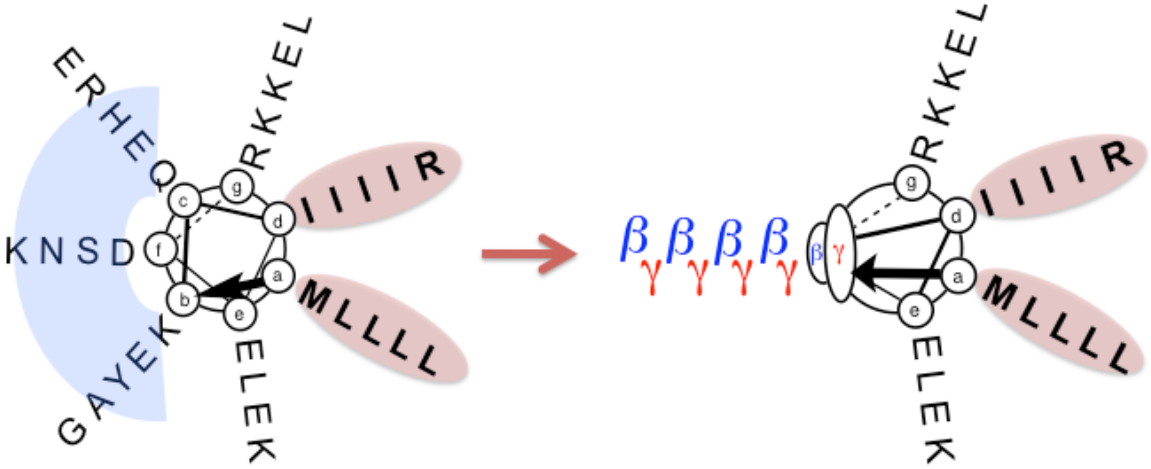

Figure 2.7 (A) Sequences of α/β/γ-peptides derived from GCN4-pLI. Peptides **2.6** and **2.7** are marked with green stars (B) Structures of β- and γ-amino acids (C) Helical wheel diagrams for the αααααααα heptads of GCN4-pLI and the αγααβα hexads version of GCN4-pLI.

The α/β/γ-peptides **2.8** and **2.11** could not be synthesized by SPPS, due to the low coupling efficiency of the cyclic γ-residue, EtACHA (Figure 2.7). The other α/β/γ-peptides (**2.6**, **2.7**, **2.9**, **2.10**, **2.12**, **2.13**) were successfully synthesized and purified (Figure 2.7). CD was used to investigate the secondary structures of four of the 31-mer or 32-mer α/β/γ-peptides **2.7**, **2.9**, **2.10**, and **2.12**, which have one or two hexads repeat with cyclic or acyclic γ-amino acids (Figure 2.8). In 50% TFE, all four peptides showed α-helix-like structures with characteristic minima between 205 nm and 210 nm of similar intensities. In water, however, the peptides with acyclic γ-residues (**2.9** and **2.10**) exhibited decreased CD intensity compared to peptides with cyclic γ-residues (**2.7** and **2.12**). These data indicate that both cyclic- and acyclic γ-residues can support helical folding by GCN4-pLI-derived α/β/γ-peptides in aqueous and/or organic-aqueous solutions. Since our purpose in using the GCN4-pLI sequence was to facilitate the crystallization of α/β/γ-peptides, we did not focus on CD observations in this chapter. Efforts to quantify the ring constraint effect of γ-residues on helicity were pursued with the backbone thioester exchange (BTE) method (Chapter 4).

All the oligomers synthesized were screened for crystallization by the hanging drop method, and two of the screened oligomers provided high-quality crystals from aqueous solution (Figure 2.7, peptide **2.6** and **2.7**). The resulting structures show that an αβααγααβα unit can indeed adopt an α-helix-like conformation when either a cyclic- or acyclic- γ-residue is used (Figure 2.9 and 2.10, peptide **2.6** and **2.7**).

Ac–RMKQIEDKLEEIILZKL(γcyc)IEZELARIKKLLYER–OH **2.9**

Ac–RMKQIEDKLEEIILZKL(γcyc)IEZEL(γcyc)IKZLLYER–OH **2.10**

Ac–RMKQIEDKLEEIILXKLγ4hAIEXELARIKKLLYER–OH **2.7**

Ac–RMKQIEDKLEEIILZKLγ4hAIEZELγ4hAIKZLLYER–OH **2.12**

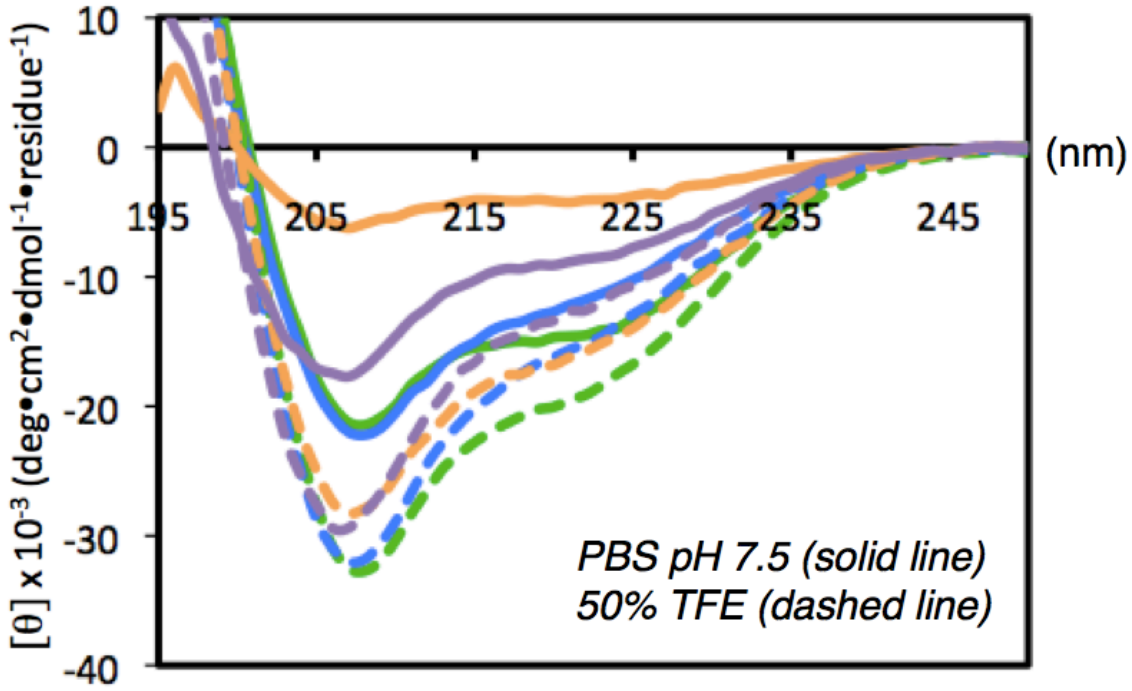

Figure 2.8 Circular dichroism spectra from peptides containing cyclic γ-amino acids (**2.9** and **2.10**) and peptides containing acyclic γ-amino acids (**2.7** and **2.12**), measured in PBS buffer pH 7.5 and in 50 % trifluoroethanol at 20 °C. Peptide concentration is 50 μM for all spectra.

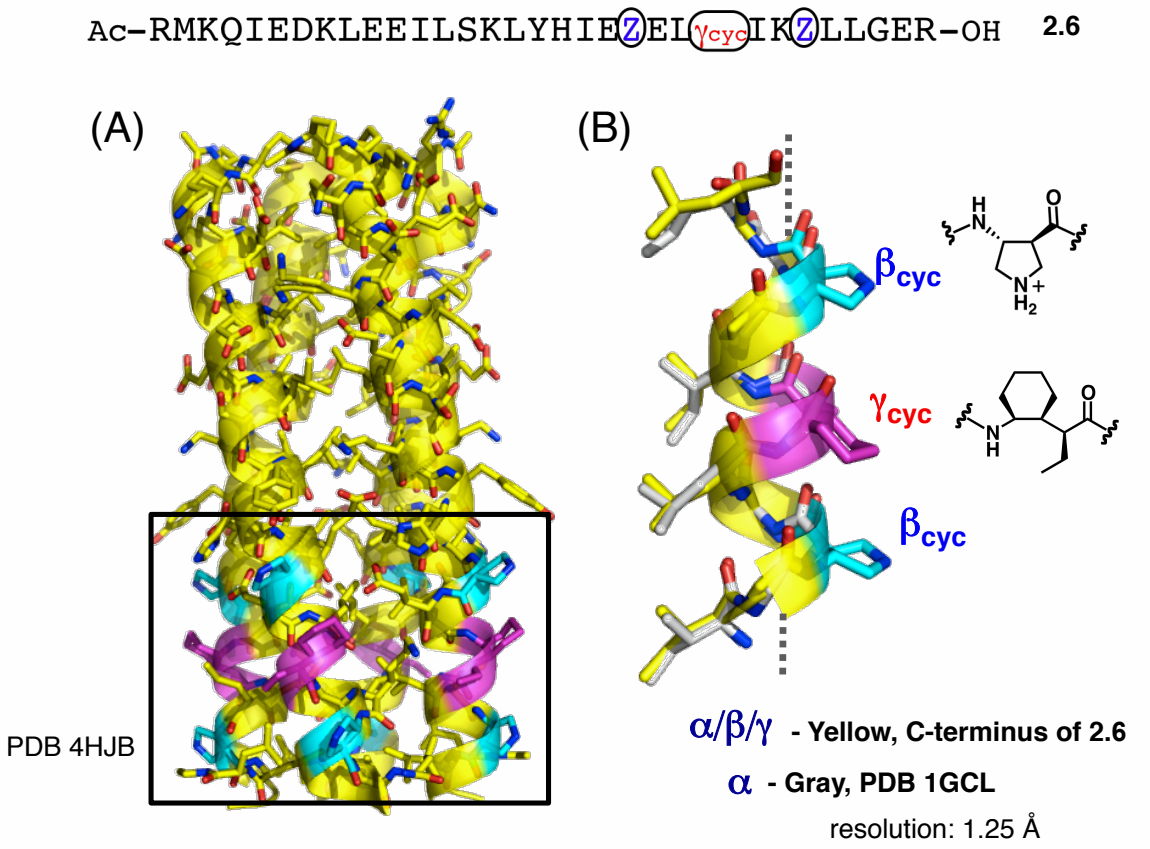

Figure 2.9 (A) Four-helix bundle formed by **2.6** (PDB 4HJB) as determined *via* x-ray crystallography (B) Overlaid structures of C-terminal α/β/γ-region of **2.6** and the analogous α-region of GCN4-pLI (PDB 1GCL). Structures are simplified for the clear view; hydrophobic core side chains and ring constraints are shown. β- and γ-residues are highlighted in cyan and purple, respectively.

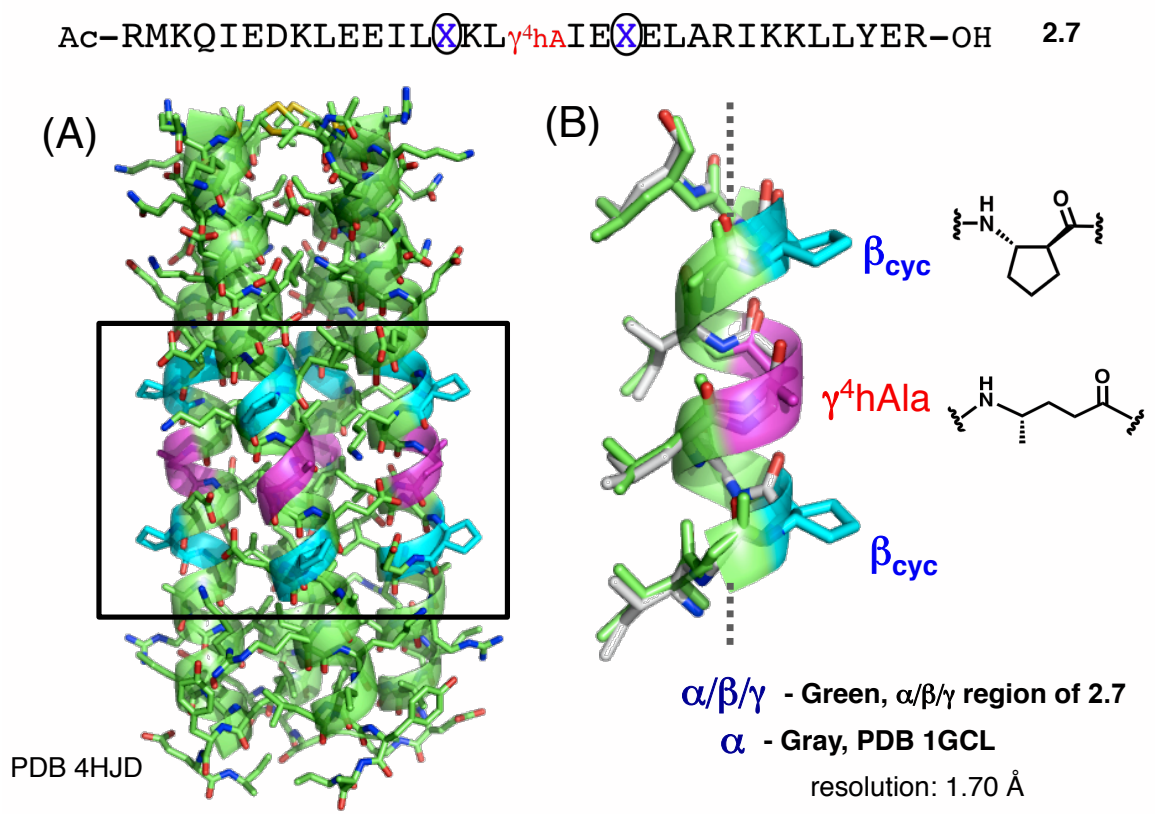

Figure 2.10 (A) Four-helix bundle formed by **2.7** (right, PDB 4HJD), as determined *via* x-ray crystallography (B) Overlaid structures of α/β/γ-region of **2.7** and the analogous α-region of GCN4-pLI (PDB 1GCL). Structures are simplified for the clear view; hydrophobic core side chains and ring constraints are shown. β- and γ-residues are highlighted in cyan and purple, respectively.

2.4.2 Structural analysis

2.4.2.1 Hydrogen bonding

The H-bonding pattern among backbone amide groups within the α/β/γ segments of **2.6** and **2.7** is somewhat more complex than the H-bonding pattern of the canonical α-helix, which features i, i+4 C=O--H-N H-bonds (13-atom rings). All backbone carbonyl groups in the α/β/γ segments of **2.6** and **2.7** form i, i+3 C=O--H-N H-bonds, which occur in 10-, 11- or 12-atom rings, depending upon the types of residues between the amide groups (Figure 2.11). Such H-bonds are typically identified based on O--N distances, with 3.3 Å as a standard upper limit;[40] in the α/β/γ segments of **2.6** and **2.7**, a few i, i+3 O--N distances exceed this limit (3.5-3.9 Å) (Table 2.1 and 2.2). Some backbone carbonyls in **2.6** and **2.7** participate in bifurcated H-bonds, involving i, i+4 C=O--H-N interactions (14-atom rings) in addition to the i, i+3 interactions (Figure 2.12).

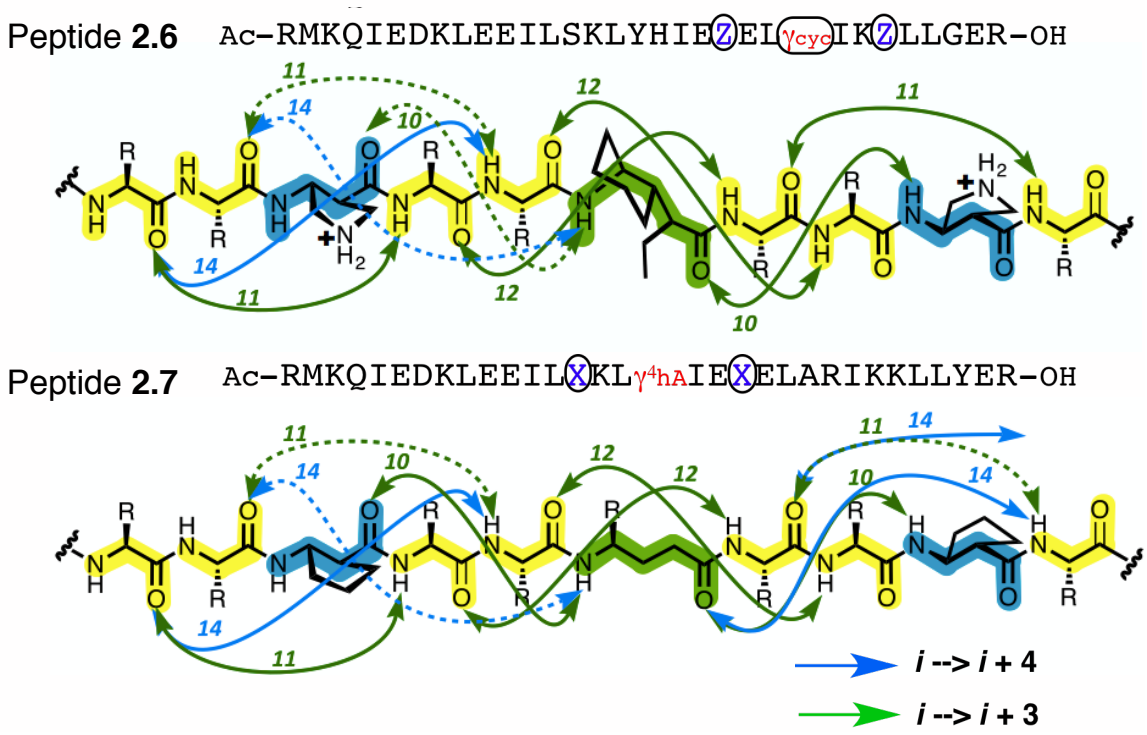

Figure 2.11. Hydrogen bonds identified in the crystal structures of **2.6** (top) and **2.7** (bottom) shown on the peptide structures. H-bonding distances (O--N distances) with 3.3 Å as upper limit are shown as plain curves; H-bonding distances between 3.5 and 3.9 Å are shown as dashed curves.

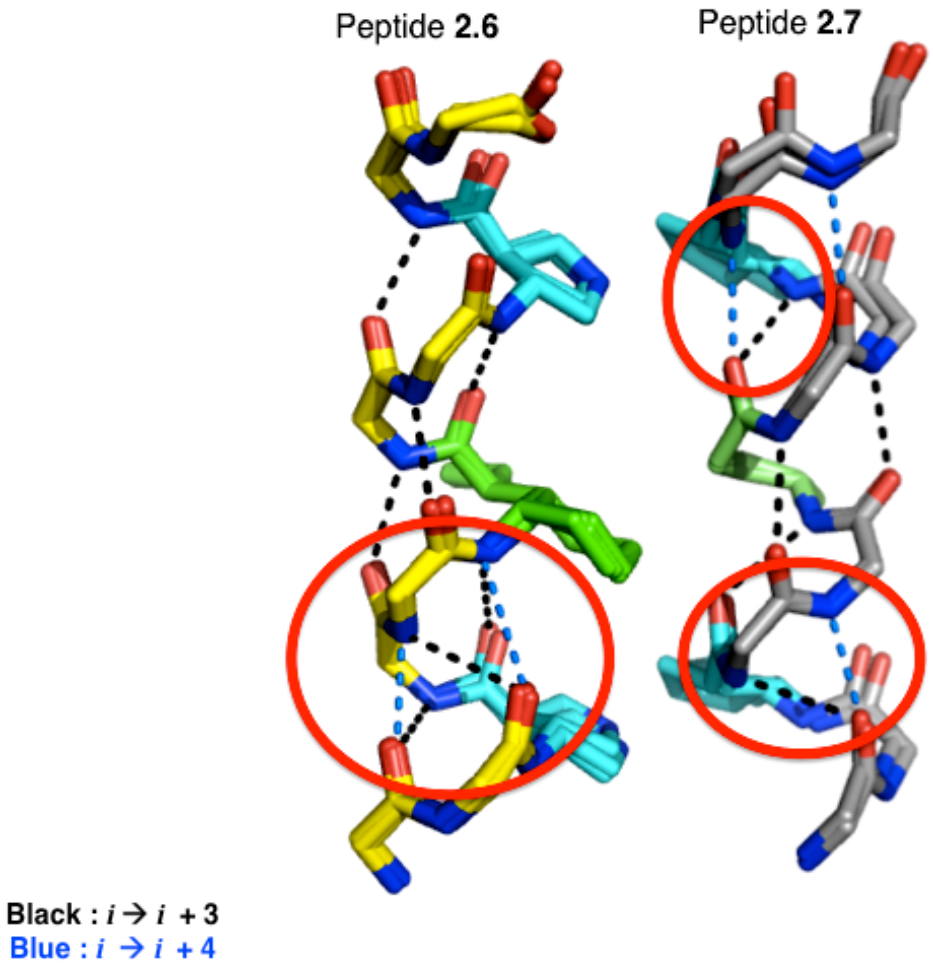

Figure 2.12 Hydrogen bonds from crystal structures of **2.6** (left) and **2.7** (right). Bifurcated H-bonds are highlighted by red circles. i,i+3 and i,i+4 H-bonds are shown as black and blue dashed lines, respectively. α-Residue side chains are omitted for clarity.

Table 2.1 Hydrogen bond distances (O--N distance) from the four independent molecules in the crystal structure of peptide **2.6**. Distances from each chain and averaged values (Å) are shown.

Peptide **2.6**, β(21), γ(24), β(27)

O		*i*	NH		*i* + n	# of atoms between H-bonding atoms	A	B	C	D	Avg.
α	19	*i*	α	22	*i* + 3	11	3.3	3.3	3.3	3.4	3.3
				23	*i* + 4	14	2.9	2.9	3	3	3.0
α	20	*i*		23	*i* + 3	11	3.6	3.4	3.4	3.6	3.5
			γ	24	*i* + 4	14	3.7	3.5	3.6	3.8	3.7
β	21	*i*	γ	24	*i* + 3	10	3.6	3.8	3.5	3.6	3.6
				25	*i* + 4	15	5.1	5.2	5.2	5.3	5.2
α	22	*i*	α	25	*i* + 3	12	3	2.9	2.9	2.9	2.9
				26	*i* + 4	15	5.3	5.3	5.3	5.3	5.3
α	23	*i*	α	26	*i* + 3	12	2.8	2.8	2.9	2.8	2.8
			β	27	*i* + 4	15	4.9	4.7	4.9	4.9	4.9
γ	24	*i*	β	27	*i* + 3	10	3	2.9	2.9	2.9	2.9
				28	*i* + 4	14	4.6	4.7	4.8	4.7	4.7
α	25	*i*		28	*i* + 3	11	3	2.9	2.9	3	3.0
				29	*i* + 4	14	4.7	4.6	4.7	4.7	4.7

Table 2.2 Hydrogen bond distances (O--N distance) from the two independent molecules in the crystal structure of peptide **2.7**. Distances from each chain and averaged values (Å) are shown.

Peptide **2.7**, β(15), γ(18), β(21)

O		*i*	NH		*i* + n	# of atoms between H-bonding atoms	A	B	Avg.
α	13	*i*	α	16	*i* + 3	11	3.3	3.3	3.3
				17	*i* + 4	14	2.9	3	3.0
α	14	*i*		17	*i* + 3	11	3.8	3.9	3.9
			γ	18	*i* + 4	14	4	4.2	4.1
β	15	*i*	γ	18	*i* + 3	10	3.1	3	3.1
				19	*i* + 4	15	5	5	5.0
α	16	*i*	α	19	*i* + 3	12	3	3.1	3.1
				20	*i* + 4	15	5.4	5.5	5.5
α	17	*i*	α	20	*i* + 3	12	3	3.1	3.1
			β	21	*i* + 4	15	4.8	5.4	5.1
γ	18	*i*	β	21	*i* + 3	10	**3.5**	**2.9**	3.2
			α	22	*i* + 4	14	**3.2**	**4**	3.6
α	19	*i*		22	*i* + 3	11	3.4	3.4	3.4
			α	23	*i* + 4	14	2.9	3	3.0

2.4.2.2 Comparison: NOEs from NMR in solution and H-H distances from crystallographic data

The crystallographic data show that NOEs detected in solution and attributed to the α-helix-like conformation are associated with pairs of backbone hydrogen atoms that are brought into proximity in this folded state, including the two medium range NOEs mentioned above for **2.3** in aqueous solution (Figure 2.5, Table 2.3). In **2.6**, the distance between the γ-residue CγH (position 24) and the β-residue NH at position 27 is 3.0 Å, while in **2.7**, the distance between the γ-residue CγH (position 18) and the β-residue NH at position 21 is 2.9 Å (H--H distance). In **2.6**, the distance between the γ-

residue CγH (position 24) and the α-residue NH at position 26 is 2.5 Å, and the same separation is observed in **2.7** between the γ–residue CγH (position 18) and the α-residue NH at position 20. We note, however, in **2.7**, the backbone (i, i+2) H-H distance between the β-residue CβH (position 15) and the α-residue NH at position 17 in the crystal structures do not give rise to NOEs for **2.3** in aqueous solution, perhaps because this conformation is only partially populated (Table 2.3).

Table 2.3 Average H-H distances in crystal structures of peptides **2.6** and **2.7** corresponding to medium/weak-range NOEs of peptides **2.1** and **2.2**, respectively.

	NOE type	residue #	Distance (Å) Crystal structure	NOEs from 2D-NMR
2.6	α–residue CαH(*i*) – α–residue NH(*i*+3)	20-23(4)[a]	3.7	weak
	β–residue CβH(*i*) – γ–residue NH(*i*+3)	21-24(4)	3.4	medium
	α–residue CαH(*i*) – α–residue NH(*i*+2)	23-25(4)	2.9	weak
	γ–residue CγH(*i*) – α–residue NH(*i*+2)	24-26(4)	2.5	medium
	γ–residue CγH(*i*) – β–residue NH(*i*+3)	24-27(4)	3.0	strong - medium
2.7	α–residue CαH(*i*) – α–residue NH(*i*+3)	14-17(2)	3.8	weak
	β–residue CβH(*i*) – α–residue NH(*i*+2)	15-17(2)	3.6	-
	β–residue CβH(*i*) – γ–residue NH(*i*+3)	15-18(2)	3.3	medium
	α–residue CαH(*i*) – α–residue NH(*i*+2)	17-19(2)	2.8	weak
	γ–residue CγH(*i*) – α–residue NH(*i*+2)	18-20(2)	2.5	medium
	γ–residue CγH(*i*) – β–residue NH(*i*+3)	18-21(2)	2.9	medium

NOE range from 2D-NMR: Weak (3.6-5 Å), Medium (2.6-3.5 Å), Strong (2-2.5 Å)
[a] Number of measurements in crystal chains shown in parentheses.

2.4.2.3 Helix parameters

The crystal structures allow a detailed comparison of α/β/γ-peptide hexads with α heptads. In addition, the crystallographic data for **2.6** and **2.7** enable comparisons with several recently reported crystal structures of peptidic oligomers that contain γ-residues and display C=O(*i*)--H-N(*i+3*) H-bonded helical secondary structures. Table 2.4 compares the standard helix parameters determined for the αβααγα hexads in **2.6** and

in **2.7** with analogous parameters for the α-helix (as represented by GCN4-pLI; PDB 1GCL), for a canonical 3_{10}-helix,[40] for α-helix-mimetic α/β-peptides (PDB 3O43, 3F87 and 3C3H), and for various oligomers containing either the cyclic γ-residue we have employed[41-43] or γ^4-residues.[44-49] Although all of these helices have generally similar geometries, the αβααγα unit does best at matching the α-helix radius.

Table 2.4 Helical parameters for α/β/γ–, γ–, α/β– and α–peptides.

Peptide	Pattern	rise/turn, ρ (Å)	radius, r (Å)
α/β/γ– **2.6**, **2.7**	αβααγα	5.7	2.3
γ^{c} [b]	γ	5.5	2.9
α/γ^{c} [c]	αγ	6.1	2.5
α/γ^{4} [d]	αγ	5.3	2.1
β^{c}/γ^{c} [e]	βγ	5.4	2.5
α/β [f]	ααβ, ααβααβ	5.2-5.4	2.4-2.5
α [g]	GCN4pLI	5.4	2.3
	3_{10}-helix	5.8	2.0

Helical parameters were calculated as previously described (ref 15a)
[a] ref 15a, [b] ref 15e, [c] ref 15b, [d] PDB 3O43, [e] PDB 3F87, [f] PDB 3C3H, [g] PDB 1GCL

2.4.2.4 γ Residue torsion angles

Table 2.5 compares the four backbone torsion angles of cyclic γ-residues and γ^4-residues in various helical contexts. As might be expected, the cyclohexane-based γ-residue generally prefers gauche torsion angles (~60°) about the backbone Cα-Cβ and Cβ-Cγ bonds, ζ and θ, respectively.[41-43] The α-helix-like conformation observed in α/β/γ-peptide **2.6**, however, seems to require a somewhat smaller Cβ-Cγ torsion angle (45.9°) in the cyclohexyl ring. Crystal structures of helical α/γ-peptides containing γ^4-residues that have recently emerged from the Gopi[47-49] and Balaram[44,45] laboratories show that in

these cases, the Cβ-Cγ torsion angles are frequently in the range of 50°, but an even smaller torsion angle is observed for the corresponding backbone bond in the γ^4-hAla residue of **2.7** (38.9°). The relatively small θ backbone torsion angles for the γ-residues in **2.6** and **2.7** raise the possibility that the cyclohexyl-constrained γ backbone may not be optimally suited to an α-helix-mimicking conformation.

Table 2.5 Backbone torsion angles (degrees) for γ–residues in various peptides.

peptides	ϕ	θ	ζ	ψ
α/β^c/γ^c– **2.6**	-135.5	45.9	56.9	-118.6
α/β^c/γ^4– **2.7**	-132.9	38.9	64.7	-107.3
γ^c [a]	-154.5	60.2	59.5	-126.8
α/γ^c [b]	143.7	-56.6	-52.5	111.7
α/γ^4 [c]	-125.8	50.8	61.9	-118.9
α/γ^4/γ^4 [d]	-124.1	53.6	65.1	-136.2
α/γ^4/α [d]	-126.7	51.0	59.6	-120.9
β^c/γ^c [e]	-134.7	60.1	59.8	-121.0

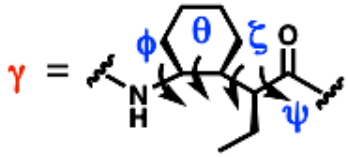

[a] ref 15a, [b] ref 15b, [c] ref 16a, [d] ref 17a, [e] ref 15d

2.5 Efforts toward synthesis of 5-membered ring-constrained γ-amino acids

EtACHA, containing a *cis*-cyclohexyl ring constraint for the Cβ-Cγ bond, can be incorporated into an α-helix-like conformation in α/β/γ-peptides, but the crystal structure of **2.6** suggests that the θ torsion angle deviates from the intrinsic preference for ~ 60° when EtACHA participates in such a helix (Table 2.5). As an alternative γ-amino acid, in

light of the initial computational results (see experimental session), we sought to prepare the analogous γ-amino acid with a *cis*-cyclopentyl ring constraint for the Cβ-Cγ bond (Figure 2.13).

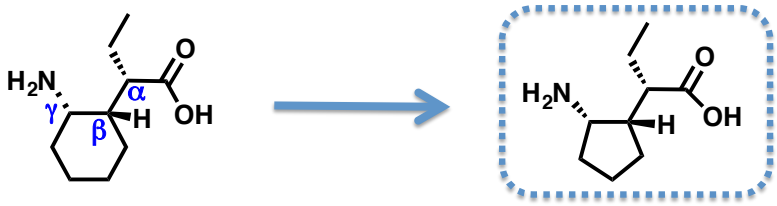

α-ethyl-cis-2-aminocyclohenxaneacetic acid (S, S, S) EtACHA

α-ethyl-cis-2-aminocyclopentaneacetic acid **(S, S, S) EtACPA**

Figure 2.13 Structures of γ-amino acids, Et-ACHA and Et-ACPA.

Efforts to synthesize the (S,S,S) α-ethyl-*cis*-2-amino cyclopentaneacetic acid (ACPA) involved Michael additions of *n*-butanal to 1-nitrocyclopentene, with catalysis L-proline[50] or the Hayashi-Jorgenson catalyst[43] (Figure 2.14). However, the Michael products were difficult to purify owing to poor diastereomeric selectivity or rapid epimerization. Reduction of crude aldehydes to alcohols, or oxidation to carboxylic acids, eliminated the epimerization problem, but the stereoisomer mixtures remained inseparable. Carful purification of the aldehyde Michael product using a silica gel column, followed immediately by oxidizing the aldehyde to the carboxylic acid, seemed to afford one pure product. However, the stereochemistry has not been identified, and optimization of this process will be necessary.

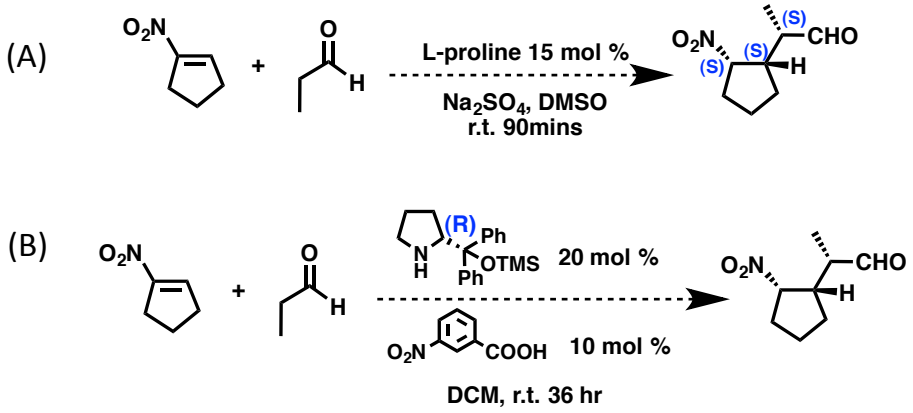

Figure 2.14 Initial efforts toward preparation of Et-ACPA (A) using L-proline [50] (B) using Hayashi-Jorgenson catalyst [43].

2.6 Conclusions

The results suggest that β^3- and γ^4-amino acid residues, which bear a single side chain and are therefore homologous to α-amino acid residues, differ in their intrinsic tendencies to adopt helical secondary structure, with γ^4-residues displaying a higher propensity than β^3-residues. Previous work has shown that short peptidic oligomers containing β^3-residues or γ^4-residues, either exclusively or in combination with α-residues, can adopt helical conformations in the crystalline state or in organic solvents.[18-31,47-49,51-53] Aqueous solution represents a more challenging environment in terms of peptidic secondary structure formation, and we have used comparisons in water to show that cyclic β-residues display substantially higher helical propensities than β^3-residues.[16,32,54-57] Considering this precedent, the relatively large helical propensity of γ^4-residues revealed by our comparisons among $\alpha/\beta/\gamma$-peptides **2.1** and **2.3-2.5** in aqueous solution is unexpected. The helical propensity of the cyclic γ-residue in **2.1** appears to be somewhat superior to that of γ^4-hAla, but the relatively small θ

backbone torsion angles documented crystallographically for the γ-residues in **2.6** and **2.7** raise the possibility that the cyclohexyl-constrained γ backbone may not be optimally suited for the α-helix mimetic conformation. In the future, alternative types of γ-residue constraints should be explored in pursuit of improved stability of the α-helix-like conformation available to α/β/γ-peptides.

2.7 Experimental

2.7.1 Materials

Fmoc α-amino acids and resin for solid phase peptide synthesis were purchased from Novabiochem or Chem-Impex, and coupling reagents and additives, O-benzotriazole-N,N,N',N'-tetramethyluronium hexafluorophosphate (HBTU), O-(7-azabenzotriazol-1yl)-N,N,N,N'-tetramethyluronium hexafluorophosphate(HATU), 1-ethyl-3-(3-dimethylaminopropyl)carbodiimide hydrochloride (EDCI), hydroxybenzotriazole (HOBt), 1-hydroxy-7-azabenzotoriazole) (HOAt), were purchased from Chem-Impex. Other reagents and solvents were purchased from Sigma Aldrich. Fmoc β- and γ- amino acids were prepared according to previous reports.[43,58]

2.7.2 Peptide synthesis

All peptides were synthesized on 25 μmol scale by previously reported microwave-assisted solid-phase methods.[17] Microwave irradiation was carried out with a CEM MARS microwave reactor with a microtiter plate turnable, fiber-optic temperature probe and magnetic stirrer. NovaPEG rink amide resin (NovaBiochem) was used for peptides **2.1**-**2.5**, and Fmoc-Arg(Pbf) loaded NovaSyn TGA resin (NovaBiochem) was

used for peptides **2.6** and **2.7**. Peptides **2.6** and **2.7** were prepared as C-terminal acids via a combination of microwave method (for $\alpha/\beta/\gamma$-region) and room-temperature peptide synthesis methods (for α-region).

2.7.3 Purification and characterization of peptides

All peptides were purified on a Shimadzu SCL-10A liquid chromatograph fitted with a C18-functionalized reverse-phase column. The binary solvent system used H_2O:CF_3CO_2H (100:0.1 v/v) as A solvent and CH_3CN:CF_3CO_2H (100:0.1 v/v) as B solvent. Following purification, fractions were lyophilized. Polypeptide identity was confirmed using matrix-assisted laser desorption ionization-time of flight (MALDI-TOF) mass spectrometry (Bruker REFLEX II). Purity was determined by analytical HPLC, and was greater than 95 % for all peptides described below.

Peptide **2.1**

Ac–E (γcyc) A R (βcyc) Y A (γcyc) Q A (βcyc) K–NH_2

Calc. 1533.9 Found 1533.7

Purification condition: 34-44 % MeCN, 20 min

HPLC purity check: 10-60 % MeCN, 50 min

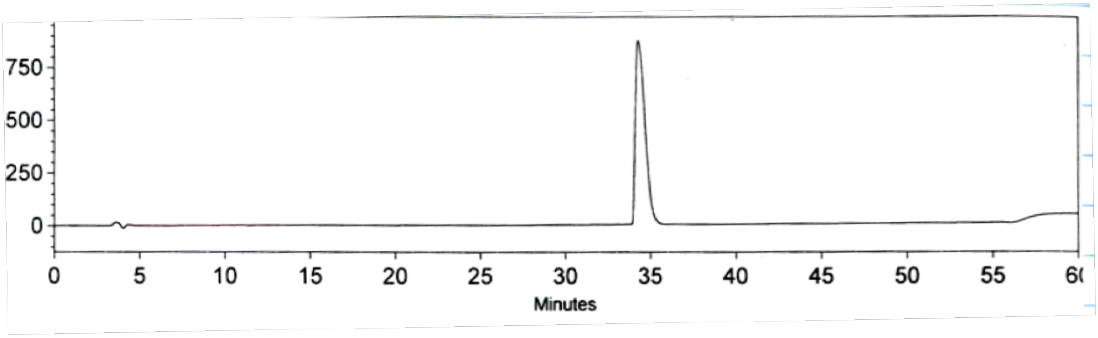

Peptide **2.2**

Ac–E L E A R Q Y A Orn Nle Q A F K–NH_2

Calc. 1722.9 Found 1721.8

Purification condition:18-28 % B, 20 min

Purity check: 10-60 % B, 50 min

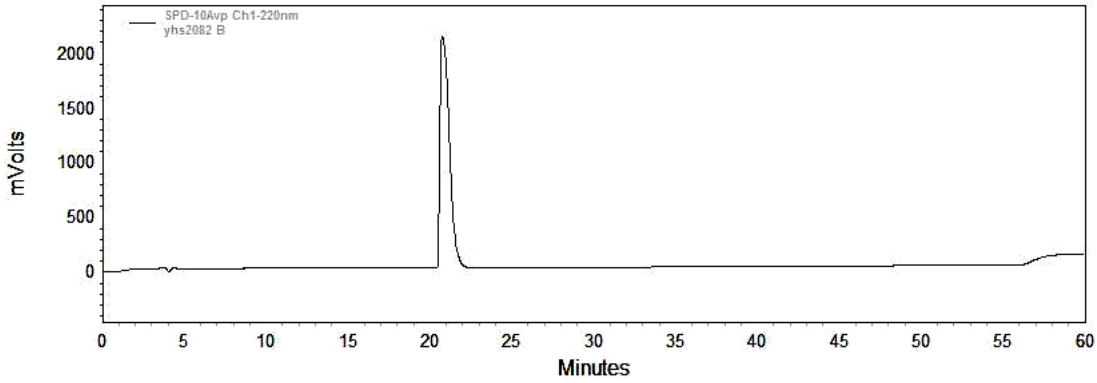

Peptide **2.3**

Ac–E γ⁴hA A R(βcyc) Y A γ⁴hA Q A(βcyc) K–NH_2

Calc. 1397.8 Found 1397.7

Purification condition: 18-29 % B, 20 min

Purity check: 10-60 % B, 50 min

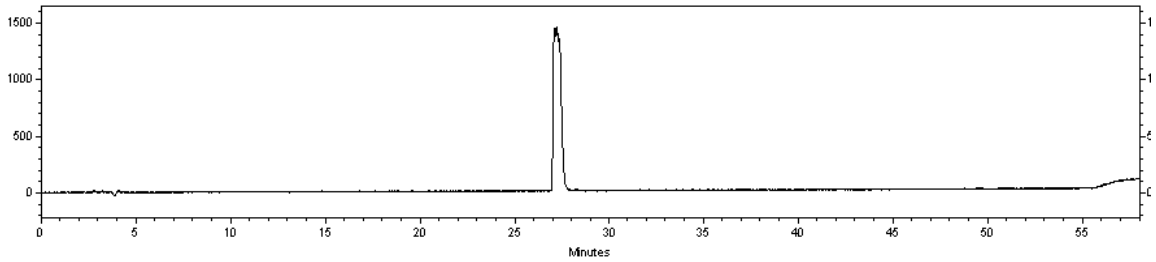

Peptide **2.4**

Ac–E (γcyc) A R γ³hQ Y A(γcyc) Q A γ³hF K–NH_2

Calc. 1615.0 Found 1614.8

Purification condition: 25-35 % B, 20 min

Purity check: 10-60 % B, 50 min

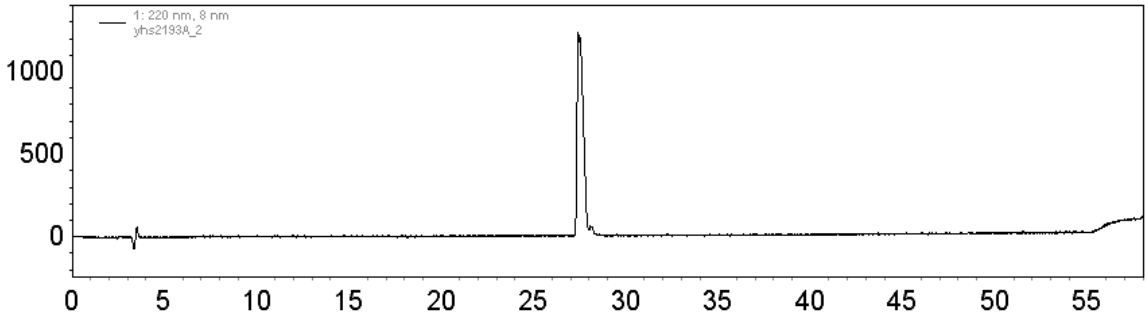

Peptide **2.5**

Ac–E γ4hA A R γ³hQ Y A γ4hA Q A γ³hF K–NH_2

Calc. 1478.8 Obsd. 1478.7

Purification condition: 15-25 % B, 20 min

Purity check: 10-60 % B, 50 min

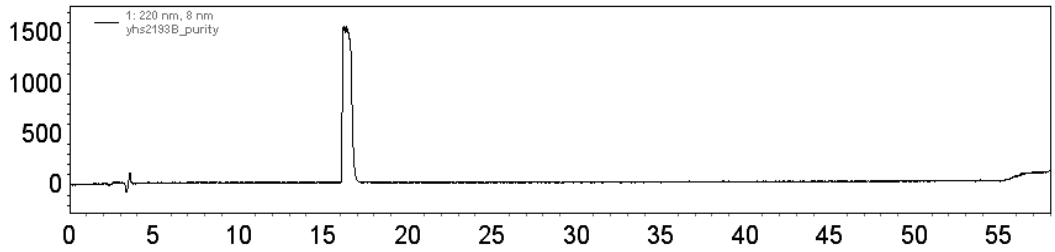

Peptide **2.6**

Ac–RMKQIEDKLEEILSKLYHIEZELγcycIKZLLGER–OH

Calc. 4000.1 Obsd. 4002.1

Purification condition: 30-45 % B, 30 min (purified twice)

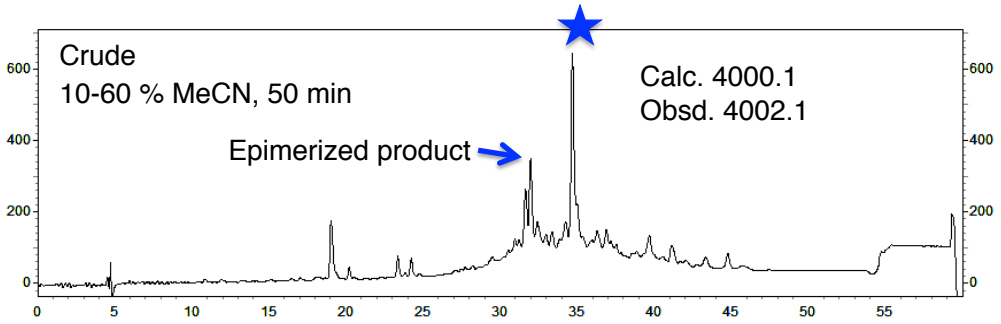

Purity check: 10-60 % B, 50 min

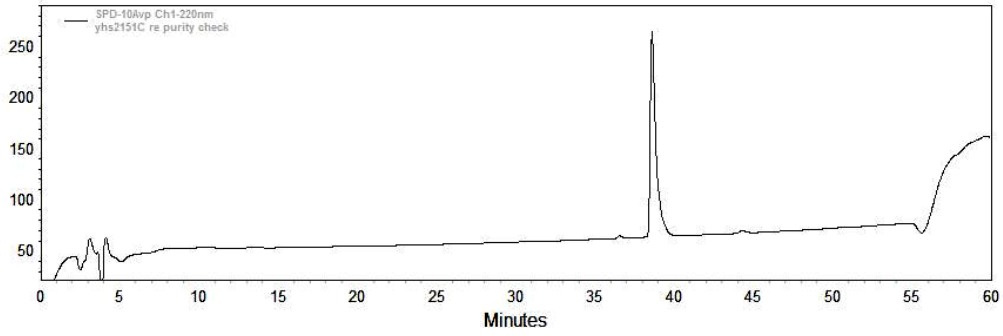

Peptide **2.7**

Ac–RMKQIEDKLEEIL(X)KLγ^4hAIE(X)ELARIKKLLYER–OH

Calc. 4004.2 Found 4005.8

Purification condition: 35-45 % B, 20 min (purified twice)

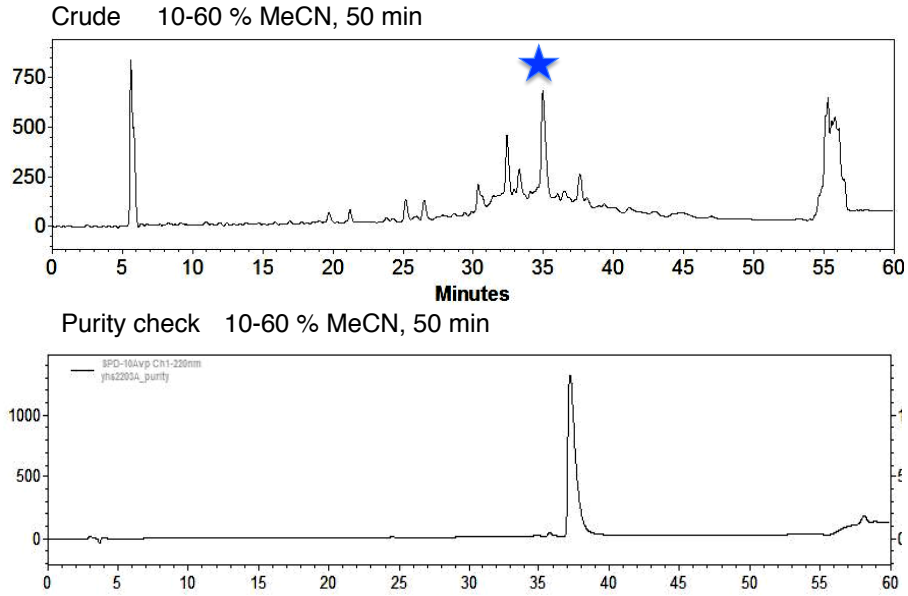

Peptide **2.9**

Ac–RMKQIEDKLEEIL(Z)KL(γcyc)IE(Z)ELARIKKLLYER–OH

Calc. 4074.3 Found 4076.5

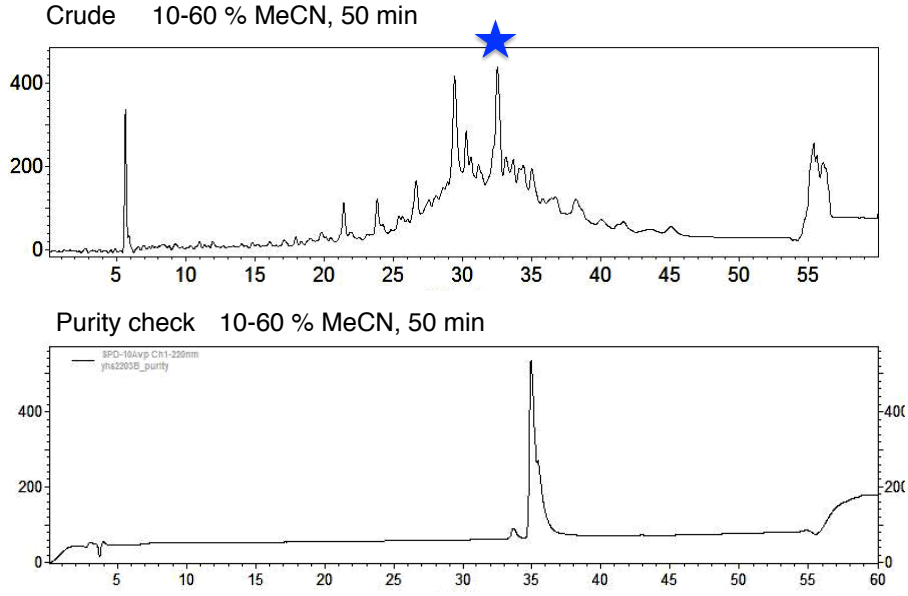

Peptide **2.10**

Ac–RMKQIEDKLEEIL(Z)KL(γcyc)IE(Z)EL(γcyc)IK(Z)LLYER–OH

Calc. 3998.2 Found 3999.9

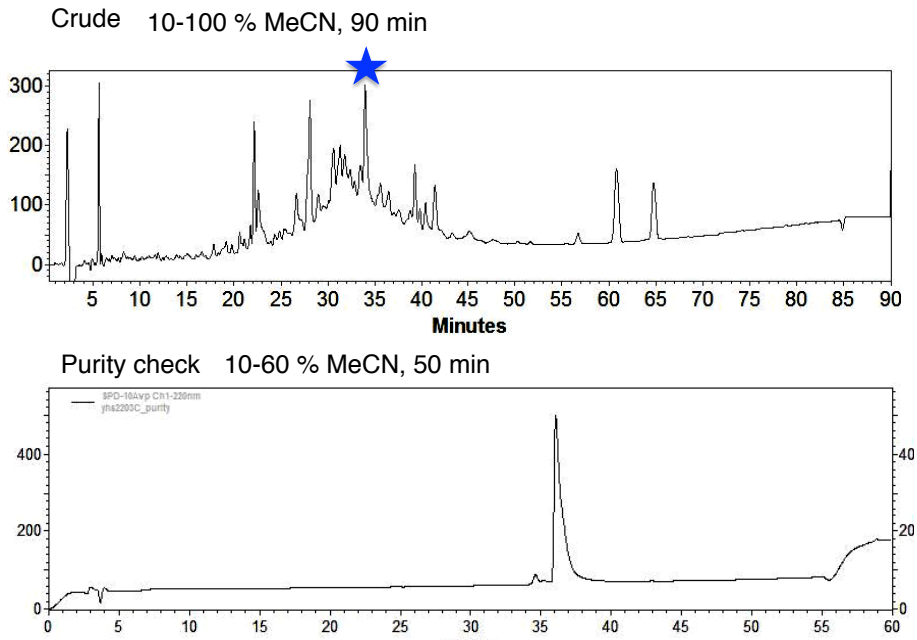

Peptide **2.12**

Ac–RMKQIEDKLEEIL(Z)KLγ4hAIE(Z)ELγ4hAIK(Z)LLYER–OH

Calc. 3862.1 Found 3864.3

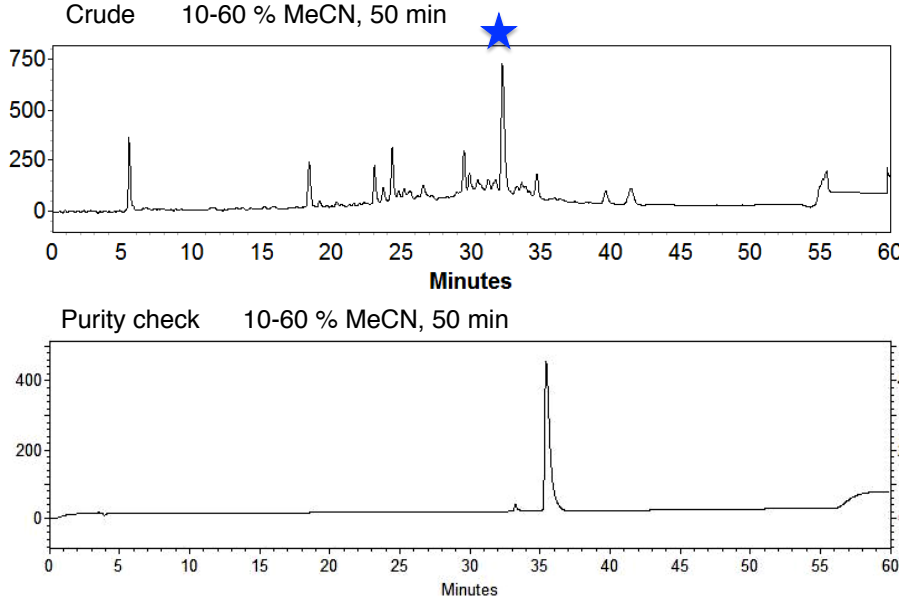

Peptide **2.13**

Ac–RMKQIEDKLEEILYKLγ^{4}hAIE(X)ELγ^{4}hAIK(X)LLγ^{4}hAR–OH

Calc. 3718.0 Found 3719.5

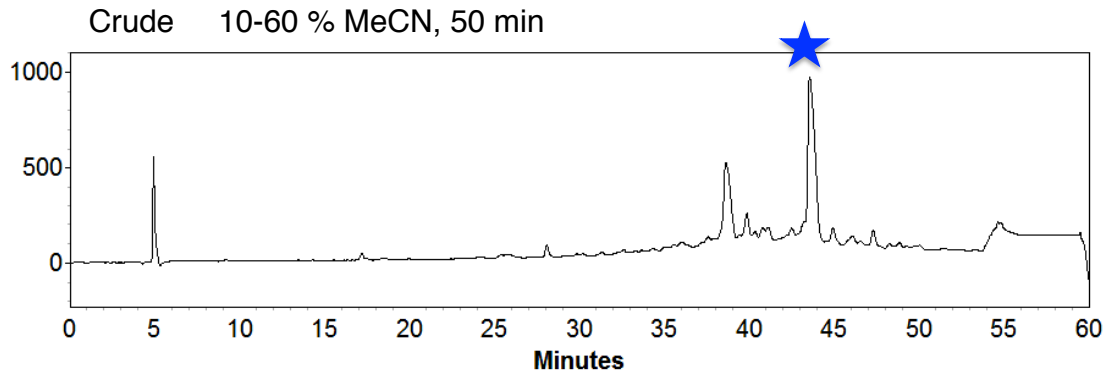

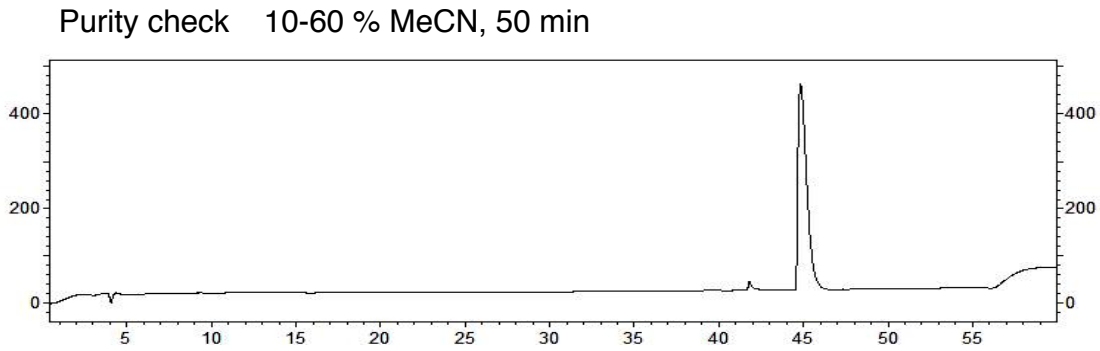

Ac–RMKQIEDKLEEILYKL(γcyc)IE(Z)EL(γcyc)IK(Z)LL(γcyc)R–OH **2.11**

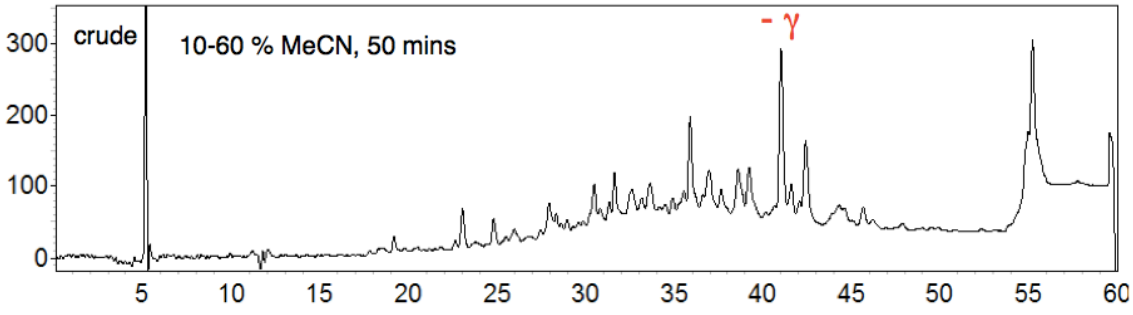

Figure 2.15 HPLC trace of crude stock of peptide **2.11**. Due to the low yield, **2.11** could not be purified.

2.1

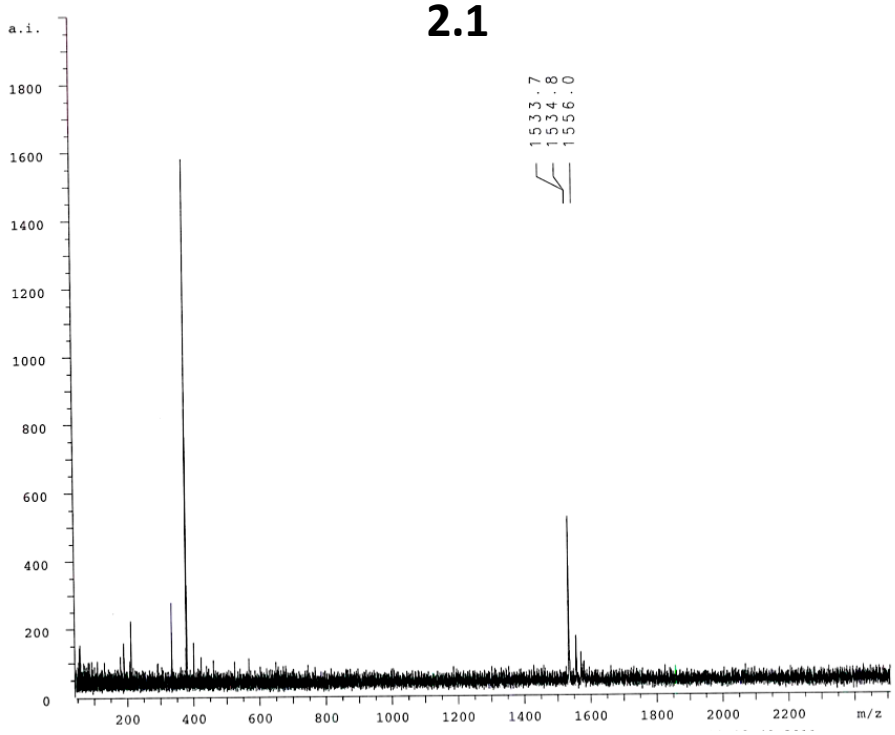

2.1

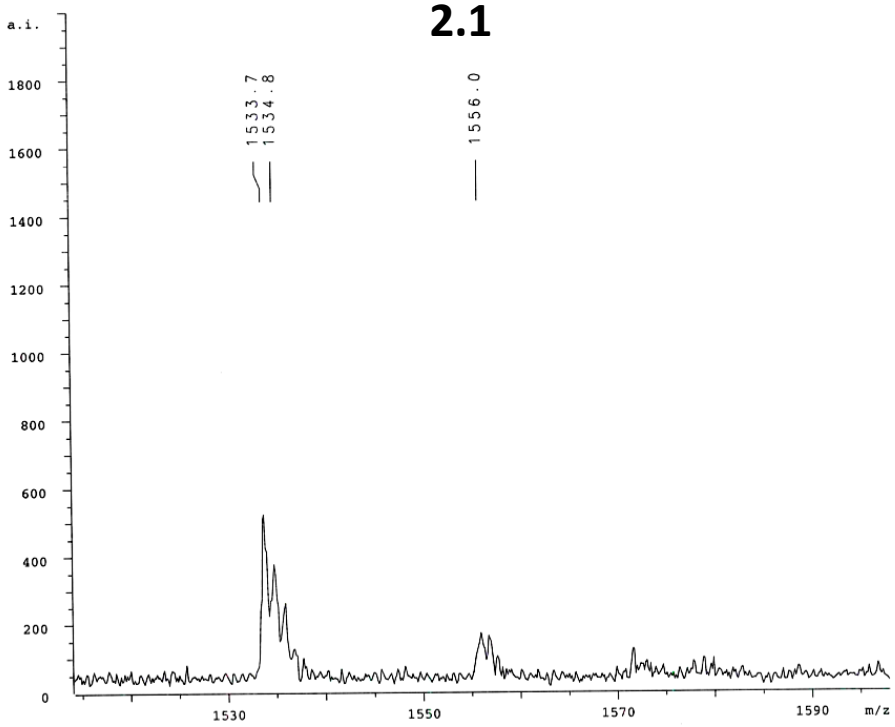

2.2

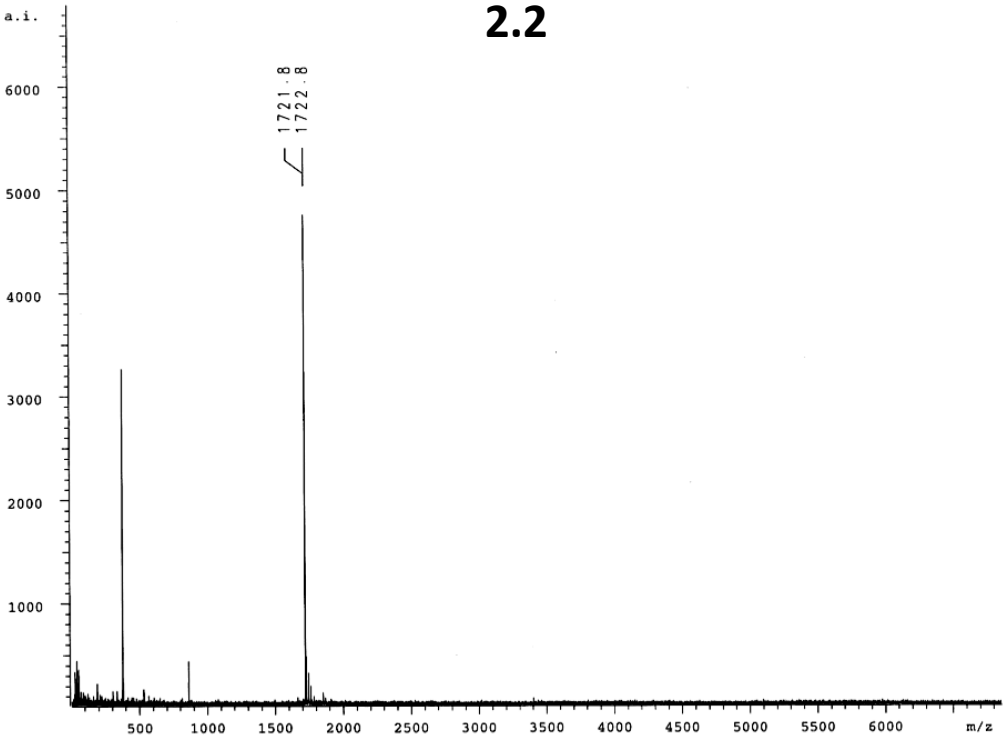
a.i.
6000
5000
4000
3000
2000
1000
1721.8
1722.8
500
1000
1500
2000
2500
3000
3500
4000
4500
5000
5500
6000
m/z

2.2

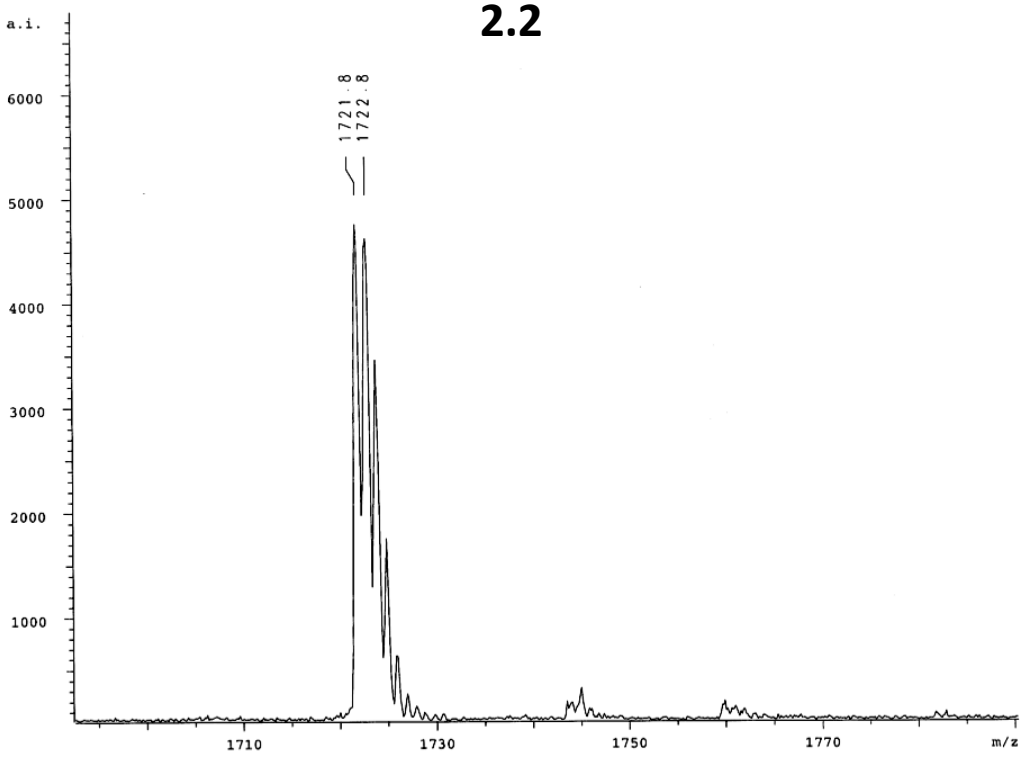
a.i.
6000
5000
4000
3000
2000
1000
1721.8
1722.8
1710
1730
1750
1770
m/z

2.3

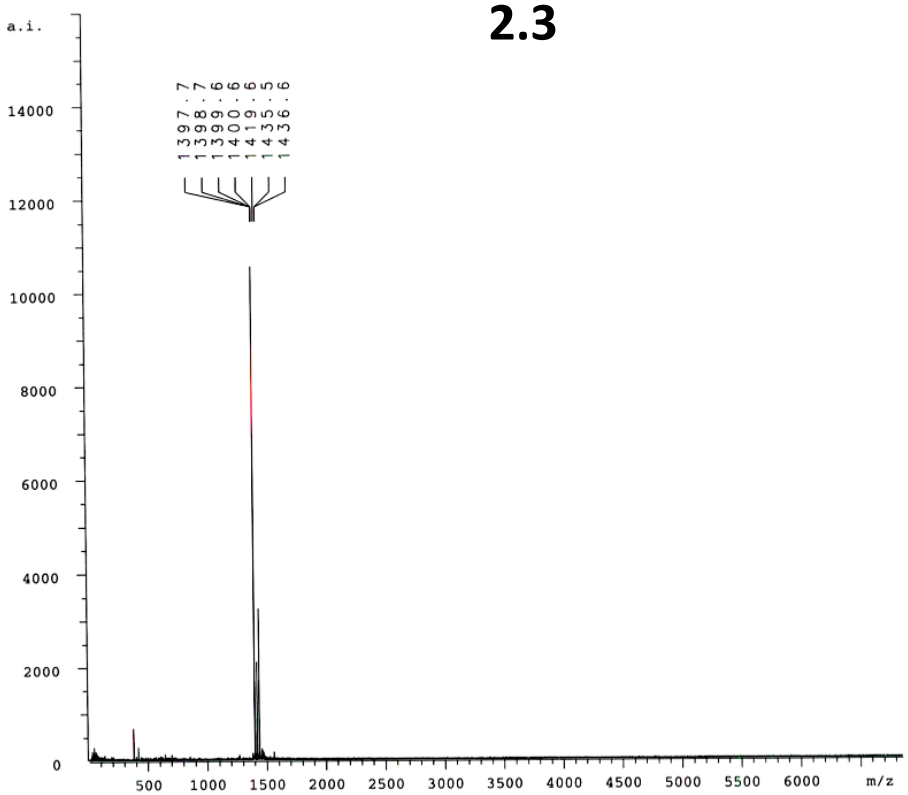
a.i.
14000
12000
10000
8000
6000
4000
2000
0
1397.7
1398.7
1399.6
1400.6
1419.6
1435.5
1436.6
500
1000
1500
2000
2500
3000
3500
4000
4500
5000
5500
6000
m/z

2.3

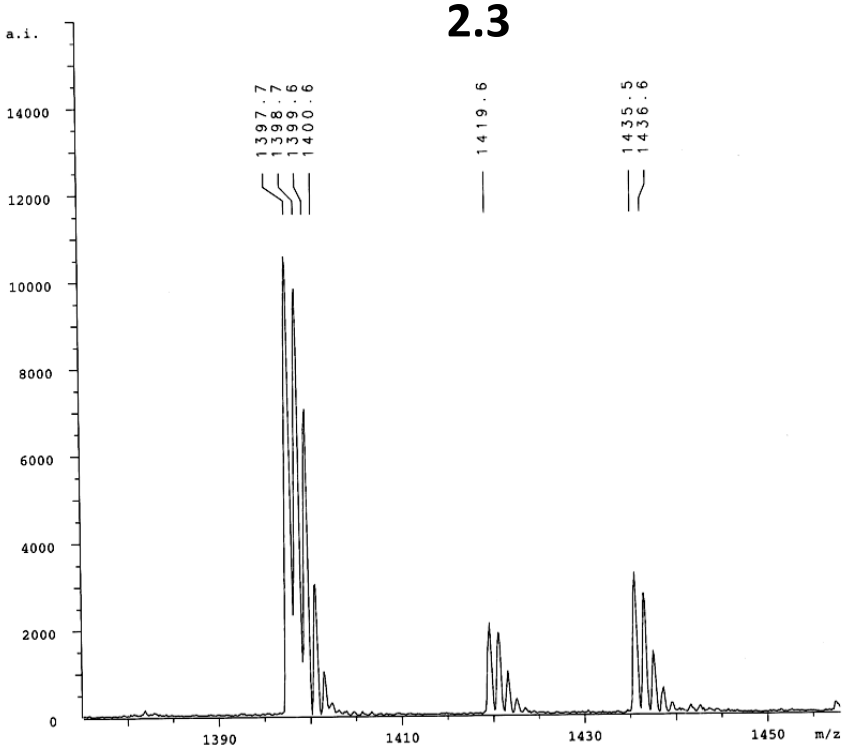
a.i.
14000
12000
10000
8000
6000
4000
2000
0
1397.7
1398.7
1399.6
1400.6
1419.6
1435.5
1436.6
1390
1410
1430
1450
m/z

2.4

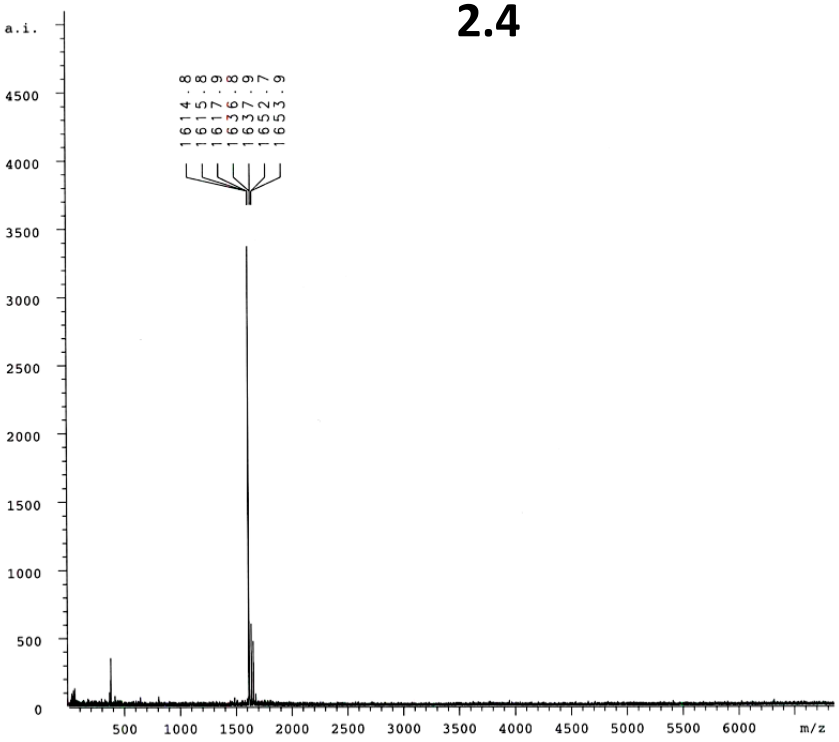
a.i.
4500
4000
3500
3000
2500
2000
1500
1000
500
0
1614.8
1615.8
1617.9
1636.8
1637.9
1652.7
1653.9
500
1000
1500
2000
2500
3000
3500
4000
4500
5000
5500
6000
m/z

2.4

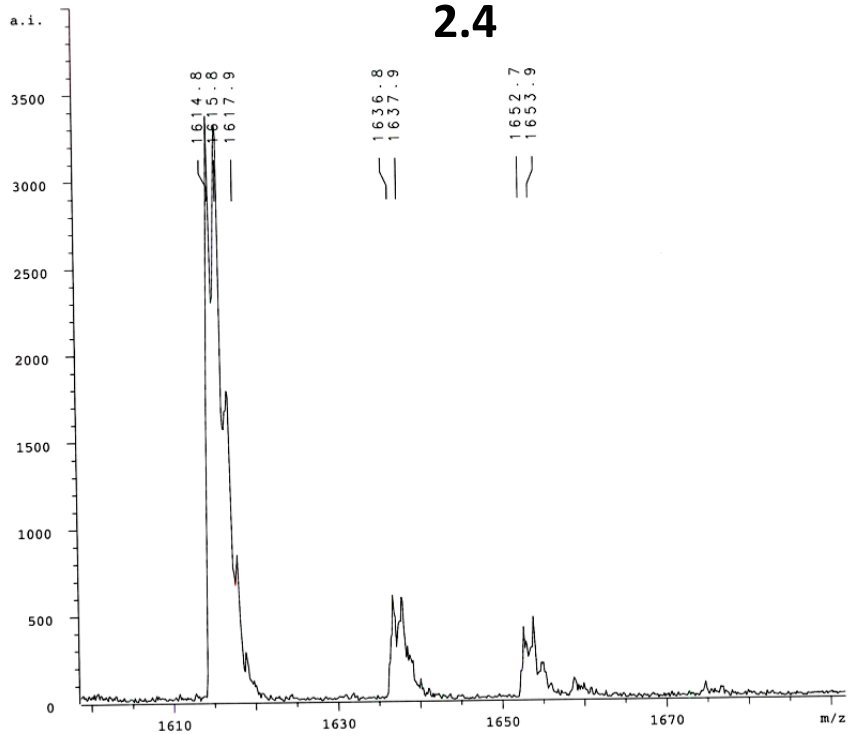
a.i.
3500
3000
2500
2000
1500
1000
500
0
1614.8
1615.8
1617.9
1636.8
1637.9
1652.7
1653.9
1610
1630
1650
1670
m/z

2.5

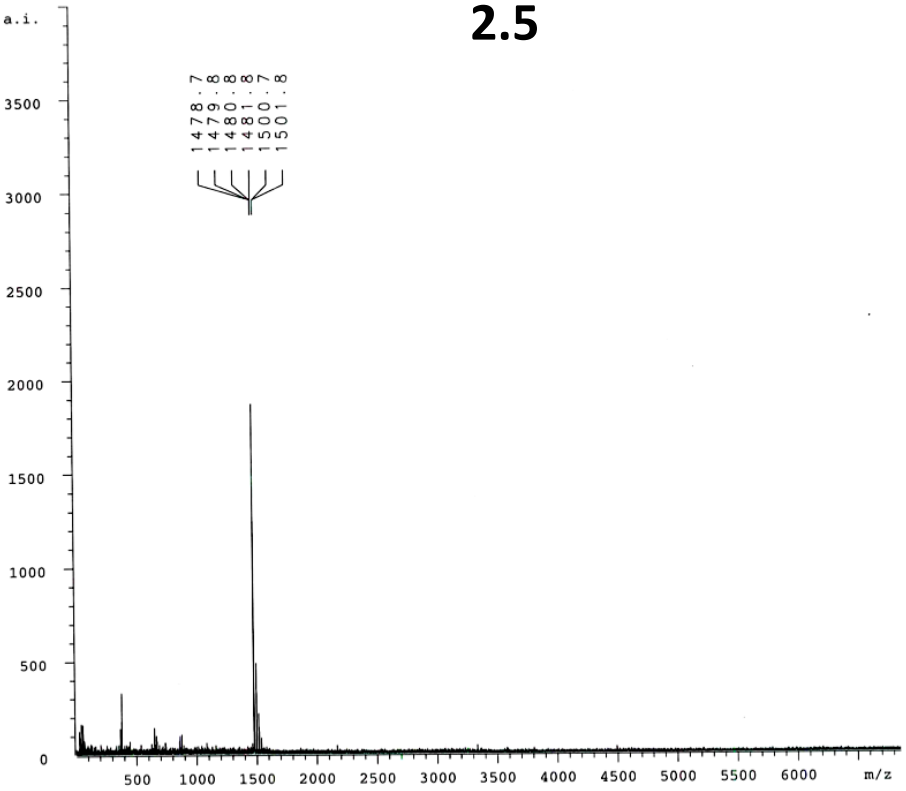
a.i.
3500
3000
2500
2000
1500
1000
500
0
1478.7
1479.8
1480.8
1481.8
1500.7
1501.8
500
1000
1500
2000
2500
3000
3500
4000
4500
5000
5500
6000
m/z

2.5

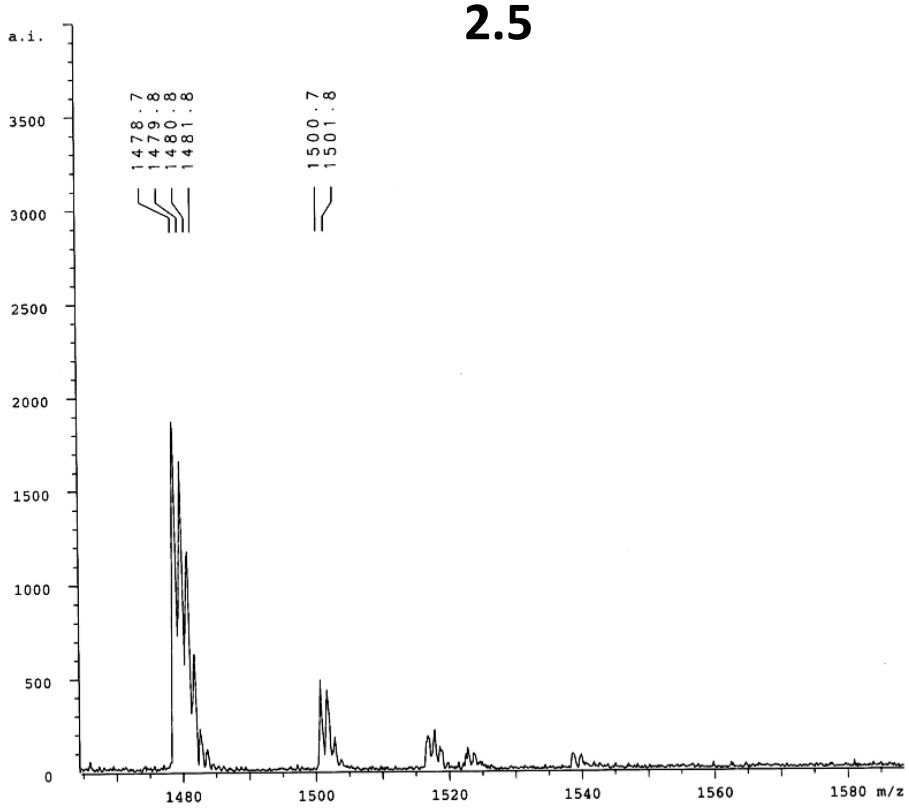
a.i.
1478.7
1479.8
1480.8
1481.8
1500.7
1501.8
3500
3000
2500
2000
1500
1000
500
0
1480
1500
1520
1540
1560
1580 m/z

2.6

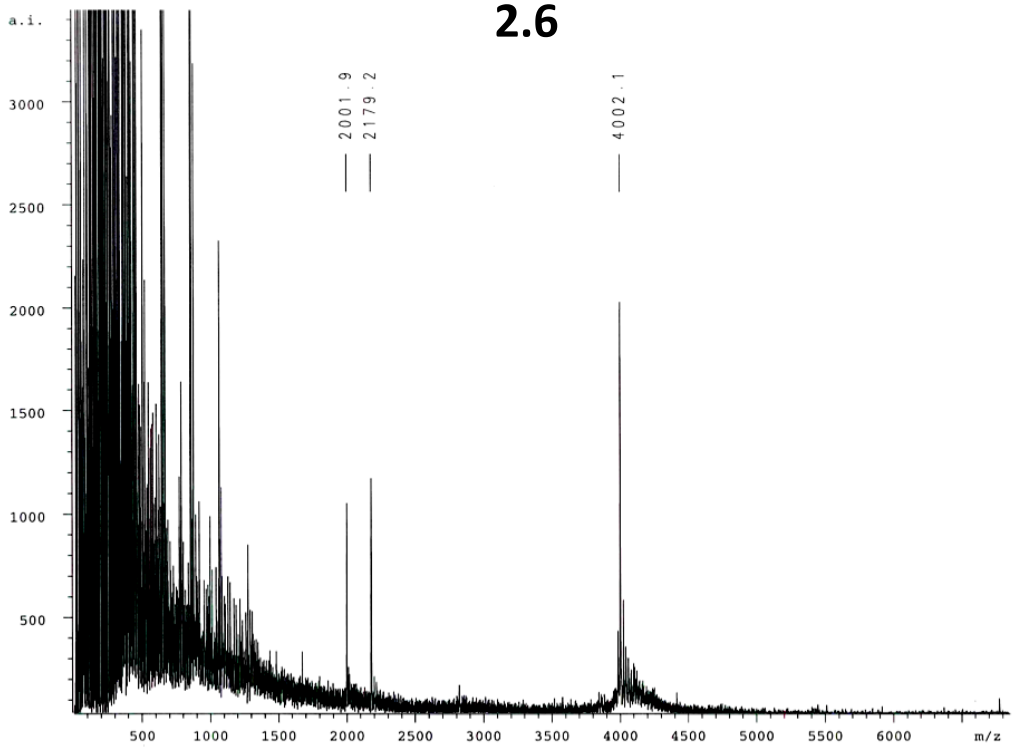
a.i.
2001.9
2179.2
4002.1
3000
2500
2000
1500
1000
500
500
1000
1500
2000
2500
3000
3500
4000
4500
5000
5500
6000
m/z

2.6

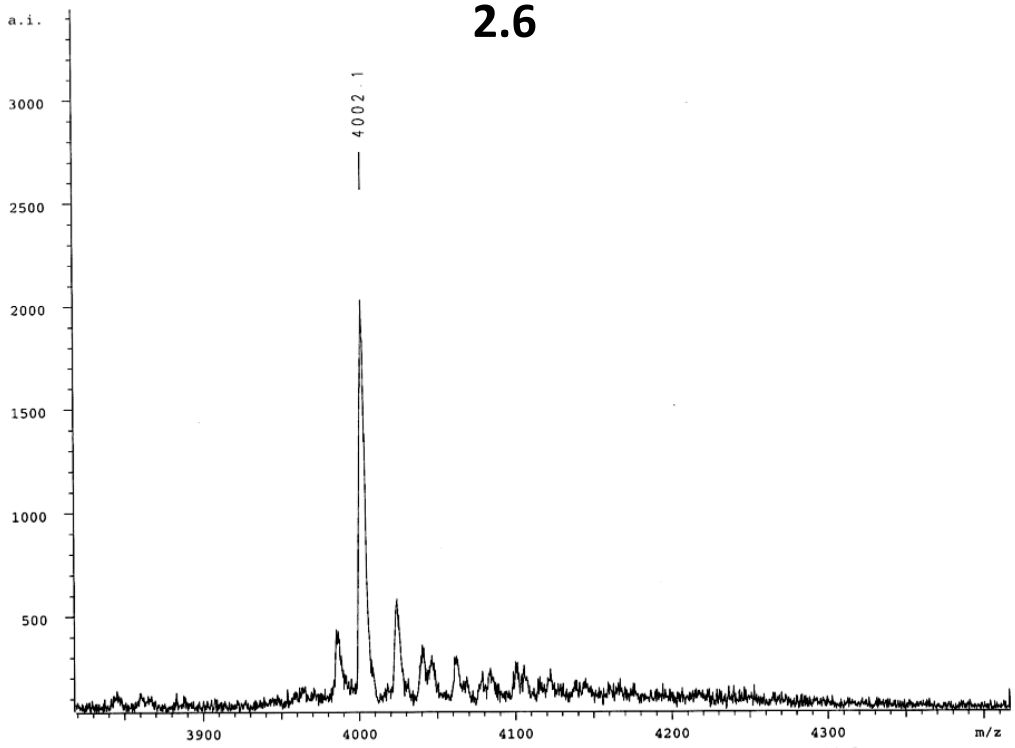
a.i.
4002.1
3000
2500
2000
1500
1000
500
3900
4000
4100
4200
4300
m/z

2.7

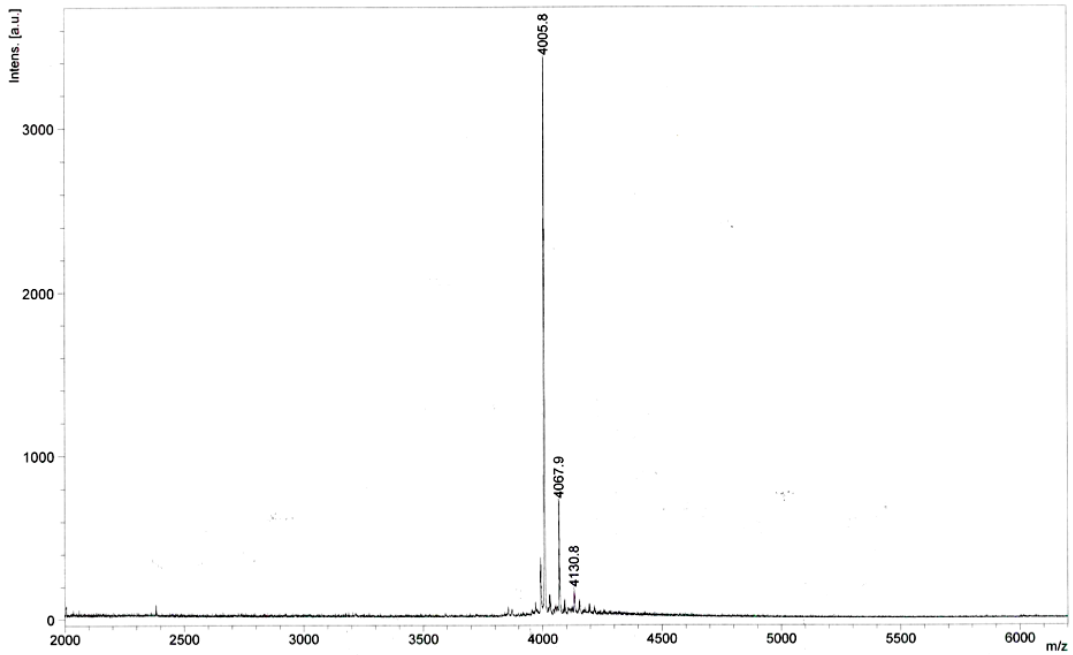
Intens. [a.u.]
4005.8
4067.9
4130.8
3000
2000
1000
0
2000
2500
3000
3500
4000
4500
5000
5500
6000
m/z

2.7

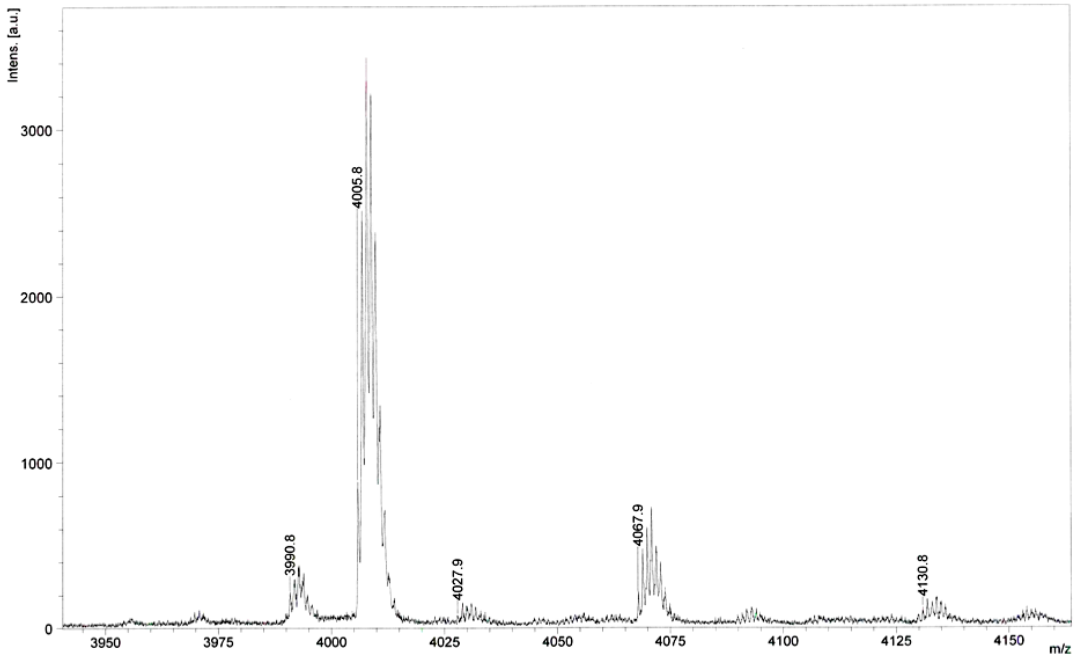
Intens. [a.u.]
3000
2000
1000
0
4005.8
3990.8
4027.9
4067.9
4130.8
3950
3975
4000
4025
4050
4075
4100
4125
4150
m/z

2.9

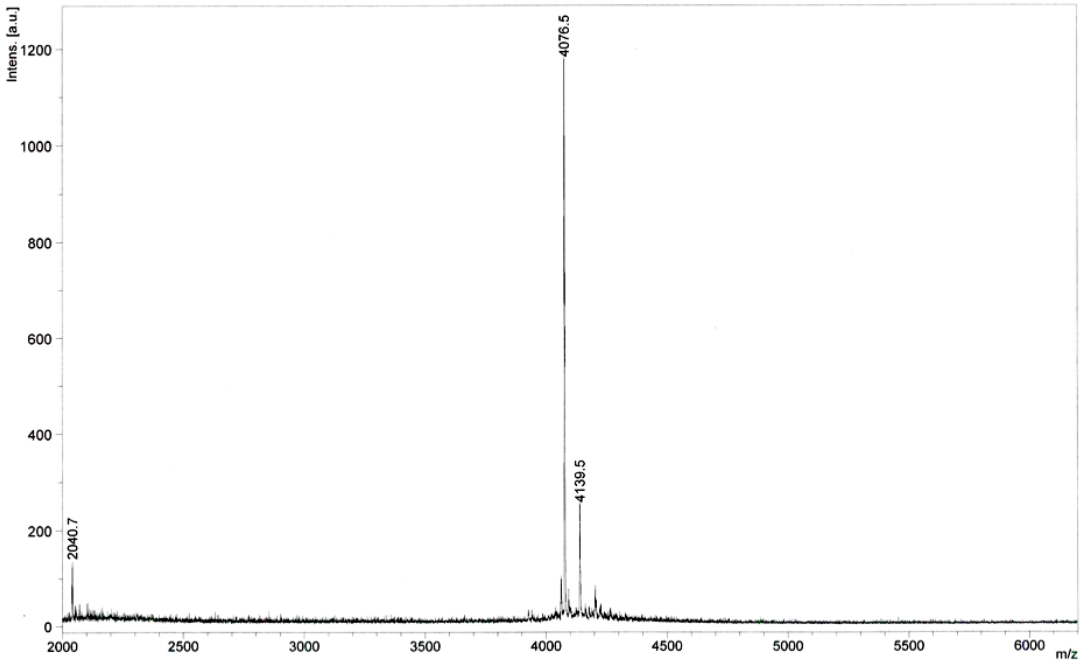
Intens. [a.u.]
1200
1000
800
600
400
200
0
4076.5
4139.5
2040.7
2000
2500
3000
3500
4000
4500
5000
5500
6000
m/z

2.9

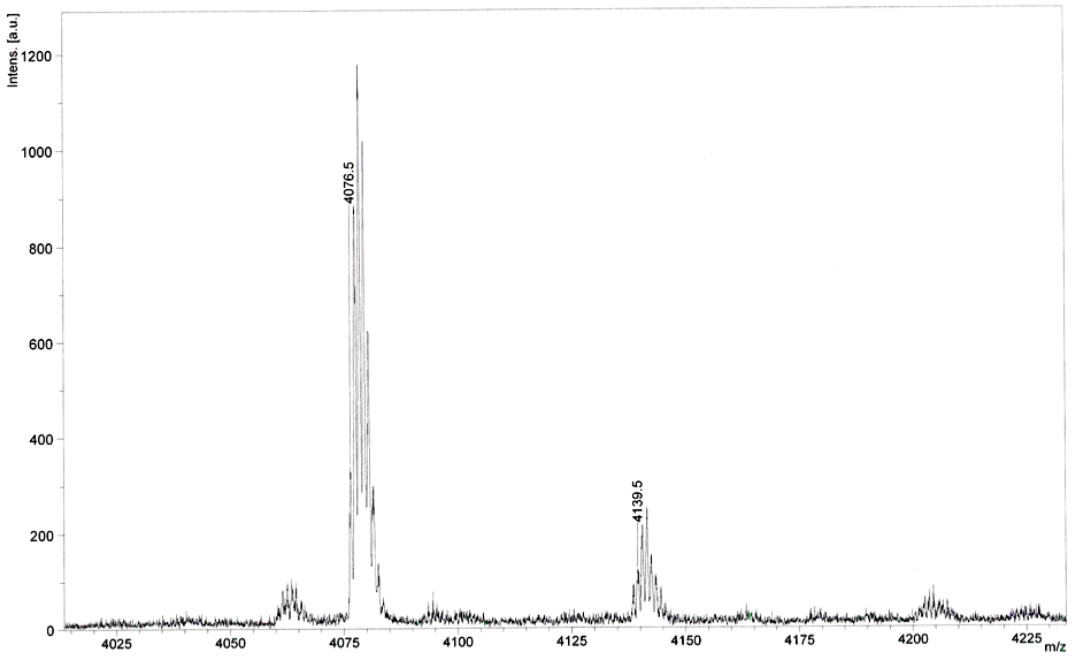
Intens. [a.u.]
1200
1000
800
600
400
200
0
4076.5
4139.5
4025
4050
4075
4100
4125
4150
4175
4200
4225
m/z

2.10

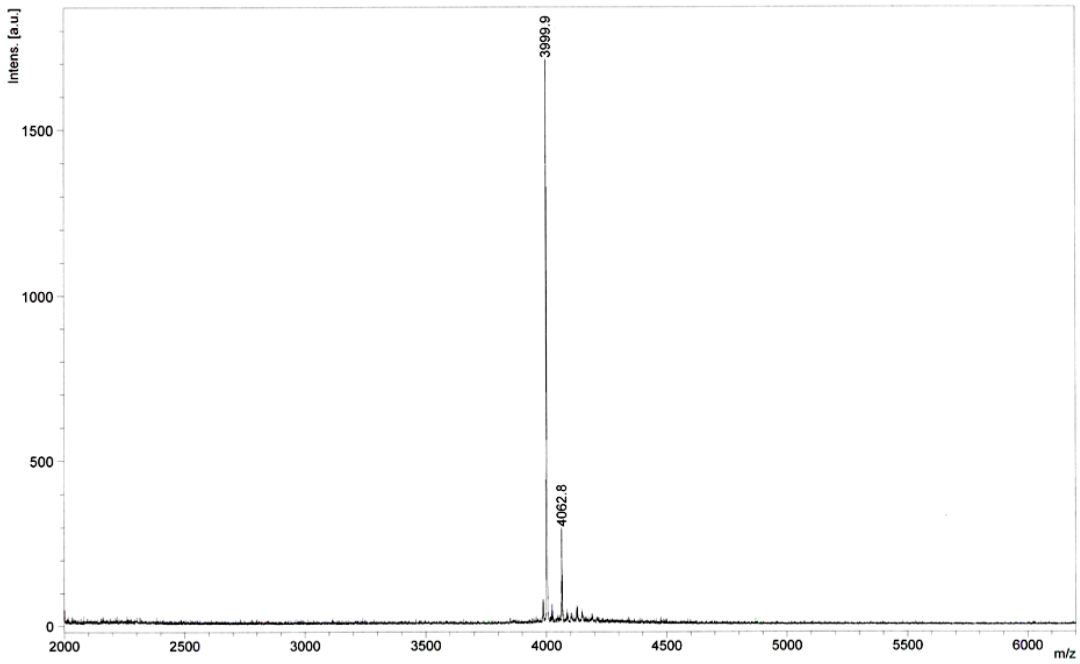
Intens. [a.u.]
1500
1000
500
0
3999.9
4062.8
2000
2500
3000
3500
4000
4500
5000
5500
6000
m/z

2.10

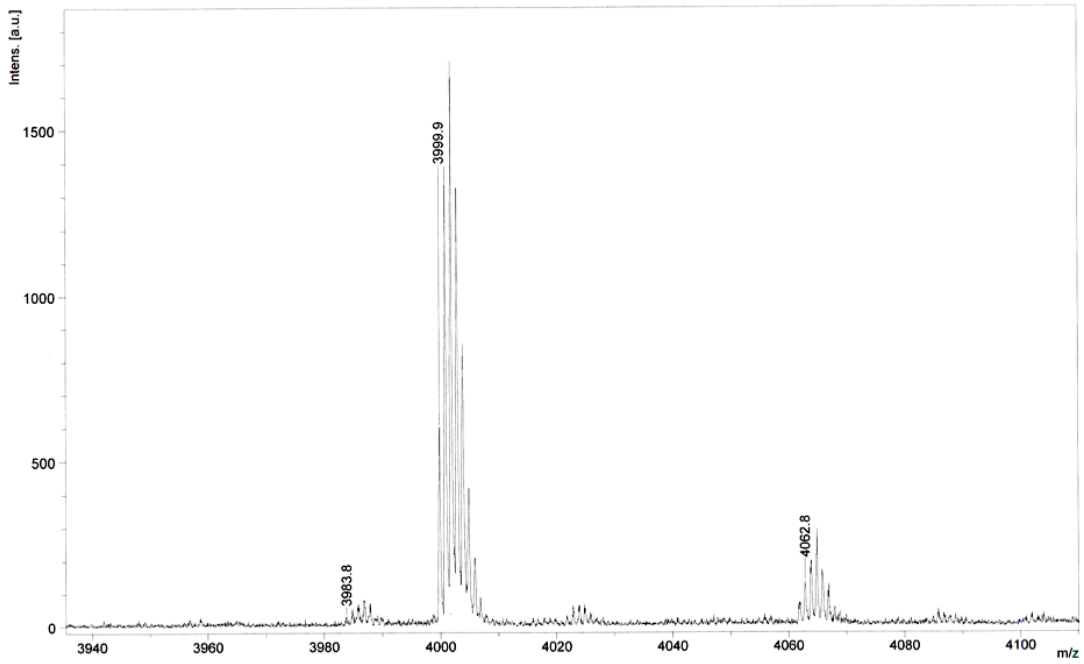
Intens. [a.u.]
1500
1000
500
0
3999.9
3983.8
4062.8
3940
3960
3980
4000
4020
4040
4060
4080
4100
m/z

2.12

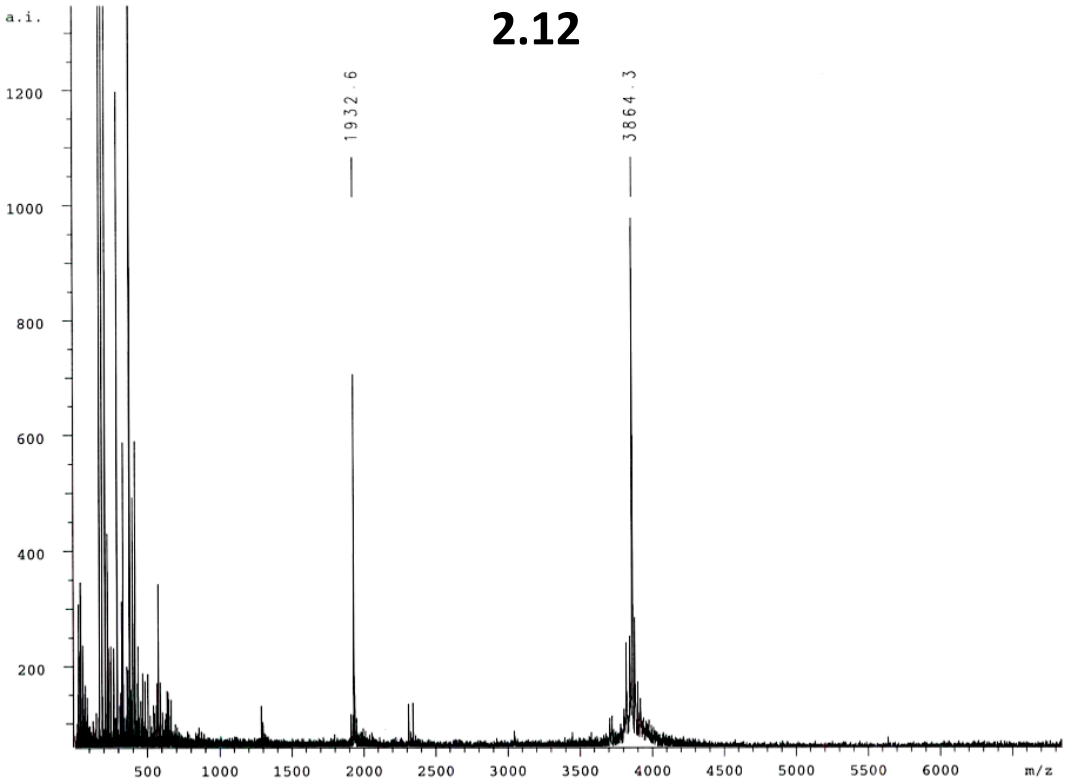
a.i.
1200
1000
800
600
400
200
1932.6
3864.3
500
1000
1500
2000
2500
3000
3500
4000
4500
5000
5500
6000
m/z

2.12

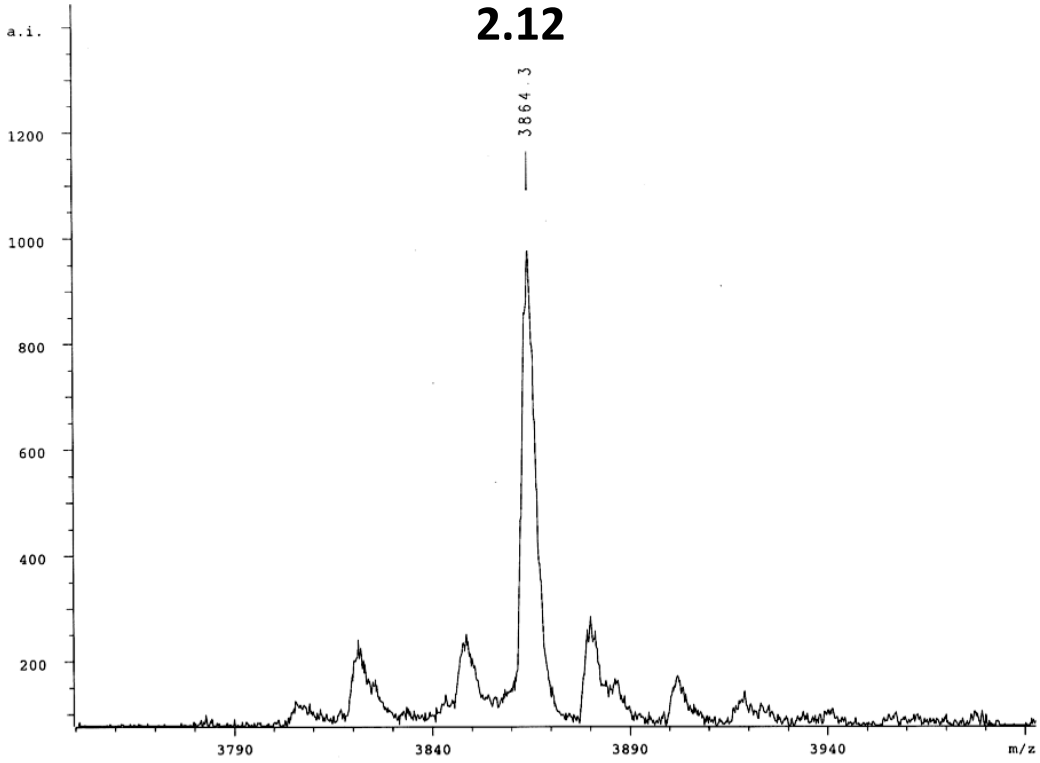
a.i.
3864.3
1200
1000
800
600
400
200
3790
3840
3890
3940
m/z

2.13

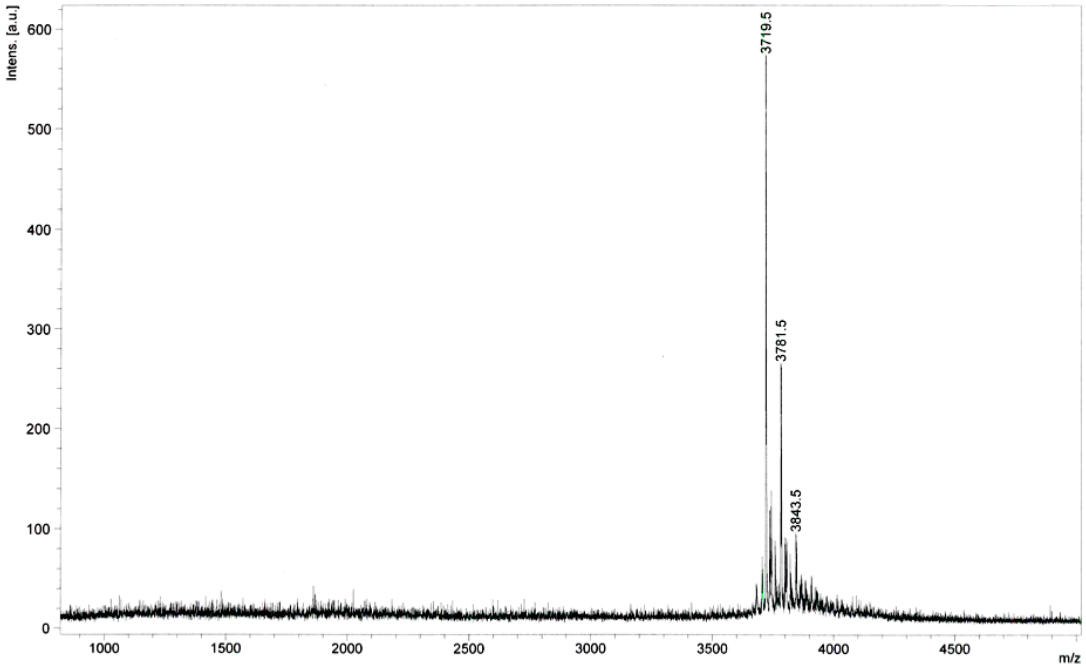
Intens. [a.u.]
3719.5
3781.5
3843.5
600
500
400
300
200
100
0
1000
1500
2000
2500
3000
3500
4000
4500
m/z

2.13

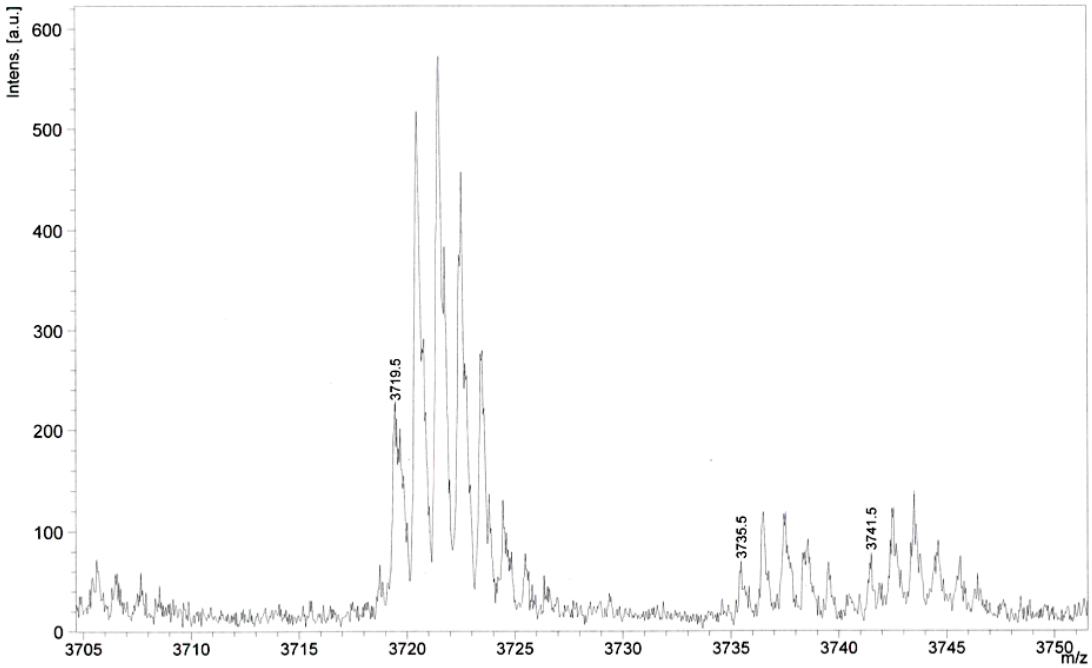

2.7.4 Circular Dichroism Spectroscopy

CD spectra were measured on an AVIV circular dichroism spectrometer model 420. Spectra were recorded in a 1 mm quartz cell with a wavelength step size of 1 nm and an averaging time of 5 sec for each measurement. Variable-temperature measurements were carried out at 10 ^{o}C intervals with an equilibration time of 10 min at each new temperature.

2.7.5 2D-NMR analysis

Two-dimensional NMR spectra were recorded on a Varian INOVA 600 MHz spectrometer equipped with a Varian 5 mm ^{1}H/^{13}C/^{15}N, 3-axis PFG probe. Data were

processed using Varian VNMR 6.1 software. All NMR samples were prepared with total volumes of approximately 0.35 mL in 5 mm Shigemi tubes. Lyophilized peptides were dissolved in 9:1 H_2O/D_2O, or CD_3OH solvent. 2,2-Dimethyl-2-silapentane-5-sulfonate (DSS) sodium salt was used as internal standard for chemical shifts. The ^1H chemical shift assignments were achieved by sequential assignment procedures using gCOSY, TOCSY, and ROESY measurements.[60] TOCSY and ROESY spectra were acquired using watergate suppression. All experiments were performed by collecting 2048 points in f2 and 300-600 points in f1. TOCSY experiments employed a standard MLEV-17 spin lock sequence with a spin lock field of 7-8 KHz and mixing time of 100 ms. ROESY experiments used spin-locking fields of ~3 kHz's and mixing times of 150-250 ms. The 2D NMR spectra data were analyzed using the program Sparky.[61] Residue designations and chemical shift data are summarized in Table 2.7 and 2.8.

Table 2.6 Chemical shift data for peptide **2.3** in CD_3OH (10 ^oC).

	Residue	NH	^1H-α	^1H-β	^1H-γ	
1	Glu	8.449	4.187			
2	γ^4hAla	7.931	2.280, 1.996	1.483	3.889	CH_3=1.111
3	Ala	8.459	4.041			
4	Arg	8.624	4.122			
5	ACPC	7.735	2.700	4.179		CH_2=1.987, 1.650
6	Tyr	8.147	4.206			
7	Ala	8.130	4.185			
8	γ^4hAla	7.361	2.129, 2.251	1.635	3.843	CH_3=1.121
9	Gln	8.381	4.019			
10	Ala	8.735	4.175			
11	ACPC	7.754	2.668	4.256		CH_2=2.001, 1.662
12	Lys	8.072	4.151			

Table 2.7 Chemical shift data for peptide **2.3** in 90% H_2O/ 10% D_2O (10 °C).

	Residue	NH	^{1}H-α	^{1}H-β	^{1}H-γ	
1	Glu	8.413	4.143			
2	γ^{4}hAla	7.996	1.876, 2.293	1.644	3.790	CH_3=1.134
3	Ala	8.371	4.148			
4	Arg	8.457	4.154			
5	ACPC	7.788	2.632	4.168		CH_2=2.032, 1.934, 1.714, 1.564
6	Tyr	8.233	4.445			
7	Ala	8.113	4.185			
8	γ^{4}hAla	7.494	1.89, 2.303	1.661	3.776	CH_3=1.122
9	Gln	8.375	4.179			
10	Ala	8.513	4.178			
11	ACPC	7.874	2.655	4.248		CH_2=2.049, 1.759, 1.584
12	Lys	8.359	4.238			

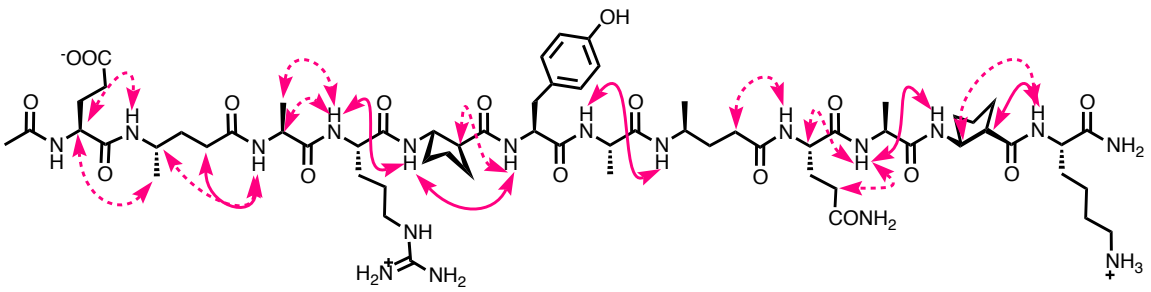

Figure 2.16 Sequential NOEs from α/β/γ-peptide **2.3** in CD_3OH at 10 °C. Medium (2.6~3.5 Å) and weak (3.6~5.5 Å) NOEs are shown as plain and dashed curves, respectively.

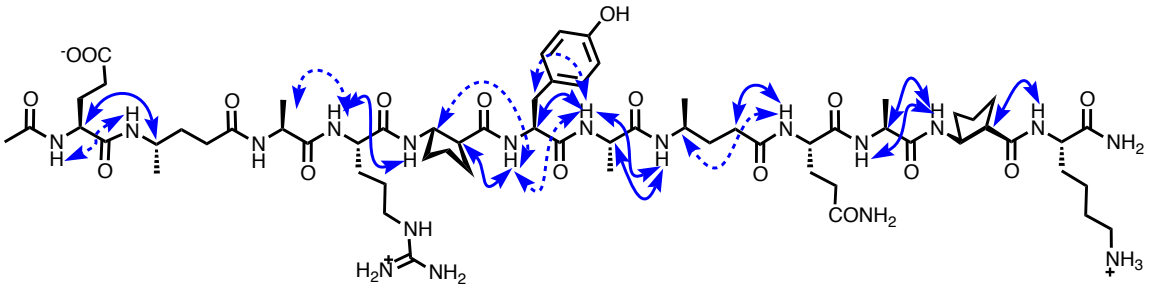

Figure 2.17 Sequential NOEs from α/β/γ-peptide **2.3** in 90% H_2O/ 10% D_2O at 10 °C. Medium (2.6~3.5 Å) and weak (3.6~5.5 Å) NOEs are shown as plain and dashed curves, respectively.

2.7.6 Peptide Crystallization and Diffraction Data Collection

(Mortenson, D. E. and Satyshur, K. A involved in collecting the diffraction data and solving the structures)

Crystallization experiments involving α + α/β/γ-peptides were carried out using the hanging-drop vapor diffusion method in 24-well Linbro-style plates (Hampton). For all crystallizations, 1 μL of a 10 mg/mL aqueous peptide stock solution was mixed with 1 μL of precipitant solution on a silanized glass slide and allowed to equilibrate over a well containing 700 μL of precipitant solution. Optimized crystals of peptide **2.6** were obtained from a precipitant solution containing 0.2 M NaCl, 0.1 M sodium acetate, pH 4.6 and 30% (v/v) 2-methyl-2,4-pentanediol (MPD). These crystals were cryoprotected by transferring to a precipitant solution supplemented with MPD (44% total v/v) before flash freezing in liquid nitrogen. For peptide **2.7**, optimized crystals were obtained from a precipitant solution containing 0.1 M sodium acetate, pH 4.6, and 8% v/v PEG 4000. Crystals of peptide **2.7** were cryoprotected by transferring to a precipitant solution supplemented with PEG4000 (24% total v/v) before flash freezing in liquid nitrogen.

Diffraction data were collected using synchrotron radiation (λ = 0.97872 Å; LS-CAT 21-ID-F) at 100 K. Data collected from crystals of peptides **2.6** and **2.7** were indexed, integrated and scaled using the XDS software package.[62] Five percent of reflections distributed randomly across resolution shells were flagged for calculation of R_{free} during model refinement.

Structures of peptides **2.6** and **2.7** were determined by molecular replacement in Phaser[63] using the structure of GCN4-pLI (PDB 1GCL)[35] as a starting model in both cases. Following structural solution, manual rebuilding of the models was carried out in Coot.[64] The monomers γ^4-homoalanine and Et-ACHA were built using the PRODRG server.[65] Refinement of both models was carried out *via* maximum likelihood methods in Refmac5[66] using anisotropic temperature factors and riding hydrogen atoms. Data processing and model refinement statistics for structures of peptides **2.6** and **2.7** are listed in Table 2.9.

Table 2.8 Data collection and refinement statistics.

	Peptide **2.6** (cyclic γ)	Peptide **2.7** (acyclic γ)
PDB accession code	4HJB	4HJD
Data Collection Temp. (K)	100	100
Beamline/Detector	21-ID-F	21-ID-F
Wavelength (Å)	0.97872	0.97872
Resolution range	46.29 – 1.25 (1.28 – 1.25)	17.62 – 1.70 (1.70 – 1.74)
Unique reflections	27036 (1056)	6350 (477)
Completeness (%)	89.1 (47.5)	98.3 (98.8)
R_{sym}	0.050 (0.324)	0.034 (0.346)
I/σ_I	28.8 (4.05)	23.4 (3.76)
Redundancy	11.3 (1.8)	3.7 (3.7)
Wilson B-factor (Å^2)	12.9	28.8
Space group	P2	C2
Unit cell parameters		
(a, b, c)	34.2, 46.3, 34.9	46.9, 51.5, 31.0
(α / β / γ)	90.0/ 91.3/ 90.0	90.0/ 128.9/ 90.0
Water content (%)	37.2	34.6
Refinement:		
# Non-H Atoms	1097	559
Resolution range (Å)	46.29 – 1.25 (1.28 – 1.25)	17.62 – 1.70 (1.74 – 1.70)
R(work)	0.139 (0.166)	0.251 (0.343)
R(free)	0.191 (0.222)	0.295 (0.322)
RMS bond length (Å)	0.025	0.005
RMS bond angle (°)	2.9	0.9
Coordinate ESU (Å)	0.04	0.11
Mean B Value (Å^2)	21.0	22.6

Table 2.9 H-H distances from the crystal structure of peptide **2.6** corresponding to NOEs recorded in solution-phase measurements. Distances from each chain and averaged values (Å) are shown.

Peptide **2.6**	Distance from crystal structure (Å)					
NOE type	residue #	A	B	C	D	avg
α-residue CαH(*i*) – α-residue NH(*i+2*)	20-23	3.7	3.4	3.4	3.4	3.5
β-residue CβH(*i*) - α-residue NH(*i+2*)	21-23	3.6	3.8	3.6	3.6	3.7
β-residue CβH(*i*) - γ-residue NH(*i+3*)	21-24	3.2	3.4	3.4	3.5	3.4
α-residue CαH(*i*) - α-residue CαH(*i+3*)	21-24	4.7	4.9	5.0	5.0	4.9
α-residue CαH(*i*) – α-residue NH(*i+3*)	22-25	4.1	4.0	4.1	4.0	4.1
α-residue CαH(*i*) – α-residue NH(*i+2*)	23-25	2.8	3.0	3.0	3.0	3.0
γ-residue CγH(*i*) – α-residue NH(*i+2*)	24-26	2.3	2.6	2.5	2.3	2.4
γ-residue CγH(*i*) - β-residue NH(*i+3*)	24-27	2.8	3.0	3.2	3.0	3.0

Table 2.10 H-H distances from the crystal structure of peptide **2.7** corresponding to NOEs recorded in solution-phase measurements. Distances from each chain and averaged values (Å) are shown.

Peptide **2.7**	Distance from crystal structure (Å)			
NOE type	residue #	A	B	avg
α-residue CαH(*i*) – α-residue NH(*i+3*)	14-17	3.7	3.8	3.8
β-residue CβH(*i*) - α-residue NH(*i+2*)	15-17	3.6	3.5	3.6
β-residue CβH(*i*) - γ-residue NH(*i+3*)	15-18	3.3	3.2	3.3
α-residue CαH(*i*) - γ-residue NH(*i+2*)	16-18	3.9	3.7	3.8
α-residue CαH(*i*) – α-residue NH(*i+3*)	16-19	4.2	4.2	4.2
α-residue CαH(*i*) – α-residue NH(*i+2*)	17-19	2.6	2.9	2.8
α-residue CαH(*i*) – α-residue NH(*i+3*)	17-20	3.7	4.1	3.9
γ-residue CγH(*i*) – α-residue NH(*i+2*)	18-20	2.7	2.2	2.5
γ-residue CγH(*i*) - β-residue NH(*i+3*)	18-21	2.7	3.1	3.3

Table 2.11 Backbone torsion angles (degrees) for the α/β/γ-peptides **2.6** and **2.7**.

	#	residue	ϕ	θ	ζ	ψ
Peptide **2.6**	21	β	-115.2	78.5		-100.1
avg(4)	24	γ	-135.5	45.9	56.9	-118.6
	27	β	-107.2	83.9		-78.6
Peptide **2.7**	15	β	-125.1	82.0		-103.7
avg(2)	18	γ	-132.9	38.9	64.7	-107.3
	21	β	-113.8	79.7		-109.4

Table 2.12 RMSD from peptide **2.6** to α-peptide GCN4-pLI.

	RMSD (Å)	Atoms used for alignments
Chain A	0.521	182
Chain B	0.578	167
Chain C	0.637	157
Chain D	0.528	174

Table 2.13 RMSD from peptide **2.7** to a-peptide GCN4-pLI.

	RMSD (Å)	Atoms used for alignment
Chain A	0.570	175
Chain B	0.726	180

Table 2.14 RMSD from peptides **2.6** and **2.7** to α-peptide GCN4-pLI for the αβααγα-hexad region.

	RMSD (Å)	Atoms used for alignments
2.6 chain A to GCN4-pLI	0.347	27
2.7 chain A to GCN4-pLI	0.507	25
2.7(13-19) to **2.6** (19-25)	0.264	41

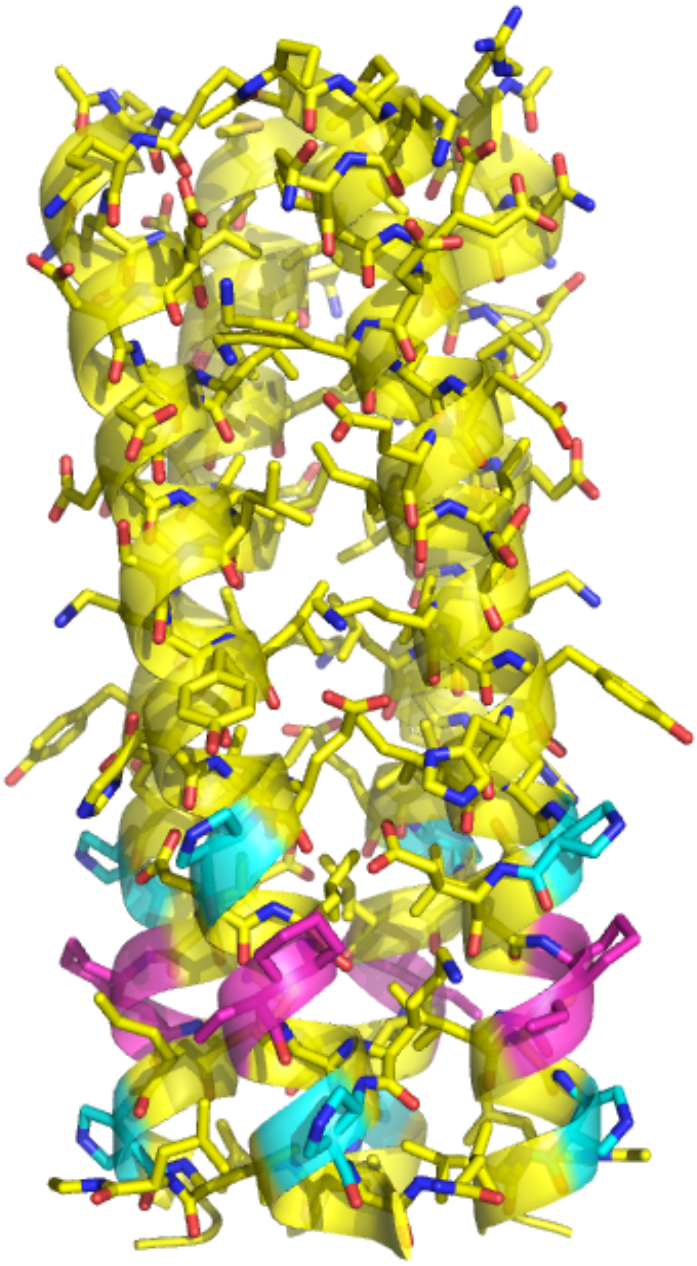

Figure 2.18 Four-helix bundle formed by peptide **2.6** as determined *via* x-ray crystallography (PDB 4HJB); β- and γ- residues are highlighted in cyan and purple, respectively. In these images the helical ribbons are based on the structure of GCN4-pLI itself (PDB 1GCL), but the sticks are from the new structures. This image is intended primarily to illustrate the positions of the β and γ -residues within the four-helix bundle.

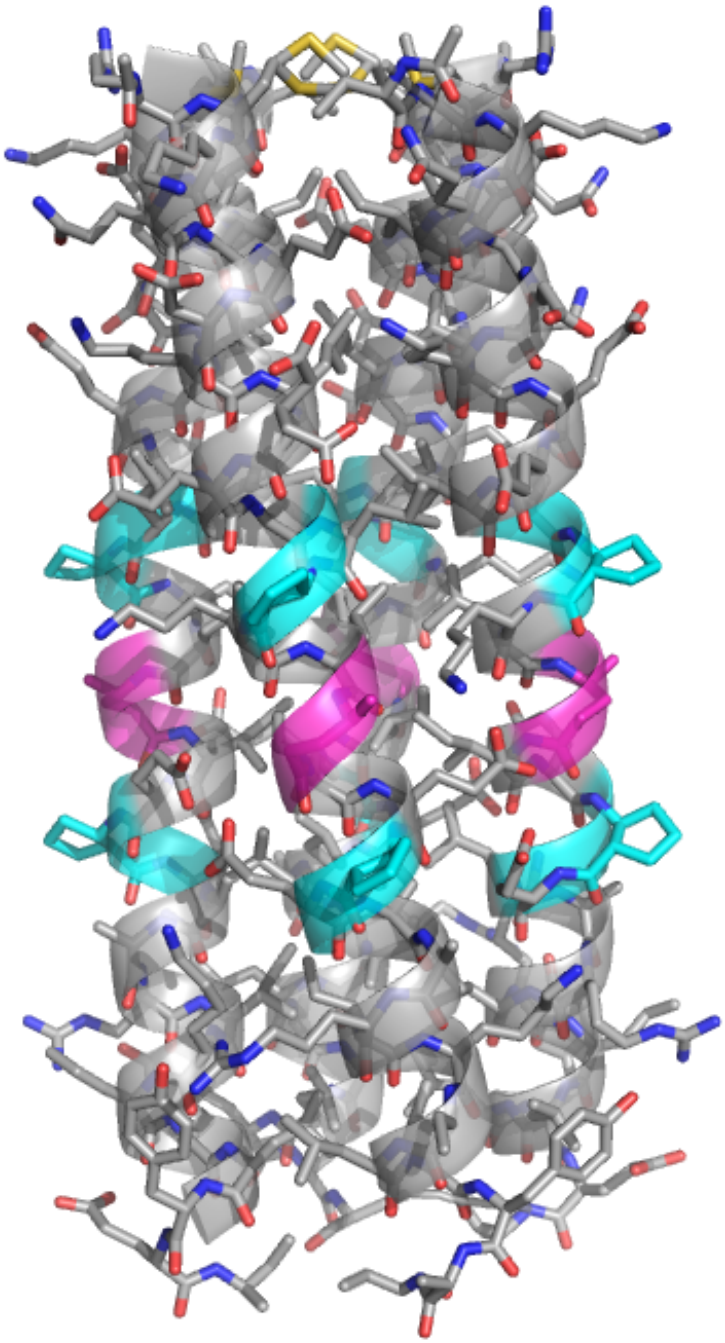

Figure 2.19 Four-helix bundle formed by peptide **2.7** as determined *via* x-ray crystallography (PDB 4HJD); β and γ -residues are highlighted in cyan and purple, respectively. In these images the helical ribbons are based on the structure of GCN4-pLI itself (PDB 1GCL), but the sticks are from the new structures. This image is intended primarily to illustrate the positions of the β and γ -residues within the four-helix bundle.

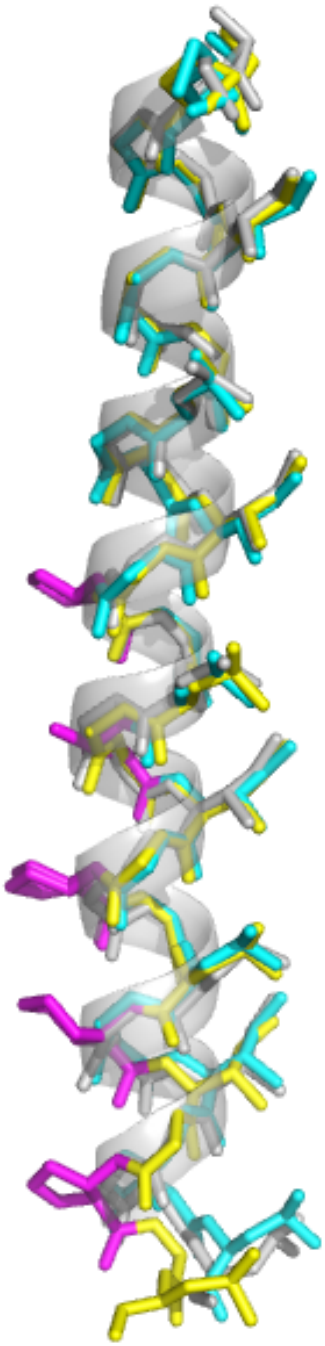

Figure 2.20 Overlaid structures of peptide **2.6** (yellow), **2.7** (cyan) and GCN4-pLI (gray). Structures are simplified for the clear view; hydrophobic core side chains and ring constraints are shown. Ring-constrained residues are highlighted in magenta.

Ac–RMKQIEDKLEEIL(X)KLγ⁴hAIE(X)ELARIKKLLYER–OH **2.7**

yhs2213A

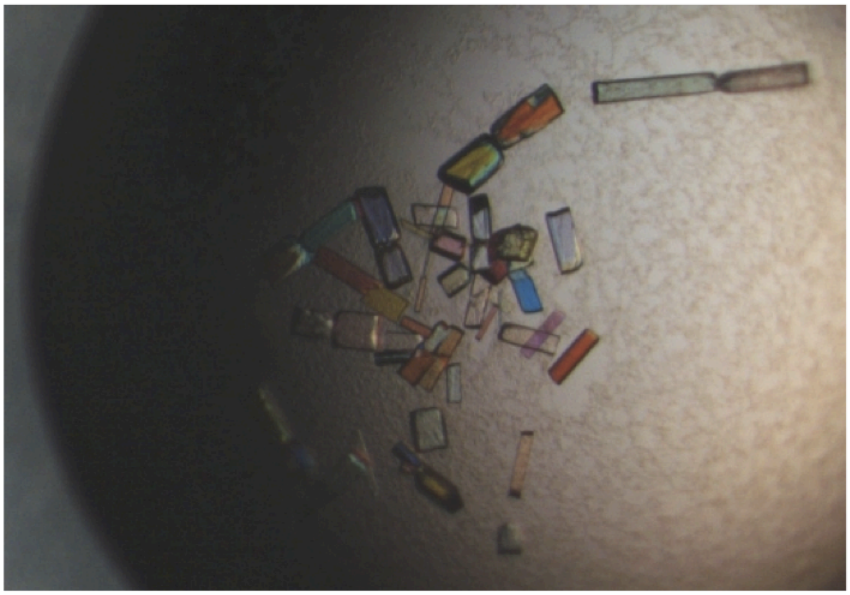

Figure 2.21 Crystal picture from peptide **2.7** under microscope, crystallized from the solution containing 0.1M Sodium acetate trihydrate pH 4.6, w/v PEG 4,000 and cryo-protected with PEG 4,000 up to about 24%.

Ac–RMKQIEDKLEEIL(Z)KLγ⁴hAIE(Z)ELγ⁴hAIK(Z)LLYER–OH **2.12**

yhs2223A

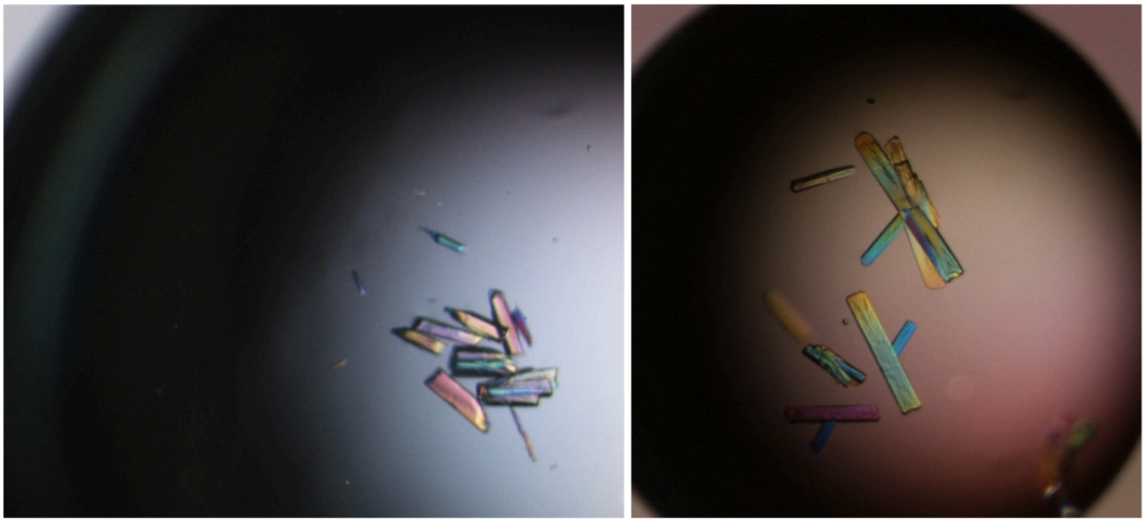

Figure 2.22 Crystal picture from peptide **2.12** under microscope, crystallized from the solution containing 0.12 M Sodium acetate trihydrate pH 4.6, 2.0 M sodium formate and cryo-protected with PEG 400 up to about 22%. However, these crystals only provided poor X-ray diffraction data.

Ac–RMKQIEDKLEEILZKL(γcyc)IEZEL(γcyc)IKZLLYER–OH **2.10**

yhs2213C

Figure 2.23 Crystal picture from peptide **2.10** under microscope, crystallized from the solution containing 0.2 M Sodium citrate tribasic dihydrate, 0.1 M Tris hydrochloride pH 8.5, and 30% PEG 400. However, we could not optimize the crystallization.

2.7.7 Torsion angles of different cyclic γ-residues predicted by computational analysis

To estimate what alternative types of γ-residue constraints might potentially lead to improved stability of the α-helix-like conformation available for α/β/γ-peptides, HF/6-31G* and then B3LYP/6-31G* levels of *ab initio* MO theory were initially applied for calculations using X-ray α/β/γ-structures (PDB 4HJB, 4HJD) as starting models. Potentially interesting γ-amino acids are those in which either the Cα-Cβ bond or the Cβ-Cγ bond is constrained by a cyclohexyl or a cyclopentyl ring with *cis*- or *trans*-configuration (Table 2.15).

Based on the backbone torsion angles of the most stable helices of α/β/γ-peptides calculated, γ-amino acids with a *cis*-cyclopentyl ring on the Cβ-Cγ bond, or with a *trans*-cyclopentyl ring on the Cα-Cβ bond showed promise in promoting an α-helix-like conformation in α/β/γ-peptides with similar torsion angles to that found in our crystal structures (Table 2.15). The γ-amino acid containing a *trans*-cyclopentyl ring on the Cα-Cβ bond has been synthesized and examined in α/γ-peptides by Dr. Giuliano, but the γ-residue yielded α/γ-peptides with flexible helical folding estimated by 2D NMR studies.[59]

Table 2.15 Backbone torsion angles of the most stable helices of α/β/γ-peptides at the B3LYP/6-31G* level of ab initio MO theory (prior to B3LYP/6-31G*, initial models were calculated by applying HF/6-31G*). Estimated θ and ζ angles close to those from the crystal structures are marked by red squares, and of those cyclopentyl ring constrained γ-residues chemical structures are shown below the table.

			ϕ	θ	ζ	ψ
Crystal structure						
6-ring	*cis*	EtACHA (4S, 3S, 2S)	-135	44	59	-119
		γ[4]hAla	-131	35	68	-108
B3LYP, 6-31G(d)						
6-ring	*cis*	EtACHA	-135	52	56	-120
		GABA	-126	51	59	-124
5-ring	*cis*	4S, 3S, 2S-Et	-128	44	60	-120
	cis	4S, 3S	-119	40	65	-127
	trans	4S, 3R	-129	61	49	-114
	cis	3R, 2S	-132	59	47	-112
	trans	3S, 2S	-123	43	76	-123

For the calculation, β= ACPC

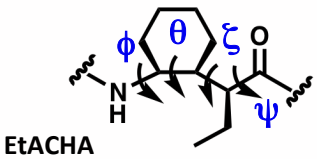

EtACHA

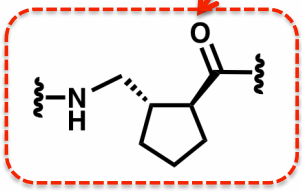

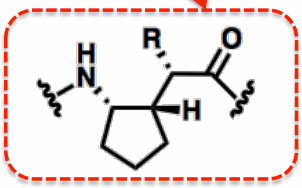

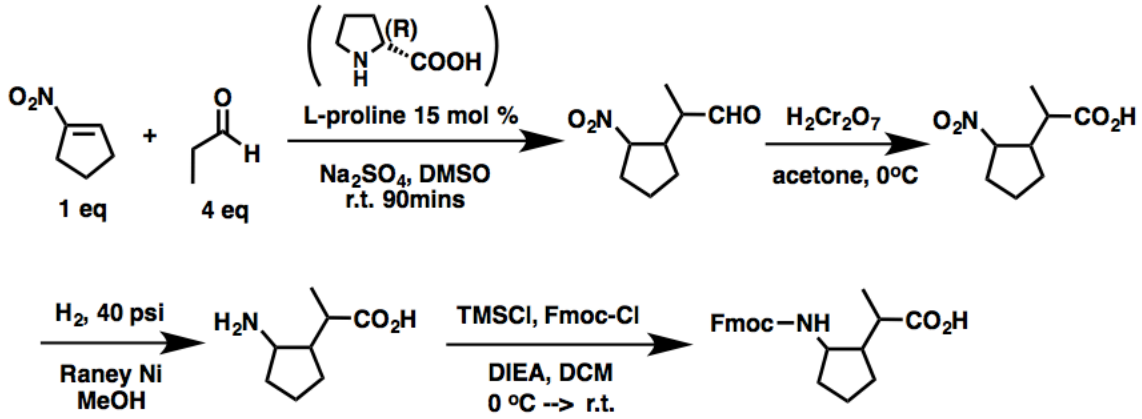

Figure 2.24 Scheme for synthesis of EtACPA

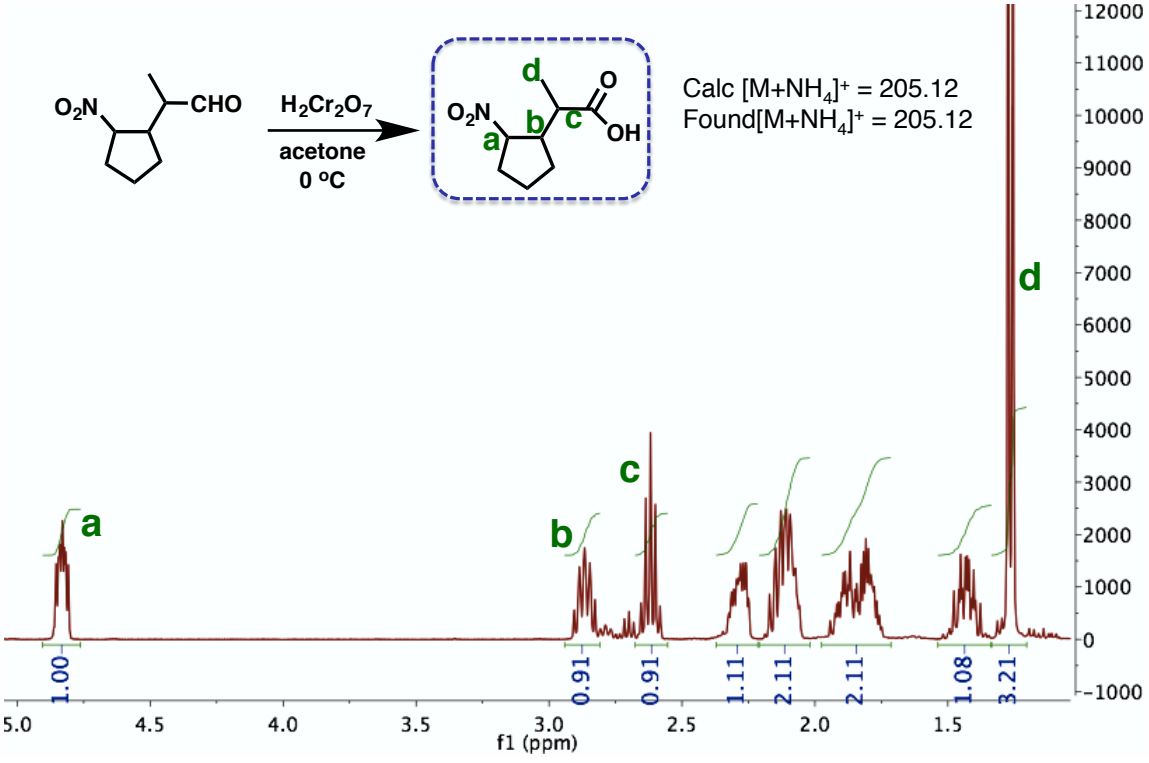

Figure 2.25 ^{1}H-NMR of oxidized intermediate, nitro-cyclopentaneacetic acid.

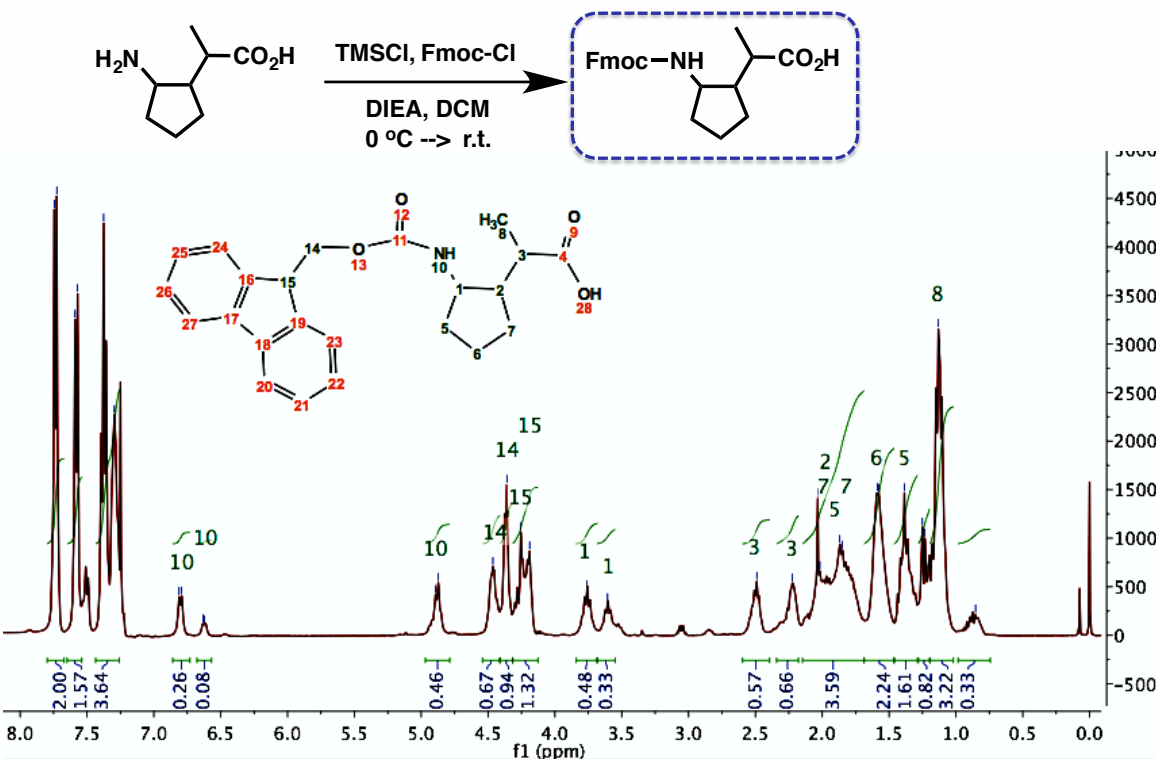

Figure 2.26 ^{1}H-NMR of Fmoc protected amino-cyclopentaneacetic acid.

2.8 References

(1) Arkin, M. R.; Wells, J. A. Small-molecule inhibitors of protein-protein interactions: Progressing towards the dream. *Nature Reviews Drug Discovery* **2004**, *3*, 301-317.

(2) Jochim, A. L.; Arora, P. S. Assessment of helical interfaces in protein-protein interactions. *Molecular Biosystems* **2009**, *5*, 924-926.

(3) Bullock, B. N.; Jochim, A. L.; Arora, P. S. Assessing Helical Protein Interfaces for Inhibitor Design. *Journal of the American Chemical Society* **2011**, *133*, 14220-14223.

(4) Azzarito, V.; Long, K.; Murphy, N. S.; Wilson, A. J. Inhibition of alpha-helix-mediated protein-protein interactions using designed molecules. *Nature Chemistry* **2013**, *5*, 161-173.

(5) Guichard, G.; Huc, I. Synthetic foldamers. *Chemical Communications* **2011**, *47*, 5933-5941.

(6) Goodman, C. M.; Choi, S.; Shandler, S.; DeGrado, W. F. Foldamers as versatile frameworks for the design and evolution of function. *Nature Chemical Biology* **2007**, *3*, 252-262.

(7) Schafmeister, C. E.; Brown, Z. Z.; Gupta, S. Shape-Programmable Macromolecules. *Accounts of Chemical Research* **2008**, *41*, 1387-1398.

(8) Yin, H.; Hamilton, A. D. Strategies for targeting protein-protein interactions with synthetic agents. *Angewandte Chemie-International Edition* **2005**, *44*, 4130-4163.

(9) Horne, W. S. Peptide and peptoid foldamers in medicinal chemistry. *Expert Opinion on Drug Discovery* **2011**, *6*, 1247-1262.

(10) Johnson, L. M.; Gellman, S. H.: alpha-Helix Mimicry with alpha/beta-Peptides. In *Methods in Protein Design*; Keating, A. E., Ed.; Methods in Enzymology, 2013; Vol. 523; pp 407-429.

(11) Horne, W. S.; Johnson, L. M.; Ketas, T. J.; Klasse, P. J.; Lu, M.; Moore, J. P.; Gellman, S. H. Structural and biological mimicry of protein surface recognition by alpha/beta-peptide foldamers. *Proceedings of the National Academy of Sciences of the United States of America* **2009**, *106*, 14751-14756.

(12) Johnson, L. M.; Mortenson, D. E.; Yun, H. G.; Horne, W. S.; Ketas, T. J.; Lu, M.; Moore, J. P.; Gellman, S. H. Enhancement of alpha-Helix Mimicry by an alpha/beta-

Peptide Foldamer via Incorporation of a Dense Ionic Side-Chain Array. *Journal of the American Chemical Society* **2012**, *134*, 7317-7320.

(13) Boersma, M. D.; Haase, H. S.; Peterson-Kaufman, K. J.; Lee, E. F.; Clarke, O. B.; Colman, P. M.; Smith, B. J.; Horne, W. S.; Fairlie, W. D.; Gellman, S. H. Evaluation of Diverse alpha/beta-Backbone Patterns for Functional alpha-Helix Mimicry: Analogues of the Bim BH3 Domain. *Journal of the American Chemical Society* **2012**, *134*, 315-323.

(14) Lee, E. F.; Smith, B. J.; Horne, W. S.; Mayer, K. N.; Evangelista, M.; Colman, P. M.; Gellman, S. H.; Fairlie, W. D. Structural Basis of Bcl-x(L) Recognition by a BH3-Mimetic alpha/beta-Peptide Generated by Sequence-Based Design. *Chembiochem* **2011**, *12*, 2025-2032.

(15) Horne, W. S.; Boersma, M. D.; Windsor, M. A.; Gellman, S. H. Sequence-based design of alpha/beta-peptide foldamers that mimic BH3 domains. *Angewandte Chemie-International Edition* **2008**, *47*, 2853-2856.

(16) Price, J. L.; Hadley, E. B.; Steinkruger, J. D.; Gellman, S. H. Detection and Analysis of Chimeric Tertiary Structures by Backbone Thioester Exchange: Packing of an alpha Helix against an alpha/beta-Peptide Helix. *Angewandte Chemie-International Edition* **2010**, *49*, 368-371.

(17) Sawada, T.; Gellman, S. H. Structural Mimicry of the alpha-Helix in Aqueous Solution with an Isoatomic alpha/beta/gamma-Peptide Backbone. *Journal of the American Chemical Society* **2011**, *133*, 7336-7339.

(18) Hanessian, S.; Luo, X. H.; Schaum, R.; Michnick, S. Design of secondary structures in unnatural peptides: Stable helical gamma-tetra-, hexa-, and octapeptides and consequences of alpha-substitution. *Journal of the American Chemical Society* **1998**, *120*, 8569-8570.

(19) Hintermann, T.; Gademann, K.; Jaun, B.; Seebach, D. gamma-peptides forming more stable secondary structures than alpha-peptides: Synthesis and helical NMR-solution structure of the gamma-hexapeptide analog of H-(Val-Ala-Leu)(2)-OH. *Helvetica Chimica Acta* **1998**, *81*, 983-1002.

(20) Seebach, D.; Brenner, M.; Rueping, M.; Schweizer, B.; Jaun, B. Preparation and determination of X-ray-crystal and NMR-solution structures of gamma(2,3,4)-peptides. *Chemical Communications* **2001**, 207-208.

(21) Baldauf, C.; Gunther, R.; Hofmann, H. J. Helix formation in alpha,gamma- and beta,gamma-hybrid peptides: Theoretical insights into mimicry of alpha- and beta-Peptides. *Journal of Organic Chemistry* **2006**, *71*, 1200-1208.

(22) Claudon, P.; Violette, A.; Lamour, K.; Decossas, M.; Fournel, S.; Heurtault, B.; Godet, J.; Mely, Y.; Jamart-Gregoire, B.; Averlant-Petit, M.-C.; Briand, J.-P.; Duportail, G.; Monteil, H.; Guichard, G. Consequences of Isostructural Main-Chain Modifications for the Design of Antimicrobial Foldamers: Helical Mimics of Host-Defense Peptides Based on a Heterogeneous Amide/Urea Backbone. *Angewandte Chemie-International Edition* **2010**, *49*, 333-336.

(23) Karle, I. L.; Pramanik, A.; Banerjee, A.; Bhattacharjya, S.; Balaram, P. omega-amino acids in peptide design. Crystal structures and solution conformations of peptide helices containing a beta-alanyl-gamma-aminobutyryl segment. *Journal of the American Chemical Society* **1997**, *119*, 9087-9095.

(24) Araghi, R. R.; Jaeckel, C.; Coelfen, H.; Salwiczek, M.; Voelkel, A.; Wagner, S. C.; Wieczorek, S.; Baldauf, C.; Koksch, B. A beta/gamma Motif to Mimic alpha-Helical Turns in Proteins. *Chembiochem* **2010**, *11*, 335-339.

(25) Hagihara, M.; Anthony, N. J.; Stout, T. J.; Clardy, J.; Schreiber, S. L. Vinylogous Polypeptides- An Alternative Peptide Backbone. *Journal of the American Chemical Society* **1992**, *114*, 6568-6570.

(26) Baldauf, C.; Gunther, R.; Hofmann, H. J. Helix formation and folding in gamma-peptides and their vinylogues. *Helvetica Chimica Acta* **2003**, *86*, 2573-2588.

(27) Farrera-Sinfreu, J.; Zaccaro, L.; Vidal, D.; Salvatella, X.; Giralt, E.; Pons, M.; Albericio, F.; Royo, M. A new class of foldamers based on cis-gamma-amino-L-proline. *Journal of the American Chemical Society* **2004**, *126*, 6048-6057.

(28) Sharma, G. V. M.; Jadhav, V. B.; Ramakrishna, K. V. S.; Jayaprakash, P.; Narsimulu, K.; Subash, V.; Kunwar, A. C. 12/10- and 11/13-mixed helices in alpha/gamma- and beta/gamma-hybrid peptides containing C-linked carbo-gamma-

amino acids with alternating alpha- and beta-amino acids. *Journal of the American Chemical Society* **2006**, *128*, 14657-14668.

(29) Khurram, M.; Qureshi, N.; Smith, M. D. Parallel sheet structure in cyclopropane gamma-peptides stabilized by C-H center dot center dot center dot O hydrogen bonds. *Chemical Communications* **2006**, 5006-5008.

(30) Baruah, P. K.; Sreedevi, N. K.; Gonnade, R.; Ravindranathan, S.; Damodaran, K.; Hofmann, H.-J.; Sanjayan, G. J. Enforcing periodic secondary structures in hybrid peptides: A novel hybrid foldamer containing periodic gamma-turn motifs. *Journal of Organic Chemistry* **2007**, *72*, 636-639.

(31) Sharma, G. V. M.; Chandramouli, N.; Choudhary, M.; Nagendar, P.; Ramakrishna, K. V. S.; Kunwar, A. C.; Schramm, P.; Hofmann, H.-J. Hybrid Helices: Motifs for Secondary Structure Scaffolds in Foldamers. *Journal of the American Chemical Society* **2009**, *131*, 17335-17344.

(32) Horne, W. S.; Price, J. L.; Gellman, S. H. Interplay among side chain sequence, backbone composition, and residue rigidification in polypeptide folding and assembly. *Proceedings of the National Academy of Sciences of the United States of America* **2008**, *105*, 9151-9156.

(33) Schmitt, M. A.; Choi, S. H.; Guzei, I. A.; Gellman, S. H. Residue requirements for helical folding in short alpha/beta-peptides: Crystallographic characterization of the 11-helix in an optimized sequence. *Journal of the American Chemical Society* **2005**, *127*, 13130-13131.

(34) Roccatano, D.; Colombo, G.; Fioroni, M.; Mark, A. E. Mechanism by which 2,2,2-trifluoroethanol/water mixtures stabilize secondary-structure formation in peptides: A molecular dynamics study. *Proceedings of the National Academy of Sciences of the United States of America* **2002**, *99*, 12179-12184.

(35) Harbury, P. B.; Zhang, T.; Kim, P. S.; Alber, T. A Switch Between 2-Stranded, 3-Stranded and 4-Stranded Coiled coils in GCN4 Leucine-Zipper Mutants. *Science* **1993**, *262*, 1401-1407.

(36) Oshea, E. K.; Klemm, J. D.; Kim, P. S.; Alber, T. X-Ray Structure of the GCN4 Leucine Zipper, a 2-Stranded, Parallel Coiled coil. *Science* **1991**, *254*, 539-544.

(37) Oshaben, K. M.; Salari, R.; McCaslin, D. R.; Chong, L. T.; Horne, W. S. The Native GCN4 Leucine-Zipper Domain Does Not Uniquely Specify a Dimeric Oligomerization State. *Biochemistry* **2012**, *51*, 9581-9591.

(38) Price, J. L.; Horne, W. S.; Gellman, S. H. Structural Consequences of beta-Amino Acid Preorganization in a Self-Assembling alpha/beta-Peptide: Fundamental Studies of Foldameric Helix Bundles. *Journal of the American Chemical Society* **2010**, *132*, 12378-12387.

(39) Horne, W. S.; Price, J. L.; Keck, J. L.; Gellman, S. H. Helix bundle quaternary structure from alpha/beta-peptide foldamers. *Journal of the American Chemical Society* **2007**, *129*, 4178.

(40) Barlow, D. J.; Thornton, J. M. HELIX GEOMETRY IN PROTEINS. *Journal of Molecular Biology* **1988**, *201*, 601-619.

(41) Guo, L.; Zhang, W.; Reidenbach, A. G.; Giuliano, M. W.; Guzei, I. A.; Spencer, L. C.; Gellman, S. H. Characteristic Structural Parameters for the gamma-Peptide 14-Helix: Importance of Subunit Preorganization. *Angewandte Chemie-International Edition* **2011**, *50*, 5843-5846.

(42) Guo, L.; Almeida, A. M.; Zhang, W.; Reidenbach, A. G.; Choi, S. H.; Guzei, I. A.; Gellman, S. H. Helix Formation in Preorganized beta/gamma-Peptide Foldamers: Hydrogen-Bond Analogy to the alpha-Helix without alpha-Amino Acid Residues. *Journal of the American Chemical Society* **2010**, *132*, 7868.

(43) Guo, L.; Chi, Y.; Almeida, A. M.; Guzei, I. A.; Parker, B. K.; Gellman, S. H. Stereospecific Synthesis of Conformationally Constrained gamma-Amino Acids: New Foldamer Building Blocks That Support Helical Secondary Structure. *Journal of the American Chemical Society* **2009**, *131*, 16018.

(44) Basuroy, K.; Dinesh, B.; Shamala, N.; Balaram, P. Structural Characterization of Backbone-Expanded Helices in Hybrid Peptides: (alpha gamma)(n) and (alpha beta)(n) Sequences with Unconstrained beta and gamma Homologues of L-Val. *Angewandte Chemie-International Edition* **2012**, *51*, 8736-8739.

(45) Basuroy, K.; Dinesh, B.; Shamala, N.; Balaram, P. Promotion of Folding in Hybrid Peptides through Unconstrained gamma Residues: Structural Characterization of

Helices in (alpha gamma gamma)(n) and (alpha gamma alpha)(n) Sequences. *Angewandte Chemie-International Edition* **2013**, *52*, 3136-3139.

(46) Dinesh, B.; Basuroy, K.; Shamala, N.; Balaram, P. Structural characterization of folded pentapeptides containing centrally positioned beta(R)Val, gamma(R)Val and gamma(S)Val residues. *Tetrahedron* **2012**, *68*, 4374-4380.

(47) Bandyopadhyay, A.; Jadhav, S. V.; Gopi, H. N. alpha/gamma(4)-Hybrid peptide helices: synthesis, crystal conformations and analogy with the alpha-helix. *Chemical Communications* **2012**, *48*, 7170-7172.

(48) Jadhav, S. V.; Bandyopadhyay, A.; Gopi, H. N. Protein secondary structure mimetics: crystal conformations of alpha/gamma(4)-hybrid peptide 12-helices with proteinogenic side chains and their analogy with alpha- and beta-peptide helices. *Organic & Biomolecular Chemistry* **2013**, *11*, 509-514.

(49) Jadhav, S. V.; Misra, R.; Singh, S. K.; Gopi, H. N. Efficient Access to Enantiopure gamma(4)-Amino Acids with Proteinogenic Side-Chains and Structural Investigation of gamma(4)-Asn and gamma(4)-Ser in Hybrid Peptide Helices. *Chemistry-a European Journal* **2013**, *19*, 16256-16262.

(50) Stevenson, B.; Lewis, W.; Dowden, J. Expedient Route to an Amine Precursor of Halichlorine and Pinnaic Acid from Nitrocyclopent-1-ene. *Synlett* **2010**, 672-674.

(51) Seebach, D.; Overhand, M.; Kuhnle, F. N. M.; Martinoni, B.; Oberer, L.; Hommel, U.; Widmer, H. beta-peptides: Synthesis by Arndt-Eistert homologation with concomitant peptide coupling. Structure determination by NMR and CD spectroscopy and by X-ray crystallography. Helical secondary structure of a beta-hexapeptide in solution and its stability towards pepsin. *Helvetica Chimica Acta* **1996**, *79*, 913-941.

(52) Seebach, D.; Ciceri, P. E.; Overhand, M.; Jaun, B.; Rigo, D.; Oberer, L.; Hommel, U.; Amstutz, R.; Widmer, H. Probing the helical secondary structure of short-chain beta-peptides. *Helvetica Chimica Acta* **1996**, *79*, 2043-2066.

(53) Daniels, D. S.; Petersson, E. J.; Qiu, J. X.; Schepartz, A. High-resolution structure of a beta-peptide bundle. *Journal of the American Chemical Society* **2007**, *129*, 1532.

(54) Cheng, R. P.; Gellman, S. H.; DeGrado, W. F. beta-peptides: From structure to function. *Chemical Reviews* **2001**, *101*, 3219-3232.

(55) Appella, D. H.; Barchi, J. J.; Durell, S. R.; Gellman, S. H. Formation of short, stable helices in aqueous solution by beta-amino acid hexamers. *Journal of the American Chemical Society* **1999**, *121*, 2309-2310.

(56) LePlae, P. R.; Fisk, J. D.; Porter, E. A.; Weisblum, B.; Gellman, S. H. Tolerance of acyclic residues in the beta-peptide 12-helix: Access to diverse side-chain arrays for biological applications. *Journal of the American Chemical Society* **2002**, *124*, 6820-6821.

(57) Raguse, T. L.; Lai, J. R.; Gellman, S. H. Environment-independent 14-helix formation in short beta-peptides: Striking a balance between shape control and functional diversity. *Journal of the American Chemical Society* **2003**, *125*, 5592-5593.

(58) LePlae, P. R.; Umezawa, N.; Lee, H. S.; Gellman, S. H. An efficient route to either enantiomer of trans-2-aminocyclopentanecarboxylic acid. *Journal of Organic Chemistry* **2001**, *66*, 5629-5632.

(59) Giuliano, M. W.; Maynard, S. J.; Almeida, A. M.; Reidenbach, A. G.; Guo, L.; Ulrich, E. C.; Guzei, I. A.; Gellman, S. H. Evaluation of a Cyclopentane-Based gamma-Amino Acid for the Ability to Promote alpha/gamma-Peptide Secondary Structure. *Journal of Organic Chemistry* **2013**, *78*, 12351.

(60) K. Wüthrich, *NMR of Proteins and Nucleic Acids*, Wiley-Interscience, New York, **1986**.

(61) T. D. Goddard, D. G. Kneller, Sparky 3, University of California, San Francisco.

(62) Kabsch, W. *Acta Cryst.* **2010**, *D66*, 125.

(63) McCoy, A. J.; Grosse-Kunstleve, R. W.; Adams, P. D.; Winn, M. D.; Storoni, L. C.; Read, R. J. *J. Appl. Cryst.* **2007**, *40*, 658.

(64) Emsley, P.; Cowtan, K. *Acta Cryst.* **2004**, *D60*, 2126.

(65) Schüttelkopf, A. W.; van Aalten, D. M. F., *Acta Crystallogr.* **2004**, *D60*, 1355.

(66) Murshudov, G. N.; Vagin, A. A.; Dodson, E. J. *Acta Cryst.* **1997**, *D53*, 240.

Chapter 3. Helical α/β/γ-Peptides: Exploration of Achiral/Acyclic γ-Residues and Different Patterns

3.1 Introduction

Previously, 12-mer α/β/γ-peptides were examined with an αγααβα hexad backbone pattern (Figure 3.1).[1,2] α/β/γ-Peptide **3.1A** is maximally pre-organized in that both β- and γ-residues are ring-constrained, and adopted an α-helix-like conformation in water according to CD and 2D NMR studies. Surprisingly, α/β/γ-peptide **3.1**, without ring-constraints on the γ-residues also showed substantial helicity in water, which is a challenging environment compared to organic solvents in terms of peptidic secondary structure formation. However, the helical conformation of **3.1** was not as highly populated as that of **3.1A** (Figure 3.1).[1,2] These surprising results suggest that ring-constraints on γ-residues might not be essential for helical stability of α/β/γ-peptides, and that γ^4-residues have substantial intrinsic tendencies to adopt helical secondary structure.

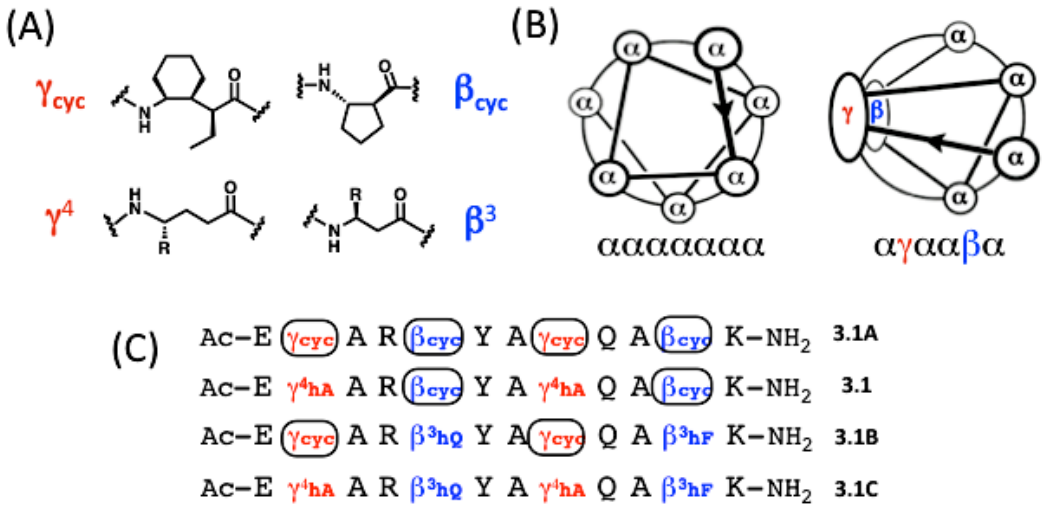

Figure 3.1 (A) Structures of cyclic- and acyclic β- and γ-residues (B) Helical wheel diagrams for the αααααααα heptad and the αγααβα hexad (C) Sequences of α/β/γ-peptides **3.1A**, **3.1**, **3.1B** and **3.1C**. β- and γ- residues are highlighted in blue and red, respectively. Ring constrained residues are marked by circles.

The importance of γ residue substitution pattern of α/β/γ-peptide helicity was initially studied using EtACHA and γ^{4}hAla within an αγααβα hexad pattern. We want to deepen our understanding of the residue-structure relationship in helical α/β/γ-peptides, especially to understand the impact of acyclic γ-residue identities on helicity. Herein, α/β/γ-peptides containing achiral and acyclic γ-amino acids have been investigated. γhGly (also known as γ-aminobutyric acid, GABA) and γ^{4}hAib (*geminal* dimethyl substitution at the γ-carbon) have been examined in 12-mer α/β/γ-peptides.[2] Further, we have investigated the effect of varying α–β–γ backbone patterns on α/β/γ-peptide helical propensities.

3.2 Exploration of achiral and acyclic γ-amino acid in an αγααβα hexad

3.2.1 Peptide design

In this chapter, we focused on acyclic and achiral residues, GABA and γ^{4}hAib, which are analogous to the α-amino acids glycine (Gly) and 2-aminoisobutyric acid (Aib), respectively. GABA and γ^{4}hAib are particularly interesting because the α-residue Gly destabilizes α–helical folding due to the flexibility that comes from a lack of sidechain,[3] whereas the α residue Aib is a strong promoter of helical folding because of its geminal dimethyl substitution[4]. GABA and γ^{4}hAib were incorporated into 12-mer α/β/γ-peptides, to enable comparison with previous studies (Figure 3.2A). α/β/γ-Peptides containing GABA (peptide **3.1D**) and γ^{4}hAib (peptide **3.1E**) were prepared by SPPS, and their conformational behavior was investigated by CD and 2D-NMR.

(A)

Ac–E γ^4hA A R β_{cyc} Y A γ^4hA Q A β_{cyc} K–NH_2 **3.1**

Ac–E GABA A R β_{cyc} Y A GABA Q A β_{cyc} K–NH_2 **3.1D**

Ac–E γ^4hAib A R β_{cyc} Y A γ^4hAib Q A β_{cyc} K–NH_2 **3.1E**

(B)

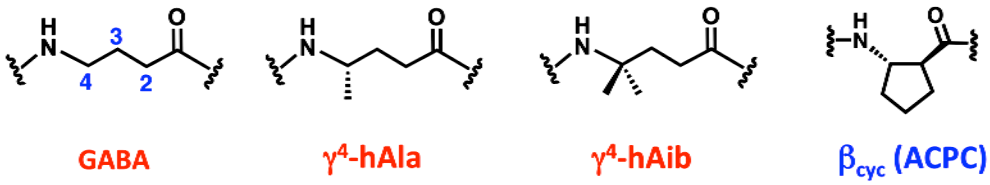

GABA γ^4-hAla γ^4-hAib β_{cyc} (ACPC)

Figure 3.2 (A) Sequences of α/β/γ-peptides **3.1** (γ= γ^4hAla), **3.1D** (γ= γhGly), and **3.1E** (γ= γ^4hAib). (B) Structures of γ- and β- amino acids.

3.2.2 Circular Dichroism and 2D-NMR experiments

Conformations of **3.1D** (γ=GABA) and **3.1E** (γ=γ^4hAib) were initially examined by circular dichroism in water and 60% TFE/water solution. The CD signature of **3.1** (γ=γ^4hAla) is a benchmark that indicates a helical population, which was previously characterized by 2D NMR, and CD spectra of **3.1C** (γ- and β- residues are acyclic) is a negative control, which indicates a lack of structure.[2] The CD signals presented by **3.1D** and **3.1E** in water and 60% TFE were not strong enough to conclude that these peptides significantly populate a helical conformation. The overall intensities of the CD curves of **3.1D** and **3.1E** were between those of **3.1** and **3.1C**, suggesting that **3.1D** and **3.1E** might be slightly helical in aqueous buffer (Figure 3.3A).

Ac–E γ⁴hA A R (βcyc) Y A γ⁴hA Q A (βcyc) K–NH_2 **3.1**

Ac–E γ⁴hA A R β³hQ Y A γ⁴hA Q A β³hF K–NH_2 **3.1C**

Ac–E GABA A R (βcyc) Y A GABA Q A (βcyc) K–NH_2 **3.1D**

Ac–E γ⁴hAib A R (βcyc) Y A γ⁴hAib Q A (βcyc) K–NH_2 **3.1E**

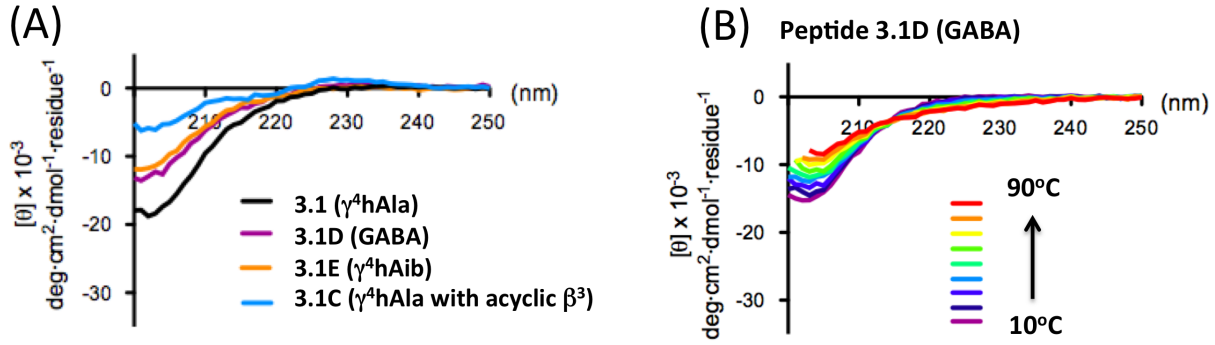

Figure 3.3 (A) Circular dichroism spectra of α/β/γ-peptides **3.1**, **3.1C**, **3.1D** and **3.1E** measured in PBS buffer pH 7.5, 20°C. (B) CD data for α/β/γ-peptide **3.1D** (γ = γhGly) measured in 50% MeOH/50% H_2O at varied temperature from 10 °C to 90 °C. Peptide concentration is 0.1 mM for all spectra.

Because the CD signals of **3.1D** and **3.1E** were very similar to each other, we chose **3.1D** for further study. Water is a very challenging environment for peptide folding.[5] Helix formation involves intramolecular hydrogen bonding from residues in i,i+3 and i,i+4 sequence relationships[6], and in an aqueous environment, these hydrogen bonds must compete with hydrogen bonding to water molecules. Addition of an organic co-solvent, such as TFE or methanol, encourages formation of internally H-bonded peptide secondary structure.[7] To encourage helical folding of **3.1D**, we used 50% methanol/water solution for CD measurements (Figure 3.3B). In 50% methanol, the CD signature of **3.1D** showed a slightly increased intensity relative to pure water. When the temperature was varied from 10°C to 90°C in 50% methanol/water, the CD intensity decreased as the temperature increased, indicating that **3.1D** becomes unfolded at

higher temperatures (Figure 3.3B). This thermal denaturation result indirectly suggests that **3.1D** might be partially structured in PBS buffer, because the CD intensity in PBS buffer lies between the CD intensities observed at 10°C and 90°C in 50% methanol/water.

The CD data for **3.1D** in 50% methanol cannot provide decisive insight on helical folding of **3.1D**. To further probe the conformation of **3.1D** in 50% methanol, we performed 2D-NMR experiments. We used 100% methanol (CD_3OH) for the 2D-NMR solvent, which is expected to induce a greater helical population than 50% methanol/water. Several critical non-adjacent NOEs indicative of helical folding were observed between residues in i,i+2 and i,i+3 relationships (Figure 3.4).

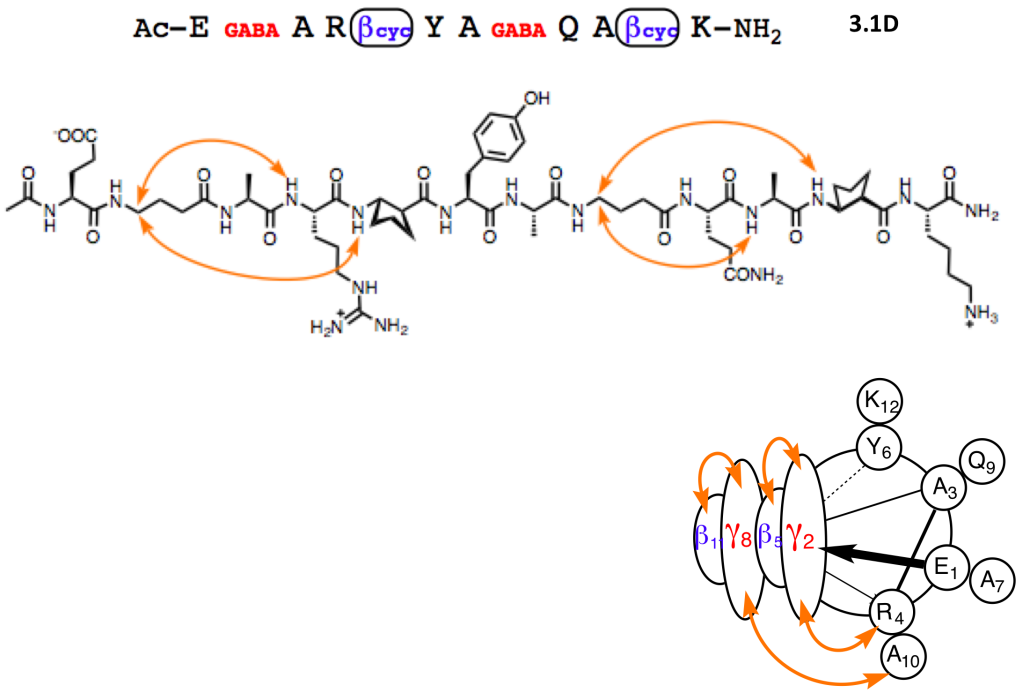

Figure 3.4 NOEs observed between non-adjacent residues for α/β/γ-peptide **3.1D**. Peptide concentration is 8 mM in CD_3OH at 10 °C. Medium intensity NOEs are shown as curved arrows on the peptide structure and on the helical wheel diagram.

Overall, these results indicate that either removing the methyl side chain of γ^4hAla (→ GABA) or adding another methyl at C4 (→γ^4hAib) causes a decline in helical propensity. The findings for γ^4hAib contrast with the known behavior of Aib, which is a strong promoter of α-peptide helicity.[4] The retention of a low level of helicity for **3.1D**, which contains highly flexible "glycine-like" γ residues, is intriguing, given the low α-helical propensity of Gly itself.[3]

3.3 Exploration of different substitution patterns in α/β/γ-peptides

3.3.1 Peptide design

The α/β/γ-peptide family is potentially very large, with many possible backbone combinations of α-, β-, and γ- residues. Among the possible patterns, the αγααβα hexad has been studied previously.[1] 2D-NMR and X-ray crystallographic results clearly showed that the αγααβα hexad pattern aligns β- and γ-residues along one face of the α/β/γ-helix, allowing α-residues displayed at the other face to interact with helical interfaces (Figure 3.5).[2] However, studies of helical α/β peptidomimetics have found that non-natural β-residues with side chains also could participate favorably in target binding.[8,9] Because various acyclic γ[4]-amino acids analogous to α-amino acids containing side chains are available, an investigation of different α/β/γ-backbone combinations is necessary for the future development of function-based α/β/γ peptidomimetics.

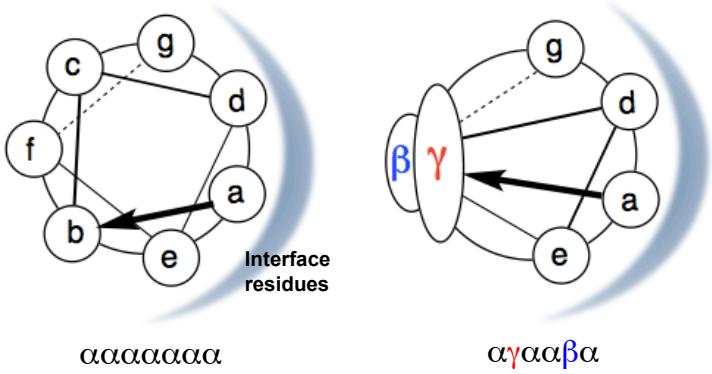

Figure 3.5 Helical wheel diagrams of the α-helix, and α/β/γ-helix in αγααβα hexads. Shadowed area indicates a hypothetical interface with a partner protein. In each case this surface is dominated by α residues.

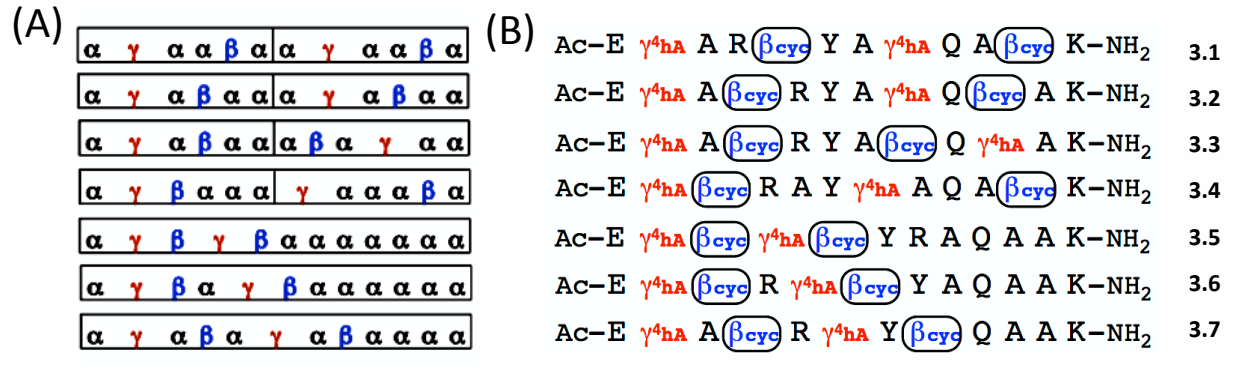

Figure 3.6 (A) Representatives of different α/β/γ-backbone combination of 12-mer α/β/γ-peptide (B) Sequences of α/β/γ-peptides **3.1**-**3.7** based on backbone patterns shown in (A).

12-mer α/β/γ-peptide **3.1**, with two hexad repeats (about four helical turns), was chosen as the parent peptide for investigating the effect of backbone pattern variation on the helicity of α/β/γ-peptides (Figure 3.6). The number of arrangements with eight α-amino acids, two β-amino acids, and two γ-amino acids in 12 positions is nearly 3000 (i.e., 12!/(2! x 2! x 8!) = 2970). This number is too great to permit study of all possible patterns. Seven different isomeric peptides, **3.1**-**3.7**, were selected. Peptide **3.1** was previously reported to be helical (Figure 3.6B).[2] Peptide **3.2** has one fewer α residue between γ and β in the hexad repeat compared to peptide **3.1**. Peptide **3.3** was designed by inverting positions of β and γ in the C-terminal hexad relative to peptide **3.2**. Locations of β and γ residues are scrambled in peptide **3.4**. Design of peptides **3.5**-**3.7** begins from (α/β/γ+α)-chimeric peptide **3.5**. Peptides **3.6** and **3.7** have different numbers of α-residues between β- and γ-residues relative to peptide **3.5** (Figure 3.6). Since acyclic γ^4-residues have been shown to support helical structure of α/β/γ-peptides[2], we prepared 7 different α/β/γ-peptides using acyclic γ- with cyclic β-amino

acids (Figure 3.6B). The use of γ^4hAla facilitates the preparation of a series of $\alpha/\beta/\gamma$-peptides because γ^4hAla is more successfully coupled onto growing peptides during solid phase peptide synthesis compared to six-membered-ring constrained γ-amino acid EtACHA.[1,2] This difference presumably reflects differences in steric hindrance.

3.3.2 Circular dichroism

The conformational behavior of the seven $\alpha/\beta/\gamma$-peptides was evaluated by CD in PBS buffer and in 60% trifluoroethanol (TFE)/40% PBS buffer solution at neutral pH (Figure 3.7). CD spectra of **3.1**-**3.7** measured in 60% TFE presented minima around 203-205 nm with strong intensities, indicative of helical structure for an $\alpha/\beta/\gamma$-peptide.[1,2] In water, CD intensities were decreased compared to those observed in 60% TFE, possibly due to a lack of secondary structure-promoting TFE, as is often observed for α-peptides. Based on the CD signature of peptide **3.1**, which was previously characterized by 2D NMR to be at least partially helical in aqueous solution, we might conclude that **3.2**-**3.7** are all partially helical in water, regardless of the backbone patterns (Figure 3.7).[2]

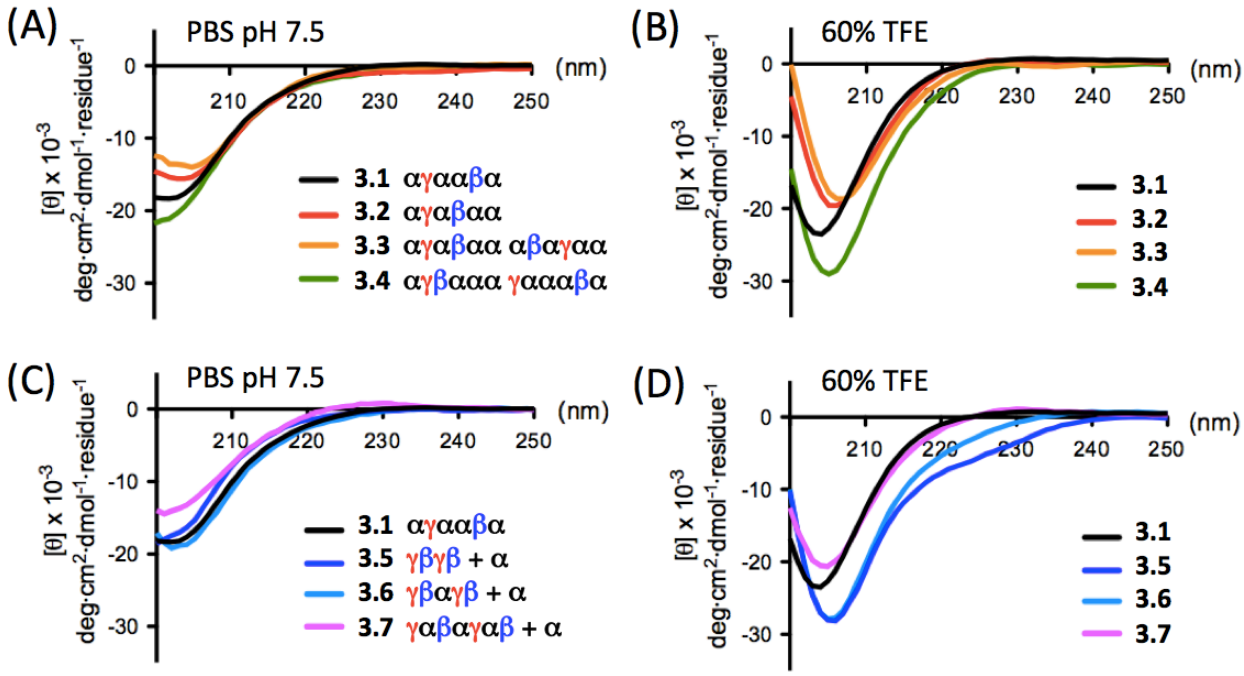

Figure 3.7 Circular dichroism data of (A) peptides **3.1**-**3.4** in PBS buffer pH 7.5, 20°C, (B) peptides **3.1**-**3.4** in 60% TFE/40% PBS buffer, (C) peptides **3.1**, **3.5**-**3.7** in PBS buffer pH 7.5, 20°C and (D) peptides **3.1**, **3.5**-**3.7** in 60% TFE/40% PBS buffer. Peptide concentration is 0.1 mM for all measurements.

3.3.3 2D-NMR studies

To test the hypothesis that an α/β/γ-peptide with a non-αγααβα backbone pattern adopts helical conformations in aqueous or aqueous-TFE solutions, we investigated NOEs of **3.4B** in water as well as in 60% CF_3CD_2OH/40% water by 2D-NMR experiments. Peptide **3.4B** is analogous to **3.4**, but two alanines have been replaced with glutamine (positon 5) and norleucine (position 8) to facilitate 2D-NMR resonance assignments (Figure 3.8B). Peptide **3.4** was chosen as a representative of non-αγααβα systems because **3.4** had the most random backbone pattern among the analogues experimented by CD. By overlaying results from gCOSY, wgTOCSY and wgROESY, we could assign all resonances from backbone amide N-Hs and backbone C-Hs of peptide

3.4B. Numerous non-sequential NOEs that are indicative of helical folding were detected in 60% TFE (Figure 3.8A and C). In contrast, in pure water, although the chemical shift dispersion among amide N-Hs and α, β, or γ backbone C-Hs was sufficient for unambiguous resonance assignment, we could not clearly assign any of non-adjacent NOEs crosspeaks due to significant peak overlaps. In random coil or unfolded peptides, it is very hard to observe good peak dispersion in backbone amide N-Hs and αC-Hs regions due to peak overlaps. In helical conformation, chemical shifts of backbone amide N-Hs and αC-Hs tend to be up-field shifted relative to their random coil values, due to helix-stabilizing intra H-bonds, and this results in a dispersion of backbone resonance peaks.[10] When a peptide is partially helical in water, it is very challenging to clearly assign NOEs from non-adjacent residues because of the dynamics of peptide folding. Taking these factors into account, 2D NMR results of **3.4B** in water suggest that **3.4B** is slightly helical in water.

It is unambiguous that **3.4B** (or **3.4**) is helical in 60% TFE/40% PBS buffer based on the CD and 2D NMR results. **3.4B** (or **3.4**) is considered to be partially helical in water based on the CD and 2D NMR results; 1) **3.4B** and **3.4** displayed a similar CD signature to **3.1**, which was previously characterized to be helical by 2D NMR, 2) a good 2D NMR peak dispersion has been shown in backbone amide N-H and αC-H region for clear resonance assignments. With a most random backbone pattern, **3.4B** (or **3.4**) manifested helicity in 60% TFE/40% PBS buffer and partially helical conformation in water (PBS buffer). The partial helicity of **3.4** implies that other α/β/γ-peptides **3.2-3.7** with non-αγααβα backbone patterns are also perhaps partially helical in water based on their similar CD characteristics in PBS buffer (Figure 3.7).

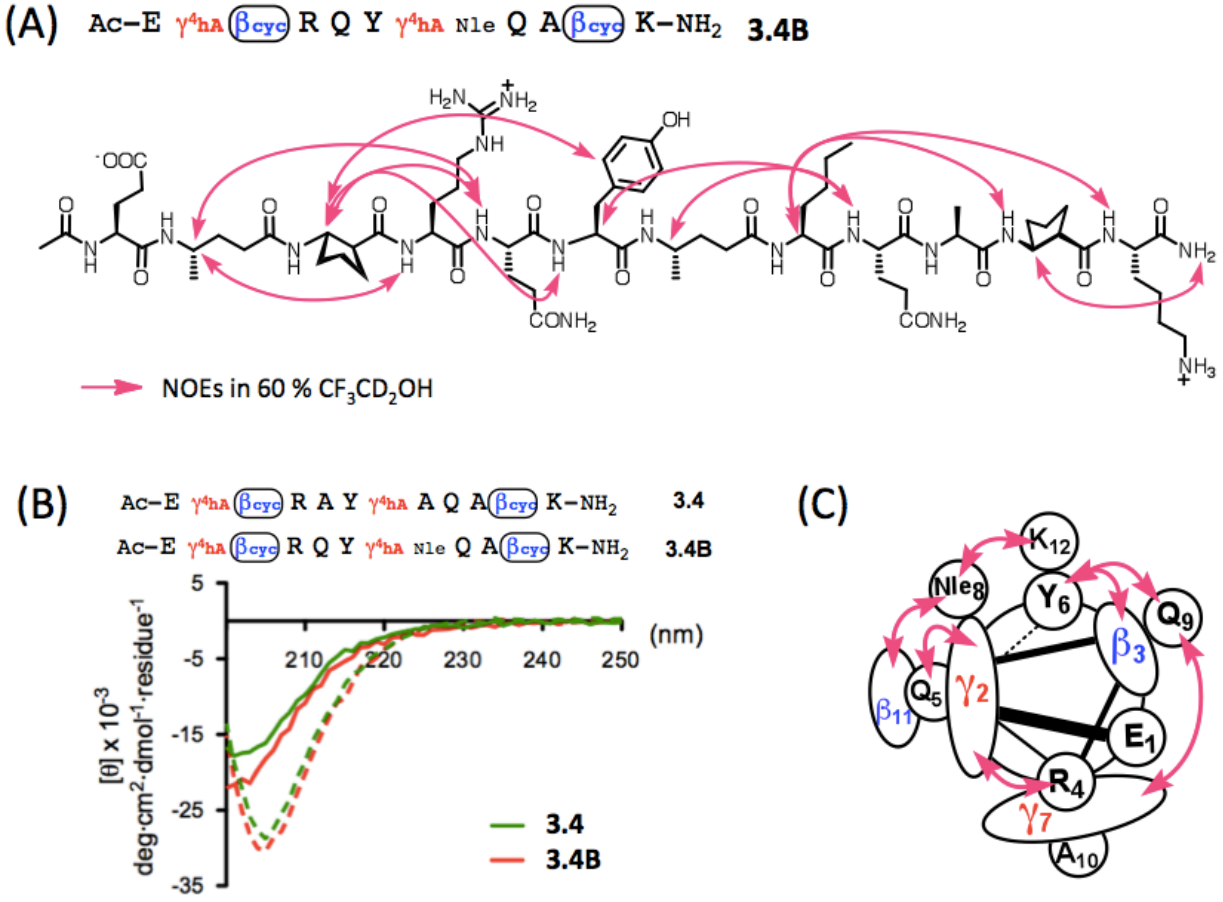

Figure 3.8 NOEs observed between non-adjacent residues for α/β/γ-peptide **3.4B** (peptide concentration 8 mM) in 60% CF_3CD_2OH/30% H_2O/10% D_2O mixture (shown in pink) at 4 °C. Medium strong and medium weak NOEs are shown as plain curved arrows (A) on the peptide structures and (C) on the helical wheel diagrams. (B) Circular dichroism spectra from **3.4** (green) and **3.4B** (red) in PBS buffer pH 7.5 (solid line) and 60% TFE/40% PBS buffer (dashed line), 20°C. Peptide concentration is 0.1 mM for all measurements. For NOE assignments see the experimental session.

We pursued 2D-NMR analysis of other α/β/γ-peptides. Peptides **3.2** and **3.5**-**3.7** were investigated by gCOSY, wgTOCSY and wgROESY in water and in 50~60% CF_3CD_2OH/water mixtures (Table 3.1, Figure 3.9). All the resonances of backbone amide N-Hs and α, β, or γ backbone C-Hs were assigned for each residue in peptides **3.2**, **3.6** and **3.7**, except for those of two alanines from **3.5** in water, which were indistinguishable. Interestingly, several non-adjacent NOEs between residues in i,i+2 and i,i+3 relationships were identified from (α/β/γ+α)-chimeric peptides **3.5**-**3.7** in water as well as in 50-60% TFE. CD data in water for peptides **3.1**-**3.7** were very similar, and peptide **3.7** exhibited the weakest CD signal in water (Figure 3.7). Based on the fact that even **3.7** presented NOEs indicative of helix formation in water, we conclude that the partial helicity of **3.4B** (or **3.4**) in water is supported. Although the helicity of α/β/γ-peptides with acyclic γ^4- and 5-membered-ring constrained β-amino acids might vary somewhat depending on the backbone substitution pattern, partial helical folding in water appears to occur regardless of the arrangement of α, β, and γ residues.

Table 3.1 NOEs from non-adjacent residues for peptides **3.2**, **3.5**, **3.6** and **3.7** measured in water and 50-60% TFE at 4 ^{o}C. Here listed non-adjacent NOEs only from backbone hydrogens.

	90% H_2O/10% D_2O		
peptide		type	distance (Å)
3.5	γ^4hAla(04)HG-Tyr(06)HN	i,i+2	3.8
3.6	γ^4hAla(02)HG-Arg(04)HN	i,i+2	3.3
	γ^4hAla(05)HG-Tyr(07)HN	i,i+2	3.5
3.7	γ^4hAla(02)HG-ACPC(04)HN	i,i+2	3.3
	γ^4hAla(06)HG-ACPC(08)HN	i,i+2	3.7
	50-60% CF_3CD_2OH/10% D_2O in H_2O		
peptide		type	distance (Å)
3.2	Glu(01)HA-ACPC(04)HN	i,i+3	4.8
3.5	γ^4hAla(02)HA-ACPC(05)HN	i,i+3	4.3
	γ^4hAla(04)HG-Tyr(06)HN	i,i+2	3.8
3.6	γ^4hAla(02)HG- γ^4hAla(05)HN	i,i+3	3.9
	γ^4hAla(02)HG-Arg(04)HN	i,i+2	3.9
3.7	γ^4hAla(02)HG-ACPC(04)HN	i,i+2	3.5
	γ^4hAla(06)HG-ACPC(08)HN	i,i+2	3.4

(A) Ac–E γ⁴hA A βcyc R Y A γ⁴hA Q βcyc A K–NH_2 **3.2**

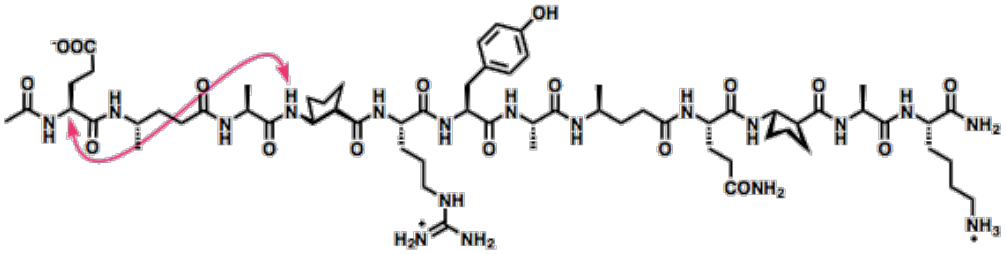

(B) Ac–E γ⁴hA βcyc γ⁴hA βcyc Y R A Q A A K–NH_2 **3.5**

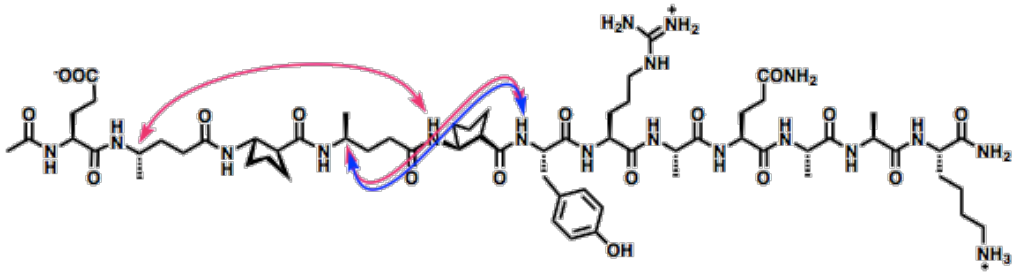

(C) Ac–E γ⁴hA βcyc R γ⁴hA βcyc Y A Q A A K–NH_2 **3.6**

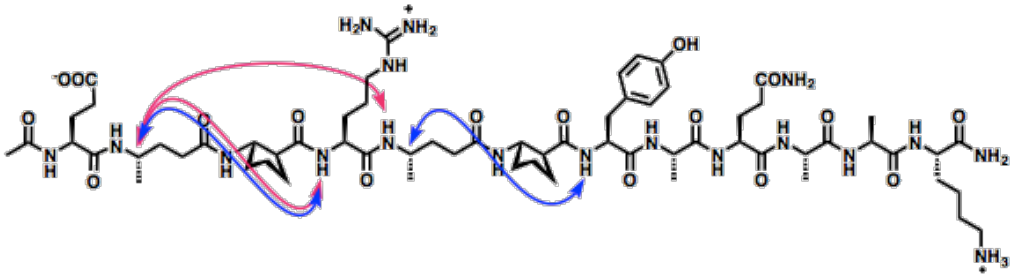

(D) Ac–E γ⁴hA A βcyc R γ⁴hA Y βcyc Q A A K–NH_2 **3.7**

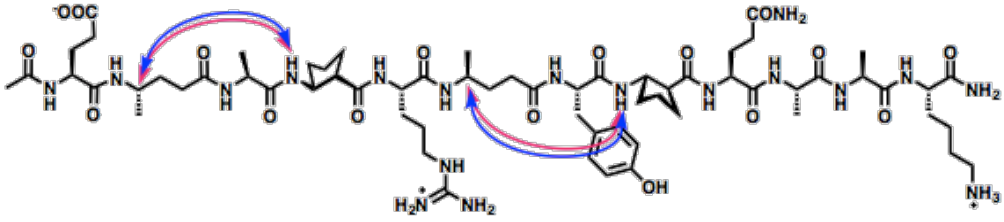

Figure 3.9 NOEs from non-adjacent residues for peptides **3.2**, **3.5**, **3.6** and **3.7** measured in 60% CF_3CD_2OH/30% H_2O/10% D_2O (shown in pink) or in 90% H_2O/10% D_2O (shown in blue) at 4 °C (Peptide concentration 5-8 mM). Medium NOEs are shown as plain curved arrows on the peptide structures.

3.4 Effect of cyclic γ- and β-residues on the helicity of α/β/γ-peptides in various backbone patterns

3.4.1 Adding ring-constraints at γ-residues

Previous studies with α/β/γ-peptide **3.1A** showed that 6-membered-ring constrained γ-amino acids and 5-membered-ring constrained β-amino acids together yielded a structurally stable α-helix-like conformation.[1] We wondered what effect a 6-membered-ring constrained γ-amino acid would have in α/β/γ-peptides with backbone patterns other than αγααβα hexad repeat. Peptides **3.2A** and **3.4A** were prepared by incorporating EtACHA at positions where γ^4hAla were in **3.2** and **3.4B**, and the helix-forming propensities of **3.2A** and **3.4A** were assessed by CD and 2D-NMR.

In 60% TFE, **3.2A** and **3.4A**, which contain cyclic γ-residues, showed very similar CD signatures to **3.2** and **3.4B**, which contain acyclic γ-residues (Figure 3.10B and C). However, in water, **3.2A** showed reduced CD intensity relative to **3.2**, while **3.4A** exhibited a similar CD intensity relative to **3.4B**. The CD minima of **3.4A** and **3.2A** in water were slightly red-shifted compared to **3.4B** and **3.2**, respectively. A shift of the CD minimum in water incurred by changing γ-residues from acyclic to cyclic has also been observed for peptides **3.1** and **3.1A**, which are known via 2D NMR to be helical in aqueous solution (Figure 3.10A). The CD result shown by **3.2A** is our first empirical observation that implies the cyclohexyl constrained γ amino acid (EtACHA) does not improve helical folding of an α/β/γ-peptide than γ^4hAla. This is consistent with our previous prediction that EtACHA might not provide optimal torsion angles to promote

helical folding of α/β/γ-peptides, based on the analyses of torsion angles in EtACHA from the X-ray crystal structure of GCN4-PLI derived α/β/γ-peptides.[2]

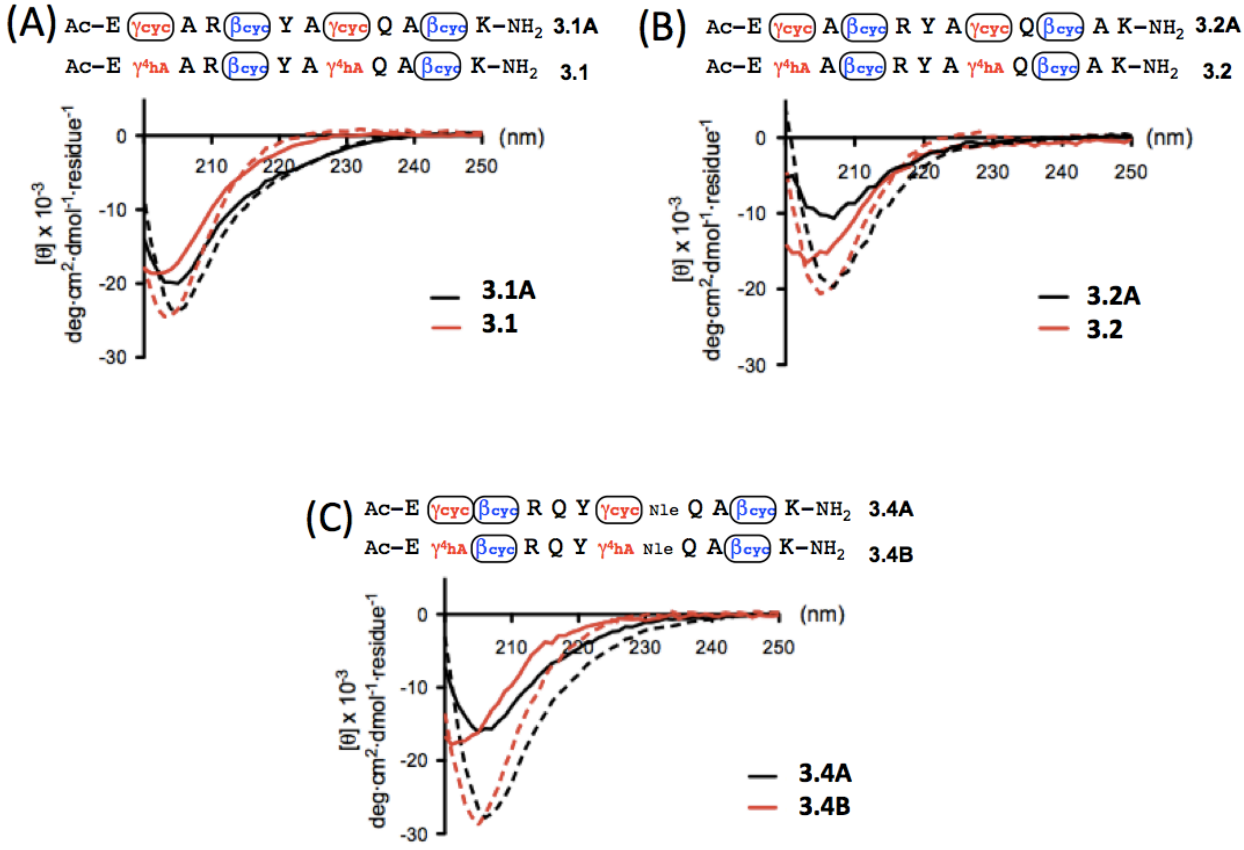

Figure 3.10. Circular dichroism data from (A) peptides **3.1A** (black) and **3.1** (red), (B) peptides **3.2A (**black) and **3.2** (red), (C) peptides **3.4A** (black) and **3.4B** (red) in PBS buffer (solid line) and in 60% TFE/40% PBS (dashed line) at pH 7.5, 20 °C. Peptide concentration is 0.1 mM for all measurements.

2D-NMR data for **3.4A** in 60% TFE/40% water showed numerous i,i+2 and i,i+3 non-adjacent NOEs indicative of helix formation (Figure 3.11). Even in water, several of the NOEs were observed (Figure 3.11). The 2D-NMR analysis indicates that a cyclohexyl ring-constrained γ-residue can consistently be used in helical α/β/γ-peptides regardless of backbone α/β/γ pattern. However, EtACHA does not appear to

significantly enhance helical folding compared to an acyclic γ^4-residue. Considering the time necessary to synthesize EtACHA, its low coupling efficiency in SPPS and the difficulties in incorporating side chain functional groups, we conclude that using γ^4-amino acids could be beneficial for function-based $\alpha/\beta/\gamma$-peptidomimetic development, especially at the initial evaluation stage.

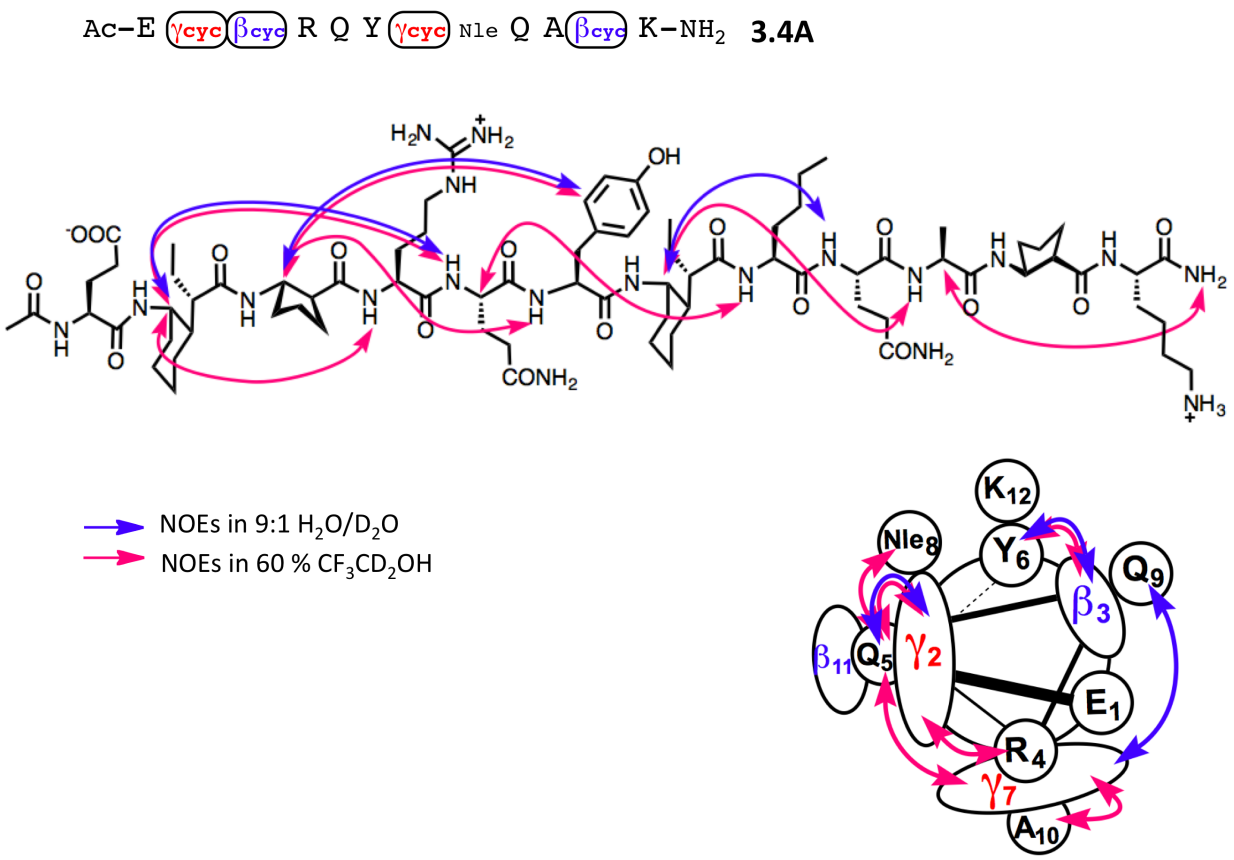

Figure 3.11 NOEs observed between non-adjacent residues for $\alpha/\beta/\gamma$-peptide **3.4A** (peptide concentration 1.5 mM) in 60% CF_3CD_2OH/30% H_2O/10% D_2O (shown in pink) or in 90% H_2O/10% D_2O (shown in blue) at 4 °C. Medium strong (2.5 Å ~ 3.5 Å) and medium weak (3.5 Å ~ 4.0 Å) NOEs both are shown as plain curved arrows on the peptide structures and on the helical wheel diagrams. For NOE assignments see the experimental session.

3.4.2 Removing ring-constraints on β-residues

12-mer α/β/γ-peptides **3.1B** and **3.1C**, which have an αγααβα pattern and lack ring-constraints on the β-residues, were mostly unstructured in water (Figure 3.1).[2] We examined whether ring-constraints on β-residues are essential for folding of α/β/γ-peptides with non-αγααβα residue patterns when there is no ring-constraint on γ-residues. The ring-constraints on β-residues were relaxed in peptides **3.2**, **3.5**, and **3.6**, resulting in **3.2B**, **3.5A**, and **3.6A**. Peptides **3.5A** and **3.6A** were potentially because of their (α/β/γ+α)-chimeric backbones. The CD spectra of **3.2B**, **3.5A**, and **3.6A** in water (Figure 3.12) clearly showed that these peptides, which do not contain helical backbone pre-organizing residues, are unstructured. In 60% TFE, significantly reduced CD intensities were exhibited by **3.2B**, **3.5A** and **3.6A** compared to **3.2**, **3.5**, and **3.6**, suggesting diminished helicity of **3.2B**, **3.5A** and **3.6A** compared to the analogous peptides containing cyclic β residues.

Previously, we have shown that α/β/γ-peptides without ring-constraints on β, but with ring-constraints on γ-residues (Figure 3.1, peptide **3.1B**), are not structured in aqueous environments.[2] These results highlighted the critical role of cyclic β residues for helicity in α/β/γ-peptides, and a strong helical structure-adopting ability of γ^4-residues in α/β/γ-peptides.[2] Since the cyclohexyl ring-constraint on γ residues did not significantly enhanced helical folding of **3.1A**, **3.2A** and **3.4A** (Figure 3.10), we assume that the α/β/γ analogues with different residue patterns will show similar trends in folding behavior to the trend among analogues of **3.1** (i.e., **3.1A**, **3.1**, **3.1B**, and **3.1C**). We have not

examined the helicity of α/β/γ-analogues with different residue patterns containing cyclic γ and acyclic β residues, but we expect them not to be helical.

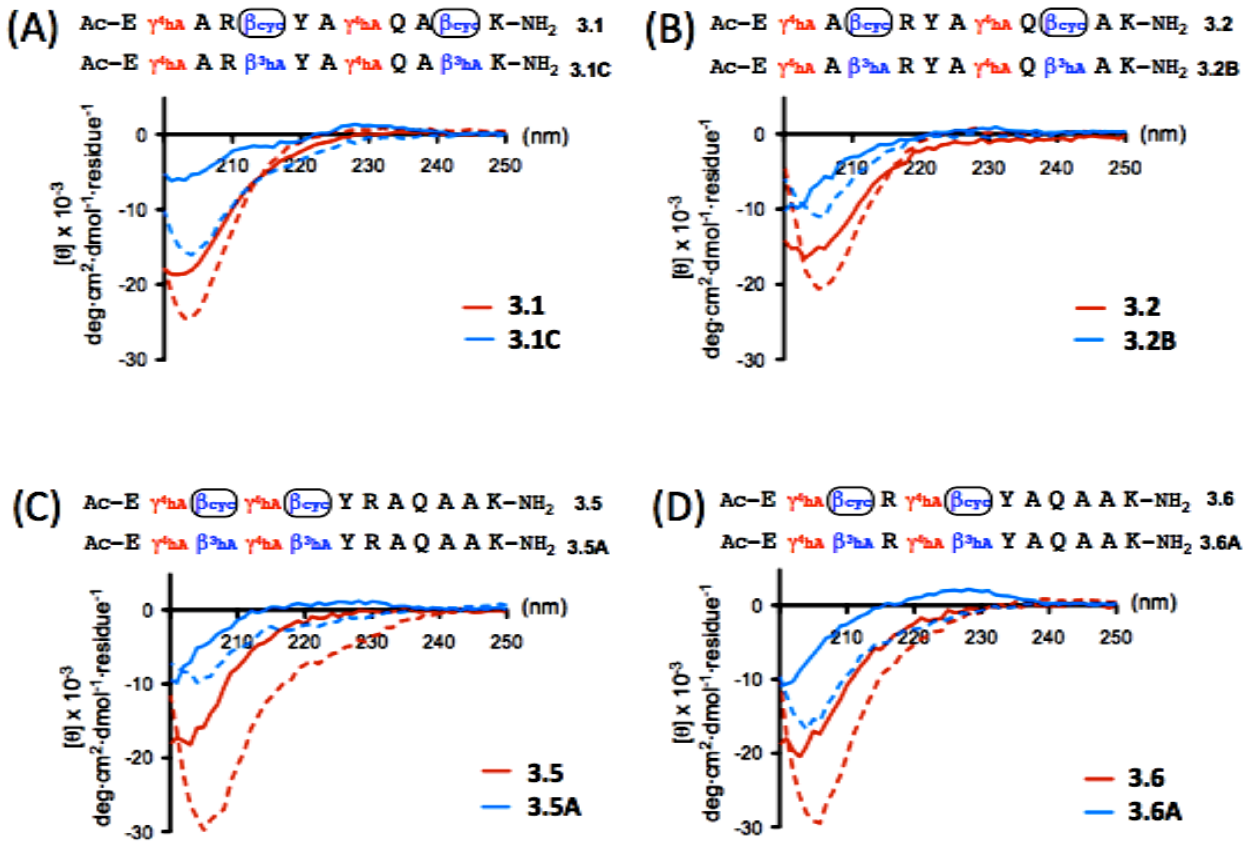

Figure 3.12 Circular dichroism data from (A) peptides **3.1** (red) and **3.1C** (blue), (B) peptides **3.2** (red) and **3.2B** (blue), (C) peptides **3.5** (red) and **3.5A** (blue), (D) peptides **3.6** (red) and **3.6A** (blue) in PBS buffer (solid line) and in 60% TFE/40% PBS buffer (dashed line) at pH 7.5, 20 °C. Peptide concentration is 0.1 mM for all measurements.

3.5 Conclusions

Helical α/β/γ-peptides with different acyclic γ residues and with various backbone patterns were explored. Achiral and acyclic γhGly and γ^{4}hAib could accommodate helical folding in α/β/γ-peptides but with reduced helicity compared to γ^{4}hAla. Further,

variations in residue arrangement in the backbone of α/β/γ-peptides were examined using acyclic γ^4hAla and cyclic β residues, and helical folding was observed for all arrangements tested. When γ residues were constrained with a cyclohexyl ring (EtACHA), peptides were helical, but helicity was not improved compared to analogous α/β/γ-peptides with acyclic γ^4-residues. Without pre-organized β residues, however the 12-mer α/β/γ-peptides were mostly unstructured in water, suggesting a critical role of ring-constrained β residues for α/β/γ-peptide helicity. With addition of helix-promoting TFE, α/β/γ-peptides with acyclic β residues showed helical folding, but with significantly reduced helical population compared to analogous α/β/γ-peptides containing cyclic β residues.

The results from this study suggest that as long as cyclically constrained β-amino acids are incorporated into α/β/γ-peptides, the α/β/γ-peptide helical propensity is not very sensitive to the nature of the acyclic γ-amino acids used (although γ^4-amino acids are the best helix-adopting acyclic residues) or the pattern of residues within the backbone. This study broadens the collection of possibly useful α/β/γ-peptides.

3.6 Experimental

3.*6.1 General*

Fmoc α-amino acids and resin for solid phase peptide synthesis were purchased from Novabiochem or Chem-Impex, and coupling reagents and additives, O-benzotriazole-N,N,N',N'-tetramethyluronium hexafluorophosphate (HBTU), O-(7-azabenzotriazol-1yl)-N,N,N,N'-tetramethyluronium hexafluorophosphate (HATU), 1-

ethyl-3-(3-dimethylaminopropyl)carbodiimide hydrochloride (EDCI), hydroxybenzotriazole (HOBt), 1-Hydroxy-7-azabenzotoriazole) (HOAt), were purchased from Chem-Impex. Fmoc β-amino acids such as Fmoc-(1*S*,2*S*)-2-aminocyclopentane carboxylic acid and acyclic Fmoc β^3-amino acids were purchased from Chem-Impex. Acyclic γ-amino acids were purchased from Polypeptide group. Ring constrained γ-amino acid, EtACHA, was synthesized according to previous reports.[11] Other reagents and solvents were purchased from Sigma-Aldrich.

3.6.2 Peptide Synthesis and Purification

3.6.2.1 Syntheses of α/β/γ-peptides (SPPS)

All of the α/β/γ-peptides described here were synthesized on Nova PEG rink amide resin (25-50 μmol scale) by microwave-assisted solid-phase method using a CEM MARS microwave reactor.[1,2,12] For α- and cyclic/acyclic β-amino acids coupling reactions, Fmoc-amino acids were pre-activated in a separated vial (4 equiv. of Fmoc-amino acids, 3.95 equiv. of HBTU, 8 equiv. of DIEA, 0.1 M HOBT in DMF solution) for 1-2 minutes, then the solution was added to resin in a filter tube, reacted under microwave irradiation (2 min ramp to 70 ^{o}C, 4 min hold at 70 ^{o}C for α-residues, 12 min hold for β-residues). For acyclic γ-amino acids coupling reactions, the same condition to β-amino acid coupling was applied but DIEA was added right before starting microwave irradiation in order to avoid intra-cyclization reaction of γ-amino acids. Cyclic γ-residue (EtACHA) coupling reactions were performed by pre-activating 4 equiv. of Fmoc-amino acid with 4 equiv. of EDCI and 8 equiv. of DIEA in 0.1M HOAt in DMF, then the mixture solution was added to resin and reacted for 14 hours at room temperature while gently

shaking. Fmoc deprotection reactions were carried out using 20 % piperidine in DMF under microwave irradiation (2 min ramp to 80 ^{o}C, 2 min hold at 80 ^{o}C). Upon completion of couplings, the N-terminus amine was capped by acetylation using Ac_2O in DMF and DIEA.[12]

3.6.2.2 Cleavage, Deprotection, HPLC Purification, and Characterization

Peptides were globally deprotected and cleaved from the resin by suspending in cleavage cocktail (95% trifluoroacetic acid (TFA), 2.5 % water, and 2.5 % triisopropylsilane) for 4~5 hours. After filtering out the TFA cleavage solution from the resin, peptides were precipitated from the TFA solution by adding cold diethyl ether, centrifuged to get a peptide pellet, and the crude peptide was purified by reverse-phase HPLC using a C18 column. Peptides identity was confirmed by matrix-assisted laser desorption/ionization time-of-flight (MALDI-TOF-MS) mass spectrometry. Peptides purity was checked on analytical reverse-phase HPLC.

3.1D

Ac–E GABA A R(βcyc) Y A GABA Q A(βcyc) K–NH_2

Estimated 1369.8, Found 1369.5

Purification condition: 13-24 % MeCN, 20 min

Purity check: 10-40 % MeCN, 30 min

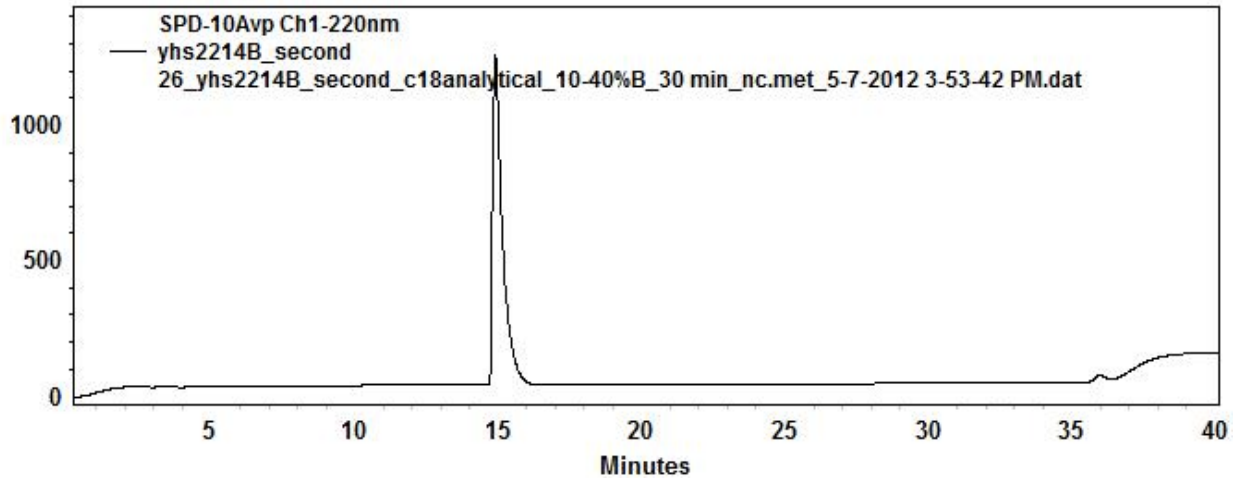

3.1E

Ac–E γ⁴hAib A R(βcyc) Y A γ⁴hAib Q A(βcyc) K–NH_2

Estimated 1425.8, Found 1425.8

Purification condition: 17-27 % MeCN, 20 min

Purity check: 10-60 % MeCN, 50 min

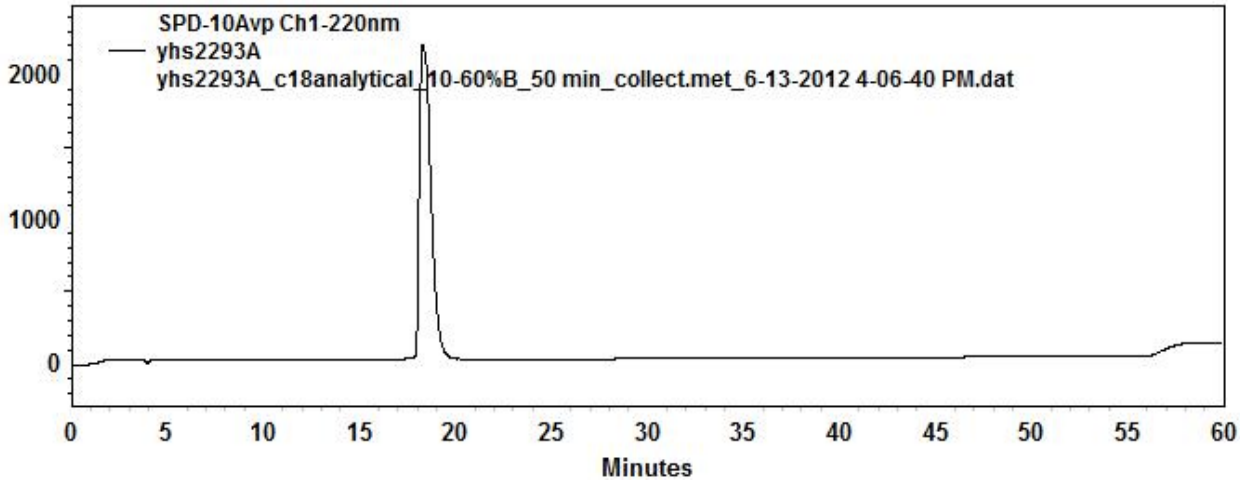

3.2

Ac–E γ⁴hA A βcyc R Y A γ⁴hA Q βcyc A K–NH_2

Estimated 1397.8, Found 1397.8

Purification condition: 17-27 % MeCN, 20 min

Purity check: 10-45 % MeCN, 35min

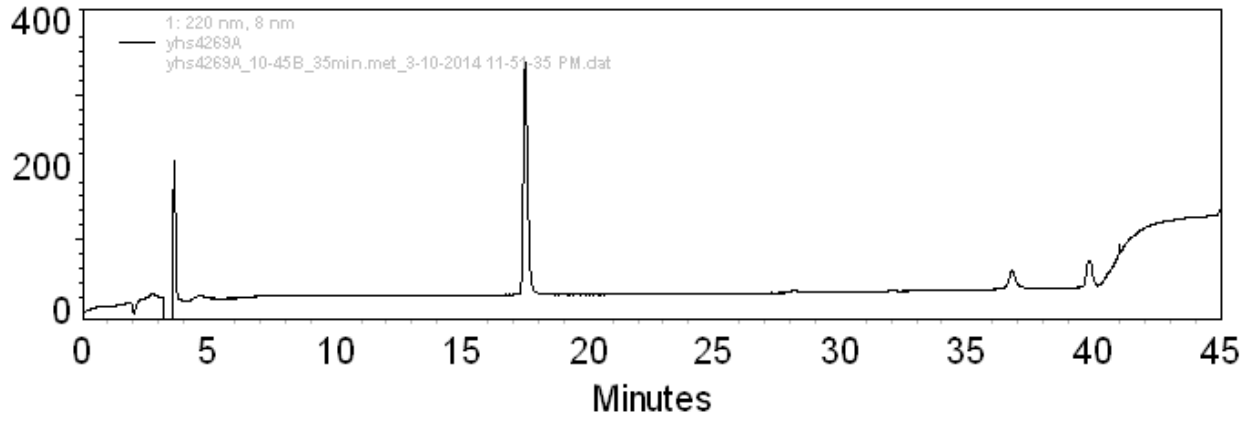

3.3

Ac–E γ⁴hA A βcyc R Y A βcyc Q γ⁴hA A K–NH_2

Estimated 1397.8, Found 1397.9

Purification condition: 17-27 % MeCN, 20 min

Purity check: 10-45 % MeCN, 35 min

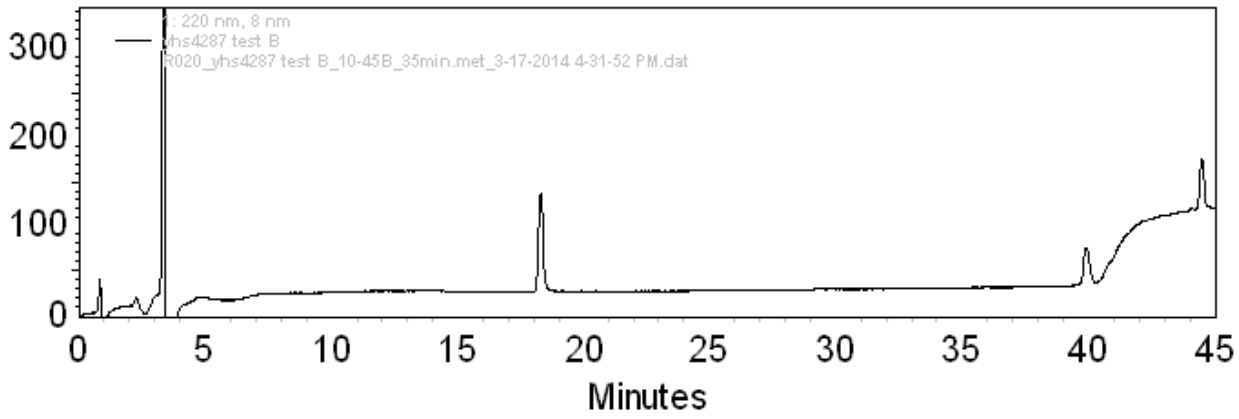

3.4

Ac–E γ⁴hA (βcyc) R A Y γ⁴hA A Q A (βcyc) K–NH_2

Estimated 1397.8, Found 1397.9

Purification condition: 17-27 % MeCN, 20 min

Purity check: 10-45 % MeCN, 35 min

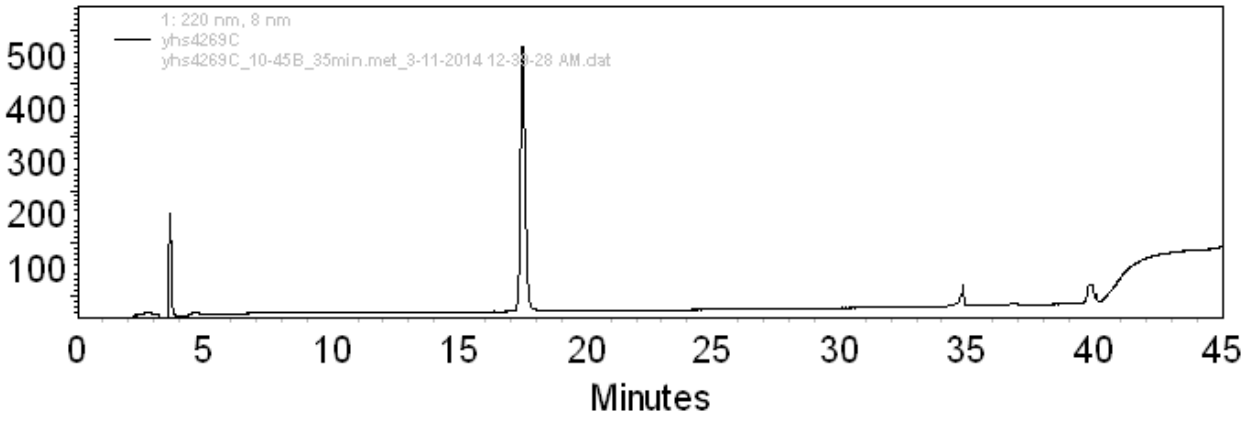

3.5

Ac–E γ⁴hA (βcyc) γ⁴hA (βcyc) Y R A Q A A K–NH_2

Estimated 1397.8, Found 1397.9

Purification condition: 17-27 % MeCN, 20 min

Purity check: 10-45 % MeCN, 35 min

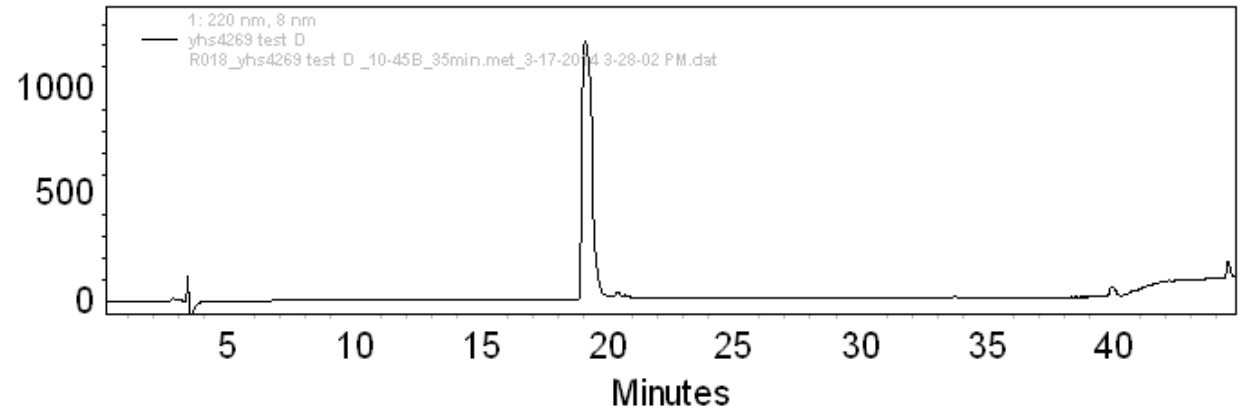

3.6

Ac–E γ⁴hA (βcyc) R γ⁴hA (βcyc) Y A Q A A K–NH_2

Estimated 1397.8, Found 1397.9

Purification condition: 17-27 % MeCN, 20 min

Purity check: 10-45 % MeCN, 35 min

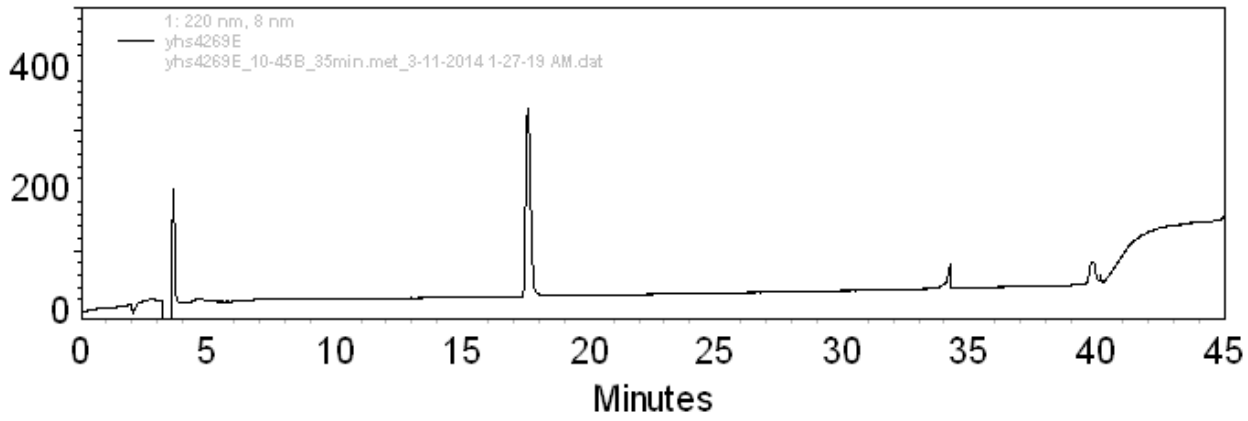

3.7

Ac–E γ⁴hA A (βcyc) R γ⁴hA Y (βcyc) Q A A K–NH_2

Estimated 1397.8, Found 1397.9

Purification condition: 17-27 % MeCN, 20 min

Purity check: 10-45 % MeCN, 35 min (used Prep column)

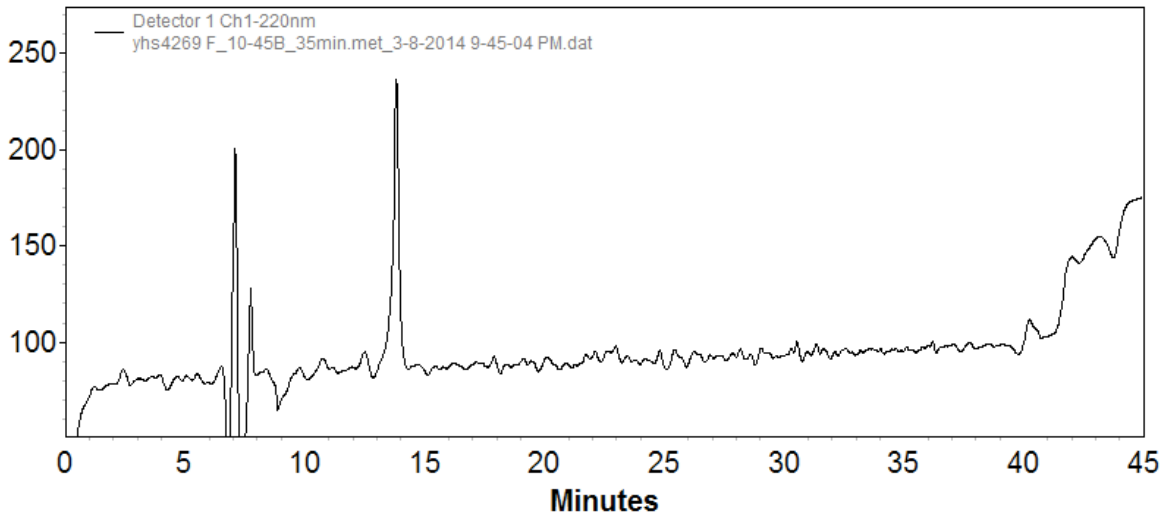

3.2A

Ac–E (γcyc) A (βcyc) R Y A (γcyc) Q (βcyc) A K–NH_2

Estimated 1533.9, Found 1534.0

Purification condition: 30-40 % MeCN, 20 min

Purity check: 10-60 % MeCN, 50 min

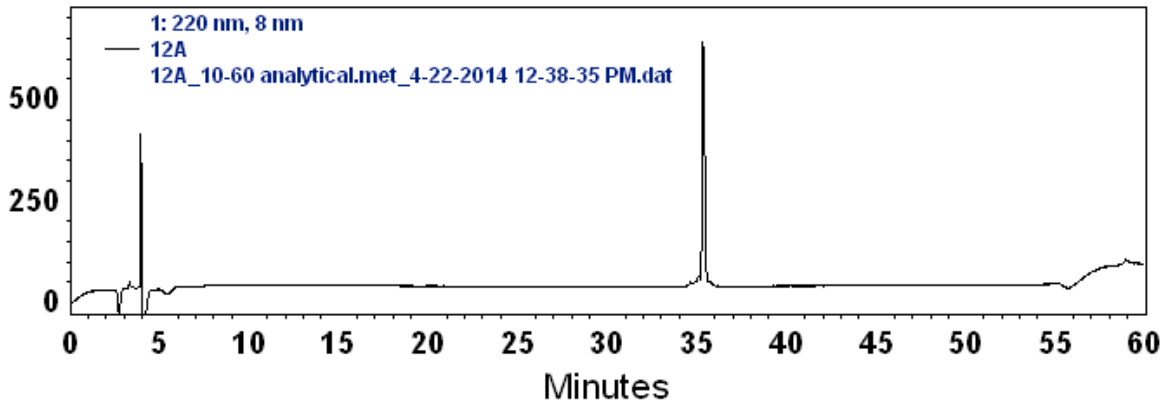

3.2B

Ac–E γ^4hA A β^3hA R Y A γ^4hA Q β^3hA A K–NH_2

Estimated 1345.8, Found 1345.8

Purification condition: 13-23 % MeCN, 20 min

Purity check: 10- % MeCN, 50 min

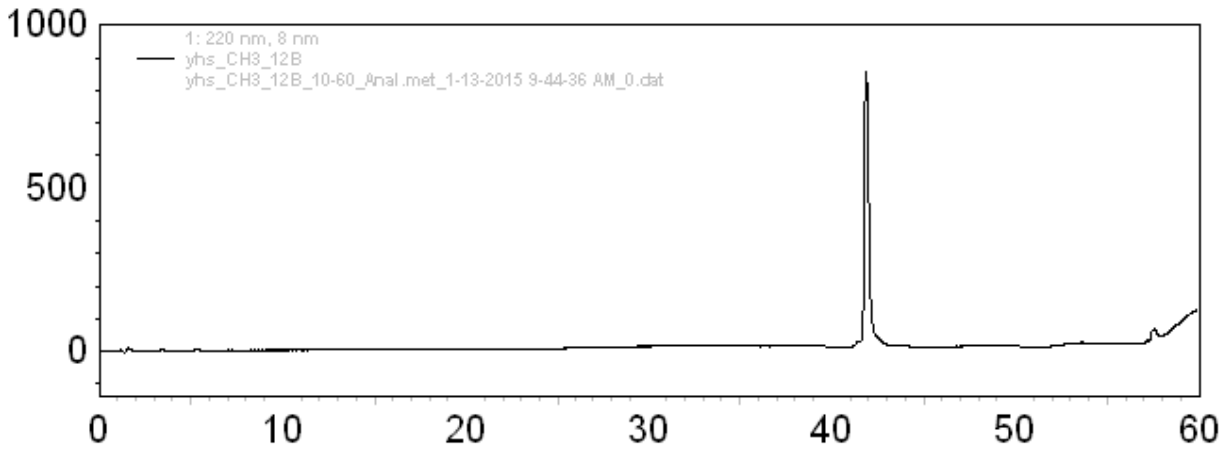

3.4A

Ac–E (γcyc)(βcyc) R Q Y (γcyc) Nle Q A (βcyc) K–NH_2

Estimated 1633.0, Found 1632.6

Purity check: 15-45 % MeCN, 30 min

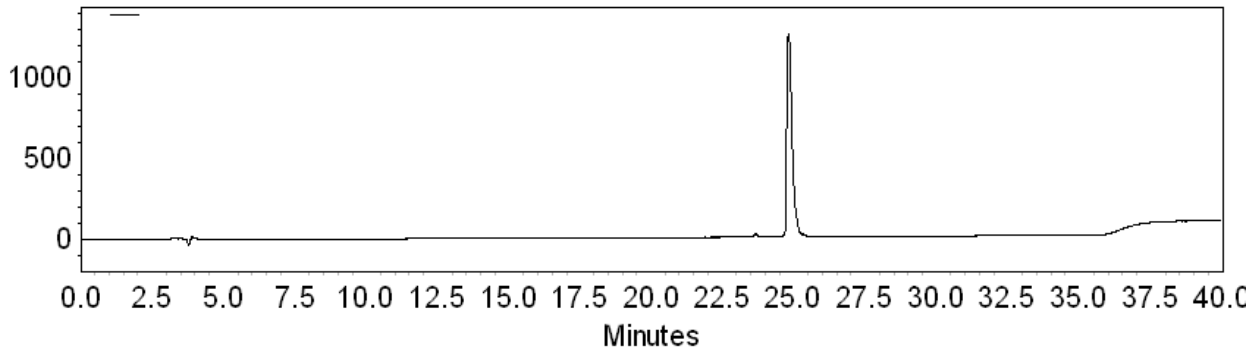

3.4B

Ac–E (γ⁴hA)(βcyc) R Q Y (γ⁴hA) Nle Q A (βcyc) K–NH_2

Estimated 1496.8, Found 1496.9

Purification condition: 19-29 % MeCN, 20 min

Purity check: 10-60 % MeCN, 50 min

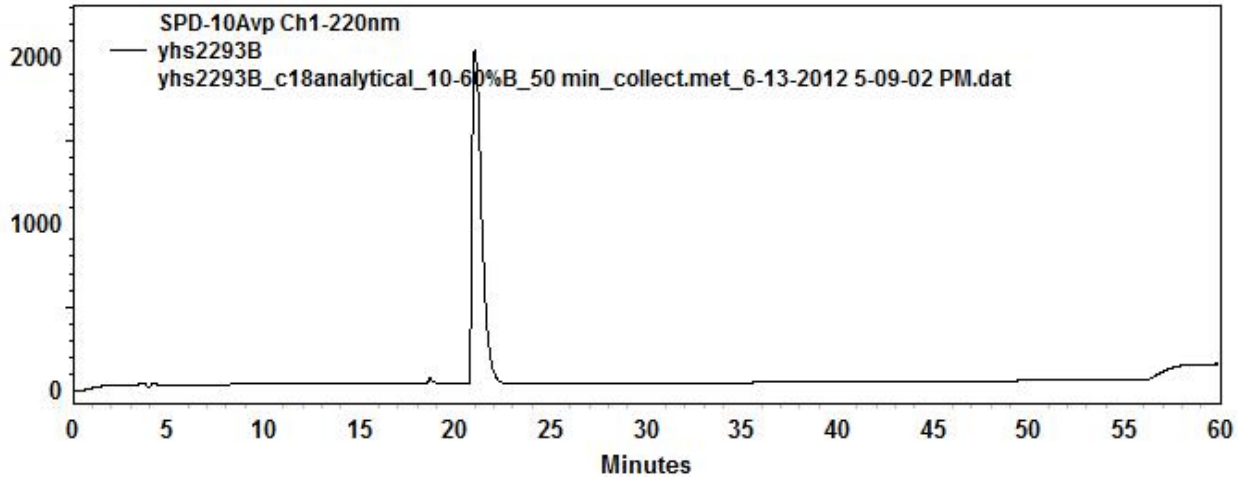

3.5A

Ac–E γ^4hA β^3hA γ^4hA β^3hA Y R A Q A A K–NH_2

Estimated 1345.8, Found 1345.8

Purification condition: 13-23 % MeCN, 20 min

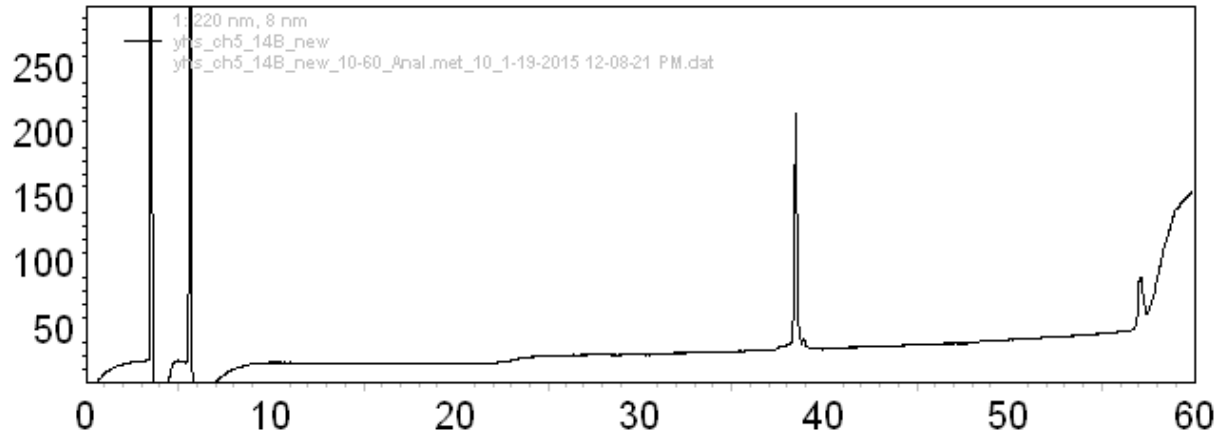

3.6A

Ac–E γ^4hA β^3hA R γ^4hA β^3hA Y A Q A A K–NH_2

Estimated 1345.8, Found 1345.8

Purification condition: 13-23 % MeCN, 20 min

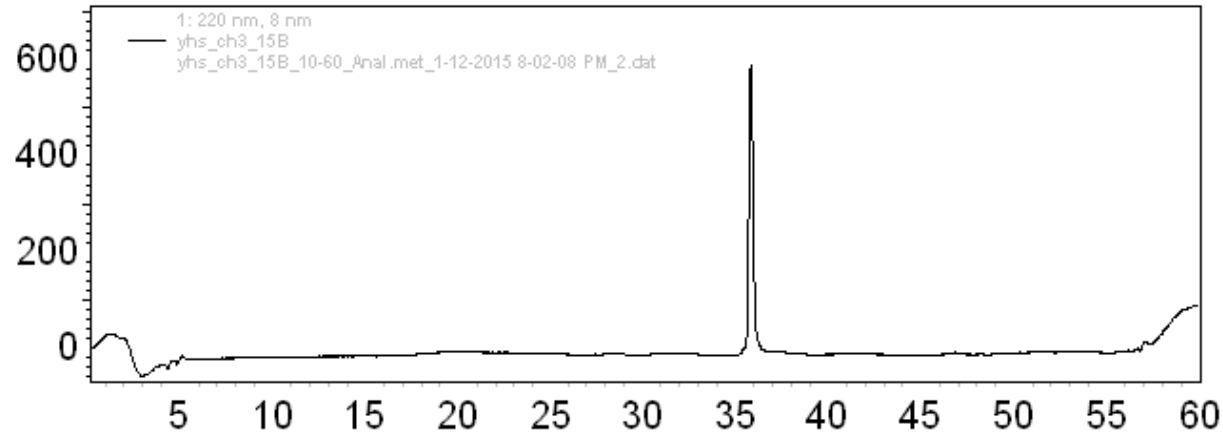

3.1D

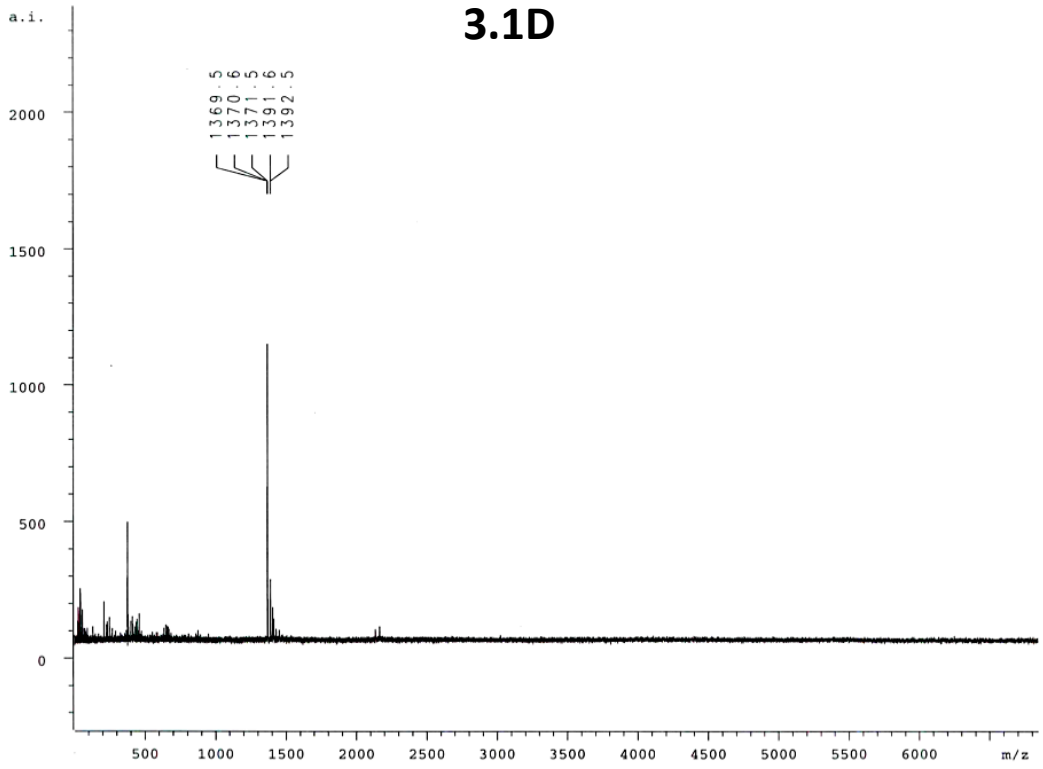
a.i.
1369.5
1370.6
1371.5
1391.6
1392.5
2000
1500
1000
500
0
500
1000
1500
2000
2500
3000
3500
4000
4500
5000
5500
6000
m/z

3.1D

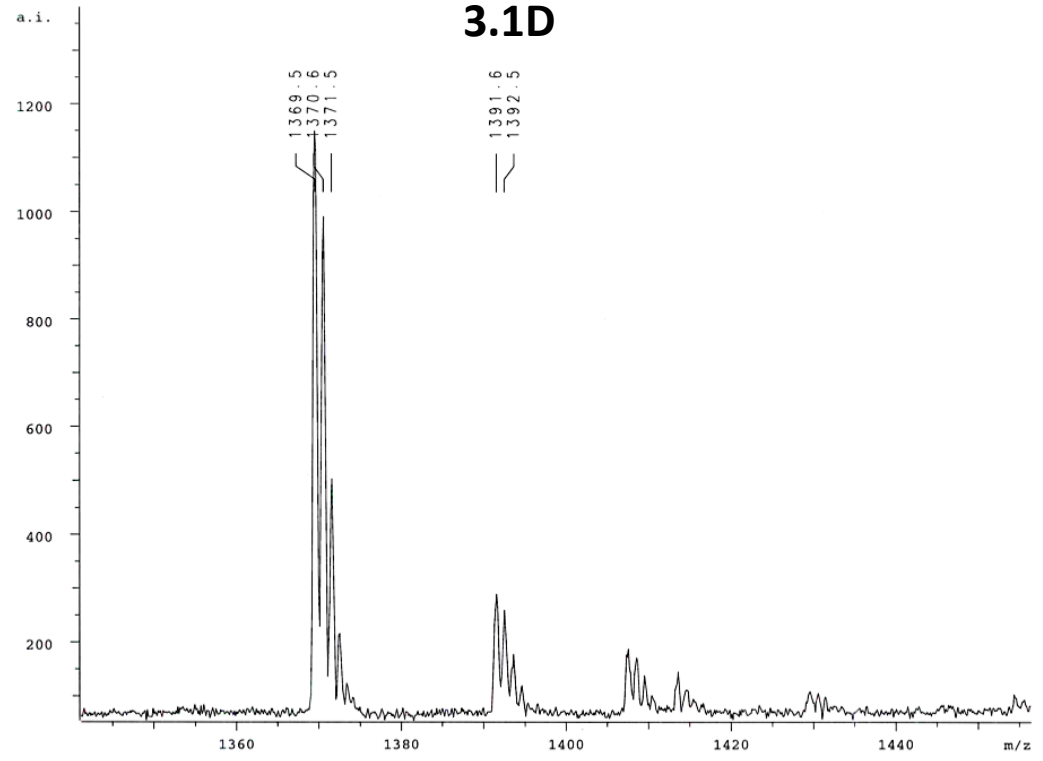
a.i.
1369.5
1370.6
1371.5
1391.6
1392.5
1200
1000
800
600
400
200
1360
1380
1400
1420
1440
m/z

3.1E

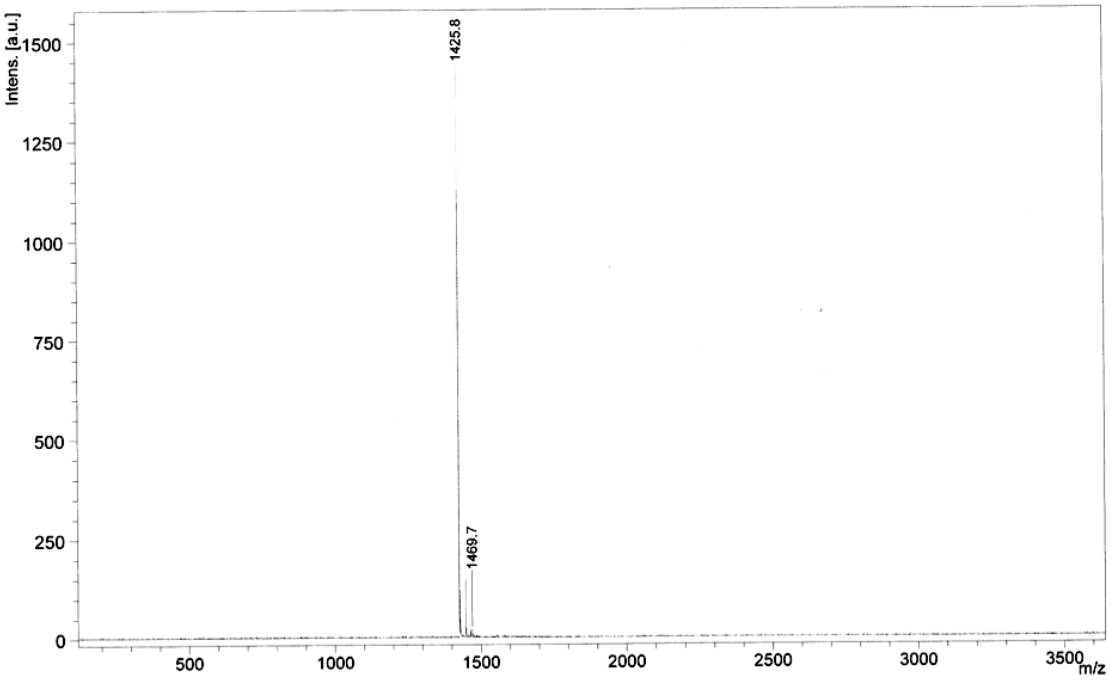
Intens. [a.u.]
1500
1250
1000
750
500
250
0
1425.8
1469.7
500
1000
1500
2000
2500
3000
3500
m/z

3.1E

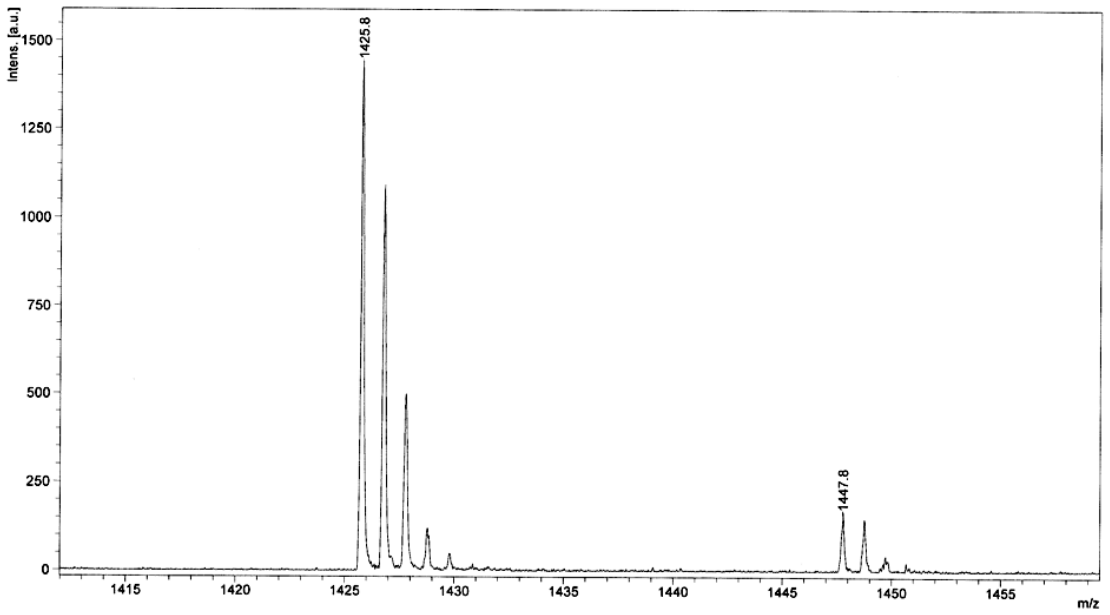
Intens. [a.u.]
1500
1250
1000
750
500
250
0
1425.8
1447.8
1415
1420
1425
1430
1435
1440
1445
1450
1455
m/z

3.2

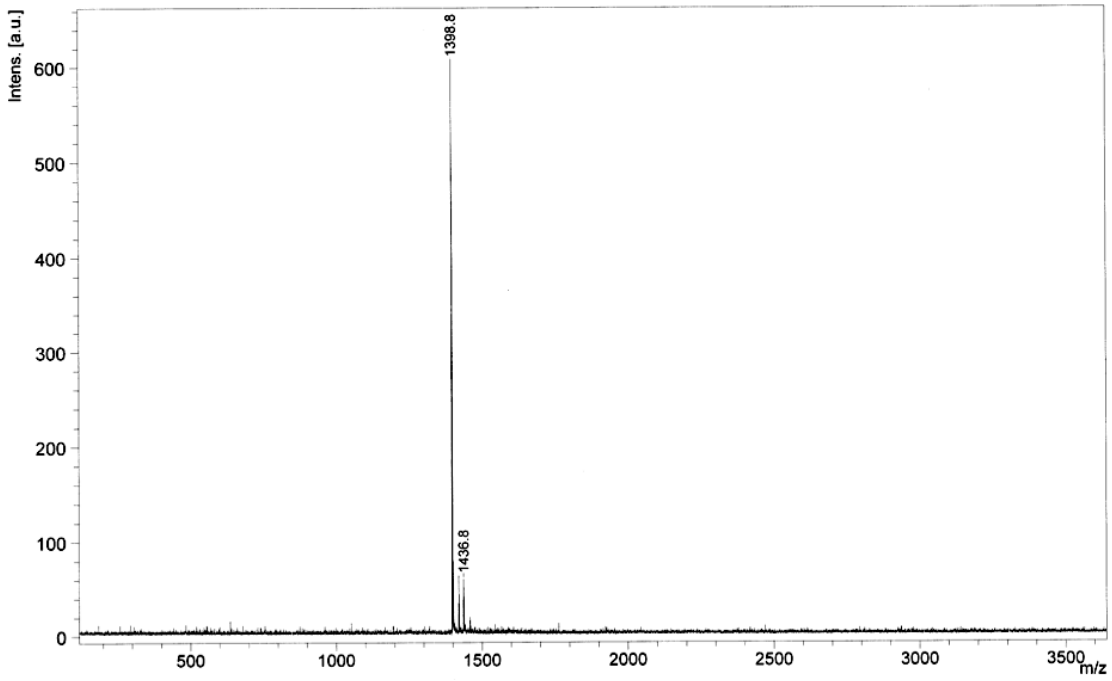
Intens. [a.u.]
600
500
400
300
200
100
0
1398.8
1436.8
500
1000
1500
2000
2500
3000
3500
m/z

3.2

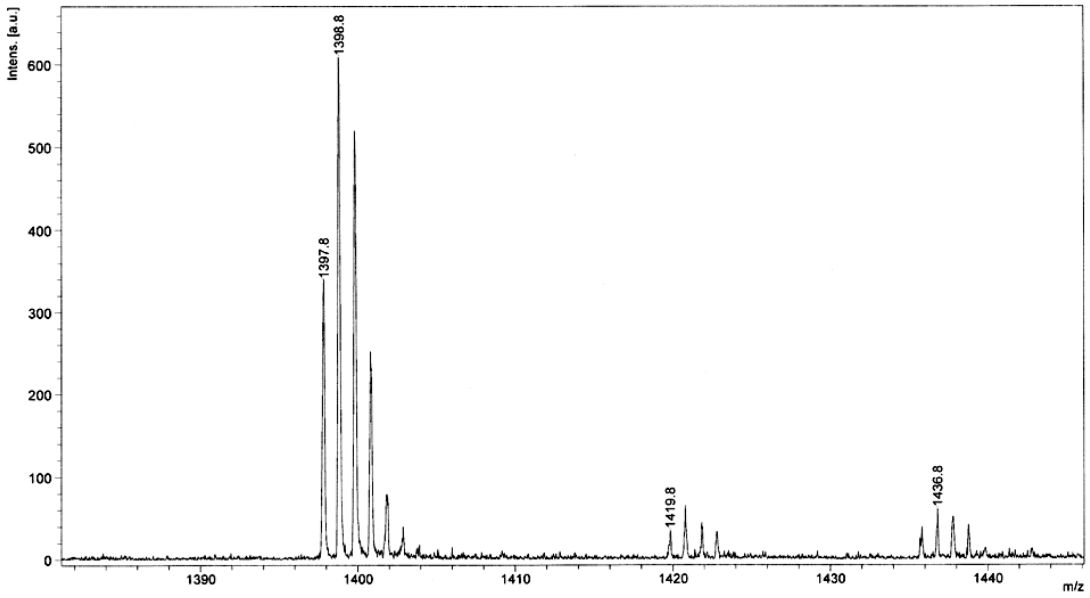
Intens. [a.u.]
600
500
400
300
200
100
0
1398.8
1397.8
1419.8
1436.8
1390
1400
1410
1420
1430
1440
m/z

3.3

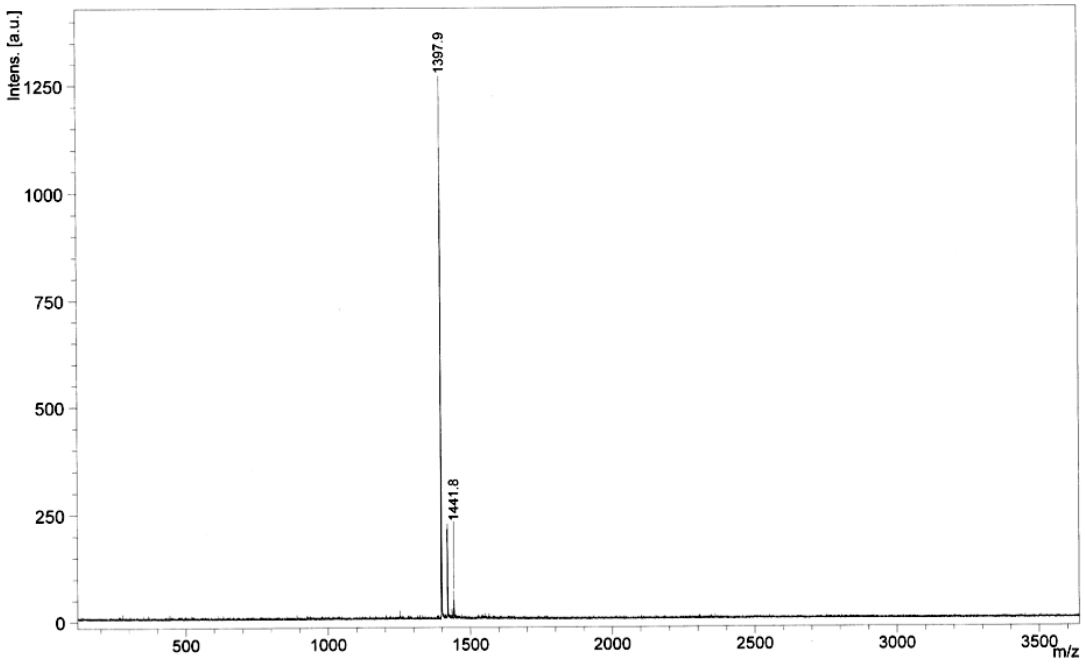
Intens. [a.u.]
1250
1000
750
500
250
0
1397.9
1441.8
500
1000
1500
2000
2500
3000
3500
m/z

3.3

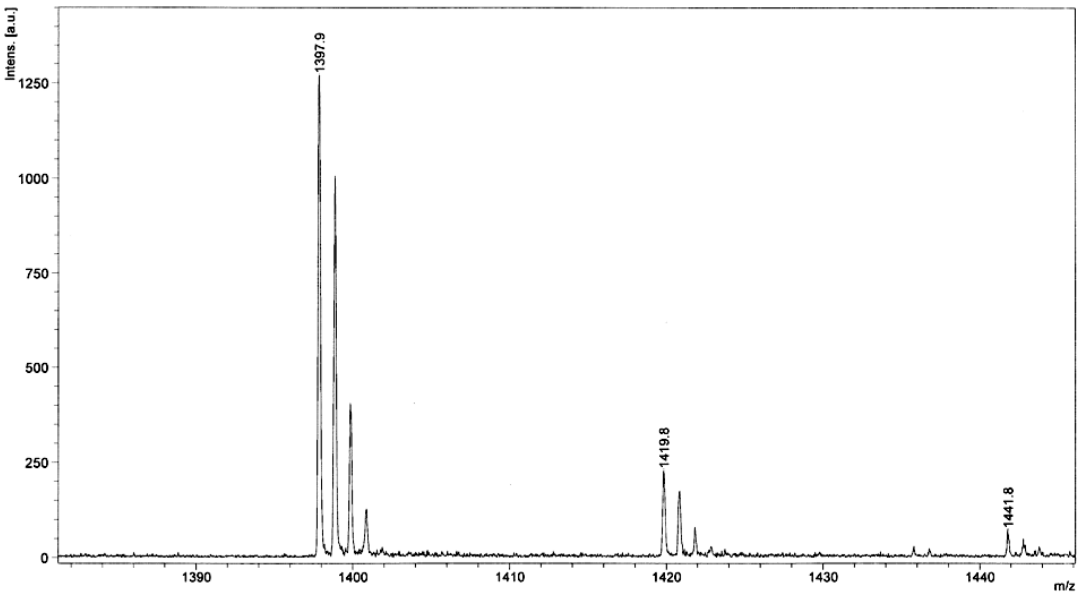
Intens. [a.u.]
1250
1000
750
500
250
0
1397.9
1419.8
1441.8
1390
1400
1410
1420
1430
1440
m/z

3.4

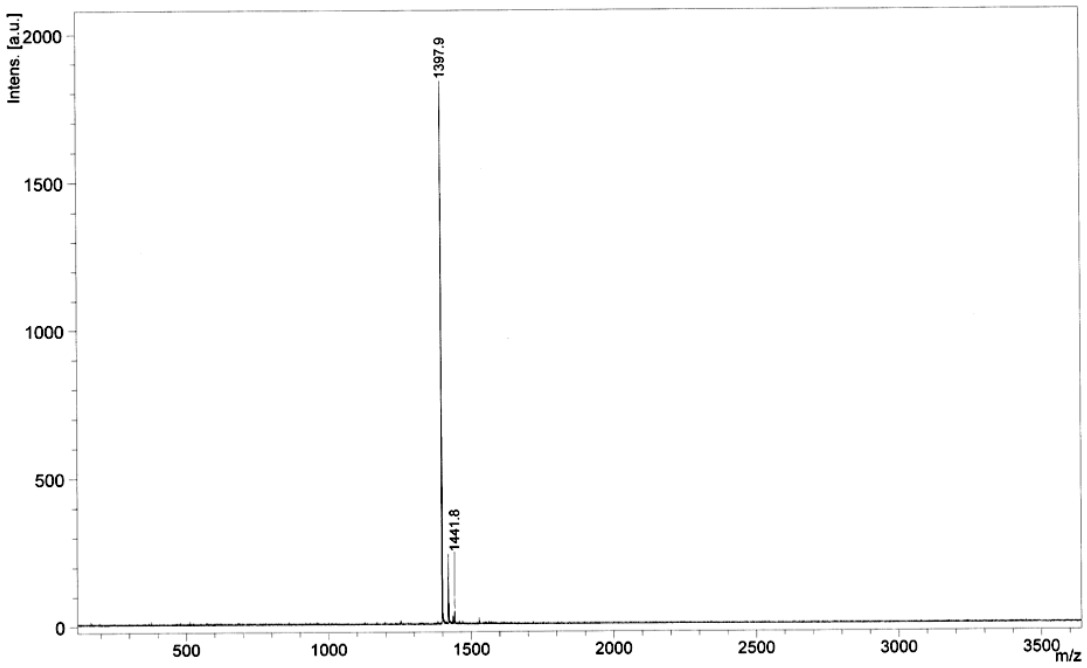
Intens. [a.u.]
2000
1500
1000
500
0
1397.9
1441.8
500
1000
1500
2000
2500
3000
3500
m/z

3.4

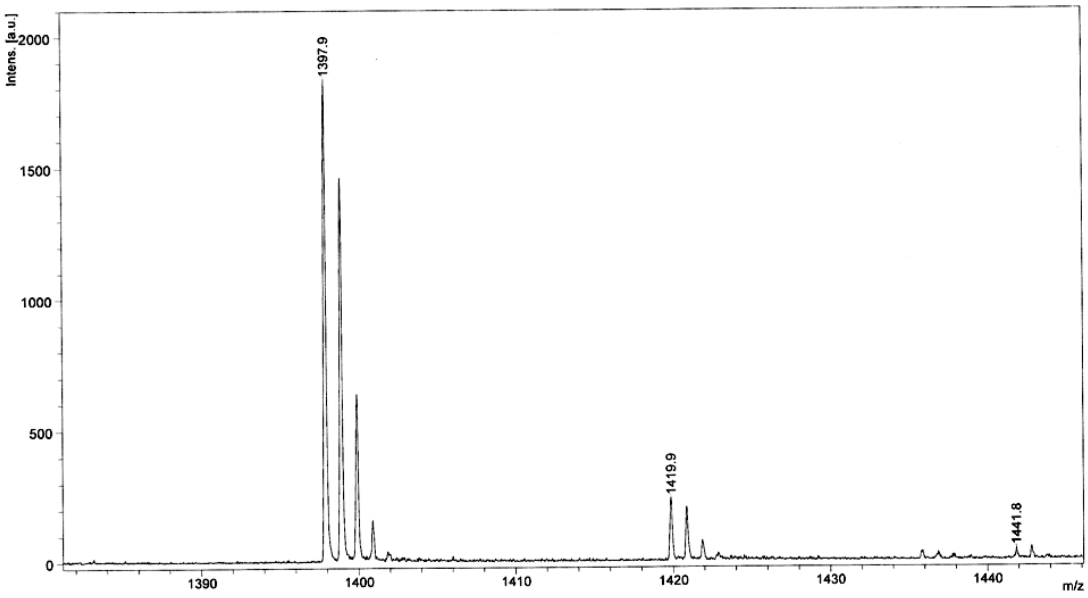
Intens. [a.u.]
2000
1500
1000
500
0
1397.9
1419.9
1441.8
1390
1400
1410
1420
1430
1440
m/z

3.5

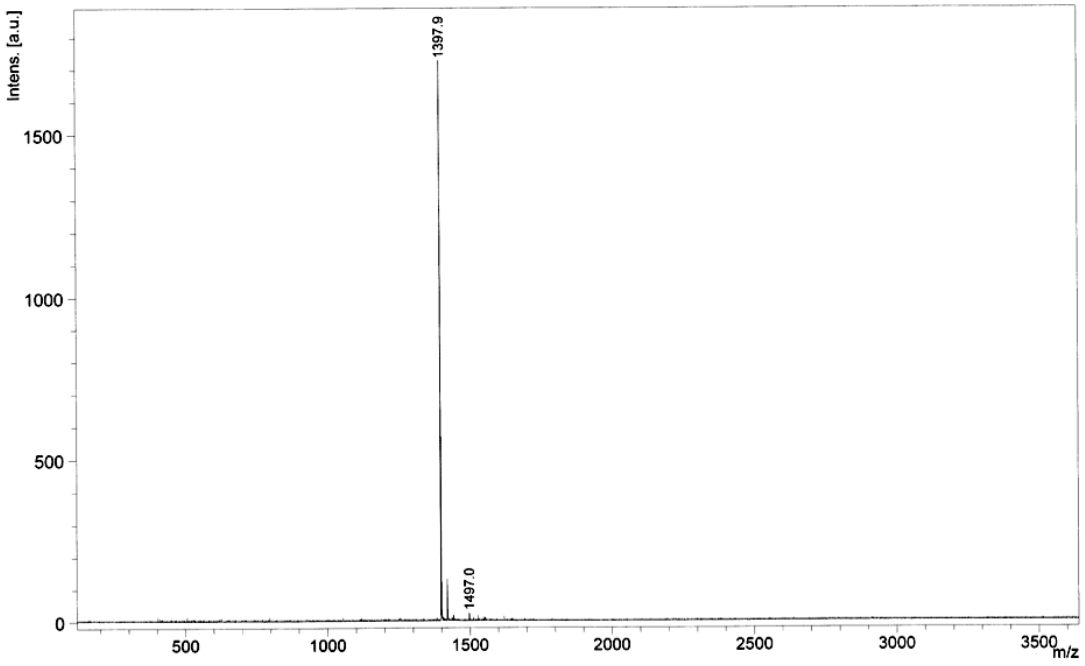
Intens. [a.u.]
1397.9
1497.0
1500
1000
500
0
500
1000
1500
2000
2500
3000
3500
m/z

3.5

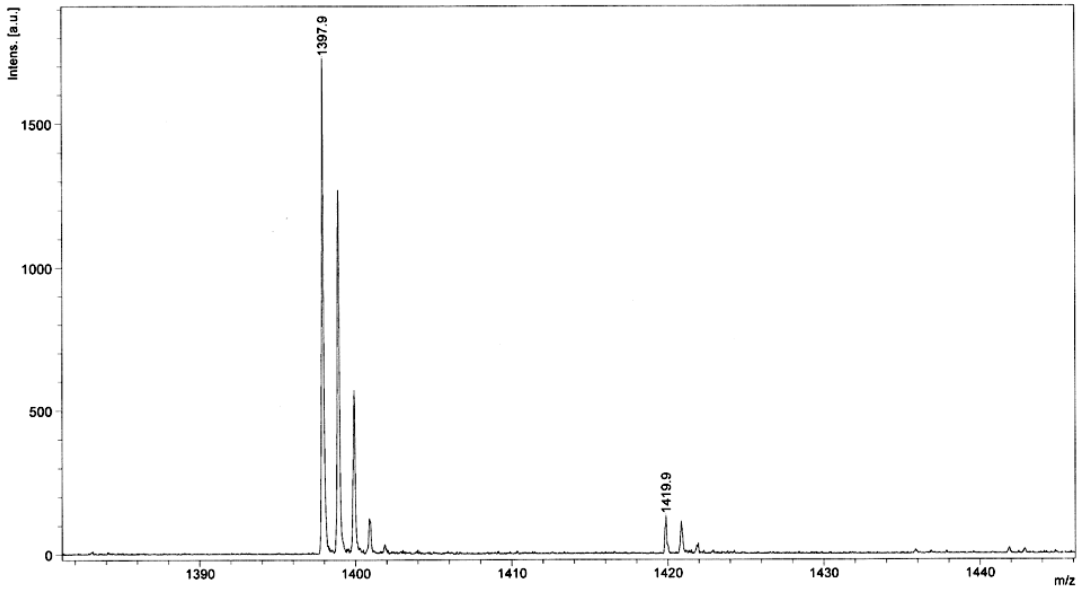
Intens. [a.u.]
1397.9
1419.9
1500
1000
500
0
1390
1400
1410
1420
1430
1440
m/z

3.6

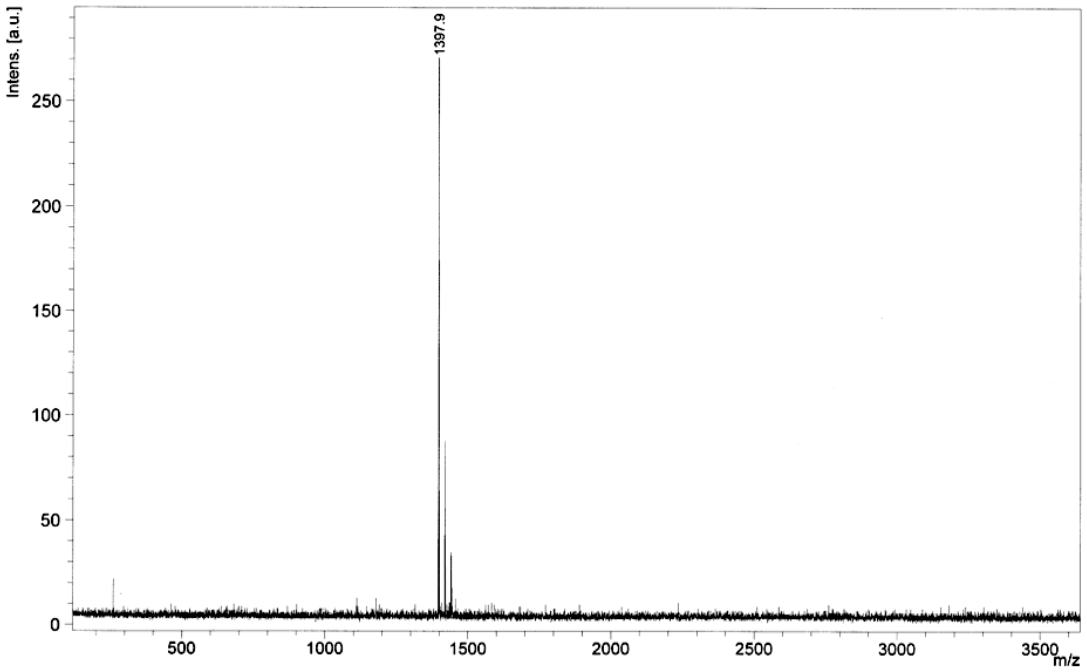
Intens. [a.u.]
1397.9
250
200
150
100
50
0
500
1000
1500
2000
2500
3000
3500
m/z

3.6

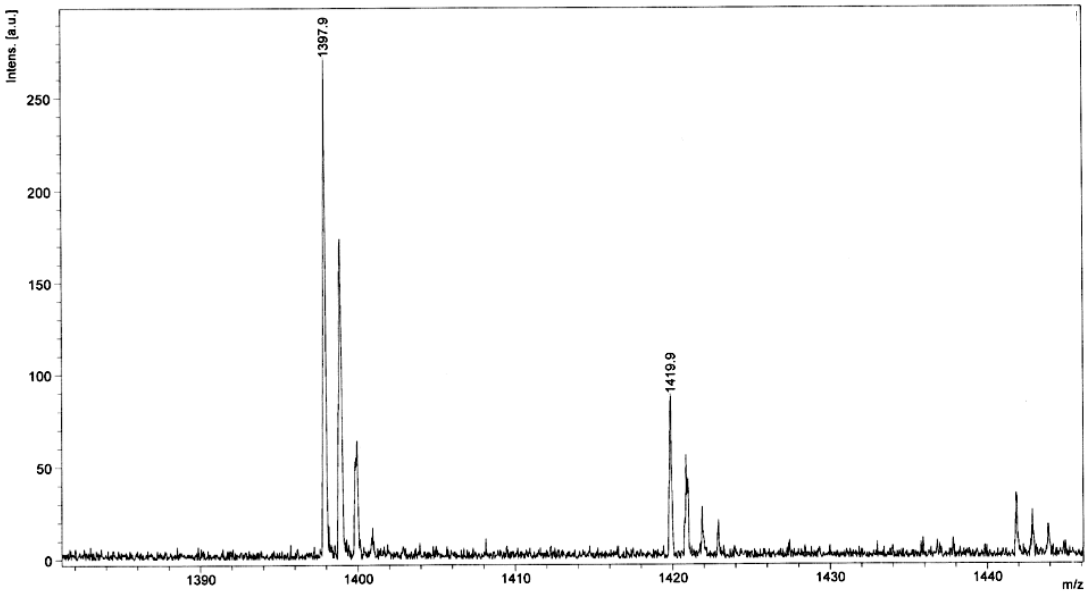
Intens. [a.u.]
1397.9
1419.9
250
200
150
100
50
0
1390
1400
1410
1420
1430
1440
m/z

3.7

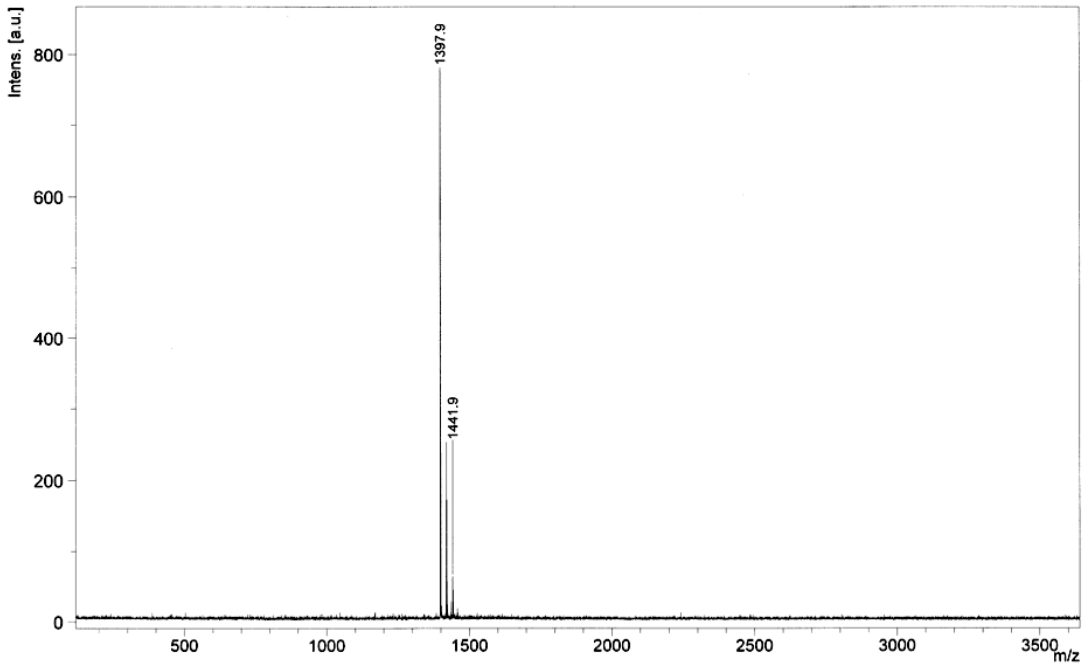
Intens. [a.u.]
800
600
400
200
0
1397.9
1441.9
500
1000
1500
2000
2500
3000
3500
m/z

3.7

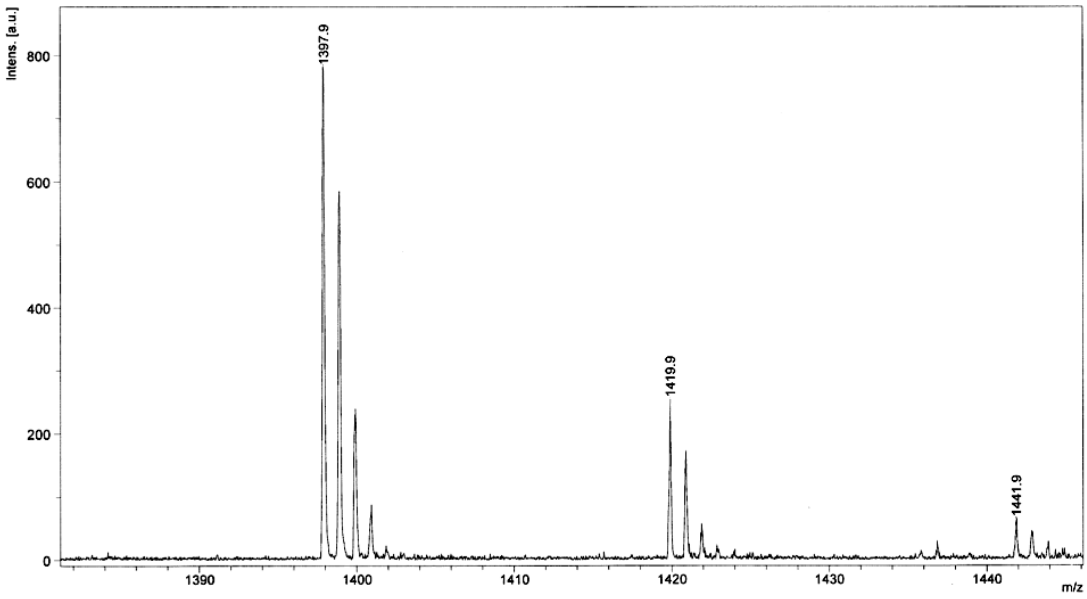
Intens. [a.u.]
800
600
400
200
0
1397.9
1419.9
1441.9
1390
1400
1410
1420
1430
1440
m/z

3.2A

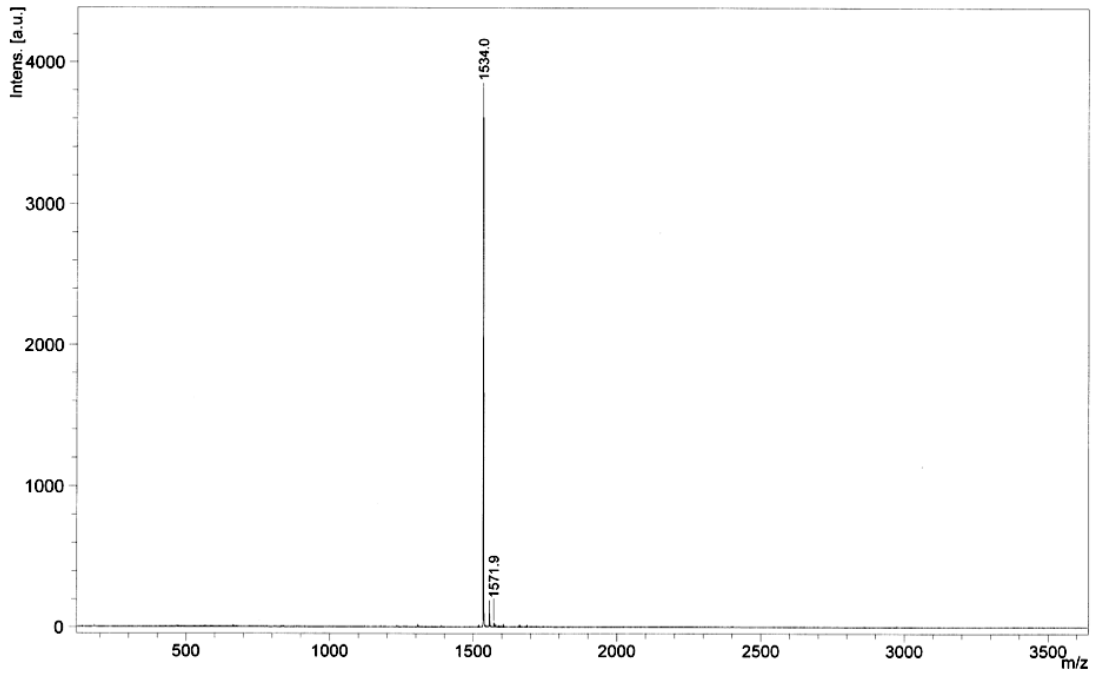
Intens. [a.u.]
4000
3000
2000
1000
0
1534.0
1571.9
500
1000
1500
2000
2500
3000
3500
m/z

3.2A

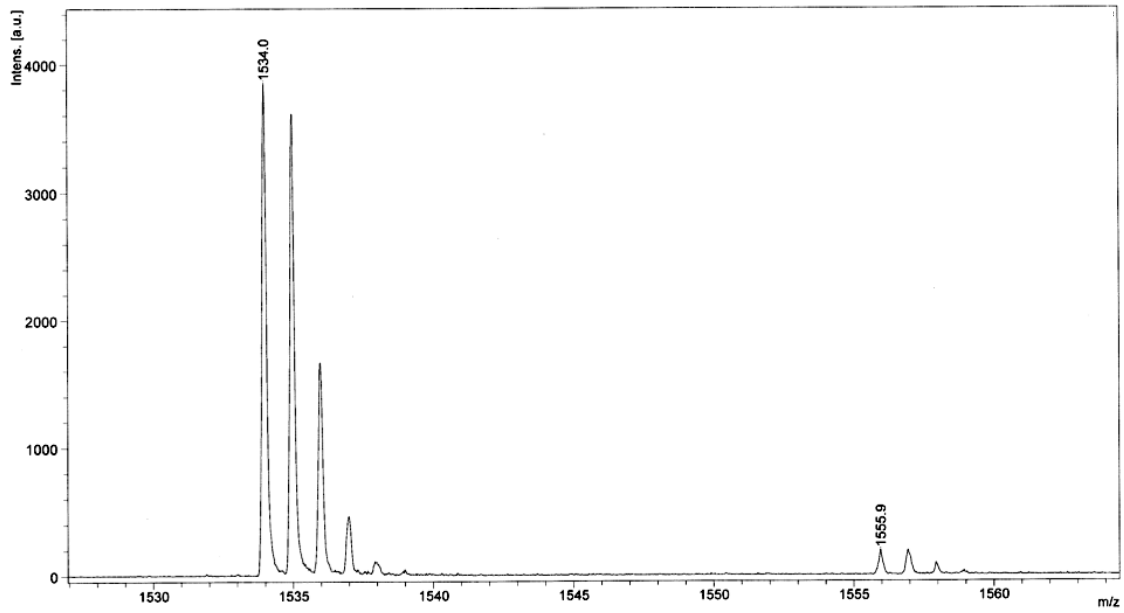
Intens. [a.u.]
4000
3000
2000
1000
0
1534.0
1555.9
1530
1535
1540
1545
1550
1555
1560
m/z

3.2B

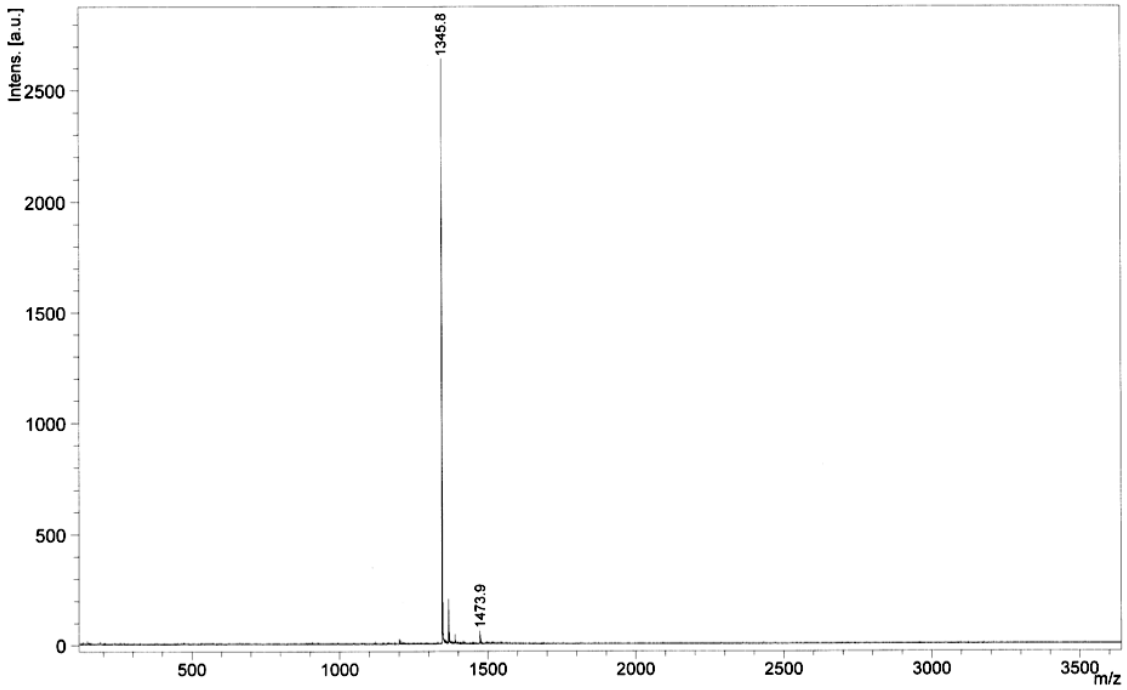
Intens. [a.u.]
2500
2000
1500
1000
500
0
1345.8
1473.9
500
1000
1500
2000
2500
3000
3500
m/z

3.2B

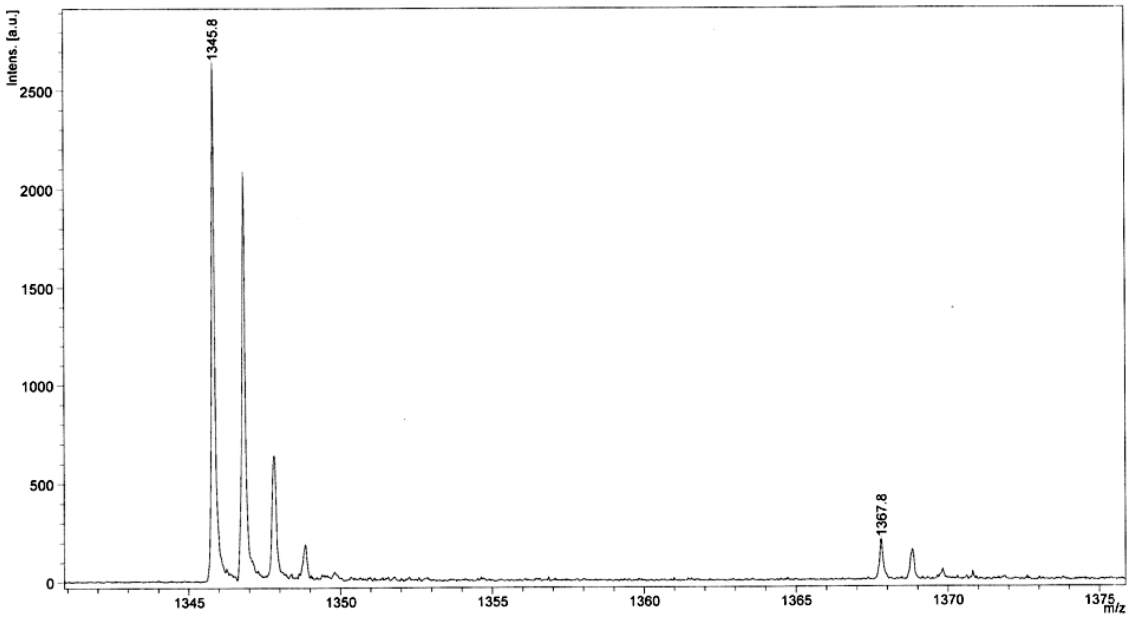
Intens. [a.u.]
2500
2000
1500
1000
500
0
1345.8
1367.8
1345
1350
1355
1360
1365
1370
1375
m/z

3.4A

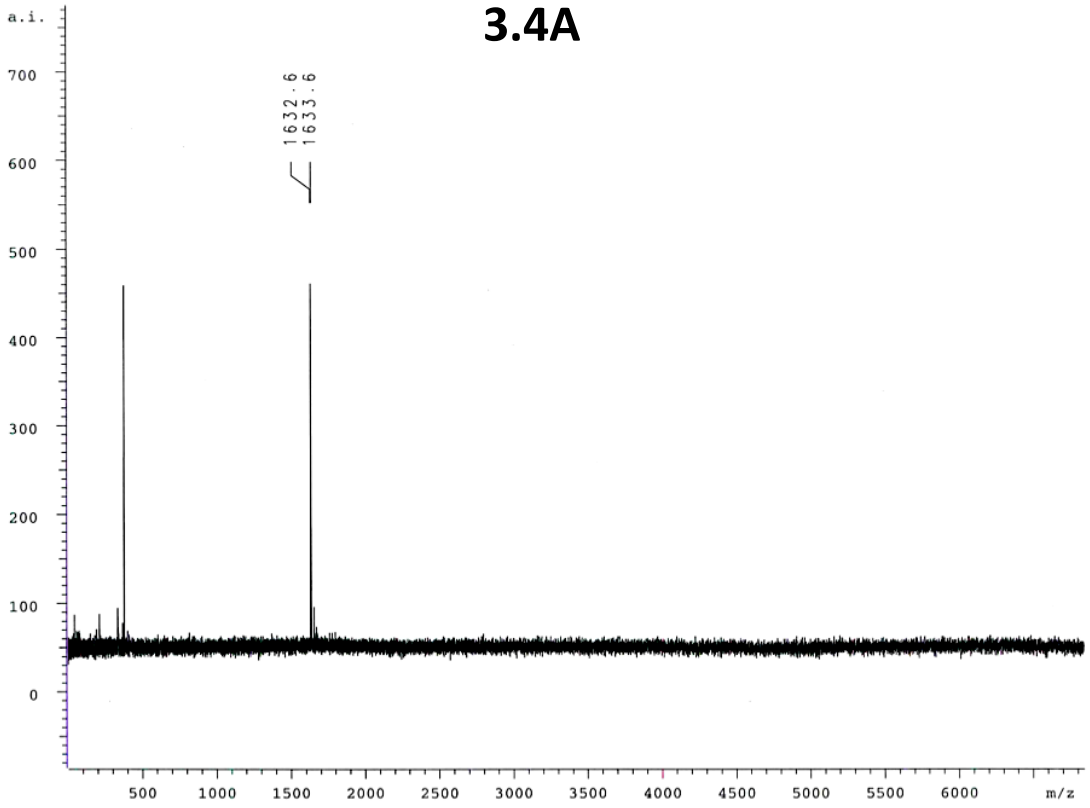
a.i.
700
600
500
400
300
200
100
0
1632.6
1633.6
500
1000
1500
2000
2500
3000
3500
4000
4500
5000
5500
6000
m/z

3.4A

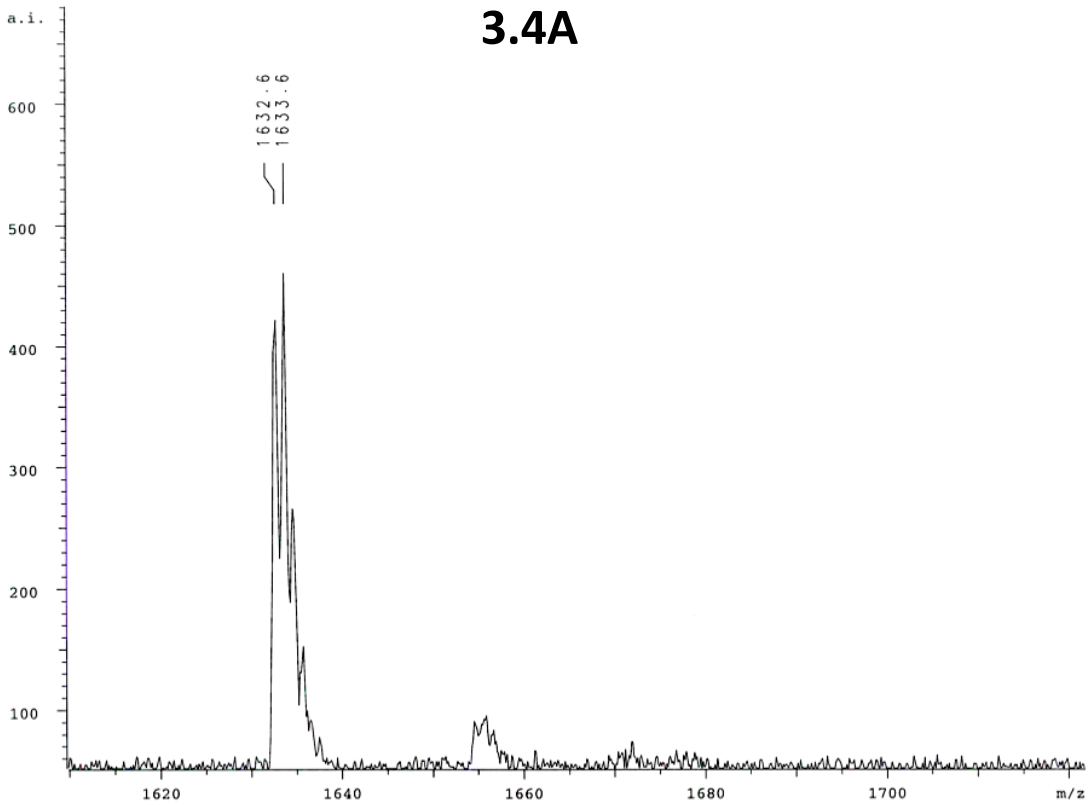
a.i.
600
500
400
300
200
100
1632.6
1633.6
1620
1640
1660
1680
1700
m/z

3.4B

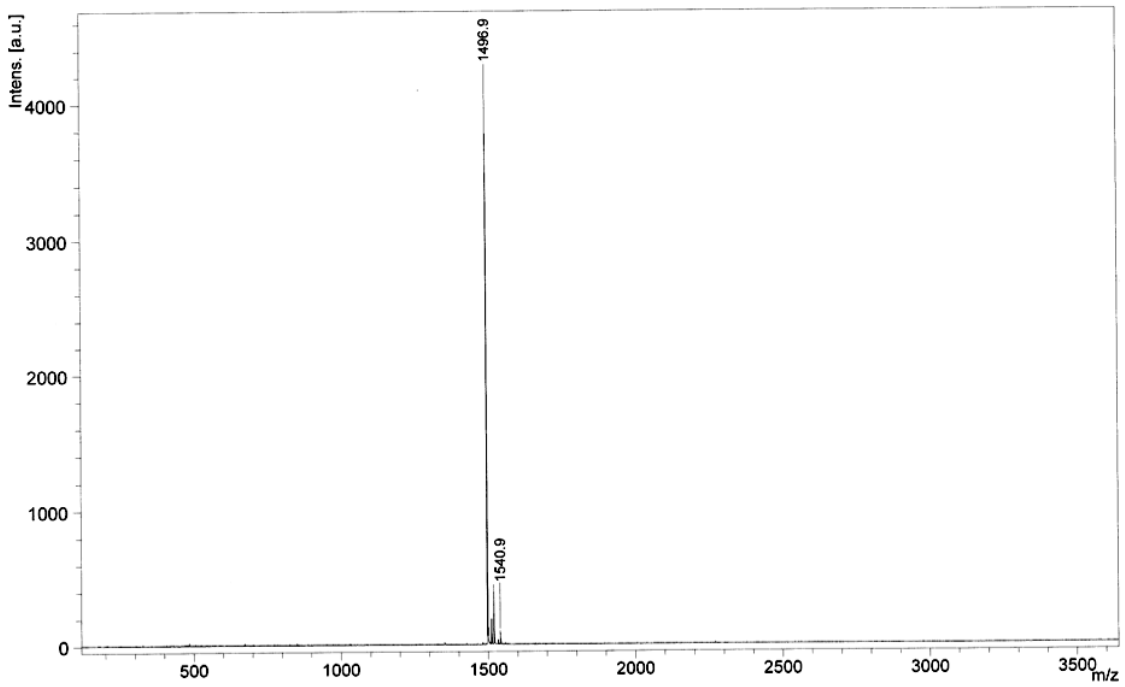
Intens. [a.u.]
4000
3000
2000
1000
0
1496.9
1540.9
500
1000
1500
2000
2500
3000
3500
m/z

3.4B

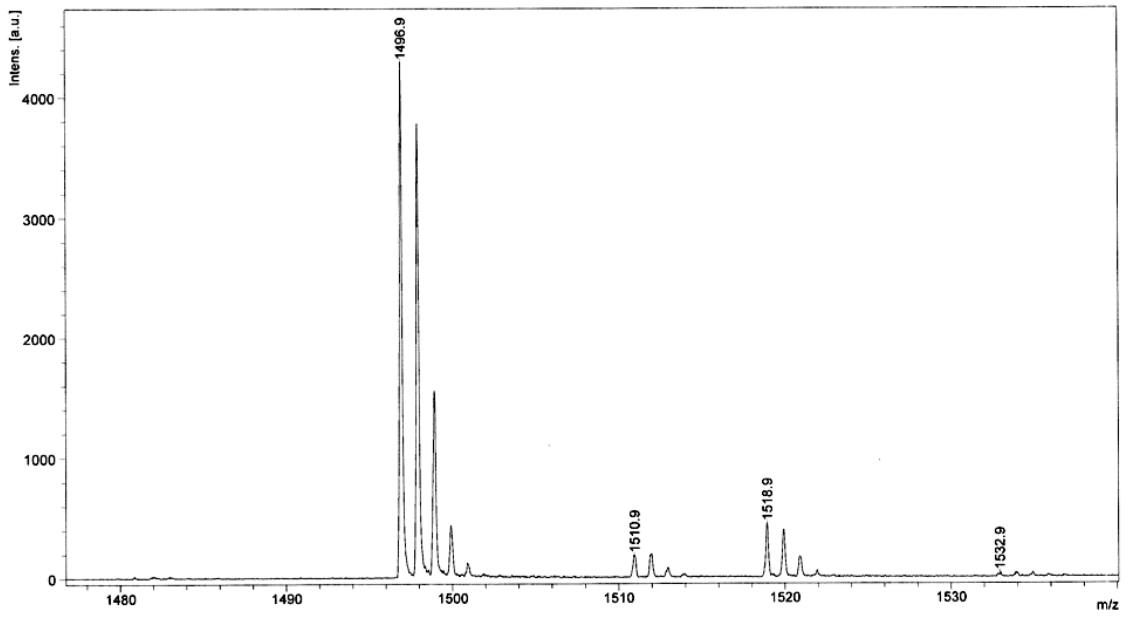
Intens. [a.u.]
4000
3000
2000
1000
0
1496.9
1510.9
1518.9
1532.9
1480
1490
1500
1510
1520
1530
m/z

3.5A

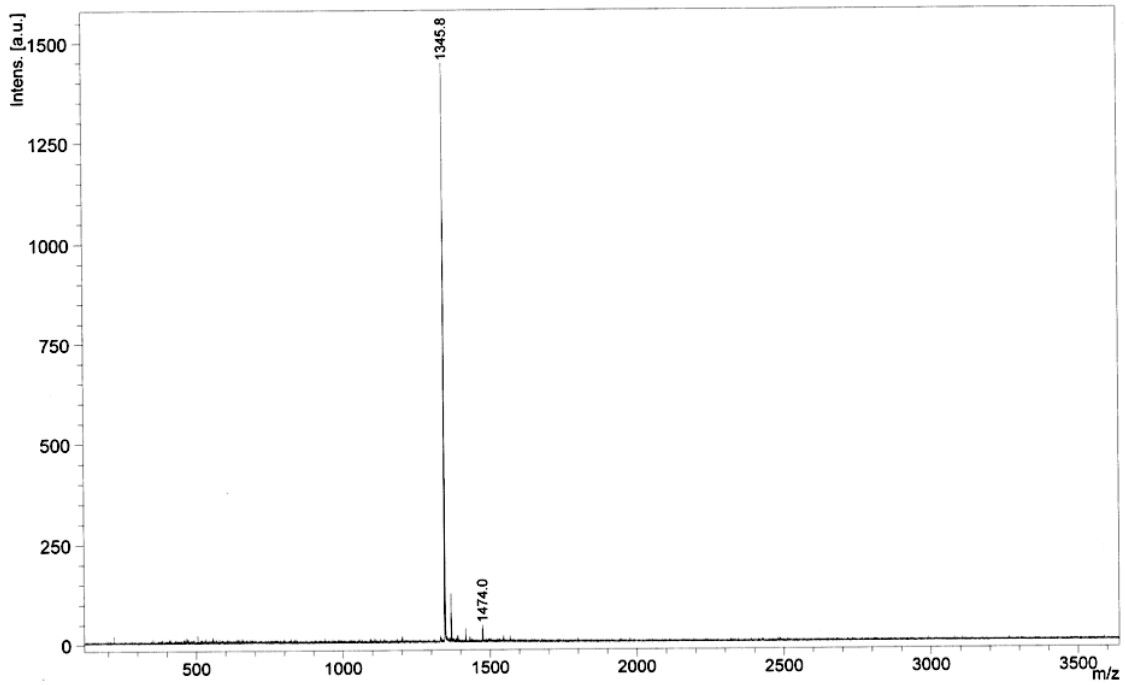
Intens. [a.u.]
1500
1250
1000
750
500
250
0
1345.8
1474.0
500
1000
1500
2000
2500
3000
3500
m/z

3.5A

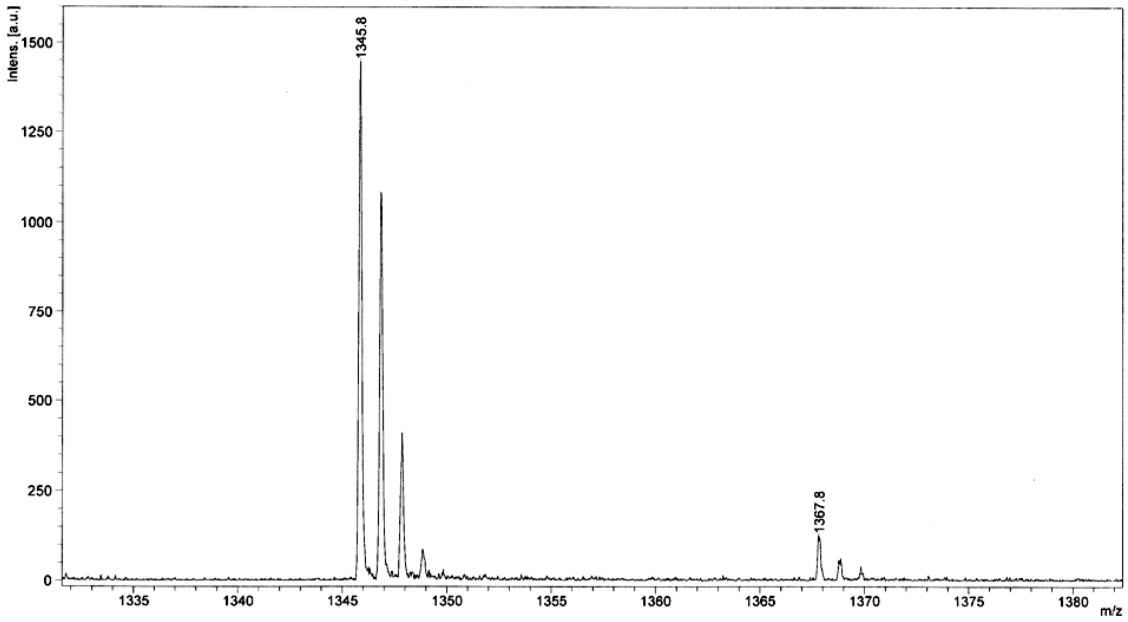
Intens. [a.u.]
1500
1250
1000
750
500
250
0
1345.8
1367.8
1335
1340
1345
1350
1355
1360
1365
1370
1375
1380
m/z

3.6A

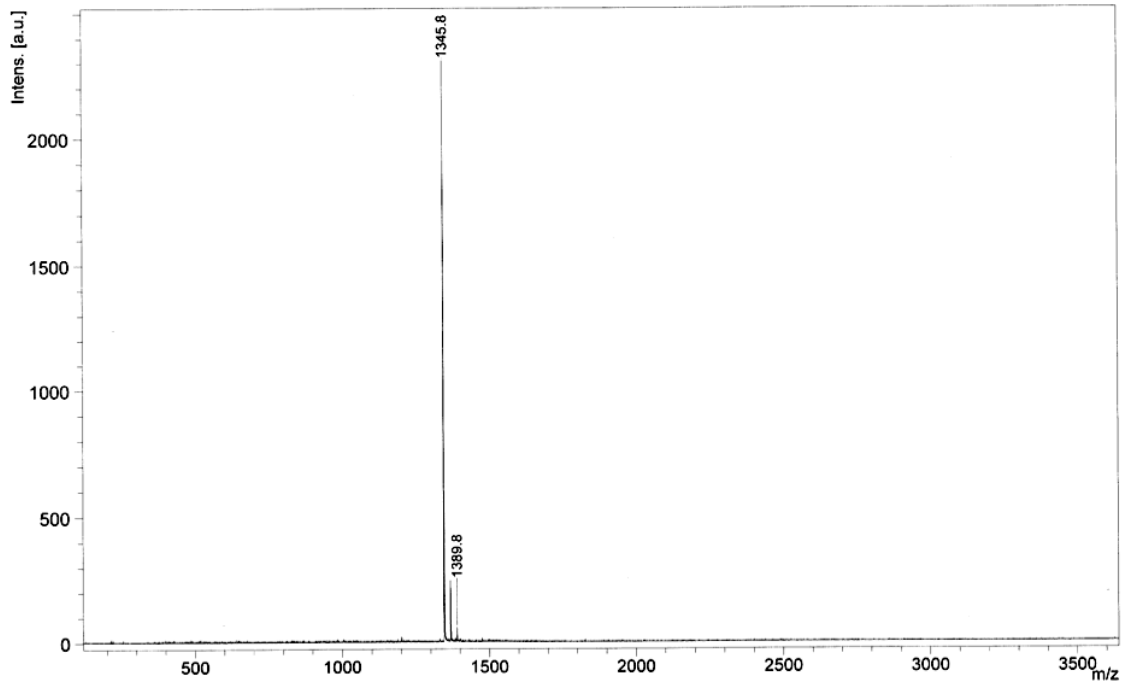

3.6A

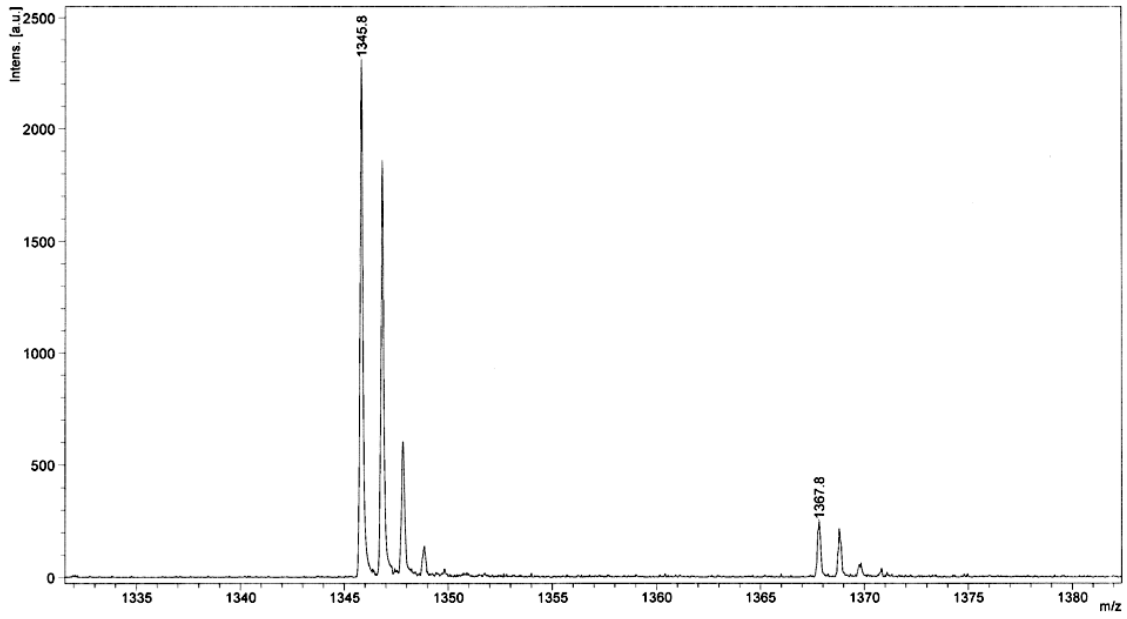

3.6.3 Circular dichroism spectroscopy

Elipticity spectra of wavelength scans (260 nm - 190 nm) were recorded in a 1 mm quartz cell with an averaging time of 6 sec for each step (1 nm step size) in pH 7.5 PBS buffer, in 50% MeOH/water mixture, and in 60% TFE/water mixture at 20 ^{o}C (AVIV circular dichroism spectrometer model 420). Thermal stability of $\alpha/\beta/\gamma$-peptides was tested by variable-temperature measurements (10 ^{o}C - 90 ^{o}C) with 10 ^{o}C intervals with an equilibration time of 10 min at each new temperature.

Plain line: CD measurements in PBS buffer pH 7.5
Dashed line: CD measurements in 60% TFE/40% PBS buffer

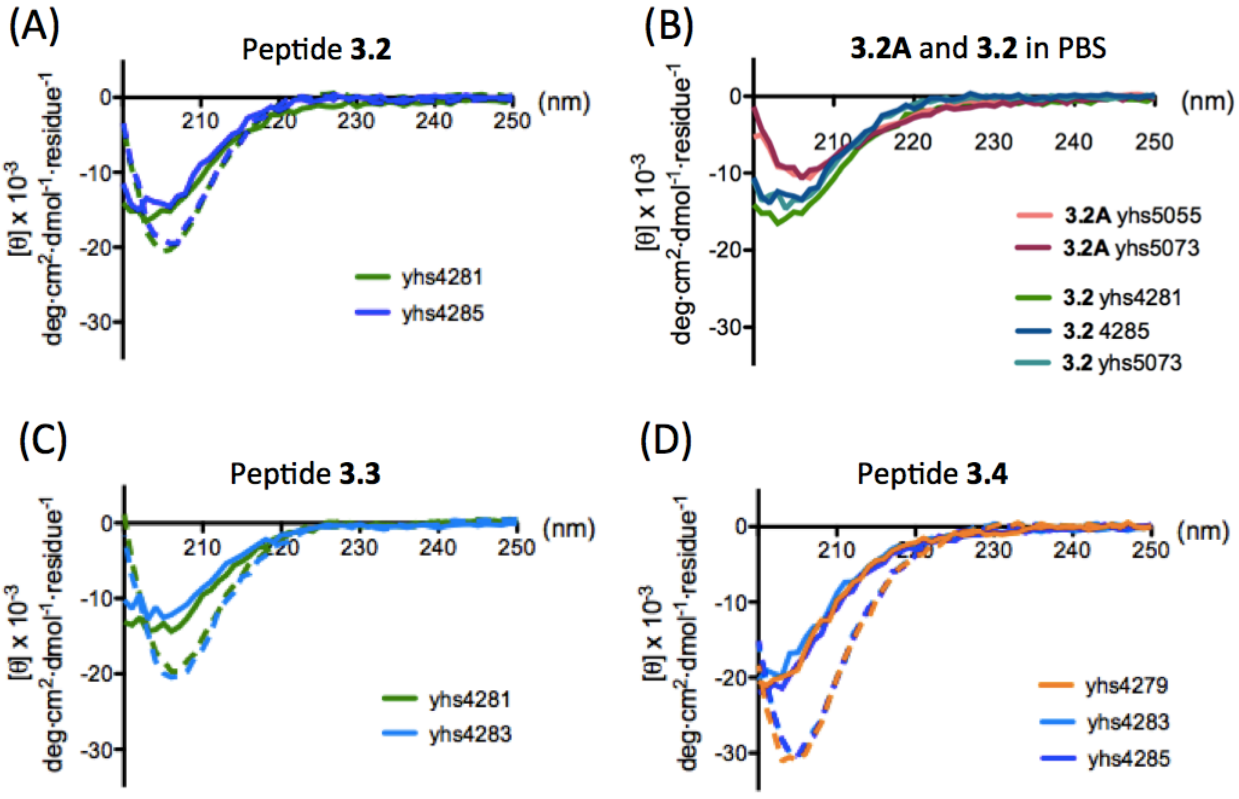

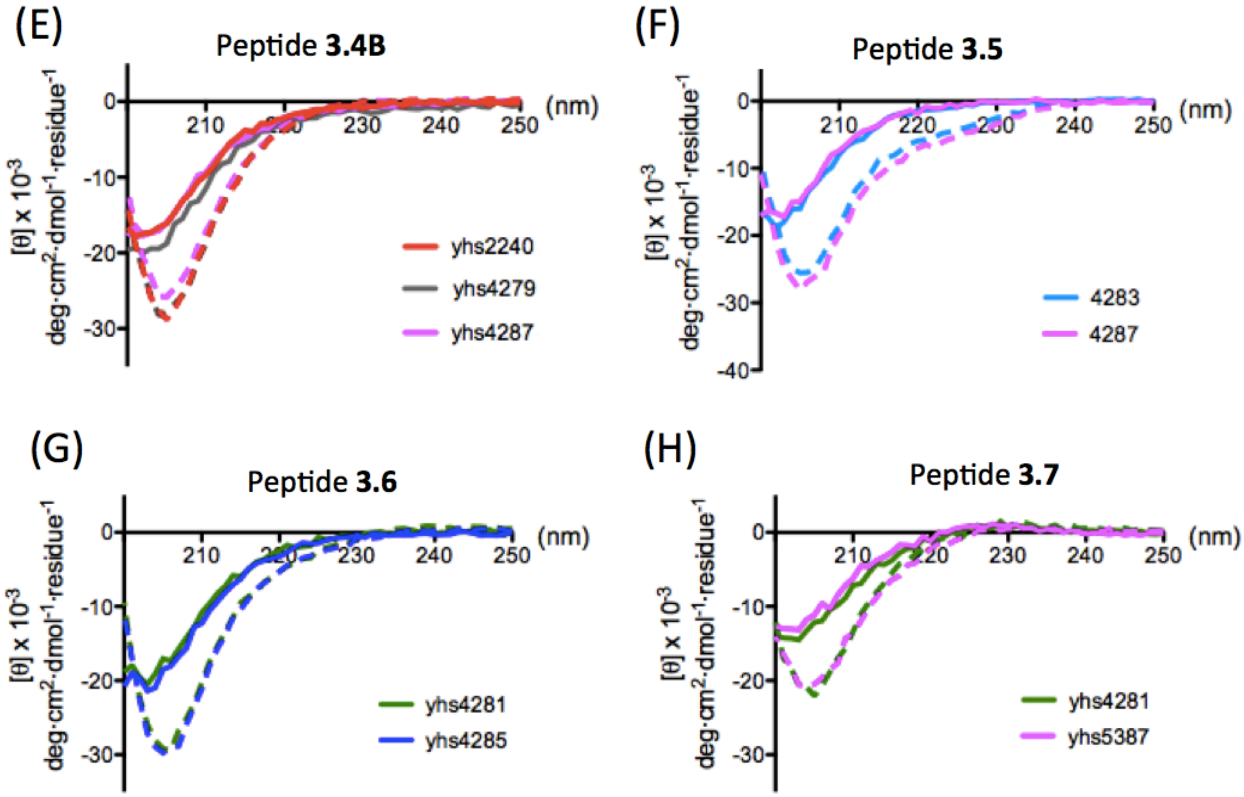

Figure 3.13 CD measurement repeats for **3.2**-**3.7**, **3.2A** and **3.4B** in PBS buffer at pH 7.5 (solid line) and in 60% TFE/40 % PBS buffer (dashed line) at 20 ^{o}C. Peptide concentration is 0.1 mM for all CD measurements. Repeat experiments have been carried out by preparing new peptide stock solutions using lyophilized peptides.

3.6.4 2D-NMR

Two-dimensional NMR study was performed on a Varian INOVA 600 MHz spectrometer equipped with a Varian 5 mm or 3 mm $^{1}H/^{13}C/^{15}N$, 3-axis PFG probes in 5 mm Shigemi tubes or in 3 mm tubes at 10 ^{o}C or at 4 ^{o}C. Peptides NMR samples were prepared as 2-8 mM in 90% H_2O/10% D_2O, in CD_3OH, or in 60 % CF_3CD_2OH/ 30 % H_2O/ 10% D_2O with 2,2-Dimethyl-2-silapentane-5-sulfonate (DSS) sodium salt as an internal standard. gCOSY, wgTOCSY, and wgROESY (watergate suppression) data were processed and analyzed using Varian VNMR 6.1 software[12] and Sparky[13], respectively.

Table 3.2 Chemical shift data for peptide **3.1D** in CD_3OH (10 ^{o}C).

Res #	aa	NH	^{1}H-α	^{1}H-β	^{1}H-γ
1	Glu	8.39	4.24		
2	GABA	8.11	2.28		3.383, 3.029
3	Ala	8.43	4.08		
4	Arg	8.48	4.15		
5	ACPC	7.77	2.65	4.18	
6	Tyr	8.12	4.34		
7	Ala	8.14	4.28		
8	GABA	7.55	2.33	1.888, 1.786	3.363, 3.034
9	Gln	8.39	4.11		
10	Ala	8.55	4.20		
11	ACPC	7.84	2.64	4.25	
12	Lys	8.14	4.22		

Table 3.3 Chemical shift data for peptide **3.2** in 90% H_2O/10% D_2O (4 ^oC).

Res #	aa	NH	^1H-α	^1H-β	^1H-γ
1	Glu	8.38	4.15		
2	γ^4Ala	8.05	2.21		3.77
3	Ala	8.32	4.18		
4	ACPC	8.37	2.60	4.23	
5	Arg	7.09	4.07		
6	Tyr	8.42	4.55		
7	Ala	7.93	4.14		
8	γ^4Ala	7.63	2.27		3.80
9	Gln	8.29	4.15		
10	ACPC	8.37	2.60	4.15	
11	Ala	8.43	4.24		
12	Lys	8.41	4.25		

Table 3.4 Chemical shift data for **3.2** in 60 % CF_3CD_2OH/30 % H_2O/10% D_2O (4 ^oC).

Res #	aa	NH	^1H-α	^1H-β	^1H-γ
1	Glu	8.02	4.15		
2	γ^4Ala	7.38	2.31		3.89
3	Ala	7.95	4.28		
4	ACPC	8.35	2.55	4.28	
5	Arg	8.09	3.96		
6	Tyr	8.39	4.60		
7	Ala	8.23	4.23		
8	γ^4Ala	7.59	2.31		3.89
9	Gln	7.99	4.25		
10	ACPC	8.36	2.61	4.30	
11	Ala	8.19	4.18		
12	Lys	8.41	4.31		

Table 3.5 Chemical shift data for peptide **3.4A** in 90% H_2O/10% D_2O (4 ^oC).

Res #	aa	NH	^1H-α	^1H-β	^1H-γ
1	Glu	8.46	4.25		
2	EtACHA	7.94			4.03
3	ACPC	8.19	2.47	4.03	
4	Arg	8.45	4.12		
5	Gln	8.85	4.31		
6	Tyr	8.18	4.63		
7	EtACHA	7.46			3.90
8	Nle	7.92	4.15		
9	Gln	8.73	4.19		
10	Ala	7.92	4.16		
11	ACPC	7.82	2.64	4.26	
12	Lys	8.41	4.21		

Table 3.6 Chemical shift data for **3.4A** in 60 % CF_3CD_2OH/30 % H_2O/10% D_2O (4 ^oC).

Res #	aa	NH	^1H-α	^1H-β	^1H-γ
1	Glu	8.21	4.29		
2	EtACHA	7.23			4.19
3	ACPC	7.79	2.60	4.32	
4	Arg	8.55	4.00		
5	Gln	8.68	4.42		
6	Tyr	8.26	4.58		
7	EtACHA	8.01			4.12
8	Nle	7.79	3.87		
9	Gln	8.40	4.08		
10	Ala	7.86	4.30		
11	ACPC	7.81	2.79	4.28	
12	Lys	8.29	4.14		

Table 3.7 Chemical shift data for peptide **3.4B** in 90% H_2O/10% D_2O (4 ^oC).

Res #	aa	NH	^1H-α	^1H-β	^1H-γ
1	Glu	8.44	4.17		
2	γ^4Ala	8.11			3.82
3	ACPC	8.04	2.65	4.17	
4	Arg	8.52	4.20		
5	Gln	8.58	4.27		
6	Tyr	8.15	4.47		
7	γ^4Ala	7.78			3.73
8	Nle	8.20	4.15		
9	Gln	8.65	4.24		
10	Ala	8.20	4.20		
11	ACPC	8.01	4.26	4.26	
12	Lys	8.43	4.24		

Table 3.8 Chemical shift data for **3.4B** in 60 % CF_3CD_2OH/30 % H_2O/10% D_2O (4 ^oC).

Res #	aa	NH	^1H-α	^1H-β	^1H-γ
1	Glu	8.00	4.29		
2	γ^4Ala	7.63	2.18		3.93
3	ACPC	7.77	2.64	4.25	
4	Arg	8.32	4.02		
5	Gln	8.50	4.35		
6	Tyr	8.08	4.56		
7	γ^4Ala	7.82	2.33		3.94
8	Nle	7.99	4.03		
9	Gln	8.75	4.13		
10	Ala	7.82	4.29		
11	ACPC	7.60	2.76	4.30	
12	Lys	8.22	4.19		

Table 3.9 Chemical shift data for peptide **3.5** in 90% H_2O/10% D_2O (4 ^oC).

Res #	aa	NH	^1H-α	^1H-β	^1H-γ
1	Glu	8.45	4.17		
2	γ^4Ala	8.15			3.77
3	ACPC	8.05	2.48	4.28	
4	γ^4Ala	8.02			3.83
5	ACPC	8.15	2.65	4.20	
6	Tyr	8.45	4.47		
7	Arg	8.20	4.21		
8	Ala-a	8.39	4.26		
9	Gln	8.40	4.24		
10a	Ala-b	8.38	4.25		
11b	Ala-c	8.26	4.19		
12	Lys	8.37	4.24		

Table 3.10 Chemical shift data for **3.5** in 60 % CF_3CD_2OH/30 % H_2O/10% D_2O (4 ^oC).

Res #	aa	NH	^1H-α	^1H-β	^1H-γ
1	Glu	8.08	4.23		
2	γ^4Ala	7.59	2.276, 2.172		3.89
3	ACPC	7.76	2.52	4.40	
4	γ^4Ala	7.69	2.28		4.08
5	ACPC	8.20	2.76	4.28	
6	Tyr	8.64	4.27		
7	Arg	8.35	4.18		
8	Ala	8.04	4.19		
9	Gln	8.23	4.14		
10	Ala	8.06	4.17		
11	Ala	7.85	4.26		
12	Lys	7.79	4.24		

Table 3.11 Chemical shift data for peptide **3.6** in 90% H_2O/10% D_2O (4 ^oC).

Res #	aa	NH	^1H-α	^1H-β	^1H-γ
1	Glu	8.46	4.18		
2	γ^4Ala	8.13			3.81
3	ACPC	8.09	2.67	4.20	
4	Arg	8.46	4.14		
5	γ^4Ala	8.03			3.85
6	ACPC	8.03	2.58	4.14	
7	Tyr	8.35	4.50		
8	Ala	8.28	4.29		
9	Gln	8.24	4.25		
10a	Ala	8.39	4.27		
11b	Ala	8.32	4.26		
12	Lys	8.37	4.24		

Table 3.12 Chemical shift data for **3.6** in 60 % CF_3CD_2OH/30 % H_2O/10% D_2O (4 ^oC).

Res #	aa	NH	^1H-α	^1H-β	^1H-γ
1	Glu	8.08	4.24		
2	γ^4Ala	7.48	2.27		3.95
3	ACPC	7.66	2.67	4.28	
4	Arg	8.36	4.09		
5	γ^4Ala	8.16	2.29		4.10
6	ACPC	7.92	2.60	4.22	
7	Tyr	8.31	4.23		
8	Ala	8.14	4.25		
9	Gln	8.01	4.18		
10	Ala	8.36	4.16		
11	Ala	7.98	4.18		
12	Lys	7.68	4.24		

Table 3.13 Chemical shift data for peptide **3.7** in 90% H_2O/10% D_2O (4 ^oC).

Res #	aa	NH	^1H-α	^1H-β	^1H-γ
1	Glu	8.43	4.18		
2	γ^4Ala	8.07	2.23		3.80
3	Ala	8.25	4.14		
4	ACPC	8.30	2.62	4.18	
5	Arg	8.30	4.15		
6	γ^4Ala	8.03	2.20		3.77
7	Tyr	8.11	4.38		
8	ACPC	8.21	2.45	4.18	
9	Gln	8.38	4.25		
10	Ala	8.45	4.14		
11	Ala	8.19	4.21		
12	Lys	8.25	4.21		

Table 3.14 Chemical shift data for **3.7** in 60 % CF_3CD_2OH/30 % H_2O/10% D_2O (4 ^oC).

Res #	aa	NH	^1H-α	^1H-β	^1H-γ
1	Glu	8.06	4.25		
2	γ^4Ala	7.50	2.30		3.90
3	Ala	7.95	4.17		
4	ACPC	8.23	2.62	4.26	
5	Arg	8.06	4.13		
6	γ^4Ala	8.08	2.29		3.92
7	Tyr	7.94	4.33		
8	ACPC	8.28	2.52	4.24	
9	Gln	8.33	4.04		
10	Ala	8.52	4.21		
11	Ala	7.96	4.20		
12	Lys	7.84	4.24		

Ac–E γcyc βcyc R Q Y γcyc Nle Q A βcyc K–NH_2 **3.4A**

(A)

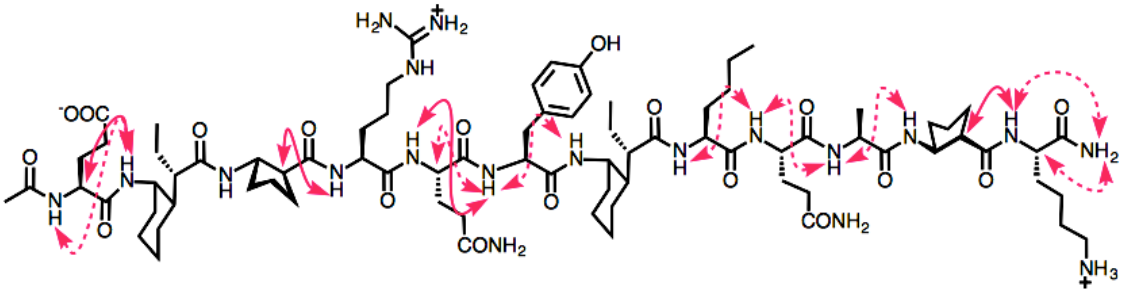

(B)

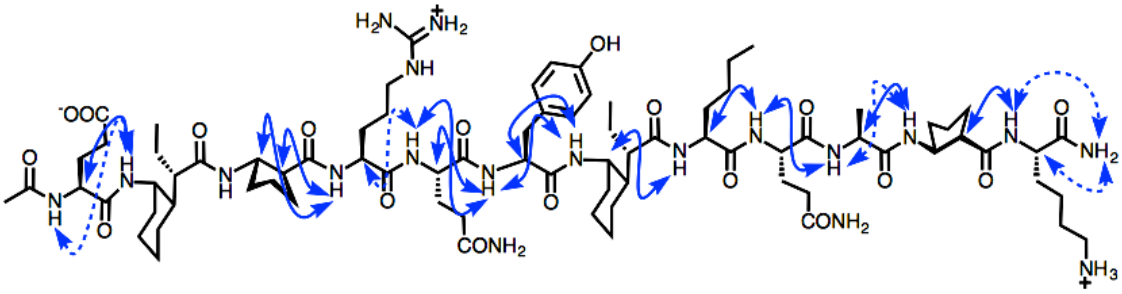

Figure 3.14 Sequential NOEs from α/β/γ-peptide **3.4A** in (A) 60 % CF_3CD_2OH/30 % H_2O/10% D_2O (shown as pink), and (B) 90% H_2O/10% D_2O (shown as blue), at 4 °C. Medium (2.6~3.5 Å) and weak (3.6~5.5 Å) NOEs are shown as plain and dashed curves, respectively.

Ac–E γ⁴hA βcyc R Q Y γ⁴hA Nle Q A βcyc K–NH_2 **3.4B**

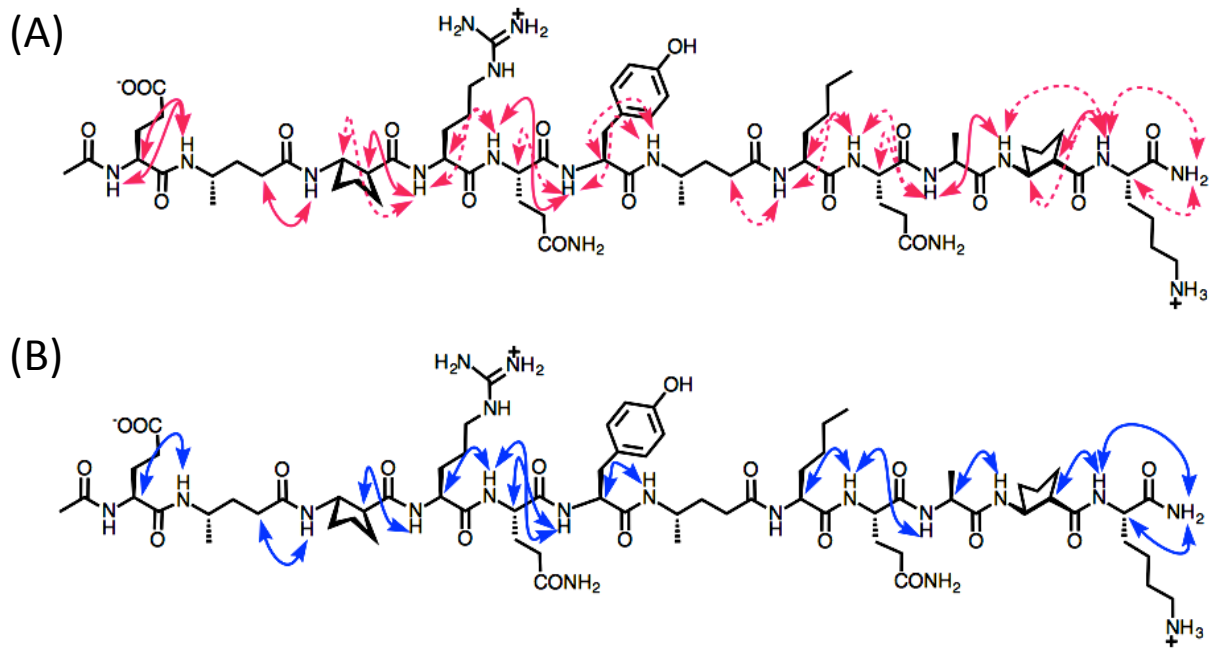

Figure 3.15 Sequential NOEs from α/β/γ-peptide **3.4B** in (A) 60 % CF_3CD_2OH/30 % H_2O/10% D_2O (shown as pink), and (B) 90% H_2O/10% D_2O (shown as blue), at 4 °C. Medium (2.6~3.5 Å) and weak (3.6~5.5 Å) NOEs are shown as plain and dashed curves, respectively.

Table 3.15 Sequential NOEs from **3.2**, measured in 60 % CF_3CD_2OH/30 % H_2O /10% D_2O and 90% H_2O/10% D_2O at 4 ^oC.

60 % CF_3CD_2OH/30 % H_2O /10% D_2O	Å	90% H_2O/10% D_2O	Å
Glu(01)HG-γ^4hAla(02)HN	3.4	Glu(01)HA- γ^4hAla(02)HN	2.9
γ^4hAla (02)HA-Glu(01)HN	4.4	γ^4hAla(02)HG-Glu(01)HN	3.6
γ^4hAla (02)HA-Ala(03)NH	3.4	γ^4hAla(02)HN-Glu(01)HN	3.5
ACPC(04)HA-Arg(05)HN	3.2	γ^4hAla(02)HA-Ala(03)NH	3.3
Ala(07)HA- γ^4hAla (08)HN	3.2	ACPC(04)HA-Arg(05)HN	2.5
γ^4hAla (08)HN-Ala(07)HN	3.5	Tyr(06)HA-Ala(07)NH	3.2
Gln(09)HN-ACPC(10)HN	3.0	Ala(07)NH-Tyr(06)HN	3.1
ACPC(10)HA-Ala(11)NH	2.9	Ala(07)HA- γ^4hAla(08)HN	2.8
Ala(11)HA-Lys(12)HN	4.2	γ^4hAla(08)HN-Ala(07)NH	3.5
NH_2(13)NH'-Lys(12)HN	3.2	γ^4hAla(08)HA-Gln(09)HN	2.9
		ACPC(10)HA-Ala(11)HN	2.5
		Lys(12)HA-NH_2(13)HN	3.3
		NH_2(13)NH'-Lys(12)HN	3.4

Table 3.16 Sequential NOEs from **3.5**, measured in 60 % CF_3CD_2OH/30 % H_2O /10% D_2O and 90% H_2O/10% D_2O at 4 ^oC.

60 % CF_3CD_2OH/30 % H_2O /10% D_2O	Å	90% H_2O/10% D_2O	Å
Glu(01)HA- γ^4hAla(02)HN	2.6	ACPC(03)HA- γ^4hAla(04)HN	2.6
γ^4hAla(02)HN-Glu(01)HN	3.4	ACPC(03)HB- γ^4hAla(04)HN	3.1
γ^4hAla(02)HA'-ACPC(03)HN	3.1	ACPC(05)HA-Tyr(06)HN	2.8
ACPC(03)HA- γ^4hAla(04)HN	2.7	Tyr(06)HA-Arg(07)HN	2.7
ACPC(03)HB- γ^4hAla(04)HN	3.0	Tyr(06)HB-Arg(07)HN	3.9
ACPC(05)HA-Tyr(06)HN	3.2	Lys(12)HA-NH_2(13)HN	3.2
Ala(08)HN-Arg(07)HN	3.6	Lys(12)HN-NH_2(13)HN	3.9
Ala(10)HN-Gln(09)HN	3.4		
Ala(11)HN-Ala(10)HN	3.9		
Lys(12)HA-NH_2(13)HN	3.7		
NH_2(13)HN-Lys(12)HN	3.6		

Table 3.17 Sequential NOEs from **3.6**, measured in 60 % CF_3CD_2OH/30 % H_2O /10% D_2O and 90% H_2O/10% D_2O at 4 ^oC.

60 % CF_3CD_2OH/30 % H_2O /10% D_2O	Å	90% H_2O/10% D_2O	Å
Glu(01)HA- γ^4hAla(02)HN	3.0	Glu(01)HA- γ^4hAla(02)HN	2.5
γ^4hAla(02)HN-Glu(01)HN	3.4	ACPC(03)HA-Arg(04)HN	2.7
ACPC(03)HA-Arg(04)HN	3.3	ACPC(06)HA-Tyr(07)HN	2.6
γ^4hAla(05)HA-ACPC(06)HN	3.8	Tyr(07)HA-Ala(08)HN	3.9
ACPC(06)HA-Tyr(07)HN	3.3	Lys(12)HA-NH_2(13)HN	3.0
Ala(10)HN-Gln(09)HN	3.8		
Ala(10)HN-Ala(11)HN	3.9		
Lys(12)HN-Ala(11)HN	4.0		
Lys(12)HA-NH_2(13)HN	3.5		
NH_2(13)HN-Lys(12)HN	4.0		

Table 3.18 Sequential NOEs from **3.7**, measured in 60 % CF_3CD_2OH/30 % H_2O /10% D_2O and 90% H_2O/10% D_2O at 4 ^oC.

60 % CF_3CD_2OH/30 % H_2O /10% D_2O	Å	90% H_2O/10% D_2O	Å
γ^4hAla(02)HN-Glu(01)HN	3.5	γ^4hAla(02)HN-Glu(01)HN	3.4
Glu(01)HA- γ^4hAla(02)HN	3.0	Glu(01)HA- γ^4hAla(02)HN	3.4
Ala(03)NH-ACPC(04)HN	4.2	γ^4hAla(02)HG-Ala(03)HN	4.4
ACPC(04)HA-Arg(05)HN	3.0	γ^4hAla(02)HA-Ala(03)HN	2.8
ACPC(08)HA-Gln(09)HN	3.0	Arg(05)HA- γ^4hAla(06)HN	3.9
Ala(10)CH_3-Tyr(07)HD	3.2	γ^4hAla(06)HN-Arg(05)HN	3.4
Gln(09)HB-Ala(10)HN	3.8	γ^4hAla(06)HA-Tyr(07)HN	2.9
Ala(11)HN-Ala(10)HN	3.5	Tyr(07)HD-ACPC(08)HN	4.3
Lys(12)HA-NH_2(13)HN	3.5	Tyr(07)HA-ACPC(08)HN	2.6
NH_2(13)HN-Lys(12)HN	3.6	Tyr(07)HB-ACPC(08)HN	3.4
		ACPC(08)HA-Gln(09)HN	2.8
		Gln(09)HG-Ala(10)HN	3.7
		Gln(09)HA-Ala(10)HN	3.1
		Ala(11)HN-Ala(10)HN	3.7
		NH_2(13)HN-Lys(12)HN	3.6
		Lys(12)HA-NH_2(13)HN	3.1

Partial wgROESY spectra of **3.1D** in CD_3OH (10 ^oC)

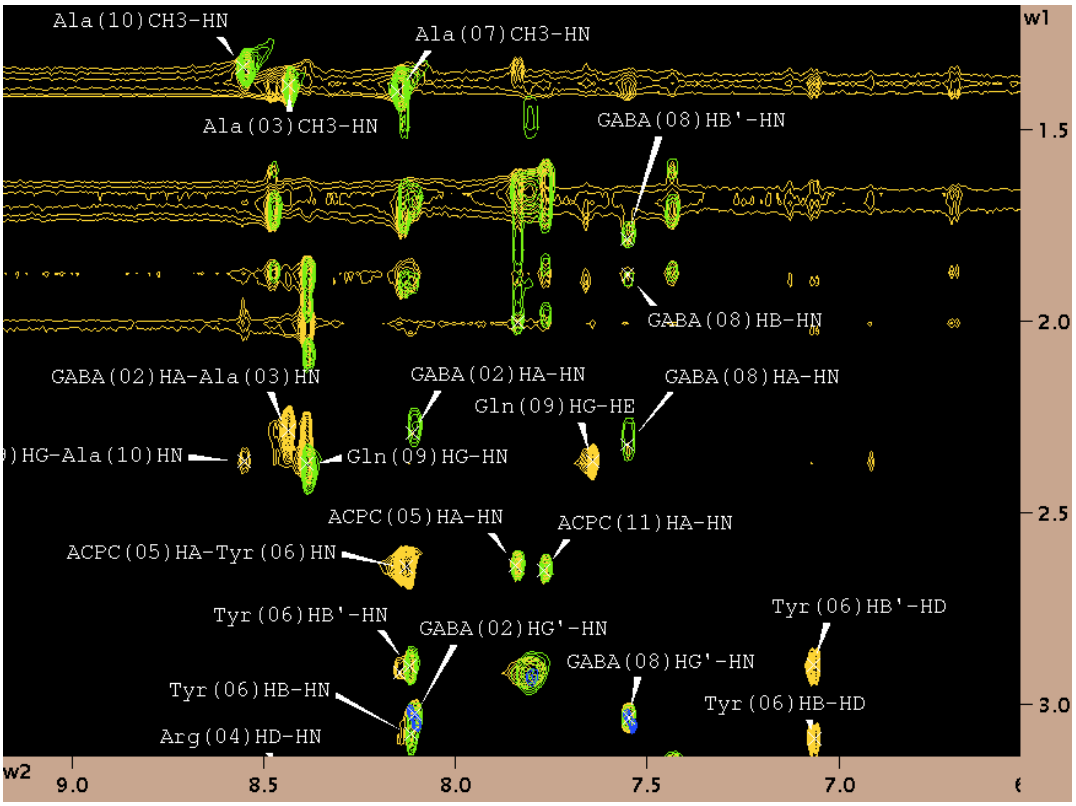

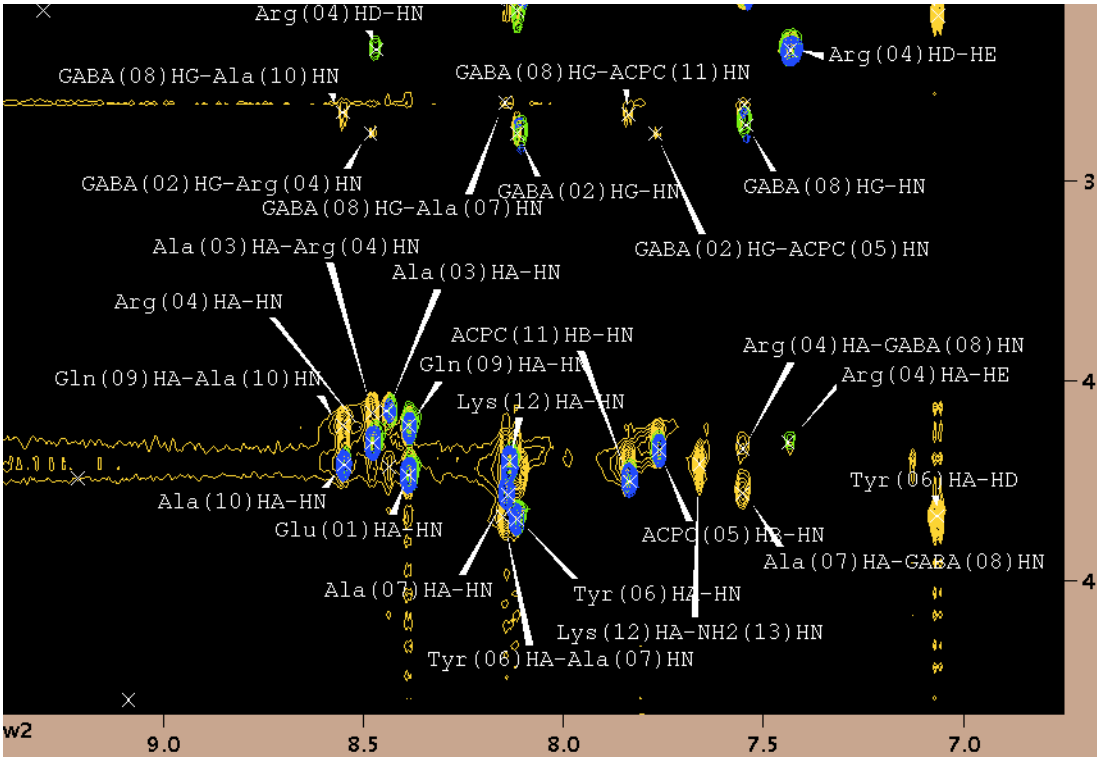

Partial wgROESY spectra of **3.2** in 90% H_2O/10% D_2O (4 ^oC)

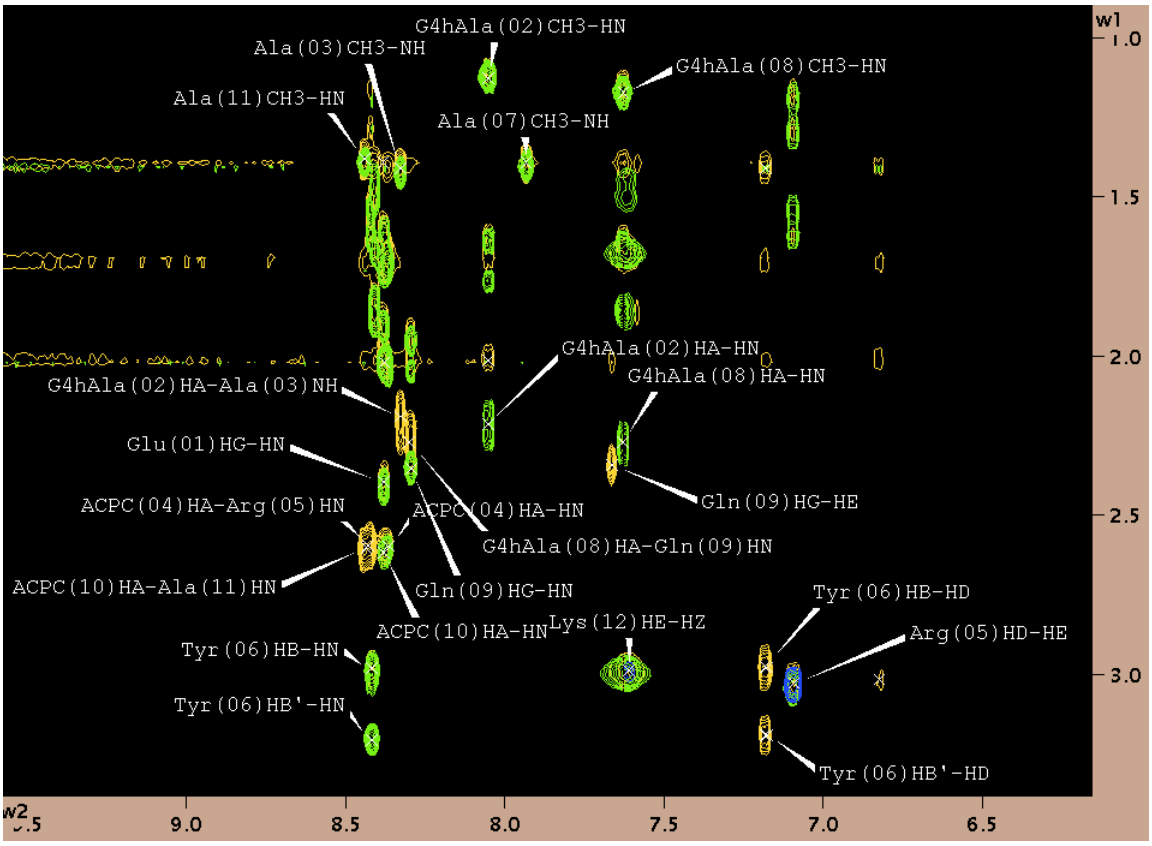

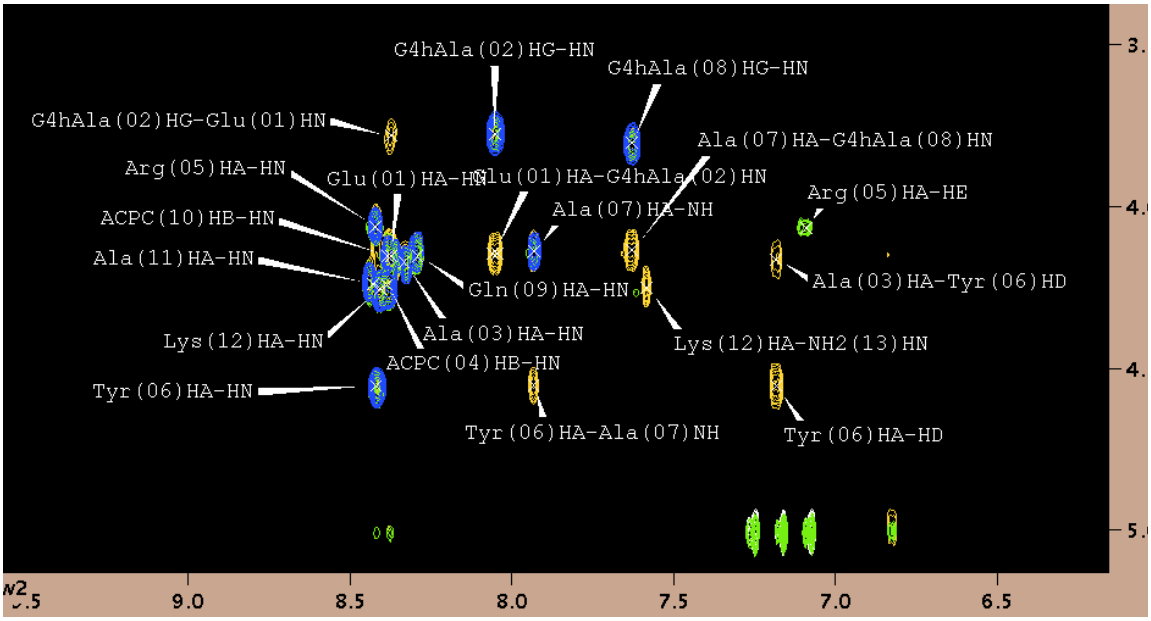

Partial wgROESY spectra of **3.2** in 60 % CF_3CD_2OH/30 % H_2O/10% D_2O (4 ^oC)

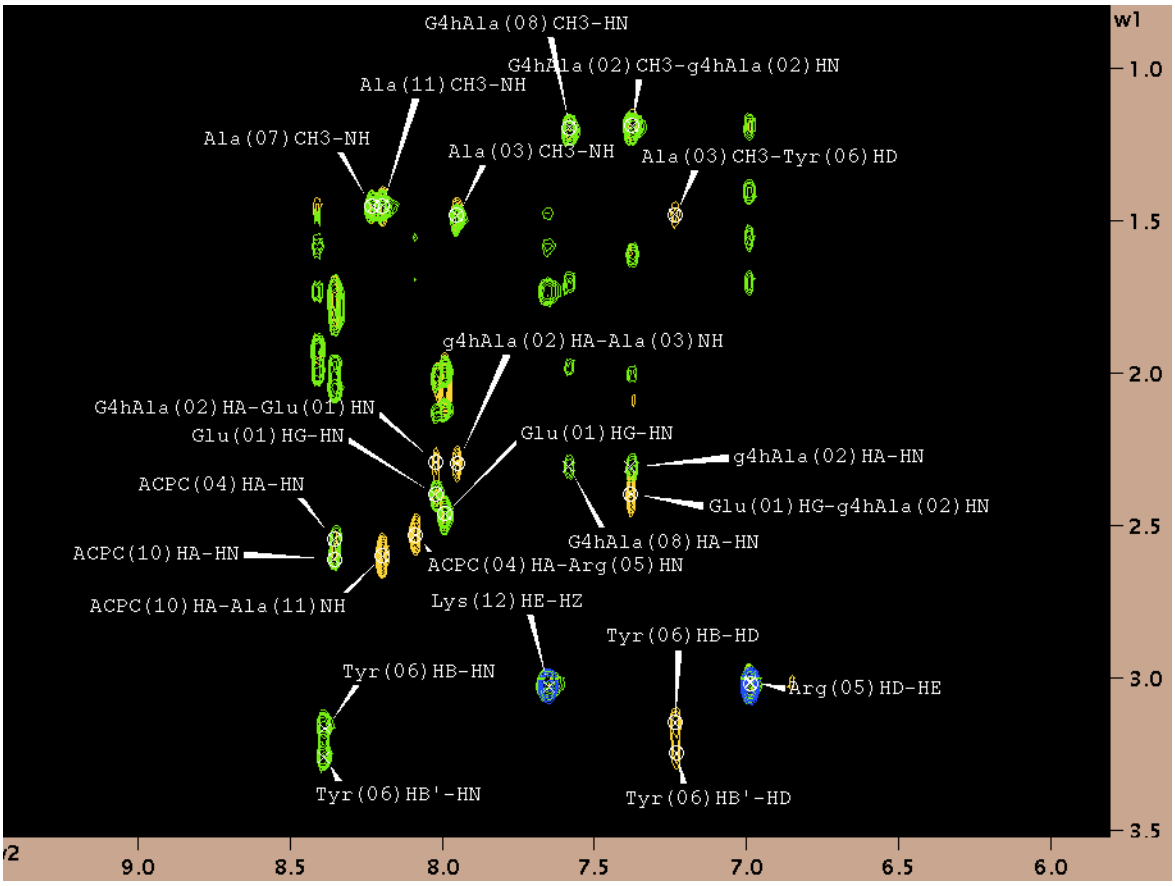

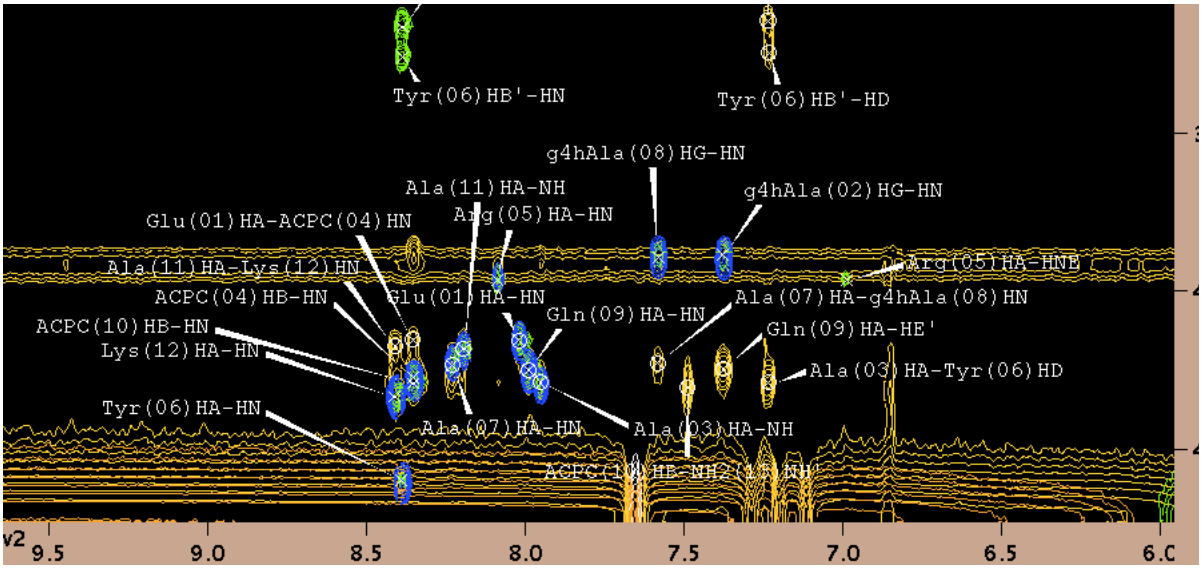

Partial wgROESY spectra of **3.4A** in 90% H_2O/10% D_2O (4 ^oC)

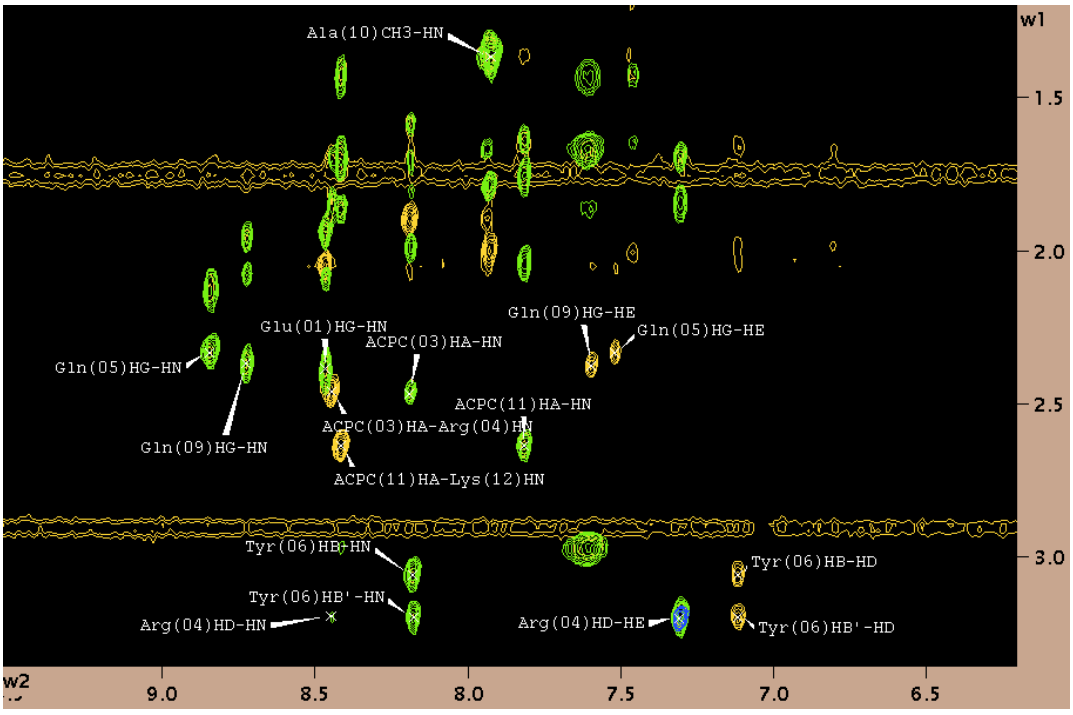

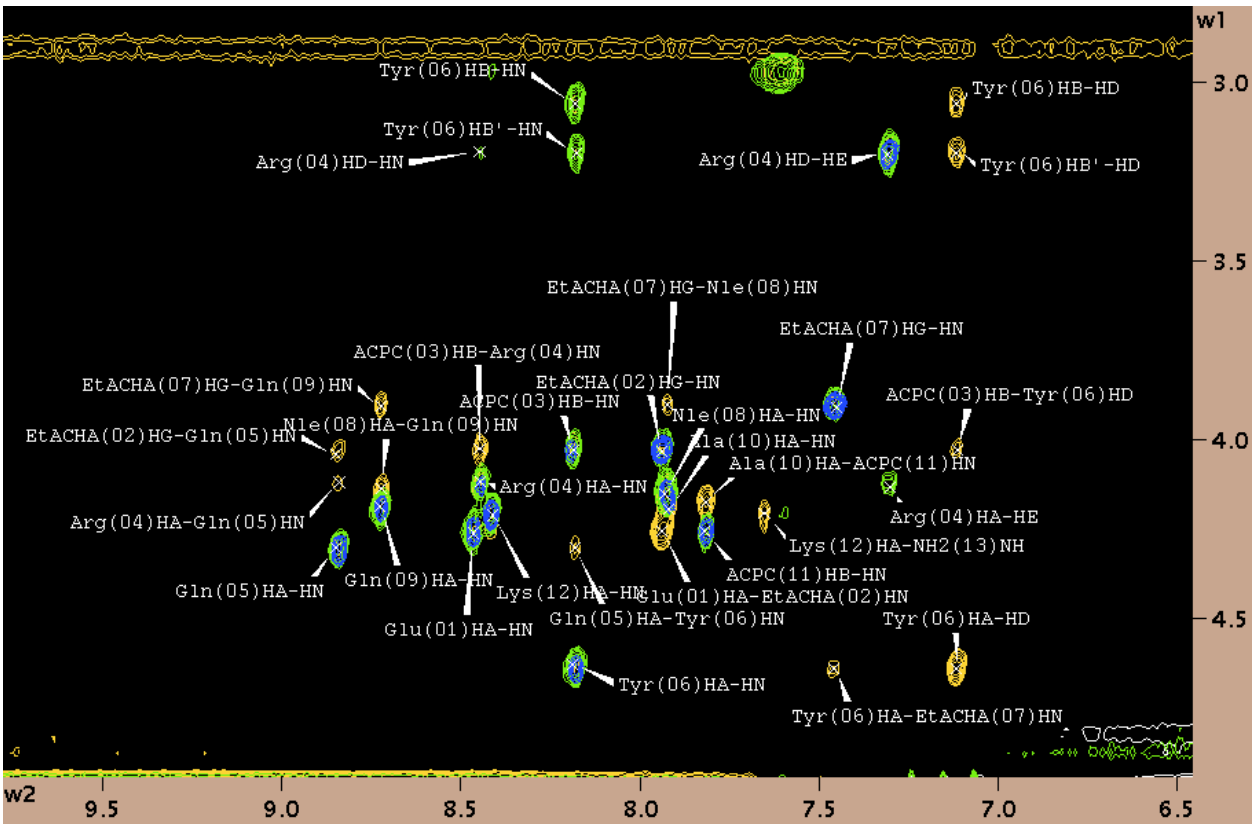

Partial wgROESY spectra of **3.4A** in 60 % CF_3CD_2OH/30 % H_2O/10% D_2O (4 ^oC)

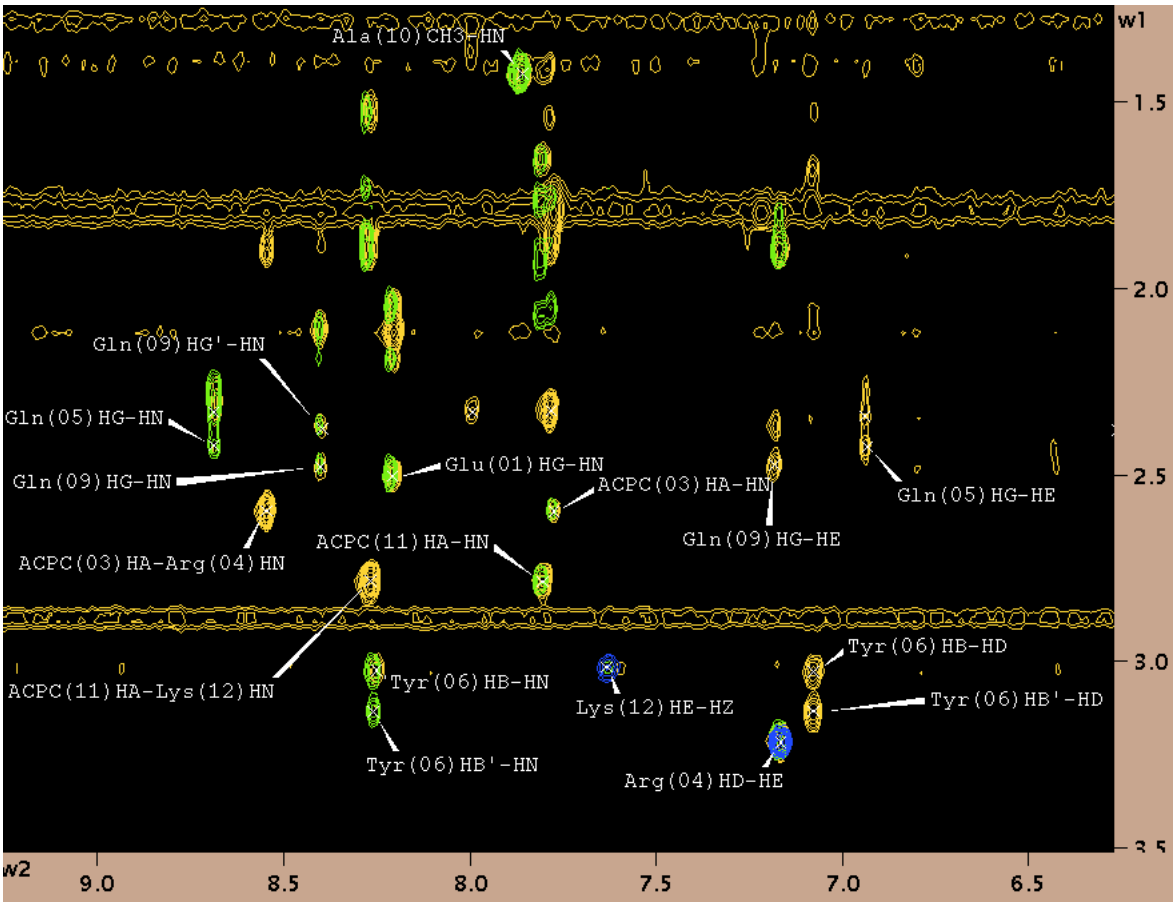

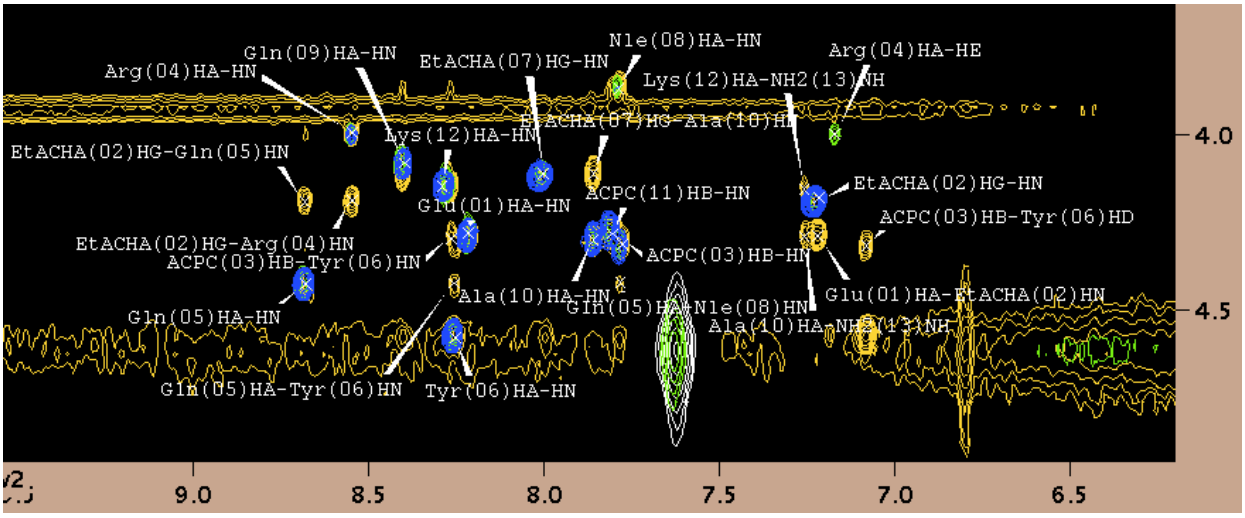

Partial wgROESY spectra of **3.4B** in 90% H_2O/10% D_2O (4 ^oC)

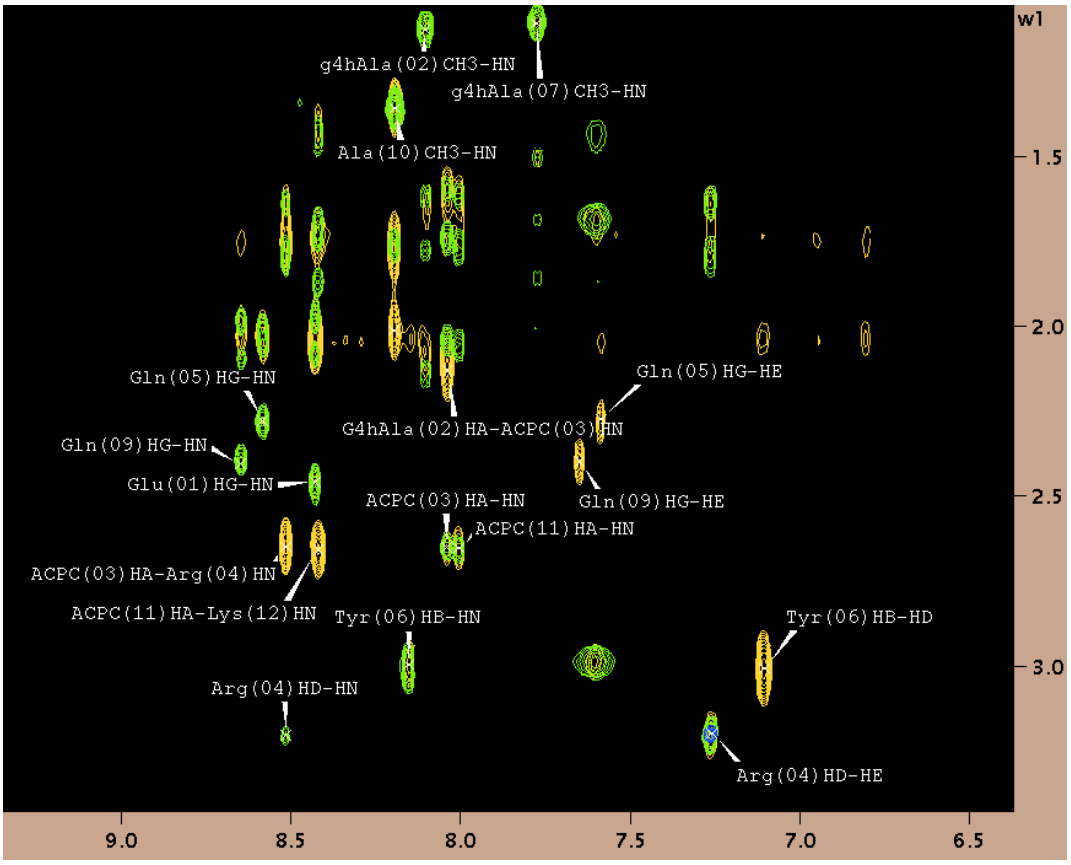

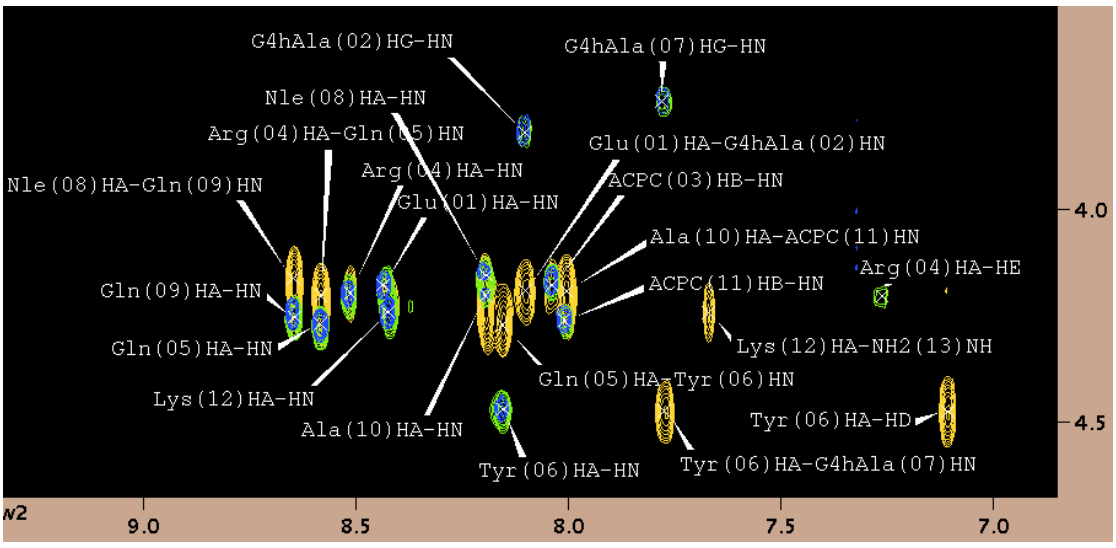

Partial wgROESY spectra of **3.4B** in 60 % CF_3CD_2OH/30 % H_2O/10% D_2O (4 ^oC)

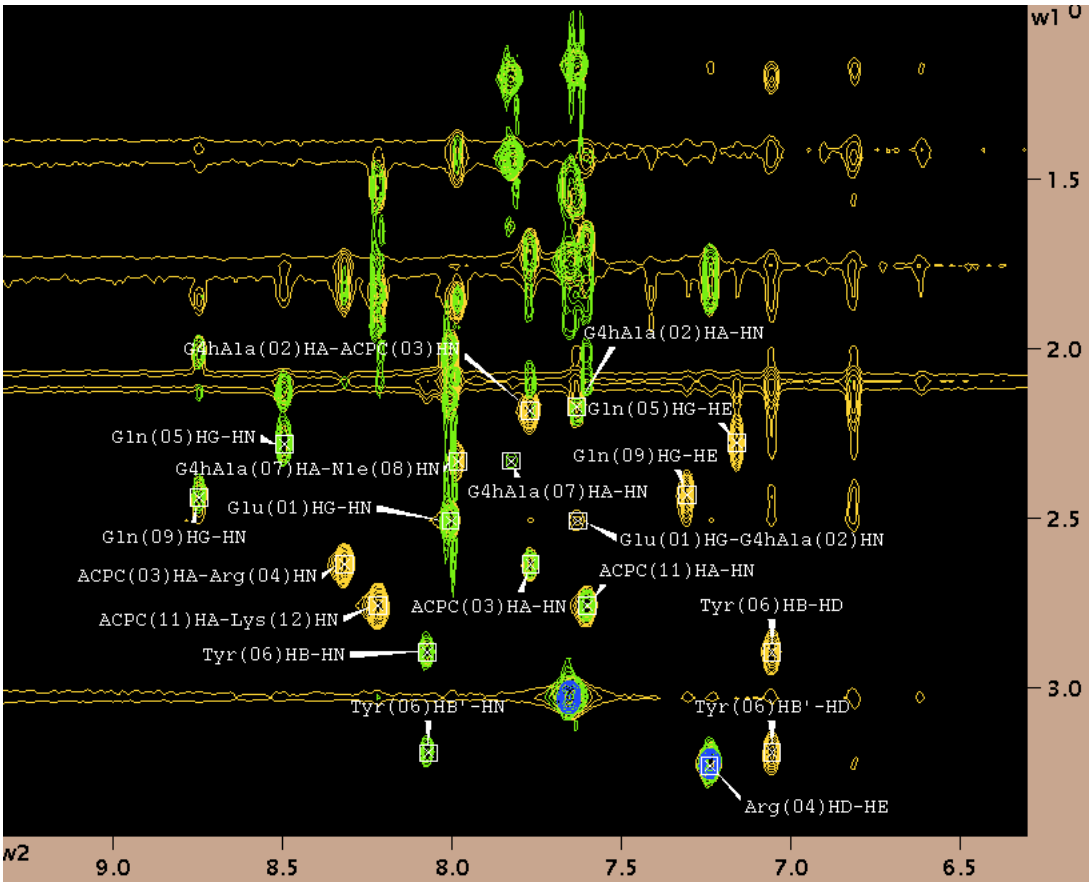

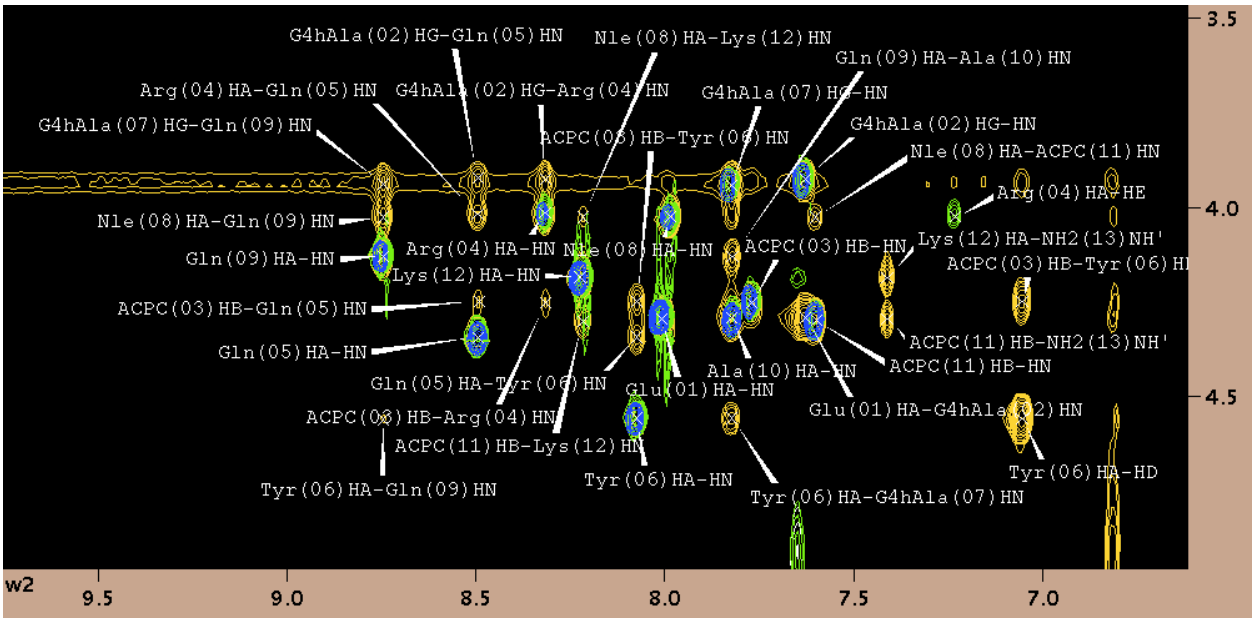

Partial wgROESY spectra of **3.5** in 90% H_2O/10% D_2O (4 ^oC)

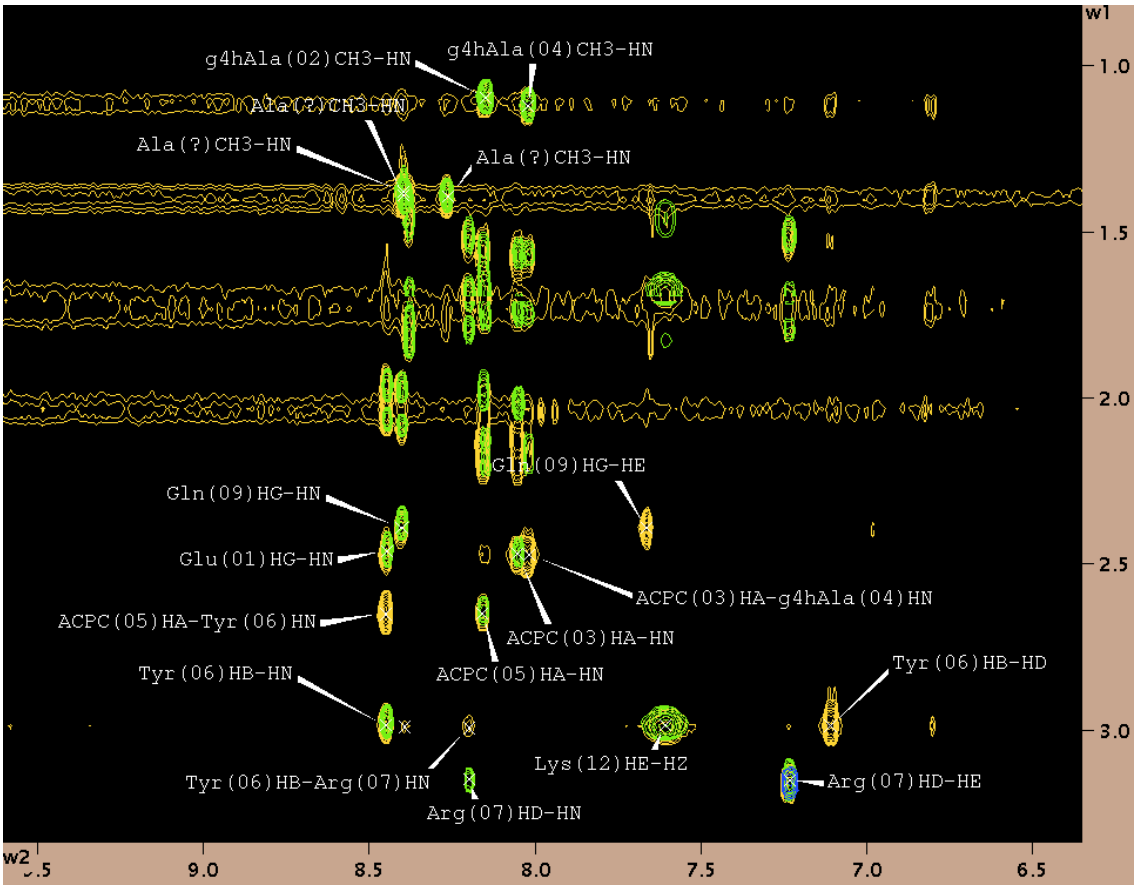

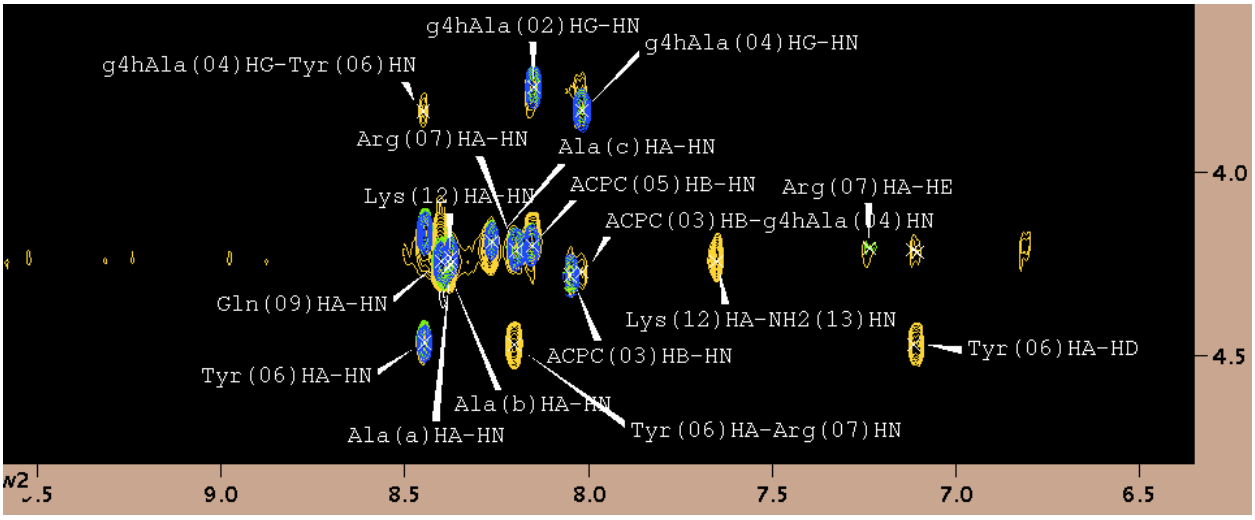

Partial wgROESY spectra of **3.5** in 60 % CF_3CD_2OH/30 % H_2O/10% D_2O (4 ^oC)

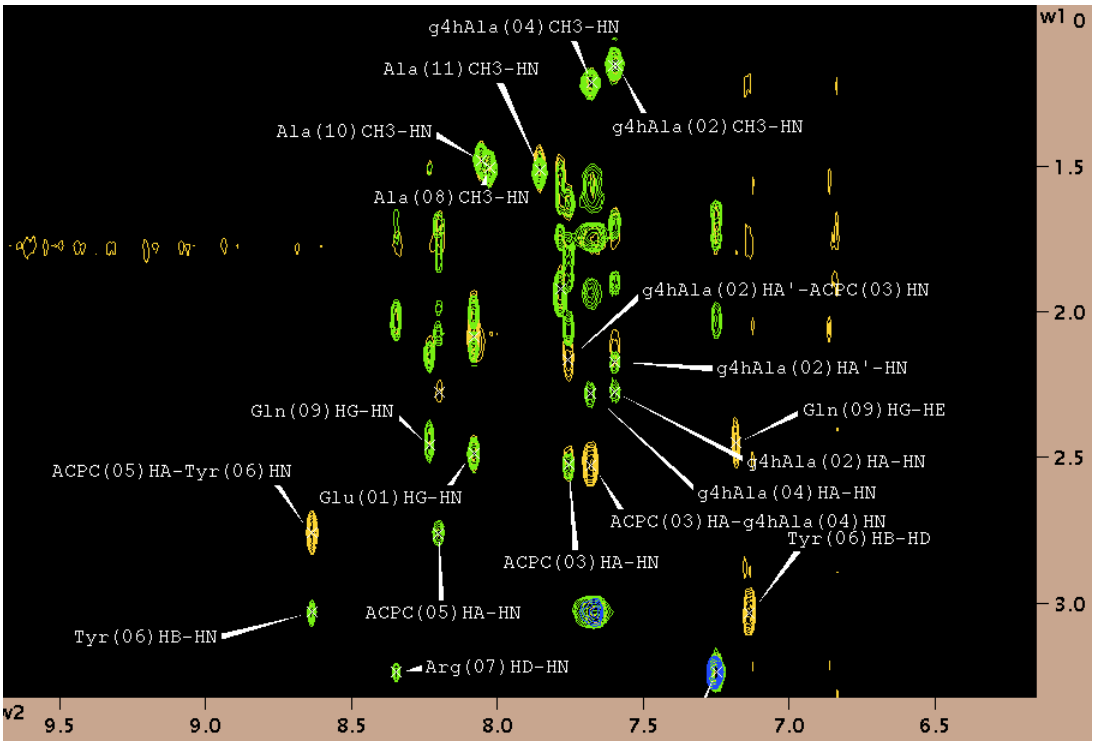

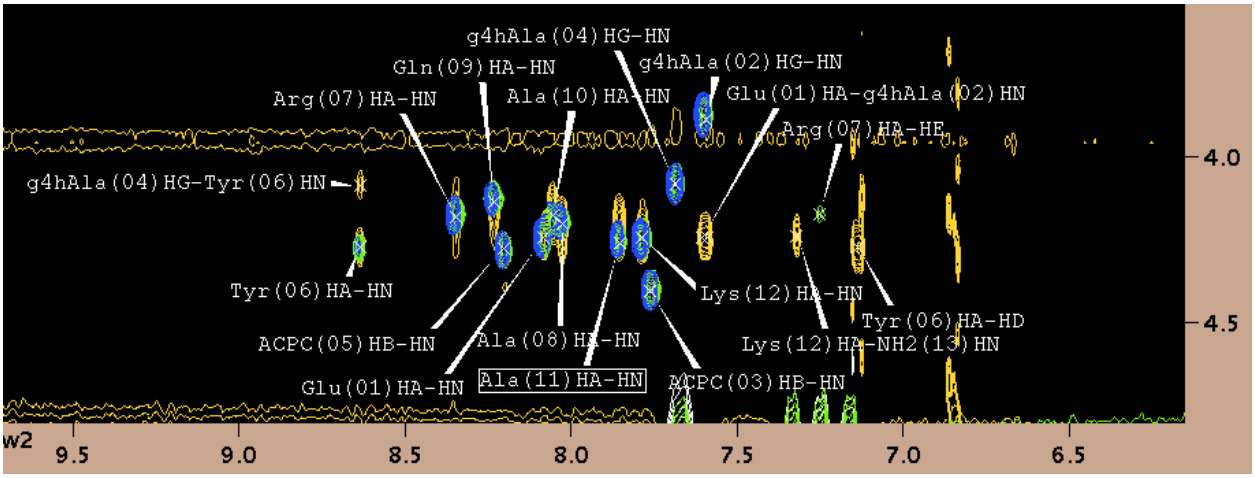

Partial wgROESY spectra of **3.6** in 90% H_2O/10% D_2O (4 ^oC)

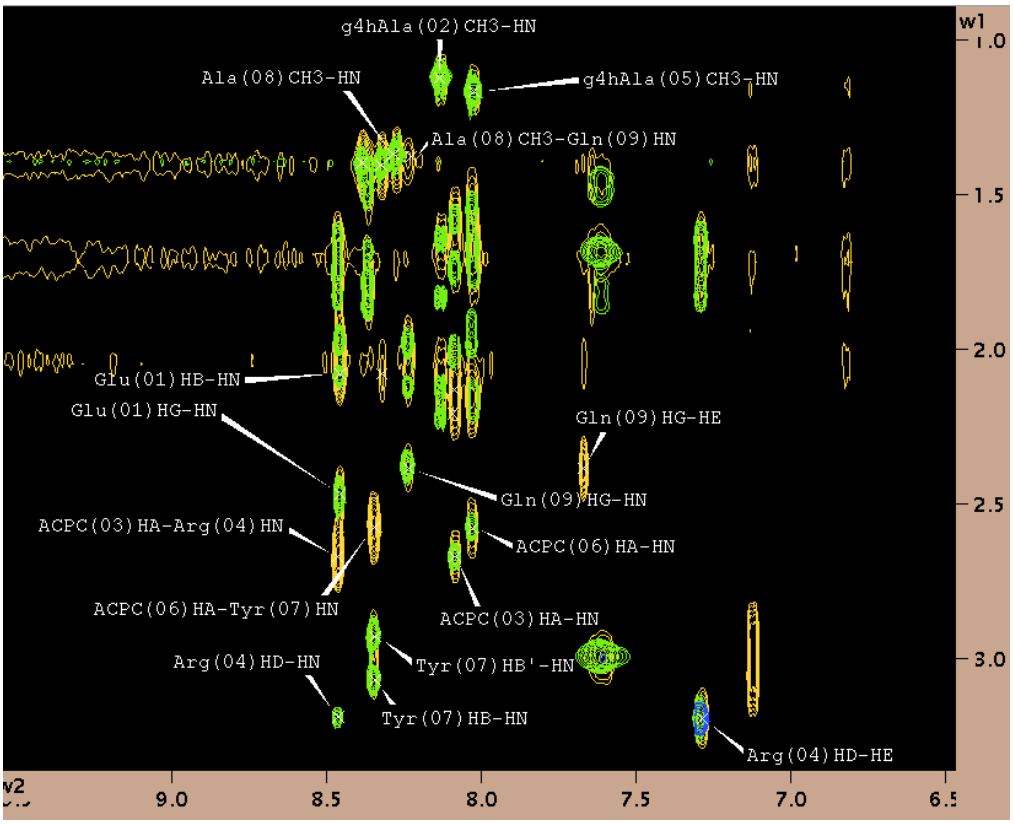

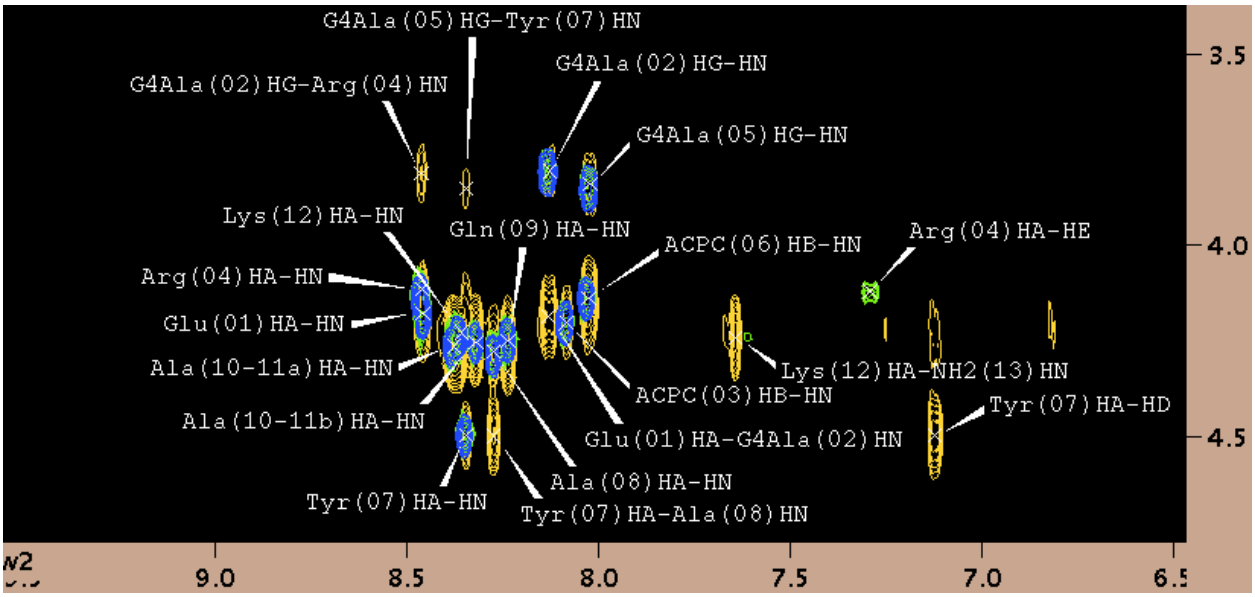

Partial wgROESY spectra of **3.6** in 60 % CF_3CD_2OH/30 % H_2O/10% D_2O (4 ^oC)

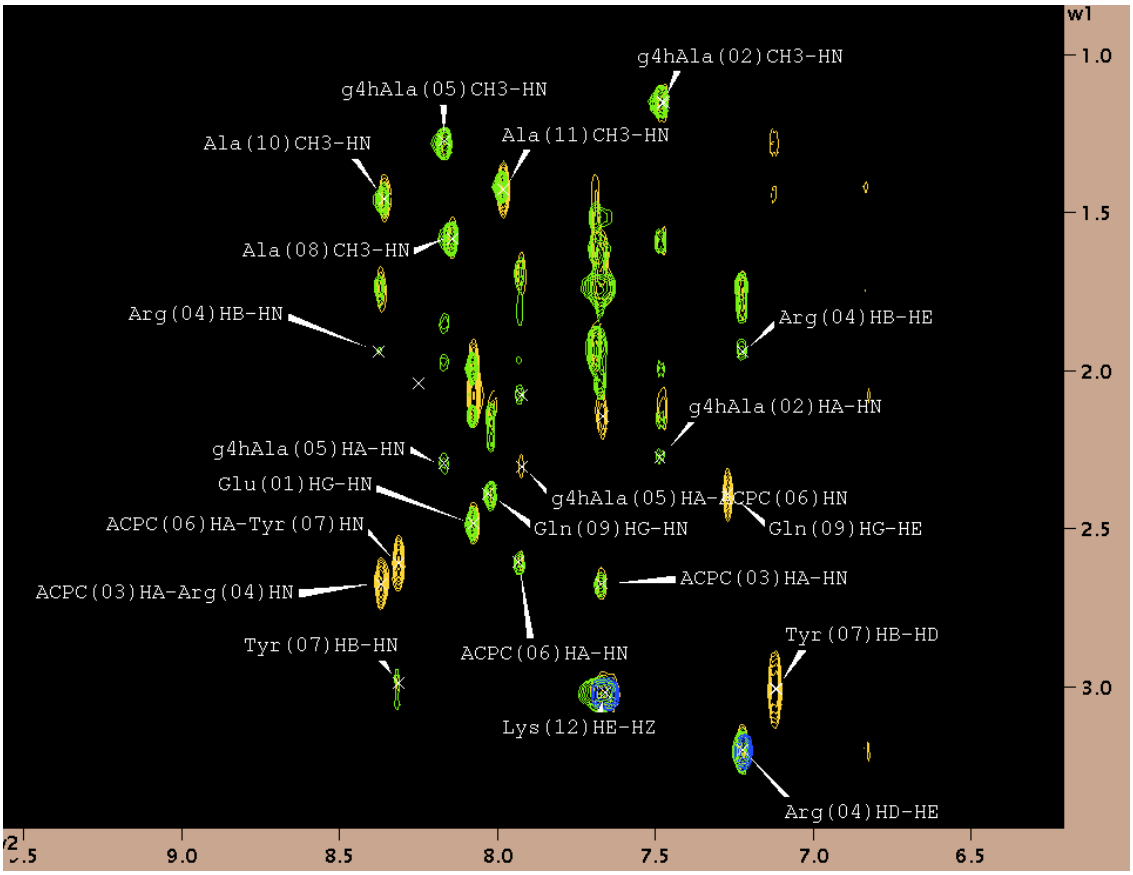

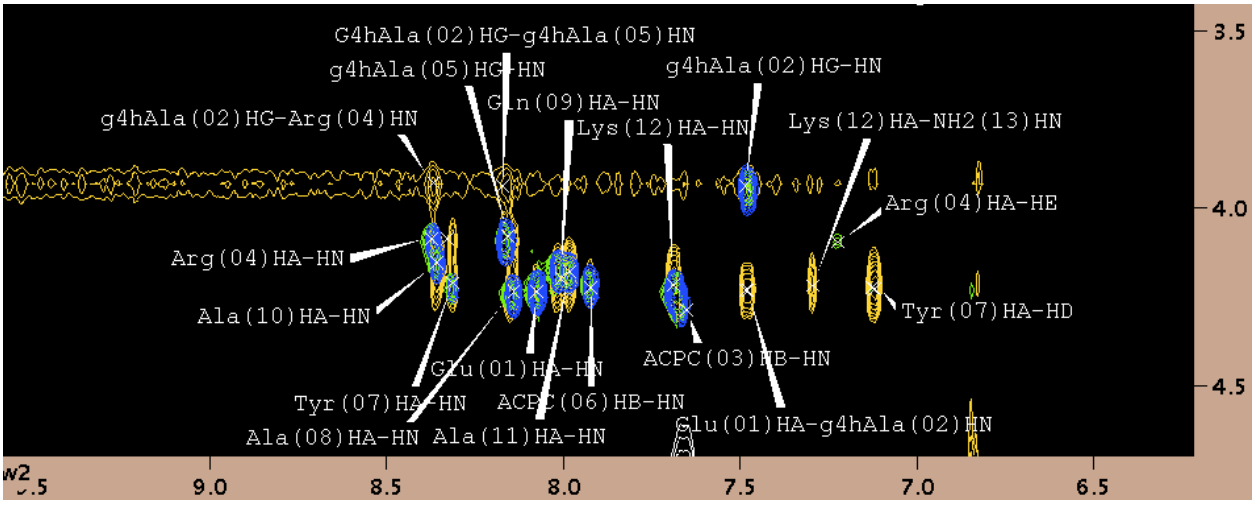

Partial wgROESY spectra of **3.7** in 90% H_2O/10% D_2O (4 ^oC)

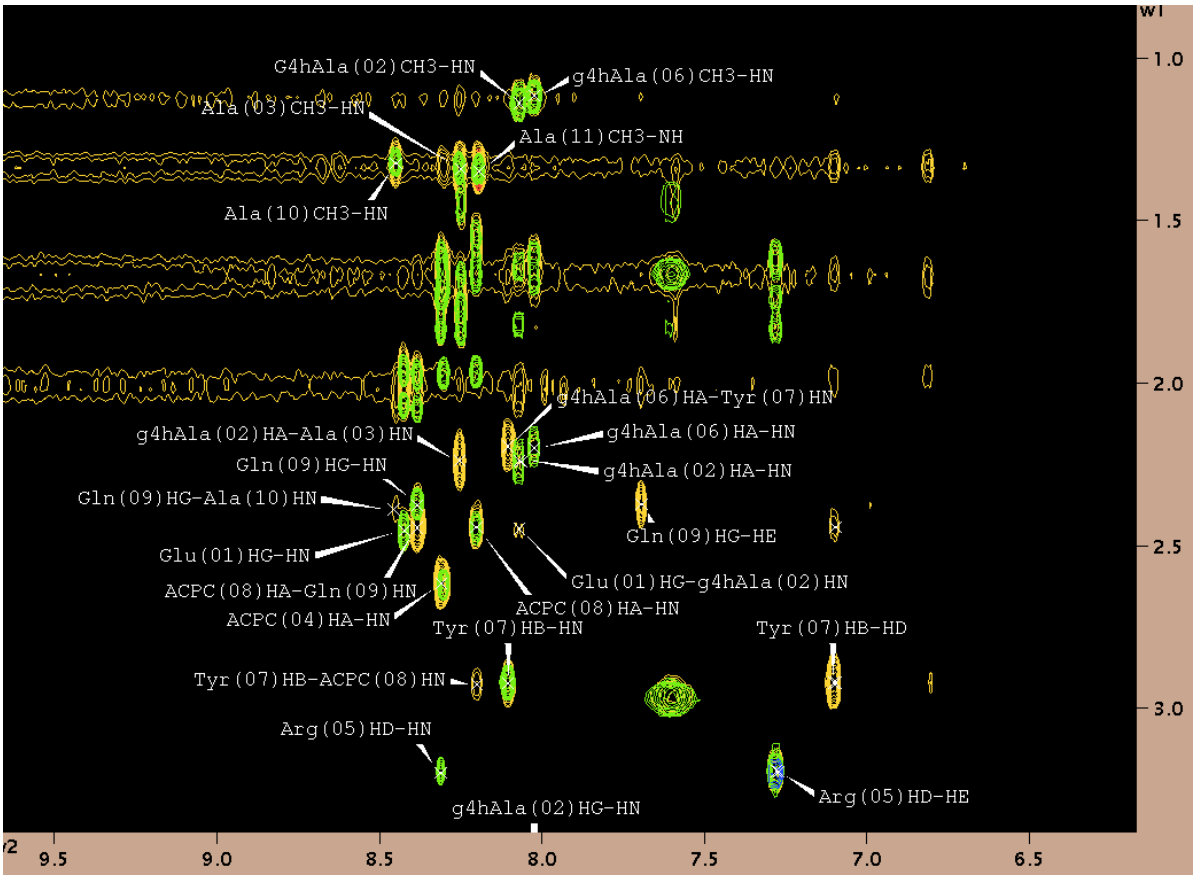

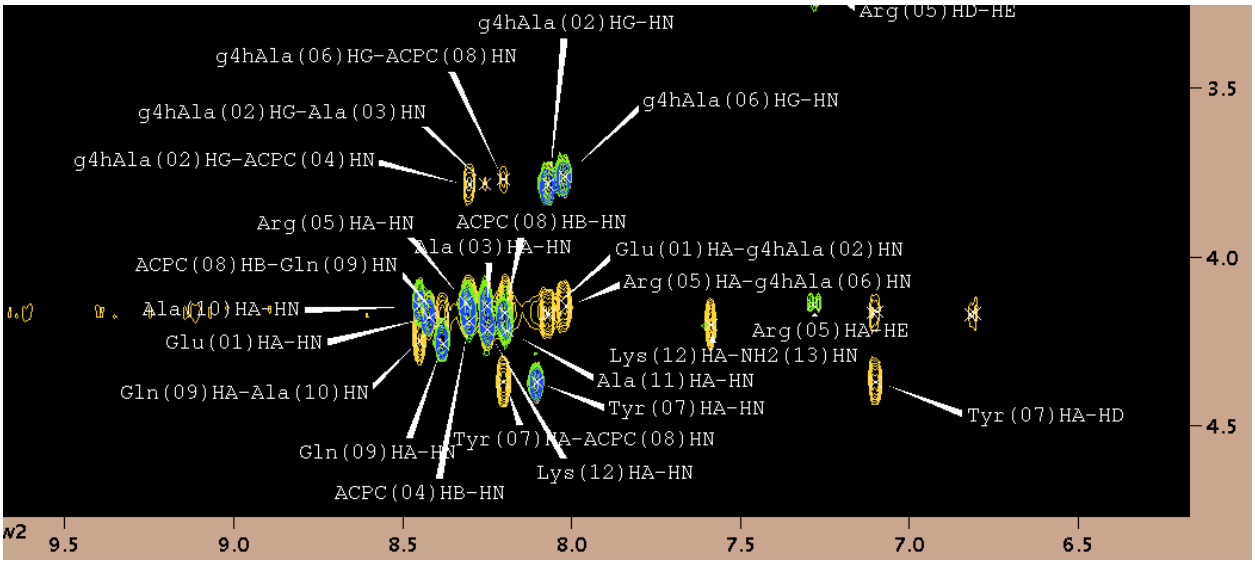

Partial wgROESY spectra of **3.7** in 60 % CF_3CD_2OH/30 % H_2O/10% D_2O (4 ^oC)

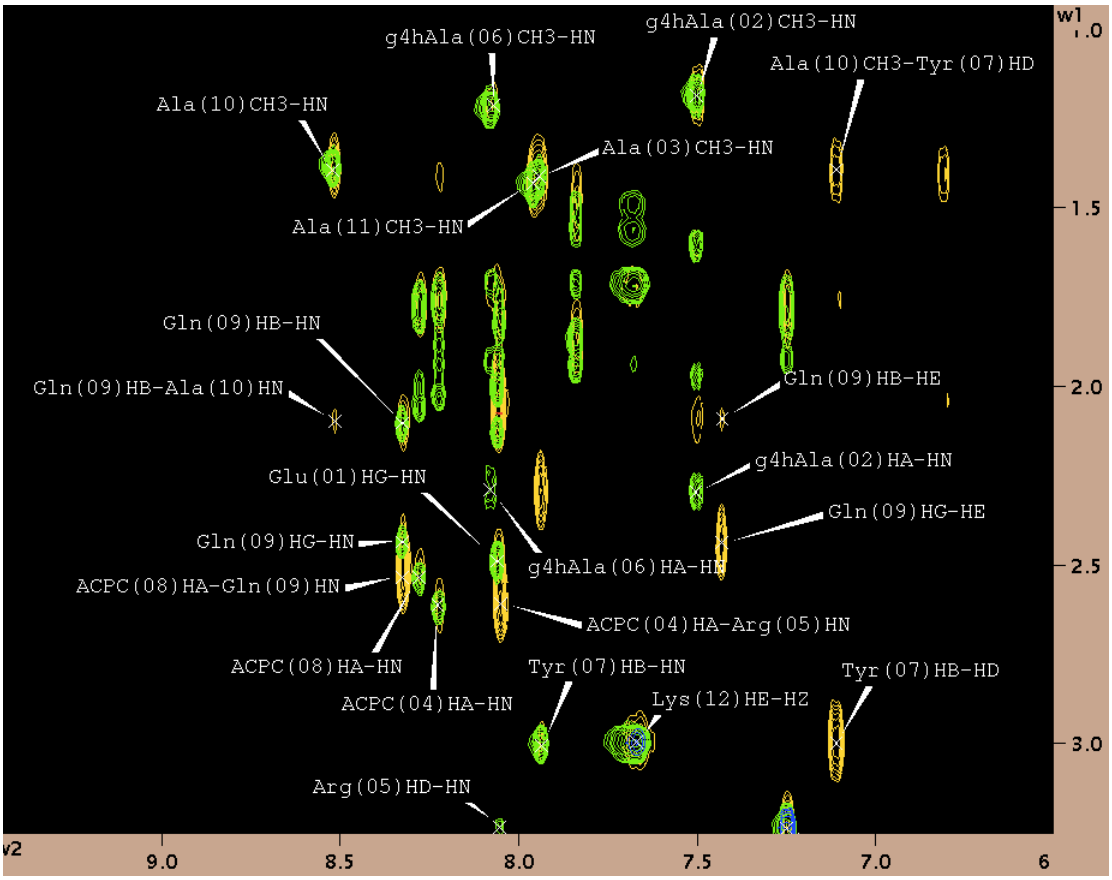

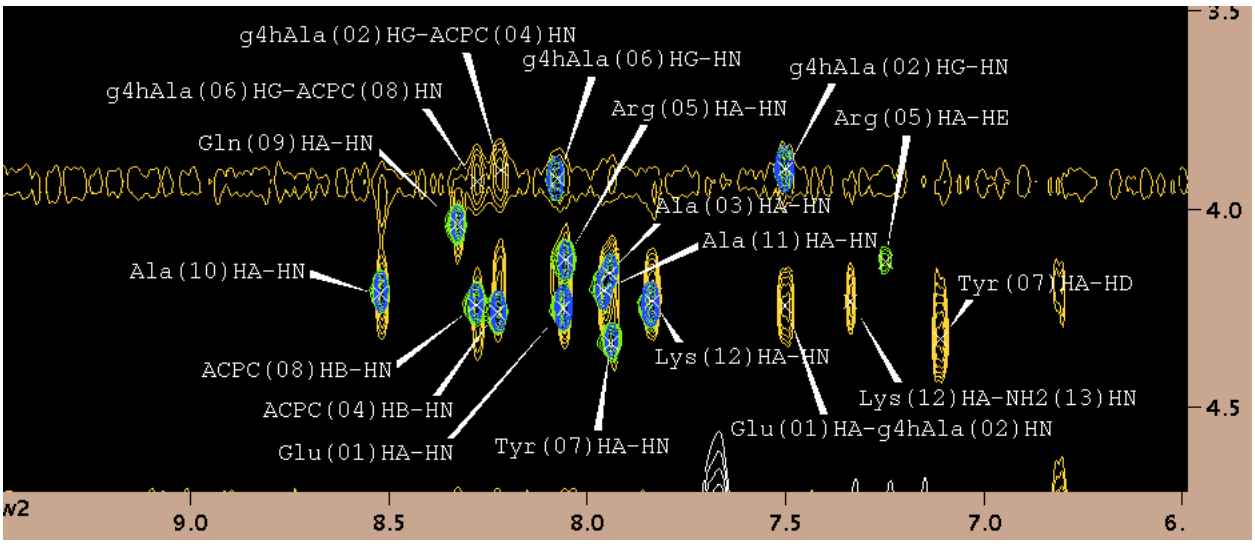

Partial gCOSY spectrum of **3.1D** in CD_3OH (10 ^oC)

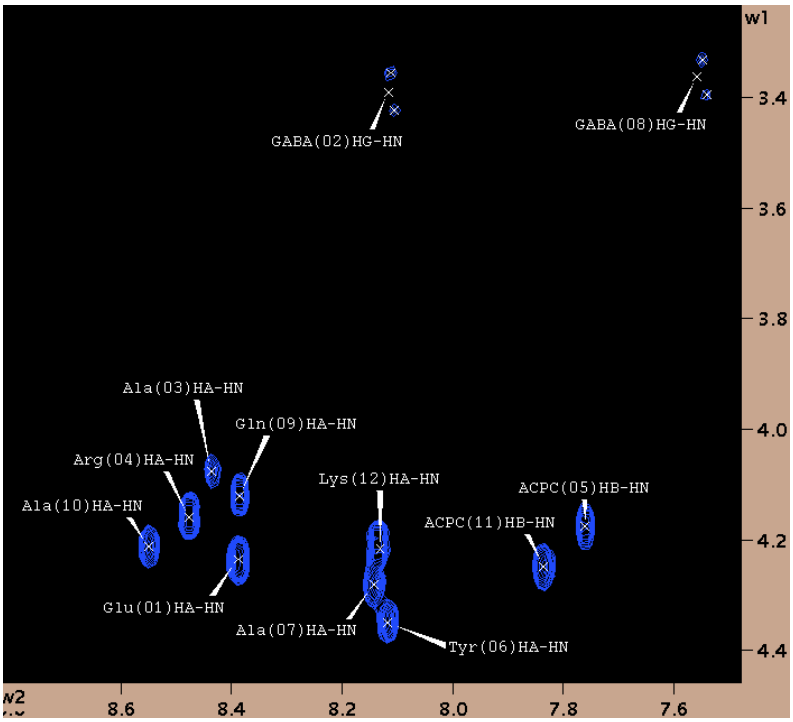

Partial gCOSY spectrum of **3.2** in 90% H_2O/10% D_2O (4 ^oC)

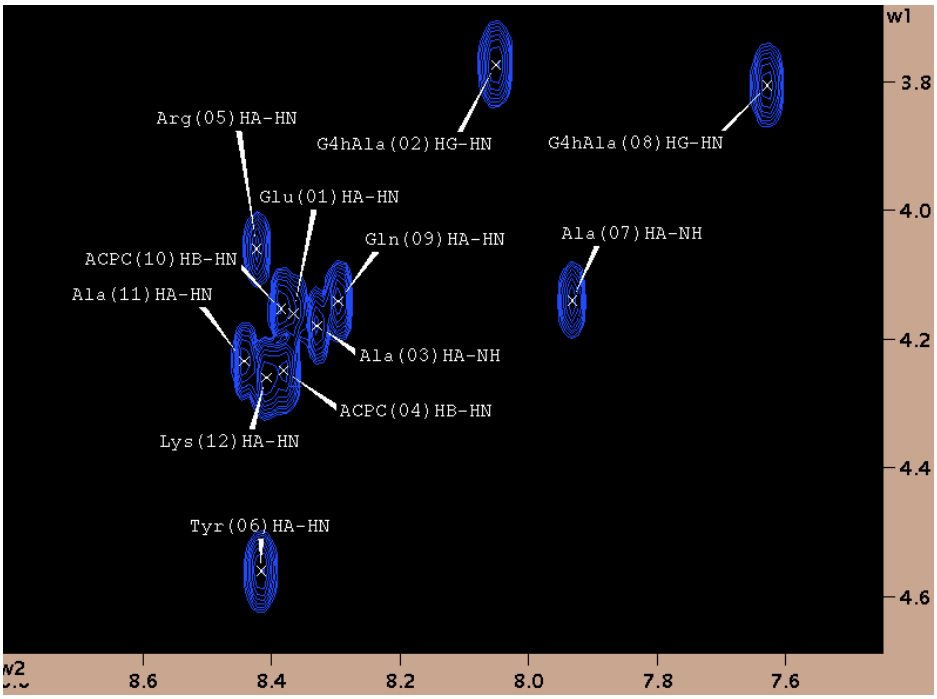

Partial gCOSY spectrum of **3.2** in 60 % CF_3CD_2OH/30 % H_2O/10% D_2O (4 ^oC)

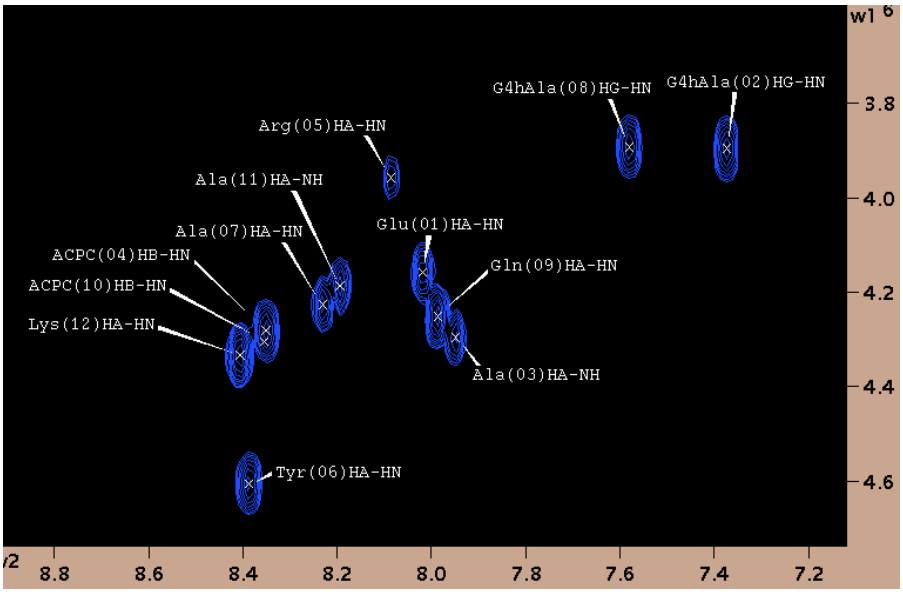

Partial gCOSY spectrum of **3.4A** in 90% H_2O/10% D_2O (4 ^oC)

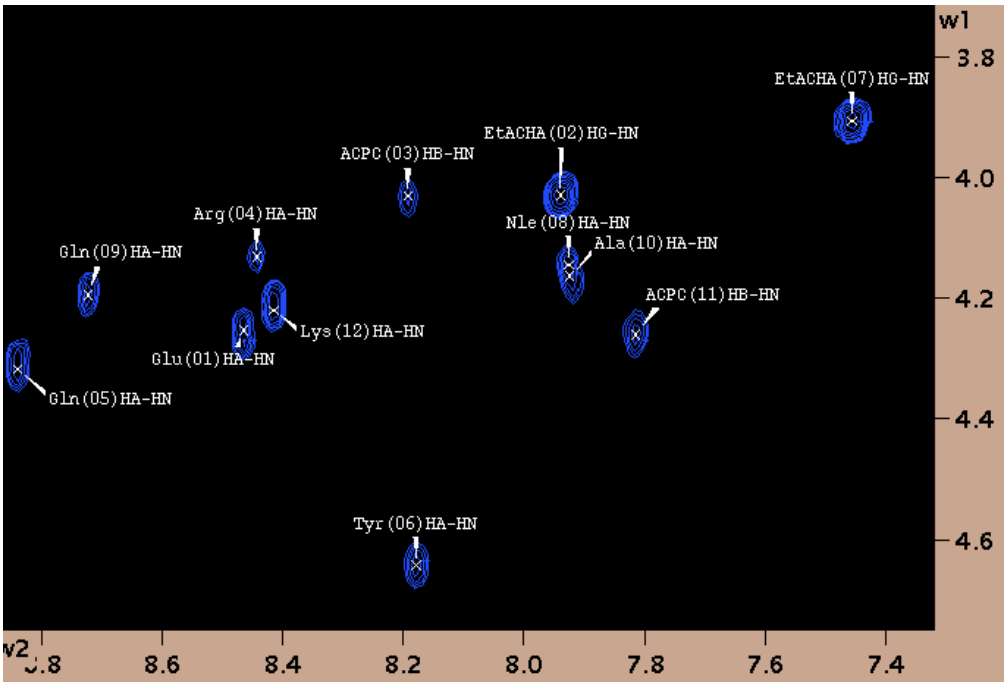

Partial gCOSY spectrum of **3.4A** in 60 % CF_3CD_2OH/30 % H_2O/10% D_2O (4 ^oC)

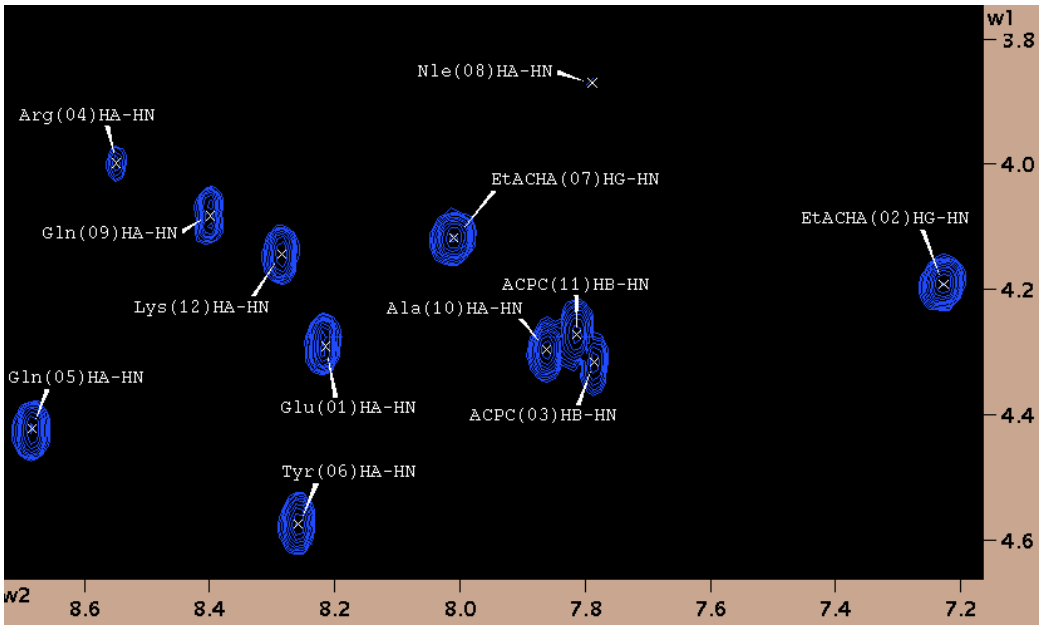

Partial wgROESY spectra of **3.4B** in 90% H_2O/10% D_2O (4 ^oC)

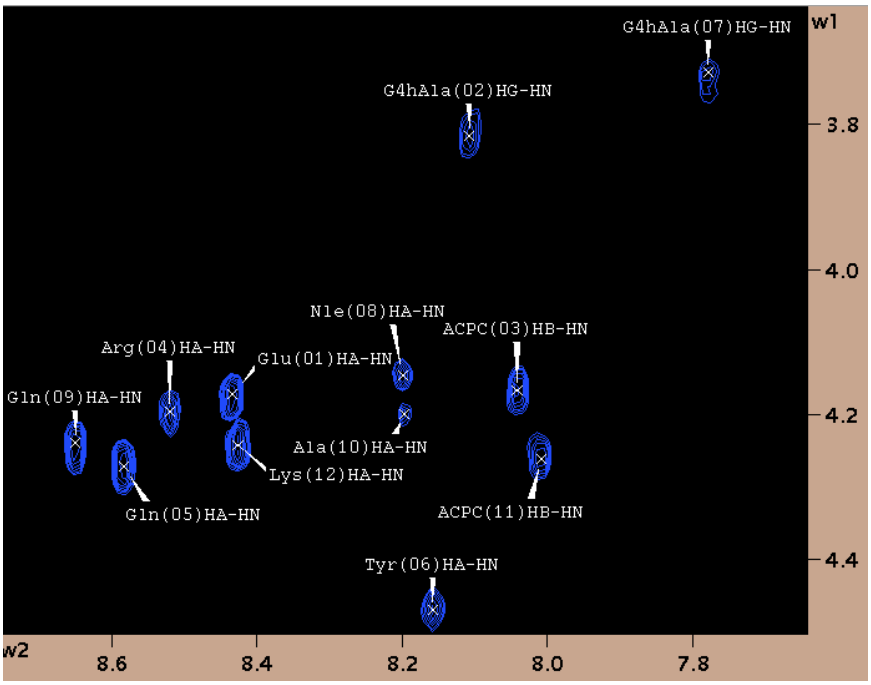

Partial gCOSY spectrum of **3.4B** in 60 % CF_3CD_2OH/30 % H_2O/10% D_2O (4 ^oC)

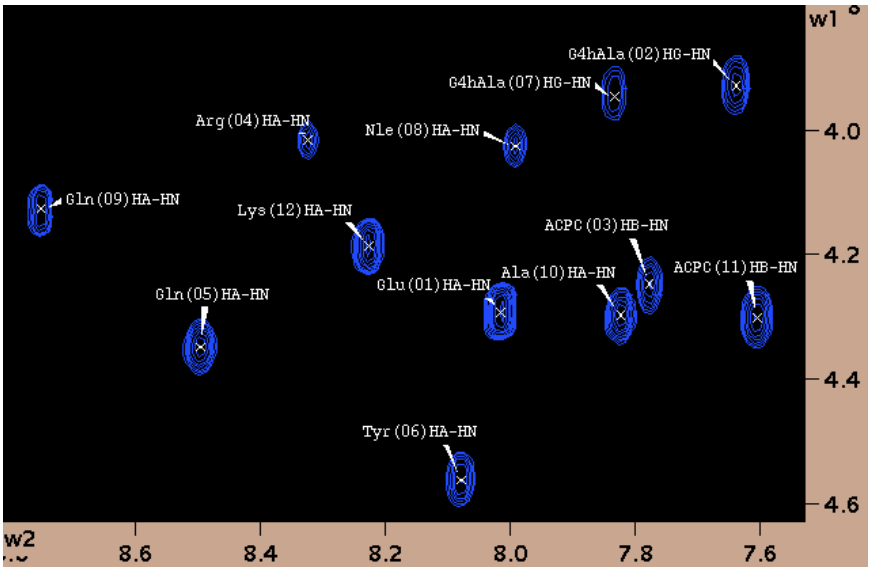

Partial gCOSY spectrum of **3.5** in 90% H_2O/10% D_2O (4 ^oC)

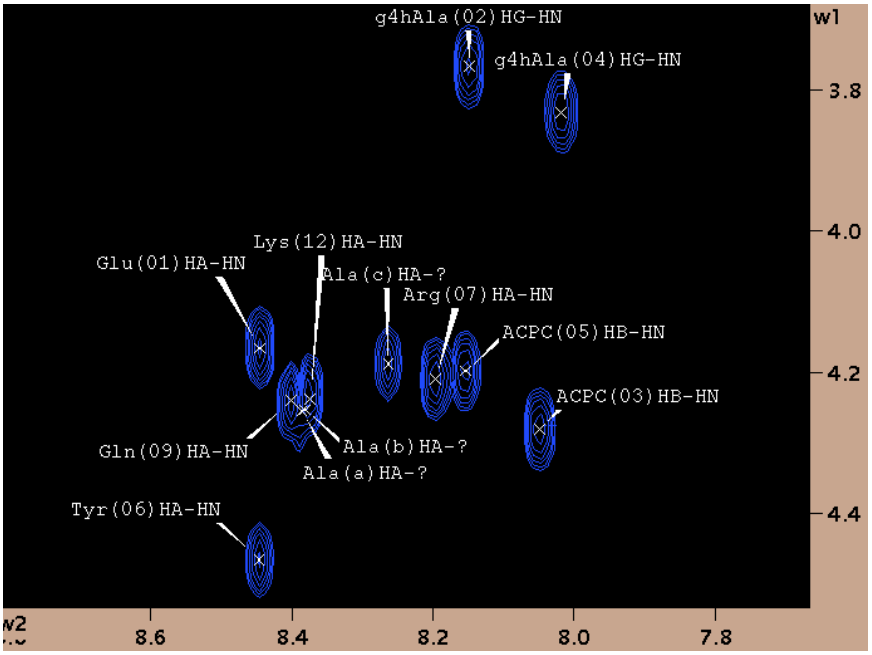

Partial gCOSY spectrum of **3.5** in 60 % CF_3CD_2OH/30 % H_2O/10% D_2O (4 ^oC)

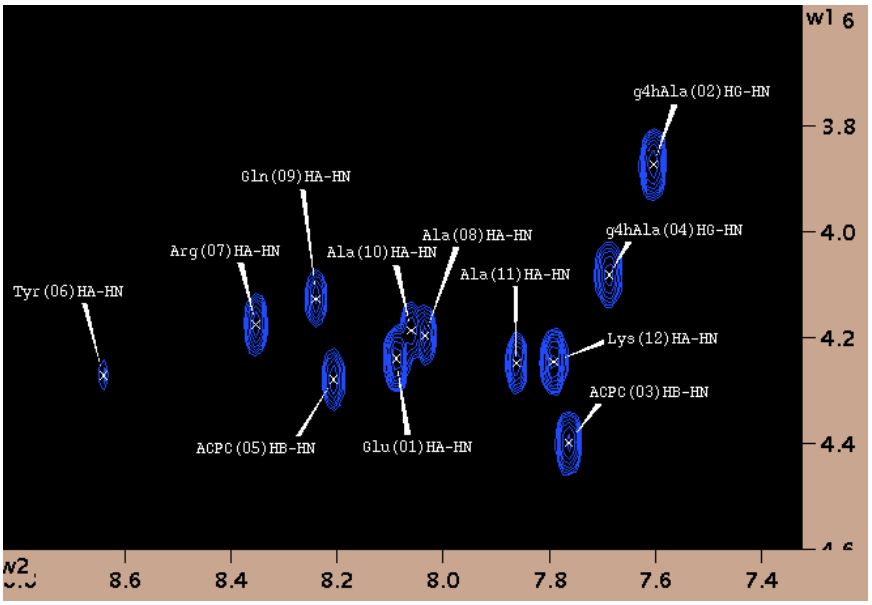

Partial gCOSY spectrum of **3.6** in 90% H_2O/10% D_2O (4 ^oC)

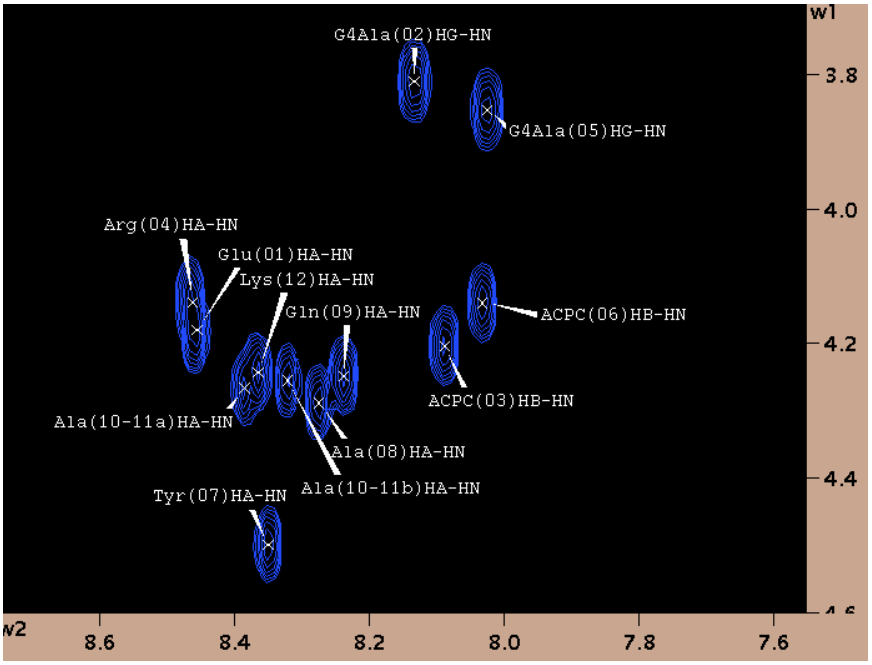

Partial gCOSY spectrum of **3.6** in 60 % CF_3CD_2OH/30 % H_2O/10% D_2O (4 ^oC)

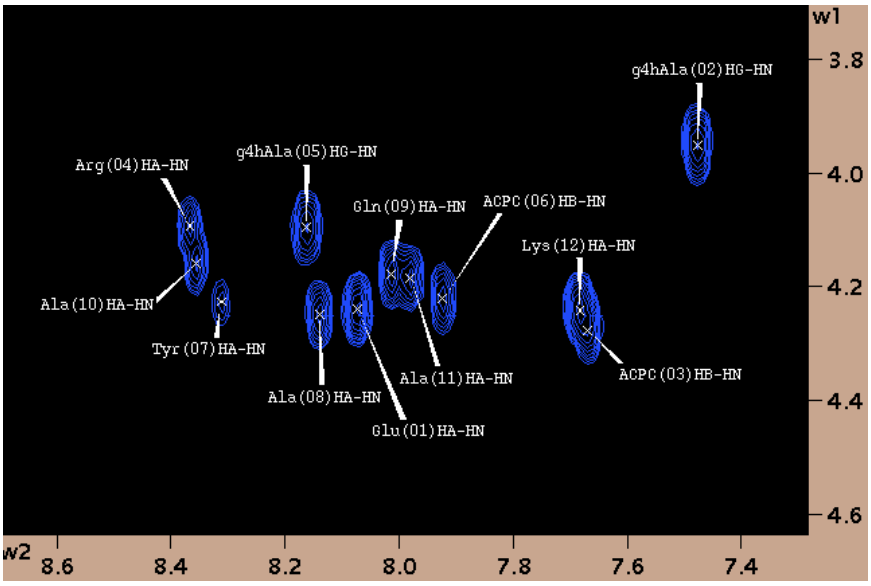

Partial gCOSY spectrum of **3.7** in 90% H_2O/10% D_2O (4 ^oC)

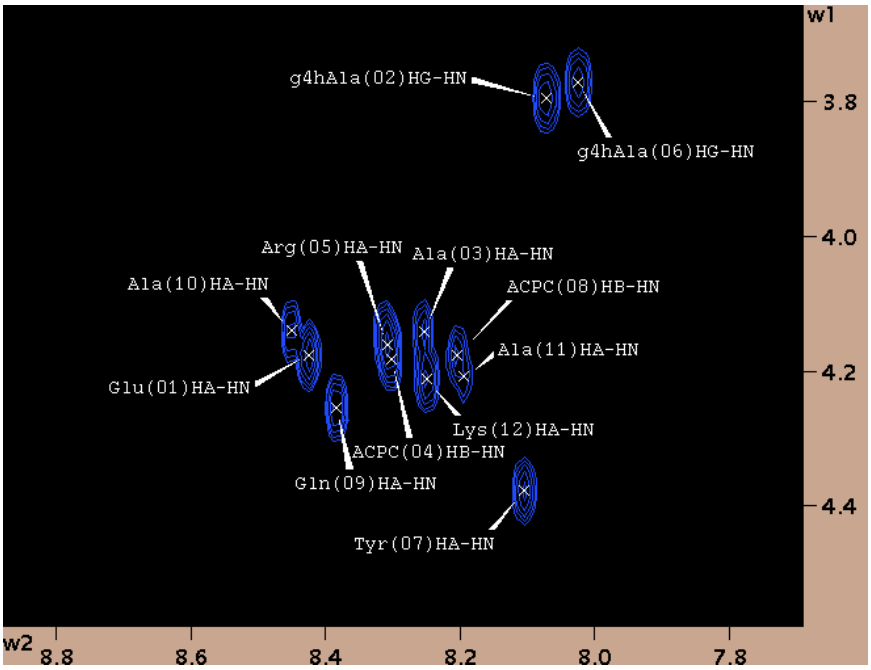

Partial gCOSY spectrum of **3.7** in 60 % CF_3CD_2OH/30 % H_2O/10% D_2O (4 ^oC)

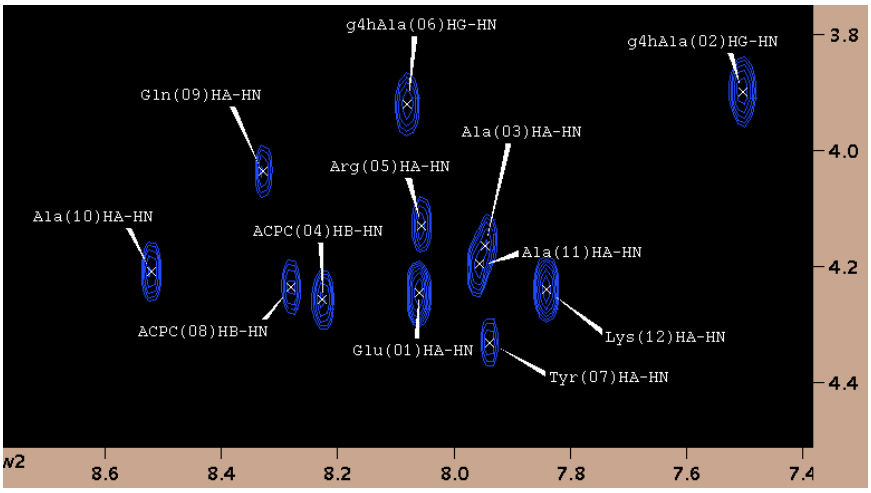

3.7 References

(1) Sawada, T.; Gellman, S. H. Structural Mimicry of the alpha-Helix in Aqueous Solution with an Isoatomic alpha/beta/gamma-Peptide Backbone. *Journal of the American Chemical Society* **2011**, *133*, 7336-7339.

(2) Shin, Y.-H.; Mortenson, D. E.; Satyshur, K. A.; Forest, K. T.; Gellman, S. H. Differential Impact of beta and gamma Residue Preorganization on alpha/beta/gamma-Peptide Helix Stability in Water. *Journal of the American Chemical Society* **2013**, *135*, 8149-8152.

(3) Chakrabartty, A.; Schellman, J. A.; Baldwin, R. L. LARGE DIFFERENCES IN THE HELIX PROPENSITIES OF ALANINE AND GLYCINE. *Nature* **1991**, *351*, 586-588.

(4) Toniolo, C.; Bonora, G. M.; Bavoso, A.; Benedetti, E.; Diblasio, B.; Pavone, V.; Pedone, C. Linear Oligopepitde. 97. Preferred Conformations of Pepties Containing alpha, alpha-Disubstituted alpha-Amino aicds. *Biopolymers* **1983**, *22*, 205-215.

(5) Cheng, R. P.; Gellman, S. H.; DeGrado, W. F. beta-peptides: From structure to function. *Chemical Reviews* **2001**, *101*, 3219-3232.

(6) Pauling, L.; Corey, R. B.; Branson, H. R. The structure of proteins; two hydrogen-bonded helical configurations of the polypeptide chain. *Proceedings of the National Academy of Sciences of the United States of America* **1951**, *37*, 205-211.

(7) Roccatano, D.; Colombo, G.; Fioroni, M.; Mark, A. E. Mechanism by which 2,2,2-trifluoroethanol/water mixtures stabilize secondary-structure formation in peptides: A molecular dynamics study. *Proceedings of the National Academy of Sciences of the United States of America* **2002**, *99*, 12179-12184.

(8) Boersma, M. D.; Haase, H. S.; Peterson-Kaufman, K. J.; Lee, E. F.; Clarke, O. B.; Colman, P. M.; Smith, B. J.; Horne, W. S.; Fairlie, W. D.; Gellman, S. H. Evaluation of Diverse alpha/beta-Backbone Patterns for Functional alpha-Helix Mimicry: Analogues of the Bim BH3 Domain. *Journal of the American Chemical Society* **2012**, *134*, 315-323.

(9) Giuliano, M. W.; Horne, W. S.; Gellman, S. H. An alpha/beta-Peptide Helix Bundle with a Pure beta(3)-Amino Acid Core and a Distinctive Quaternary Structure. *Journal of the American Chemical Society* **2009**, *131*, 9860.

(10) Wishart, D. S.; Sykes, B. D.; Richards, F. M. The Chemical-shift Index- A Fast and Simple Method for The Assignment of Protein Secondary Structure throught NMR-Spectroscopy. *Biochemistry* **1992**, *31*, 1647-1651.

(11) Guo, L.; Chi, Y.; Almeida, A. M.; Guzei, I. A.; Parker, B. K.; Gellman, S. H. Stereospecific Synthesis of Conformationally Constrained gamma-Amino Acids: New Foldamer Building Blocks That Support Helical Secondary Structure. *Journal of the American Chemical Society* **2009**, *131*, 16018.

(12) Murray, J. K.; Gellman, S. H. Parallel synthesis of peptide libraries using microwave irradiation. *Nature Protocols* **2007**, *2*, 624

(13) K. Wüthrich, *NMR of Proteins and Nucleic Acids*, Wiley-Interscience, New York, **1986**.

(14) T. D. Goddard, D. G. Kneller, Sparky 3, University of California, San Francisco.

Chapter 4: Efforts to Develop a Coiled-coil System for Thermodynamic Study of α/β/γ-Peptide Helix Stability via Backbone Thioester Exchange (BTE)

4.1 Introduction

4.1.1 Helical α/β/γ-peptide in αγααβα hexads

Helical peptidomimetics have been extensively developed to regulate pharmacologically important protein-protein interactions (PPIs) involving helical interfaces.[1-3] The utilization of foldamers containing unnatural backbone subunits that show discrete conformational propensities serves as a promising strategy for the development of helical peptidomimetics.[4-6] To develop therapeutically useful helical foldamers that can bind to specific sites on target proteins *in vivo*, it is essential to examine secondary structures of designed foldamers and to further characterize the tertiary and quaternary structures formed by interactions between the foldamers themselves and with canonical α-peptides.

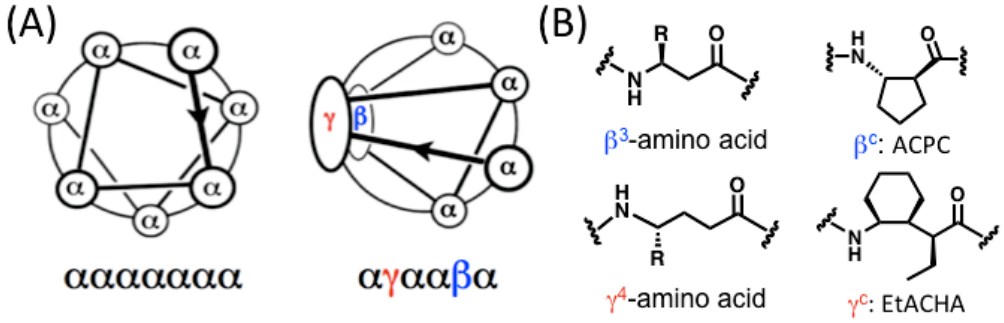

Figure 4.1 (A) Helical wheel diagrams of α heptads and αγααβα hexads. (B) Structures of cyclic/acyclic- β- and γ- amino acid residues.

Recently, we have found that an α/β/γ-peptide with an αγααβα hexad repeat pattern exhibited α-helix-like folding in water (Figure 4.1).[7,8] The αγααβα hexad mimics the natural α-helix heptad by positioning β- and γ-residues along one face of the helix,

allowing the α residues to define the other face of the helix (Figure 4.1A). The β- and γ- residues, collectively, contain the same number of backbone atoms as the three α residues they replace, resulting in a hexad repeat in helical α/β/γ-peptides that accurately mimics the heptad repeat of natural α-helical peptides.[7]

The cyclopentyl-constrained β- and cyclohexyl-constrained γ-residues together promote helical folding of α/β/γ-peptides (Figure 4.1B).[7] Interestingly, acyclic γ^4-amino acids also show same propensity to promote a helical structure in α/β/γ-peptides when ring-constrained β-residues are used.[8] The helical secondary structure of α/β/γ-peptides is clearly supported by circular dichroism (CD), 2D-NMR and X-ray crystallographic data.[8] However, those methods do not allow us to quantitatively evaluate relative helix stabilities of the α/β/γ-peptides with varying the identities of the β- and γ-residues. Herein, we pursue quantification of the contributions of cyclic β- and γ-residues to α/β/γ-peptide helical stability using the backbone thioester exchange (BTE) method in an α+α/β/γ chimeric coiled-coil system.

4.1.2 Thermodynamic analysis of tertiary structural stability using the BTE method (Backbone Thioester Exchange)

Quantitative analysis of peptide or protein conformational stability in solution has been commonly pursued by methods such as thermal and chemical denaturation, monitored by CD, and hydrogen-deuterium exchange experiments, monitored by 2D-NMR.[9] However, these methods rely on a massive empirical database of α-peptides and proteins and thus cannot be readily extended to unnatural foldamers.

Previously, Woll and Gellman[10,11] developed the backbone thioester exchange (BTE) experiment to probe the stability of α-peptide secondary and tertiary structures, and this strategy has also been successfully applied to measurement of the thermodynamic stability of α+α and α+α/β antiparallel coiled-coils.[12-14] Our aim is to use the BTE strategy to investigate the stability of the α-helix-like conformation of $\alpha/\beta/\gamma$-peptides using an α+$\alpha/\beta/\gamma$ chimeric antiparallel coiled-coil system.

4.1.2.1 Introduction to BTE

In the BTE experiment, thermodynamic stability of polypeptide folding (ΔG_{Fold}) can be derived by indirectly measuring the equilibrium constant of polypeptide folding (K_{Fold}) (Figure 4.2). In order to measure K_{Fold} for a coiled-coil structure (helix-loop-helix), one replaces one amide bond in the loop region with a thioester bond. The resulting thiodepsipeptide (N_TC: N-terminal segment and C-terminal segment linked by a thioester bond) is added to a solution containing a small thiol peptide ($_{HS}Y$: thiol on a Tyr-derived small peptide). $_{HS}Y$ participates in thiol-thioester exchange reaction with N_TC, liberating the C-terminal thiol peptide ($_{HS}C$) and generating new thioester peptide

N_TY (N-terminal segment and Tyr-derivative linked by thioester bond) (Figure 4.2). When a thioester exchange reaction reaches equilibrium, the reaction mixture is characterized by analytical HPLC to determine the populations of four species, $_{HS}C$, N_TY, N_TC, and $_{HS}Y$. Each species contains one Tyr residue, enabling them all to be detected by UV-Vis absorption at 275 nm. The relative concentration of each species at equilibrium is determined by comparing the integrated peak areas, which are used to calculate the equilibrium constant (K_{BTE}). The K_{Fold} is determined from the simple relationship $K_{Fold} = K_{BTE} - 1$ (Figure 4.3, eq 4.5).

The relationship $K_{Fold} = K_{BTE} - 1$ is based on the hypothetical condition expressed in eq 4.4 ($[_{HS}Y][N_TC_U]/[N_TY][_{HS}C]=1$). Eq 4.4 is based on a few key assumptions concerning the model system. 1) The thioester bonds in N_TY and N_TC_U are iso-energetic. 2) The Tyr-derived segment in N_TY does not engage in energetically significant packing interactions with the rest of the molecule. 3) The full-length thioester peptide N_TC_F does not self-associate intermolecularly.

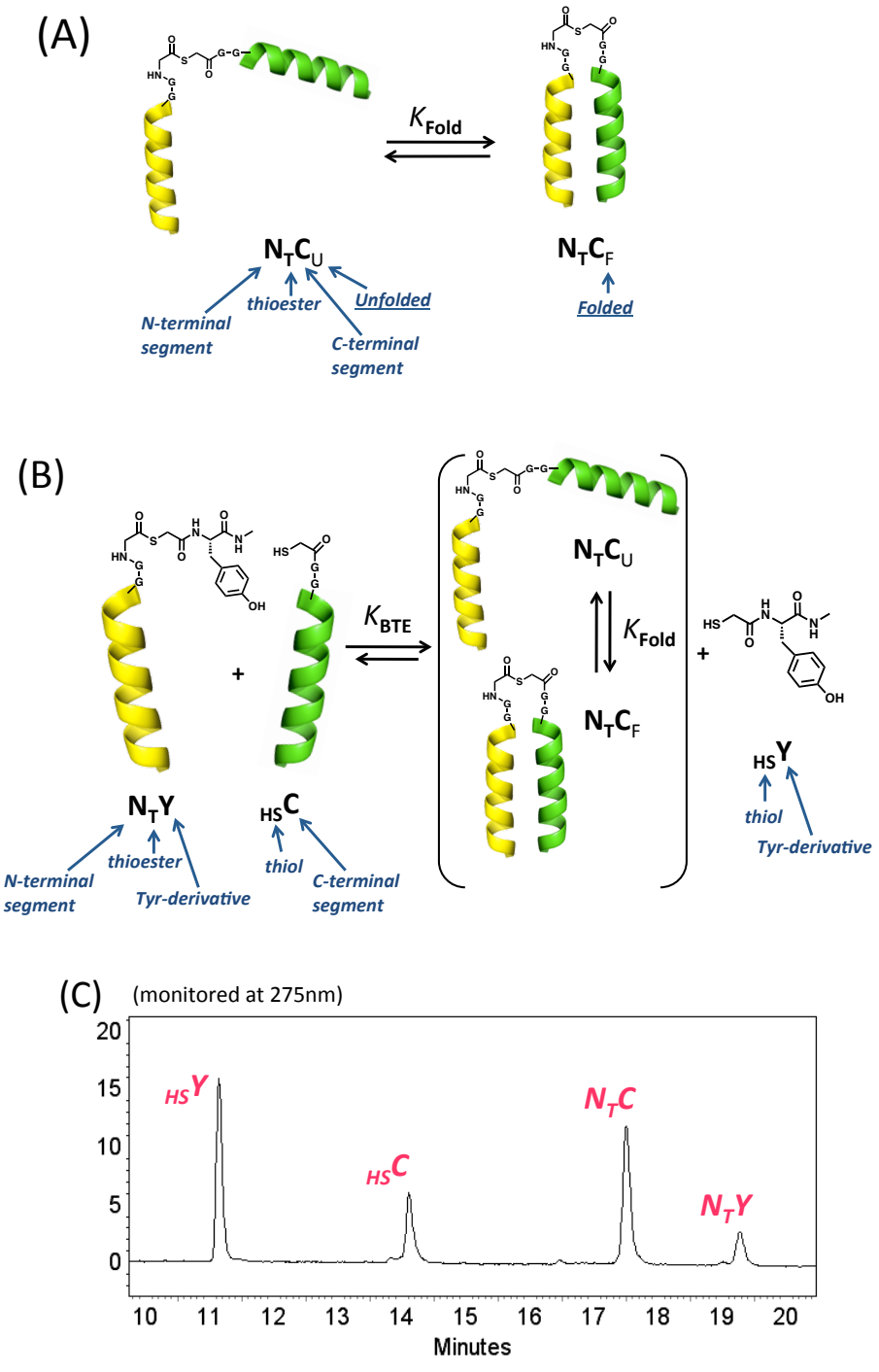

Figure 4.2 (A) A coiled-coil model N_TC in a two-state folding equilibrium. (B) Cartoon depicting a thioester exchange assay. Parentheses show a two-state folding equilibrium for thiodepsipeptide. (C) Representative analytical HPLC profile for a thioester exchange assay. Peaks are labeled as part (B) of the figure.

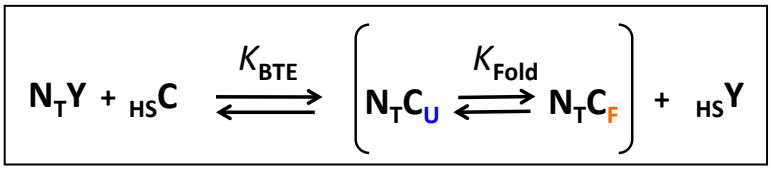

$$K_{BTE} = \frac{([N_TC_F]+[N_TC_U])\,[_{HS}Y]}{[N_TY][_{HS}C]} \qquad (4.1)$$

$$K_{Fold} = [N_TC_F]/[N_TC_U] \qquad (4.2)$$

$$K_{BTE} = \frac{(K_{Fold}+1)\,[_{HS}Y][N_TC_U]}{[N_TY][_{HS}C]} \qquad (4.3)$$

$$\frac{[_{HS}Y][N_TC_U]}{[N_TY][_{HS}C]} = 1 \qquad (4.4)$$

$$K_{BTE} = K_{fold} + 1 \qquad (4.5)$$

$$\Delta G_{Fold} = -\,RT\ \ln(K_{fold}) \qquad (4.6)$$

Figure 4.3 Derivation of the relationship between K_{BTE} and K_{Fold}.

-Terminology summary-

$_{HS}$Y: a tyrosine-containing small thiol peptide

N_TY: a thioester helical peptide containing a small Tyr derivative, which becomes the N-terminal helix of **N_TC**

$_{HS}$C: a thiol helical peptide, which becomes a C-terminal helix of **N_TC**

N_TC: a coiled-coil thiodepsipeptide resulted from a BTE reaction between **N_TY** and **$_{HS}$C**. In this chapter, numbering designation of **N_TC** peptides corresponds to numbering of **$_{HS}$C**. (e.g., **N_TC<u>10</u>** is generated from BTE between **N_TY** and **$_{HS}$C<u>10</u>**.)

N_TC_F: folded state of **N_TC**

N_TC_U: unfolded state of **N_TC**

Those conditions must be verified by control experiments. To assess the first and second conditions, we perform BTE experiments with N_TY and small thiol molecules other than $_{HS}Y$ that cannot form significant non-covalent interactions with the N-terminal helix in N_TY (e.g., methyl thioglycolate). In this case the expected equilibrium constant is near 1 (Figure 4.4A). To assess adherence to the third condition, we carry out analytical ultracentrifugation experiments (AU, sedimentation equilibrium test) on a full-length N_AC peptide to determine whether the peptide is monomeric when the BTE reaction is executed.[14] A full-length N_AC peptide contains an amide bond instead of a thioester bond in the loop region of N_TC (Figure 4.4B). The N_TC peptide cannot be analyzed by AU, a process that requires several days, due to slow thioester hydrolysis. Prior to AU analysis, the similarity of N_AC and N_TC is evaluated by CD measurements.

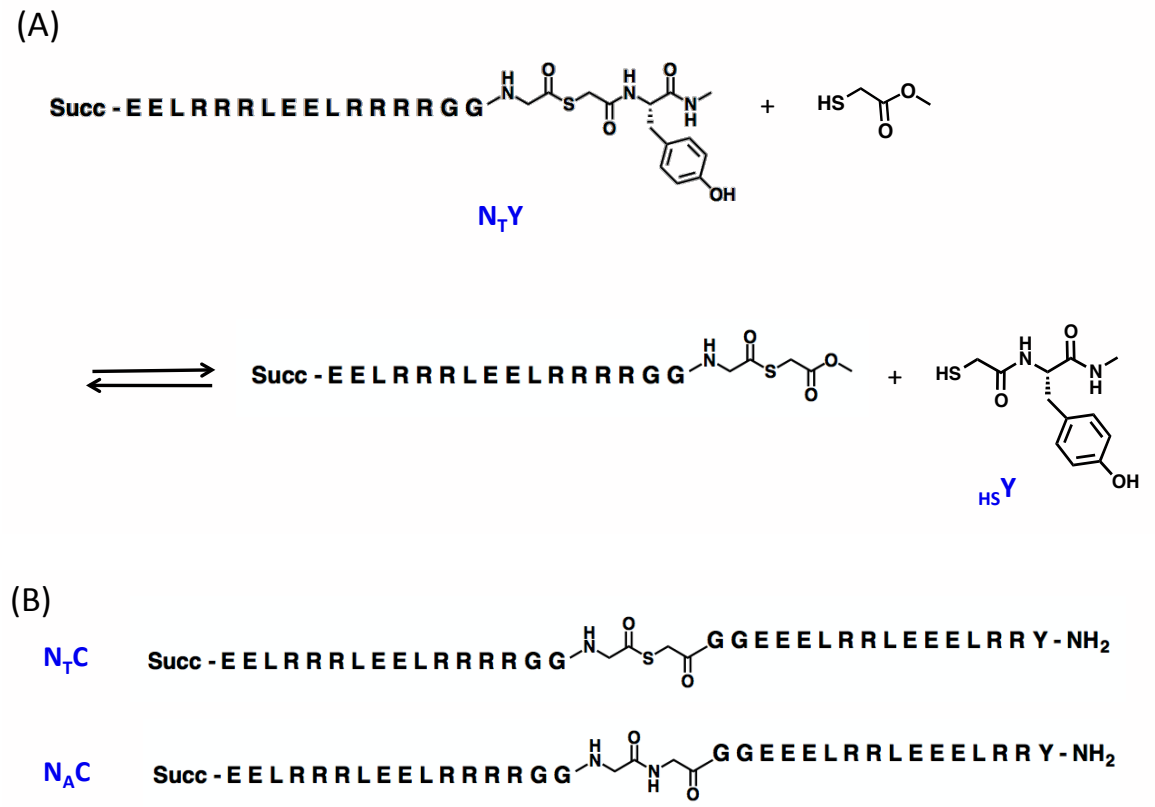

Figure 4.4 (A) A representative control BTE experiment to determine whether the Tyr fragment engages in energetically significant packing interactions with the rest of the molecule within N_TY. The expected equilibrium constant is 1. (B) Representative sequences of N_TC and N_AC analogues. N_AC is used for AU analysis because the thioester bond in N_TC is slowly hydrolyzed during AU analysis, which requires several days of sample centrifugation.

4.1.2.2. Antiparallel α-helical coiled-coils

The α-helical coiled-coil is a common structural motif found in protein tertiary and quaternary structure.[15] In order to elucidate the factors that control interhelical affinity in coiled-coils, Hadley and Gellman designed an antiparallel helix-loop-helix coiled-coil model and performed BTE studies (Figure 4.5).[15,16] Coiled-coil dimerization is driven largely by the "knobs-into-holes" interdigitation of hydrophobic side chains at the coiled-coil interface.[17] Hydrophobic residues are placed at core *a* and *d* positions within the

abcdefg heptad repeat to drive a dimeric association. In the design used by Hadley and Gellman, charged residues were placed at the other positions (*b, c, e, f* and *g*) to stabilize the secondary- and tertiary-structures by intrahelical- and interhelical-electrostatic interactions, respectively (Figure 4.5).[18] To prevent intermolecular assembly, one Leu at a core position was replaced with Arg (Figure 4.5, R_{14} in a N-terminal helix).[14] The central six Gly residues form a flexible interhelical loop, and in N_TC, the fourth Gly is replaced with a thioglycolic acid (sC) residue, which enables a thiol-thioester exchange.

Succ - E E L R R R L E E L R R R R G G G [sG] G G L E E E L R R L E E E L R R Y - NH_2 $N_TC\alpha$ 1

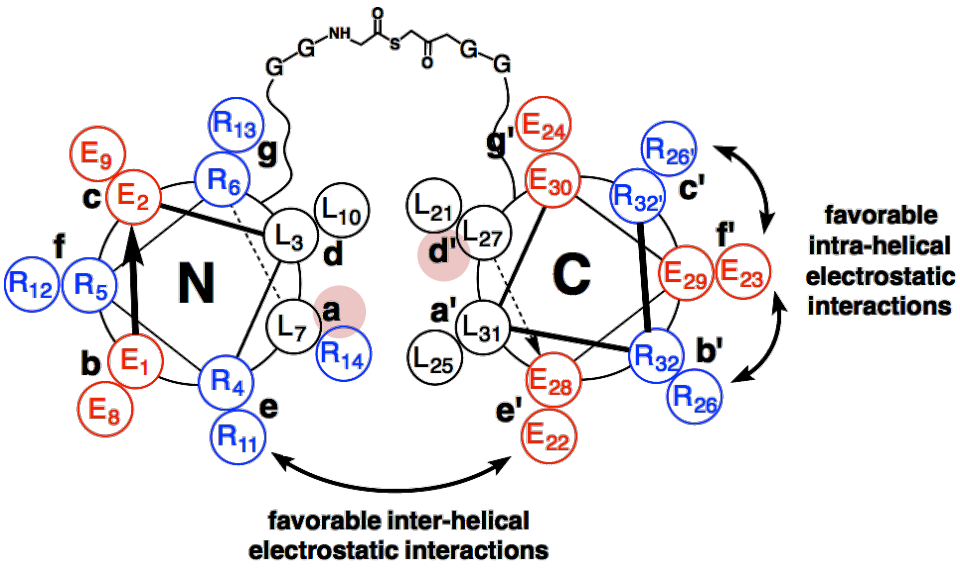

Figure 4.5 $\alpha+\alpha$ Thiodepsipeptide **$N_TC\alpha$1**, which can form an anti-parallel coiled-coil tertiary structure. The sequence of **$N_TC\alpha$1** is shown with thioglycolic acid highlighted in a rectangle. The helical wheel diagram indicates the anti-parallel coiled-coil model of **$N_TC\alpha$1**. Stabilizing inter- and intra-helical electrostatic interactions are shown by curved arrows. Residues at *a* and *d'* positions in the hydrophobic core of the coiled-coil (marked in pink circles) were systematically substituted with different residues (Leu, Ile, Val, Ala, and Asn).

The relationship between sequence and structural stability within the antiparallel coiled-coil was examined by comparing ΔG_{Fold} values derived from BTE experiments, in which hydrophobic interface residues at *a* and *d'* positions were systematically substituted with different residues (Leu, Ile, Val, Ala, and Asn) (Figure 4.5). The BTE strategy was shown to provide data that correlated well with the results found by bioinformatic analysis of coiled-coil interactions.[13,19-21]

4.1.2.3. (α + α/β) Coiled-coil design for BTE analysis

Price *et al.* demonstrated that α+α/β chimeric coiled-coil packing could be studied using the BTE method.[12] This α+α/β BTE study was motivated by the finding that backbones containing alternating α- and β-residues can adopt an α-helix-like conformation that is designated the 14/15-helix.[22,23] The design of the α+α/β antiparallel coiled-coil model was based on the α+α coiled-coil model used by Hadley to explore sequence-stability relationships among coiled-coils via BTE (Figure 4.6).[13,14] In the $N_TC\alpha\beta$ thiodepsipeptide the N-terminal segment is an α-helical fragment containing only α-residues and identical to the N-terminal segment of the previous α+α BTE model. The C-terminal segment is an α/β-peptide fragment designed to form a 14/15-helix, which is expected to pack against the N-terminal α-helix. The N-terminal α-helix and C-terminal α/β-peptide helix are connected by a linker that contains five Gly residues and one thioglycolate (sG) residue, which allows the BTE reaction occur (Figure 4.6). The results from the BTE analysis of $N_TC\alpha\beta$ suggested that ΔG_{Fold} = -1.1 kcal/mol, which indicates that at equilibrium about 85% of the peptide $N_TC\alpha\beta$ is in the folded state (α+α/β coiled-

coil packing), and that α+α/β helix packing is favored by 1.1 kcal/mol relative to a lack of such packing.[12] This value is comparable to ΔG_{Fold} from the analogous α+α coiled coil model, -1.4 kcal/mol.[14]

(A)

Succ - E E L R R R L E E L R R R R G G G ^{s}G G G L E E E L R R L E E E L R R Y - NH_2 $N_TC\alpha$ **1**

Succ - E E L R R R L E E L R R R R G G G ^{s}G G G E E E X L Z E L E X E L R Z Y - NH_2 $N_TC\alpha\beta$ **1**

(B)

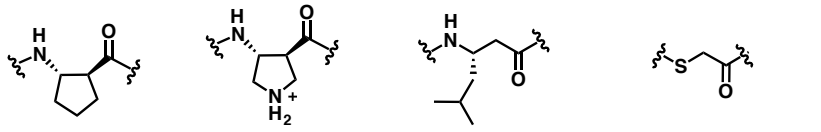

(C)

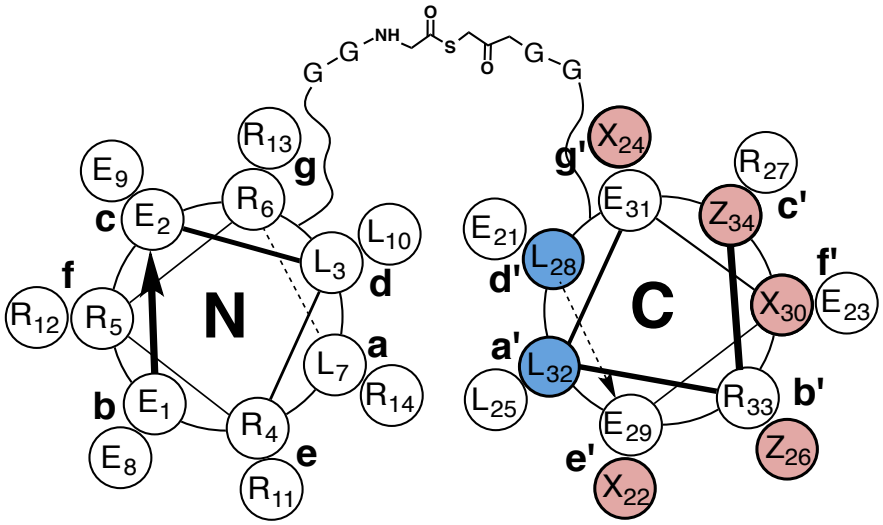

Figure 4.6 (A) Sequences of α-peptide antiparallel coiled-coil **$N_TC\alpha$1** and chimeric (α + α/β)-peptide **$N_TC\alpha\beta$1**. (B) Structures of β-amino acids and thioglycolic acid. (C) Helical wheel diagrams of the antiparallel coiled-coil for **$N_TC\alpha\beta$1** (acyclic β- in blue, cyclic β- in red).

4.2 Efforts to design an α+ α/β/γ coiled coil model system for BTE studies

4.2.1 Initial α+ α/β/γ coiled coil model 1: not suitable for BTE study

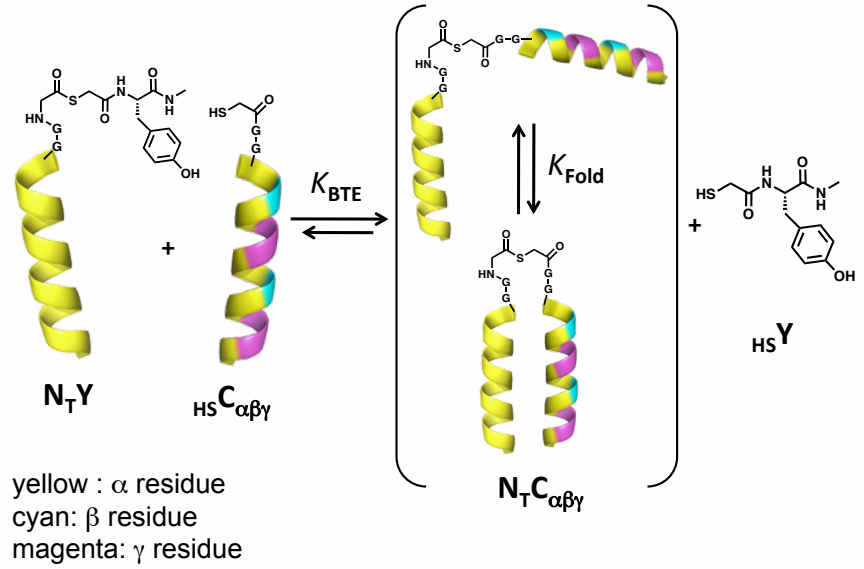

Figure 4.7 Cartoon depicting a thioester exchange assay using an α/β/γ-thiol peptide designs. Parentheses show the two-state folding equilibrium for the thiodepsipeptide.

To quantitatively evaluate contributions of ring-constraints on β- and γ-residues to α/β/γ-peptide helix stability, we sought to conduct thermodynamic analyses of the folded *vs.* unfolded equilibria of (α-helix--loop--α/β/γ-helix)-peptides (Figure 4.7). Our α+α/β/γ coiled-coil model design was based on the previously reported coiled-coil system **$N_TC\alpha1$**,[14] and uses positively charged, or uncharged cyclic β-residues, APC and ACPC, and an uncharged cyclic γ-residue, EtACHA (Figure 4.8).[14] We used ACPC on the β position near the loop region because the ring nitrogen of APC has been shown to carry out nucleophilic attack on the thioester bond. However, these α→ β or γ replacements cause local and global changes in charge and charge distribution between the C-

terminal segment of **$N_TC\alpha$1** and the C-terminal segment of **$N_TC\alpha\beta\gamma$1** (Figure 4.8). To minimize charge inequality between the corresponding C-terminal α-peptide and $\alpha/\beta/\gamma$-peptide segments, we chose a coiled-coil system that switches the charged residues at the C- and N-termini, resulting in **$N_TC\alpha\beta\gamma$2** (Figure 4.8).

In the α+$\alpha/\beta/\gamma$ chimeric thiodepsipeptide **$N_TC\alpha\beta\gamma$2**, the N-terminal segment is identical to the N-terminal α-helix-forming segment of **$N_TC\alpha$2**, and the C-terminal portion is an $\alpha/\beta/\gamma$-peptide with an $\alpha\gamma\alpha\alpha\beta\alpha$ motif analogous to the C-terminus of **$N_TC\alpha$2** (Figure 4.8). The central glycine-rich segment is positioned to form a flexible interhelical loop. The C-terminal segment can be varied systematically by incorporating different β and γ residues, with and without ring constraints.

(A)

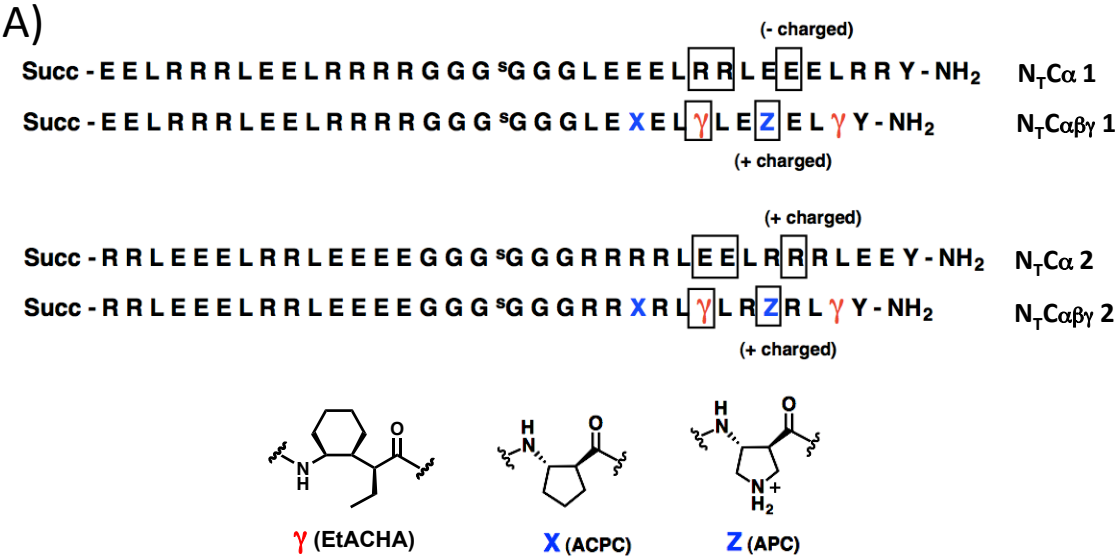

(B)

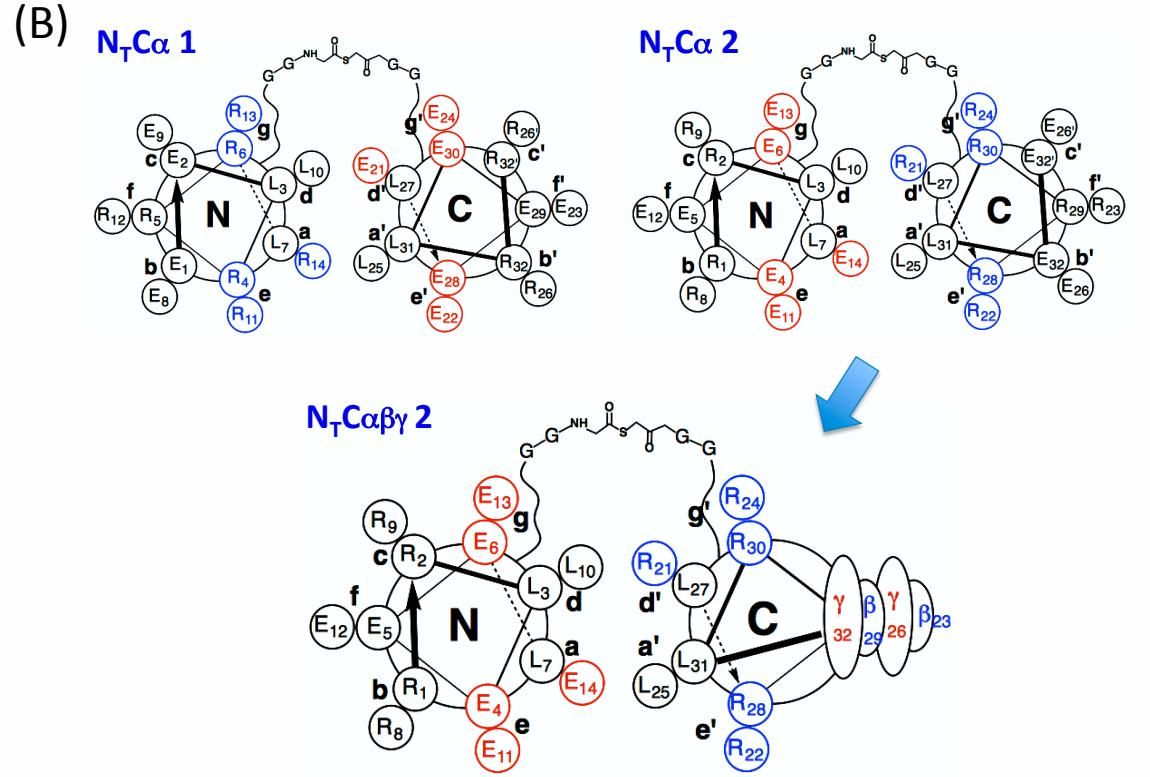

Figure 4.8 (A) Sequences of α+α and α+α/β/γ thiodepsipeptides in the N_TC series (sG=thioglycolic acid). (B) Helical wheel diagrams of the anti-parallel coiled-coil tertiary structures that should be available to **$N_TC\alpha1$**, **$N_TC\alpha2$**, and **$N_TC\alpha\beta\gamma2$**.

Several control experiments are necessary to determine whether the $\alpha+\alpha/\beta/\gamma$ model system is suitable for BTE analysis. The coiled-coil should adhere to the key relationship in eq. 4.4 ($[_{HS}Y][N_TC_U]/[N_TY][_{HS}C]=1$), the full-length N_TC should not self-associate, and $_{HS}Y$ should not have a favorable interaction with the N-terminal helix N_TY. For an $\alpha+\alpha/\beta/\gamma$ model system, another critical control experiment is required in order to determine whether the coiled-coil folding is exclusively driven by the six Leu residues that are intended to form the hydrophobic core (at positions 3, 7, 10, 25, 27, and 31, Figure 4.8). These control experiments include testing analogous $\alpha+\alpha$ coiled-coil models. A positive control $\alpha+\alpha$ coiled-coil model, which contains six Leu residues in the intended hydrophobic core of the tertiary structure, is expected to show favorable coiled-coil folding, with $\Delta G_{Fold} \leq$ -1 kcal/mol. A negative control $\alpha+\alpha$ coiled-coil model, which contains one hydrophilic Asn and five Leu residues in the intended hydrophobic core, is expected to show little tendency for coiled-coil forming ($\Delta G_{Fold} \approx 0$ kcal/mol).[12,14]

In previous BTE coiled-coil model systems with $\alpha+\alpha$ and $\alpha+\alpha/\beta$ peptides, a single core substitution from Leu to Asn in the C-terminal helix resulted in a drastic coiled-coil destabilization, with a ΔG_{Fold} increase of about 1 kcal/mol compared to the analogous system without the Asn substitution (Figure 4.9).[12,14] A similar trend is expected for an $\alpha+\alpha/\beta/\gamma$ coiled-coil model if the full-length thioester peptide folding depends on packing within the intended hydrophobic core.

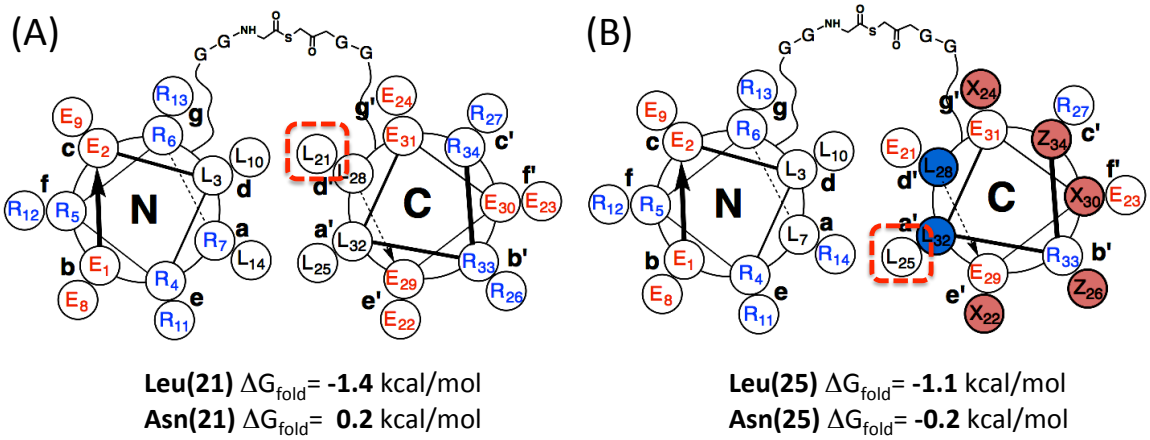

Figure 4.9 Coiled-coil disruption by replacing Leu with Asn in hydrophobic interface. (A) α+α thiodepsipeptide model[14]. (B) α+α/β thiodepsipeptide model[12].

To establish a positive control α+α model based on the α+α/β/γ model **N_TCαβγ 2**, we used two Ala to substitute for one γ, one Ala for ACPC, and one Arg for APC (Figure 4.10). The resulting α+α model, **N_TCα3**, and the analogous negative control α+α model, **N_TCα3_L27N**, which contains one Asn at position 27, were tested by BTE experiments. BTE with **N_TCα3_L27N** resulted in ΔG_{Fold} ≈ -1 kcal/mol, indicating that the intended negative control **N_TCα3_L27N** experiences a significant driving force for association of the N- and C- terminal segments (Figure 4.10). This unexpected result may rise because since five of the charged residues in **N_TCα2** (Figure 4.8A) are substituted with Ala residues in **N_TCα3_L27N**, and the Ala-rich "back face" of the C-terminal helix may engage in hydrophobic association with the Leu-rich face of the N-terminal helix or with other molecules in the system. These control experiments indicate the α+α/β/γ model **N_TCαβγ2** is not suitable for BTE study. Indeed, several preliminary BTE experiment using C-terminal α/β/γ-peptides **$_{HS}$Cαβγ3**, **$_{HS}$Cαβγ4**, and **$_{HS}$Cαβγ4_L27N** all resulted in ΔG_{Fold} ≈ -1 kcal/mol (Figure 4.10). These results suggest that the back face of the C-

terminal α/β/γ-peptide helix, where β and γ residues are dominant, can participate in hydrophobically driven packing against the N-terminal α-helix.

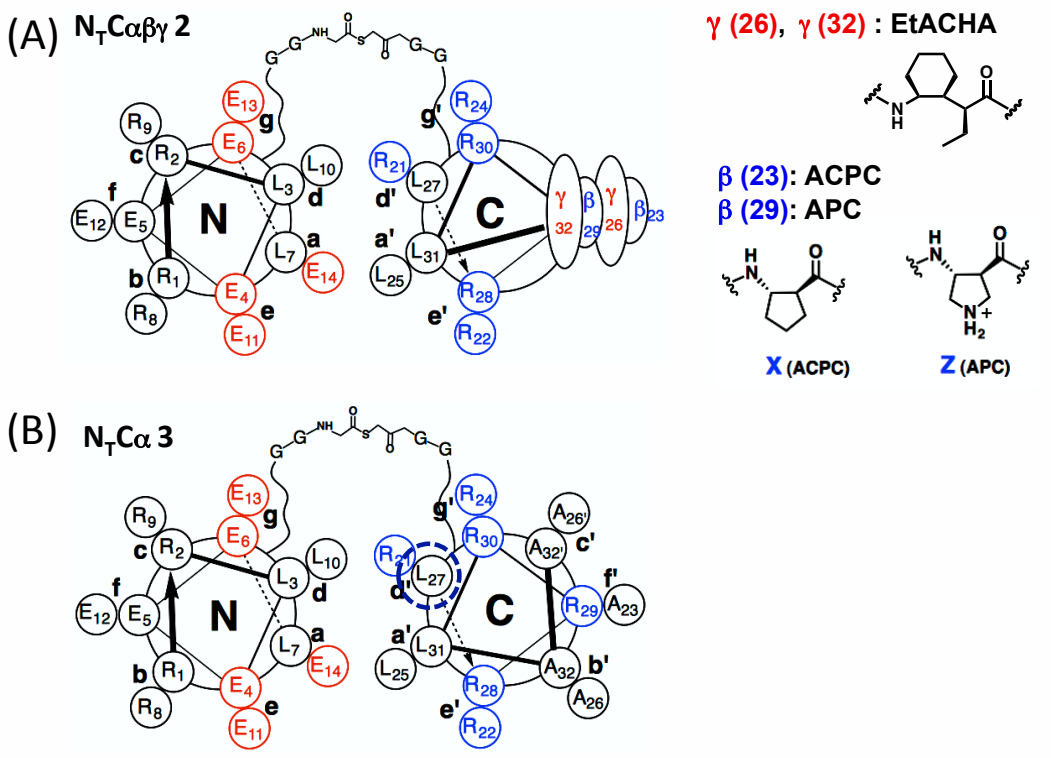

N_TCα 3_L27N From N_TCα 3, Leu at 27 is replaced by Asn

(C)

	21					25			27				31				ΔG$_{fold}$ (kcal/mol)
$_{HS}$Cα2	sG	G	G	R	R	R	R	L	E	E	L	R	R	R	L	E	E	Y	-1.4
$_{HS}$Cα3_L27N	sG	G	G	R	R	A	R	L	A	A	N	R	R	R	L	A	A	Y	-1.1

(D)

	21					25			27				31				ΔG$_{fold}$ (kcal/mol)
$_{HS}$Cαβγ 3	sG	G	G	R	R	X	R	L	γ^c	L	R	Z	R	L	γ^4A	Y	-1.3
$_{HS}$Cαβγ 4	sG	G	G	R	R	βA	R	L	γ^4A	L	R	βR	R	L	γ^4A	Y	-1.1
$_{HS}$Cαβγ 4_L27N	sG	G	G	R	R	βA	R	L	γ^4A	N	R	βR	R	L	γ^4A	Y	-0.9

Figure 4.10 (A) Helical wheel diagrams of the anti-parallel coiled-coil tertiary structures for **N_TCαβγ2** and the α analogue. (B) **N_TCα3**; Leu at 27 position is replaced by Asn for the negative control α analogue **N_TCα3_L27N**. (C) Sequences of thiol peptides **$_{HS}$Cα2** and **$_{HS}$Cα3_L27N**, and ΔG_{Fold} values from BTE assays using them. (D) Sequences of thiol α/β/γ-peptides **$_{HS}$Cαβγ3**, **$_{HS}$Cαβγ4** and **$_{HS}$Cαβγ4_L27N**, and ΔG_{Fold} values from BTE assays using them.

4.2.2 α+ α/β/γ Coiled coil model 2: not suitable for BTE study

In order to try to generate a suitable α+α/β/γ coiled-coil model, in which folding is solely driven by the intended hydrophobic core interactions, we sought to introduce charged residues on the back face of the C-terminal α/β/γ helix. For charged cyclic β residues, APC could not be used because of its tendency to carry out nucleophilic attack on the thioester bond. Instead, a 5-membered-ring-constrained β-residue containing a guanidinium group, gAPC, was chosen (**N_TCαβγ5**) (Figure 4.11A). If this substitution does not prevent the back face of the C-terminal helix from engaging in hydrophobic interactions, then an anionic 6-membered-ring constrained γ residue could be incorporated (**N_TCαβγ6**) (Figure 4.11A).

The α+α coiled-coil peptides analogous to the new α+α/β/γ coiled-coil models are **N_TCα5** and **N_TCα6** (Figure 4.11B and C). However, the negative control α+α systems **N_TCα5_L25N** and **N_TCα6_L25N**, which contain Asn at position 25, both showed only small changes in ΔG_{Fold} relative to **N_TCα5** and **N_TCα6**, respectively (Figure 4.11D). ΔG_{Fold} values for **N_TCα5_L25N** and **N_TCα6_L25N** were ~ -1.3 kcal/mol, suggesting significant packing between the N- and C-terminal segments (Figure 4.11D). These results suggest that the intended hydrophobic core interaction was minimally disrupted by single replacement with a hydrophilic residue at position 25, indicating that the analogous α+α/β/γ coiled-coil **N_TCαβγ5** and **N_TCαβγ6** are not suitable as coiled-coil models for BTE studies (Figure 4.11).

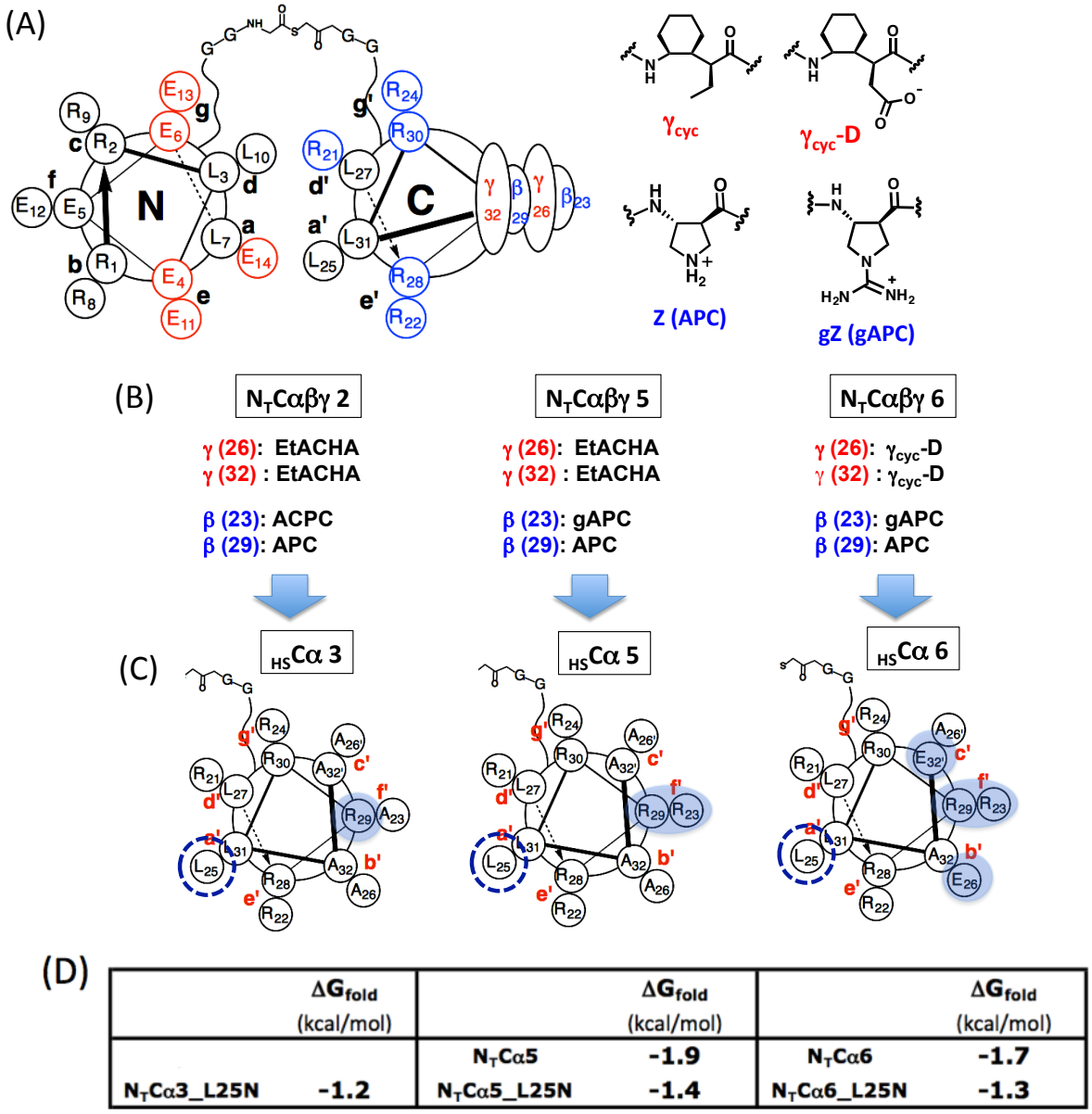

	ΔGfold (kcal/mol)		ΔGfold (kcal/mol)		ΔGfold (kcal/mol)
		NTCα5	-1.9	NTCα6	-1.7
NTCα3_L25N	-1.2	NTCα5_L25N	-1.4	NTCα6_L25N	-1.3

Figure 4.11 (A) Representative helical wheel for **$N_TC\alpha\beta\gamma$**, and structures of cyclic β and γ residues. (B) **$N_TC\alpha\beta\gamma$ 3**, **5**, and **6**. (C) Helical wheel diagrams of C-terminal thiol α-peptides **$_{HS}C\alpha$ 3**, **5**, and **6**, which are analogous to C-terminal α/β/γ-helices of **$N_TC\alpha\beta\gamma$ 2**, **5**, and **6**, respectively. Leu25 is replaced by Asn in negative control α analogues. (D) ΔG_{Fold} values from positive and negative control peptides.

4.2.3 α+ α/β/γ Coiled-coil model 3

Since we could not find a functional model system from the α-sequences containing negatively charged residues at the *e* and *g* heptad positions of the N-terminal helix and positively charged residues at these positions of the C-terminal helix, we turned to refining the original α+α coiled-coil system with the opposite heterodimer-specifying charged residues (Figure 4.12). To maximize charge density on the back face of the C-terminal α/β/γ helix, we used charged β- and γ-residues, including the guanidinium-containing cyclic β (gAPC), β^3-hArg, anionic cyclic γ (γ_{cyc}-D), and γ^4-hAsp. For the analogous control α+α models, the C-terminal α-helix that corresponds to the α/β/γ helix **Cαβγ7** is **Cα7** (Figure 4.12). ΔG_{Fold} values measured for **N_TCα7** and **N_TCα7_L25N** were about -0.8 and -0.1 kcal/mol, respectively. These results suggest that this α+α model may fold driven by the intended hydrophobic core interaction, and thus encouraging the further use of this sequence as a starting point for BTE studies (Figure 4.12).

We performed preliminary BTE experiments using analogous α/β/γ-thiol peptides containing acyclic β- and acyclic γ-residues (**$_{HS}$Cαβγ8**), which might have limited helicity due to the lack of constrained residues (Figure 4.12). The resulting ΔG_{Fold} values for **N_TCαβγ8** and negative control **N_TCαβγ8_L25N** were about 0.2 and 0.4 kcal/mol, respectively. Since the C-terminal segment within **N_TCαβγ8** is not expected to be very helical, and thus the coiled-coil folding is not expected to be favorable, the ΔG_{Fold} value of 0.2 kcal/mol for **N_TCαβγ8** is reasonable. The negative control, **N_TCαβγ8_L25N**, lacking a hydrophobic residue in the expected core, also resulted in a reasonable ΔG_{Fold}

value of 0.4 kcal/mol. The current coiled-coil model system could be adequate for BTE study with a helical α/β/γ motif. However, it is important to determine if the full-length thioester peptide **$N_TC\alpha\beta\gamma8$** is monomeric. The possibility of self-association will be addressed by analytical ultracentrifugation (AU) experiments using the analogous full-length amide peptides **$N_AC\alpha\beta\gamma8$**.

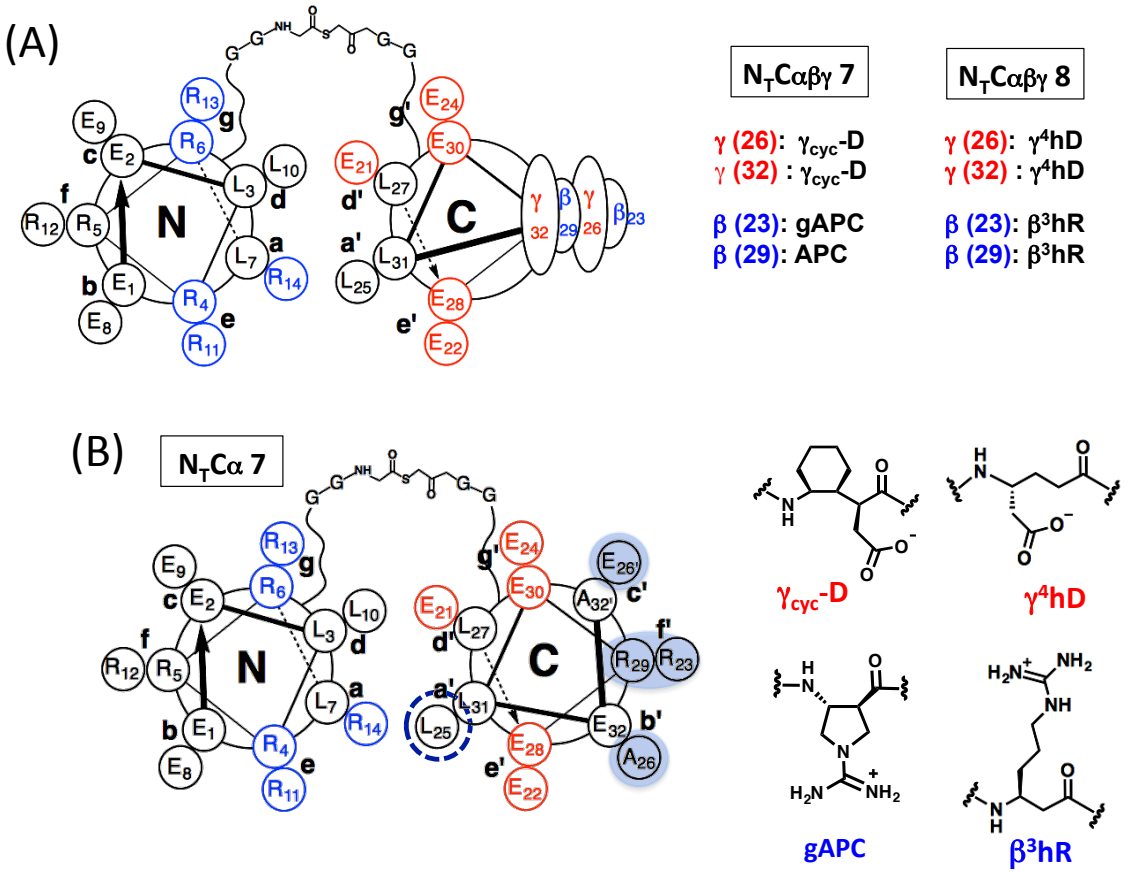

(C)

	ΔG_{fold} (kcal/mol)		ΔG_{fold} (kcal/mol)
$N_TC\alpha7$	-0.8	$N_TC\alpha\beta\gamma$ 8	0.2
$N_TC\alpha7$_L25N	-0.1	$N_TC\alpha\beta\gamma$ 8_L25N	0.4

Figure 4.12 (A) Representative helical wheel diagrams of the anti-parallel coiled-coil tertiary structures for **$N_TC\alpha\beta\gamma$**, and designation of **$N_TC\alpha\beta\gamma7$**, and **8**. (B) Helical wheel diagram of **$N_TC\alpha7$**. Leu25 is replaced by Asn in negative control. (D) ΔG_{Fold} values from positive and negative control peptides.

4.3 Conclusions and Future directions

In order to quantitatively evaluate the contributions of ring constraints to α/β/γ peptide helix stability, we attempted to modify an α+α coiled-coil model that had been previously used for BTE studies. However, in our initial α/β/γ design, one γ-residue replaces two charged α-residues on the back face of the C-terminal helix, sacrificing two charges per one γ-replacement. This caused the back face of the C-terminal helix to be quite hydrophobic, which might cause unexpected interactions with the N-terminal helix.

To maximize charge density on the back face (b',c', and f' positions) of the α/β/γ-peptide helix, guanidinium-containing cyclic β- and anionic cyclic γ- residues can be incorporated in C-terminal α/β/γ helix.[24] Negative control BTE experiments have been carried out with different α+α and α+α/β/γ coiled-coil models using acyclic β- and γ-residues, *i.e.*, γ^4hAsp and β^3hArg. One Leu at the hydrophobic interface on the C-terminal helix was substituted with Asn to destabilize coiled-coil folding. After several trials, we found one system that was significantly destabilized by Leu → Asn substitution in the α+α system, **N_TCα7** and **N_TCα7_L25N**, analogous to α+α/β/γ system **N_TCαβγ7**, which might thus be suitable for future BTE studies.

In the future, AU analysis must be performed for **N_ACαβγ7** and **N_ACαβγ8**; if the α+α and α+α/β/γ full-length peptides (containing all-amide backbone) from this system are monomeric, the model is appropriate for BTE analysis. However, if the full-length molecules self-associate as determined by AU, we should search further for a BTE system. Ongoing BTE studies will allow us to quantitatively evaluate the effect of cyclic vs. acyclic β- and γ-residues on α/β/γ-peptide helix folding and stability. These studies

will improve our understanding of α/β/γ-peptidomimetics and enable their use to control specific protein-protein interactions.

4.4 Experimental

4.4.1 General

Fmoc α-amino acids and resin for solid phase peptide synthesis were purchased from Novabiochem or Chem-Impex, and coupling reagents and additives, O-benzotriazole-N,N,N',N'-tetramethyluronium hexafluorophosphate (HBTU), O-(7-azabenzotriazol-1yl)-N,N,N,N'-tetramethyluronium hexafluorophosphate (HATU), 1-ethyl-3-(3-dimethylaminopropyl)carbodiimide hydrochloride (EDCI), hydroxybenzotriazole (HOBt), 1-Hydroxy-7-azabenzotoriazole) (HOAt), were purchased from Chem-Impex. Fmoc β-amino acids such as Fmoc-(1*S*,2*S*)-2-aminocyclopentane carboxylic acid and acyclic Fmoc β^3-amino acids were purchased from Chem-Impex. Acyclic γ-amino acids were purchased from Polypeptide group. Ring constrained γ-amino acid, EtACHA, was synthesized according to previous reports.[24] Other reagents and solvents were purchased from Sigma-Aldrich.

4.4.2 Peptide Synthesis and Purification

4.4.2.1 Synthesis of thiol peptide ($_{HS}$C)

All of the α- and α/β/γ-peptide thiols described here were synthesized on Nova PEG rink amide resin (25-50 μmol scale) by microwave-assisted solid-phase method using a CEM MARS microwave reactor.[7,8,25] For α- and cyclic/acyclic β-amino acids

coupling reactions, Fmoc-amino acids were pre-activated in a separated vial (4 equiv. of Fmoc-amino acids, 3.95 equiv. of HBTU, 8 equiv. of DIEA, 0.1 M HOBT in DMF solution) for 1-2 minutes, then the solution was added to resin in a filter tube, reacted under microwave irradiation (2 min ramp to 70 ^{o}C, 4 min hold at 70 ^{o}C for α-residues, 12 min hold for β-residues). For acyclic γ-amino acids coupling reactions, the same condition to β-amino acid coupling was applied but DIEA was added right before starting microwave irradiation in order to avoid intra-cyclization reaction of γ-amino acids. Cyclic γ-residue (EtACHA) coupling reactions were performed by pre-activating 4 equiv. of Fmoc-amino acid with 4 equiv. of EDCI and 8 equiv. of DIEA in 0.1M HOAt in DMF, then the mixture solution was added to resin and reacted for 14 hours at room temperature while gently shaking. Fmoc deprotection reactions were carried out using 20 % piperidine in DMF under microwave irradiation (2 min ramp to 80 ^{o}C, 2 min hold at 80 ^{o}C). The N-terminal thiols were obtained by the coupling of S-trityl-thioglycolic acid as the last residue. Peptides were globally deprotected and cleaved from the resin by suspending in cleavage cocktail (95% trifluoroacetic acid (TFA), 2.5 % water, and 2.5 % triisopropylsilane) for 4~5 hours. After precipitating peptides in cold diethyl ether, peptides were purified by HPLC.

4.4.2.2 Synthesis of thioester peptide (N_TY)

To prepare thioester peptides **N_TY(1)** and **N_TY(2)**, **N_{TE}(1)** and **N_{TE}(2)** were synthesized by safety catch method[26,27] on H-Gly-sulfamyl-butyryl Nova Syn TG resin (50 μmol scale) by microwave-assisted solid-phase method using a CEM MARS

microwave reactor.[7,8,25] Cleaved and purified **N_{TE}(1)** and **N_{TE}(2)** were reacted with $_{HS}$**Y** to yield **N_TY(1)** and **N_TY(2)**.

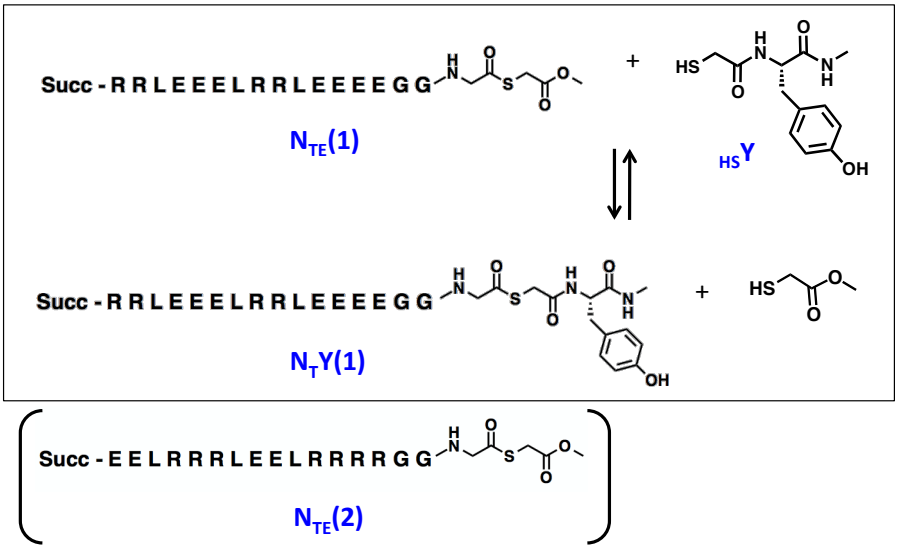

For α-amino acids coupling reactions, Fmoc-amino acids were pre-activated in a separated vial (4 equiv. of Fmoc-amino acids, 3.95 equiv. of HBTU, 8 equiv. of DIEA, 0.1 M HOBT in DMF solution) for 1-2 minutes, then the solution was added to resin in a filter tube, reacted under microwave irradiation (2 min ramp to 70 °C, 4 min hold at 70 °C for α-residues, 12 min hold for β-residues). Fmoc deprotection reactions were carried out using 20 % piperidine in DMF under microwave irradiation (2 min ramp to 80 °C, 2 min hold at 80 °C). Upon completion of couplings, the N-terminus amine was reacted with mono-*tert*-butyl succinate under the same condition for the α-amino acid couplings. A sulfonamide nitrogen was alkylated by reacting the resin with iodoacetonitrile (180 μL, 50 equiv., filtered through basic alumina prior to use) and 1.0 M DIEA in DMF (6 mL) under microwave irradiation (1 hour at 50 °C). The reaction was washed with DMF. To cleave the peptide from the resin, methyl thioglycolate (54 μL, 12 equiv.) and DMF (1

mL) were added to the resin and reacted under microwave (1 hour at 50 ^{o}C) The liquid was filtered into a flask, and the resin was then washed three times with CH_2Cl_2 (5 mL), and the combined filtrate was rotary evaporated. Peptides were globally deprotected by suspending in cleavage cocktail (95% trifluoroacetic acid (TFA), 2.5 % water, and 2.5 % triisopropylsilane) for 4~5 hours. After precipitating peptides in cold diethyl ether, peptides were purified by HPLC to give $\mathbf{N_{TE}(1)}$ and $\mathbf{N_{TE}(2)}$.

$\mathbf{N_{TE}(1)}$ and $\mathbf{N_{TE}(2)}$ were combined with peptide thiol $_{HS}\mathbf{Y}$ (~ 10 fold excess) in aqueous (pH 7, 50 mM phosphate buffer, 2 mM triscarboxyethyl phosphine) solution, which allowed thioester exchange. After 2 hours of exchange at room temperature, $\mathbf{N_TY(1)}$ and $\mathbf{N_TY(2)}$ were collected by HPLC.

4.4.3 Backbone thioester exchange

4.4.3.1 BTE method

Thioester exchange assays were performed by mixing 200 μM of an N-terminal a-peptide thioester ($\mathbf{N_TY}$) and 200 μM of a C-terminal α- or α/β/γ-peptide thiol ($_{HS}\mathbf{C}$) in BTE buffer composed of 50 mM sodium phosphate and 2 mM tris(2-carboxyethyl)phosphine hydrochloride (TCEP) to allow 100 μM BTE reaction condition. Each peptide stock solution was prepared in BTE buffer and quantified by UV. Two peptides ($\mathbf{N_TY}$ and $_{HS}\mathbf{C}$) were combined to give 200 μM solution, and mixed thoroughly. About 30 μL of the BTE reaction mixture was injected onto an analytical HPLC, and the equilibrating species ($_{HS}\mathbf{C}$, $\mathbf{N_TY}$, $\mathbf{N_TC}$, and $_{HS}\mathbf{Y}$) were detected by UV-Vis absorption at 275 nm. The relative concentration of each species at equilibrium is determined by comparing the integrated peak areas, which are used to calculate the equilibrium

constant (K_{BTE}). The K_{BTE} allows to determine K_{Fold} and ΔG_{Fold} from the relationships $K_{Fold} = K_{BTE} - 1$ (Figure 4.3, eq 4.5) and $\Delta G_{Fold} = -RTlnK_{Fold}$.

4.4.3.2 BTE data (HPLC traces and MALDI-MS)

Sequences of peptides used for BTE assays and ΔG_{Fold} (kcal/mol) values

				3				7			10				14				
N_TY(1)	succ	R	R	L	E	E	E	L	R	R	L	E	E	E	E	G	G	G	sY-*N*-Me
				21				25			27				31				**ΔG_{fold}** (kcal/mol)
$_{HS}$Cα2	sG	G	G	R	R	R	R	L	E	E	L	R	R	R	L	E	E	Y	**-1.4**
$_{HS}$Cα3_L27N	sG	G	G	R	R	A	R	L	A	A	N	R	R	R	L	A	A	Y	**-1.1**
$_{HS}$Cα3_L25N	sG	G	G	R	R	A	R	N	A	A	L	R	R	R	L	A	A	Y	**-1.2**
$_{HS}$Cα5	sG	G	G	R	R	**R**	R	L	A	A	L	R	R	R	L	A	A	Y	**-1.9**
$_{HS}$Cα5_L25N	sG	G	G	R	R	**R**	R	N	A	A	L	R	R	R	L	A	A	Y	**-1.4**
$_{HS}$Cα6	sG	G	G	R	R	**R**	R	L	**E**	A	L	R	R	R	L	A	**E**	Y	**-1.7**
$_{HS}$Cα6_L25N	sG	G	G	R	R	**R**	R	N	**E**	A	L	R	R	R	L	A	**E**	Y	**-1.3**
$_{HS}$Cαβγ 3	sG	G	G	R	R	**X**	R	L	**γ^c**		L	R	**Z**	R	L	**γ^4A**		Y	**-1.3**
$_{HS}$Cαβγ 4	sG	G	G	R	R	**βA**	R	L	**γ^4A**		L	R	**βR**	R	L	**γ^4A**		Y	**-1.1**
$_{HS}$Cαβγ 4_L27N	sG	G	G	R	R	**βA**	R	L	**γ^4A**		N	R	**βR**	R	L	**γ^4A**		Y	**-0.9**

				3				7			10				14				
N_TY(2)	succ	E	E	L	R	R	R	L	E	E	L	R	R	R	R	G	G	G	sY-*N*-Me
				21				25			27				31				**ΔG_{fold}** (kcal/mol)
$_{HS}$Cα7	sG	G	G	E	E	R	E	L	A	E	L	E	R	E	L	E	A	Y	**-0.8**
$_{HS}$Cα7_L25N	sG	G	G	E	E	R	E	N	A	E	L	E	R	E	L	E	A	Y	**-0.1**
$_{HS}$Cαβγ8	sG	G	G	E	E	**βR**	E	L	**γ^4D**		L	E	**βR**	E	L	**γ^4D**		Y	**0.2**
$_{HS}$Cαβγ8_L25N	sG	G	G	E	E	**βR**	E	N	**γ^4D**		L	E	**βR**	E	L	**γ^4D**		Y	**0.4**

Table of BTE data in ΔG_{Fold} (kcal/mol) values

	Run1	Run2	Run3	Run4	Run5	Run6	Run7	Avg	Std
$_{HS}$Cα2	-1.31	-1.28	-1.37	-1.36	-1.40	-1.43	-1.36	-1.4	0.05
$_{HS}$Cα3_L27N	-1.30	-1.11	-0.99	-1.10	-0.99			-1.1	0.13
$_{HS}$Cα3_L25N	-1.11	-1.17	-1.13	-1.26				-1.2	0.06
$_{HS}$Cα5	-1.90	-2.00	-1.87					-1.9	0.07
$_{HS}$Cα5_L25N	-1.47	-1.45	-1.39	-1.39				-1.4	0.04
$_{HS}$Cα6	-1.65	-1.74	-1.70	-1.65				-1.7	0.04
$_{HS}$Cα6_L25N	-1.38	-1.20	-1.28					-1.3	0.09
$_{HS}$Cαβγ 3	-1.29	-1.27	-1.38	-1.23				-1.3	0.06
$_{HS}$Cαβγ 4	-1.07	-1.13	-1.10	-1.13				-1.1	0.03
$_{HS}$Cαβγ 4_L27N	-0.78	-0.96	-0.95					-0.9	0.10
$_{HS}$Cα7	-0.83	-0.65	-0.81	-0.90				-0.8	0.11
$_{HS}$Cα7_L25N	-0.08	-0.11	-0.07	-0.19	-0.25			-0.1	0.08
$_{HS}$Cαβγ8	0.34	-0.03	0.10	0.40				0.2	0.20
$_{HS}$Cαβγ8_L25N	0.41	0.20	0.64					0.4	0.22

MALDI Data

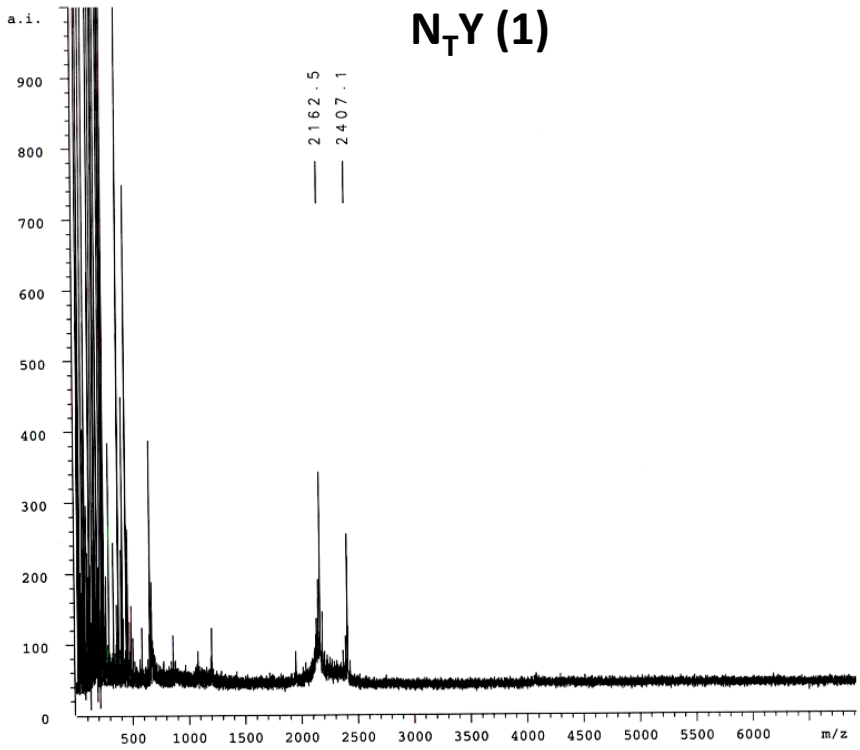

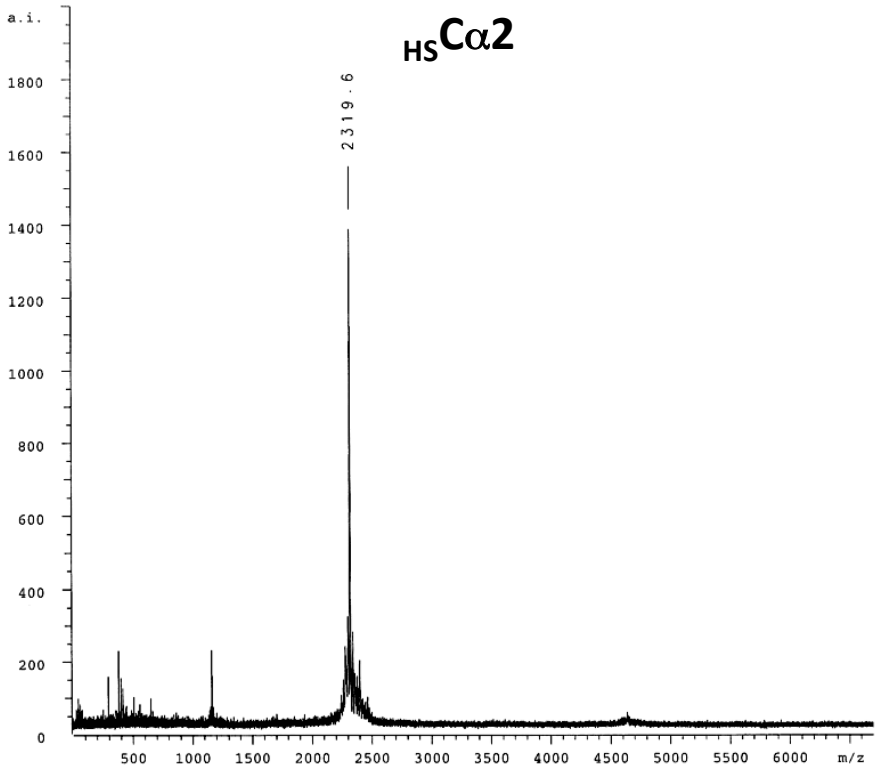
HSCα2
a.i.
2319.6
m/z

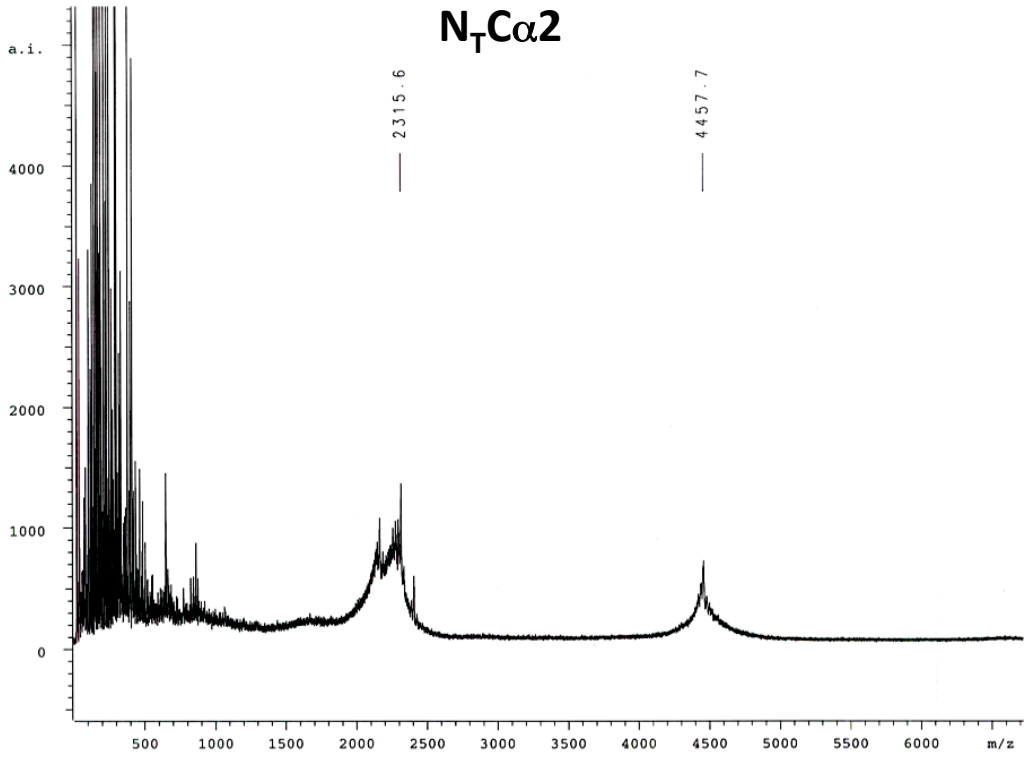
NTCα2
a.i.
2315.6
4457.7
m/z

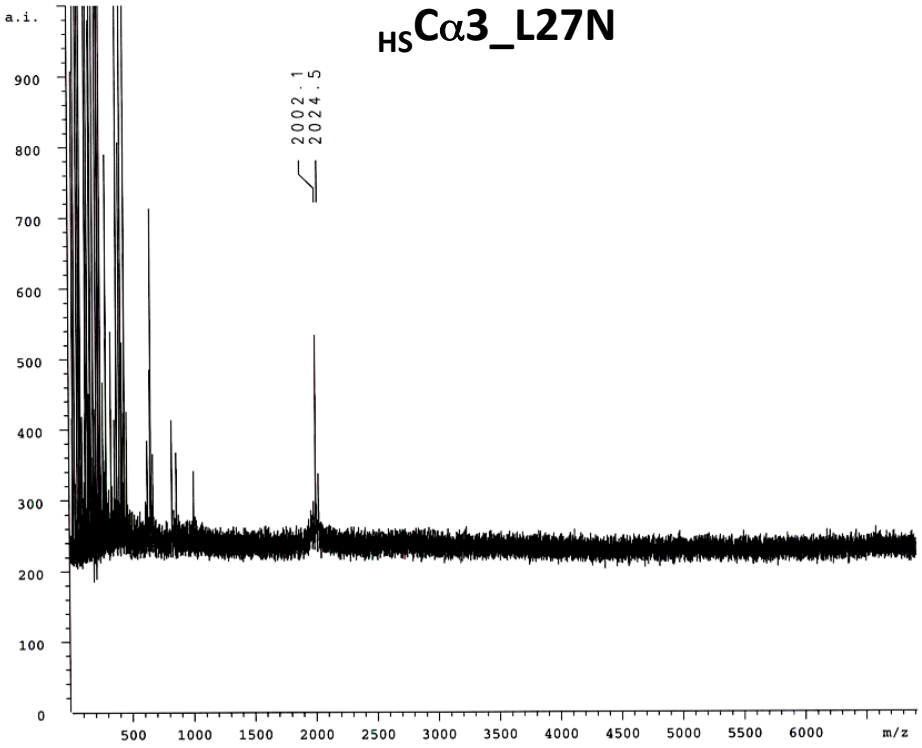
$_{HS}$Cα3_L27N
a.i.
2002.1
2024.5
m/z

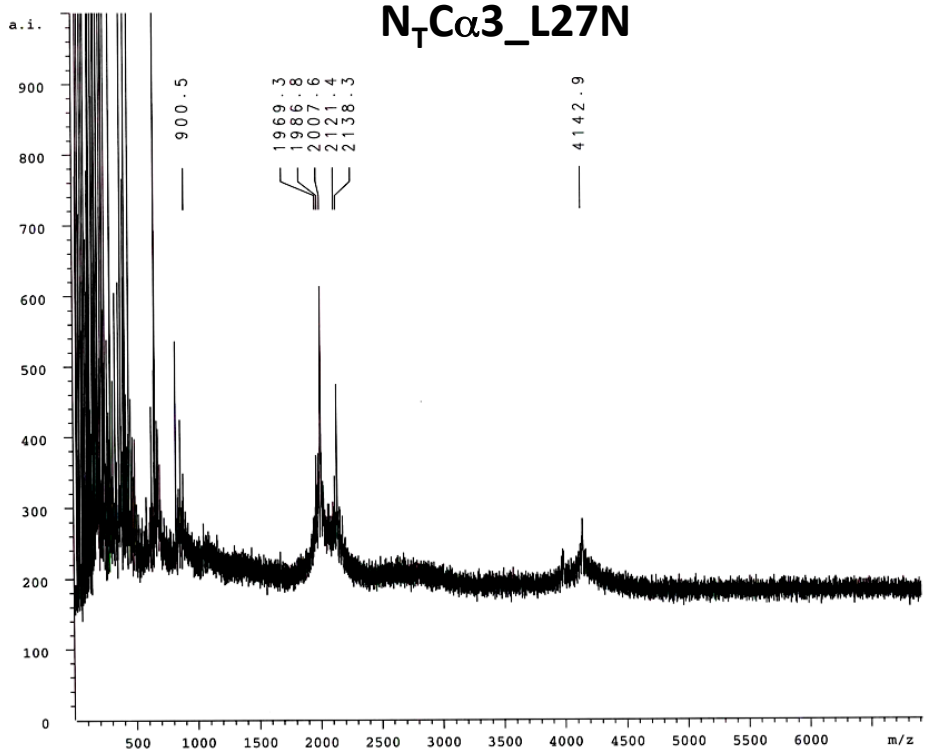
N_TCα3_L27N
a.i.
900.5
1969.3
1986.8
2007.6
2121.4
2138.3
4142.9
m/z

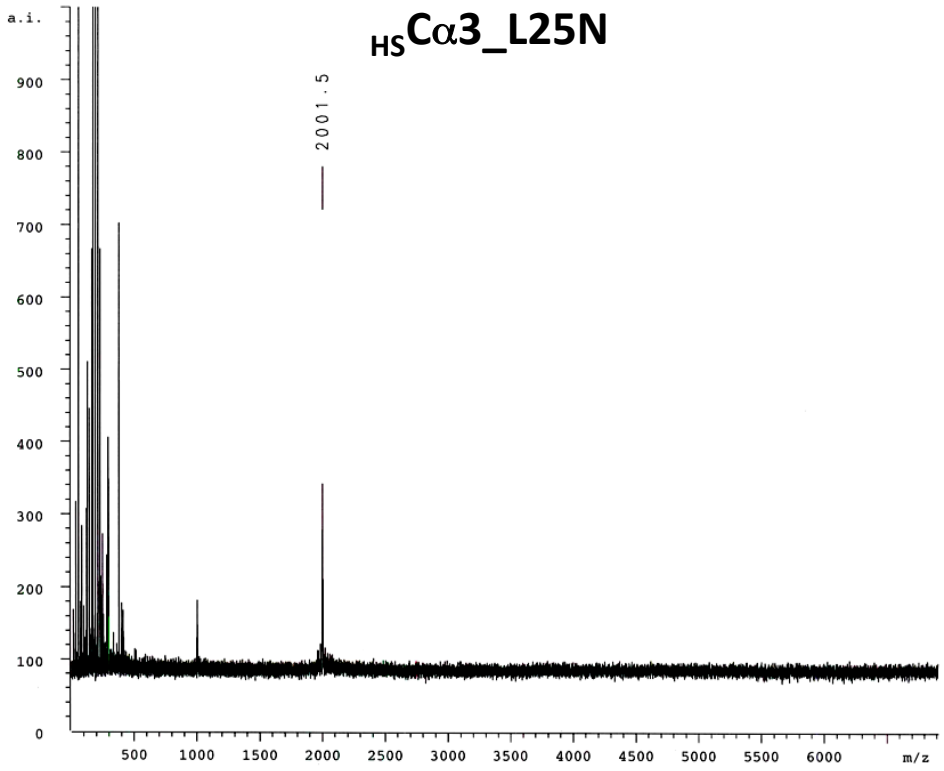
HSCα3_L25N
a.i.
2001.5
m/z

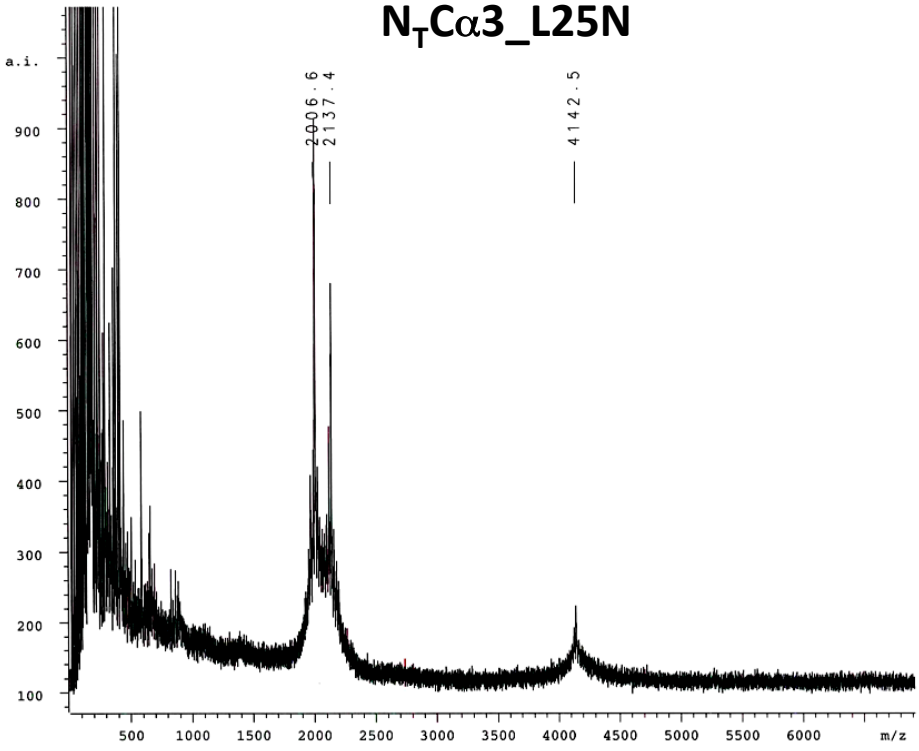
NTCα3_L25N
a.i.
2006.6
2137.4
4142.5
m/z

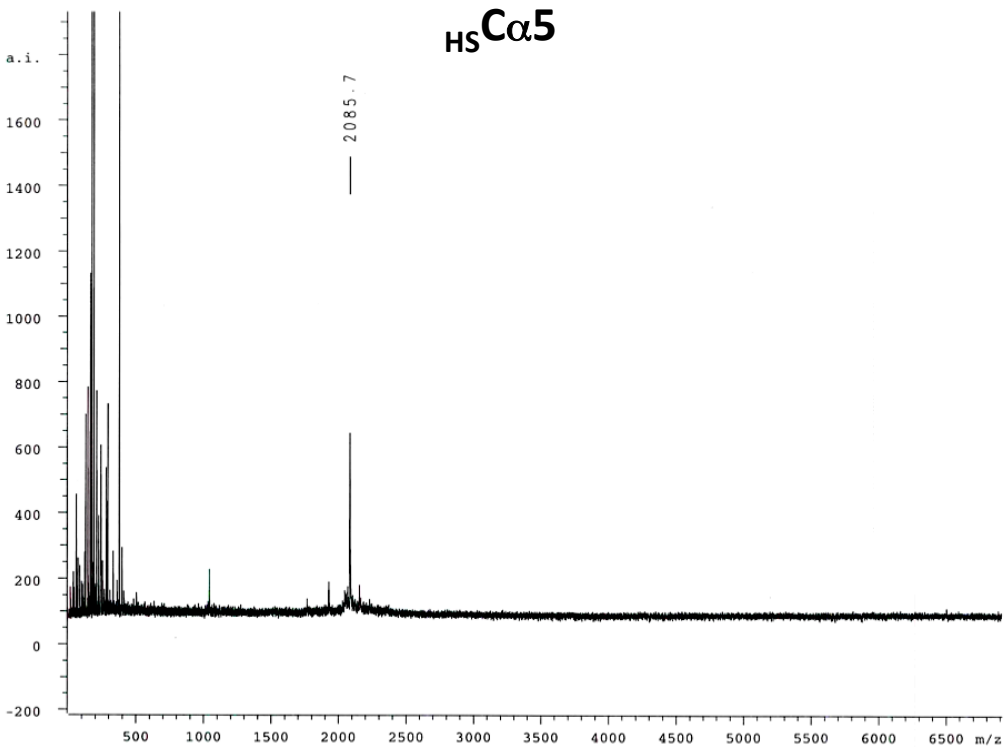
HSCα5
a.i.
2085.7
1600
1400
1200
1000
800
600
400
200
0
-200
500
1000
1500
2000
2500
3000
3500
4000
4500
5000
5500
6000
6500
m/z

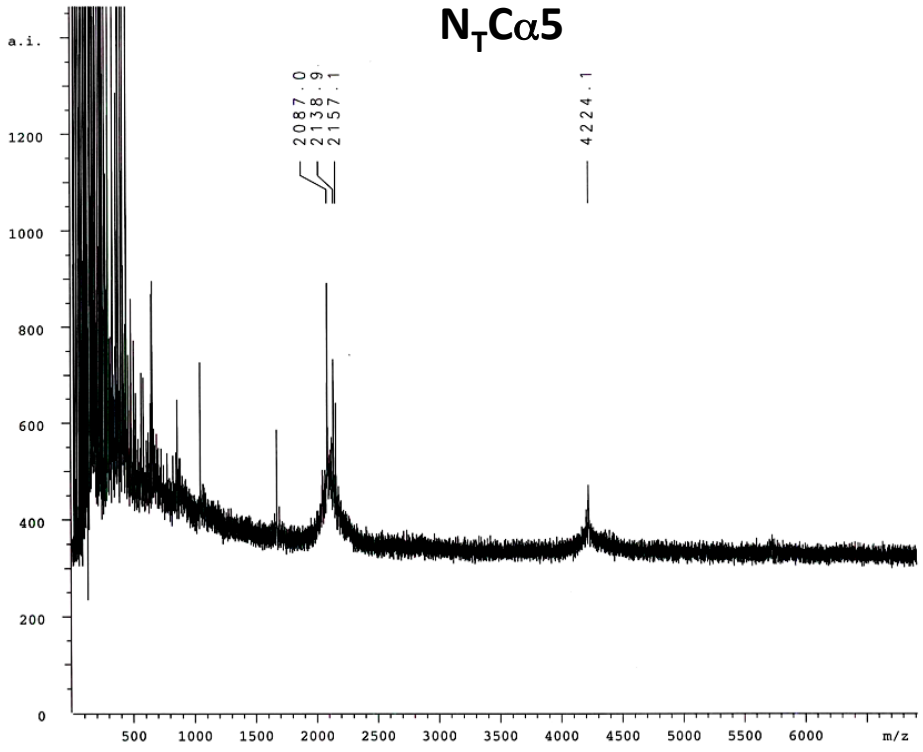
NTCα5
a.i.
2087.0
2138.9
2157.1
4224.1
1200
1000
800
600
400
200
0
500
1000
1500
2000
2500
3000
3500
4000
4500
5000
5500
6000
m/z

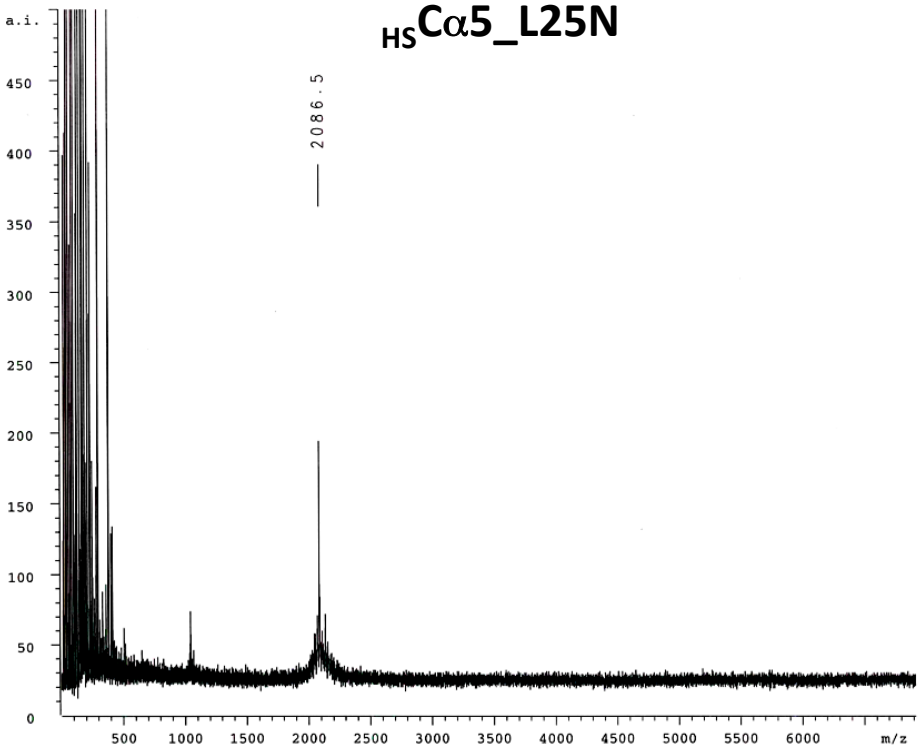
$_{HS}$Cα5_L25N
a.i.
2086.5
m/z

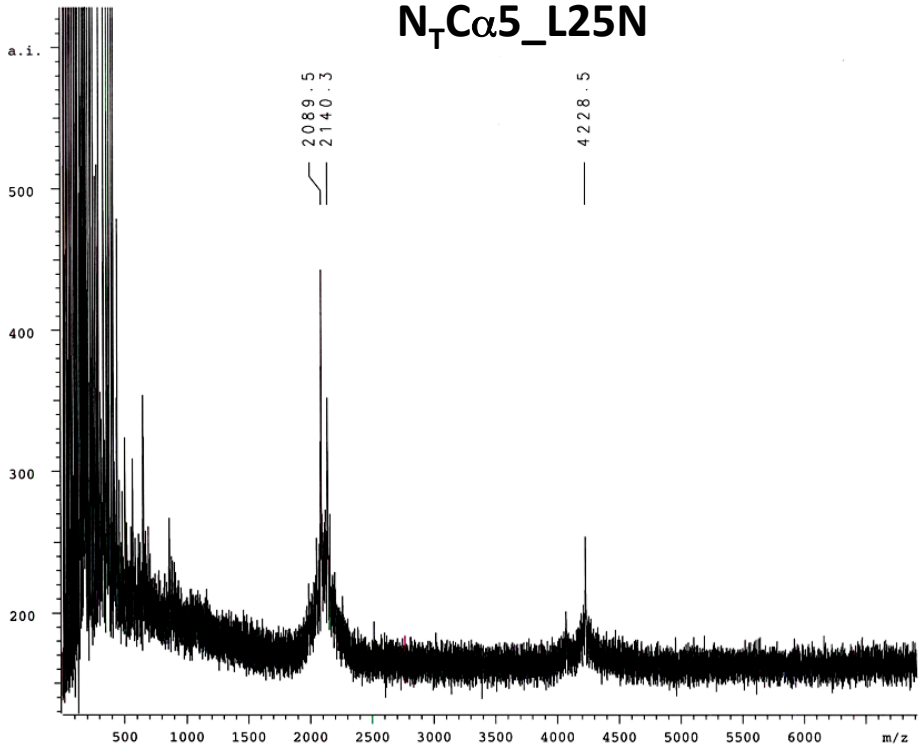
N_TCα5_L25N
a.i.
2089.5
2140.3
4228.5
m/z

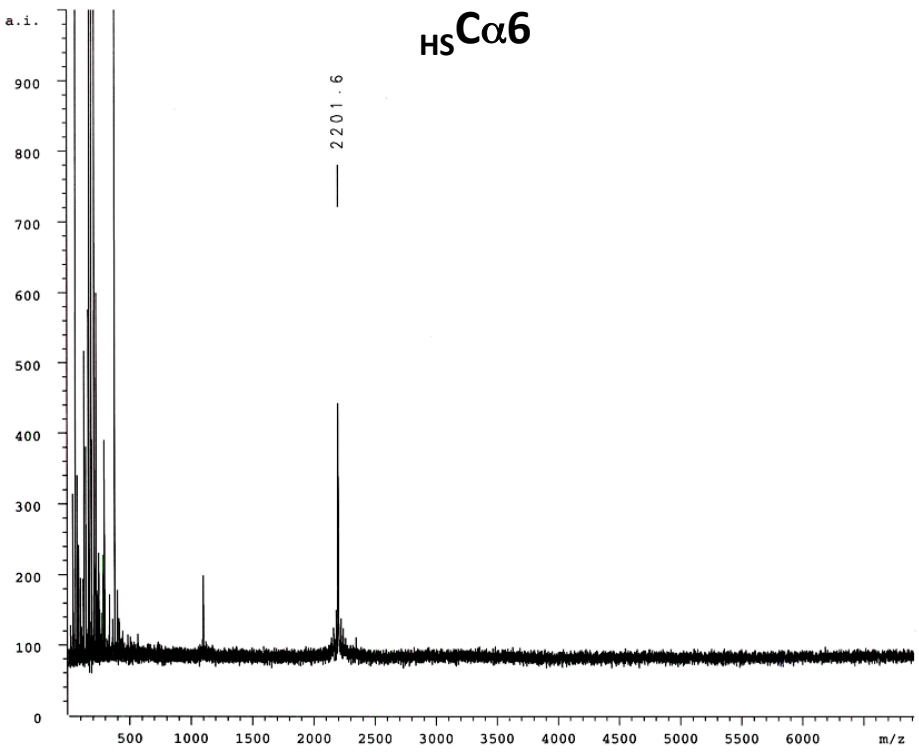
$_{HS}$Cα6
a.i.
2201.6
m/z

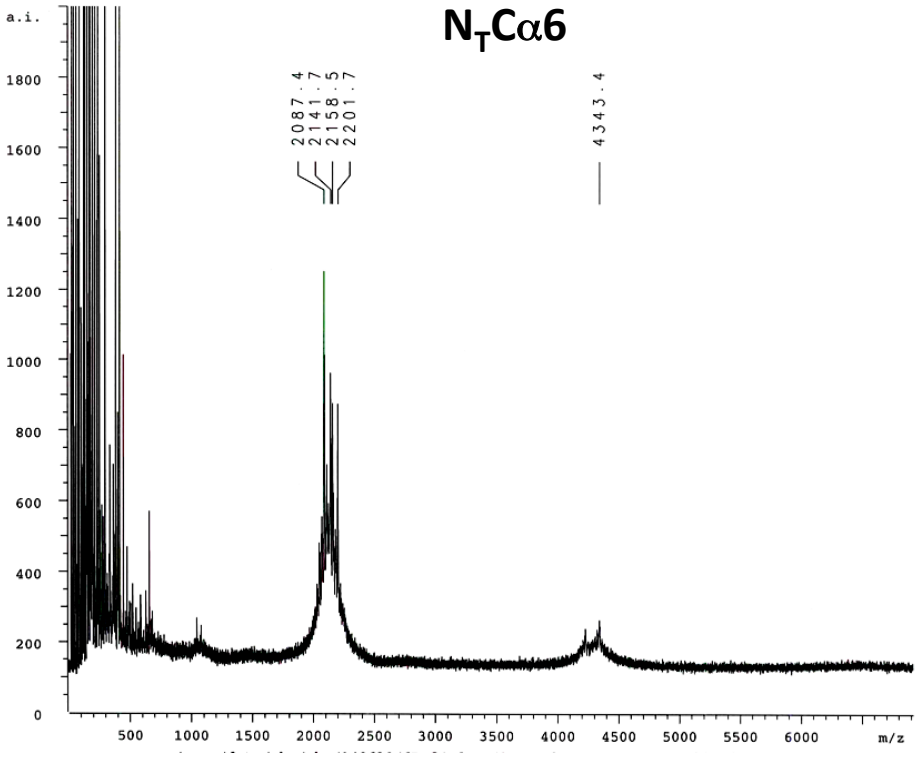
N_TCα6
a.i.
2087.4
2141.7
2158.5
2201.7
4343.4
m/z

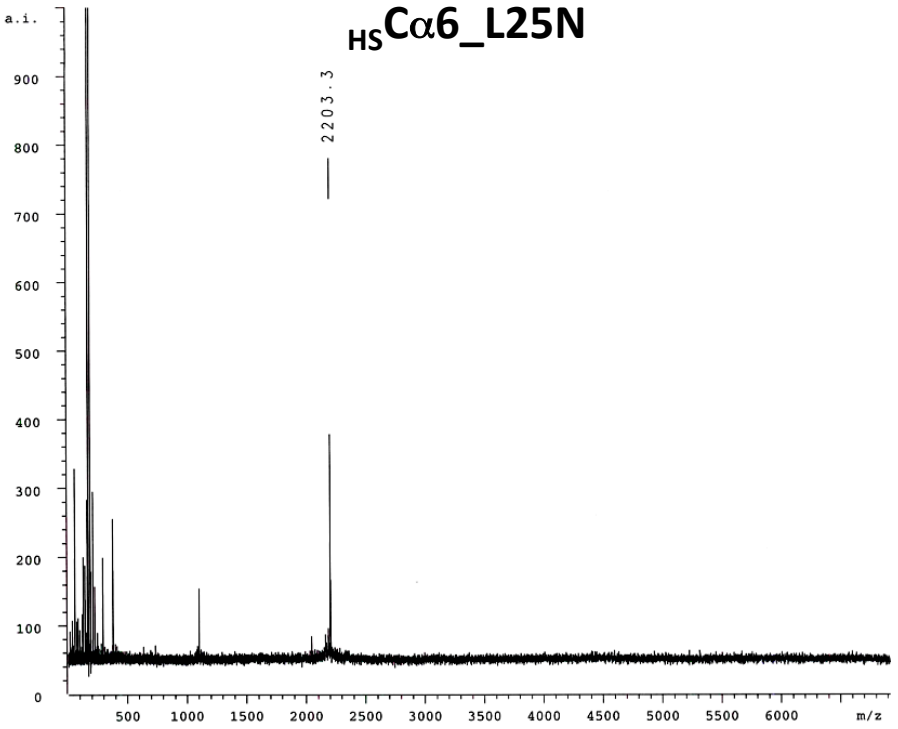
HSCα6_L25N
a.i.
2203.3
m/z

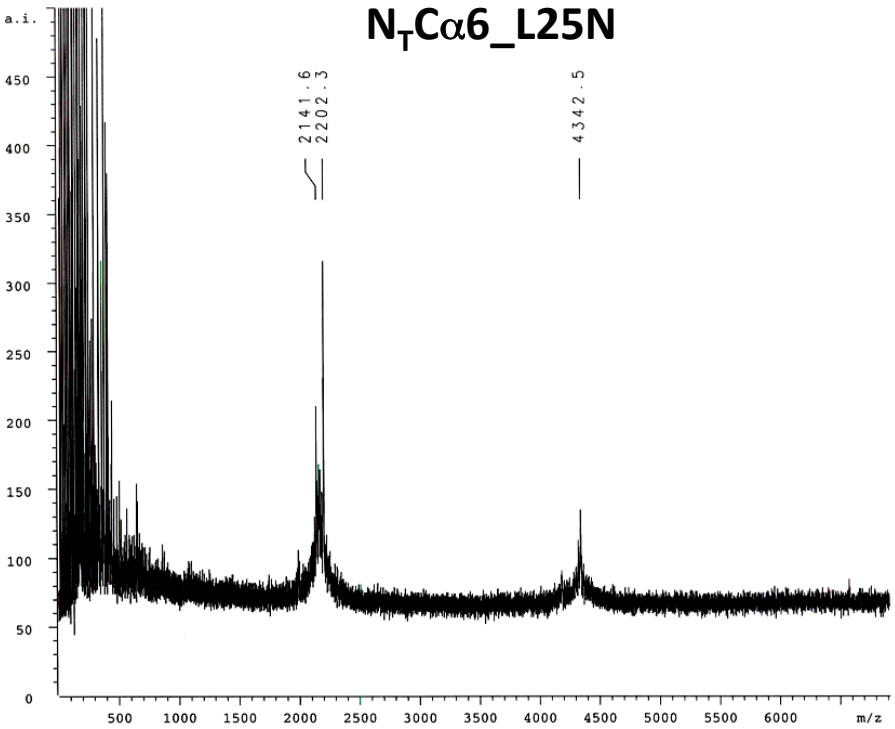
NTCα6_L25N
a.i.
2141.6
2202.3
4342.5
m/z

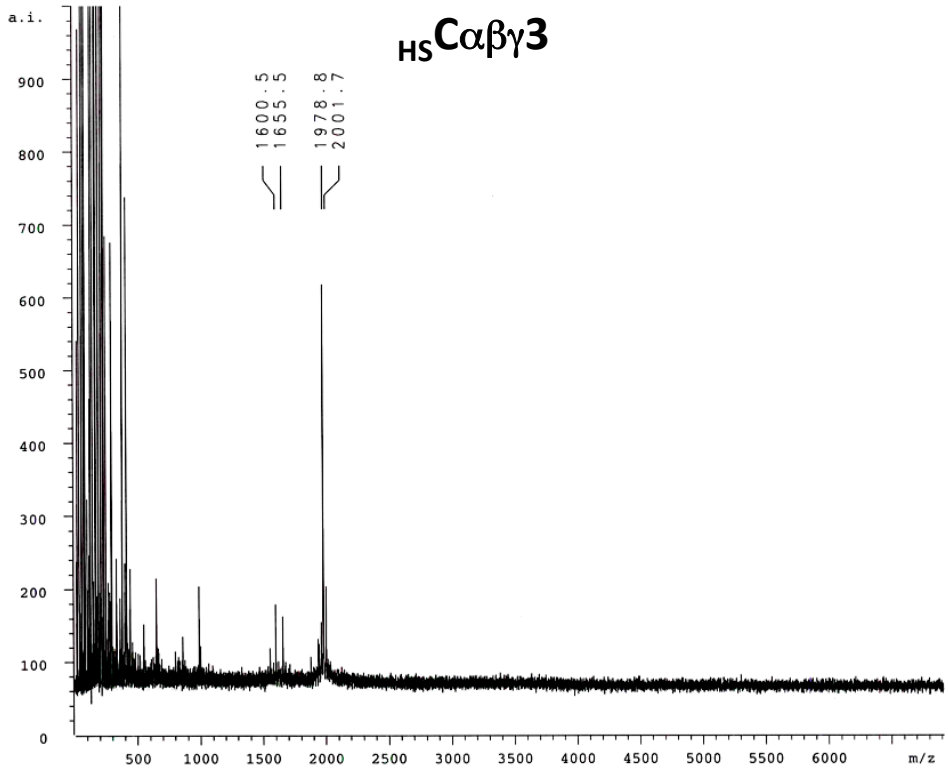
HSCαβγ3
a.i.
1600.5
1655.5
1978.8
2001.7
m/z

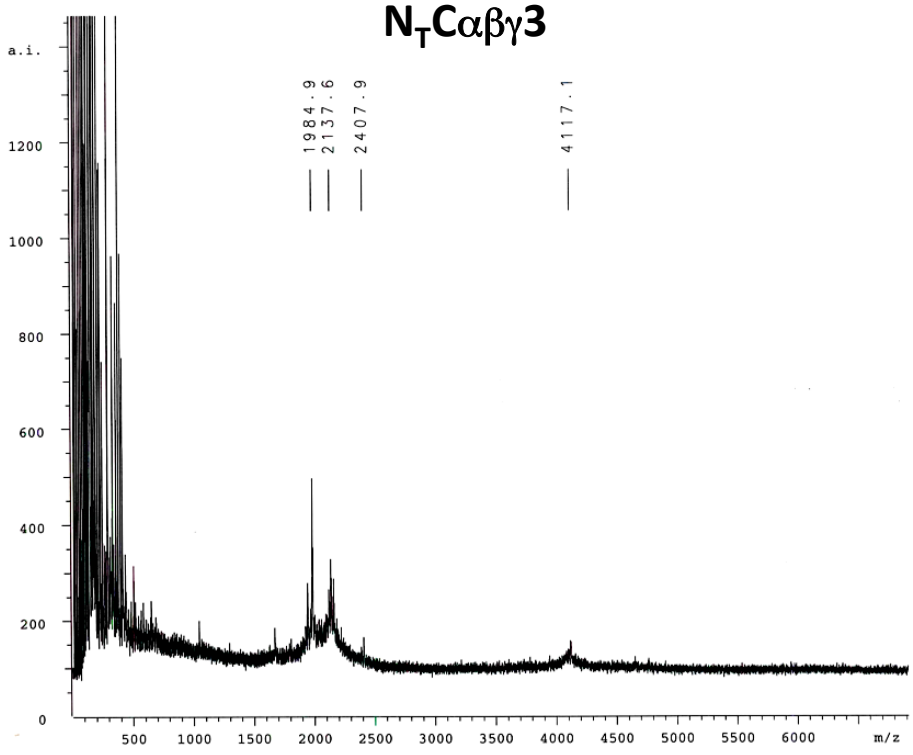
NTCαβγ3
a.i.
1984.9
2137.6
2407.9
4117.1
m/z

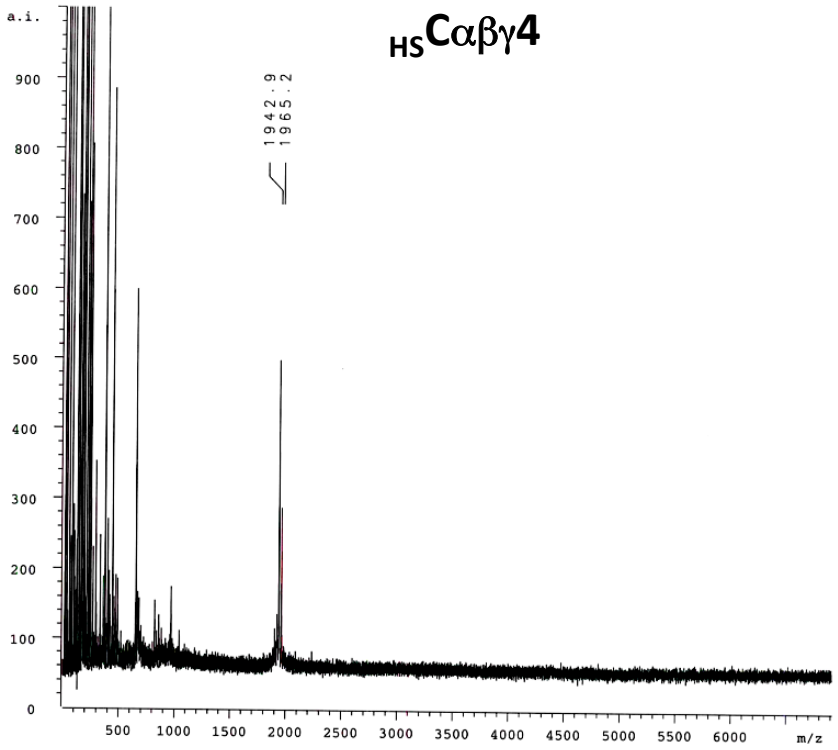
HSCαβγ4
a.i.
1942.9
1965.2
m/z

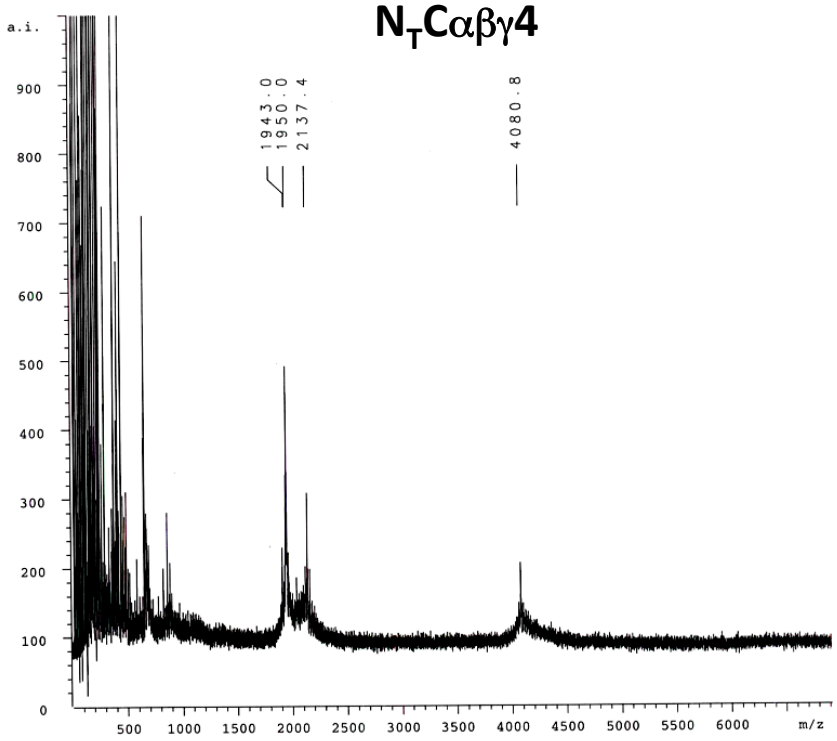
NTCαβγ4
a.i.
1943.0
1950.0
2137.4
4080.8
m/z

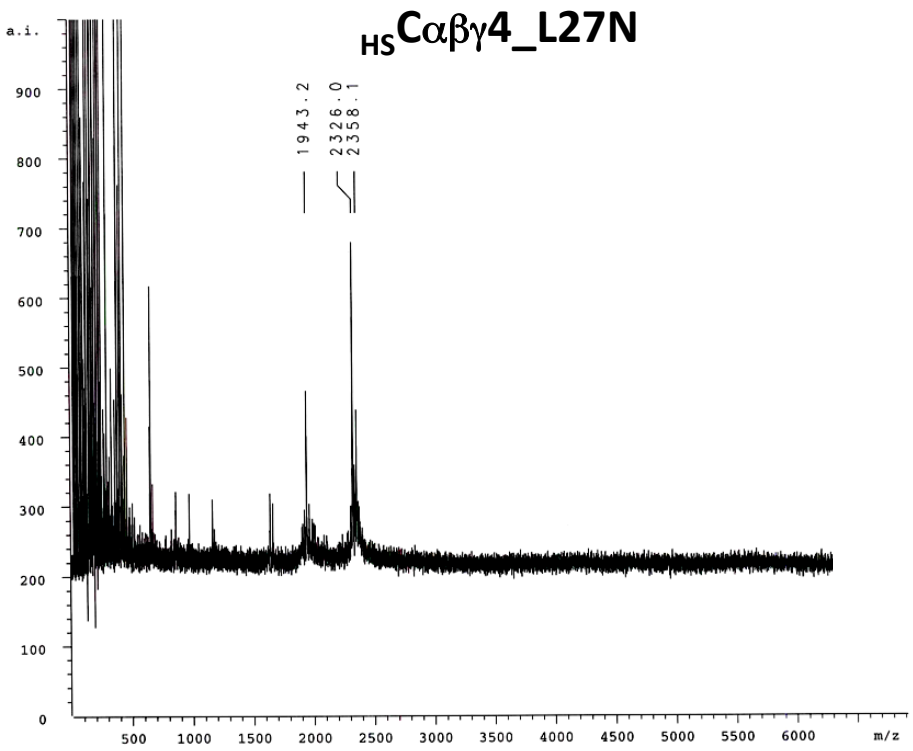
HSCαβγ4_L27N
a.i.
1943.2
2326.0
2358.1
m/z

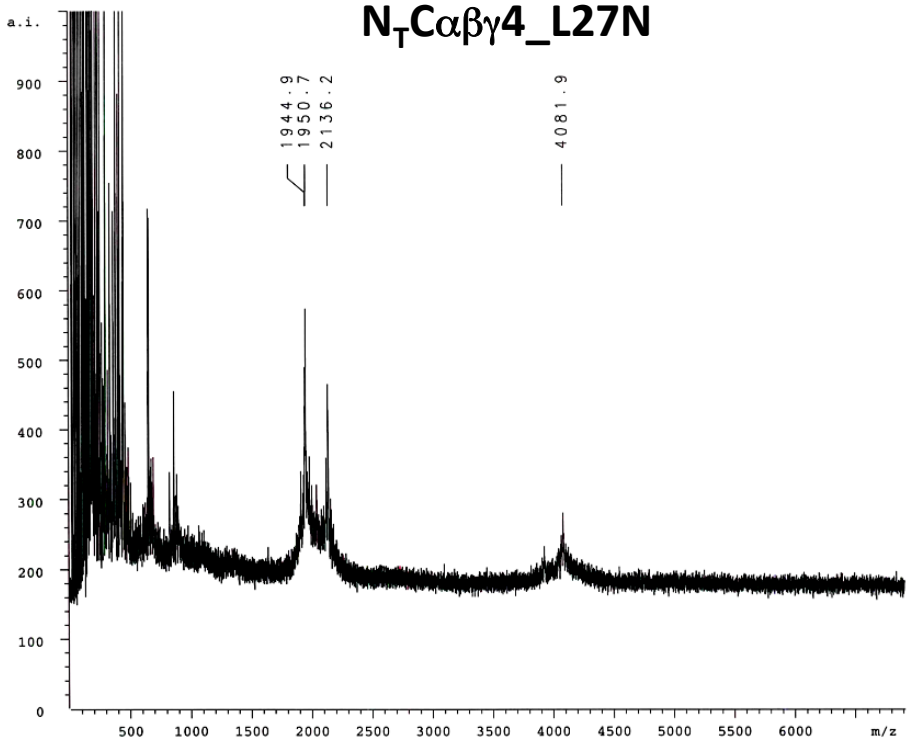
NTCαβγ4_L27N
a.i.
1944.9
1950.7
2136.2
4081.9
m/z

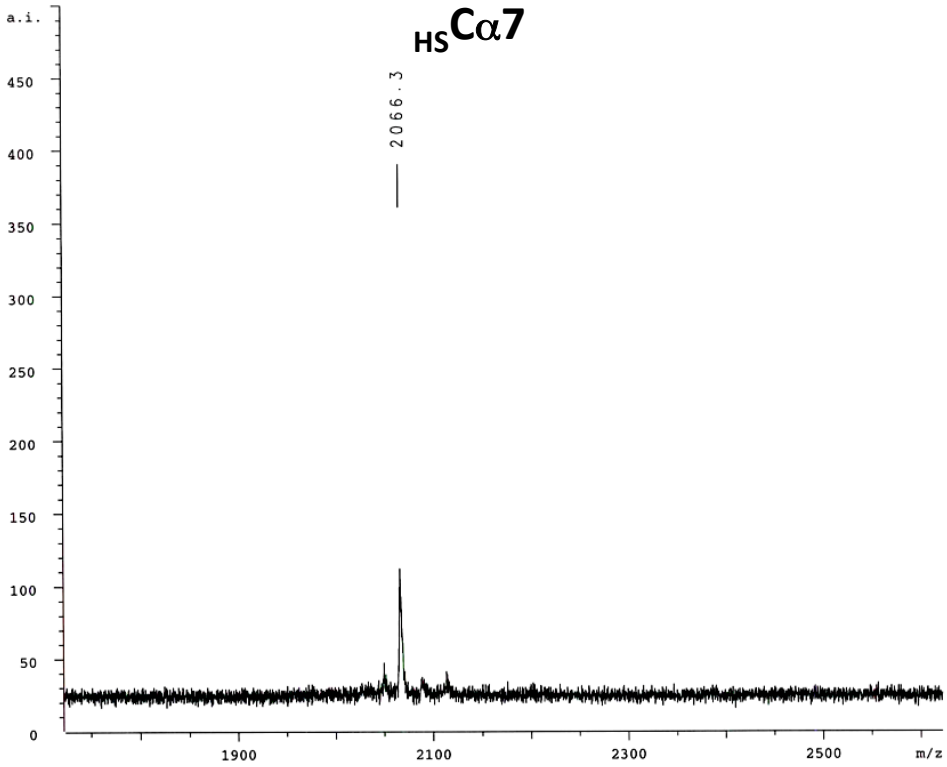
HSCα7
a.i.
2066.3
0
50
100
150
200
250
300
350
400
450
1900
2100
2300
2500
m/z

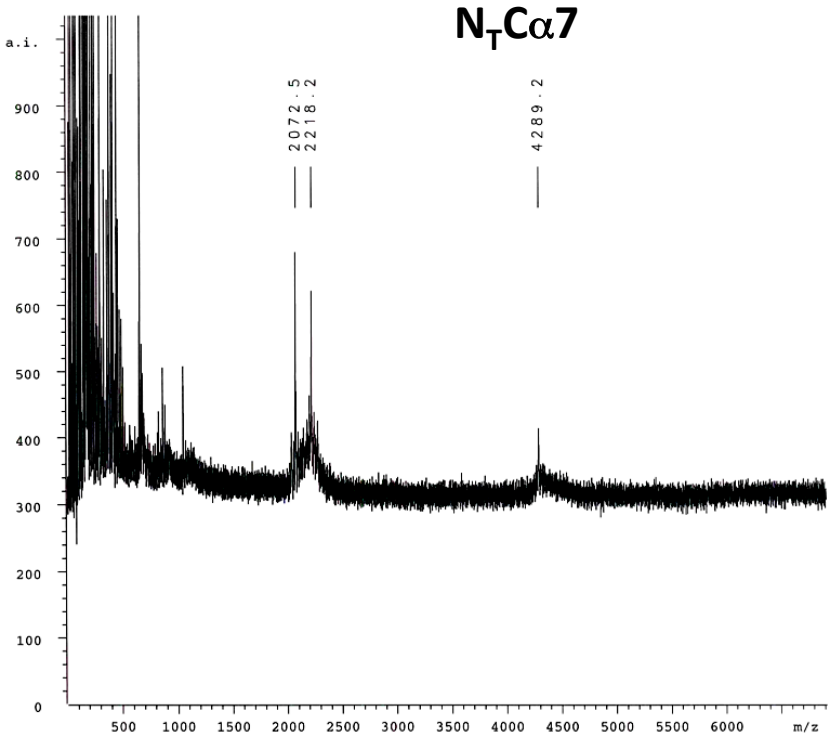
NTCα7
a.i.
2072.5
2218.2
4289.2
0
100
200
300
400
500
600
700
800
900
500
1000
1500
2000
2500
3000
3500
4000
4500
5000
5500
6000
m/z

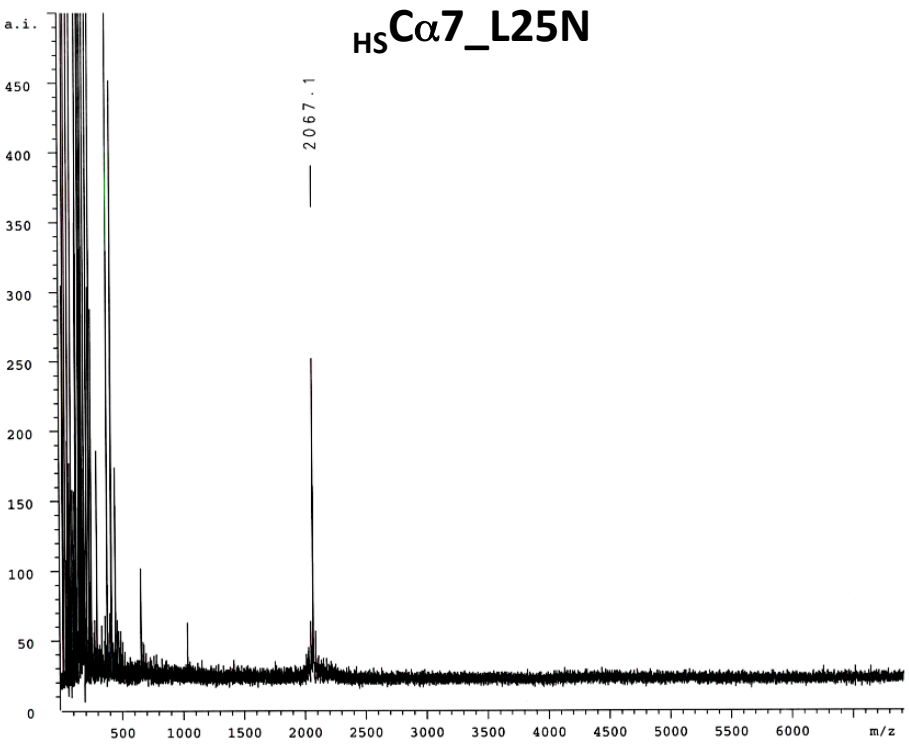
HSCα7_L25N
a.i.
2067.1
m/z

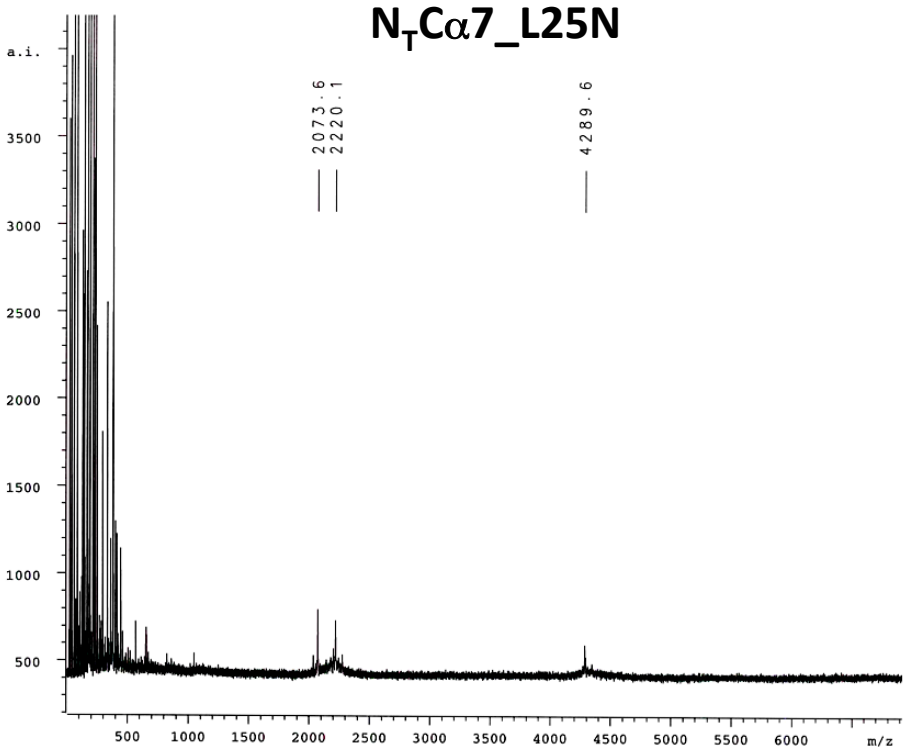
NTCα7_L25N
a.i.
2073.6
2220.1
4289.6
m/z

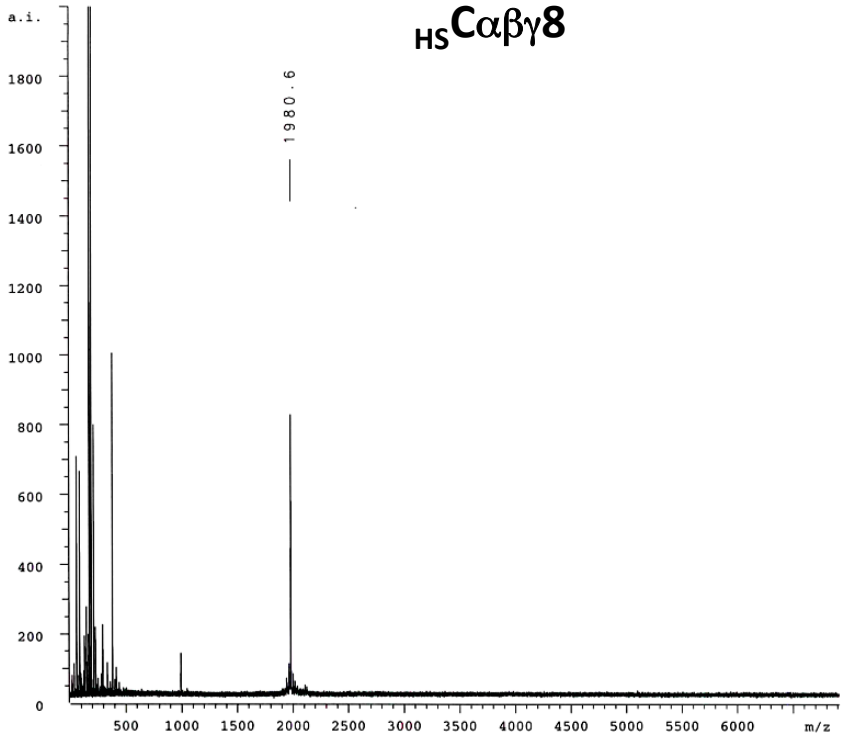
HSCαβγ8
a.i.
1980.6
m/z

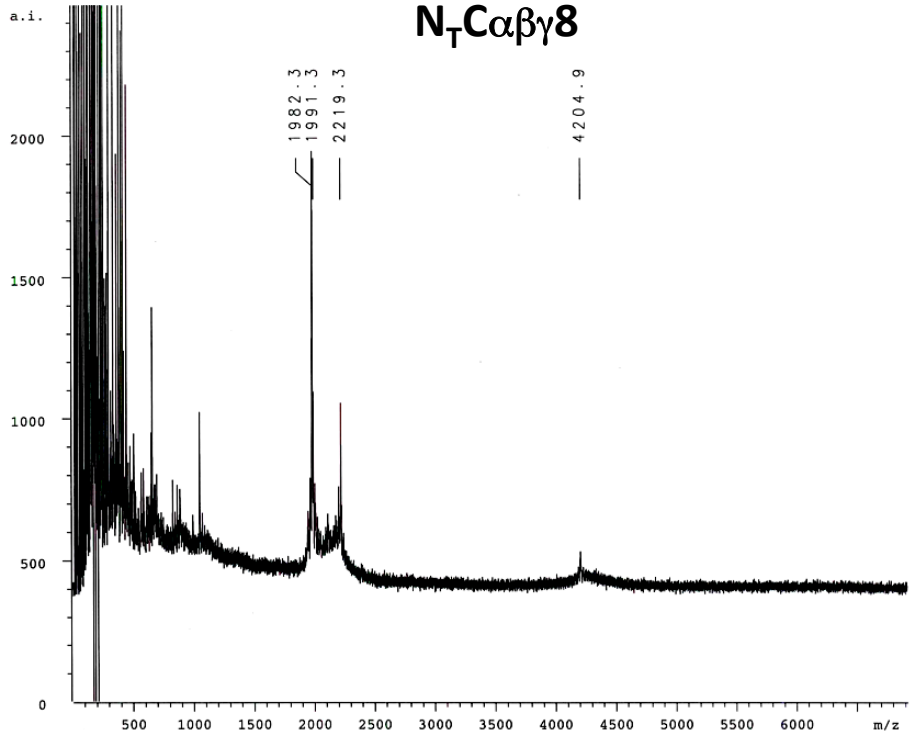
NTCαβγ8
a.i.
1982.3
1991.3
2219.3
4204.9
m/z

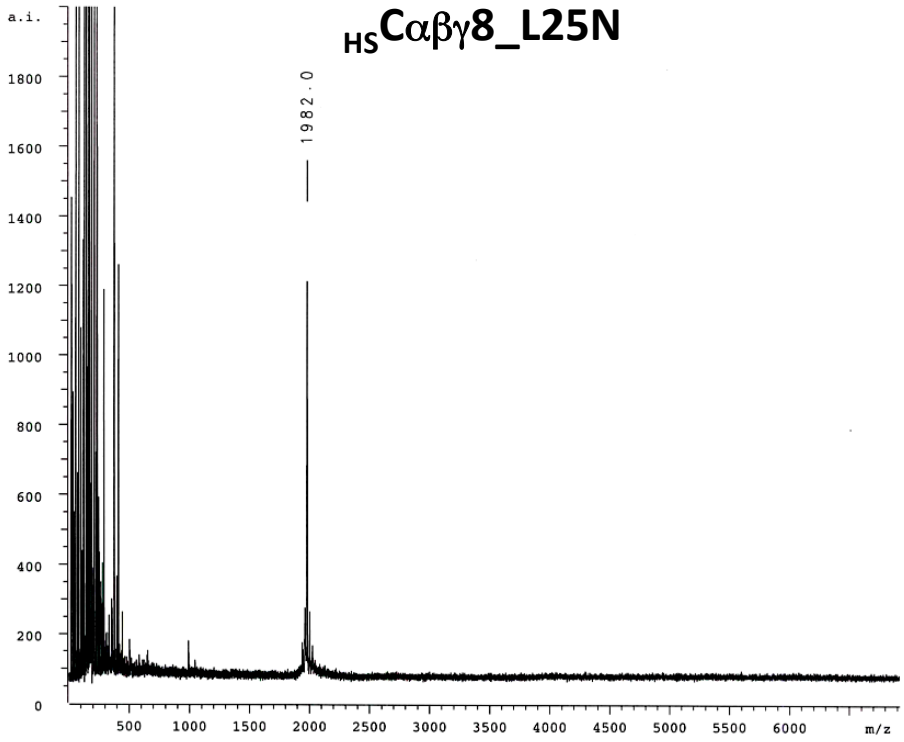
HSCαβγ8_L25N
a.i.
1982.0
m/z

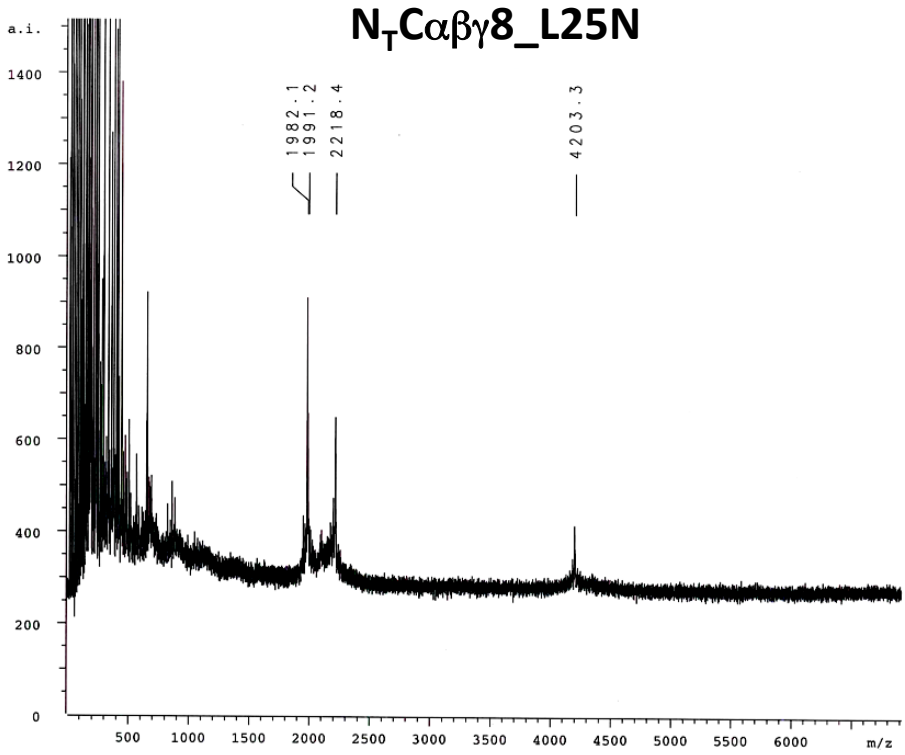
NTCαβγ8_L25N
a.i.
1982.1
1991.2
2218.4
4203.3
m/z

Representative HPLC traces for thioester exchange assays

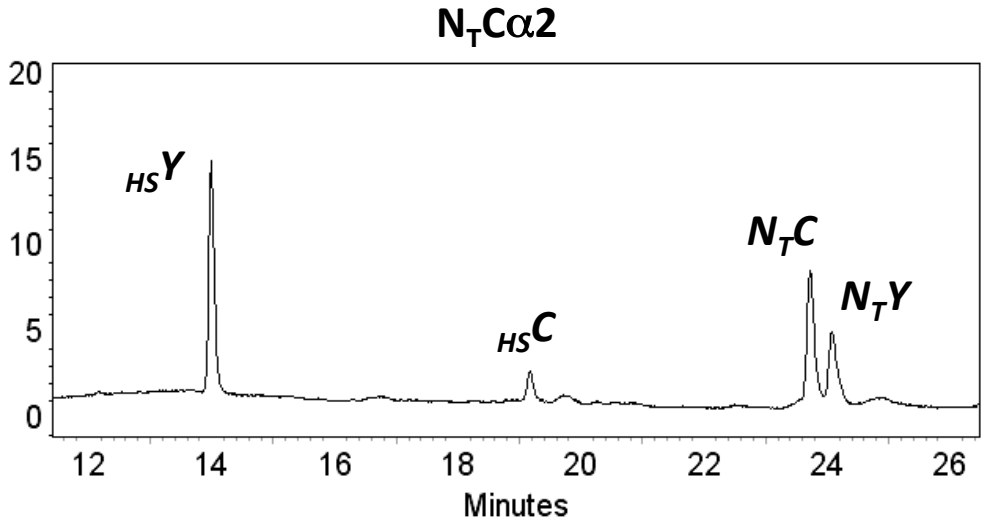

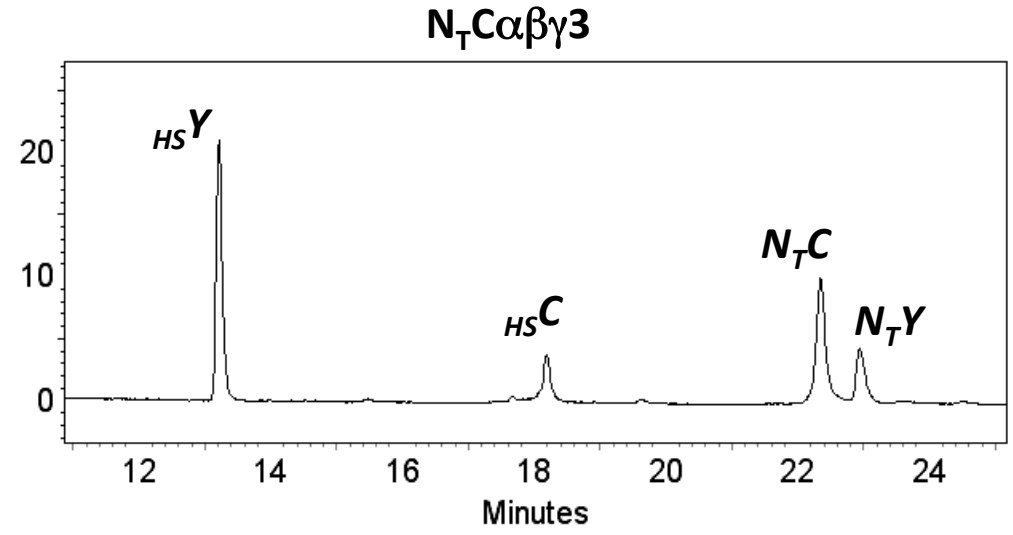

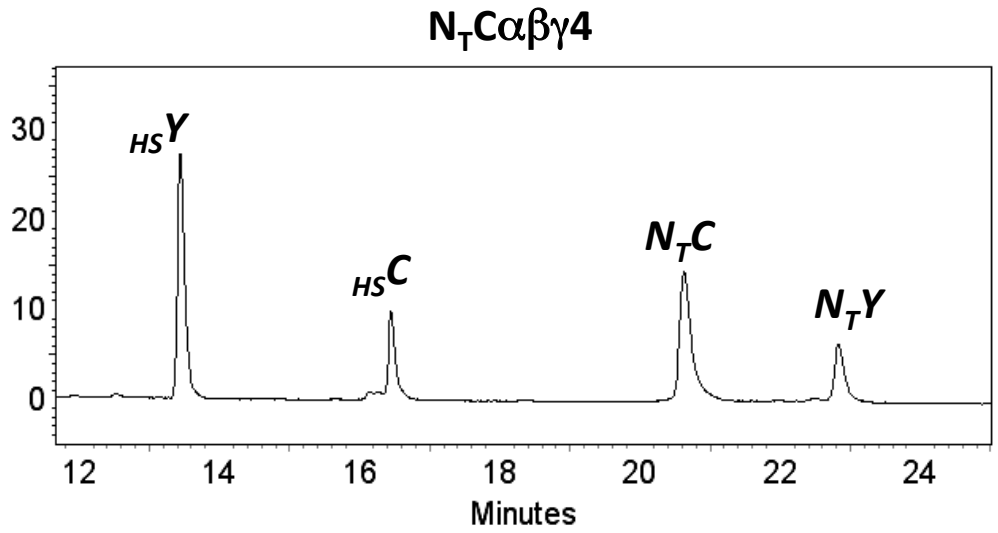
$N_TC\alpha\beta\gamma4$
30
20
10
0
$_{HS}Y$
$_{HS}C$
N_TC
N_TY
12
14
16
18
20
22
24
Minutes

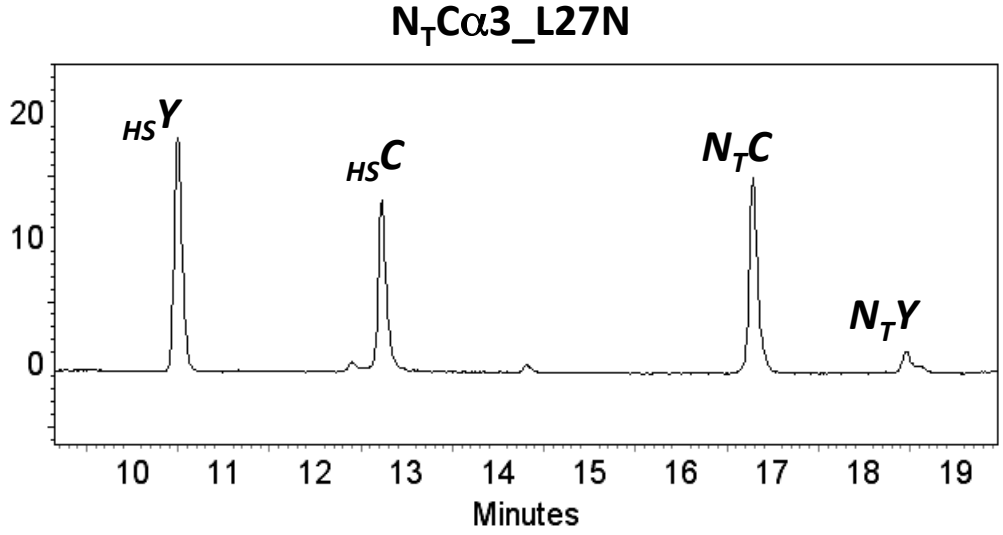
$N_TC\alpha3\_L27N$
20
10
0
$_{HS}Y$
$_{HS}C$
N_TC
N_TY
10
11
12
13
14
15
16
17
18
19
Minutes

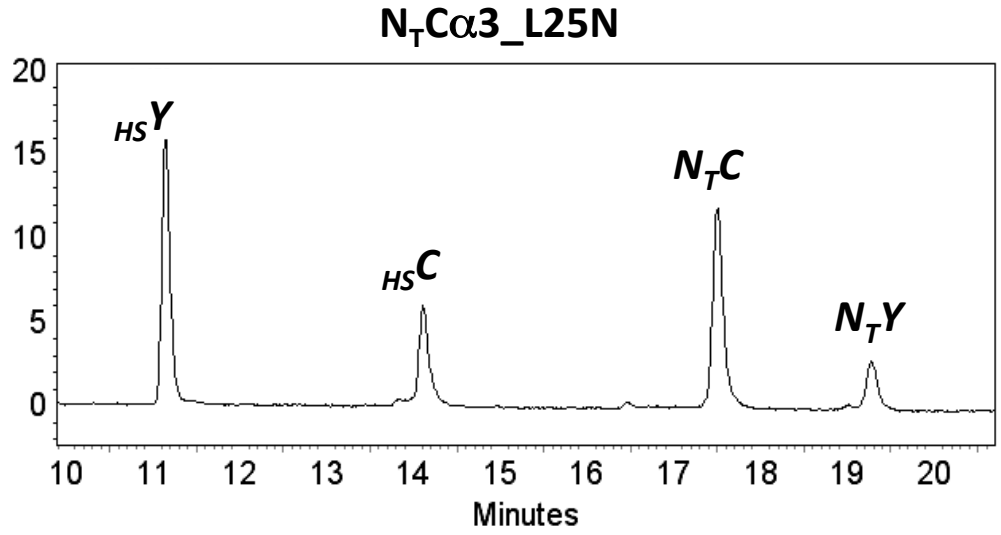
$N_TC\alpha3\_L25N$
20
15
10
5
0
$_{HS}Y$
$_{HS}C$
N_TC
N_TY
10 11 12 13 14 15 16 17 18 19 20
Minutes

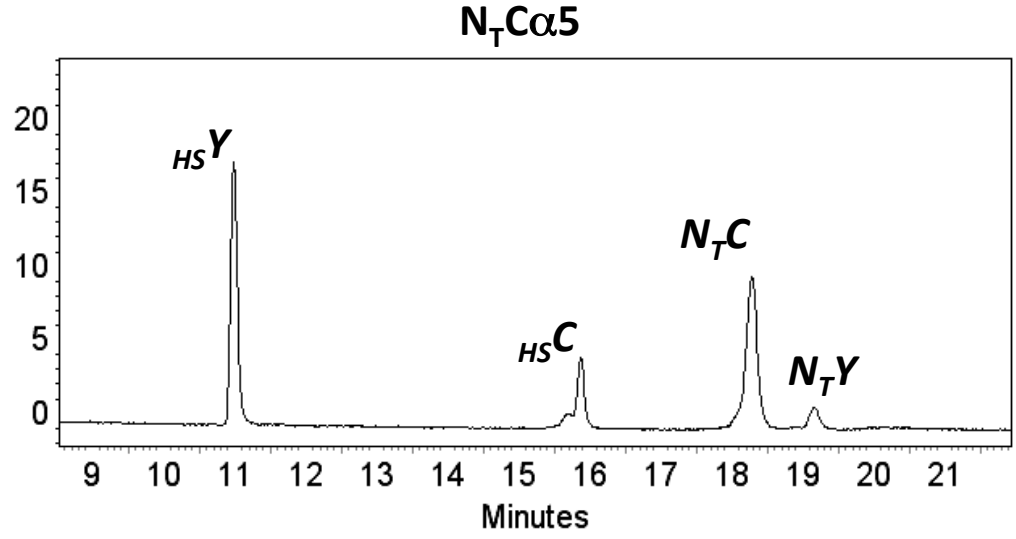
$N_TC\alpha5$
20
15
10
5
0
$_{HS}Y$
$_{HS}C$
N_TC
N_TY
9 10 11 12 13 14 15 16 17 18 19 20 21
Minutes

$N_TC\alpha6$

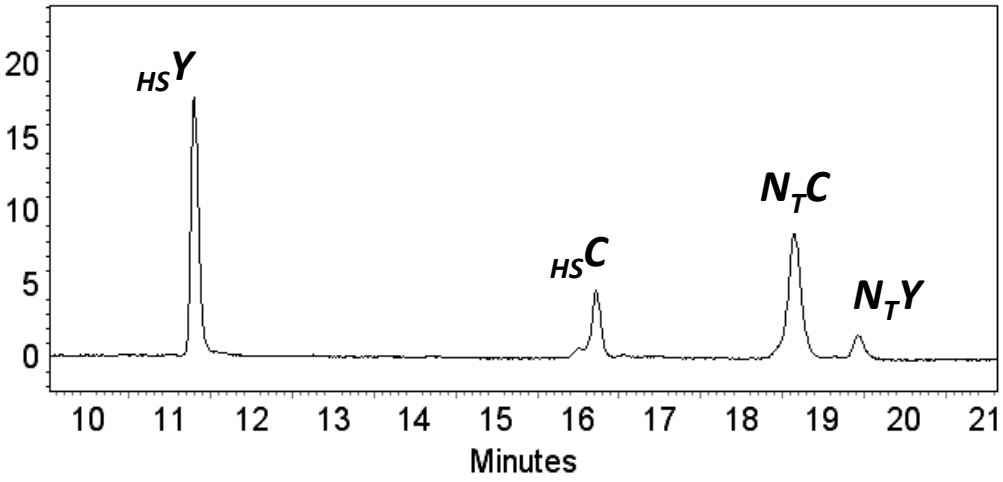

$N_TC\alpha7$

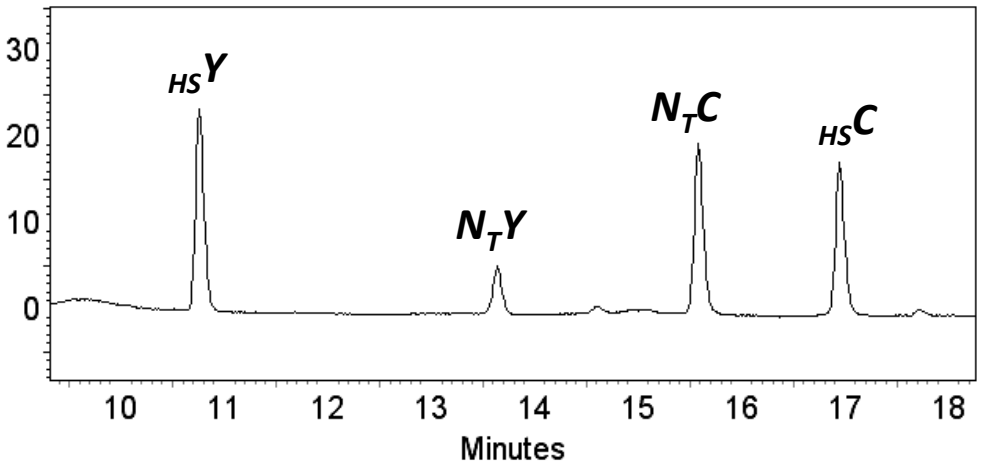

4.5 References

(1) Azzarito, V.; Long, K.; Murphy, N. S.; Wilson, A. J. Inhibition of alpha-helix-mediated protein-protein interactions using designed molecules. *Nature Chemistry* **2013**, *5*, 161-173.

(2) Jochim, A. L.; Arora, P. S. Assessment of helical interfaces in protein-protein interactions. *Molecular Biosystems* **2009**, *5*, 924-926.

(3) Wilson, A. J. Inhibition of protein-protein interactions using designed molecules. *Chemical Society Reviews* **2009**, *38*, 3289-3300.

(4) Horne, W. S.; Gellman, S. H. Foldamers with Heterogeneous Backbones. *Accounts of Chemical Research* **2008**, *41*, 1399-1408.

(5) Cheng, R. P.; Gellman, S. H.; DeGrado, W. F. beta-peptides: From structure to function. *Chemical Reviews* **2001**, *101*, 3219-3232.

(6) Gellman, S. H. Foldamers: A manifesto. *Accounts of Chemical Research* **1998**, *31*, 173-180.

(7) Sawada, T.; Gellman, S. H. Structural Mimicry of the alpha-Helix in Aqueous Solution with an Isoatomic alpha/beta/gamma-Peptide Backbone. *Journal of the American Chemical Society* **2011**, *133*, 7336-7339.

(8) Shin, Y.-H.; Mortenson, D. E.; Satyshur, K. A.; Forest, K. T.; Gellman, S. H. Differential Impact of beta and gamma Residue Preorganization on alpha/beta/gamma-Peptide Helix Stability in Water. *Journal of the American Chemical Society* **2013**, *135*, 8149-8152.

(9) Chakrabartty, A.; Baldwin, R. L.; Eisenberg, D. S.; Richards, F. M. Stability of alpha-helices. *Advances in Protein Chemistry; Protein stability* **1995**, *46*, 141-176.

(10) Woll, M. G.; Hadley, E. B.; Mecozzi, S.; Gellman, S. H. Stabilizing and destabilizing effects of phenylalanine -> F-5-phenylalanine mutations on the folding of a small protein. *Journal of the American Chemical Society* **2006**, *128*, 15932-15933.

(11) Woll, M. G.; Gellman, S. H. Backbone thioester exchange: A new approach to evaluating higher order structural stability in polypeptides. *Journal of the American Chemical Society* **2004**, *126*, 11172-11174.

(12) Price, J. L.; Hadley, E. B.; Steinkruger, J. D.; Gellman, S. H. Detection and Analysis of Chimeric Tertiary Structures by Backbone Thioester Exchange: Packing of an alpha Helix against an alpha/beta-Peptide Helix. *Angewandte Chemie-International Edition* **2010**, *49*, 368-371.

(13) Hadley, E. B.; Testa, O. D.; Woolfson, D. N.; Gellman, S. H. Preferred side-chain constellations at antiparallel coiled-coil interfaces. *Proceedings of the National Academy of Sciences of the United States of America* **2008**, *105*, 530-535.

(14) Hadley, E. B.; Gellman, S. H. An antiparallel alpha-helical coiled-coil model system for rapid assessment of side-chain recognition at the hydrophobic interface. *Journal of the American Chemical Society* **2006**, *128*, 16444-16445.

(15) Woolfson, D. N. The design of coiled-coil structures and assemblies. *Fibrous Proteins: Coiled-Coils, Collagen and Elastomers* **2005**, *70*, 79.

(16) Lupas, A. N.; Gruber, M. The structure of alpha-helical coiled coils. *Fibrous Proteins: Coiled-Coils, Collagen and Elastomers* **2005**, *70*, 37.

(17) Crick, F. H. C. The packing of alpha -helices: simple coiled-coils. *Acta Crystallographica* **1953**, *6*, 687-697.

(18) Burkhard, P.; Ivaninskii, S.; Lustig, A. Improving coiled-coil stability by optimizing ionic interactions. *Journal of Molecular Biology* **2002**, *318*, 901-910.

(19) Steinkruger, J. D.; Bartlett, G. J.; Woolfson, D. N.; Gellman, S. H. Strong Contributions from Vertical Triads to Helix-Partner Preferences in Parallel Coiled Coils. *Journal of the American Chemical Society* **2012**, *134*, 15652-15655.

(20) Steinkruger, J. D.; Bartlett, G. J.; Hadley, E. B.; Fay, L.; Woolfson, D. N.; Gellman, S. H. The d '-d-d ' Vertical Triad Is Less Discriminating Than the a '-a-a ' Vertical Triad in the Antiparallel Coiled-Coil Dimer Motif. *Journal of the American Chemical Society* **2012**, *134*, 2626-2633.

(21) Steinkruger, J. D.; Woolfson, D. N.; Gellman, S. H. Side-Chain Pairing Preferences in the Parallel Coiled-Coil Dimer Motif: Insight on Ion Pairing between Core and Flanking Sites. *Journal of the American Chemical Society* **2010**, *132*, 7586.

(22) Choi, S. H.; Guzei, I. A.; Gellman, S. H. Crystallographic Characterization of the alpha/beta-Peptide 14/15-Helix. *Journal of the American Chemical Society* **2007**, *129*, 13780.

(23) Choi, S. H.; Guzei, I. A.; Spencer, L. C.; Gellman, S. H. Crystallographic characterization of helical secondary structures in alpha/beta-peptides with 1 : 1 residue alternation. *Journal of the American Chemical Society* **2008**, *130*, 6544-6550.

(24) Guo, L.; Chi, Y.; Almeida, A. M.; Guzei, I. A.; Parker, B. K.; Gellman, S. H. Stereospecific Synthesis of Conformationally Constrained gamma-Amino Acids: New Foldamer Building Blocks That Support Helical Secondary Structure. *Journal of the American Chemical Society* **2009**, *131*, 16018.

(25) Murray, J. K.; Gellman, S. H. Parallel synthesis of peptide libraries using microwave irradiation. *Nature Protocols* **2007**, *2*, 624-631.

(26) Ingenito, R.; Bianchi, E.; Fattori, D.; Pessi, A. Solid phase synthesis of peptide C-terminal thioesters by Fmoc/t-Bu chemistry. *Journal of the American Chemical Society* **1999**, *121*, 11369-11374.

(27) Shin, Y.; Winans, K. A.; Backes, B. J.; Kent, S. B. H.; Ellman, J. A.; Bertozzi, C. R. Fmoc-based synthesis of peptide-(alpha)thioesters: Application to the total chemical synthesis of a glycoprotein by native chemical ligation. *Journal of the American Chemical Society* **1999**, *121*, 11684.

Chapter 5: Functional $\alpha/\beta/\gamma$ peptides: Efforts toward BH3 domain/Bcl-x$_L$ protein-protein interaction modulation

5.1 Introduction

5.1.1 Regulation of apoptosis by Bcl-2 family of proteins [1-3]

Apoptosis, or programmed cell death, is a crucial mechanism for balancing cell death and life. Misregulation leads to severe human diseases due to excessive cell accumulation (e.g., neoplasia, autoimmune disorders, etc.) or excessive loss (e.g., neurodegenerative diseases).[1-3] Apoptosis is activated through extrinsic (started from a ligation of specific cell-surface death receptors) or intrinsic (mitochondrial) pathways, both of which result in the activation of members of the caspase family, leading to cell death (Figure 5.1). Most cell death in vertebrates proceeds through the intrinsic apoptotic pathway and is achieved by the permeabilization of the mitochondrial outer cell membrane (Figure 5.1).[1-3]

The intrinsic signaling pathway is known to be regulated by three subsets within the B-cell lymphoma 2 (Bcl-2) family of proteins: 1) effector pro-apoptotic proteins such as Bax (Bcl2-associated X protein) and Bak (Bcl-2-antagonist/killer protein), 2) anti-apoptotic proteins such as Bcl-2, Bcl-xL (B-cell lymphoma-extra large), Mcl-1 (myeloid cell leukemia sequence-1), Bcl-2/Bcl2L2 (Bcl-2-like protein-2), and 3) Bcl-homology 3 domain (BH3)-only proteins such as Bim (Bcl-2-interacting mediator of cell death), Bid (BH3-interacting-domain death agonist), Bad (Bcl-2-associated death promoter), Noxa (the latin word for damage), Puma (p53-upregulated modulator of apoptosis), and others (Figure 5.1).[2] In unstressed cells, inactive killer protein Bak (or Bax) is loosely associated with the outer mitochondrial membrane (or with anti-apoptotic proteins such as Bcl-xL and Mcl-1), preventing apoptosis.[2,4,5] In response to death signals, the BH3-only members (i.e., Bim, Bid, Puma, etc) bind to the anti-apoptotic proteins, releasing

and activating pro-apoptotic proteins such as Bak and Bax, which go on to initiate apoptosis (Figure 5.1).[1-3]

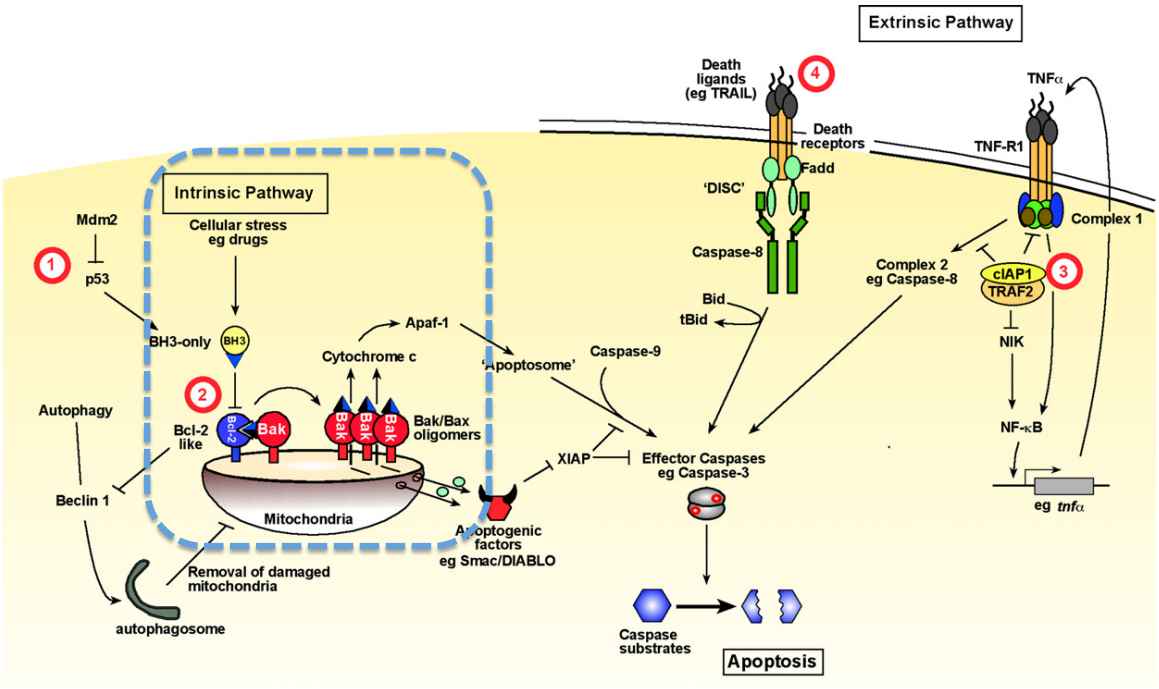

Figure 5.1 Intrinsic and extrinsic pathways of caspase activation and apoptosis. The interactions between Bcl-2 family proteins, which we aim to intervene for therapeutic purposes, are highlighted by a blue box.[3] (Figure is adapted from Ref.3)

The anti-apoptotic proteins display a hydrophobic cleft that can accommodate the α-helical BH3 domain of a pro-apoptotic protein or a BH3-only proteins (Figure 5.2). Many peptidic/oligomeric and small molecule mimics of α-helical BH3 domains have been developed to regulate the interactions between pro- and anti-apoptotic proteins, but further improvements are necessary for designed mimetics to be functional therapeutics.[6-8]

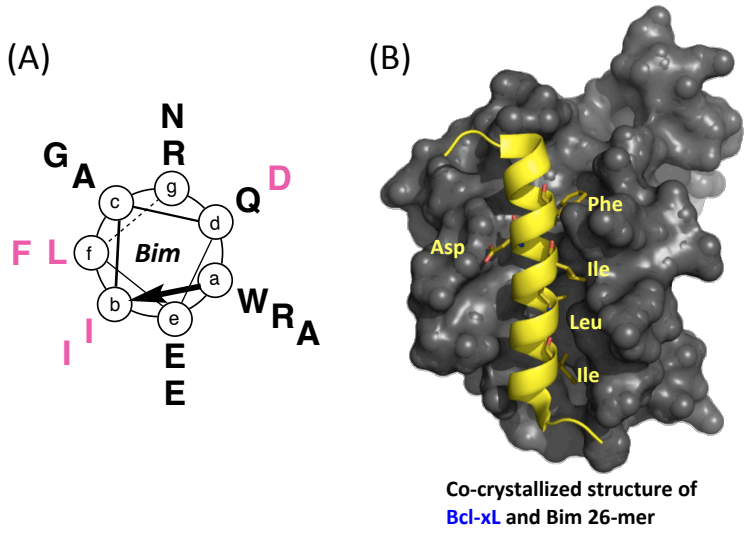

Figure 5.2 (A) α-Helical wheel diagram of the Bim BH3 domain. Important residues for binding to Bcl-xL are highlighted in pink. (B) Co-crystal structure of Bim 26mer bound to Bcl-xL (PDF 3FDL).[9]

5.1.2 Bim mimic α/β peptidomimetics

All BH3-only proteins share structural similarities required for binding to the hydrophobic cleft of the anti-apoptotic proteins of Bcl-2 family; however, each BH3-only protein has its own selectivity among the different anti-apoptotic members.[2,10] Some BH3-only proteins, such as Bim, Bid and Puma, promiscuously bind to all anti-apoptotic members of the Bcl-2 family, whereas others bind only to specific anti-apoptotic proteins. For example, Bad binds to Bcl-xL and Bcl-2, but not to Mcl-1; Noxa binds to Mcl-1, but not to Bcl-xL and Bcl-2. A limitation of ABT-737, a small molecule inhibitor developed by Abbott Laboratories, is that it does not bind to Mcl-1, even though it binds tightly to other anti-apoptotic proteins (K_d < 1 nM).[11]

A critical limitation of canonical α-peptides is their rapid proteolytic degradation in physiological environments (Figure 5.3, α-peptide Bim 26-mer half-life is less than 1 minute). The Gellman group has developed unnatural oligomers with well-defined

folding behavior, or so called foldamers, containing non-natural backbone subunits such as β-amino acids. Foldamers, such as β-peptides (containing exclusively β-residues) and α/β-peptides (heterogeneous backbone with α- and β-residues), have been shown to adopt helical conformations with significantly increased resistance to proteolysis.[12-18] Function-based α/β-peptides have been developed that mimic α-helical BH3 domains, and bind to the BH3-recognition cleft of both Bcl-xL and Mcl-1. Sadowsky *et al.* evaluated hundreds of β-peptides and α/β-peptides for their ability to mimic α-helical BH3 domains, and developed the (α/β+α)-chimeric peptide with a strong affinity for Bcl-xL (K_i ≈ 5 nM by Fluorescent Polarization (FP) assay); however, the α-segment at the C-terminus was susceptible to proteolytic digestion.[19] Horne *et al.* designed α/β-foldamers containing β^3-amino acids in an ααβααβ heptad pattern based on the Puma sequence, and showed that by aligning β-residues on one side of the helix, the amphipathic α-helix could be effectively mimicked (K_i < 1 nM for Bcl-xL, K_i ≈ 150 nM for Mcl-1, by FP).[17]

Boersma *et al.* have explored Bim-derived α/β-peptides with different patterns (i.e., ααβααβ, αβ and αααβ) incorporating β^3-amino acids (Figure 5.3).[9] A Bim 18-mer-derived α/β-peptide (peptide **α/β 2**, Figure 5.3B) with one of the four possible αααβ patterns binds to both Bcl-xL and Mcl-1 (K_i ≈ 50 nM for Bcl-xL, K_i ≈ 130 nM for Mcl-1, by FP), and the analogous Bim 26-mer α/β-peptide (peptide **α/β 4**, Figure 5.3B) binds with high affinity to both Bcl-xL and Mcl-1 (IC_{50} ≈ 7.5 nM for Bcl-xL, IC_{50} ≈ 2.4 nM for Mcl-1, by SPR).[9] Bim 18-mer-derived α/β-peptides in ααβααβ pattern (**α/β 1**), and αααβ pattern (**α/β 2**) were co-crystallized with Bcl-xL (PDB ID; **α/β1** with Bcl-xL: 4A1U, **α/β2**

with Bcl-xL: 4A1W, Figure 5.3A).[9] Both two structures show that these α/β-peptides form a network of contacts with Bcl-xL that mimics remarkably well those of the natural Bim BH3 domain. Later, Peterson-Kaufman and Hasse incorporated ring-constrained β-residues (ACPC and APC) to enhance helical propensity of the α/β-foldamers (Peterson-Kaufman dissertation, Chapter 3; Hasse dissertation Chapter 4). By using anionic 5-membered-ring-constrained β-residues in selected positions, and by altering several α-residues, these workers developed a Bim 18-mer derived α/β-foldamer with the ααβααβ pattern that displayed improved binding relative to the analogous α/β-foldamer containing acyclic β^3-residues (Figure 5.3). The α/β-peptide and protein interaction model based on the interactions among Bcl-2 family proteins has provided crucial information and guiding principles to help develop successful α/β-peptidomimetics for other protein-protein interaction targets.[14-16,20,21]

(A)

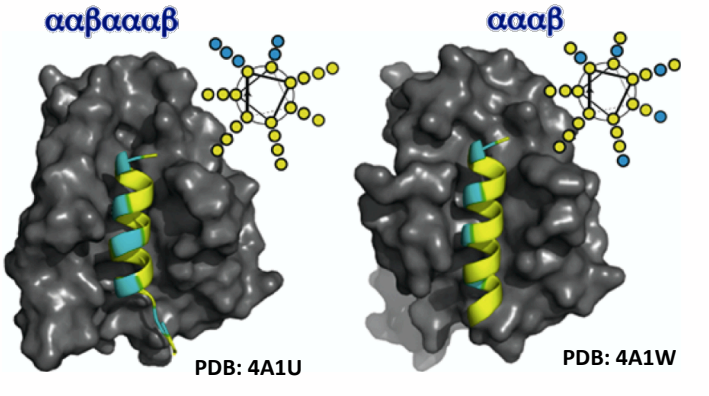

(B)

		K_i (nM)		$t_{1/2}$ (min)
		Bcl-xL	Mcl-1	
Bim 18-mer	Ac–I W I A Q E L R R I G D E F N A Y Y–NH_2	23	<26	
α/β 1 (αaβaaaβ)	Ac–I W I A Q E L R R I G D E F N A Y Y–NH_2	540	230	
α/β 2 (aaaβ)	Ac–I W I A Q E L R R I G D E F N A Y Y–NH_2	50	130	
Bim 26-mer	Ac–D M R P E I W I A Q E L R R I G D E F N A Y Y A R R–NH_2	13[a]	1.1[a]	0.76
α/β 3 (αaβaaaβ)	Ac–D M R P E I W I A Q E L R R I G D E F N A Y Y A R R–NH_2	34[a]	1.7[a]	29
α/β 4 (aaaβ)	Ac–D M R P E I W I A Q E L R R I G D E F N A Y Y A R R–NH_2	7.5[a]	2.4[a]	220
α/β 5 (αaβaaaβ)	Ac–I X I A Q U L R Z I G D U F N X Y Y–NH_2	70	7.9	
α/β 6 (αaβaaaβ)	Ac–I X I A *E U L R Z I G D U F N X *K Y–NH_2	24	2.5	

(C)

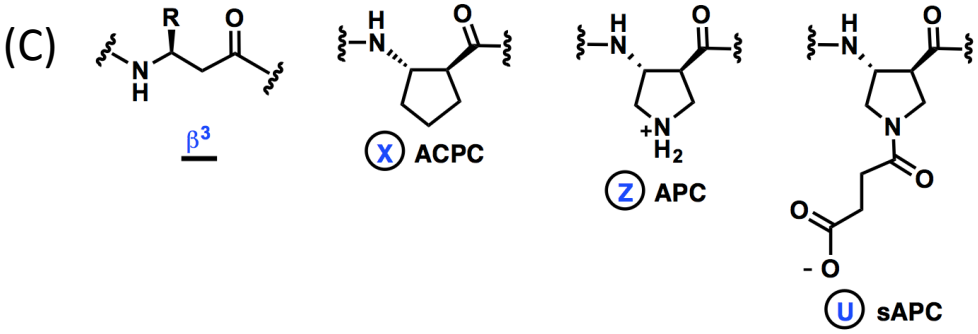

Figure 5.3 (A) Bcl-xL and Bim-derived α/β-peptides wtih αaβaaaβ and aaaβ patterns.[9] β in blue, α in yellow, Bcl-xL in gray (B) Sequences of the Bim-derived α/β-peptides wtih αaβaaaβ and aaaβ patterns. β Residues are in blue color. K_i values determined by FP competition assay or SPR (marked as [a] K_i), and the half-life values ($t_{1/2}$) determined by proteolysis assay are shown. Proteolysis: 50 μM solutions of peptides in the presence of proteinase K (10 μg/mL) in TBS buffer, pH 7.5, with 5% DMSO.[9] (C) Structures of cyclic β-amino acids.

5.1.3 α-Helix-like α/β/γ-peptides

We have shown that an α/β/γ-peptide containing ring-constrained β residues with the αγααβα hexad repeat pattern adopts a stable, helical secondary structure in water whether cyclic- or acyclic- γ residues are used (Figure 5.4).[22,23] The helix formed by the αγααβα hexad pattern was designed to mimic the recognition surface of a natural α-helix, with β- and γ-residues aligned along one side of the helix, allowing the α-residues to define the other face of the helix (Figure 5.4). Structural data from X-ray and 2D-NMR showed that an α/β/γ-helix can mimic a canonical α-helix with bifurcated C=O(i)/H-N(i+3) and C=O(i)/H-N(i+4) hydrogen bonds.[22] Herein, as an extended study of the structural analysis for the helical α/β/γ-peptides, we have examined the application of helical α/β/γ-peptidomimetics to modulate protein-protein interactions. We designed α/β/γ-foldamers to mimick helical BH3 domain peptides, and we assessed the design strategy by measuring binding to Bcl-xL (Figure 5.4C).

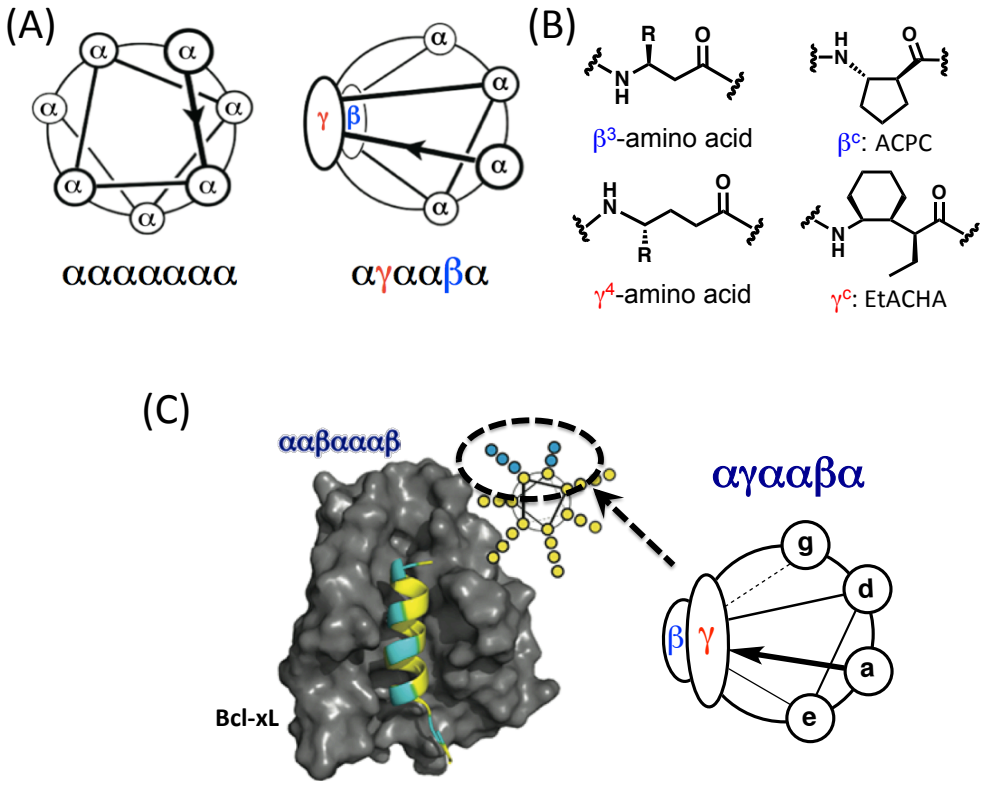

Figure 5.4 Helical wheel diagrams of α heptad and αγααβα hexad. (B) Structures of cyclic and acyclic β- and γ- amino acid residues (C) Co-crystal structure of the Bim-derived "β-stripe" α/β-peptide bound to Bcl-xL (PDB ID: 4A1U) [9], and helical wheel diagram of α/β/γ-helix. The design of the Bim-derived α/β/γ-peptides is intended to parallel the design of Bim-derived "β-stripe" α/β-peptides.

5.2 Bim mimic α/β/γ-peptides containing cyclic β- and cyclic γ-residues

Initially, Dr. Tomohisa Sawada screened helical α/β/γ-peptides based on the Bim BH3 15-mer sequence, a Bim segment containing five residues important for binding to Bcl-xL (Ile, Leu, Ile, Asp and Phe; shown as pink, Figure 5.5). The Bim mimic 13-mer α/β/γ-peptides were designed by systematically replacing α-residues of Bim 15-mer with ring-constrained β- and γ- residues in an αγααβα pattern (Figure 5.5). The binding of α/β/γ-peptides to Bcl-xL was evaluated by competition FP assay using a fluorescently labeled Bak-derived 16-mer peptide (Bodipy-GQVGRQLAIIGDDINR-NH_2) as the ligand to be displaced. The FP results showed that the α/β/γ-peptides tested did not effectively inhibit binding of the Bak-tracer to Bcl-xL. The Bcl-xL binding constant (K_i) of **5.3** was about two orders of magnitude weaker than for the analogous α-Bim 15-mer peptide (Bim K_i = 0.15 μM; **5.3** K_i = 13 μM; values from Dr. Sawada), and **5.1** did not bind at all to Bcl-xL. Peptide **5.2** showed a better binding to Bcl-xL than **5.1** and **5.3** at lower concentrations (< 10 μM); however, the binding was limited in that the FP curve of **5.2** only could reach 50% of the inhibition before aggregation with the tracer peptide occurred (> 10 μM).

We considered several hypotheses for the poor binding exhibited by α/β/γ-peptides **5.1**, **5.2**, and **5.3**. 1) Absence of the Asp on back face of the α/β/γ-helix weakened affinity for Bcl-xL. 2) Incorporation of the ring-constrained β- and γ-amino acids distorted the helical structure. 3) α/β/γ-Peptides caused partial distortion of Bcl-xL cleft upon binding. To test these hypotheses, we have examined Bim-mimicking α/β/γ-

peptides that contain cyclic and acyclic β- and γ- residues with different side chain functional groups.

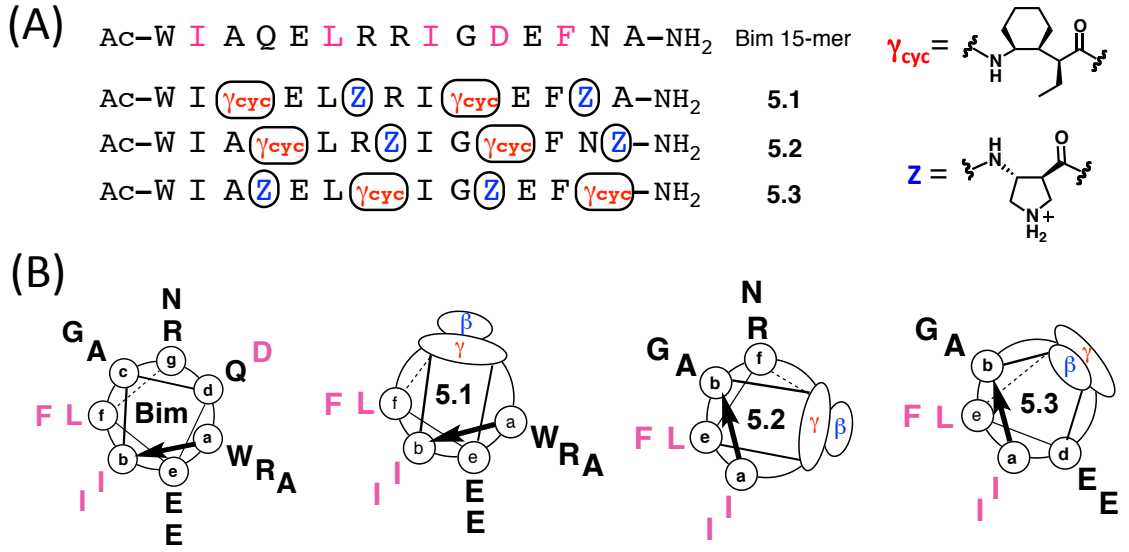

Figure 5.5 (A) Sequences of α-Bim 15-mer and α/β/γ-peptides **5.1**-**5.3** analogous to α-Bim 15-mer (B) Helical wheel diagrams of α-Bim 15-mer and α/β/γ peptides **5.1**-**5.3**.

5.3 Bim-derived *α/β/γ*-peptides containing acyclic γ-residues

5.3.1 Incorporation of acyclic γ-residues

To test the hypothesis that the absence of Asp on back face of the α/β/γ-helix formed by **5.1**-**5.3** led to weak affinity for Bcl-xL, we incorporated acyclic γ^4-hAsp or β^3-hAsp to restore the carboxylate side chain. Sequence alignment of the Asp region for the Bim 15-mer and α/β/γ-peptides containing γ^4-hAsp and β^3-hAsp suggests that the αγααβα register of **5.1** may cause the carboxylate group position to deviate from the position in the analogous Bim 15-mer (Figure 5.6). α/β/γ-Peptides **5.4** and **5.5**,

containing γ^4-hAsp, and **5.6**-**5.9**, containing β^3-hAsp, were designed based on the $\alpha\gamma\alpha\alpha\beta\alpha$ registers of **5.2**, and **5.3**, respectively. We also varied the number of ring-constrained γ-residues in $\alpha/\beta/\gamma$-peptides **5.4**-**5.9** to test if acyclic γ^4-residues can substitute cyclic γ-residues in this system, which have been reported to promote helical conformations in $\alpha/\beta/\gamma$-peptides (Figure 5.7). [22]

The Bcl-xL competition binding FP assay revealed that $\alpha/\beta/\gamma$-peptides **5.4** and **5.5** are relatively promising candidates for inhibiting interaction of Bak and Bcl-xL although K_i values of **5.4** and **5.5** could not be calculated because the FP curves did not reach to the full inhibition (Figure 5.7). **5.2** (two EtACHA) and the analogue **5.5** (one γ^4-hAsp, and one EtACHA) exhibit similar binding to Bcl-xL by FP at lower peptide concentrations (< 10 μM). However, **5.2** aggregates with the tracer peptide at higher concentrations (>10 μM) under the FP assay conditions whereas **5.5** does not. The similar affinity for Bcl-xL observed for **5.2** and **5.5** suggests that the lack of a side chain carboxylate group might not be a major factor in the weak binding of **5.2** to Bcl-xL. However, since γ^4-hAsp (**5.5**) does not decrease Bcl-xL binding compared to EtACHA (**5.2**), and more importantly since γ^4-hAsp helps prevent aggregation, we decided to continue to refine Bcl-xL binding $\alpha/\beta/\gamma$-peptides starting from **5.5** (Figure 5.7).

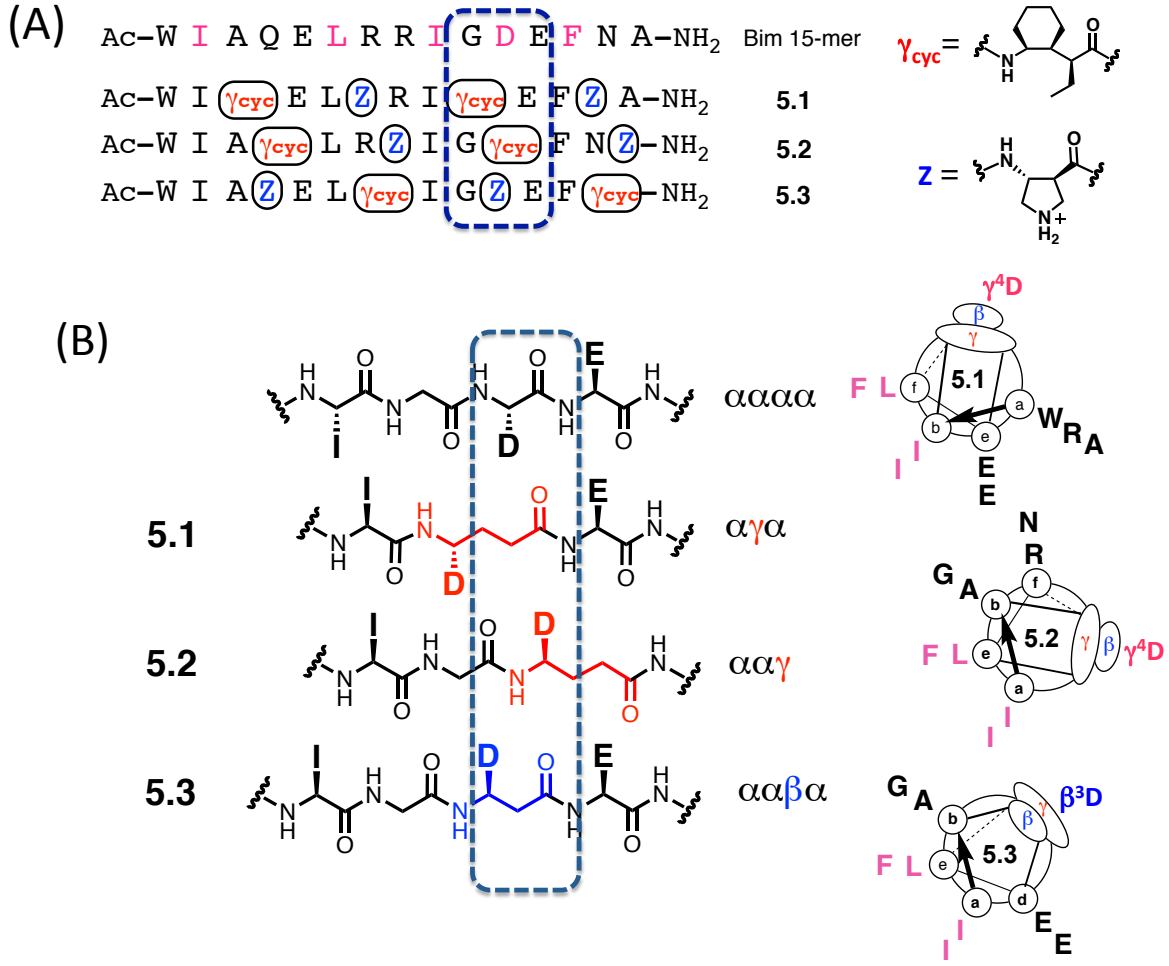

Figure 5.6 (A) Sequences of α-Bim 15-mer and the analogous α/β/γ-peptides **5.1**-**5.3**. The Asp region in each peptide is highlighted with a rectangular box. (B) Peptide sequence alignments of the regions containing γ^4-hAsp and β^3-hAsp in peptides **5.1**-**5.3** compared to the α-Bim 15-mer.

(A)

Ac–W I A Q E L R R I G D E F N A–NH_2	Bim 15-mer
Ac–W I A γ^4hA L R(Z) I G γ^4hD F N(Z)–NH_2	5.4
Ac–W I A(γcyc) L R(Z) I G γ^4hD F N(Z)–NH_2	5.5
Ac–W I A(Z) E L γ^4hA I G β^3hD E F γ^4hA–NH_2	5.6
Ac–W I A(Z) E L(γcyc) I G β^3hD E F(γcyc)–NH_2	5.7
Ac–W I A(Z) E L(γcyc) I G β^3hD E F γ^4hA–NH_2	5.8
Ac–W I A(Z) E L γ^4hA I G β^3hD E F(γcyc)–NH_2	5.9

(B)

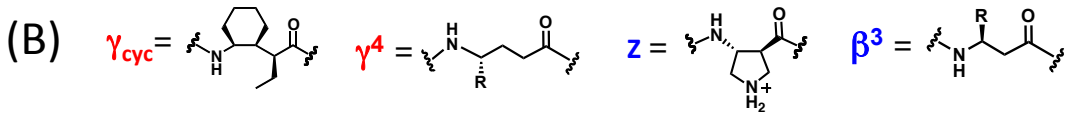

(C)

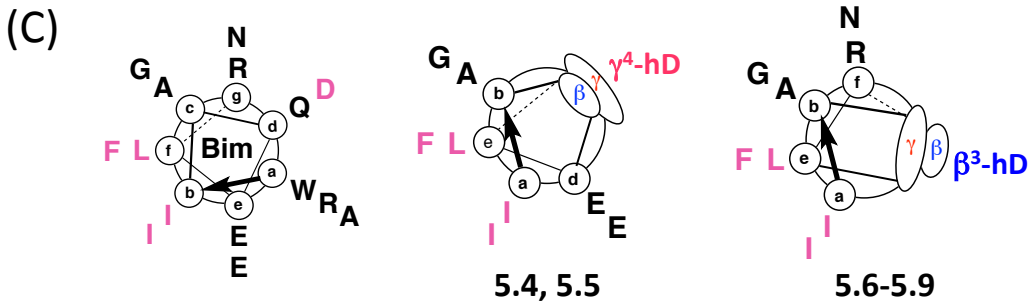

(D)

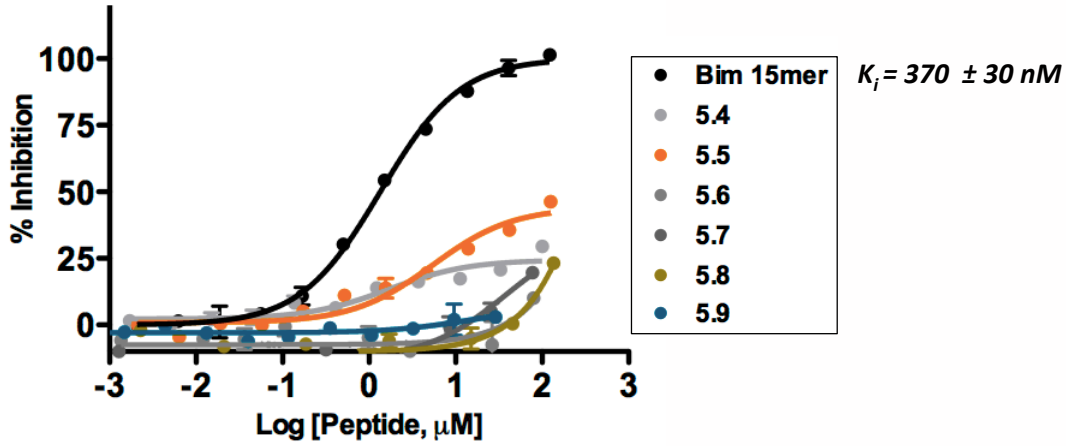

Figure 5.7 (A) Sequences of α-Bim 15-mer and the analogous α/β/γ-peptides **5.4**-**5.9**. (B) Structures of cyclic and acyclic β- and γ-amino acid residues. (C) Helical wheel diagrams of α-Bim 15-mer and α/β/γ-peptides **5.4**-**5.9** (D) Inhibition curves from the Bcl-xL competition binding FP assays using α-Bim 15-mer and α/β/γ-peptides **5.4**-**5.9**.

5.3.2 α/β/γ-Peptides with extended lengths

To further expand on α/β/γ-peptide **5.5**, α/β/γ-peptides derived from the α-Bim 18-mer and 26-mer were prepared (**5.11**-**5.16**; Figure 5.8A). The Bim α-peptide 26-mer displayed far tighter binding to Bcl-xL than the analogous 18-mer α-peptide (K_i ≈ 23 nM for α-Bim 18-mer, K_i < 3 nM for α-Bim 26-mer, by FP)[9,24,25], and thus longer versions of α/β/γ-peptides were expected to result in higher affinity for Bcl-xL than α/β/γ-peptides derived from the Bim 15-mer. Importantly, enhanced binding from the longer peptides would suggest that the α/β/γ-peptides fold into secondary structures similar to an α-helix.

Bim 18-mer-derived α/β/γ-peptides **5.12** and **5.13** with an αγααβα pattern, showed improved affinity for Bcl-xL compared to **5.5**, though only three residues were added relative to **5.5** (13-mer) to generate **5.12** or **5.13** (16-mers) (Figure 5.8B). K_i values of **5.12** and **5.13** could not be calculated because the FP curves did not reach full inhibition of the Bcl-xL/Bak-tracer interaction. The FP data suggest that at the highest α/β/γ-peptide concentration (10 μM) **5.5** reached 50% inhibition, and **5.12** and **5.13** reached 70% inhibition. Peptide **5.13**, which contains an uncharged ACPC in place of positively charged APC near the N-terminus of **5.12**, showed a similar FP curve to that of **5.12**, implying that the charge of the residue incorporated where Ala is found in the α-Bim 18-mer does not significantly affect the interaction of α/β/γ-peptides and Bcl-xL, at least for this set of Bim-derived α/β/γ-peptides.

Interestingly, when the ring constraint on a γ-residue near the C-terminus of the α/β/γ-peptide is relaxed (**5.14** vs. **5.11**-**5.13**), binding to Bcl-xL was significantly

diminished (Figure 5.8B). This observation implies that the rigid helical folding achieved by using EtACHA and ACPC together in α/β/γ-peptides **5.12** and **5.13** is beneficial for binding of the α/β/γ-peptides to Bcl-xL. α/β/γ-Peptide **5.11**, containing Trp instead of ACPC near the N-terminus, aggregated.

Before inserting β- and/or γ-residues into Bim 26-mer analogues, we evaluated α/β/γ-peptides extended using only α-resides, as shown in **5.15** and **5.16**. If Bim 26-mer analogue (α+α/β/γ)-chimeric peptides show good affinity for Bcl-xL, then elongation of an α/β/γ-Bim 18-mer analogue to an α/β/γ-Bim 26-mer analogue using an αγααβα pattern in the C- and N-terminal extensions should be the next step. One limitation of the peptide backbone transformation from α heptads to αγααβα hexads is the difficulty of mimicking longer α-peptide sequences. Conversion of α heptads to α/β/γ hexads causes a loss of one side chain per one repeating unit, and side chain functionality is further lost in incorporating EtACHA and ACPC in αγααβα hexads.

Bim 26-mer derived (α+α/β/γ)-chimeric peptide **5.16** showed slightly increased affinity for Bcl-xL relative to **5.12** and **5.13** (Figure 5.8C; FP curves of **5.12** and **5.13** reached 70% inhibition, and FP curve of **5.16** reached 80% inhibition). However, the affinity improvement shown by **5.16** was minimal considering that longer α-Bim peptides exhibited substantial affinity increases compared to shorter analogues (K_i ≈ 350 nM for α-Bim 15-mer, K_i ≈ 23 nM for 18-mer, K_i < 3 nM for 26-mer)[9], indicating that the current α/β/γ-design is not suitable for Bcl-xL binding. This problem may indicate that the α/β/γ-peptide helix is an imperfect mimic of the α-helix, or the problem may arise because of

the loss of side chain functional groups caused by replacement of α-amino acid residues with cyclic β- or γ- amino acid residues.

(A)

Ac–W I A Q E L R R I G D E F N A–NH_2 Bim 15-mer
Ac–W I A (γcyc) L R (Z) I G γ⁴hD F N (Z)–NH_2 **5.5**
Ac–W I A (γcyc) L R (Z) I G γ⁴hD F N (X)–NH_2 **5.10**

Ac–I W I A Q E L R R I G D E F N A Y Y–NH_2 Bim 18-mer
Ac–I W I A (γcyc) L R (Z) I G γ⁴hD F N (Z) K Y–NH_2 **5.11**
Ac–I (X) I A (γcyc) L R (Z) I G γ⁴hD F N (Z) K Y–NH_2 **5.12**
Ac–I (X) I A (γcyc) L R (Z) I G γ⁴hD F N (X) K Y–NH_2 **5.13**
Ac–I (X) I A γ⁴hA L R (Z) I G γ⁴hD F N (X) K Y–NH_2 **5.14**

Ac–D M R P E I W I A Q E L R R I G D E F N A Y Y A R R–NH_2 Bim 26-mer
Ac–D M R P E I W I A (γcyc) L R (Z) I G γ⁴hD F N (X) K Y A R R–NH_2 **5.15**
Ac–D M R P E I (X) I A (γcyc) L R (Z) I G γ⁴hD F N (X) Y K A R R–NH_2 **5.16**

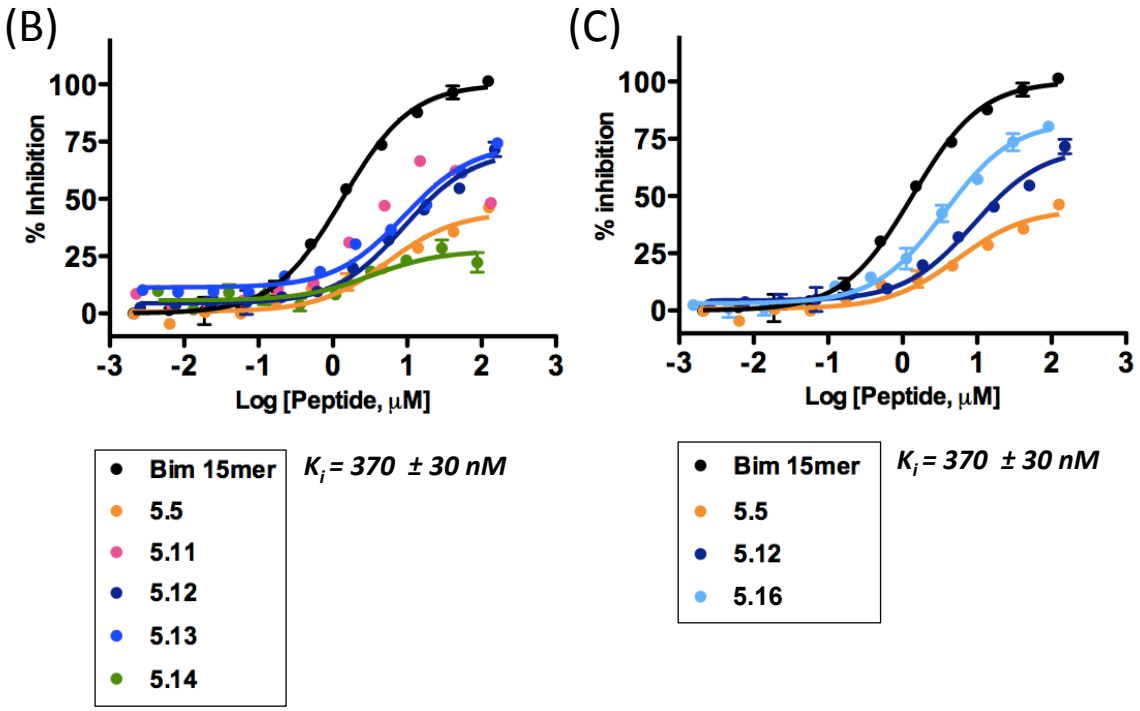

Figure 5.8 (A) Sequences of α-Bim and the analogous α/β/γ-peptides **5.10**-**5.16**. (B) Bcl-xL competition binding FP data converted to % inhibition for 16-mer α/β/γ-peptides **5.11**-**5.14**, and (C) for 24-mer α/β/γ-peptide **5.16**. Inhibition curves from the Bim 15-mer and α/β/γ-peptide **5.5** are overlaid in these graphs (B and C) for the comparison with other α/β/γ-peptides. (FP data for **5.15** in Figure 5.12.)

5.4 α/β/γ-Peptides containing acyclic β-residues

The previous study of Bim-derived α/β-foldamers by Boersma *et al.* indicates that Arg residues at positions 8 and 9 (Bim 18-mer, Figure 5.9B) are important for binding to Bcl-xL.[9] In α/β/γ-peptide **5.17**, β^3-hArg replaced APC from **5.5** to recover the Arg side chain of the parent α-Bim 15-mer (Figure 5.9A). However, without β-residue ring constraints, α/β/γ-peptides show diminished helical propensities.[22] Surprisingly, however, Bim 15-mer derived α/β/γ-peptide **5.17** showed slightly improved binding to Bcl-xL relative to **5.5** (Figure 5.9A; FP curve of **5.5** reached 50% inhibition, while FP curve of **5.17** reached to 80% inhibition).

Starting from **5.17**, we varied the number of ring constraints at γ positions in Bim 18-mer-derived α/β/γ-peptides **5.18**-**5.20** (Figure 5.9B). **5.18** showed affinity for Bcl-xL comparable to that of the α-Bim 15-mer (Figure 5.9, K_i of Bim 15-mer ≈ 370 nM, K_i of **5.18** ≈ 640 nM). Since **5.18** bound with higher affinity to Bcl-xL than did the analogue **5.13**, which contains APC at the site corresponding to β^3-hArg in **5.18**, we conclude that the side chain β^3-hArg in **5.18** is favorably positioned to interact with Bcl-xL, whereas cyclic β residue APC cannot form these favorable contacts.

Without a ring constraint on the γ-residue near the N-terminus of the α/β/γ-peptide, **5.20** showed significantly decreased binding to Bcl-xL relative to **5.18** (FP curve of **5.20** reached only 30% inhibition), suggesting that the low helical propensity of **5.20** is due to the flexibility of the backbone containing acyclic β- and γ- residues (Figure 5.9B).

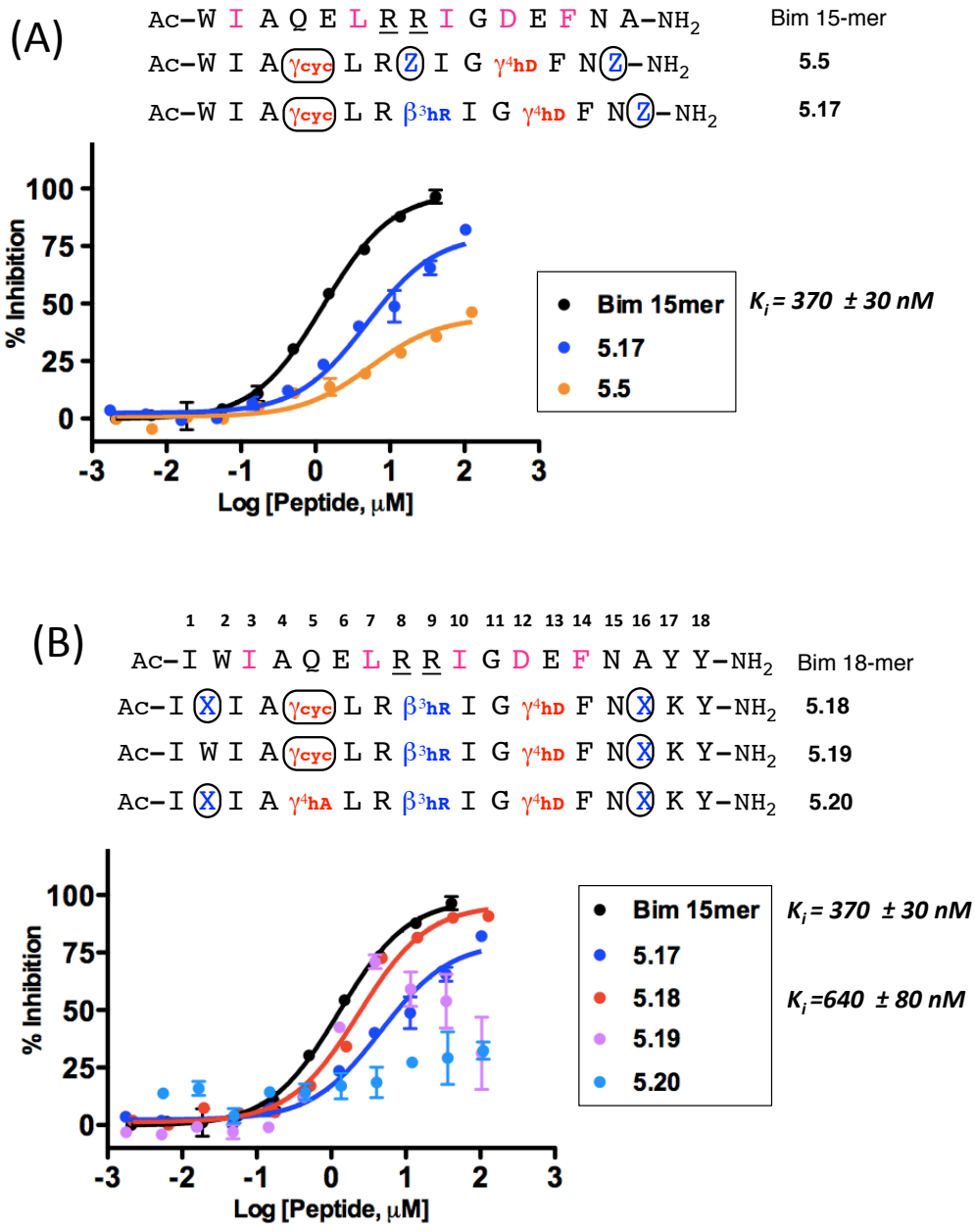

Figure 5.9 (A) Bcl-xL competition binding FP data converted to % inhibition for Bim 15-mer-derived α/β/γ-peptides **5.5** and **5.17** containing β^3-hArg and γ^4-hAsp. (B) FP data for Bim 18-mer-derived α/β/γ-peptides **5.18**-**5.20**.

Encouraged by the success of α/β/γ-peptide **5.18**, we prepared Bim 26-mer-derived α/β/γ-peptides **5.21**-**5.23** by extending **5.18** using α-residues (**5.21**), or by incorporating acyclic γ-residues near the C-terminus (**5.22**) or near both the C- and N-

termini (**5.23**) (Figure 5.10). The results from a Bcl-xL competition binding FP assay using **5.21**, however, showed weaker binding compared to **5.18** (Figure 5.10, K_i of **5.18** ≈ 640 nM, the FP curve of **5.21** reached 80% inhibition). FP assays for **5.22** and **5.23** showed even worse binding (FP curves of **5.22** and **5.23** reached 40-45% inhibition), possibly because of the lack of helicity caused by incorporation of the flexible acyclic γ-residue, or the loss of side chains.

Perhaps the origin of the weak binding to Bcl-xL by α/β/γ-peptides discussed here could be elucidated if a co-crystal structure of Bcl-xL and α/β/γ-peptide **5.18** were available. Such a structure might enable us to improve α/β/γ-peptide affinity by rational design.

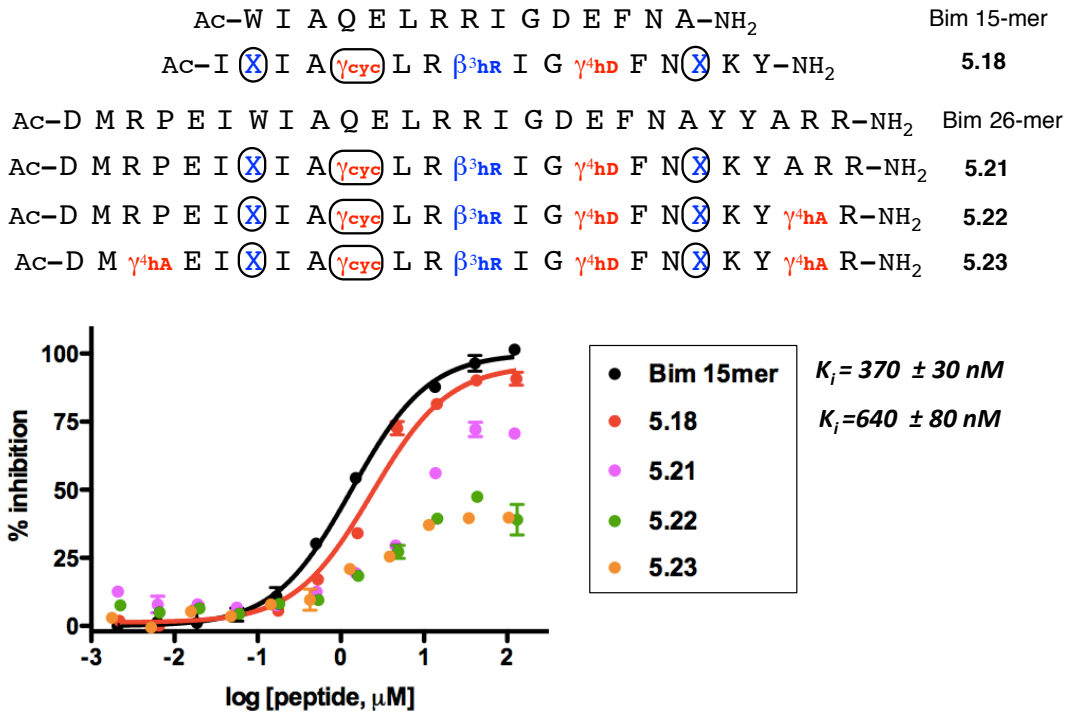

Figure 5.10 Bcl-xL competition binding FP data converted to % inhibition for the Bim 15-mer, **5.18**, and Bim 26-mer-derived α/β/γ-peptides **5.21**-**5.23**.

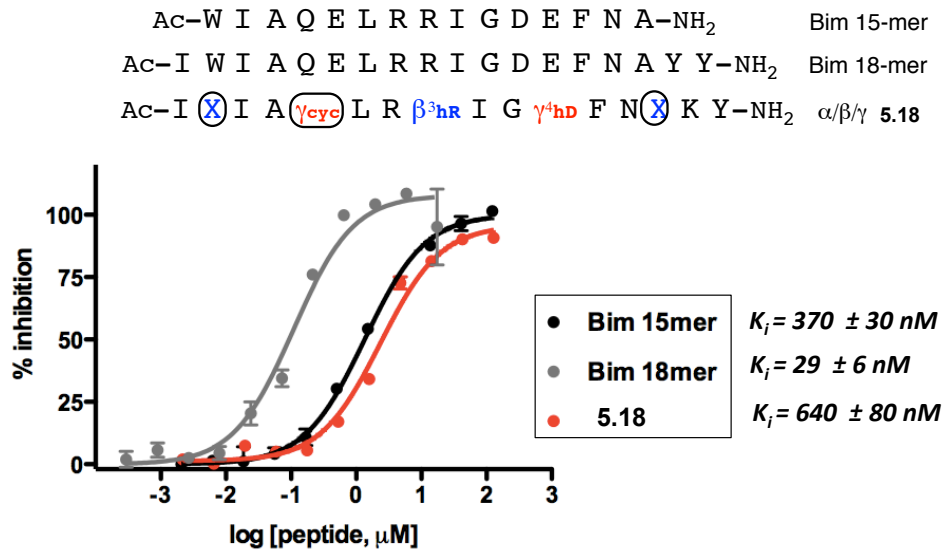

Figure 5.11 Bcl-xL competition binding FP data converted to % inhibition for the α-Bim 18-mer, the α-Bim 15-mer and α/β/γ-peptide **5.18 (**analogous to the Bim 18-mer).

5.5 Aggregation from Bim derived α/β/γ-peptides containing Trp

While evaluating the Bcl-xL binding of Bim-derived α/β/γ-peptides by FP assays, **5.11**, **5.15**, and **5.19**, each of which contains Trp near the N-terminus, showed increases of FP signal at higher concentrations (> 10 μM) (Figure 5.12). When a low molecular weight tracer peptide, such as BODIPY^{TMR}-Bak, is bound to a large, slowly rotating molecule, such as Bcl-xL, high FP is observed. If an inhibitor molecule, such as a Bim-derived α/β/γ-peptide, displaces the tracer peptide from the large binding partner (Bcl-xL), then the freed tracer peptide rotates rapidly, resulting in a low FP signal. FP assays using **5.11**, **5.15**, and **5.19** give rise to datasets in which the apparent % inhibition first increases and then decreases as the α/β/γ-peptide concentration increases. This behavior indicates that the tracer peptide (BODIPY^{TMR}-Bak) tumbles more slowly at higher competitor concentration, suggesting that the tracer peptide

aggregates with each α/β/γ-peptide at high concentrations of the latter. Bim 15-mer-derived α/β/γ-peptides **5.5** and **5.17** did not show any evidence of aggregation with the tracers, unlike the analogous Bim 18-mer-derived **5.11** and **5.19**, implying that extension from 15-mer-derived to 18-mer-derived α/β/γ-peptides by incorporating an Ile next to the Trp at the N-terminus of **5.5** and **5.17**, made the peptides significantly more hydrophobic and prone to aggregation. Bim-derived peptides have been previously shown to aggregate; Peterson-Kaufman found that some Bim-derived α/β-peptides interact with the BODIPY^{TMR}-Bak tracer peptides (Peterson-Kaufman dissertation, Chapter 3.4.1, page 72).

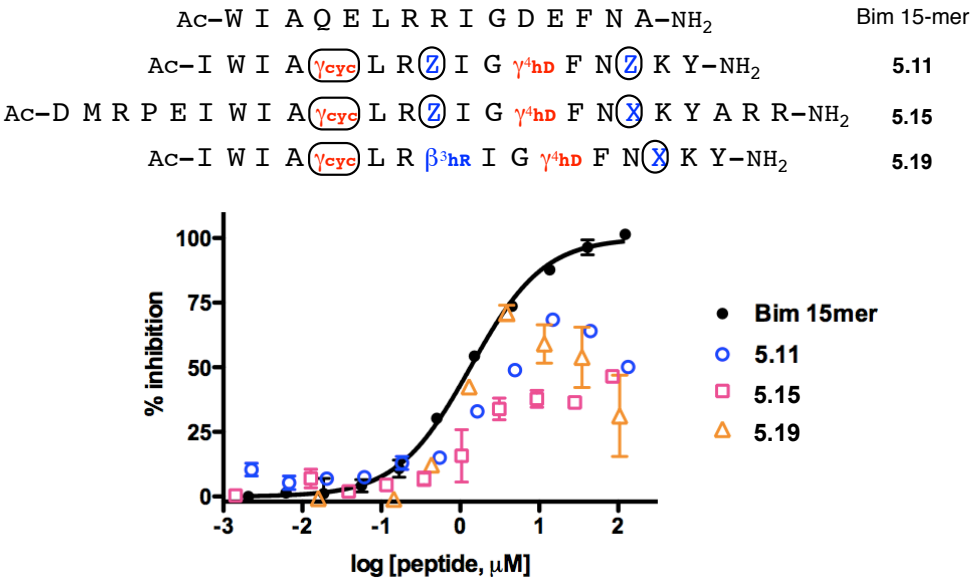

Figure 5.12 Bcl-xL competition binding FP data for α-Bim 15mer and α/β/γ-peptides **5.11**, **5.14** and **5.19**, suggesting that the α/β/γ peptides aggregate with the tracer at higher peptide concentration (> ca. 10 μM).

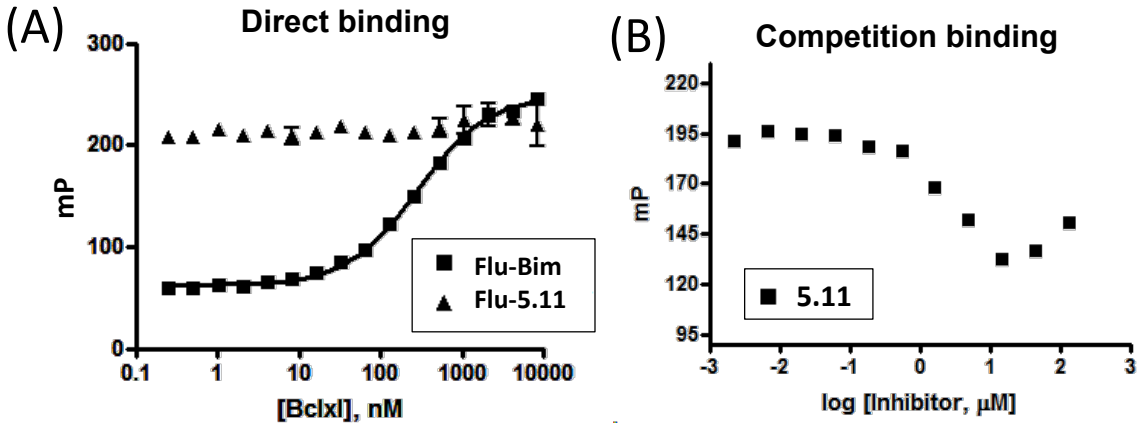

peptides concentration 10 nM

***Flu-5.11** alone showed high signal by FP assay (mp >200), suggesting self-aggregation*

Tracer (BODIPY-Bak) = 3 nM
Bcl-xL= 2 nM

Figure 5.13 (A) Bcl-xL direct-binding FP data for Flu-Bim and Flu-**5.11** (B) Bcl-xL competition binding FP data for α/β/γ-peptide **5.11**.

To prevent aggregation with the tracer peptide, a direct binding FP assay with Bcl-xL was attempted using a fluorescein-labeled derivative of α/β/γ-peptide **5.11**. However, aggregation could not be avoided as indicated by the high mP values observed at all concentrations of Bcl-xL in Figure 5.13A. **Flu-5.11** in Figure 5.13 showed self-aggregating behavior, which was tested by measuring FP of this peptide alone. We could not identify any α/β/γ-peptides that do not aggregate when the α/β/γ-peptide is derived from the Bim 18-mer or longer α-peptide, and contains Trp.

5.6 Proteolysis assay with Bim derived α/β/γ-peptides

The heterogeneous backbone in peptides containing β-residues offers therapeutic promise owing to its α-helix-like folding propensity and its proteolytic stability in physiological environments.[9] To test the susceptibility of the Bim-derived α/β/γ-

peptides to enzymatic cleavage, α-Bim and the analogous α/β/γ-peptides were incubated with a promiscuous protease, proteinase K, and the cleavage process was monitored by HPLC.

α-Bim 15-mer, as expected, was rapidly degraded in the presence of proteinase K, with a half-life of approximately 3 minutes (Figure 5.14B and C). We did not observe any degradation of α/β/γ-peptide **5.5** after about 20 hours of exposure to proteinase K (Figure 5.14D). The Bim 18-mer-derived α/β/γ-peptide **5.13** did not show any significant proteolytic degradation within 92 hours (Figure 5.14E). **5.18** may have given rise to trace cleavage products after 92 hours (Figure 5.14F). If we assume the half-lives of α/β/γ–peptides are at least 15 hours, and the half-life of the α–Bim peptide is 3 minutes, then the half-life of the α/β/γ-peptides is 300-fold longer than that of the α-peptide, suggesting that an α/β/γ-heterogeneous backbone could be useful as a basis for the design of peptide-mimics that display long-term activity *in vivo*.

(A)

Ac–W I A Q E L R R I G D E F N A–NH_2	Bim 15mer	$t_{1/2}$= 3.1 min
Ac–W I A (γcyc) L R (Z) I G γ⁴hD F N (Z)–NH_2	5.5	$t_{1/2}$ > 15 hrs
Ac–I (X) I A (γcyc) L R (Z) I G γ⁴hD F N (X) K Y–NH_2	5.13	No degradation after 24 hrs
Ac–I (X) I A (γcyc) L R β³hR I G γ⁴hD F N (X) K Y–NH_2	5.18	

(B)

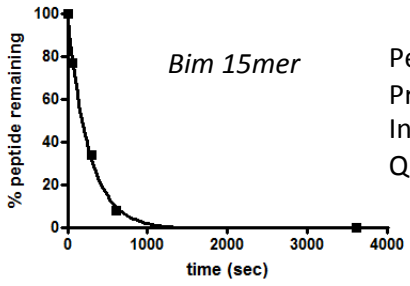

Bim 15mer

Peptide conc. 50 μM
Proteinase K (5 μg/mL)
In pH 7.5 TBS with 5% DMSO
Quenched with 1% TFA in 50:50 MeCN: H_2O

(C)

Ac–W I A Q E L R R I G D E F N A–NH_2 Bim 15mer

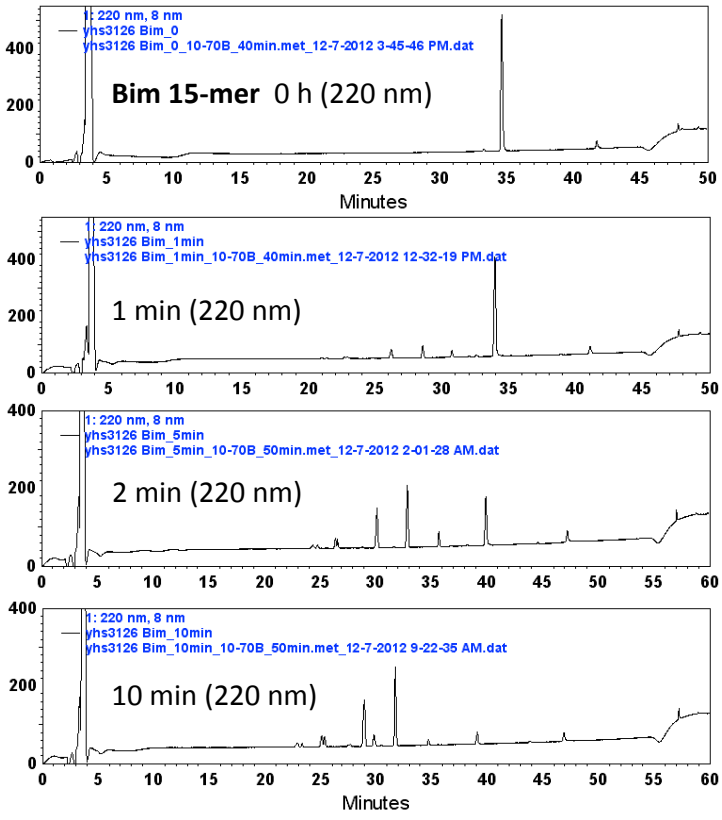

(D) Ac–W I A(γcyc) L R(Z) I G γ⁴hD F N(Z)–NH_2 **5.5**

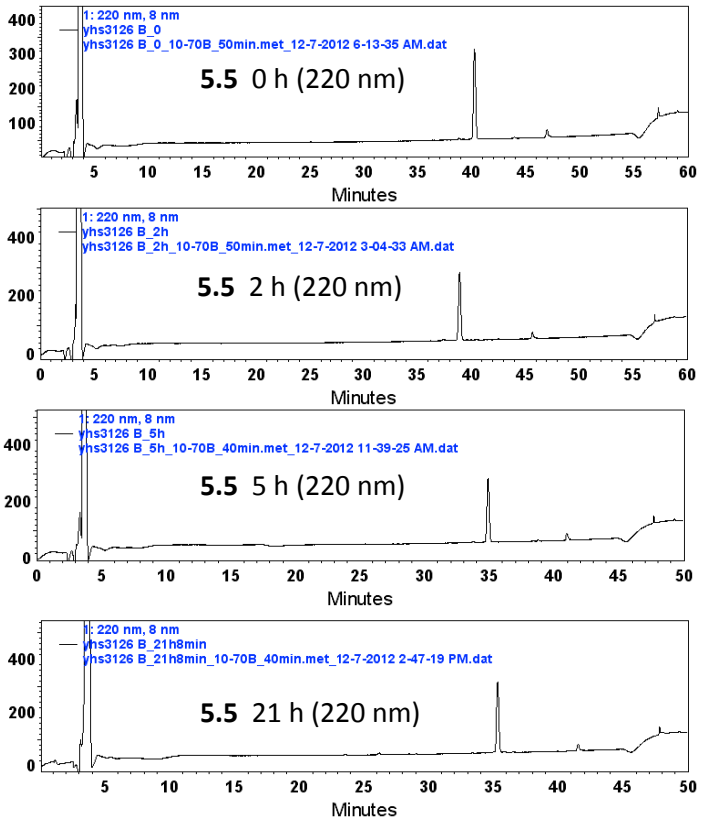

(E) Ac–I (X) I A (γcyc) L R (Z) I G γ⁴hD F N (X) K Y–NH_2 **5.13**

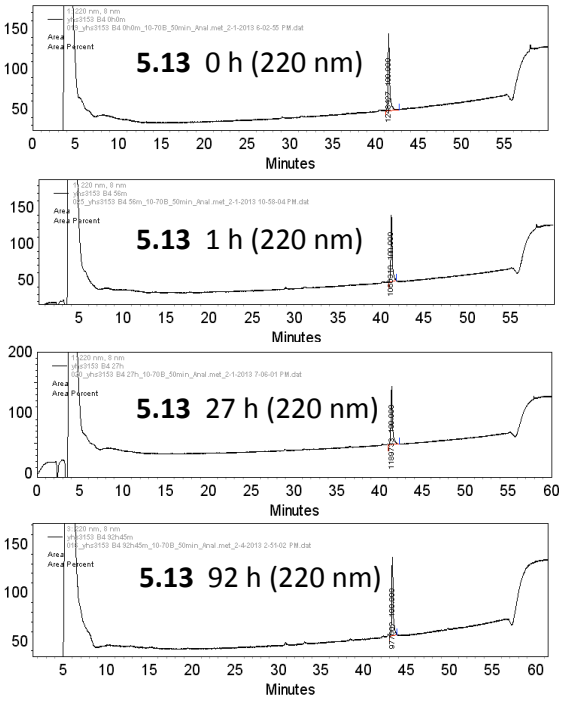

(F) Ac–I X I A γ_{cyc} L R β^3hR I G γ^4hD F N X K Y–NH_2 **5.18**

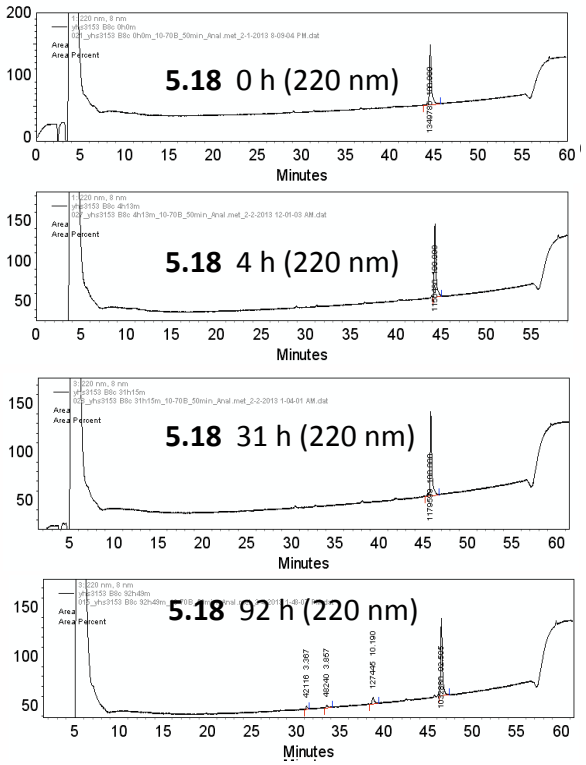

Figure 5.14 (A) Sequences of the α-Bim 15-mer and α/β/γ-peptides **5.5**, **5.13**, and **5.18**. (B) Curve resulting from proteolysis of α-Bim 15-mer in the presence of proteinase K as a function of time; the data were fit to an exponential decay model in GraphPad Prism. HPLC traces of (C) the α-Bim 15-mer, (D) **5.5** (E) **5.13** and (F) **5.18** at different time points during incubation in proteinase K solution. No noticeable degradation was observed from the solutions of **5.5**, **5.13** and **5.18** in the presence of proteinase K within ~ 30 hours.

5.7 Circular dichroism analysis

We have previously shown that a CD spectrum with a minimum around 203-205 nm is indicative of helical structure in α/β/γ-peptide.[22,23] The folding of Bim-derived α/β/γ-peptides **5.13**, **5.18**, **5.19** and the α-Bim 15-mer were examined by CD.

α/β/γ-Peptides **5.13** and **5.18** were compared to evaluate the effect of replacing cyclic APC with acyclic β^3-hArg on helical propensity. α/β/γ-Peptides **5.13** and **5.18** display similar CD behavior in PBS buffer and in 50% methanol solution, with an ellipticity minimum around 205 nm, indicating helical folding (Figure 5.15). Replacing a cyclic β (**5.13**) with an acyclic β residue (**5.18**) does not cause a noticeable change in the extent of helix formation based on the CD results. However, **5.18** is a tighter binder to Bcl-xL than **5.13**, suggesting that the acyclic β^3-hArg in **5.18** is superior to the cyclic APC in **5.13** for binding to Bcl-xL.

Although **5.19** seemed to aggregate with the tracer peptide during FP assays, we were interested in its folding behavior since **5.19** showed resonable binding at non-aggregating concentrations (< 8 μM) in the FP assay (Figure 5.15C). α/β/γ-Peptide **5.19** shows a significant CD signal around 220 nm in PBS buffer and in 50% methanol/PBS solution (Figure 5.15). Tryptophan residues have been reported to cause a CD signal in the regions 280-300 nm and 220-230 nm due to the indole rotation.[26] Even if the signal around 220-230 nm was due to the Trp residue however, the CD spectra of **5.19** in PBS buffer and 50 % methanol seem to suggest α-helix-like folding. Therefore, it might be productive to evaluate the binding of **5.19** to Bcl-xL using tools other than FP assay.

Ac–W I A Q E L R R I G D E F N A–NH_2 Bim 15mer

Ac–I (X) I A (γcyc) L R (Z) I G γ⁴hD F N (X) K Y–NH_2 5.13

Ac–I (X) I A (γcyc) L R β³hR I G γ⁴hD F N (X) K Y–NH_2 5.18

Ac–I W I A (γcyc) L R β³hR I G γ⁴hD F N (X) K Y–NH_2 5.19

(A)

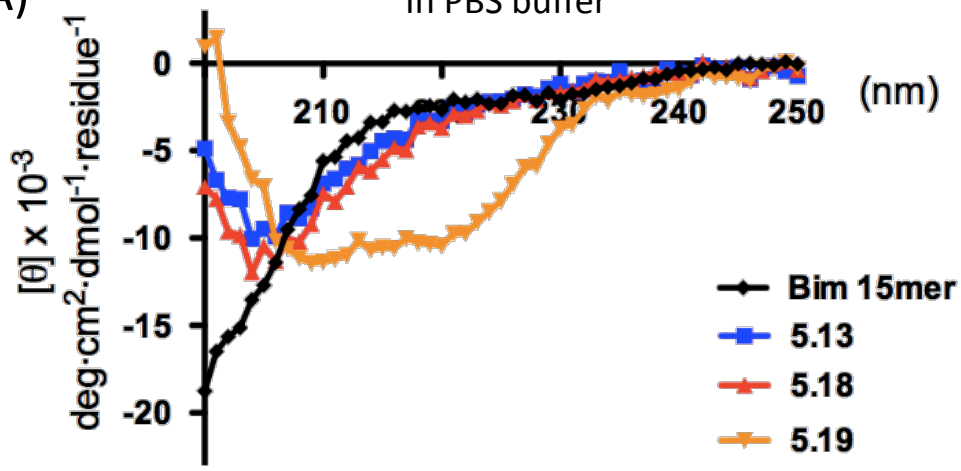

(B)

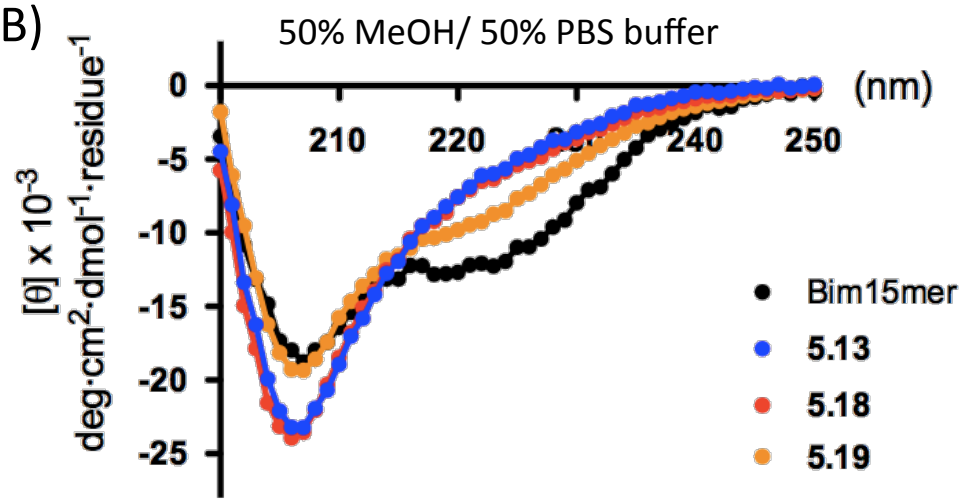

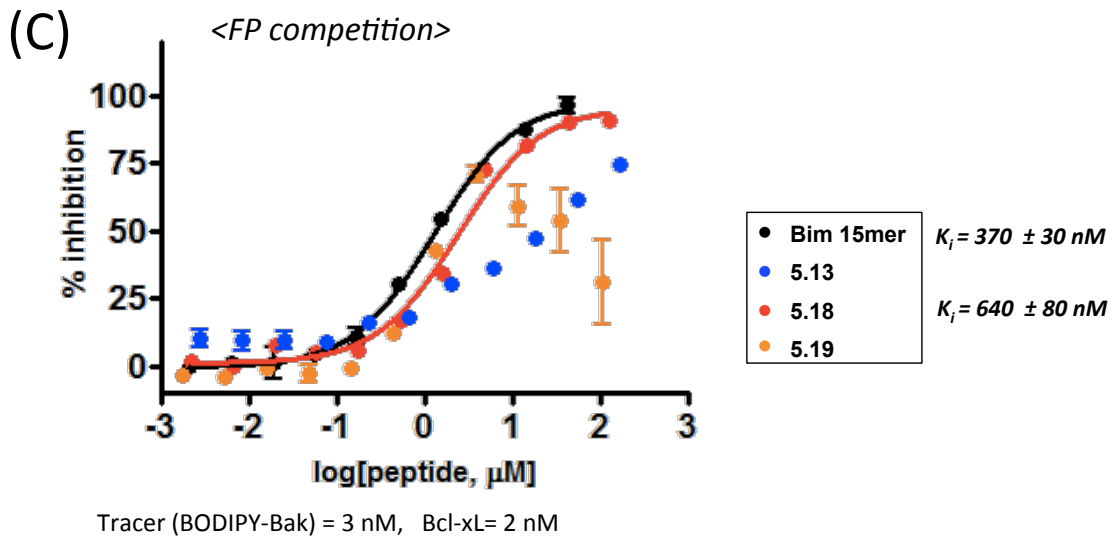

Figure 5.15 Circular dichroism spectra of the α-Bim 15-mer and α/β/γ-peptides **5.13**, **5.18**, and **5.19** (A) in PBS buffer pH 7.4 and (B) in 50% MeOH at 20 °C. (C) Bcl-xL competition binding FP data for the α-Bim 15-mer and α/β/γ-peptides **5.13**, **5.18**, and **5.19**. For circular dichroism measurements, concentrations of α/β/γ-peptides **5.13**, **5.18**, and **5.19** were 50 μM, and of the Bim 15-mer was 100 μM.

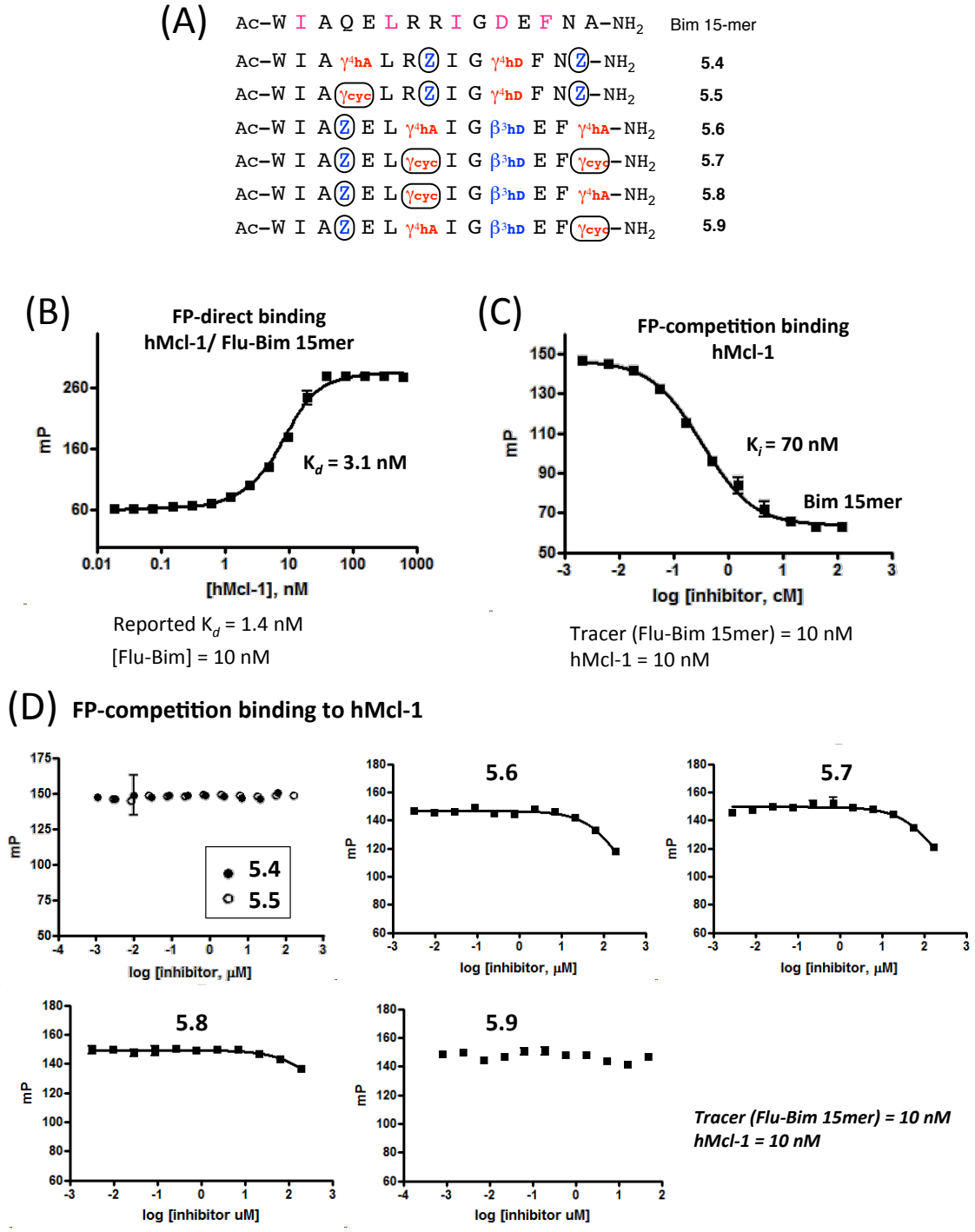

Figure 5.16 (A) α/β/γ-Peptide **5.4**-**5.9** used for the hMcl-1 binding FP assays (B) hMcl-1 direct-binding FP data for the Flu-Bim 15-mer (Bim 15-mer: WIAQELRRIGDEFNA). (C) hMcl-1 competition-binding FP data for the α-Bim 15-mer (D) hMcl-1 competition-binding FP data for α/β/γ-peptides **5.4**-**5.9**.

5.8 α/β/γ-Peptides mimicking Bim do not bind to hMcl-1

Some BH3-only proteins, such as Bim, Bid and Puma, promiscuously bind to all anti-apoptotic members of the Bcl-2 family, whereas others bind only to specific anti-apoptotic proteins either Bcl-xL or Mcl-1 .[2,10] To test the specificity of Bim-derived α/β/γ-peptides to the anti-apoptotic proteins, we evaluated the affinity of Bim 15-mer derived α/β/γ-peptides **5.4**-**5.9** for hMcl-1 by competition FP assay using a fluorescein-Bim (15-mer) tracer peptide (Figure 5.16). However, none of α/β/γ-peptides **5.4**-**5.9** showed significant binding to hMcl-1, suggesting the current α/β/γ-peptide strategy needs to be applied to different parent sequences to find hMcl-1 and Bcl-xL binding α/β/γ-peptides.

5.9 Effort toward Co-crystallization of Bcl-xL with α/β/γ-peptide 5.18

Among the Bim-derived α/β/γ-peptides, **5.18** showed the highest affinity for the Bcl-xL. A co-crystal structure of the complex between α/β/γ-peptide **5.18** and Bcl-xL would elucidate their interaction at the atomic level. To facilitate Bcl-xL protein crystallization, a "loop-deleted" form of human Bcl-xL (Δ27-82 and without membrane anchor), which forms an α-1 domain-swapped dimer yet retains BH3 domain binding activity, was used.[9,27-29] The plasmid for the "loop-deleted" form of Bcl-xLΔ27-82 (from here abbreviating to Bcl-xLΔ) was obtained from the Fairlie lab in Australia, and was expressed in RIPL Escherichia coli cells, and purified.

The proper folding of Bcl-xLΔ was confirmed by direct binding FP assay using BODIPY^{TMR}-Bak peptide (Figure 5.17A). The Bcl-xLΔ competition binding FP assay

with α-Bim 15-mer was consistent with results from full-length Bcl-xL; however, α/β/γ-peptides **5.13** and **5.18** showed somewhat reduced binding to Bcl-xLΔ relative to full-length protein (Figure 5.17B and C). While valuable insights that would be gained from a co-crystal structure of the Bcl-xLΔ/**5.18** complex, the diminished affinity of **5.18** for Bcl-xLΔ will likely make crystallizing the complex quite challenging. Therefore, this effort was abandoned.

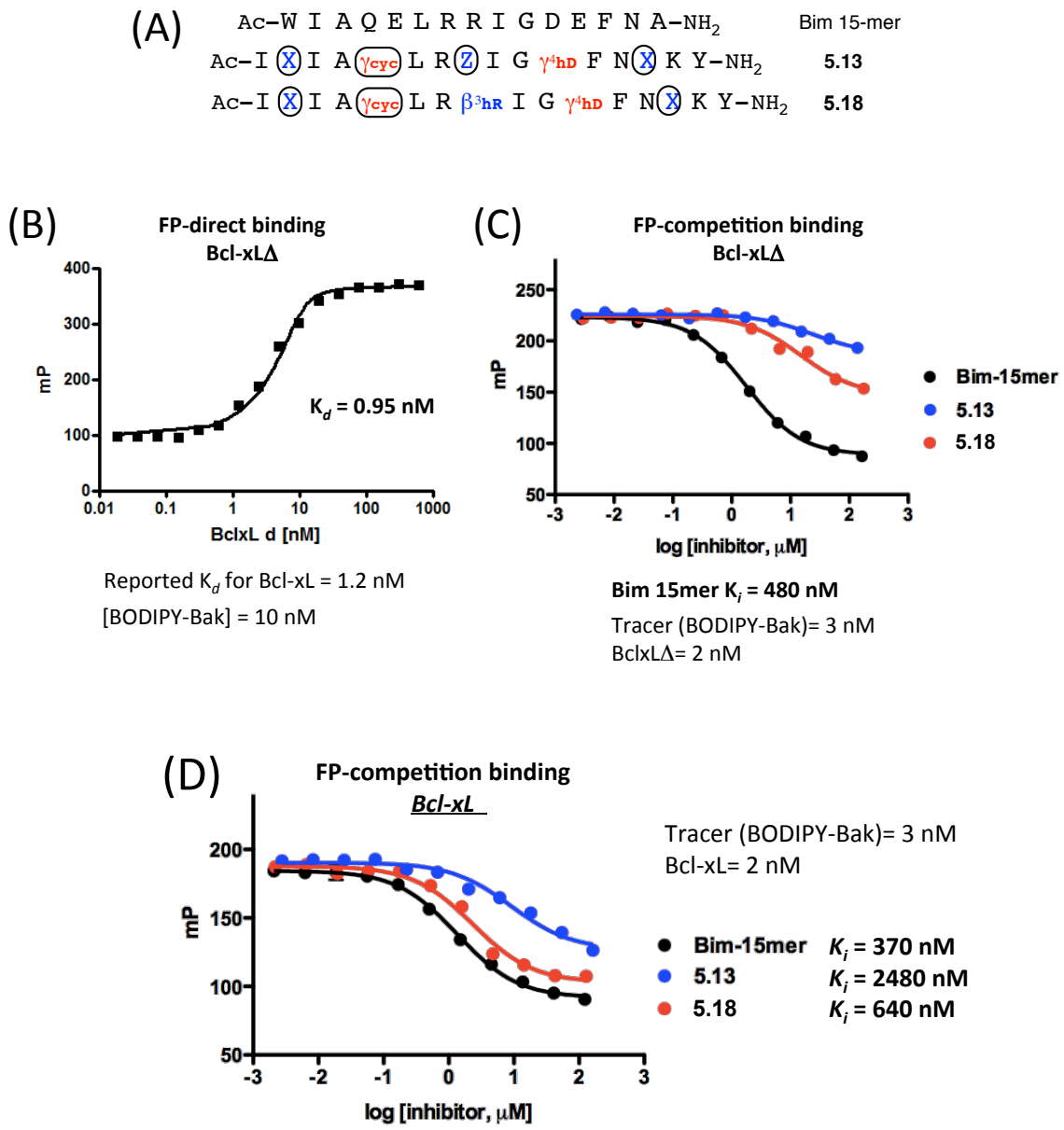

Figure 5.17 (A) Sequences of the α-Bim 15-mer and α/β/γ-peptides **5.13** and **5.18**. (B) Loop-deleted Bcl-xLΔ direct-binding FP data for BODIPY^{TMR}-Bak. (C) Loop-deleted Bcl-xLΔ competition-binding FP data for the α-Bim 15-mer and α/β/γ-peptides **5.13** and **5.18**. (D) Full length Bcl-xL competition-binding FP data for the α-Bim 15-mer and α/β/γ-peptides **5.13** and **5.18**.

5.10 Future Directions

There are several problems to address in the future of this project. 1) Aggregation of Bim 18-mer- or 26-mer-derived α/β/γ-peptides containing Trp was always observed during FP assays. 2) Bcl-xL-binding α/β/γ-peptides did not show affinity for hMcl-1. 3) Longer α/β/γ-peptides based on the sequence of **5.18** did not present improved affinity to Bcl-xL. 4) The results of FP assays from the original form of Bcl-xL and loop-deleted Bcl-xLΔ with α/β/γ-peptides **5.13** and **5.18** are not consistent.

Since Bim-derived α/β-peptides also have shown aggregation problems, it might be easier to avoid this problem by designing α/β/γ-peptides based on the Puma sequence.[17] A Puma-derived α/β-foldamer with a ααβααβ pattern, which places β-residues along one face of the helix, showed high affinity for both Bcl-xL and hMcl-1, and the analogous α/β/γ-peptide might show similar behavior to the Puma-derived α/β-peptides.[17] Alternatively, because the pattern of β- and γ- incorporation in α/β/γ-peptides does not require use of a specific replacement pattern, it may be worth optimizing Bim-derived α/β/γ-peptides by placing β- and γ-residues in different patterns than the αγααβα hexad repeat.

5.11 Conclusions

Herein, we explored α/β/γ-peptides for functionally mimicking α-helices using a model interaction between Bcl-xL and the α-helical BH3 domain peptide Bim. Starting from the Bim 15-mer-derived α/β/γ-peptides containing cyclic β (APC, ACPC) and cyclic γ residues (EtACHA), we modified α/β/γ-peptides by varying the length, and by

incorporating acyclic β and γ residues containing side chain functional groups considered to be important for binding to Bcl-xL. The most promising Bim 18-mer-derived α/β/γ-peptide, **5.18**, showed comparable K_i values to the α-Bim 15-mer for Bcl-xL binding by FP assay (Figure 5.18). Bim-derived α/β/γ-peptides exhibited significant resistance to enzymatic digestion. To gain a more detailed understanding of the interaction between Bim-derived α/β/γ-peptides and Bcl-xL, co-crystallization of their complex should be pursued.

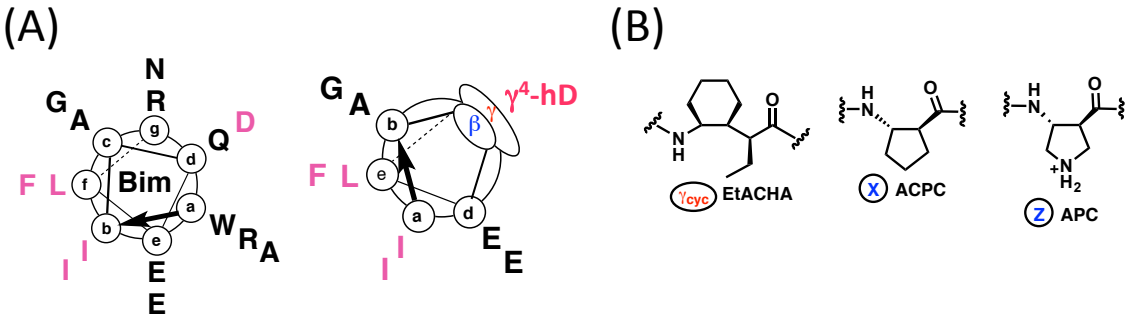

(C)

		K_i (nM) Bcl-xL
Bim 15-mer	Ac–W I A Q E L R R I G D E F N A–NH_2	370
5.5	Ac–W I A (γcyc) L R (Z) I G γ4hD F N (X) –NH_2	-
5.17	Ac–W I A (γcyc) L R β3hR I G γ4hD F N (Z) –NH_2	(1300)
Bim 18-mer	Ac–I W I A Q E L R R I G D E F N A Y Y–NH_2	29
5.13	Ac–I (X) I A (γcyc) L R (Z) I G γ4hD F N (X) K Y–NH_2	-
5.18	Ac–I (X) I A (γcyc) L R β3hR I G γ4hD F N (X) K Y–NH_2	640
5.21	Ac–D M R P E I (X) I A (γcyc) L R β3hR I G γ4hD F N (X) K Y A R R–NH_2	(3000)

Figure 5.18 Summary of Bim-derived α/β/γ-peptides. (A) Helical wheels of α-Bim and an analogous α/β/γ-helix. Important residues for binding to Bcl-xL are highlighted in pink. (B) Structures of cyclic γ- and β-residues. (C) Sequences of Bim-derived α/β/γ-peptides and K_i values obtained from the Bcl-xL competition binding FP assays. K_i values in parentheses are approximate.

5.12 Experimental

5.12.1 Materials

Fmoc α-amino acids and resin for solid phase peptide synthesis were purchased from Novabiochem or Chem-Impex, and coupling reagents and additives, O-benzotriazole-N,N,N',N'-tetramethyluronium hexafluorophosphate (HBTU), O-(7-azabenzotriazol-1yl)-N,N,N,N'-tetramethyluronium hexafluorophosphate(HATU), 1-ethyl-3-(3-dimethylaminopropyl)carbodiimide hydrochloride (EDCI), hydroxybenzotriazole (HOBt), 1-hydroxy-7-azabenzotoriazole) (HOAt), were purchased from Chem-Impex. 6-((4,4-Difluoro-1,3-dimethyl-5-(4-methoxyphenyl)-4-bora-3a,4a-diaza-s-indacene-2- propionyl)amino)hexanoic acid, succinimidyl ester (BODIPY-TMR-X-SE) was purchased from Invitrogen. Other reagents and solvents were purchased from Sigma Aldrich. Fmoc β- and γ- amino acids were prepared according to previous reports.[30,31]

5.12.2 Peptides synthesis and purification

All the α- and α/β/γ-peptides described in this chapter were synthesized on Nova PEG rink amide resin (25-50 μmol scale) by microwave-assisted solid-phase method using a CEM MARS microwave reactor.[22,23,32] For α- and cyclic/acyclic β-amino acids coupling reactions, Fmoc-amino acids were pre-activated in a separated vial (4 equiv. of Fmoc-amino acids, 3.95 equiv. of HBTU, 8 equiv. of DIEA, 0.1 M HOBT in DMF solution) for 1-2 minutes, then the solution was added to resin in a filter tube, reacted under microwave irradiation (2 min ramp to 70 ^{o}C, 4 min hold at 70 ^{o}C for α-residues, 12 min hold for β-residues). For acyclic γ-amino acid coupling reactions, the same condition

with β-amino acid coupling was applied but DIEA was added just before starting microwave irradiation in order to avoid intra-cyclization reaction of γ-amino acids. Cyclic γ-residue (EtACHA) coupling reactions were performed by pre-activating 4 equiv. of Fmoc-amino acid with 4 equiv. of EDCI and 8 equiv. of DIEA in 0.1M HOAt in DMF, then the mixture solution was added to resin and reacted for 14 hours at room temperature while gently shaking. Fmoc deprotection reactions were carried out using 20 % piperidine in DMF under microwave irradiation (2 min ramp to 80 ^{o}C, 2 min hold at 80 ^{o}C). Upon completion of couplings, the N-terminus amine was capped by acetylation using Ac_2O in DMF and DIEA.[32]

Peptides were globally deprotected and cleaved from the resin by suspending in cleavage cocktail (95% trifluoroacetic acid (TFA), 2.5 % water, and 2.5 % triisopropylsilane) for 4~5 hours. After filtering out the TFA cleavage solution from the resin, peptides were precipitated from the TFA solution by adding cold diethyl ether, centrifuged to get a peptide pellet.

BODIPY^{TMR}-Bak (BODIPY^{TMR}-GQVGRQLAIIGDDINR-NH_2)

Flu-Bim (6-carboxyfluorescein- WIAQELRRIGDEFNA-NH_2)

Flu-5.11 (6-carboxyfluorescein- IWIAγ_{cyc}LR**Z**IGγ^4**D**FN**X**KY-NH_2)

Peptides Bak, Bim and **5.11** were prepared as described above and labeled with BODIPY-TMR or Fluorescein using previously reported methods.[17] For labeling **5.11**, peptide **5.11** was synthesized, and as a last step 6-carboxyfluorescein was coupled overnight at room temperature with the same coupling condition for the α-amino acid couplings. For BODIPY labeling, Bak was synthesized with N-terminus as free amine,

cleaved, purified and lyophilized. Bak and BODIPY-TMR-SE were dissolved in 0.1 M $NaHCO_3$, and reacted for 8 hours on mechanical shaker.

Crude peptides were purified by reverse-phase HPLC using a C18 column. Peptides identity was confirmed by matrix-assisted laser desorption/ionization time-of-flight (MALDI-TOF-MS) mass spectrometry. Peptides purity was checked on analytical reverse-phase HPLC.

		Mass expected	Mass measured
5.4	Ac–W I A γ^4hA L R(Z) I G γ^4hD F N(Z)–NH_2	1596.8	1596.8
5.5	Ac–W I A(γcyc) L R(Z) I G γ^4hD F N(Z)–NH_2	1664.9	1664.8
5.6	Ac–W I A(Z) E L γ^4hA I G β^3hD E F γ^4hA–NH_2	1557.7	1557.7
5.7	Ac–W I A(Z) E L(γcyc) I G β^3hD E F(γcyc)–NH_2	1693.7	1693.7
5.8	Ac–W I A(Z) E L(γcyc) I G β^3hD E F γ^4hA–NH_2	1626.0	1626.0
5.9	Ac–W I A(Z) E L γ^4hA I G β^3hD E F(γcyc)–NH_2	1626.5	1626.5
5.10	Ac–W I A(γcyc) L R(Z) I G γ^4hD F N(X)–NH_2	1664.0	1663.7
5.11	Ac–I W I A(γcyc) L R(Z) I G γ^4hD F N(Z) K Y–NH_2	2069.2	2069.2
5.12	Ac–I(X) I A(γcyc) L R(Z) I G γ^4hD F N(Z) K Y–NH_2	1944.2	1944.1
5.13	Ac–I(X) I A(γcyc) L R(Z) I G γ^4hD F N(X) K Y–NH_2	1993.2	1993.3
5.14	Ac–I(X) I A γ^4hA L R(Z) I G γ^4hD F N(X) K Y–NH_2	1925.1	1924.8
5.15	Ac–D M R P E I W I A(γcyc) L R(Z) I G γ^4hD F N(X) K Y A R R–NH_2	3079.7	3079.0
5.16	Ac–D M R P E I(X) I A(γcyc) L R(Z) I G γ^4hD F N(X) Y K A R R–NH_2	3004.7	3004.2
5.17	Ac–W I A(γcyc) L R β^3hR I G γ^4hD F N(Z)–NH_2	1723.0	1723.1
5.18	Ac–I(X) I A(γcyc) L R β^3hR I G γ^4hD F N(X) K Y–NH_2	2051.2	2051.1
5.19	Ac–I W I A(γcyc) L R β^3hR I G γ^4hD F N(X) K Y–NH_2	2126.2	2127.0
5.20	Ac–I(X) I A γ^4hA L R β^3hR I G γ^4hD F N(X) K Y–NH_2	1983.2	1983.0
5.21	Ac–D M R P E I(X) I A(γcyc) L R β^3hR I G γ^4hD F N(X) K Y A R R–NH	3062.7	3062.0
5.22	Ac–D M R P E I(X) I A(γcyc) L R β^3hR I G γ^4hD F N(X) K Y γ^4hA R–NH	2934.7	2934.2
5.23	Ac–D M γ^4hA E I(X) I A(γcyc) L R β^3hR I G γ^4hD F N(X) K Y γ^4hA R–NH_2	2780.6	2780.2
Flu-5.11	Flu–I W I A(γcyc) L R(Z) I G γ^4hD F N(X) K Y–NH_2	2418.4	2418.4

Purity check: 10-60 % MeCN, 50 min

Ac–W I A γ⁴hA L R(Z) I G γ⁴hD F N(Z)–NH_2 **5.4**

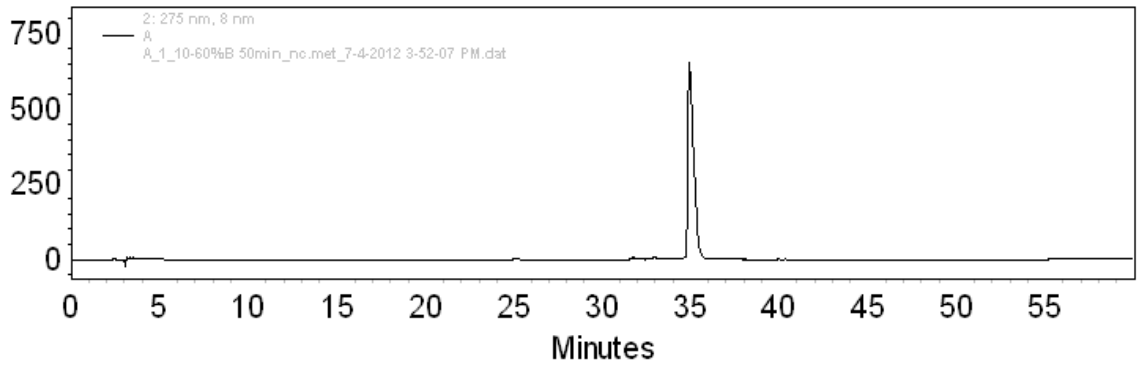

Purity check: 10-60 % MeCN, 50 min

Ac–W I A(γcyc) L R(Z) I G γ⁴hD F N(Z)–NH_2 **5.5**

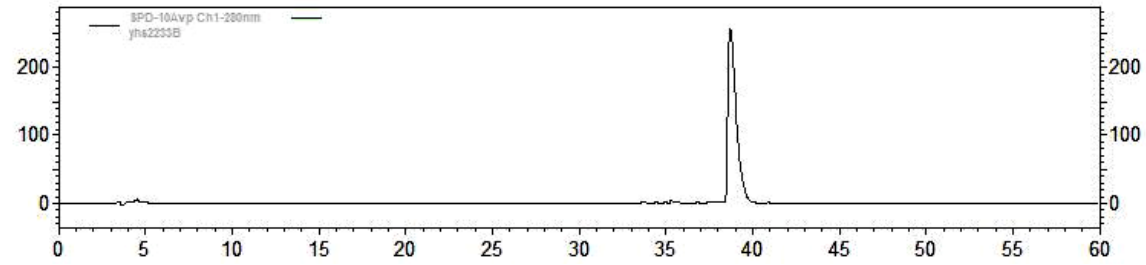

Purity check: 10-60 % MeCN, 50 min

Ac–W I A(Z) E L γ⁴hA I G β³hD E F γ⁴hA–NH_2 **5.6**

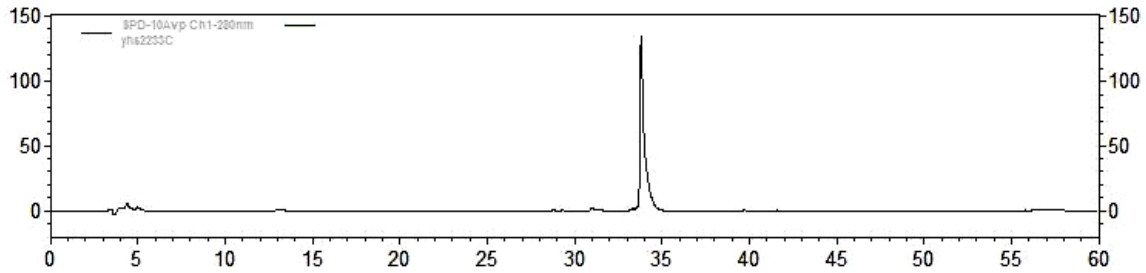

Purity check: 10-60 % MeCN, 50 min

Ac–W I A(Z) E L(γcyc) I G β³hD E F(γcyc)–NH_2 **5.7**

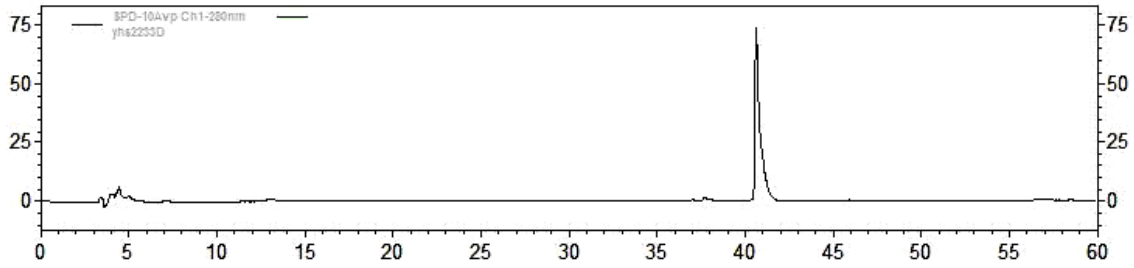

Purity check: 10-60 % MeCN, 50 min

Ac–W I A(Z) E L(γcyc) I G β³hD E F γ⁴hA–NH_2 **5.8**

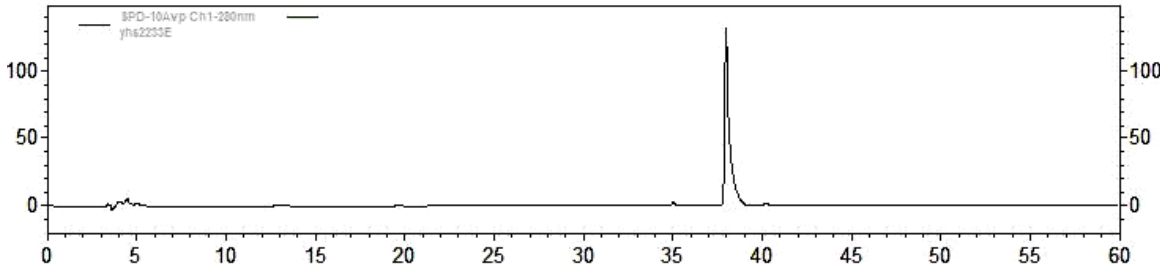

Purity check: 10-60 % MeCN, 50 min

Ac–W I A(Z) E L γ⁴hA I G β³hD E F(γcyc)–NH_2 **5.9**

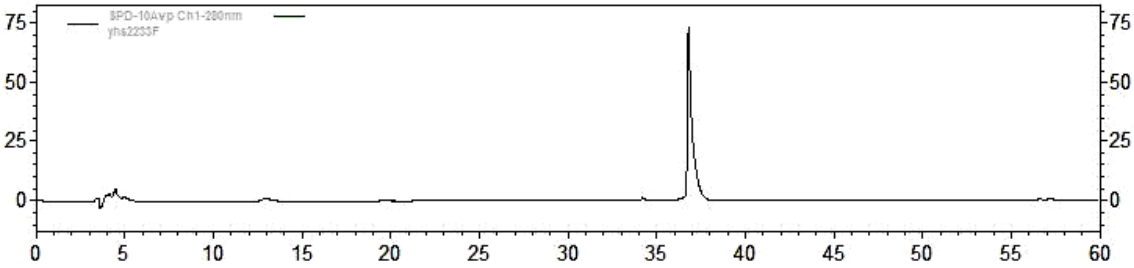

Purity check: 10-60 % MeCN, 50 min

Ac–W I A (γcyc) L R (Z) I G γ⁴hD F N (X)–NH_2 **5.10**

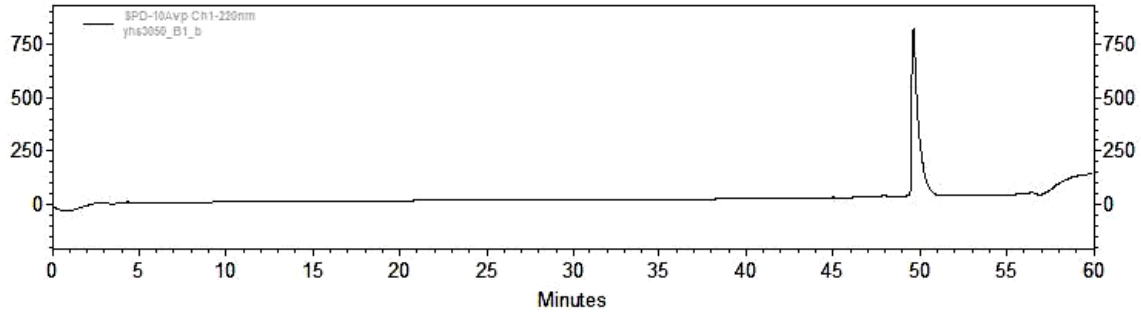

Purity check: 10-70 % MeCN, 35 min

Ac–I W I A (γcyc) L R (Z) I G γ⁴hD F N (Z) K Y–NH_2 **5.11**

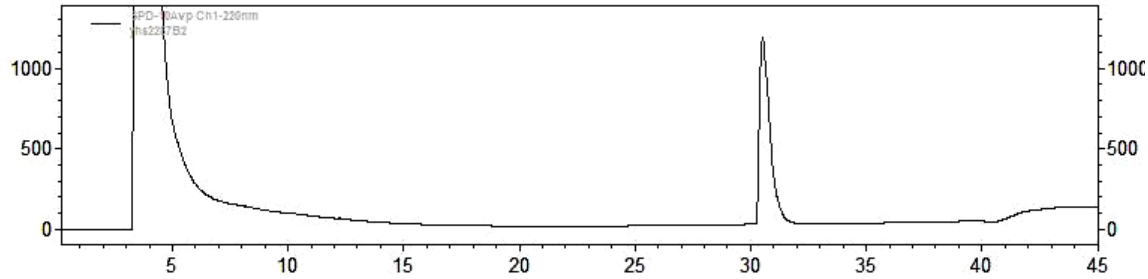

Purity check: 10-70 % MeCN, 35 min

Ac–I (X) I A (γcyc) L R (Z) I G γ⁴hD F N (Z) K Y–NH_2 **5.12**

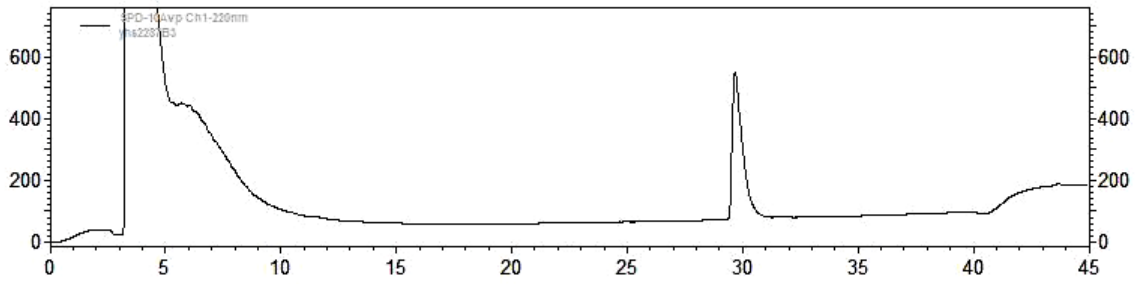

Purity check: 10-70 % MeCN, 35 min

Ac–I (X) I A (γcyc) L R (Z) I G γ⁴hD F N (X) K Y–NH_2 **5.13**

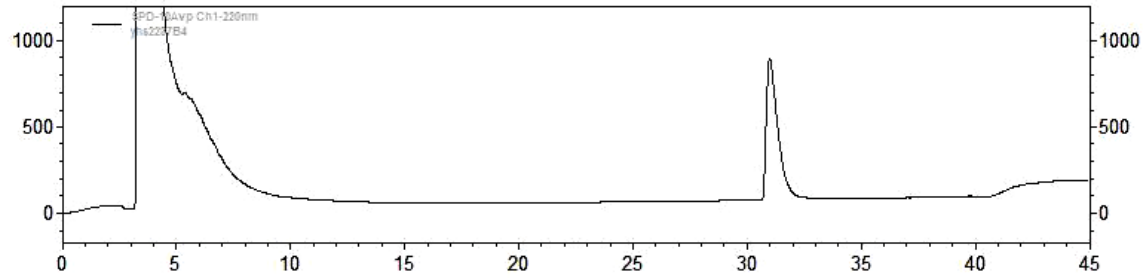

Purity check: 10-90 % MeCN, 60 min

Ac–I (X) I A γ⁴hA L R (Z) I G γ⁴hD F N (X) K Y–NH_2 **5.14**

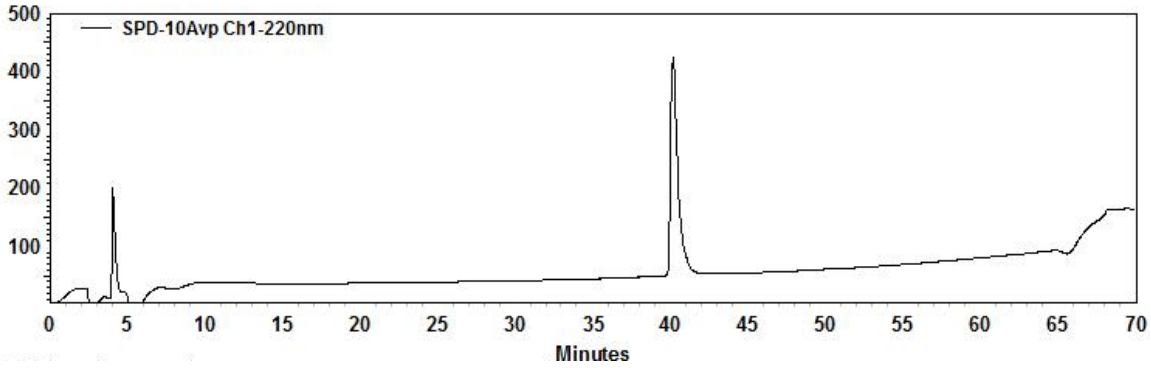

Purity check: 10-90 % MeCN, 60 min

Ac–D M R P E I W I A (γcyc) L R (Z) I G γ⁴hD F N (X) K Y A R R–NH_2 **5.15**

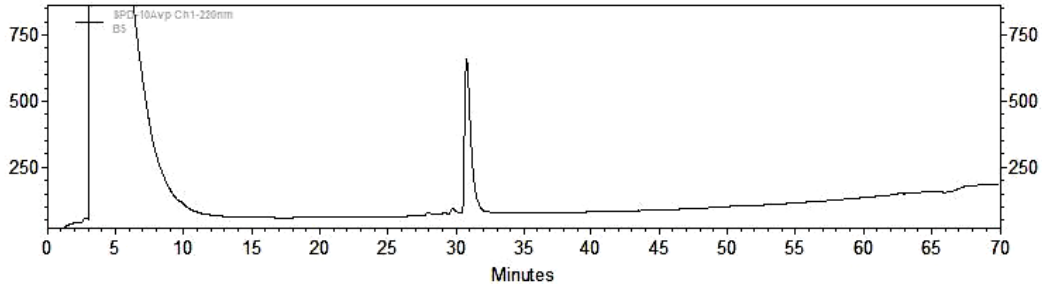

Purity check: 10-60 % MeCN, 50 min

Ac–D M R P E I (X) I A (γcyc) L R (Z) I G γ⁴hD F N (X) Y K A R R–NH_2 **5.16**

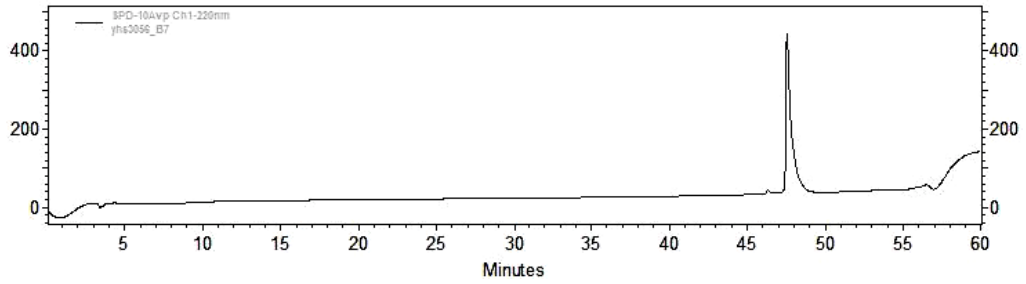

Purity check: 10-60 % MeCN, 50 min

Ac–W I A (γcyc) L R β³hR I G γ⁴hD F N (Z)–NH_2 **5.17**

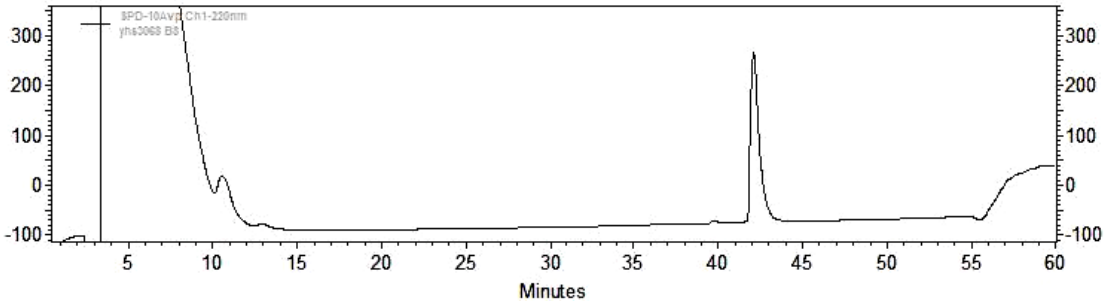

Purity check: 10-80 % MeCN, 70 min

Ac–I (X) I A (γcyc) L R β³hR I G γ⁴hD F N (X) K Y–NH_2 **5.18**

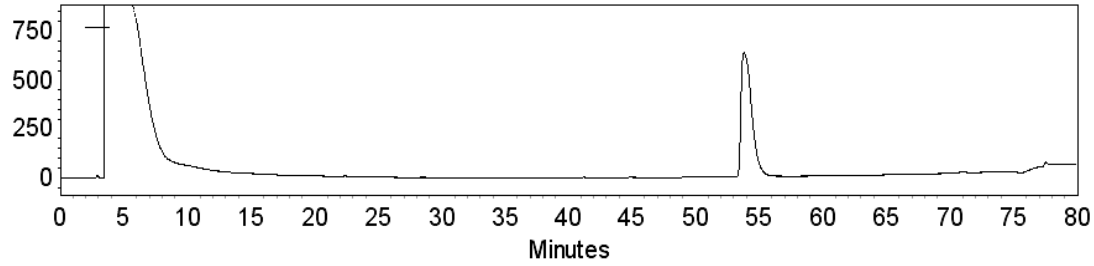

Purity check: 10-80 % MeCN, 70 min

Ac–I W I A(γcyc) L R β³hR I G γ⁴hD F N(X) K Y–NH_2 **5.19**

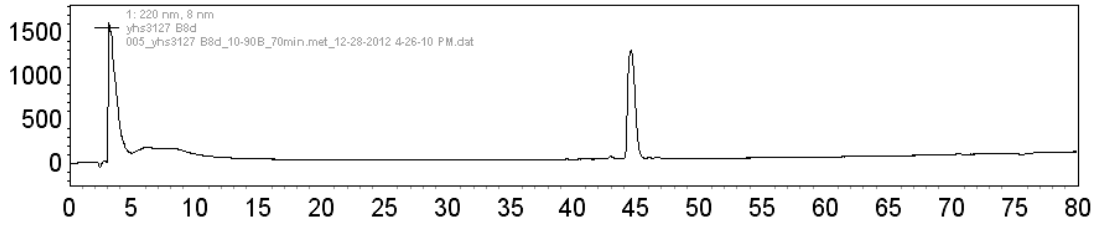

Purity check: 15-75 % MeCN, 60 min

Ac–I (X) I A γ⁴hA L R β³hR I G γ⁴hD F N(X) K Y–NH_2 **5.20**

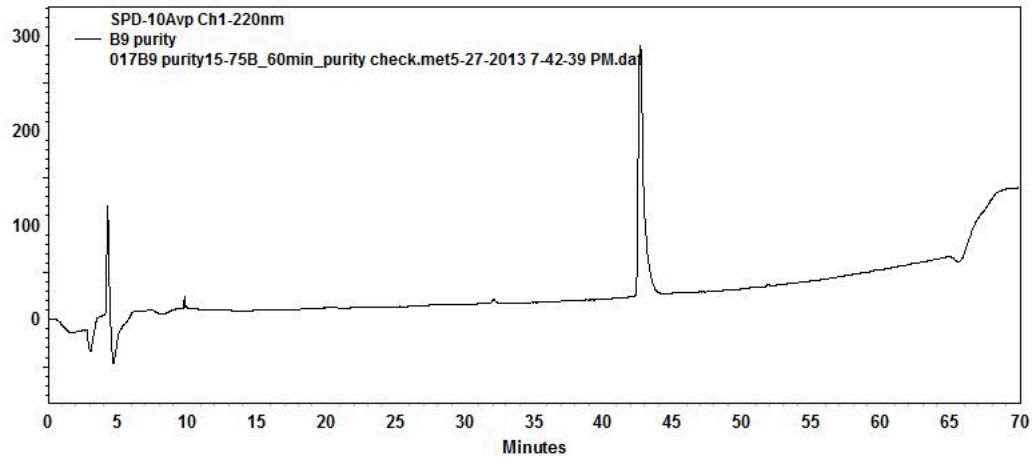

Purity check: 10-80 % MeCN, 70 min

Ac–D M R P E I (X) I A(γcyc) L R β³hR I G γ⁴hD F N(X) K Y A R R–NH_2 **5.21**

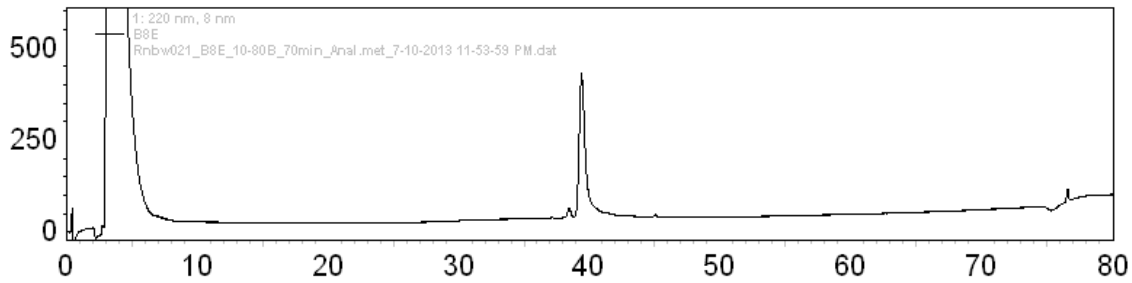

Purity check: 10-80 % MeCN, 70 min

Ac–D M R P E I (X) I A (γcyc) L R β³hR I G γ⁴hD F N (X) K Y γ⁴hA R–NH_2 **5.22**

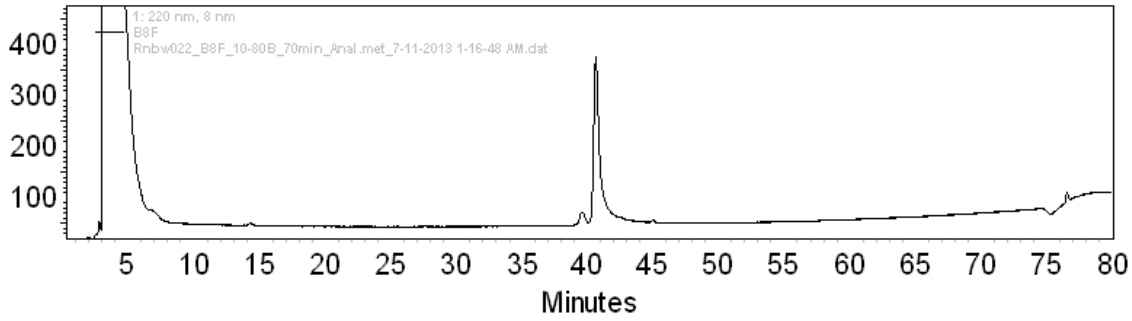

Purity check: 10-80 % MeCN, 70 min

Ac–D M γ⁴hA E I (X) I A (γcyc) L R β³hR I G γ⁴hD F N (X) K Y γ⁴hA R–NH_2 **5.23**

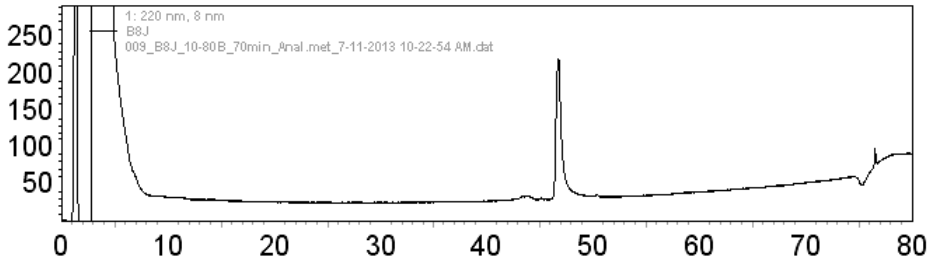

Purity check: 15-75 % MeCN, 60 min

Flu–I W I A (γcyc) L R (Z) I G γ⁴hD F N (X) K Y–NH_2 **Flu-5.11**

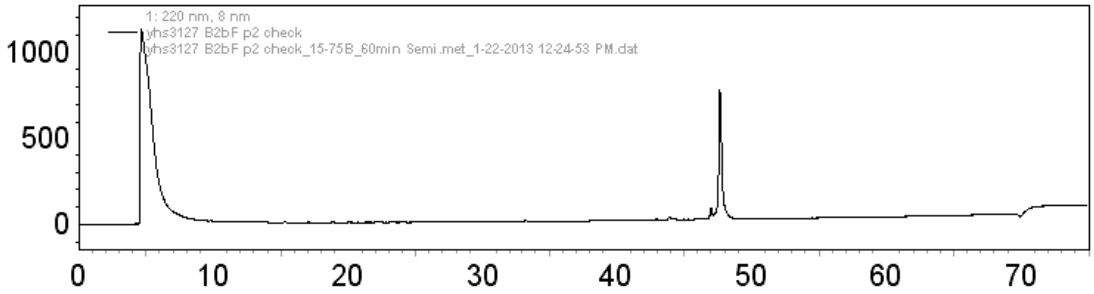

5.4

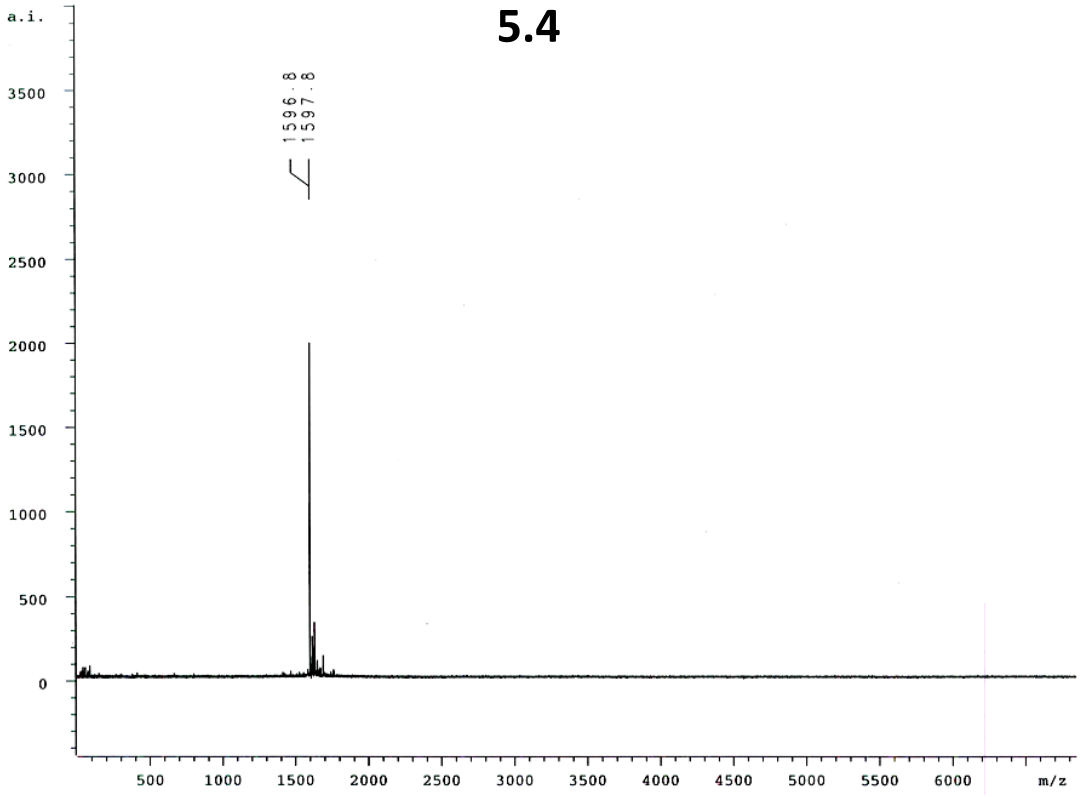
a.i.
1596.8
1597.8
3500
3000
2500
2000
1500
1000
500
0
500
1000
1500
2000
2500
3000
3500
4000
4500
5000
5500
6000
m/z

5.4

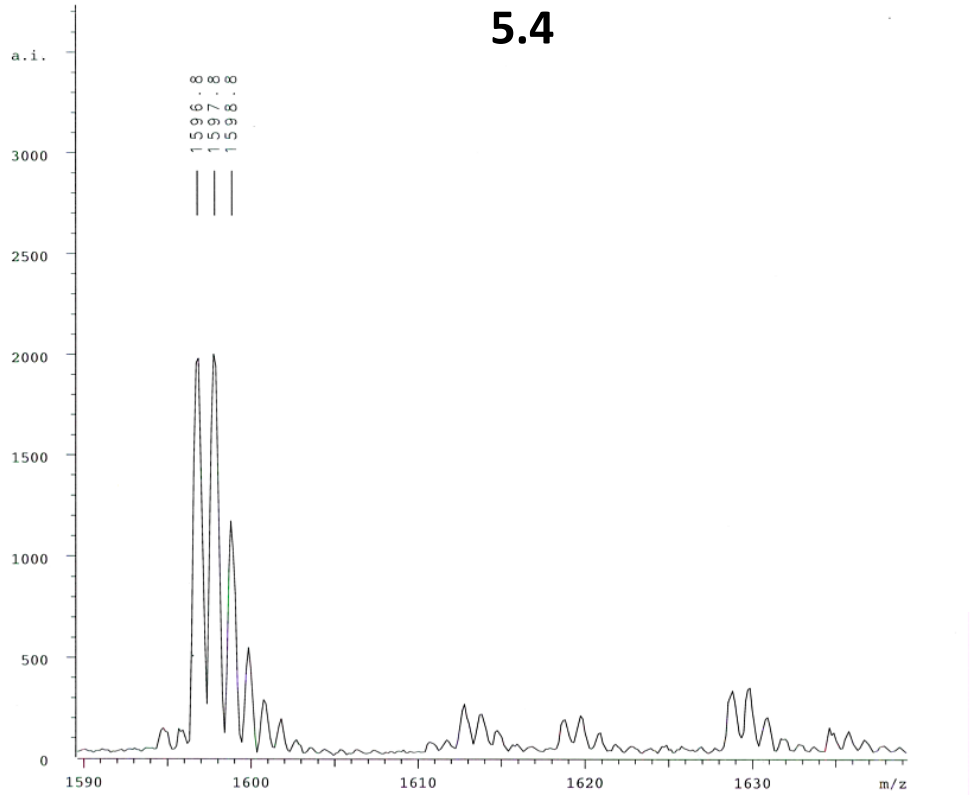
a.i.
1596.8
1597.8
1598.8
3000
2500
2000
1500
1000
500
0
1590
1600
1610
1620
1630
m/z

5.5

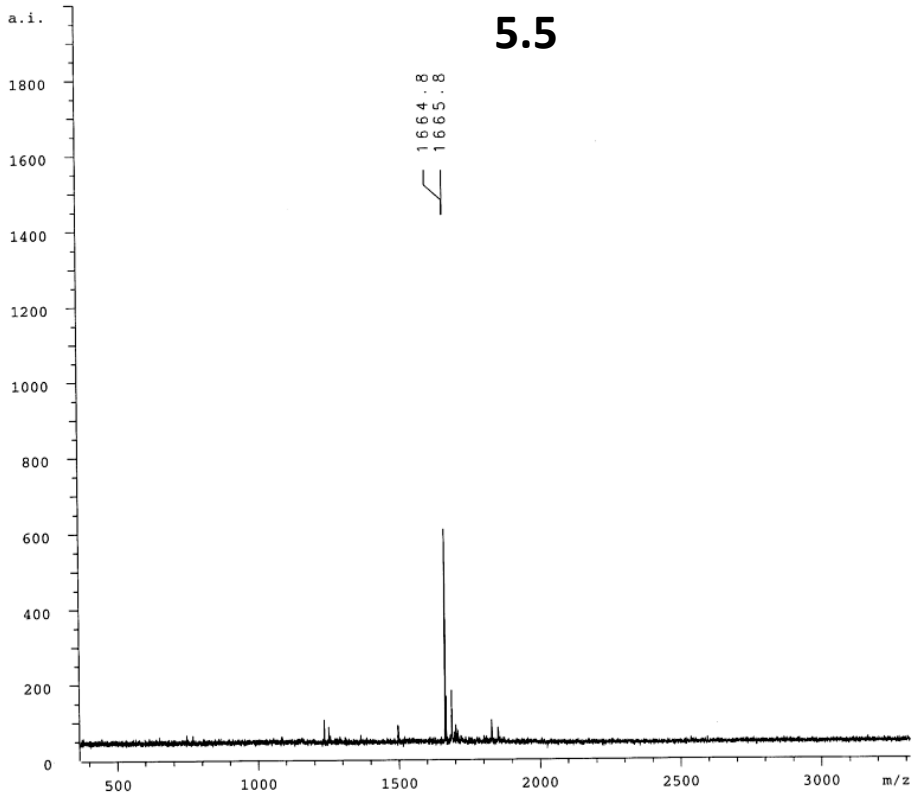
a.i.
1800
1600
1400
1200
1000
800
600
400
200
0
1664.8
1665.8
500
1000
1500
2000
2500
3000
m/z

5.5

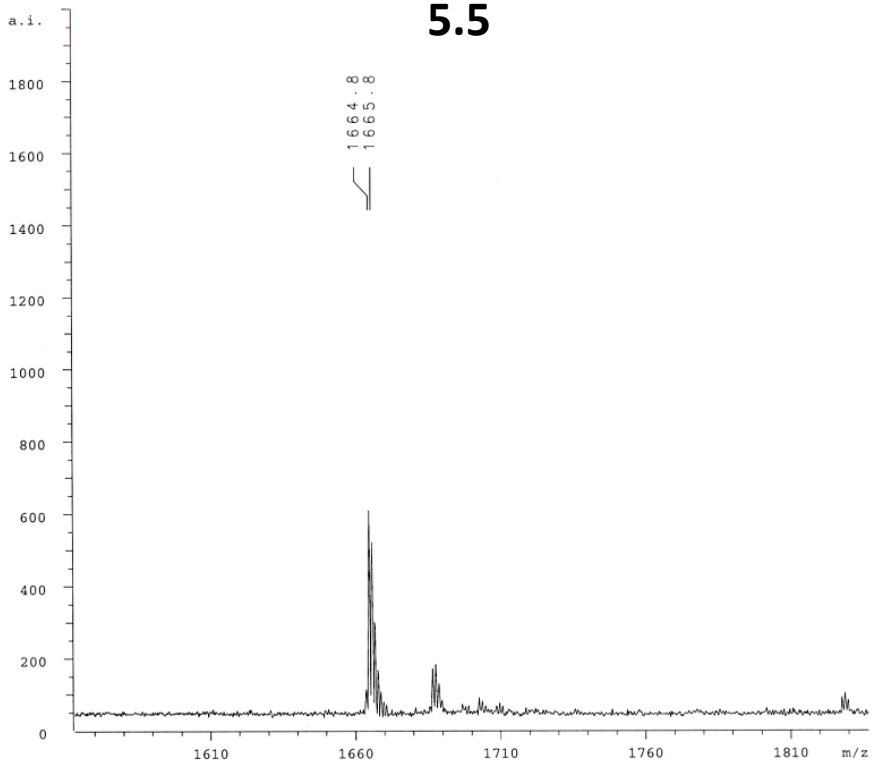
a.i.
1800
1600
1400
1200
1000
800
600
400
200
0
1664.8
1665.8
1610
1660
1710
1760
1810
m/z

5.6

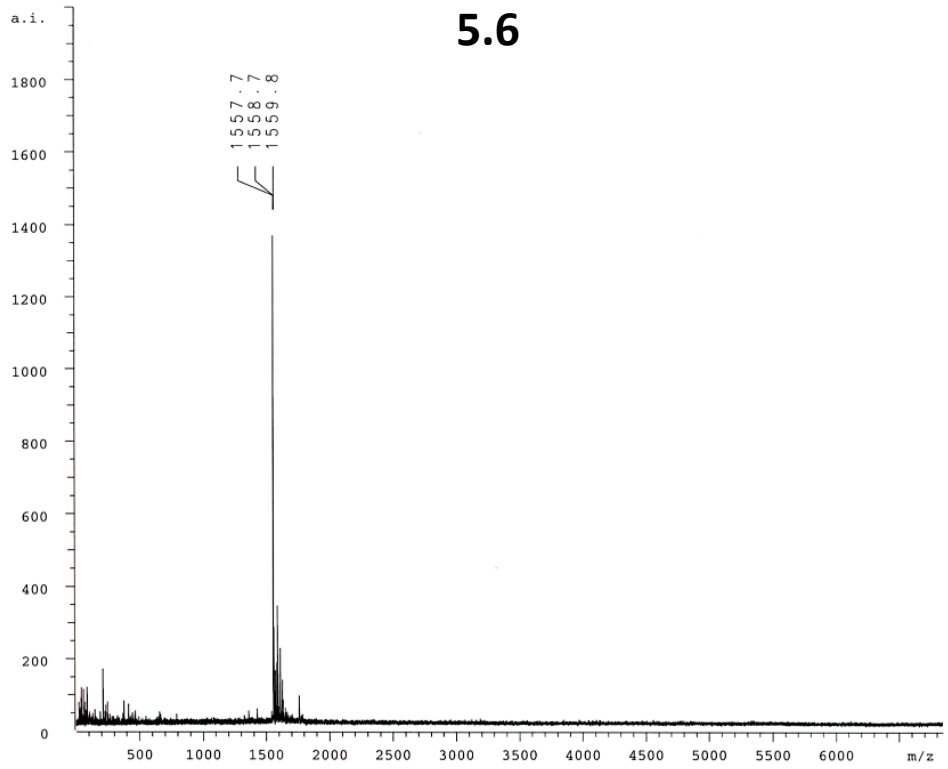
a.i.
1800
1600
1400
1200
1000
800
600
400
200
0
1557.7
1558.7
1559.8
500
1000
1500
2000
2500
3000
3500
4000
4500
5000
5500
6000
m/z

5.6

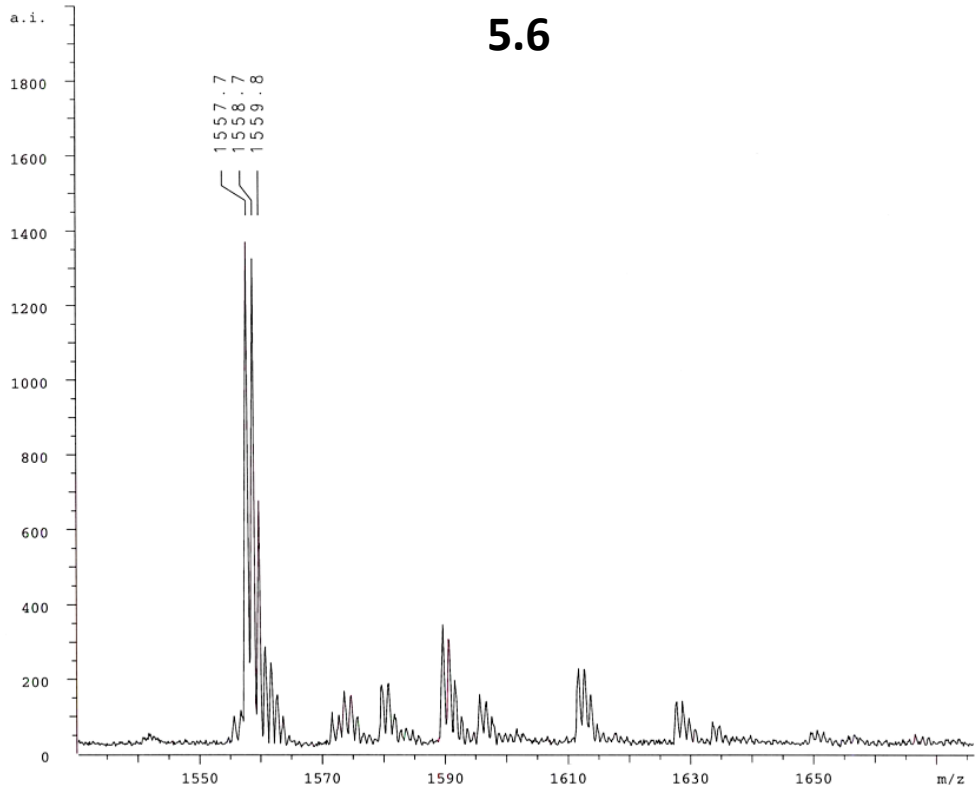
a.i.
1800
1600
1400
1200
1000
800
600
400
200
0
1557.7
1558.7
1559.8
1550
1570
1590
1610
1630
1650
m/z

5.7

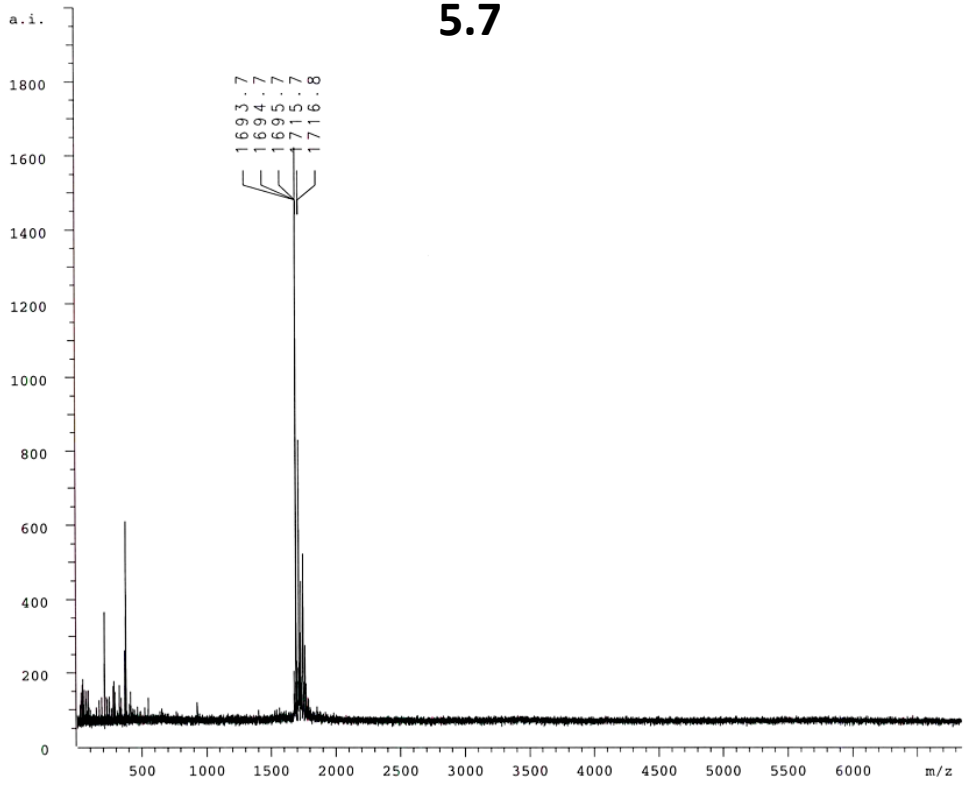
a.i.
1800
1600
1400
1200
1000
800
600
400
200
0
1693.7
1694.7
1695.7
1715.7
1716.8
500
1000
1500
2000
2500
3000
3500
4000
4500
5000
5500
6000
m/z

5.7

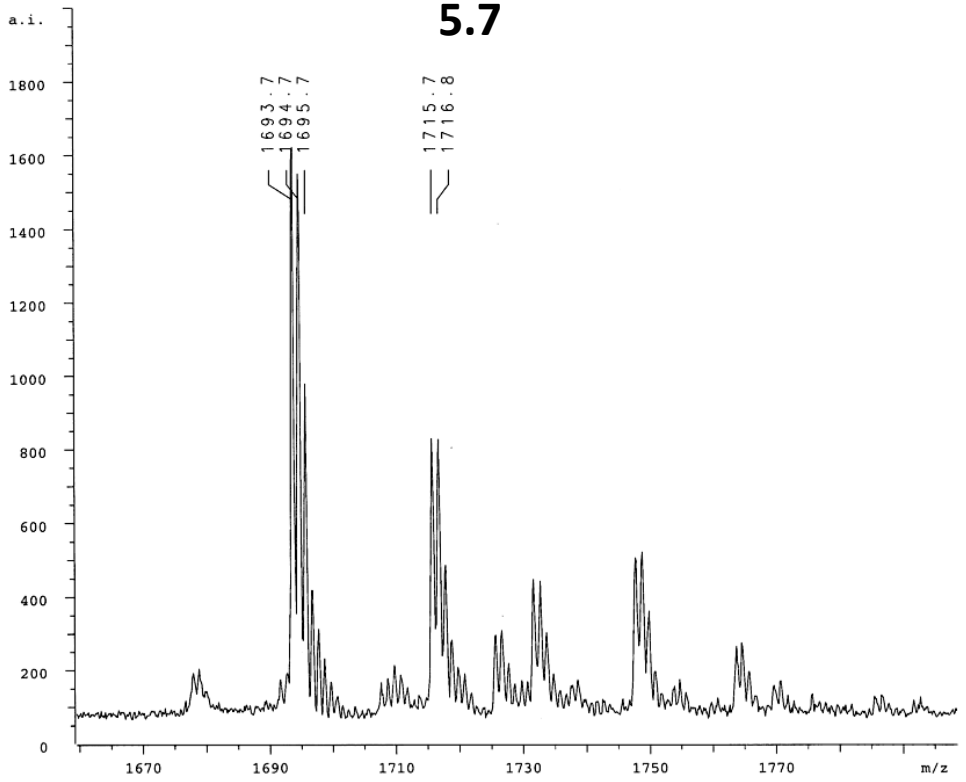
a.i.
1800
1600
1400
1200
1000
800
600
400
200
0
1693.7
1694.7
1695.7
1715.7
1716.8
1670
1690
1710
1730
1750
1770
m/z

5.8

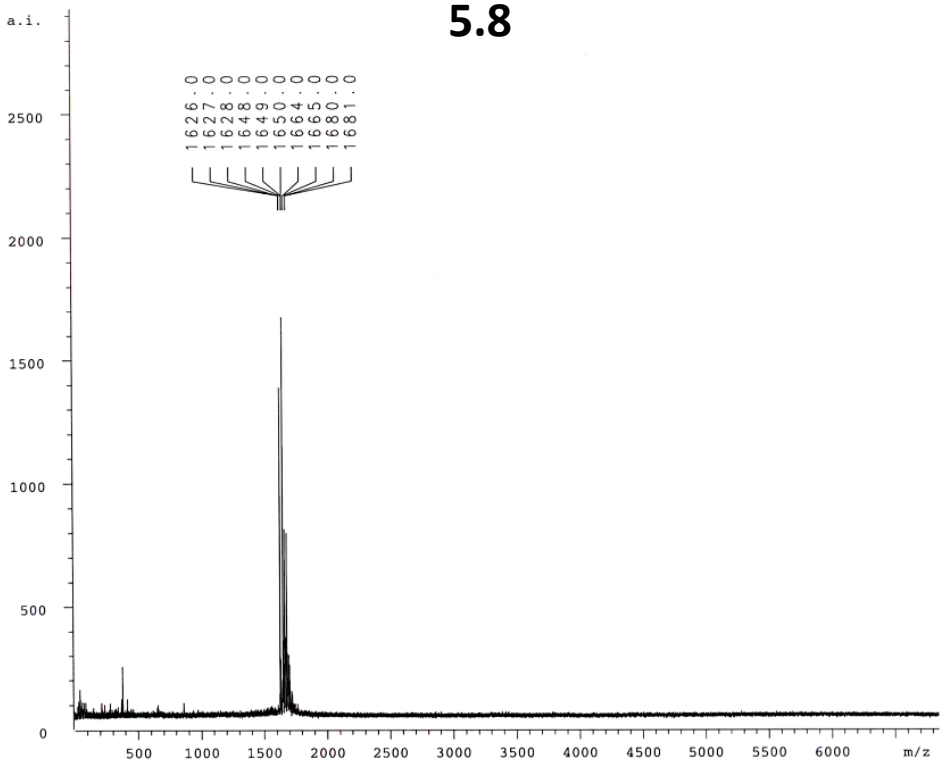
a.i.
1626.0
1627.0
1628.0
1648.0
1649.0
1650.0
1664.0
1665.0
1680.0
1681.0
2500
2000
1500
1000
500
0
500 1000 1500 2000 2500 3000 3500 4000 4500 5000 5500 6000 m/z

5.8

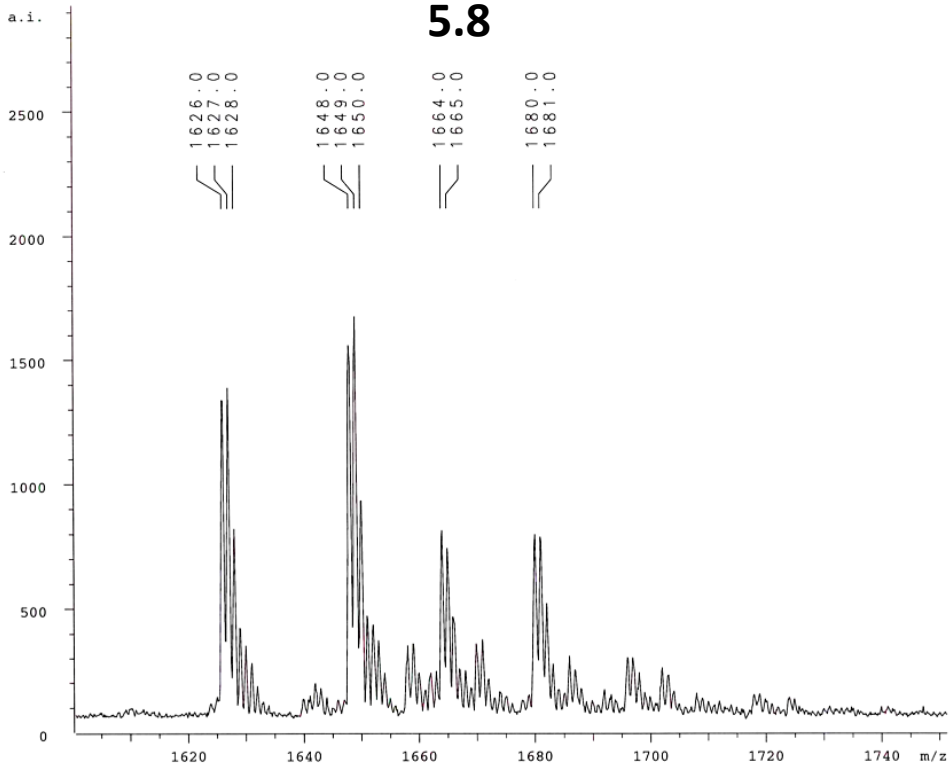
a.i.
1626.0
1627.0
1628.0
1648.0
1649.0
1650.0
1664.0
1665.0
1680.0
1681.0
2500
2000
1500
1000
500
0
1620 1640 1660 1680 1700 1720 1740 m/z

5.9

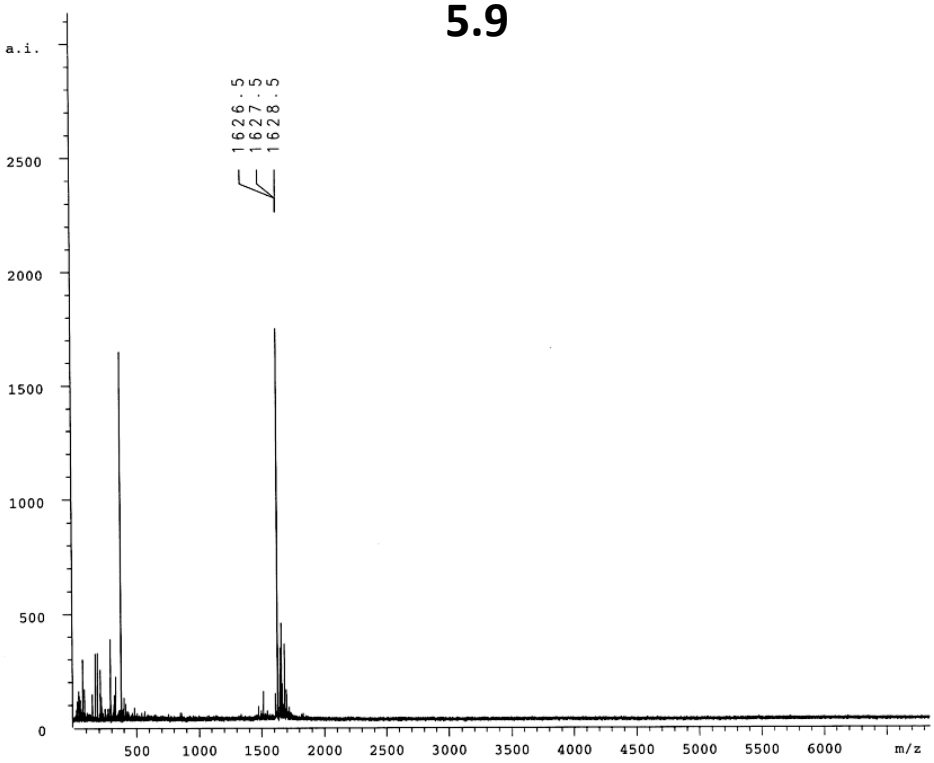
a.i.
1626.5
1627.5
1628.5
2500
2000
1500
1000
500
0
500
1000
1500
2000
2500
3000
3500
4000
4500
5000
5500
6000
m/z

5.9

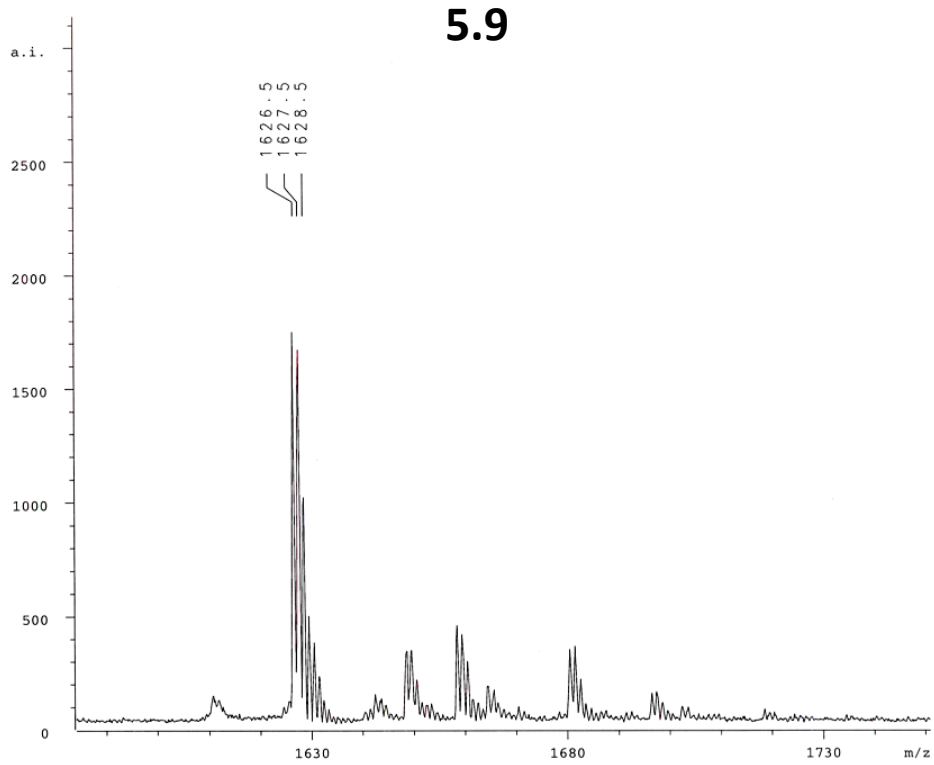
a.i.
1626.5
1627.5
1628.5
2500
2000
1500
1000
500
0
1630
1680
1730
m/z

5.10

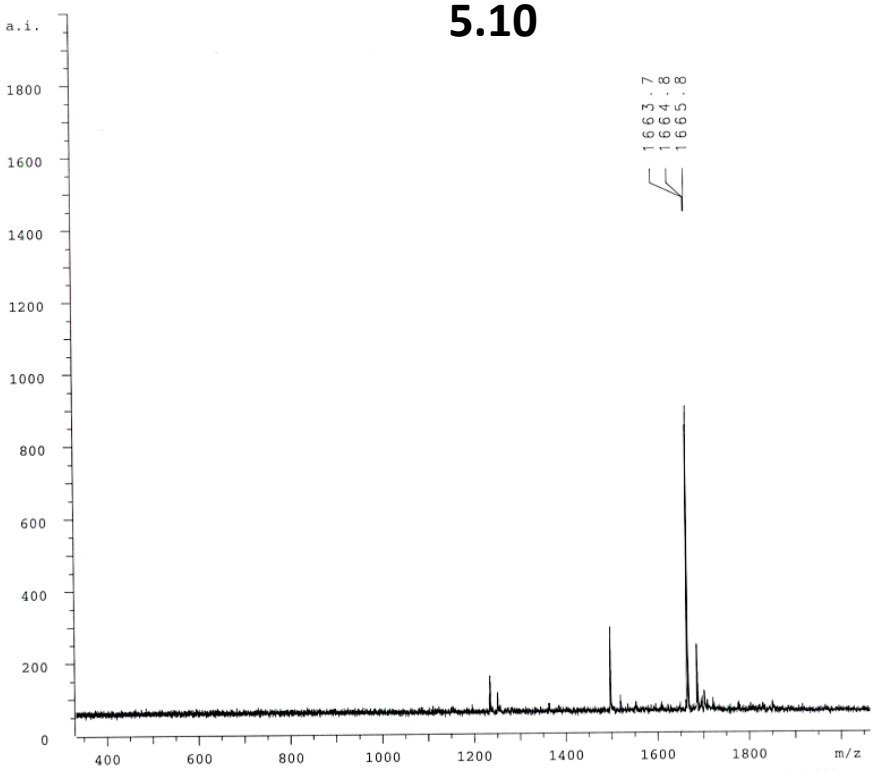
a.i.
1800
1600
1400
1200
1000
800
600
400
200
0
1663.7
1664.8
1665.8
400
600
800
1000
1200
1400
1600
1800
m/z

5.10

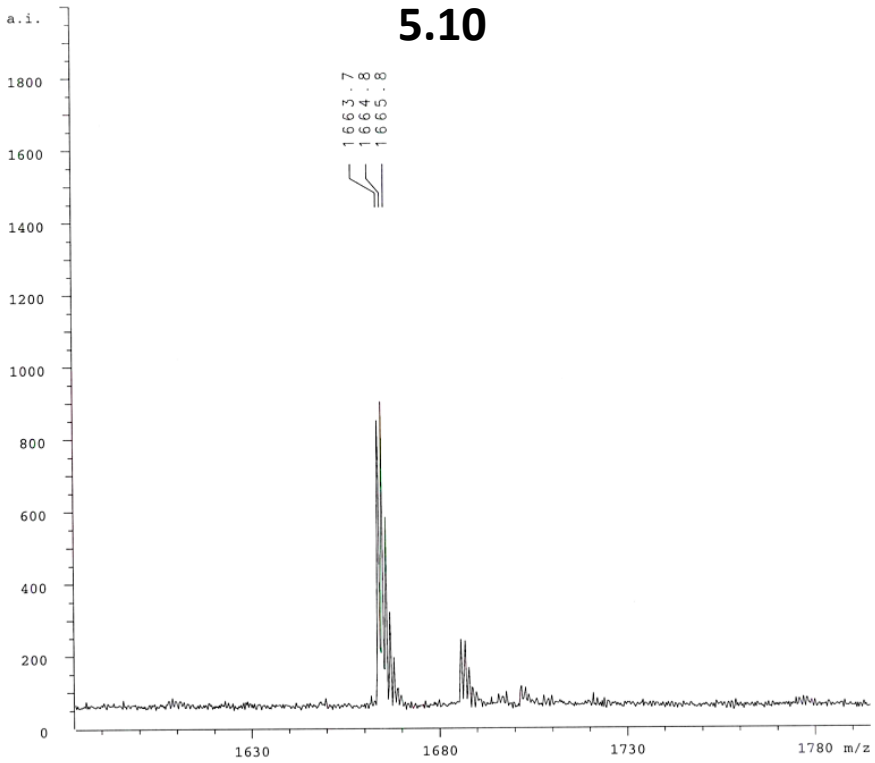
a.i.
1800
1600
1400
1200
1000
800
600
400
200
0
1663.7
1664.8
1665.8
1630
1680
1730
1780 m/z

5.11

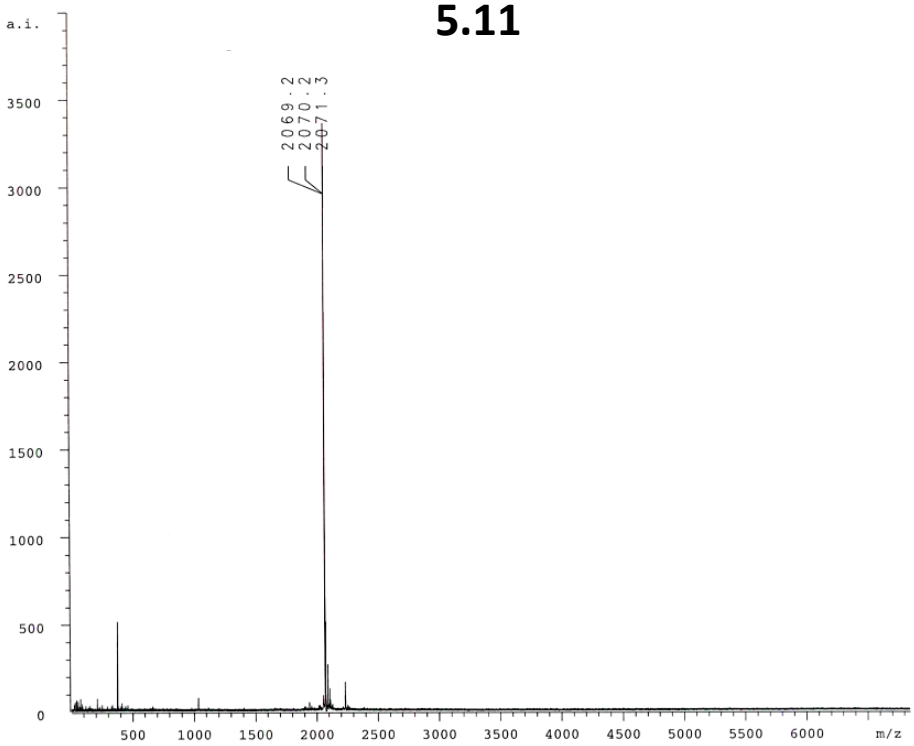
a.i.
3500
3000
2500
2000
1500
1000
500
0
2069.2
2070.2
2071.3
500
1000
1500
2000
2500
3000
3500
4000
4500
5000
5500
6000
m/z

5.11

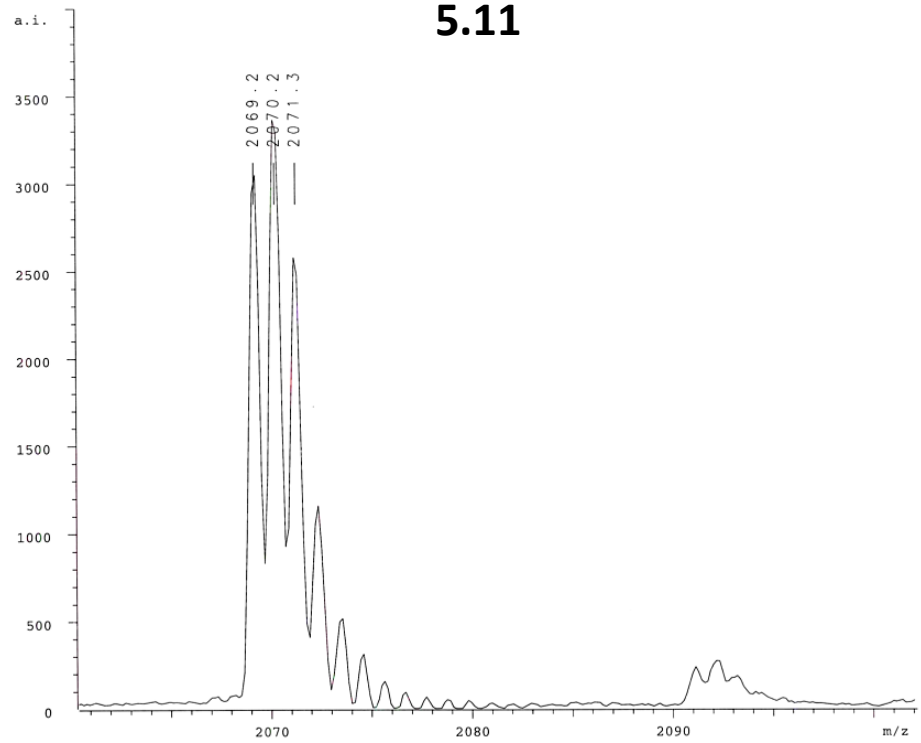
a.i.
3500
3000
2500
2000
1500
1000
500
0
2069.2
2070.2
2071.3
2070
2080
2090
m/z

5.12

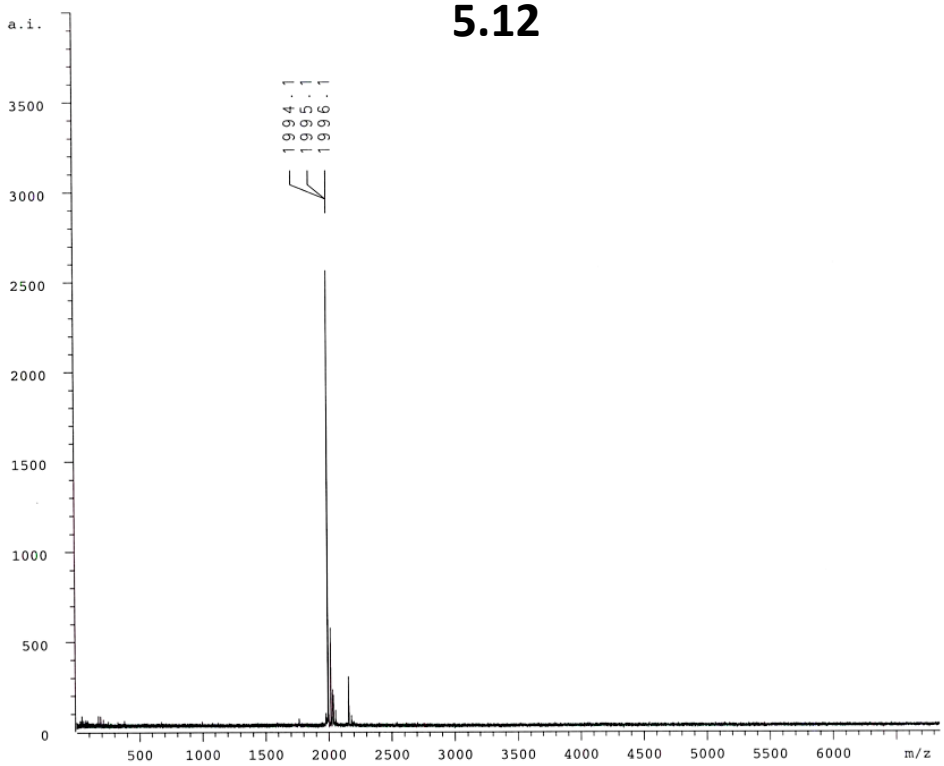
a.i.
1994.1
1995.1
1996.1
3500
3000
2500
2000
1500
1000
500
0
500
1000
1500
2000
2500
3000
3500
4000
4500
5000
5500
6000
m/z

5.12

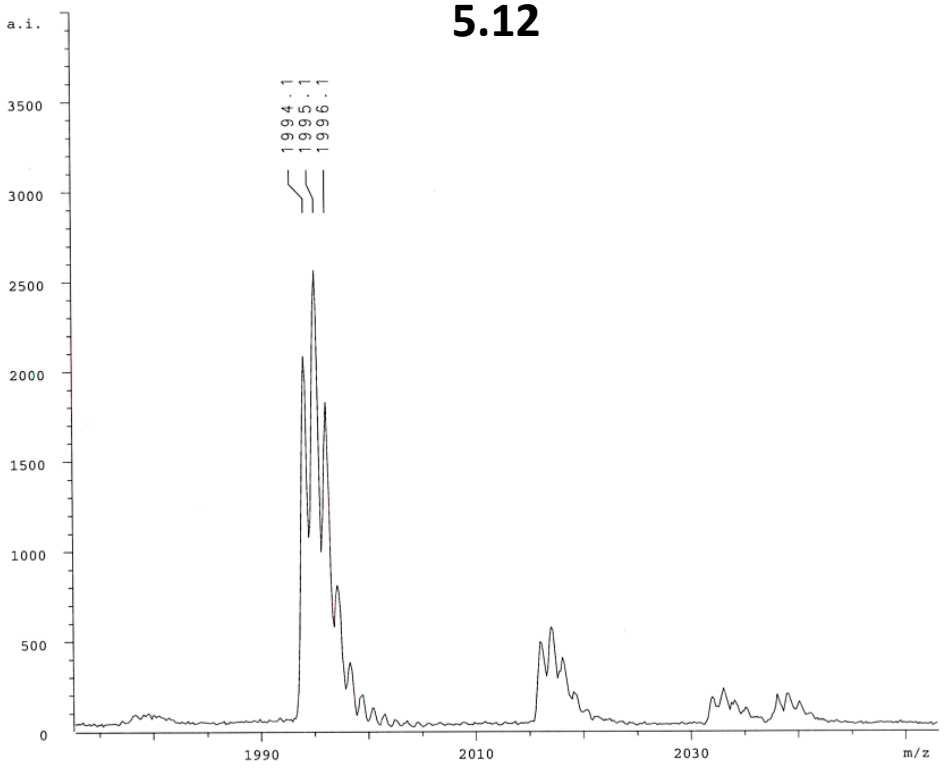
a.i.
1994.1
1995.1
1996.1
3500
3000
2500
2000
1500
1000
500
0
1990
2010
2030
m/z

5.13

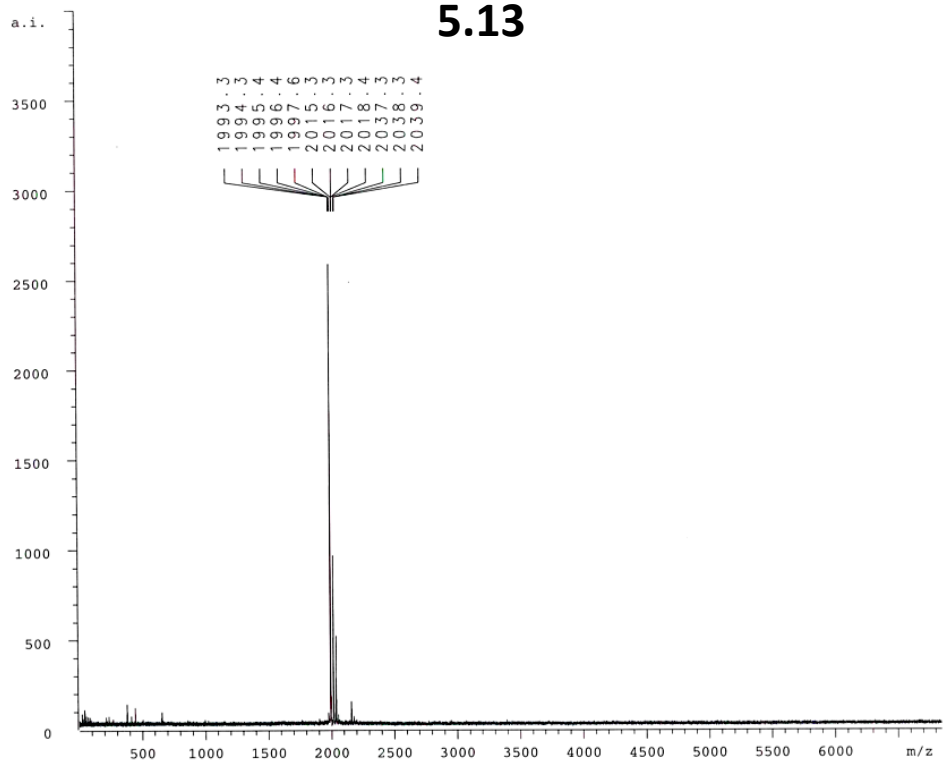
a.i.
1993.3
1994.3
1995.4
1996.4
1997.6
2015.3
2016.3
2017.3
2018.4
2037.3
2038.3
2039.4
3500
3000
2500
2000
1500
1000
500
0
500
1000
1500
2000
2500
3000
3500
4000
4500
5000
5500
6000
m/z

5.13

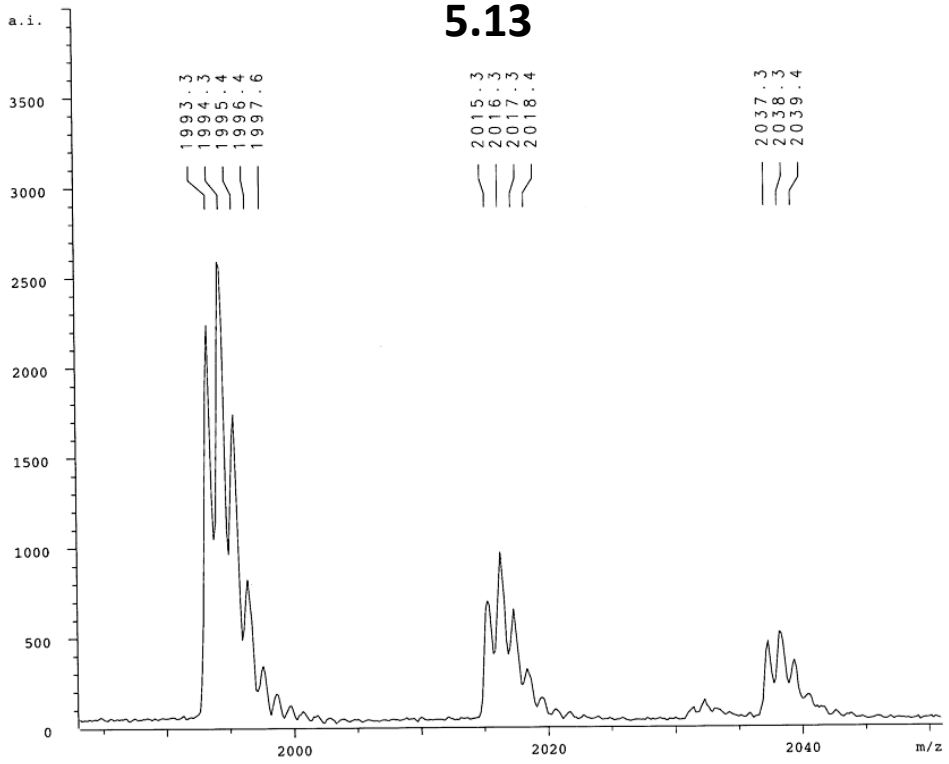
a.i.
1993.3
1994.3
1995.4
1996.4
1997.6
2015.3
2016.3
2017.3
2018.4
2037.3
2038.3
2039.4
3500
3000
2500
2000
1500
1000
500
0
2000
2020
2040
m/z

5.14

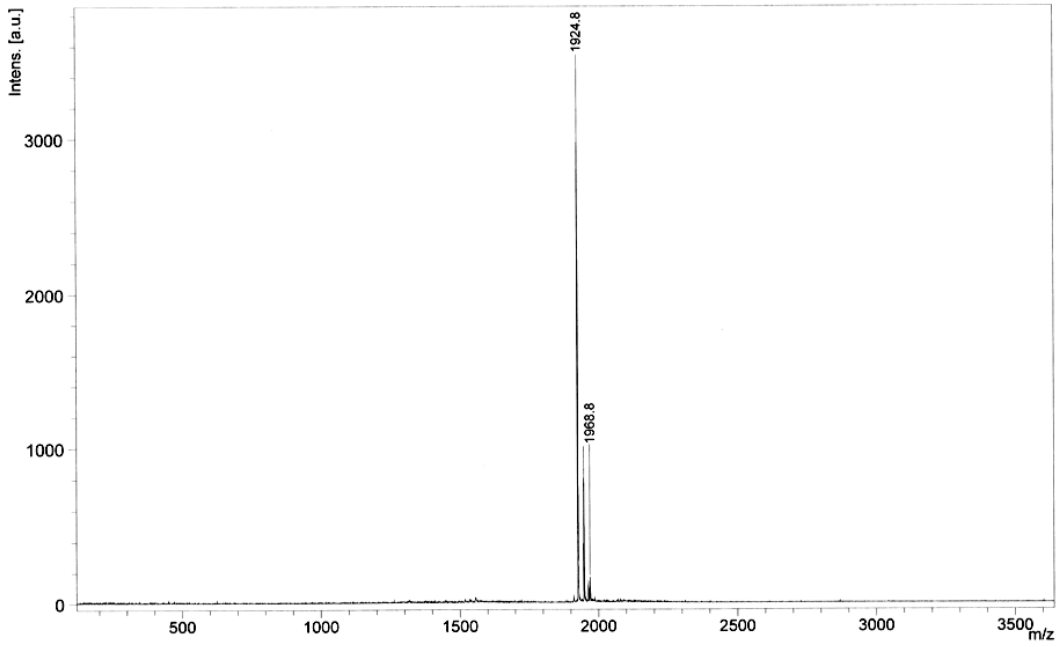
Intens. [a.u.]
3000
2000
1000
0
1924.8
1968.8
500
1000
1500
2000
2500
3000
3500
m/z

5.14

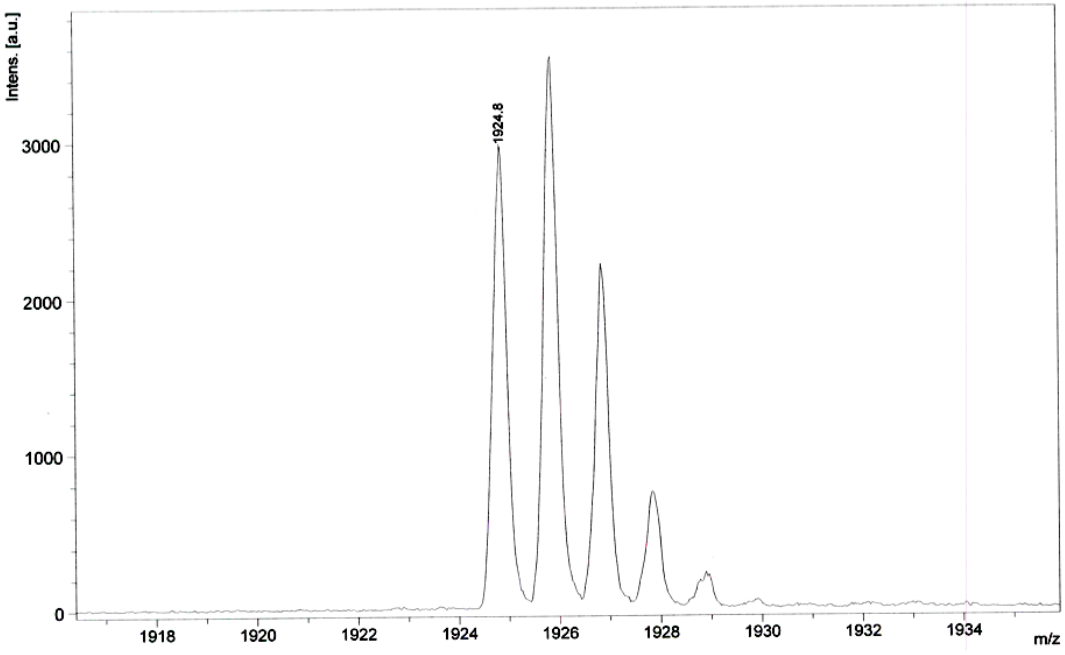
Intens. [a.u.]
3000
2000
1000
0
1924.8
1918
1920
1922
1924
1926
1928
1930
1932
1934
m/z

5.15

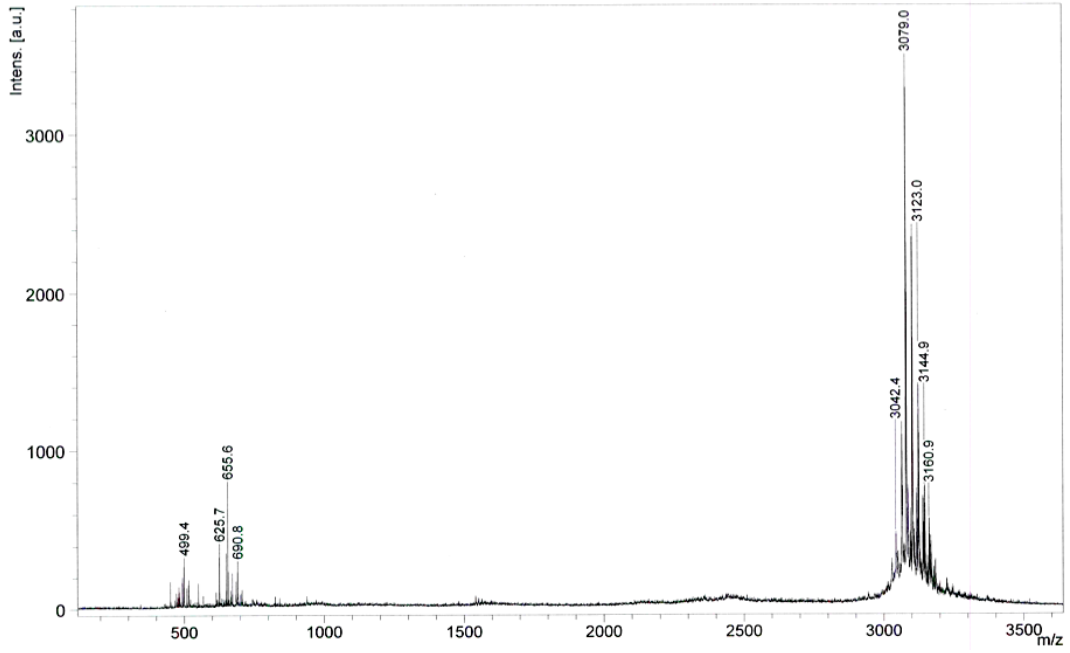
Intens. [a.u.]
3000
2000
1000
0
500
1000
1500
2000
2500
3000
3500
m/z
3079.0
3123.0
3144.9
3042.4
3160.9
655.6
625.7
690.8
499.4

5.15

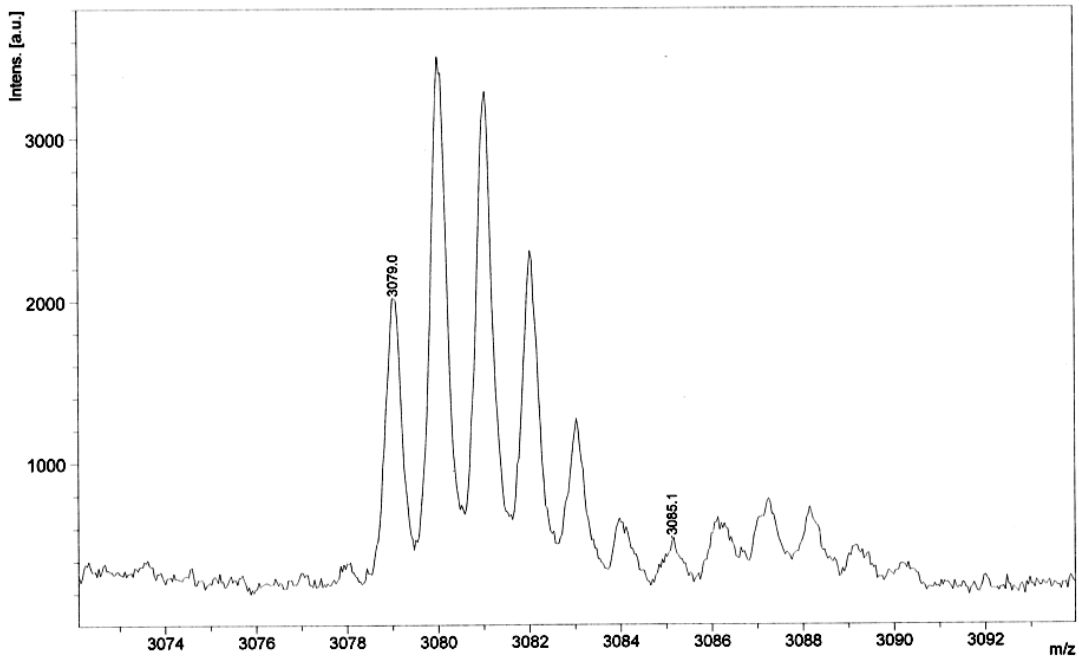
Intens. [a.u.]
3000
2000
1000
3074
3076
3078
3080
3082
3084
3086
3088
3090
3092
m/z
3079.0
3085.1

5.16

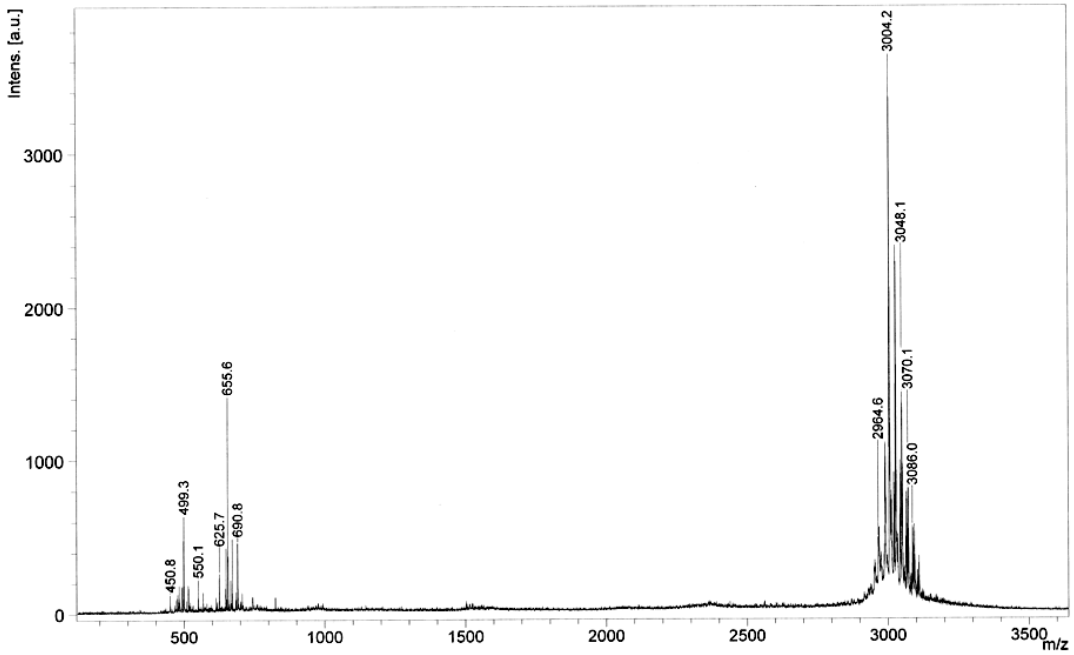
Intens. [a.u.]
3000
2000
1000
0
500
1000
1500
2000
2500
3000
3500
m/z
3004.2
3048.1
3070.1
3086.0
2964.6
655.6
499.3
625.7
690.8
450.8
550.1

5.16

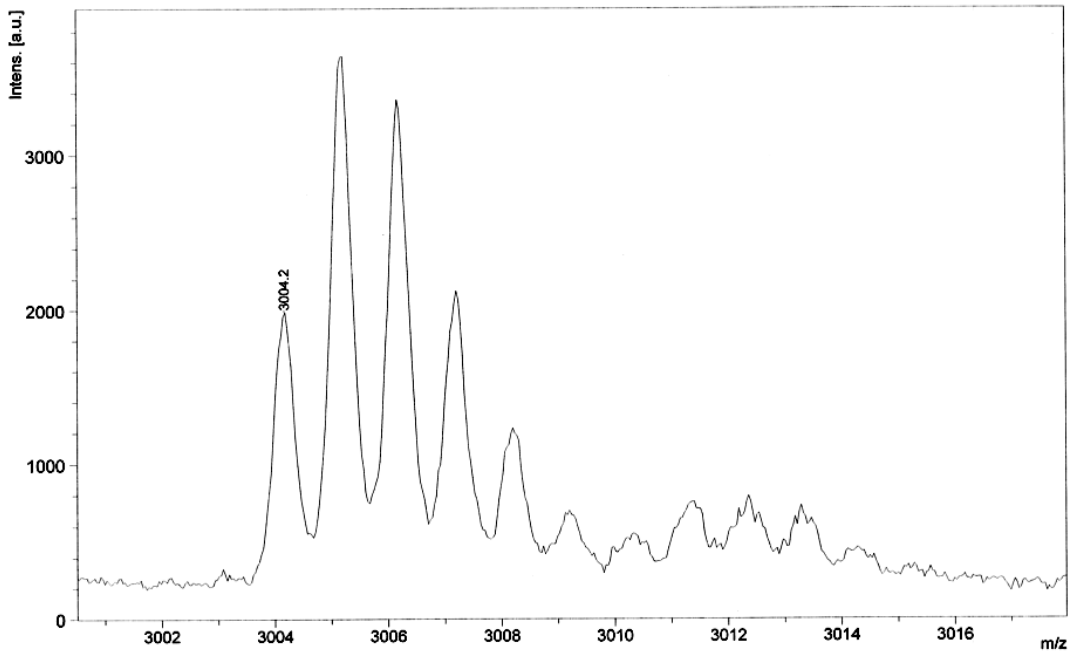
Intens. [a.u.]
3000
2000
1000
0
3002
3004
3006
3008
3010
3012
3014
3016
m/z
3004.2

5.17

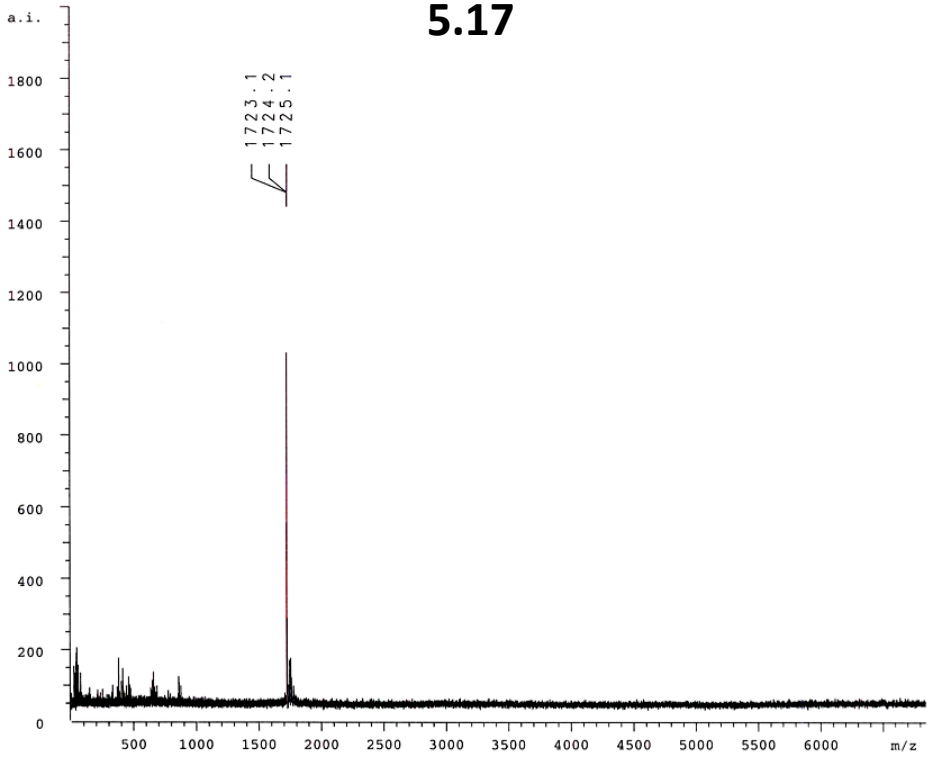
a.i.
1723.1
1724.2
1725.1
1800
1600
1400
1200
1000
800
600
400
200
0
500
1000
1500
2000
2500
3000
3500
4000
4500
5000
5500
6000
m/z

5.17

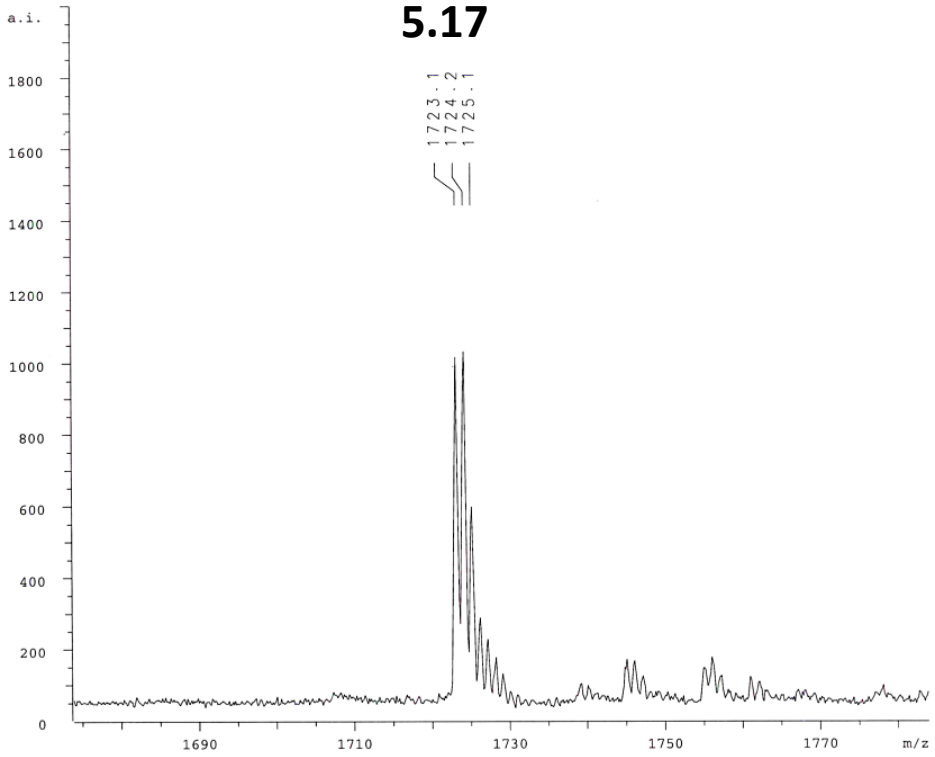
a.i.
1723.1
1724.2
1725.1
1800
1600
1400
1200
1000
800
600
400
200
0
1690
1710
1730
1750
1770
m/z

5.18

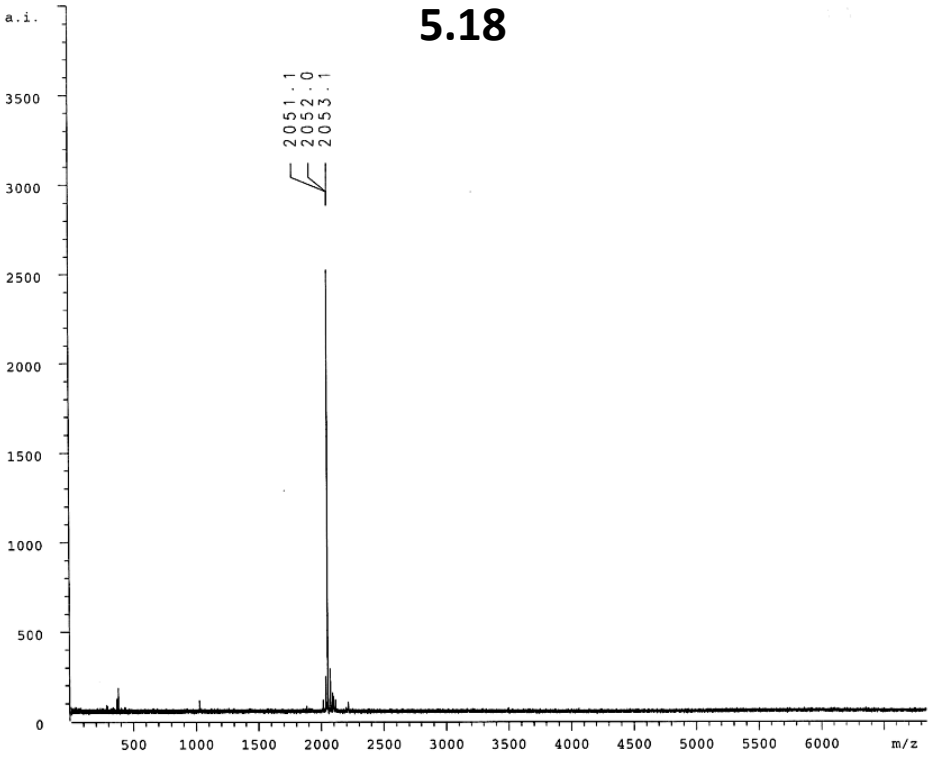
a.i.
2051.1
2052.0
2053.1
3500
3000
2500
2000
1500
1000
500
0
500
1000
1500
2000
2500
3000
3500
4000
4500
5000
5500
6000
m/z

5.18

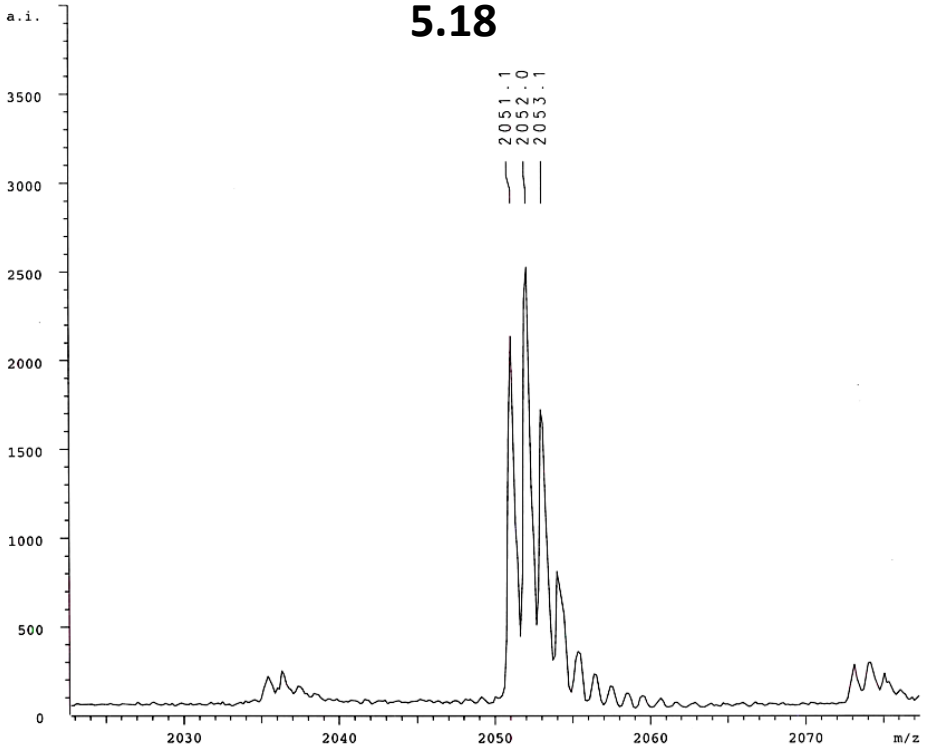
a.i.
2051.1
2052.0
2053.1
3500
3000
2500
2000
1500
1000
500
0
2030
2040
2050
2060
2070
m/z

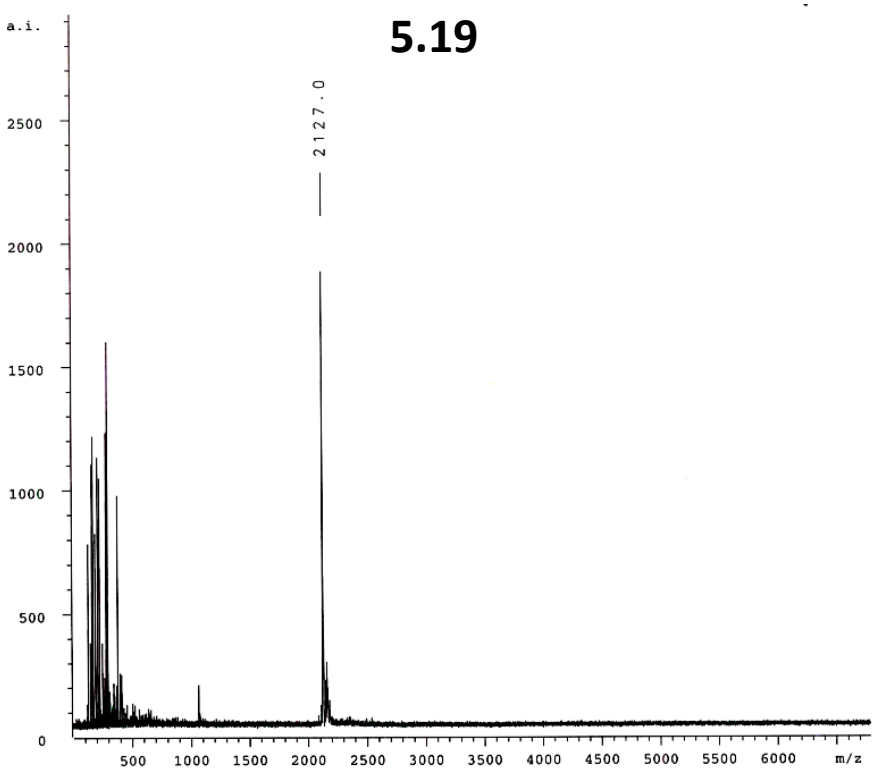
5.19
a.i.
2127.0
2500
2000
1500
1000
500
0
500 1000 1500 2000 2500 3000 3500 4000 4500 5000 5500 6000 m/z

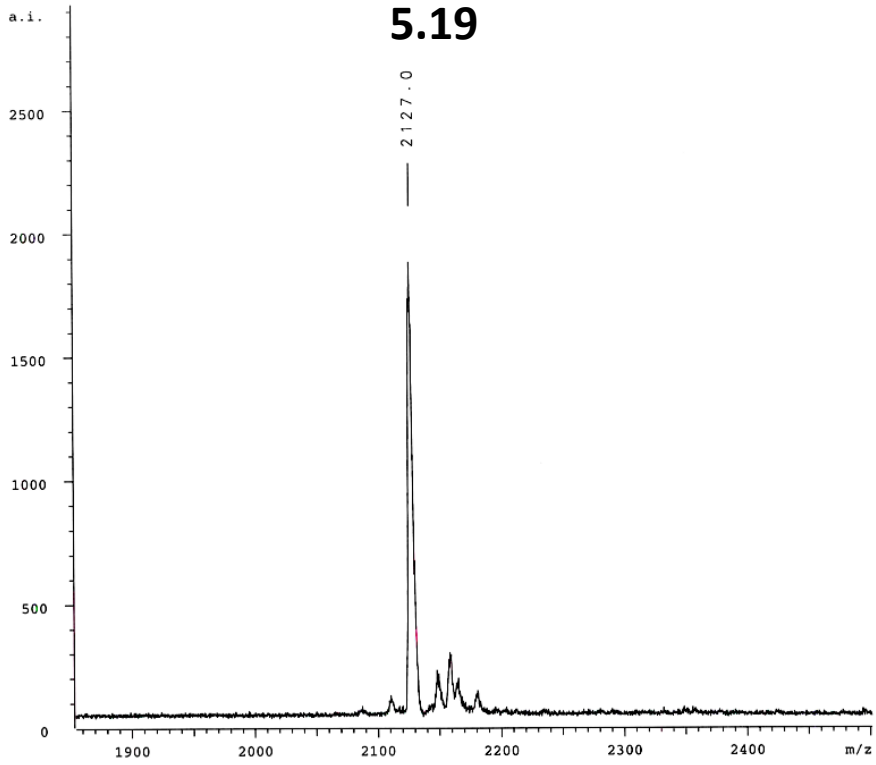
5.19
a.i.
2127.0
2500
2000
1500
1000
500
0
1900 2000 2100 2200 2300 2400 m/z

5.20

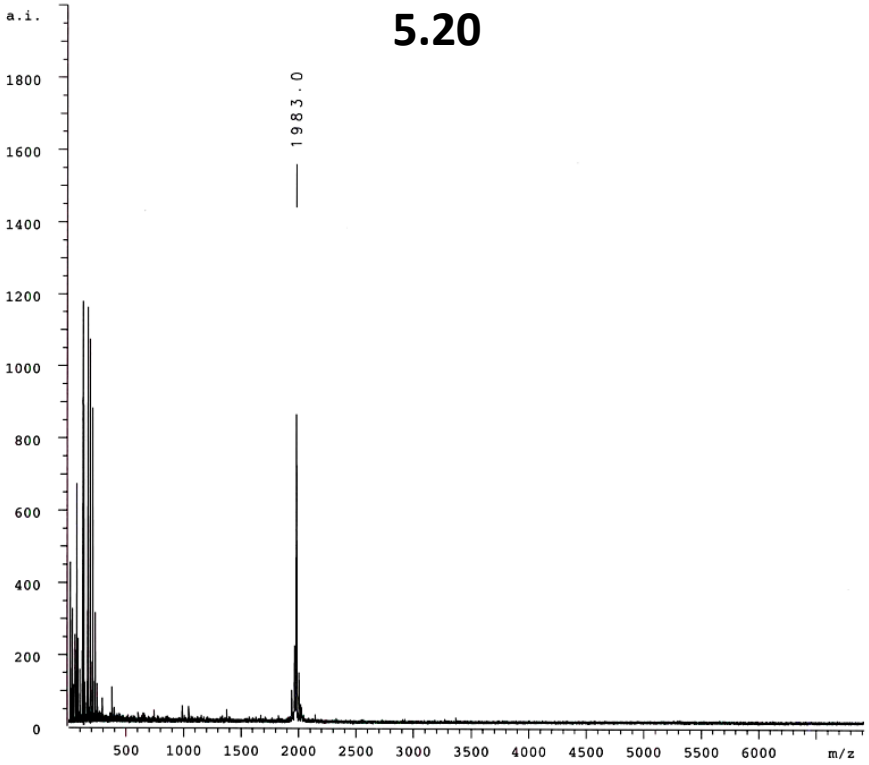

5.20

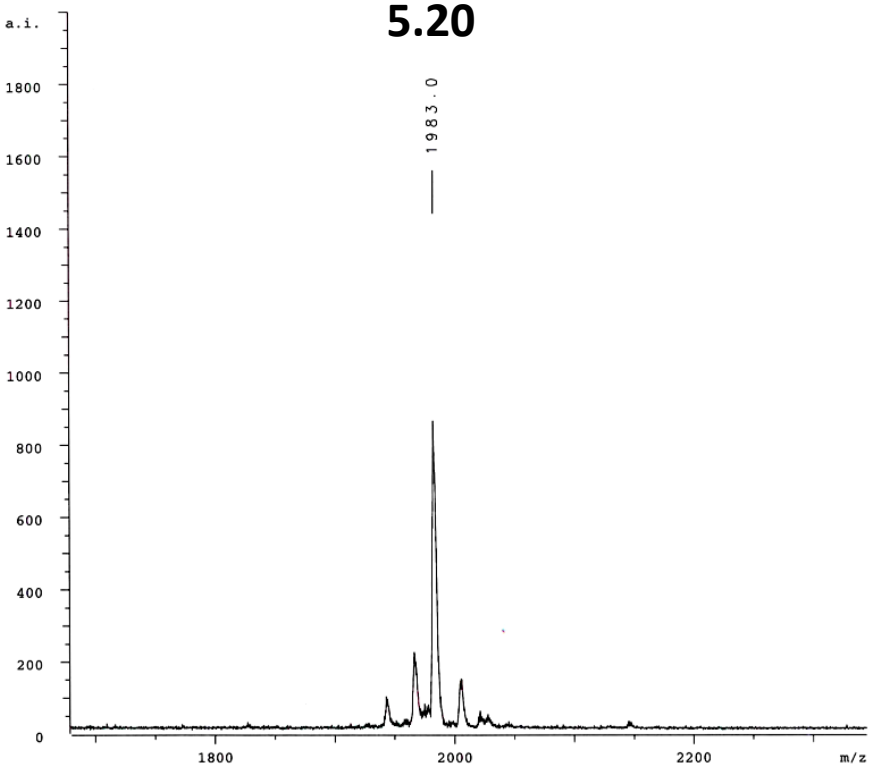

5.21

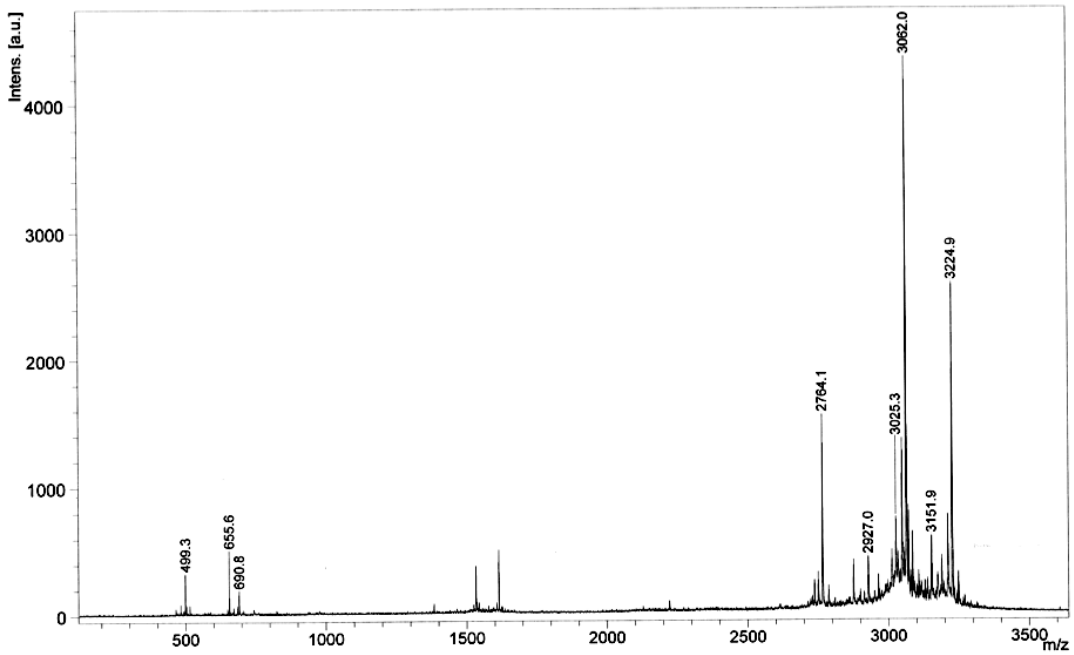
Intens. [a.u.]
4000
3000
2000
1000
0
499.3
655.6
690.8
2764.1
2927.0
3025.3
3062.0
3151.9
3224.9
500
1000
1500
2000
2500
3000
3500
m/z

5.21

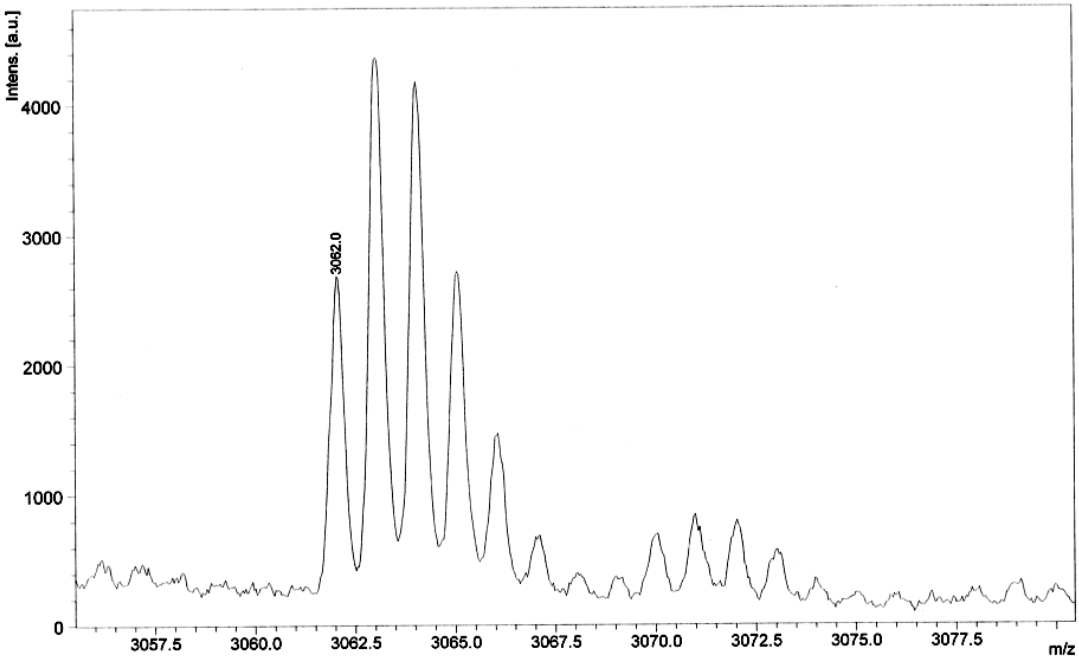
Intens. [a.u.]
4000
3000
2000
1000
0
3062.0
3057.5
3060.0
3062.5
3065.0
3067.5
3070.0
3072.5
3075.0
3077.5
m/z

5.22

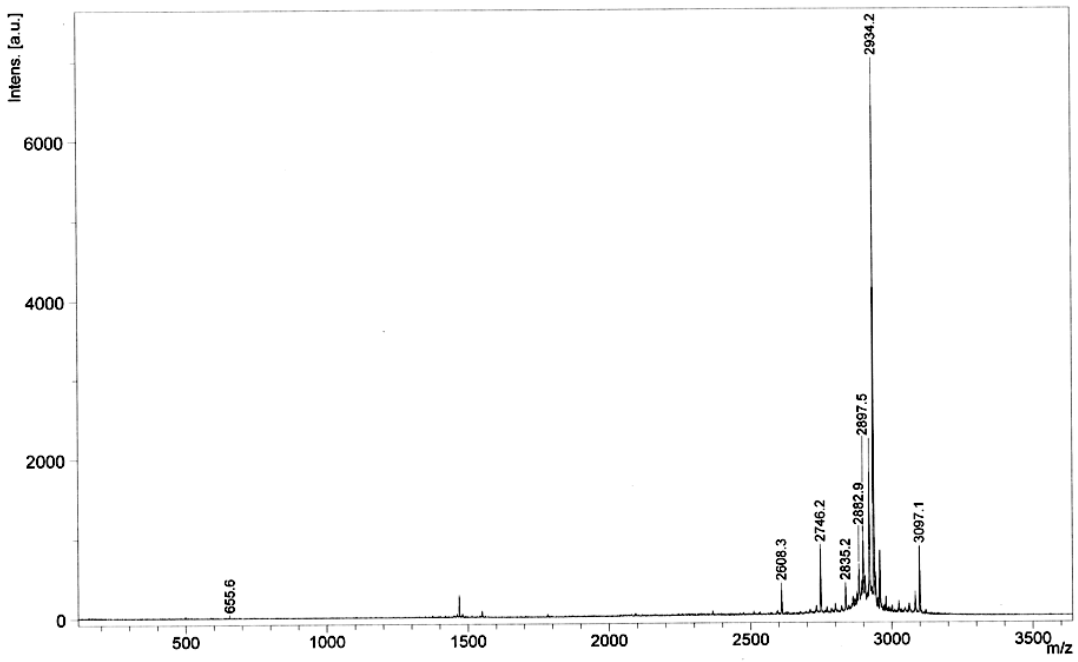
Intens. [a.u.]
6000
4000
2000
0
655.6
2608.3
2746.2
2835.2
2882.9
2897.5
2934.2
3097.1
500
1000
1500
2000
2500
3000
3500
m/z

5.22

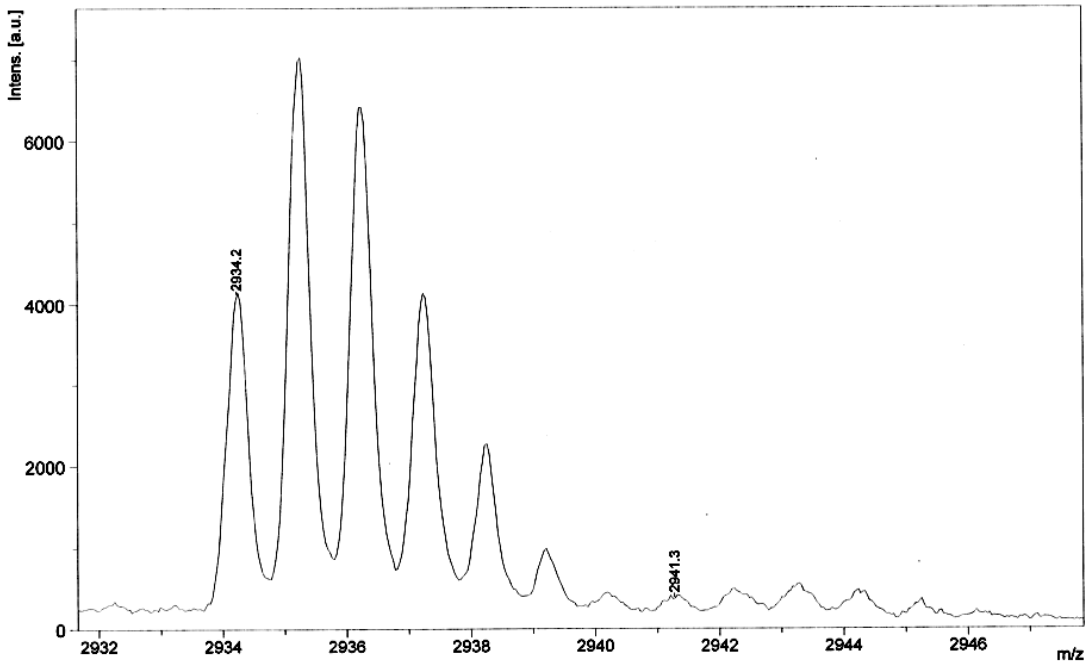
Intens. [a.u.]
6000
4000
2000
0
2934.2
2941.3
2932
2934
2936
2938
2940
2942
2944
2946
m/z

5.23

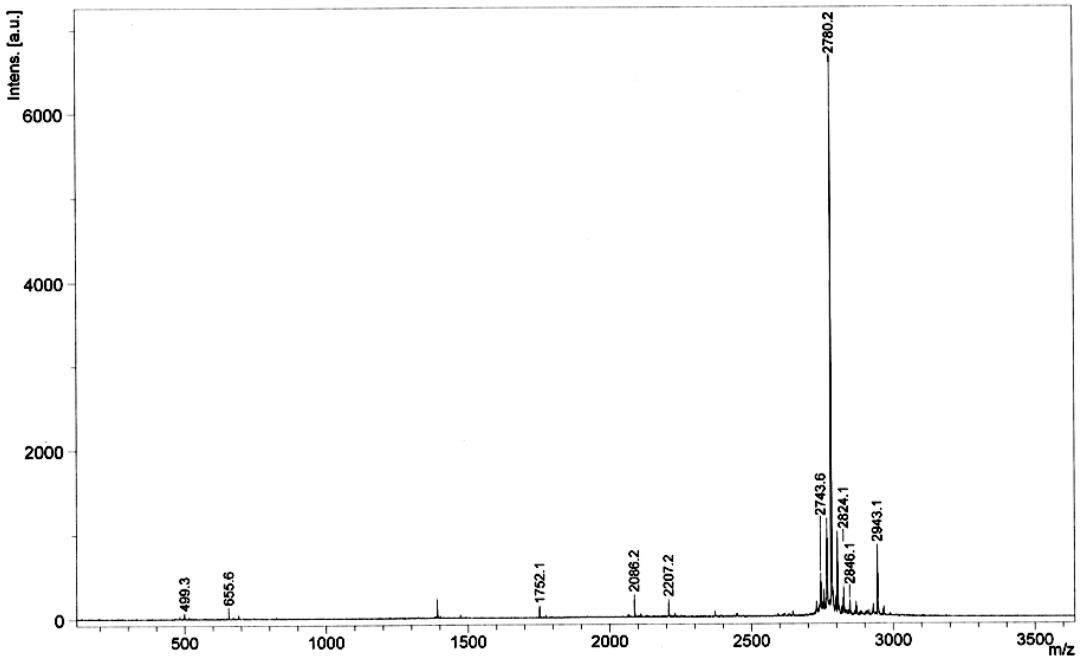
Intens. [a.u.]
6000
4000
2000
0
500
1000
1500
2000
2500
3000
3500
m/z
499.3
655.6
1752.1
2086.2
2207.2
2743.6
2780.2
2824.1
2846.1
2943.1

5.23

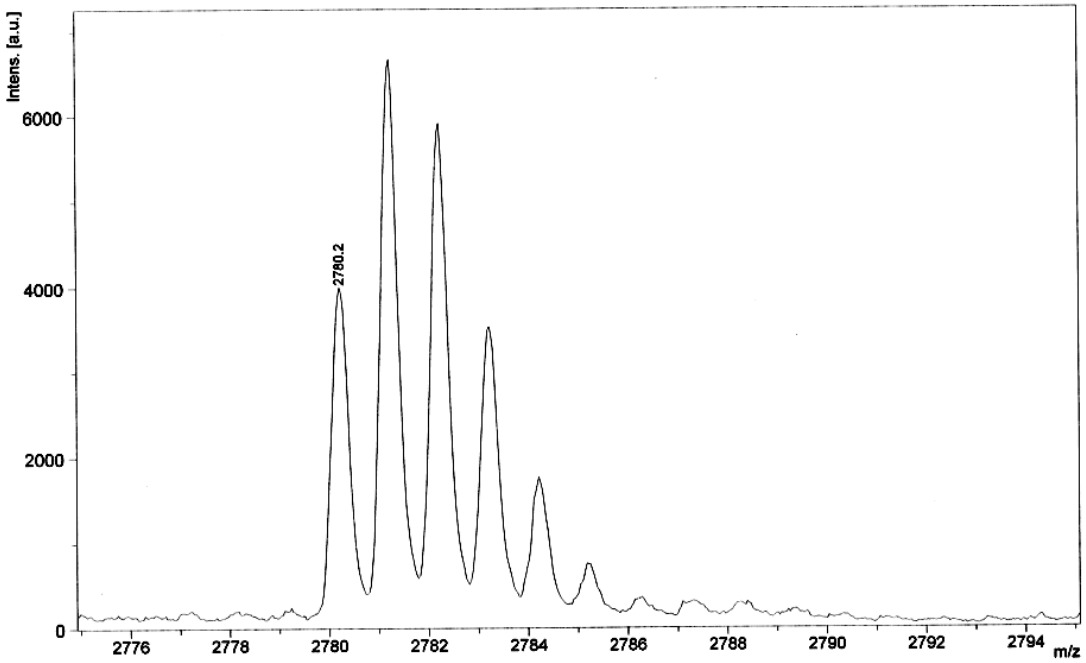
Intens. [a.u.]
6000
4000
2000
0
2776
2778
2780
2782
2784
2786
2788
2790
2792
2794
m/z
2780.2

Flu-5.11

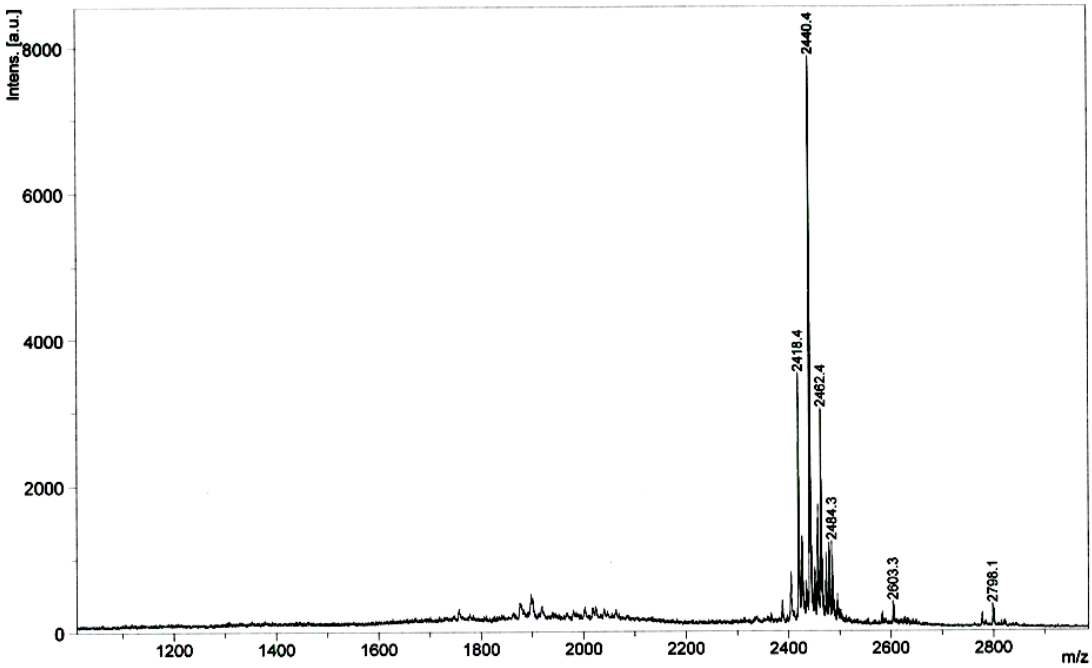

Flu-5.11

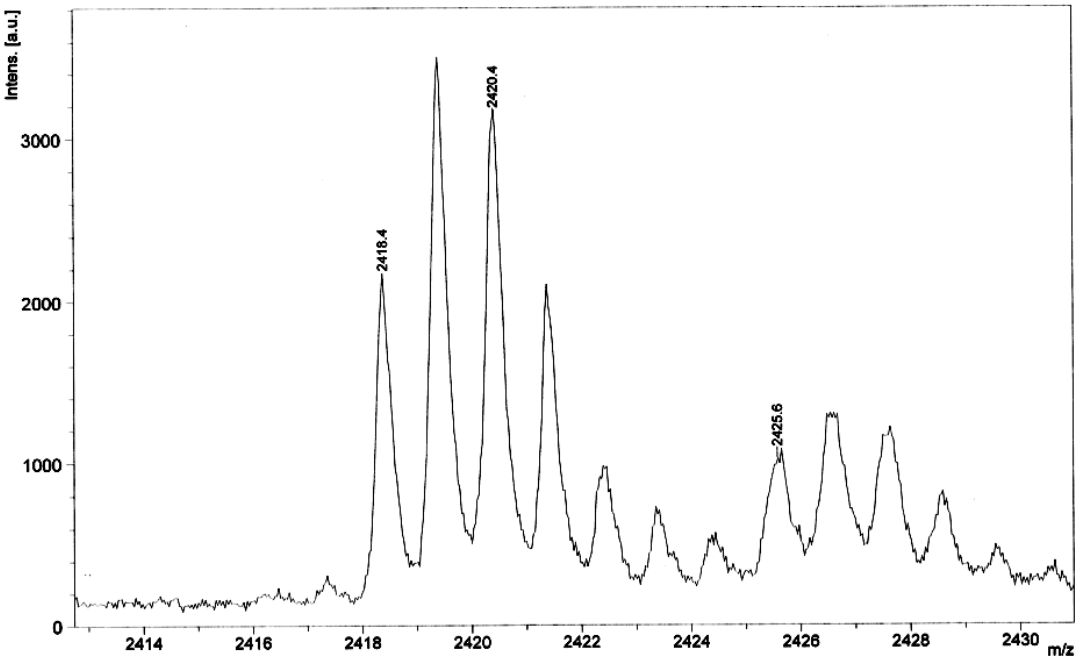

5.12.3 *Protein expression and purification*

Bcl-xL (plasmid: human His-EK-Bcl-xL, residue 1-196) and Mcl-1 (plasmid: human His-TEV-Mcl-1, residue 171-327) were expressed in BL21(DE3) *E. coli* cells, and purified using Ni-NTA agarose (Qiagen) column and FF Q column (GE healthcare) as previously described.[17]

A "loop-deleted" form of human Bcl-xL (Δ27-82 and without membrane anchor), which forms an α-1 domain-swapped dimer yet retains BH3 domain binding activity, was prepared as previously described.[9,27-29] The plasmid for the "loop-deleted" form of Bcl-xLΔ27-82 (from here abbreviating to Bcl-xLΔ) was obtained from the Fairlie lab in Australia, and was expressed in RIPL Escherichia coli cells, and purified. RIPL *E. coli* cells were grown in Luria Broth with 10 μg/mL ampicillin to an OD_{600} of 0.6-0.9. Cells were induced with 1.0 mM isopropyl-D-thiogalactoside (IPTG) and incubated for 4 hr. After harvesting, cells were lysed in 50 mM Tris pH 8.0, 150 mM NaCl, 2 mM dithiothreitol (DTT) (buffer 1) and centrifuged. The supernatant was applied to glutathione sepharose column, and washed with buffer 1. The GST-tag was cleaved on the column by adding prescission protease (GE Healthcare) and incubated 2 days in cold room. The filtrate was further purified on a Superdex 75 column in 20 mM Tris pH 8.0, 150 mM NaCl, 2 mM DTT.

Bcl-xL

MHHHH HHSSG LVPRG SGMKE TAAAK FERQH MDSPD LGTDD DDKAM S//MSQS NRELV VDFLS YKLSQ KGYSW SQFSD VEENR TEAPE GTESE METPS AINGN PSWHL ADSPA VNGAT GHSSS LDARE VIPMA AVKQA LREAG DEFEL RYRRA

FSDLT SQLHI TPGTA YQSFE QVVNE LFRDG VNWGR IVAFF SFGGA LCVES VDKEM QVLVS RIAAW MATYL NDHLE PWIQE NGGWD TFVEL YG

Bcl-xLΔ27-82

GPLGS MSQSN RELVV DFLSY KLSQK GYSWS QMAAV KQALR EAGDE FELRY RRAFS DLTSQ LHITP GTAYQ SFEQV VNELF RDGVN WGRIV AFFSF GGALC VESVD KEMQV LVSRI AAWMA TYLND HLEPW IQENG GWDTF VELYG NNAAA ESRKG QER

Mcl-1

MGSHH HHHHH HGSDY DIPTT ENLYF QGSED ELYRQ SLEII SRYLR EQATG AKDTK PMGRS GATSR KALET LRRVG DGVQR NHETA FQGML RKLDI KNE D DVKSL SRVMI HVFSD GVTNW GRIVT LISFG AFVAK HLKTI NQESC IEP LA ESITD VLVRT KRDWL VKQRG WDGFV EFFHV EDLEG G

5*.12.4 Fluorescence polarization assays*

Fluorescence polarization (FP) assays were conducted at room temperature in 384-well, black polystyrene plates (Costar). Competitive and direct binding FP assays were conducted as reported previously.[9] Briefly, for direct binding, binding affinity (K_d) of a tracer peptide for protein was measured by titrating a fixed concentration (10 nM) of tracer (BODIPY^{TMR}-Bak, Flu-Bim) with increasing concentrations (0.019 – 625 nM) of protein (Bcl-x_L, Mcl-1, and Bcl-xLΔ) in assay buffer (50 mM NaCl, 16.2 mM Na_2HP0_4, 3.8 mM KH_2PO_4, 0.15 mM NaN_3, 0.15 mM EDTA, 0.5 mg/mL Pluoronic-F68, pH 7.5) in a total volume of 50 μL per well. The binding reaction was allowed to equilibrate in for ~5 hours, and analyzed on an Envision 2100 plate reader. The data were fit using Graphpad Prism to a FP direct binding model.[33] The resulting K_d values were used for

the calculation of inhibitor dissociation constant (K_i) values after the competition FP assays.

For competition FP assays using Bcl-x_L (or Bcl-$x_L\Delta$,), the final concentrations of BODIPY-TMR-Bak tracer and Bcl-x_L (or Bcl-$x_L\Delta$) was 3 nM and 2 nM, respectively in FP buffer, and was added 2 μL aliquots of serial dilutions of α- or α/β/γ- Bim mimic peptides in DMSO with final concentrations ranging from 1.7 nM to 100 μM. For Mcl-1 competition FP assays, the final concentrations of Flu-Bim tracer and Mcl-1 were 10 nM each. The binding reaction was allowed to equilibrate in for ~5 hours, and plates were analyzed on an Envision 2100 plate reader. Inhibition constants (K_i) were determined by a competitive binding model using Graphpad Prism.[34] % Inhibition curves were plotted as previously described.[17]

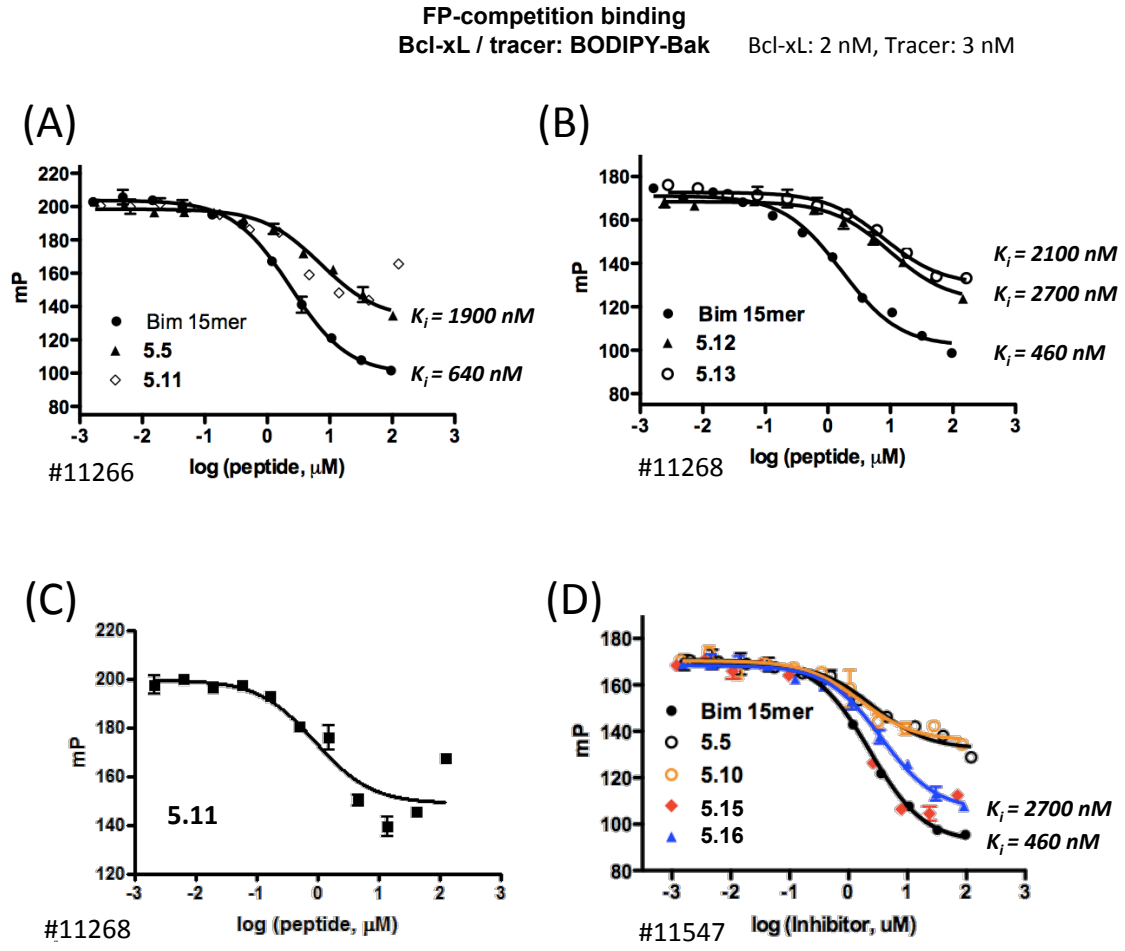

Figure 5.18 Bcl-xL competition binding FP data for α-Bim 15-mer and α/β/γ-peptides **5.11**-**5.16**. The curves result from fitting experimental data to the competitive binding model in GraphPad Prism.[34] (K_i values from **5.5** are not reliable because the FP curves did not reach the fully bound state)

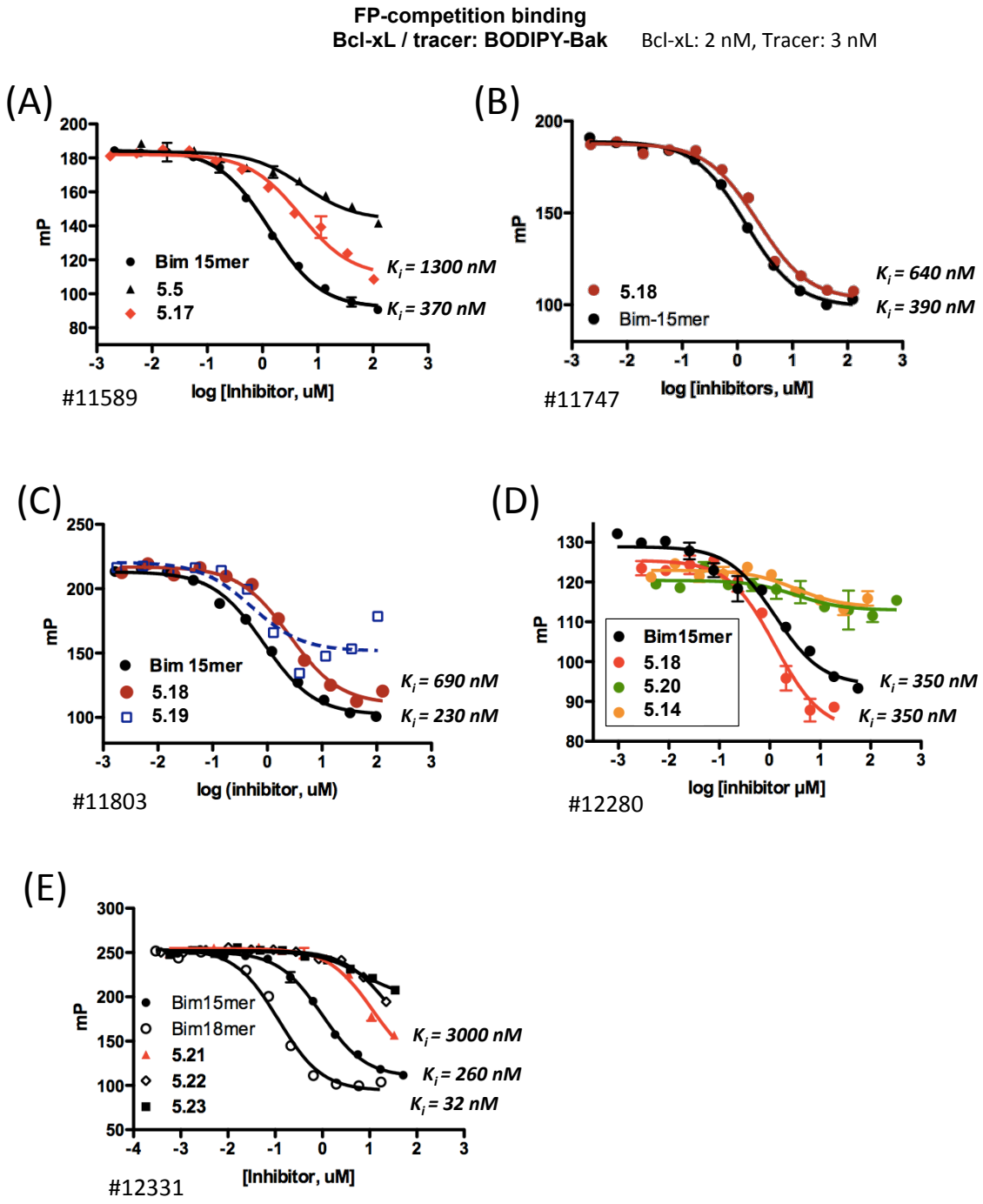

Figure 5.19 Bcl-xL competition binding FP data for α-Bim 15-mer and 18-mer, and α/β/γ-peptides **5.17**-**5.23**. Curves result from fitting experimental data to the competitive binding model in GraphPad Prism.[34]

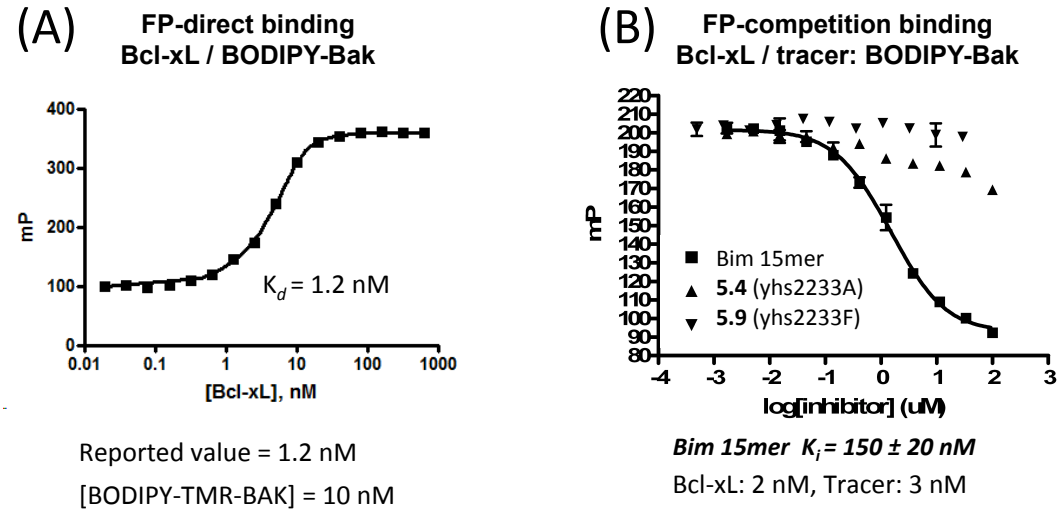

Figure 5.20 (A) Bcl-xL direct binding FP data for BODIPY^{TMR}-labeled Bak 16-mer (Bak 16-mer: GQVGRQLAIIGDDINR). Curves result from fitting the experimental data to analytical expressions for FP direct binding.[33] (B) Bcl-xL competition binding FP data for α-Bim 15-mer and $\alpha/\beta/\gamma$-peptides **5.4** and **5.9**. Curves result from fitting experimental data to the competitive binding model in GraphPad Prism.[34]

5.12.5 Circular dichroism spectroscopy

Elipticity spectra of wavelength scans (260 nm - 190 nm) were recorded in a 1 mm quartz cell with an averaging time of 6 sec for each step (1 nm step size) in pH 7.5 PBS buffer and in 50 % methanol/50% PBS buffer at 20 ^{o}C (AVIV circular dichroism spectrometer model 420). Peptides were prepared as 50-100 μM for the CD measurements.

5.13 References

(1) Kim, H.; Rafiuddin-Shah, M.; Tu, H.-C.; Jeffers, J. R.; Zambetti, G. P.; Hsieh, J. J. D.; Cheng, E. H. Y. Hierarchical regulation of mitochondrion-dependent apoptosis by BCL-2 subfamilies. *Nature Cell Biology* **2006**, *8*, 1348.

(2) Ghiotto, F.; Fais, F.; Bruno, S. BH3-Only Proteins: The Death-Puppeteer's Wires. *Cytometry Part A* **2010**, *77A*, 11-21.

(3) Meier, P.; Vousden, K. H. Lucifer's labyrinth - Ten years of path finding in cell death. *Molecular Cell* **2007**, *28*, 746-754.

(4) Willis, S. N.; Fletcher, J. I.; Kaufmann, T.; van Delft, M. F.; Chen, L.; Czabotar, P. E.; Ierino, H.; Lee, E. F.; Fairlie, W. D.; Bouillet, P.; Strasser, A.; Kluck, R. M.; Adams, J. M.; Huang, D. C. S. Apoptosis initiated when BH3 ligands engage multiple Bcl-2 homologs, not Bax or Bak. *Science* **2007**, *315*, 856-859.

(5) Willis, S. N.; Chen, L.; Dewson, G.; Wei, A.; Naik, E.; Fletcher, J. I.; Adams, J. M.; Huang, D. C. S. Proapoptotic Bak is sequestered by Mcl-1 and Bcl-x(L), but not Bcl-2, until displaced by BH3-only proteins. *Genes & Development* **2005**, *19*, 1294-1305.

(6) Lessene, G.; Czabotar, P. E.; Colman, P. M. BCL-2 family antagonists for cancer therapy. *Nature Reviews Drug Discovery* **2008**, *7*, 989-1000.

(7) van Delft, M. F.; Wei, A. H.; Mason, K. D.; Vandenberg, C. J.; Chen, L.; Czabotar, P. E.; Willis, S. N.; Scott, C. L.; Day, C. L.; Cory, S.; Adams, J. M.; Roberts, A. W.; Huang, D. C. S. The BH3 mimetic ABT-737 targets selective Bcl-2 proteins and efficiently induces apoptosis via Bak/Bax if Mcl-1 is neutralized. *Cancer Cell* **2006**, *10*, 389-399.

(8) Konopleva, M.; Contractor, R.; Tsao, T.; Samudio, I.; Ruvalo, P. P.; Kitada, S.; Deng, X.; Zhai, D.; Shi, Y.-X.; Sneed, T.; Verhaegen, M.; Soengas, M.; Ruvolo, V. R.; McQueen, T.; Schober, W. D.; Watt, J. C.; Jiffar, T.; Ling, X.; Marini, F. C.; Harris, D.; Dietrich, M.; Estrov, Z.; McCubrey, J.; May, W. S.; Reed, J. C.; Andreeff, M. Mechanisms of apoptosis sensitivity and resistance to the BH3 mimetic ABT-737 in acute myeloid leukemia. *Cancer Cell* **2006**, *10*, 375-388.

(9) Boersma, M. D.; Haase, H. S.; Peterson-Kaufman, K. J.; Lee, E. F.; Clarke, O. B.; Colman, P. M.; Smith, B. J.; Horne, W. S.; Fairlie, W. D.; Gellman, S. H. Evaluation

of Diverse alpha/beta-Backbone Patterns for Functional alpha-Helix Mimicry: Analogues of the Bim BH3 Domain. *Journal of the American Chemical Society* **2012**, *134*, 315-323.

(10) Certo, M.; Moore, V. D.; Nishino, M.; Wei, G.; Korsmeyer, S.; Armstrong, S. A.; Letai, A. Mitochondria primed by death signals determine cellular addiction to antiapoptotic BCL-2 family members. *Cancer Cell* **2006**, *9*, 351-365.

(11) Oltersdorf, T.; Elmore, S. W.; Shoemaker, A. R.; Armstrong, R. C.; Augeri, D. J.; Belli, B. A.; Bruncko, M.; Deckwerth, T. L.; Dinges, J.; Hajduk, P. J.; Joseph, M. K.; Kitada, S.; Korsmeyer, S. J.; Kunzer, A. R.; Letai, A.; Li, C.; Mitten, M. J.; Nettesheim, D. G.; Ng, S.; Nimmer, P. M.; O'Connor, J. M.; Oleksijew, A.; Petros, A. M.; Reed, J. C.; Shen, W.; Tahir, S. K.; Thompson, C. B.; Tomaselli, K. J.; Wang, B. L.; Wendt, M. D.; Zhang, H. C.; Fesik, S. W.; Rosenberg, S. H. An inhibitor of Bcl-2 family proteins induces regression of solid tumours. *Nature* **2005**, *435*, 677-681.

(12) Gellman, S. H. Foldamers: A manifesto. *Accounts of Chemical Research* **1998**, *31*, 173-180.

(13) Horne, W. S.; Gellman, S. H. Foldamers with Heterogeneous Backbones. *Accounts of Chemical Research* **2008**, *41*, 1399-1408.

(14) Johnson, L. M.; Gellman, S. H.: alpha-Helix Mimicry with alpha/beta-Peptides. In *Methods in Protein Design*; Keating, A. E., Ed.; Methods in Enzymology, 2013; Vol. 523; pp 407-429.

(15) Johnson, L. M.; Mortenson, D. E.; Yun, H. G.; Horne, W. S.; Ketas, T. J.; Lu, M.; Moore, J. P.; Gellman, S. H. Enhancement of alpha-Helix Mimicry by an alpha/beta-Peptide Foldamer via Incorporation of a Dense Ionic Side-Chain Array. *Journal of the American Chemical Society* **2012**, *134*, 7317-7320.

(16) Horne, W. S.; Johnson, L. M.; Ketas, T. J.; Klasse, P. J.; Lu, M.; Moore, J. P.; Gellman, S. H. Structural and biological mimicry of protein surface recognition by alpha/beta-peptide foldamers. *Proceedings of the National Academy of Sciences of the United States of America* **2009**, *106*, 14751-14756.

(17) Horne, W. S.; Boersma, M. D.; Windsor, M. A.; Gellman, S. H. Sequence-based design of alpha/beta-peptide foldamers that mimic BH3 domains. *Angewandte Chemie-International Edition* **2008**, *47*, 2853-2856.

(18) Horne, W. S.; Price, J. L.; Keck, J. L.; Gellman, S. H. Helix bundle quaternary structure from alpha/beta-peptide foldamers. *Journal of the American Chemical Society* **2007**, *129*, 4178.

(19) Sadowsky, J. D.; Douglas Fairlie, W.; Hadley, E. B.; Lee, H.-S.; Umezawa, N.; Nikolovska-Coleska, Z.; Wang, S.; Huang, D. C. S.; Tomita, Y.; Gellman, S. H. (alpha/beta+alpha)-Peptide antagonists of BH3 Domain/Bcl-x(L) recognition: Toward general strategies for foldamer-based inhibition of protein-protein interactions. *Journal of the American Chemical Society* **2007**, *129*, 139-154.

(20) Cheloha, R. W.; Maeda, A.; Dean, T.; Gardella, T. J.; Gellman, S. H. Backbone modification of a polypeptide drug alters duration of action in vivo. *Nature Biotechnology* **2014**, *32*, 653.

(21) Johnson, L. M.; Horne, W. S.; Gellman, S. H. Broad Distribution of Energetically Important Contacts across an Extended Protein Interface. *Journal of the American Chemical Society* **2011**, *133*, 10038-10041.

(22) Shin, Y.-H.; Mortenson, D. E.; Satyshur, K. A.; Forest, K. T.; Gellman, S. H. Differential Impact of beta and gamma Residue Preorganization on alpha/beta/gamma-Peptide Helix Stability in Water. *Journal of the American Chemical Society* **2013**, *135*, 8149-8152.

(23) Sawada, T.; Gellman, S. H. Structural Mimicry of the alpha-Helix in Aqueous Solution with an Isoatomic alpha/beta/gamma-Peptide Backbone. *Journal of the American Chemical Society* **2011**, *133*, 7336-7339.

(24) Lee, E. F.; Czabotar, P. E.; Van Delft, M. F.; Michalak, E. M.; Boyle, M. J.; Willis, S. N.; Puthalakath, H.; Bouillet, P.; Colman, P. M.; Huang, D. C. S.; Fairlie, W. D. A novel BH3 ligand that selectively targets Mcl-1 reveals that apoptosis can proceed without Mcl-1 degradation. *Journal of Cell Biology* **2008**, *180*, 341-355.

(25) Chen, L.; Willis, S. N.; Wei, A.; Smith, B. J.; Fletcher, J. I.; Hinds, M. G.; Colman, P. M.; Day, C. L.; Adams, J. M.; Huang, D. C. S. Differential targeting of prosurvival Bcl-

2 proteins by their BH3-only ligands allows complementary apoptotic function. *Molecular Cell* **2005**, *17*, 393-403.

(26) Woody, R. W. Contributions of Tryptophan Side-chains to the Far-ultraviolet Circular-Dichroism of Protiens. *European Biophysics Journal with Biophysics Letters* **1994**, *23*, 253-262.

(27) Smith, B. J.; Lee, E. F.; Checco, J. W.; Evangelista, M.; Gellman, S. H.; Fairlie, W. D. Structure-Guided Rational Design of /-Peptide Foldamers with High Affinity for BCL-2 Family Prosurvival Proteins. *Chembiochem* **2013**, *14*, 1564-1572.

(28) Lee, E. F.; Smith, B. J.; Horne, W. S.; Mayer, K. N.; Evangelista, M.; Colman, P. M.; Gellman, S. H.; Fairlie, W. D. Structural Basis of Bcl-x(L) Recognition by a BH3-Mimetic alpha/beta-Peptide Generated by Sequence-Based Design. *Chembiochem* **2011**, *12*, 2025-2032.

(29) Lee, E. F.; Sadowsky, J. D.; Smith, B. J.; Czabotar, P. E.; Peterson-Kaufman, K. J.; Colman, P. M.; Gellman, S. H.; Fairlie, W. D. High-Resolution Structural Characterization of a Helical alpha/beta-Peptide Foldamer Bound to the Anti-Apoptotic Protein Bcl-x(L). *Angewandte Chemie-International Edition* **2009**, *48*, 4318-4322.

(30) LePlae, P. R.; Umezawa, N.; Lee, H. S.; Gellman, S. H. An efficient route to either enantiomer of trans-2-aminocyclopentanecarboxylic acid. *Journal of Organic Chemistry* **2001**, *66*, 5629-5632.

(31) Guo, L.; Chi, Y.; Almeida, A. M.; Guzei, I. A.; Parker, B. K.; Gellman, S. H. Stereospecific Synthesis of Conformationally Constrained gamma-Amino Acids: New Foldamer Building Blocks That Support Helical Secondary Structure. *Journal of the American Chemical Society* **2009**, *131*, 16018.

(32) Murray, J. K.; Gellman, S. H. Parallel synthesis of peptide libraries using microwave irradiation. *Nature Protocols* **2007**, *2*, 624-631.

(33) Zhang, R. M.; Mayhood, T.; Lipari, P.; Wang, Y. L.; Durkin, J.; Syto, R.; Gesell, J.; McNemar, C.; Windsor, W. Fluorescence polarization assay and inhibitor design for MDM2/p53 interaction. *Analytical Biochemistry* **2004**, *331*, 138-146.

(34) Roehrl, M. H. A.; Wang, J. Y.; Wagner, G. A general framework for development and data analysis of competitive high-throughput screens for small-molecule inhibitors

of protein - Protein interactions by fluorescence polarization. *Biochemistry* **2004**, *43*, 16056.